Amélioration des propriétés rhéologiques et à jeune âge des laitiers alcali-activés au carbonate de sodium

Artur Kiiashko

université PARIS-SACLAY

NNT : 2019SACLN033

Thèse de doctorat

école normale supérieure paris-saclay

Improving the rheological and early age properties of sodium carbonate alkali-activated GGBS

Thèse de doctorat de l'Université Paris-Saclay
préparée à L'École normale supérieure Paris-Saclay

École doctorale n◦579 : Sciences Mécaniques et Énergétiques, Matériaux et Géosciences (SMEMAG)
Spécialité de doctorat: Génie Civil

Thèse présentée à Cachan, le 10 septembre 2019, par

M. Artur Kiiashko

Composition du Jury :

M Pavlo KRYVENKO Professeur, Kyiv National University of Construction and Architecture, Directeur SRIBM	Rapporteur
M Martin CYR Professeur, Université de Toulouse, LMDC	Rapporteur
M Mohend CHAOUCHE Directeur de recherche CNRS, ENS Paris-Saclay, LMT	Directeur de thèse
M Farid BENBOUDJEMA Professeur, ENS Paris-Saclay, LMT	Président du jury
M Laurent FROUIN Directeur R&D, ECOCEM Materials Ltd.	Examinateur
M François CUSSIGH Directeur R&D, Vinci Construction France	Examinateur
M Donal O'RIAN Directeur Général, ECOCEM Group	Invité
M Nicolas MUSIKAS Directeur Technique, ECOCEM Group	Invité

Titre : Amélioration des propriétés rhéologiques et à jeune âge des laitiers alcali-activés au carbonate de sodium

Mots clés : Laitier de hauts fourneaux ; ciment à base de laitier ; liant alkali-activé ; Carbonate de sodium ; ciment écologique ; ciment à faible impact CO_2

Résumé : Aujourd'hui, les problèmes environnementaux sont plus graves que jamais. Des mesures urgentes devraient être prises dans tous les domaines de l'activité humaine, y compris la construction. L'un des principaux contributeurs à l'impact négatif de cette industrie sur l'environnement est la fabrication du ciment Portland ordinaire (OPC) nécessaire à la production de béton et d'autres matériaux cimentaire. Malgré son importance, il présente un inconvénient important: sa production est accompagnée par de grandes quantités de gaz à effet de serre. Ils représentent 5 à 8% des émissions mondiales totales de CO_2. Des matériaux cimentaires plus écologiques sont maintenant nécessaires.

Des réductions significatives de l'impact sur l'environnement ne peuvent être obtenues que par l'utilisation de liants de nouvelle génération dont la fabrication ne nécessite pas beaucoup de processus et de traitements supplémentaires. L'une d'elles consiste à utiliser des déchets industriels comme liants (différentes laitiers, cendres volantes, cendres de biomasse, etc.). De cette manière, il y a non seulement une réduction de l'impact de processus tels que l'extraction minière ou la calcination, mais également le recyclage des déchets (un principe de l'économie circulaire).

Une possibilité consiste à utiliser du laitier de haut fourneau (GGBS) comme base pour ce ciment de nouvelle génération. En raison de sa réactivité relativement faible avec l'eau, des suppléments (également appelés activateurs) doivent être utilisés pour favoriser le processus d'hydratation. Le carbonate de sodium (Na_2CO_3) est l'un des activateurs les plus prometteurs et en même temps les moins étudiés. Un tel ciment alkali-activé présente des propriétés mécaniques et de durabilité élevées, ainsi qu'une empreinte CO_2 très faible. Parmi les principaux problèmes qui entravent son utilisation à l'échelle industrielle, on peut mentionner une évolution de la résistance lente à jeune âge et de rhéologie médiocre.

L'objectif de la présente thèse est de développer une nouvelle conception du liant à base de laitier activé par Na_2CO_3, qui répondrait à toutes les exigences modernes du secteur de la construction, en particulier les propriétés rhéologiques et le développement de la résistance à jeune âge. Ce liant doit toujours répondre à au moins trois critères principaux: faible impact environnemental, faibles risques de danger dans les applications sur le terrain et être économiquement compétitif à l'échelle industrielle.

Dans le présent travail, l'influence de différents paramètres tels que le rapport eau/liant, la concentration de Na_2CO_3, la finesse du laitier et les conditions de durcissement sur les propriétés du mélange à jeune âge et à long terme a été étudiée. Sur la base des résultats du processus d'hydratation, les additifs à base de phosphonate qui permettent de contrôler efficacement la rhéologie de tels liants ont été testé avec succès. Ils permettent non seulement de contrôler le temps de prise, mais fournissent également un effet plastifiant.

En ce qui concerne l'amélioration des propriétés de résistance au jeune âge, différentes méthodes ont été utilisées. L'utilisation d'un traitement thermique ou d'une augmentation de la finesse du GGBS s'est avérée efficace. L'exploration des causes d'une longue période d'induction a montré que l'accélération pouvait également être obtenue par l'ajout d'une source de calcium à cinétique de dissolution contrôlée. En conséquence, le liant est devenu plus réactif et plus robuste à certains facteurs (concentration d'activateur, rapport eau/liant, conditions de durcissement, etc.). Pour compenser l'empreinte carbone supplémentaire de la source de calcium ajoutée, le liant a été dilué avec succès par le calcaire sans aucune dégradation des propriétés à un certain pourcentage de dilution.

Université Paris-Saclay
Espace Technologique / Immeuble Discovery
Route de l'Orme aux Merisiers RD 128 / 91190 Saint-Aubin, France

ÉCOLE DOCTORALE
Sciences mécaniques et énergétiques, matériaux et géosciences (SMEMAG)

Title : Improving the rheological and early age properties of sodium carbonate alkali-activated GGBS

Keywords : Ground granulated blast-furnace slag (GGBS); slag cement; Alkali-activated binder; Sodium carbonate; eco-friendly cement; low CO_2 binder

Abstract : Today, environmental problems are more acute than ever. Urgent measures should be taken in all spheres of human activity including construction and civil engineering. One of the major contributors of negative environmental impacts from this industry is the manufacturing of ordinary Portland cement (OPC) required for concrete and other cementitious materials. Although, vital to economical development, it has a significant drawback - its production is accompanied by the emission of large quantities of greenhouse gases. They account for 5-8% of total world CO_2 emissions. More environmentally friendly cementitious materials are now required.

Significant reductions of the environmental impact can be achieved only through the use of new-generation binders whose manufacture does not require a lot of additional processes and treatments. One route is through the use of industrial wastes as binders (different slags, fly ash, biomass bottom ash, etc.). In this way there is not only a reduction in the impact of processes such as mining or calcination, but also the recycling of waste materials (circular economy principle).

One possibility is to use ground granulated blast furnace slag (GGBS) as the basis for such a new generation cement. Due to its rather low reactivity with water, additional supplements (also called activators) should be used to promote the hydration process. One of the most promising, and at the same time least studied, activators is sodium carbonate (Na_2CO_3). Such alkali-activated cements present high mechanical and durability properties, as well as a very low CO_2 footprint. Among the main problems hindering its industrial scale adoption are their poor rheology and slow strength gain within the first days of hardening.

The objective of this thesis is to develop a new binder based on Na_2CO_3 activated GGBS that meets all the modern requirements of the construction industry, with particular regard to its rheological properties and early age strength development. In addition this binder should always respond to at least three main criteria: low environmental impact, low health and safety concerns in field applications, and be economically competitive at industrial scale.

In the present work, the influence of different parameters like water/binder ratio, Na_2CO_3 concentration, slag fineness and curing conditions on both early age and long term properties of the mixture were studied. Based on the results of the hydration process analysis, phosphonate based additives that allow for the effective control of the rheology of such binders were successfully tested. They not only allow control over the setting time, but also provide a plasticizing effect.

Regarding the improvement of early age strength properties, various methods have been used. The use of heat treatment or an increase of GGBS fineness turned out to be efficient. Exploring the causes of the long induction period has shown that acceleration can also be achieved by the addition of a calcium source with controlled dissolution kinetics. As a result, the binder became more reactive and robust against certain factors (activator concentration, Water/Binder ratio, curing conditions, etc.). To compensate for the additional carbon footprint from the added calcium source, the binder was successfully diluted by limestone without any degradation of the properties below some dilution percentages.

Université Paris-Saclay
Espace Technologique / Immeuble Discovery
Route de l'Orme aux Merisiers RD 128 / 91190 Saint-Aubin, France

Acknowledgment

Climate change is a threat to humanity, but it's not too late to prevent it. I acknowledge ECOCEM for the opportunity to realise this research. It is very valuable when people share a common idea of a better future. I'm grateful to all of my colleagues from ECOCEM. Specifically, I want to thank Mr Laurent Frouin for his support, his advice and the great experience he shares. His faith was the engine of this work.

I would like to express my sincere gratitude to my supervisor Mr Mohend Chaouche. His knowledge, great support and sometimes mad enthusiasm was another engine for this work. But especially I would like to thank him for showing me how to see the things from a different angle and how to not think like everyone else. This skill is a driving force for progress and is a rarity in the modern world.

This PhD work was developed at the Laboratory of Mechanics and Technology (LMT) at the ENS Paris-Saclay in France. I would like, first of all, to thank all colleagues and staff at the LMT for the excellent working conditions and research facilities provided to me during this period. I would especially like to thank Rémy and Olivier for their great patience and assistance.

Last but not least, I wish to thank my parents, Irina and Dmytro, for their sacrifices in life so that I could be where I am today and special thanks to my grandmother, Alexandra.

Contents

General introduction

A basic principle adopted by many countries in recent years is sustainable and durable development. This principle also applies to the construction industry, which has a significant influence on the large aspects of society. Today, environmental issues are among the top priorities. Significant human activity (mining, excessive soil depletion, greenhouse gas, plastic, etc.) has already led to climate change~~s~~, problems with access to potable water, and the disappearance of a large number of animal~~s~~ and plant species. Decisive action must be taken to stop the degradation of the planet and prevent human extinction.

Being one of the biggest and most important sectors of the economy, the construction and civil engineering industry is one of the least active sectors in promoting innovation. Nevertheless, today it is becoming not only an option, but is gradually becoming mandatory by government regulation. More environmentally-friendly materials, good thermal insulation of buildings, and increasing the percentage of construction waste recycling are now required.

One of the major contributors of negative environmental impacts from this industry is the manufacturing of ordinary Portland cement (OPC) required for concrete production. Portland cement is the second most used resource in the world after water: its consumption is about 0.5 ton/person/year. With the increasing of the world's population and continued urbanization, from year to year the need for concrete will grow to meet the needs of new construction and the reconstruction of old buildings/infrastructure. It is worth noting that the average life expectancy of OPC based concrete, before major repairs or complete replacement, is between 50 and 100 years (depending on concrete composition and operating conditions). Of course, the cement industry is able to satisfy these needs. However, the negative effect of increasing greenhouse gas (GHG) emissions will affect climate change~~s~~. The production of cement inherently generates CO_2 during the calcination of the raw materials at very high temperature (about 1450°C.) in a kiln through the decarbonation of limestone (1):

$$CaCO_3\ (s) \rightarrow CaO\ (s) + CO_2\ (g) \qquad (1)$$

In addition, carbon dioxide is released as a result of the fossil fuels combustion needed to heat the kiln. By adding the emissions from the grinding process, almost 0.8-1 ton of CO_2 per ton of OPC is generated. Overall, the cement industry is responsible for 5-8% of the global carbon dioxide emissions (Naik, 2005; Turner and Collins, 2013; Davidovits, 2015). Various strategies employed to decrease CO_2 emissions, such as the dilution of OPC by different

supplementary cementitious materials (SCM), lowering the calcination temperature, burning of urban wastes, etc. doesn't leads to a serious decrease in CO_2 emissions or could even lead to a degradation of the cement properties (Papadakis and Tsimas, 2002; Rahman et al., 2012; Oliveira et al., 2017). The lowest quality cement led to a lower durability with a shorter concrete serving-life, which in the long term leads to a more negative environmental impact.

Significant reductions on the environmental impact of this industry can be achieved only by the use of new-generation binders whose manufacture does not require a lot of additional processes and treatments. One route is through using resources such as industrial wastes as binders (different slags, fly ash, biomass bottom ash, etc.). In this way there is not only a reduction in the impact of processes such as mining or calcination, but also the recycling of waste materials. Therefore, such materials become "co-products": waste for one industry, but a primary resource for others (principle of the circular economy).

The most reported-on group is alkali-activated industrial co-products based binders (Shi. et al., 2006; Provis and Deventer, 2014). Nonetheless, their carbon footprint strongly depends on the binder mix design, which can be significantly lower than OPC, as well as higher in some cases (depending on co-product nature, the choice of alkaline activator and its amount). One of the most prospective binders in this group is ground granulated blast furnace slag (GGBS) alkali-activated by sodium carbonate. This type of alkali activation provides the lowest price and the highest safety (low hazard risk), as well as excellent long term mechanical and durability properties. Among the main problems hindering its industrial-scale adoption are a rather slow strength evolution in the first days of hardening and poor rheology, improvement of these aspects are the main goal of this work.

The aims of the work

The objective of this investigation is to develop a new binder based on GGBS activated with sodium carbonate, which meets all the modern requirements of the construction industry with particular regard to the rheological properties and early age strength development.

Notwithstanding this, the binder should respond to at least three main criteria: low environmental impact, low hazardous concerns in field applications, and economically competitive at industrial scale. These three points are developed hereafter.

i) Low environmental impact

This is the case of slag which is a by-product of iron industry. By grinding this product into fine powder, one can obtain a cementitious material (GGBS). Nowadays, at the most modern ECOCEM plant in Dunkerque, the production of 1t of standard GGBS (4400 cm^2/g) generates only about 18 kg of CO_2 (information from www.ecocem.fr).

It is important to note that the use of GGBS as the main binder component is not only environmentally-friendly, but also leads to several enhanced technical properties such as high resistance to sulphate attacks and alkali-silica reaction, low chloride permeability, good behaviour in a chemically aggressive environments (various acids), low heat of hydration (required in massive structures to reduce thermal cracking), possible self-healing, etc. This means that such products require much less repair works and have a longer serving-life, which gives a supplementary economic and ecological benefit in long term.

Another benefit of GGBS, which not sufficiently considered in the literature, is its low water demand to achieve the appropriate rheological properties. Indeed the hydration product that is characterized by the highest water-consumption is ettringite, which is absent in a GGBS-Na_2CO_3 based binder. This is also important from both the environmental and societal point of view. Indeed, there is a dramatic reduction of water resources all over the world, not only in arid regions, leading in particular to geopolitical tensions and wars. In this regard, the benefits of decreasing the amount of mixing water used in cementitious materials is not anecdotal taking into account the huge amount of cementitious materials consumed globally.

Considering the activator Na_2CO_3 from ecological point of view, it is worth noting that Na_2CO_3 production's carbon footprint can be between 100 (from natural trona deposit, 25% of world production) and 800 kg (Solway process) per ton without transportation and other

additional processes (Houghton et al., 1996; Provis and Deventer, 2014). This is much lower than sodium silicate manufacturing, for example (Turner and Collins, 2013). Moreover (Parker et al., 2013; Harrabin, 2017) report a creation of industrial plants that could transform CO_2 emissions from some industrial process into soda ash. Which again leads to the principles of a circular economy.

In addition, the possible dilution of such binders by another co-product with even lower environmental impacts or with other local wastes/products to minimise the GHG emissions from transportation, should lead to an even greater decrease in environmental impact, provided all required properties are satisfied. For example, GGBS-limestone binders activated with Na_2CO_3 have already been considered in the literature (Moseson et al., 2012; Rakhimova et al., 2016; B. Yuan et al., 2017). However, the mixes were not optimized and the performances were mediocre in some cases. For instance, sufficiently high strength development before 3 days was not reported. Many parameters still require additional studies.

ii) Low hazardous concerns

Handling Portland cement may lead to health issues (such as allergies) due in particular to its high alkalinity (pH higher than 13.5). In addition, hazardous elements such as hexavalent Chromium may be released upon mixing, which is also toxic for the workers. Although Cr reducing agents (such as ferrous sulfate) are normally included in the cement powder, their efficiency is limited (Klemm, 1994). Builders, in particular those in the developing world, are not expected to often check the deadline related to such treatments (date to which cement should be used). The presence of GGBS in the binder is known to participate in reducing Cr (VI) in Portland cement (Bae et al., 2018), considering its absence in GGBS itself. The presence of GGBS is also known to enhance the binding capacity of Cr, as well as other heavy metals (Cd, Pb, As, etc.), in the case of various waste treatments (Akhter et al., 1990; Allan and Kukacka, 1995). This is a definite advantage when it was proposed to dilute this binder by local wastes for higher ecological benefit.

Alkali-activated binders, in particular those based on alkali-silicates, can perform better than those based on Portland cement, including at early age. However, besides economical reasons, these binders are highly alkaline, and cannot be safely handled in the field without specific equipment. This is not the case of the binder based on Na_2CO_3 activation. Activation with sodium carbonate actually leads to relatively lower alkalinity before the start of setting and hardening, even compared to OPC. That is why this activator was chosen.

iii) An economically valuable binder

The binder developed in the present study is based on raw materials that are relatively cheap and available almost everywhere around the world. The availability of GGBS may turn out to be the most problematic. For the moment, the widest application of GGBS is in combination with Portland cement (CEM II/III). If its use as an independent binder is to be popularized, the fact that it is a limited resource may turn out to be an issue. Its production is materially advantageous under the current economic conditions only in countries producing cast iron. Therefore, its dilution with a high amount of limestone or another local materials will increase the *virtual* availability of GGBS.

Actually, the amount of effective binder used in cementitious materials is often over-estimated. In most cases, the hydration degree of the binder is quite low, even at long term. This suggests that it should be possible to achieve the required performance~~s~~ even at much lower effective binder contents, provided that full hydration by the addition of some supplementary materials or chemical additives is achieved. By optimizing the rheology of the binder, it would be possible to minimize the amount of active binder (GGBS) content used in concrete and use it only as a glue.

Outline of this thesis

This document comprises seven chapters. Chapter 1 gives an overview on GGBS based alkali-activated binders. It is highlighted that Na_2CO_3 activation is the most promising provided two main issues are addressed: poor rheology and low early age strength development. This is actually the main objective of this investigation. .

In Chapter 2 the rheological properties and the early age hydration kinetics of Na_2CO_3 activated GGBS are considered. The influence of several factors including slag fineness, sodium carbonate amount and water/binder ratio are highlighted. These results are subsequently used as a reference for the forthcoming studies. Detailed study of the hydration process at different stages, starting from the very first slag contact with the alkaline solution (using *in-situ* synchrotron XRD), coupled with various other experimental methods, allowed to determine possible solutions to deal with the delayed induction period of this type of activation.

Chapter 3 focuses precisely on improving the rheological properties of these binders by addition of phosphonate based additives. Detailed investigation of the impact of such additives on the fresh state properties and their eventual delay in hydration kinetics is considered. Their impact on the hydration products is further considered to unravel their working mechanisms.

The impact of the phosphonate retarder on the long term properties as strength evolution and shrinkage is considered in more details in Chapter 4. The impact of various factors on these properties in the presence of the phosphonate including slag fineness, activator concentration, storage conditions, etc. are also investigated.

Chapter 5 is devoted to an investigation of the way to improve the early age strength development of these binders. Clinker addition in low amount turned out to be the best way to improve early strength. The properties of the final mix including rheology, hydration process, strength development, shrinkage, etc. are then investigated in detail.

To compensate for the negative effects of all the various additives used (supplementary CO_2 footprint and cost) and the limited availability of GGBS, the possibility of diluting the GGBS with limestone is investigated in Chapter 6. Both fresh and hardened states properties of the previous mixes in which GGBS is partially replaced at different levels by limestone with different fineness grades are then considered

The last Chapter 7 is devoted to the impact of alumina additives with different solubilities on the hydration process of Na_2CO_3 activated GGBS. The case of NaOH is also considered for comparison. The objective was originally to improve the early age strength of such binders. Just the opposite was obtained. At the same time this study allows highlighting one possible origin

of the blockage of the hydration of GGBS when associated with a too highly reactive clinker as shown in the previous chapters.

Chapter 1 An overview of the state of knowledge regarding GGBS and GGBS-based binders

This chapter provides a basic literature review about GGBS production and its alkali-activation for the production of independent binders. Some information about the influence of some parameters (storage conditions, chemistry, fineness, etc.) on the properties of such mixes is presented.

1.1 General information and production of GGBS

Blast furnace slag is a by-product of pig iron production in the metallurgical industry. In blast furnaces, lightweight elements that make up part of the iron ore and various additives float to the surface of the molten metal (Figure 1.1). Slag protects the metal from the harmful effects of the gas environment of the blast furnace. It also has absorbent properties and removes various impurities that can negatively affect the properties of the iron. That is why the slag has a rich chemical composition, which contains various oxides of silicon, calcium, aluminium, manganese, magnesium and some sulphides. Depending on the raw materials used, the final composition of the slag differs from plant to plant and may vary slightly even on the same production line. The average chemical composition of blast furnace slag used in civil engineering works is presented in Table 1.

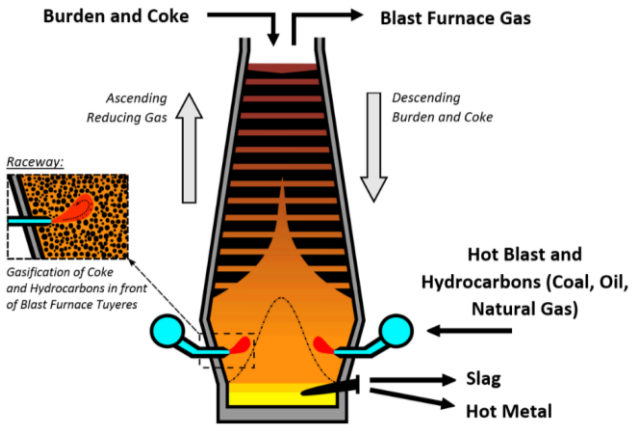

Figure 1.1: Blast furnace process overview (Spanlang et al., 2016)

Table 1: General chemical composition of slag (Moranville-Regourd, 1998)

Constituents	CaO	SiO_2	Al_2O_3	MgO	Fe_2O_3+MnO	S	TiO	Na_2O+K_2O
Proportion, %	30-50	28-38	8-24	1-18	1-3	1-2.5	<4	<2

A century ago, the production of one ton of iron resulted in almost one ton of slag, which led to significant problems in the storage and utilisation of such waste. Today, due to progress in the metallurgical industry and especially due to the enrichment of iron ore, a modern blast furnace generates between 200 and 500 kg of slag per 1t of iron. Nevertheless, even in this case, slag valorisation is an issue, since one steel plant can produce up to one million tons of slag per year (Malhotra, 1987; Laar et al., 2014).

At the exit from the blast furnace, the slag undergoes cooling. Depending on the method of cooling, different properties are obtained which are correspondingly suitable for different applications. In the case of slow air-cooling, its structure becomes crystalline. This slag after crushing is mostly used in road and civil engineering construction as soil foundation (Malhotra, 1987; Jahanshahi et al., 2012). On the other hand, rapidly water-cooled slag has an amorphous or glass structure and turns into what is called *slag sand* or *granulated blast furnace slag* (solid particles ≤ 10 mm). This slag acquires latent hydraulic properties (reaction with water under certain conditions). Cooling parameters greatly affect slag characteristics and significantly affect its subsequent reactivity. One of these parameters is the amount of the vitreous component, which for maximum reactivity must exceed 95% (Malhotra, 1987; Shi. et al., 2006). Nevertheless, due to its low solubility, a slag sand needs grinding to increase the area of its contact with solution and accordingly its reactivity. From this moment, such product is called *ground granulated blast furnace slag* (GGBS or GGBFS).

Nowadays the main use of such a product is its mixing with ordinary Portland cement to obtain a new blended binder with up to 95% GGBS (Type II and III cements). Such mixes provide a lower environmental impact, as well as some advantageous technical properties (lower released heat, higher long term strength, advanced durability in some cases, etc.). In this case, the characteristic of the slag to react relatively quickly with water is ensured not only by its fineness, but also by the presence of Portland cement. OPC dissolution provides a rapid rise of the pH and temperature inside the mix to accelerate the slag dissolution rate, as well as provide some compounds for the precipitation of the early hydrates.

Nevertheless, boosting the reaction of the slag with water by OPC addition is not the only method available. The addition of some chemical additives and modifying some parameters also make it possible to transform the GGBS into an independent hydraulic binder with similar or even greater mechanical properties than OPC.

1.2 Chemical activation and hydration process of non-OPC GGBS based binders

Slag-based binders consist of a GGBS powder blended with a chemical activator added in powder form or in aqueous solution. The chemical activation processes is highly dependent upon the type of activator. Nevertheless, they can all be characterised by the dissolution/precipitation reaction. During slag particle dissolution, the increase in the ions concentration of leached elements leads at some moment to their saturation and condensation, resulting in the formation of new solid precipitates (hydrates). This process can occur in acid, neutral or alkaline water solution, but only alkaline environments are considered in this work. The dissolution of the slag can be described by two processes (Shi. et al., 2006; Michel, 2009; Kouassi, 2011):

- ***Hydrolysis***

Immediately after the particles slag comes in contact with the aqueous solution, the leaching of the alkalis (Na^+ and K^+, Ca^{2+}, etc.) takes place. This will lead the hydrolysis of the water molecules and the H^+ ions play the role of charge compensators. This process leads to rise of the pH level and explains the alkaline self-reaction of the slag in water (Eq. 1 and 2).

$$[\equiv Si - O - Ca - O - Si \equiv] + 2H_2O \rightarrow 2[\equiv Si - OH] + Ca^{2+} + 2OH^- \quad \textit{Eq.1}$$

$$[\equiv Si - O - Na, K] + H_2O \rightarrow [\equiv Si - OH] + Na^+, K^+ + OH^- \quad \textit{Eq.2}$$

- ***Hydroxylation***

The OH^- ions, due to their high nucleophilic character (polarisation effect), break the Si-O and Al-O bonds, leading to an increase of the silicate and aluminates species concentration in the aqueous solution. The rate of silicate/aluminate leaching is significant only at high level of OH^- concentration (pH ≥ 10). Regarding the silica, in this case after the dissolution of $Si(OH)_4$ monomers, they undergo ionization to form highly soluble $SiO(OH)_3^-$ and $SiO_2(OH)_2^{2-}$ ions (alternatively written as H_3SiO^{4-} and $H_2SiO_4^{2-}$) (Maraghechi et al., 2016). Otherwise, only the first stage (hydrolysis) takes place and the Si/Al network plays the role of a protective layer against the complete dissolution of the slag surface. Assuming that no protective layer is formed on the surface of the slag grains, this process is monotonic until complete dissolution. This process is presented by the sketch in Figure 1.2.

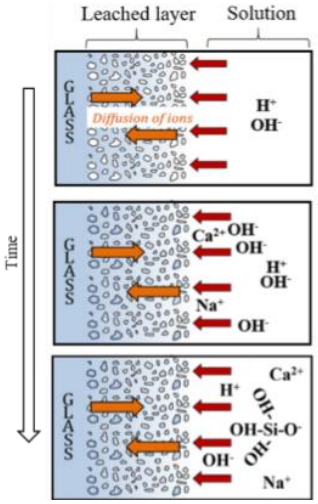

Figure 1.2: Schematic representation of leached layer model (Newlands et al., 2016)

Nevertheless, in reality simultaneous increasing of the Ca and Si/Al concentrations in solution leads to the formation of calcium-aluminium (CAH), calcium-silicate (C-S-H) and calcium-alumina-silicate (C-A-S-H) hydrate types. At the beginning, this process should mostly take place close to the slag surface where the concentration of the ionic species is high. It might be responsible for the latent hydraulic behaviour of GGBS (noticeable slowing down of the hydration process) due to the formation this passivation layer composed of hydrates (Figure 1.3). However due to the porosity of this layer, the solution can still penetrate to the slag surface and maintain leaching (Newlands et al., 2016). From this moment, the dissolution-precipitation process is radically slowed down and additional methods are required to unlock it (speed up). The influence of other factors can also take place and this theory can then be modified.

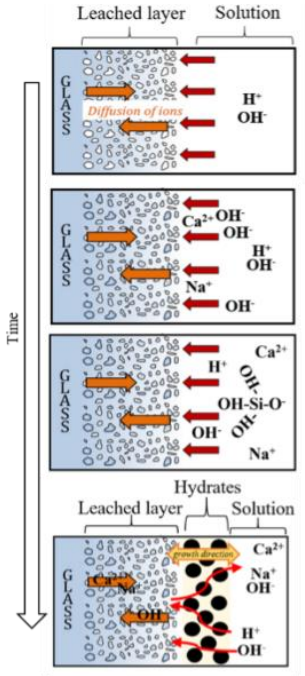

Figure 1.3: Schematic representation of dissolution-precipitation leached layer model (Newlands et al., 2016)

The influence of the presence of calcium in solution on glass dissolution is illustrated in Figure 1.4, where a deposit of hydrates occurs on the glass surface and is strongly bonded to it (Maraghechi et al., 2016). This phenomenon is responsible for the setting and hardening of such a mix, which is the main criteria for civil engineering applications. In addition, the presence of calcium in a slag glass increases its solubility (Shi. et al., 2006). Depending on the other parameters of the reaction, a compromise between the dissolution and precipitation rate can be found to obtain an alternative binder.

Figure 1.4: Left: soda-lime glass exposed for 14 days to 1 M NaOH in the absence of $Ca(OH)_2$; Right: Soda-lime glass exposed for 14 days to 1 M NaOH saturated with $Ca(OH)_2$; all slides are washed after exposure. (Maraghechi et al., 2016)

It can be concluded that the introduction of additives is necessary to maintain a high level of slag glass dissolution. Different approaches are used. The main ones are presented below.

1.2.1 Pure alkali-activation

In the case of pure alkali-activation, the addition of soluble alkali metal hydroxides (Li^+, Na^+ and K^+) leads to a rise in pH. Increasing the alkalinity provokes faster dissolution of the slag particles. In this case, the binder can be characterised by very fast setting and a rapid rise in compressive strength, depending of the alkaline concentration and slag characteristics. Nevertheless, due to this rapid reaction, hydration products are formed mainly on the slag surface, creating big passivation rings (Figure 1.5, Gebregziabiher et al., 2015), which decrease the accessibility of the alkaline solution to the slag surface and consequently slow down further dissolution and strength gain as was described previously.

Regarding the heat evolution (in an isothermal microcalorimetry test) during the hydration process, two main stages can be observed. The first one is related to the dissolution of sodium hydroxide, wetting of the slag surface and first dissolution/precipitation. The second peak (or the main peak) after very short induction period is attributed to a massive precipitation reaction (Shi and Day, 1995; Gebregziabiher et al., 2015; Sun and Vollpracht, 2018).

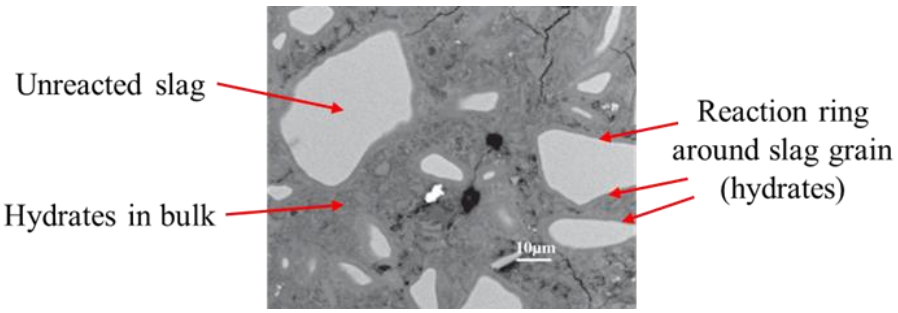

Figure 1.5: 8 M NaOH activated slag after 6 h of hydration (Gebregziabiher et al., 2015)

One common alkali-activator is NaOH. This is one of the most reported type of slag activation in the literature (Gebregziabiher et al., 2015; Hashim et al., 2015; Shi et al., 2017; Mohamed, 2019). It is also worth noting that the associated cation (here Na^+) of the activator may also play a role in the reaction process (for example through its introduction in the C-(A)-S-H for charge compensation). Actually a very limited amount of research has considered this issue (J. K. Song et al., 2010), The strength development of NaOH activated binders is characterised by a rapid growth at early age and poor values at long term. This will be discussed in the last chapter of this document.

1.2.2 Silicate activation

To avoid the problems of the hydrate precipitation on the slag surface, a combination of pure alkaline activation with the addition of supplementary chemical elements can be used. In this case, activation occurs with a solution of $M_2O{\bullet}nSiO_3$, where an alkaline metal is used (generally Na^+ or K^+) in combination with silicate. Regarding isothermal calorimetry measurements, right after the first peak of released heat (dissolution of activator and surface wetting) a clear small supplementary peak can be observed before the main induction period. According to (Brough and Atkinson, 2002; Shi. et al., 2006) at this stage the leached Ca^{2+} reacts with the dissolved silica from the activator to form the first hydrates of C-(A)-S-H type. This precipitation occurs not only on the slag surface, but also in bulk further playing the role of nucleation seeds. These seeds may limit the accumulation of calcium ions on the slag surface leading to maintain continuous Si/Al glass dissolution. As a result, compared to pure alkaline activation (only with M_2O), a very high compressive strength is usually achieved with sufficiently high evolution rate in time. This is mostly related to more homogeneous hydration in bulk resulting in a very fine porosity and a more advanced degree of slag dissolution as shown in Figure 1.6 (Brough and Atkinson, 2002; Haha et al., 2011; San et al., 2014; Shi, 1996). At the same time too fine porosity and continuous strength growth of such binders present a more significant shrinkage compared to OPC-based binders (Thomas et al., 2017).

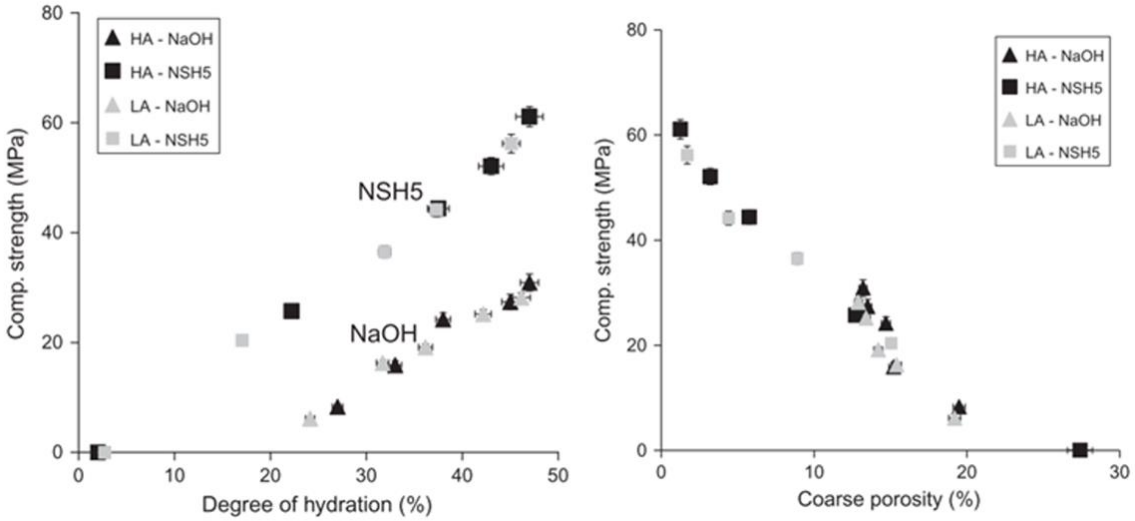

*Figure 1.6: Compressive strength vs. degree of hydration/coarse porosity measured by SEM-IA. NSH5 – Na_2SiO_3*5H_20 activator. HA or LA- high and low Al content in slag respectively (Haha et al., 2011)*

1.2.3 Calcium based activation

This type of activation is largely reported in the literature. In this case oxide/hydroxide or sulphate salts of calcium are used (CaO, $Ca(OH)_2$ and $CaSO_4$*$x$$H_2O$). The main advantage of these additives is their low cost compared to the previously cited additives. In addition, in the case of $CaSO_4$*$x$$H_2O$, a moderate pH level and very low CO_2 footprint can be mentioned.

In the case of lime (hydrated or not), the mechanism is quite similar to pure alkaline activation. The dissolution of these additives leads to a rise in pH promoting the slag dissolution. Leached Si and Al ions react with dissolved calcium to precipitate the C-S-H type hydrates. This activation can be characterised by fast setting and strength evolution. Nevertheless, the addition of a highly soluble calcium source interferes with slag calcium leaching. A fast setting leads to poor rheological properties (faster flowability loss with increasing lime dosage) (Yang et al., 2010). A lower slag dissolution and fast hardening leads in general to a quite low long term strength evolution rate (J. K. Song et al., 2010; Yang et al., 2010; Jeong et al., 2016), as it can be observed in Figure 1.7. From a practical point of view, even if the rheology issue can be addressed using appropriate (super-) plasticizers, the long term strength does not generally fulfil even low grade concrete requirements.

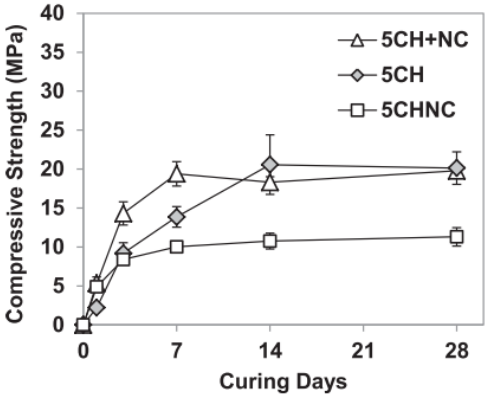

Figure 1.7: Compressive strength evolution of slag activated by 6.25% $Ca(OH)_2$ (5CH), 6.25% $Ca(OH)_2$ + 3%Na_2CO_3 (5CH+NC) or 3% $Ca(OH)_2$ + 3.25%Na_2CO_3 (5CHNC) weighted by slag at W/B=0.5 (Jeong et al., 2016)

In the case of $CaSO_4*xH_2O$ activation, also called *super-sulphated cement*, a completely different mechanism of slag activation occurs. In the case of anhydrite (x=0), the first reaction upon wetting is its transformation to gypsum. The gypsum particles play the role of nucleating sites for the further precipitated hydrates, protecting the slag surface from a dense passivation layer. Further dissolution of this gypsum provides calcium and sulphate ions to the solution. During slag dissolution, leached Si/Al ions react with leached Ca^{2+} from slag and Ca^{2+}/SO_4^{2-} from anhydrite to form different calcium-sulfo-aluminates hydrates (ettringite, monosulfooaluminate), followed by the formation of C-(A)-S-H (Singh and Garg, 1995; Gruskovnjak et al., 2008). Such reactions provide a moderate short term, but sufficiently high long term compressive strength (Gruskovnjak et al., 2008; Magallanes-Rivera and Escalante-Garcia, 2014; Masoudi and Hooton, 2019). This type of activation confirms that GGBS has a sufficiently high dissolution rate to react with water as independent binder, even at moderate pH. Its latent hydraulic behaviour should be only related to an eventual formation of some dense protective (passivation) layer on its surface during the first minutes after contact with water. By preventing this phenomenon with the addition of the right nucleating seeds and some supplementary low soluble calcium source (to maintain Si/Al consumption all time), a high compressive strength can be achieved.

1.2.4 Alkali-activation based on acid salts of alkaline metals

A variety of activators compose this category: M_2CO_3, M_2SO_4, M_3PO_4 and MF, where the alkali metal is in most cases Na^+ and K^+. The main mechanism of their activation is very similar to the silicate based one. Immediately after mixing the leached Ca^{2+} combines with the anion from the activator to form low soluble salts, depending on the activator type. This limits the re-adsorption of the leached Ca^{2+} on the slag surface preventing the precipitation of hydration

products onto this surface and thereafter promoting the slag continuous dissolution. In addition, consumption of the calcium increases the concentration gradient between solid and liquid fractions, promoting further leaching. Due to the consumption of the anions and a stable cation (Na^+ or K^+ from the activator) concentration, an imbalance is created which leads to an increase of the pH level (through in-situ formation of NaOH or KOH) (Shi. et al., 2006; Bernal et al., 2015). In contrast to pure alkali activation with hydroxides, this process is slow and so does not lead to a sharp rise in alkalinity. Increasing the pH level more slowly prevents the rapid dissolution and precipitation of hydrates on the slag surface. Moreover, precipitated calcium salts particles play the role of nucleation sites, which leads to a more homogeneous hydration in bulk.

The specific case of sodium carbonate activation

The most reported activation method (based on metal salts) in literature is that based on sodium carbonate, due to its low price and worldwide availability. Various authors (Fernández-Jiménez et al., 1999; Shi. et al., 2006; Jacquemot, 2014; Jin et al., 2014; Abdalqader and Al-tabbaa, 2015; Krivenko, 2017; Tan et al., 2019) indicate that such binders also provide high mechanical and durability properties approaching those of silicate activation and significantly higher compared to NaOH activation (Figure 1.8). Regarding the heat evolution during the hydration process, three heat peaks can be distinguished as in the case of silicate activation (Figure 1.10), with the second additional peak before the main induction period related to the precipitation of mainly calcium-based hydrates (Shi. et al., 2006). Due to a slower hydration rate and lower total heat released, such binders are used as part of low and very low heat cement. At the same time, a lower shrinkage can be expected, in contrast with the case of silicate based activation. In addition due to the moderate pH level at the beginning, (pH level of sodium carbonate solution itself is about 11.8), such a binder can be used for civil engineering work without any special security management compared to NaOH or Na_2SiO_3.

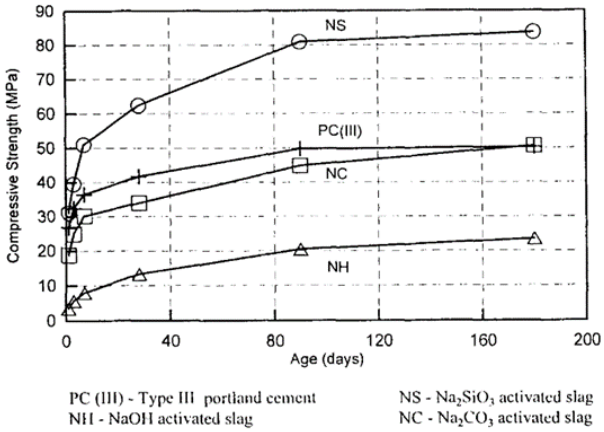

Figure 1.8: Comparison of activator type influence on compressive strength evolution (Shi, 1996)

Na_2CO_3 activated GGBS based products were largely used in the former Soviet Union. In an example of a residential high-rise building built in the late eighties is presented (Figure 1.9). Some elements like floor slabs and stairways were made from pre-cast concrete with steam curing, whereas the walls were manufactured on the construction site in an ordinary way with post-temperature treatment for acceleration (electrical heat elements) (Shi. et al., 2006; Provis and Deventer, 2014). The similar binder was also used for pre-cast elements production for a multi-storey building in Krakow, Poland in 1974. Results of (Deja, 2002) indicated that the compressive strength of such concrete was doubled after 27 years compared to the 28 days strength. This observation proves that such binders have a great internal reserve for long term hydration. This reserve can not only contribute to the increasing of the strength through continuous precipitation of hydration products, but also prevent the concrete from aggressive attacks from the environment (high durability, self-healing).

Figure 1.9: A 24-storey building built with alkali-activated slag cement concrete on Berezinsa street 2, city of Lipetsk, Russia, 1994 (Shi. et al., 2006)

The utilization of this binder over large-scale civil engineering projects is however hindered due to two main issues. The first issue is related to their rather long induction period (Bernal et al., 2016; Ke et al., 2016), which leads to a significantly slower strength evolution in the first days of hardening (Figure 1.10). In most of the cases in the literature, this induction period is often much longer compared to silicate activation and can take up to 3-5 days depending of different factors. At the same time, favourable hardening conditions can be employed, like steam curing in pre-cast or heating concrete moulds, to promote the strength development like it was used previously on real projects (Provis and Deventer, 2014; Shi. et al., 2006). In combination with another activator(s) or additive(s), a noticeable acceleration can be achieved (Jacquemot, 2014; Kovtun et al., 2015; J. Song et al., 2010; Wang et al., 2017). However, such solutions often result in the deterioration of some properties, especially with respect to rheology.

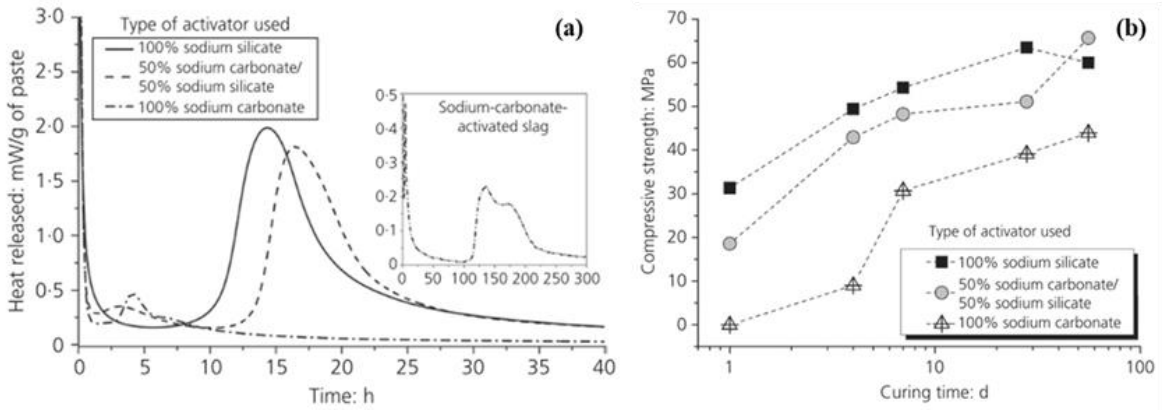

Figure 1.10: Hydration kinetic (a) and compressive strength evolution (b) of GGBS 4100 cm^2/g activated by sodium silicate, sodium carbonate or mix of thereof at W/B=0.40 (Bernal et al., 2016)

The second important drawback of these binders is related to the their poor rheology including rapid loss of flowability (Provis and Deventer, 2014; Humad et al., 2017; Yuan, 2017). In these works, some results of standard tests are presented which confirm the low followability and fast setting. Nevertheless, in this few literature sources there are no deeper studies of this issue, as well as the influence of different parameters such as slag chemistry, fineness, curing temperature, etc. The causes of the rheological problems are still not clear. Their understanding can help in finding solutions to improve it, since nowadays flowability is an important factor for the modern construction industry with the large scale utilisation of highly fluid concretes.

The main objective of the investigation reported in this document is to address these two issues.

1.3 Factors affecting the hydration process of GGBS based binders

1.3.1 Chemical composition of GGBS

The chemical composition plays an important role on the reactivity of the slag. A large amount of research work showed that the reactivity increases with lime and magnesia content, but decreases with silica and aluminium oxide content (Wang et al., 1994; Shi. et al., 2006; Winnefeld et al., 2015; Black et al., 2016). These observations are related to slag dissolution, which is highly affected by its glass structure. Previously it was described that during the hydrolysis, the leaching of Ca^{2+} and Mg^{2+} occurs due to their weak ionic bonds. On the other hand for the breaking of the strong covalent bonds of Si and Al, a high pH level is required. Increasing the Ca/Mg as well as Na/K content leads to a high level of silico-aluminate network depolymerisation (structural defects) and so higher glass solubility.

To facilitate the comparison of slags with a different chemical composition, in practice, two indicators are used: Basicity modulus M_o (Eq. (3)) and Activity modulus M_a (Eq. (4)):

$$M_0 = \frac{CaO + MgO}{SiO_2 + Al_2O_3 + Fe_2O_3} \qquad Eq.\ 3$$

$$M_a = \frac{Al_2O_3}{SiO_2} \qquad Eq.4$$

Depending on the value of the basicity modulus, the slag is divided into three groups: basic (Mo> 1), acid (Mo <1) and neutral (Mo≈0) (Kuznetsov, 1963). The higher the basicity modulus and the smaller the activity modulus, the greater the slag reactivity (Figure 1.11).

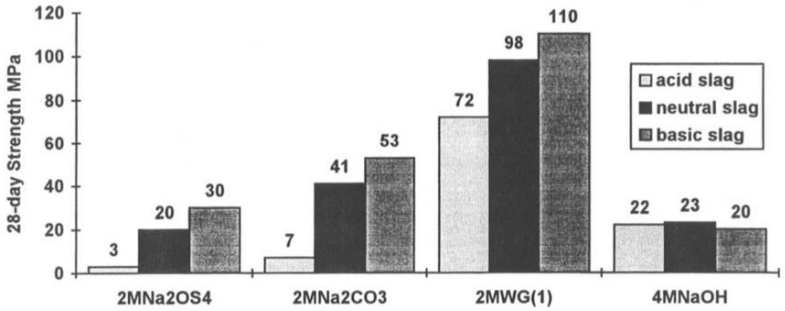

Figure 1.11: 28-day compressive strength for different types of slag and activators (20 °C; fineness=4500+300 cm^2/g; alkali solution/slag=0.41;sand/slag=2.0) (Wang et al., 1994)

Nevertheless, it is not possible to clearly distinguish the influence of every element on the final properties because decreasing one element means increasing another one. Moreover, in reality a large number of parameters change simultaneously during the actual slag production process, which complicates experimental investigations of the composition impact. In addition, not only slag dissolution rate, but also the hydration products like C-S-H are affected by the chemical composition. The results of (Kunther et al., 2017; Li et al., 2019) indicate that decreasing the Ca/Si ratio (lower amount of calcium) of C-S-H positively affects both mechanical and durability properties. While it was shown before, increasing this parameter in slag increases its solubility. Therefore, it is impossible to clearly determine an eventual correlation between the chemical composition and mechanical properties (Provis and Deventer, 2014). Only trends can be predicted.

1.3.2 GGBS fineness

One of the important factors that has a significant impact on the rate of reaction of the slag and, accordingly, the final properties of the binder is its fineness. Some authors even use the term of *mechanical* activation of the slag to deal with the fineness parameter (Kumar et al., 2008;

Allahverdi and Ahmadnezhad, 2014; Bouaziz et al., 2017). As it was already mentioned before, the granulated blast furnace sand should be ground to a certain fineness level to get cementitious properties. It is related to the glass structure that has low rate of dissolution in water or moderately alkaline solution. Increasing the particle wetting area will lead to an increase of the dissolution rate. It should be noted that this effect is non-linear (Figure 1.12). It has been already reported by (Kumar et al., 2005) that at a sufficient level of grinding, the slag reacts with pure water leading to C-S-H type hydrates precipitation within a reasonable time period.

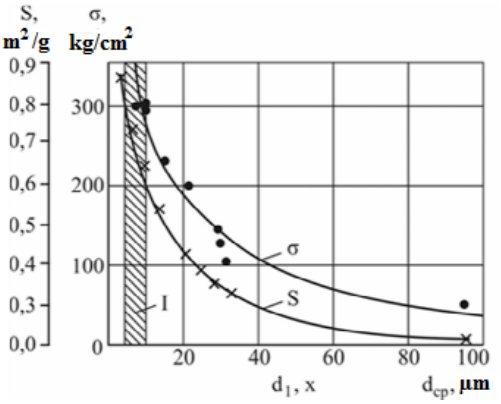

*Figure 1.12: The dependence of the activity **σ** and the specific surface **S** of the particle size **d** of GGBS (Kravchenko and Gankevich, 2013)*

During grinding (in order to increase specific surface area), damage of the grains may also occur. Figure 1.13 represents the idealized model of the defect structure. According to the theory of active surface, during the breakage of a solid particle under an external charge, a chemical modification of the atoms at the created surface may occur due to the mechanical stress. In such disordered regions, the electrostatic interaction is weakened, ensuring the stability of the ions. Loss of stability may lead to the loss of an electron, i.e. for instance to the transformation of an O^{2-} ion into a chemically high active radical O^{-*}. The valence-unsaturated atoms appear, which in turn causes a stronger reactivity (Kravchenko and Gankevich, 2013). That is why the grinding method, co-grinding of different components, moisture content of materials and the presence of modifying additives during this process have a significant impact on the subsequent properties of the solid particles (Hodakov, 1972; Ghiasvand et al., 2014; Li and Gao, 2017).

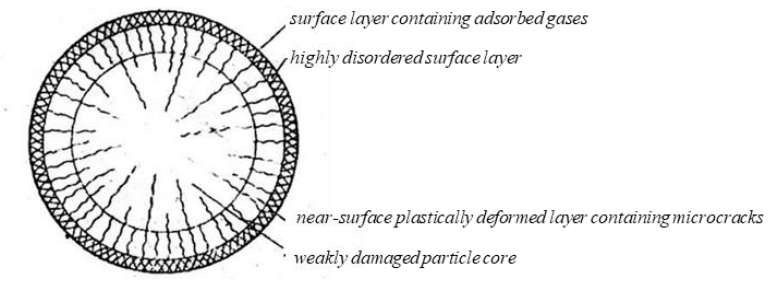

Figure 1.13: Model of the defect structure of the particle, formed during grinding (Kravchenko and Gankevich, 2013)

Some works, whose purpose was to study precisely alkali-activated slags, showed that the influence of fineness is valid for all cases. As it can be seen in Figure 1.14, increasing fineness positively affects the compressive strength regardless of the chemical composition of the used slag (Wang et al., 1994). It can also be noted that beyond a certain level of Blaine fineness, a decrease in the strength values can be observed. However, this phenomena should be related to precipitation of the hydrates on its surface which occurs too quickly, which can be tuned by the addition of some nucleation seeds. Poor rheological properties were also observed and can at the origin of this phenomenon.

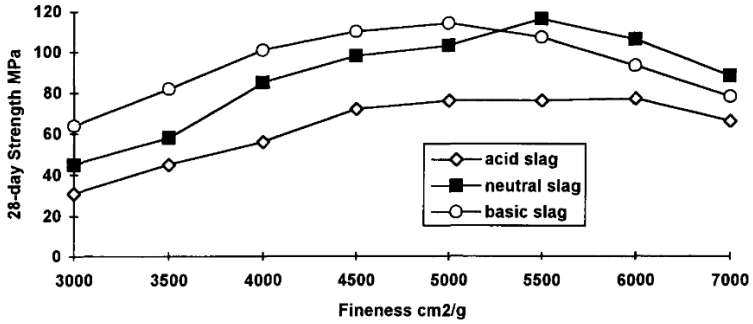

Figure 1.14: Fineness vs. 28-day strength for different types of slag (Waterglass activator, Na_20=5.5%; Ms=1; sand/slag=2; slag fineness variation=±300 cm2/g) (Wang et al., 1994)

The results of (Yuan, 2017) presented in Figure 1.15 also indicate that increasing slag fineness has a significant accelerating effect on the hydration process in the case of both Na_2CO_3 and Na_2SiO_3 activations.

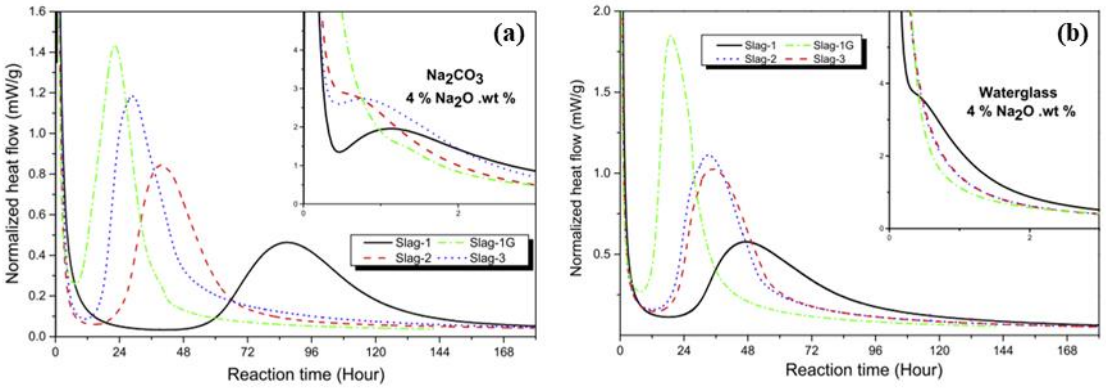

Figure 1.15: Hydration kinetics of Na_2CO_3 (a) or Na_2SiO_3 (b) slag activated. Slag 1 and 1G has same chemical composition, but Blaine fineness is 3730 and 7220 cm^2/g respectively (Yuan, 2017)

However increasing the fineness is very often associated with increasing the grinding time. This not only reduces the production capacity, but also increases energy consumption and carbon footprint. To achieve ultra-high fineness (8000 cm^2/g and more) a simple increase of grinding time will not be sufficient and additional separation processes are required. Nevertheless, if this allows for a reduction in the consumption of additional chemical additives,

as well as a decrease in the amount of binder per $1m^3$ of concrete, increasing the slag fineness can contribute overall to lowering the carbon footprint of the final concrete.

1.3.3 Impact of curing temperature

A large number of research works indicate that alkali-activated slag based binders (Bakharev et al., 1999; Fernández-Jiménez et al., 1999; Altan and Erdogan, 2012; Medina et al., 2016) or OPC-GGBS binders of CEM III type (Barnett et al., 2006; Turu'Allo, 2013) are particularly sensitive to curing temperature. Increasing the curing temperature leads firstly to a faster slag dissolution and then to an acceleration of the precipitation process due to an increased ion mobility (activation energy). The results represented in the book of (Shi. et al., 2006) indicate that the rate of the chemical reaction can be significantly accelerated by increasing the curing temperature (Figure 1 .16).

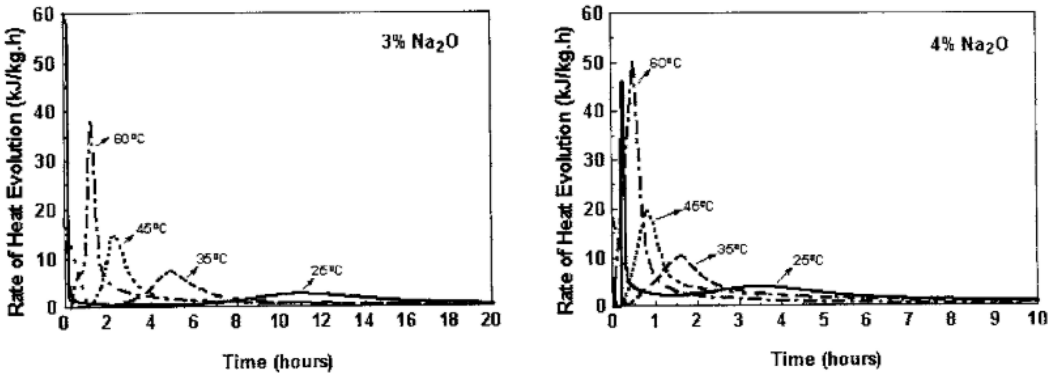

Figure 1.16: Effect of temperature on heat evolution rate of sodium silicate-activated slag cements (Fernandez-Jimenez and Puertas, 1997) as in (Shi. et al., 2006)

Nevertheless, the influence of the temperature on the mechanical properties is also related to the binder composition (its reactivity) (Black et al., 2016). As was mentioned before, increasing the hydration rate at the very beginning may lead to a faster slag surface blockage by heterogeneous (on the slag particle surface) precipitation of hydration products, which has a negative consequence on long term hydration as it will be demonstrated in the present work.

Regarding the alkali-activated slag, the results illustrated in Figure 1.17 indicate that the influence of the curing temperature depends on the activator type. In the case of NaOH activation, acceleration of the reaction by T° leads to a further slower strength evolution. With sodium silicate or sodium carbonate, an increasing of the compressive strength was observed at early age (up to 7 days) with no significant changes on long term strength (Fernandez-Jimenez and Puertas, 1997). This phenomenon was largely used in the case of pre-

cast production of concrete elements (Shi. et al., 2006), where a high strength at early age is required. It can also be observed that activator dosage has a qualitative impact.

Increasing the storage temperature has a more pronounced effect in the case of lower activator dosage (higher percentage increase for the binder with lower reactivity). It means that additional CO_2 footprint from heat treatment may be compensated by a lower amount of added activator, as well as a lower amount of binder, coarser GGBS, etc. At the same time, decreasing the temperature (less than 20°C) might cause a serious delay in setting and hardening.

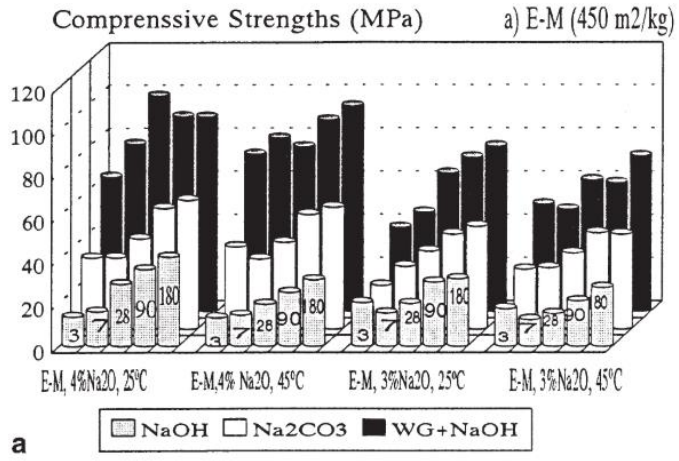

Figure 1.17: Compressive strength evolution as a function of alkaline concentration and temperature for 3 types of alkali-activators (Fernández-Jiménez et al., 1999)

1.3.4 Influence of storage humidity

As well as temperature, the storage humidity can affect the mechanical and durability properties of alkali-activated GGBS. When the Relative Humidity (RH) is lower than 100% a hydric gradient between the solid part of mortar/concrete and the air occurs, which leads to drying (water evaporation). Depending on several parameters, drying can lead not only to a slowing down of the hydration process, but even to complete cessation and/or degradation. Firstly, decreasing the water amount may cause alkaline-activator crystallisation (and even efflorescence) and the loss of water/solution contact with slag surface (dewetting). In addition, it increases the capillary pressure in the micro-pores, which is the main cause of pore collapse and drying shrinkage. As was mentioned before, alkali-activated GGBS can be characterised by a finer porosity compared to OPC. This means that for the equal amount of water evaporated a higher internal capillary pressure appears causing higher drying shrinkage (Thomas et al., 2017). This shrinkage is also responsible for cracking. Cracks that appear can not only reduce the mechanical properties, but also significantly affect the durability properties (increasing of water/gas permeability, higher carbonation, etc.). In the case of very low relative humidity

(<10%) a degradation of the structure at the hydrates level (C-S-H) occurs, leading to more significant degradation of the product properties (Shi. et al., 2006).

Nevertheless, in general the ambient humidity is approximately 40-50% or higher. It means that only drying shrinkage and all associated processes take place. Loss of capillary water is related with pore structure. A greater porosity and a developed pore bonding system, intensifies the drying. This is one of the reasons why in the majority of cases even for OPC based binders, it is required to keep the concrete in the formwork until the structure is sufficiently compacted (when there are less bound pores), moistening it after demoulding or covering it with a special protective curing-agent for some period. One of the important factors is not only %RH, but also the initial W/B ratio. High values lead to excessive water and, accordingly, supplementary porosity. In Table 2 an approximate time period before the pores become closed (no pore inter-connexions) as a function of the W/C ratio is reported in the case OPC. In the case of Na_2CO_3 slag activation at standard curing conditions due to the slower reaction, this period should be longer.

Table 2: Approximate time until capillarity pore discontinuity for OPC ((Powers, 1958) as cited in (Shi. et al., 2006))

Water/Cement ratio	Time required (days)
0.40	3
0.45	7
0.50	14
0.60	180
0.70	365
Over 0.70	infinite

Several parameters should be taken into account (slag chemistry, type of activator and its dosage, W/B ratio, porosity, curing temperature, etc.) to evaluate the actual influence of the humidity conditions and the period of moisture curing on the alkali-activated GGBS binder properties (Shi. et al., 2006; Jin and Al-Tabbaa, 2015; Thomas et al., 2017; B Yuan et al., 2017).

1.3.5 Influence of Water/Binder ratio

One of the factors that significantly affects the hydration process, as well as further mechanical and durability properties is Water/Binder ratio (Bernal et al., 2018; Jeong et al., 2016; Shi, 1996). Increasing this parameter generally leads to a slowing down of the reaction process (Figure 1.18). Once the solution becomes saturated, the process of condensation and precipitation

take place. Increasing the water amount requires a higher amount of ions to trigger this process. So with all other parameters constant, a longer period of dissolution is required. At the same time acceleration of dissolution (increasing of activator dosage, addition of some additives, increasing the curing temperature) might compensate for the retardation effect of the higher W/B ratio.

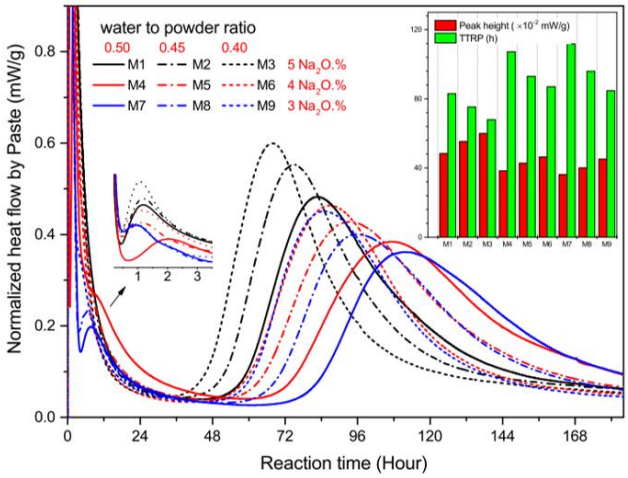

Figure 1.18: Heat release of GGBS-Na_2CO_3 activated slags at 20°C with different W/B ratio and Na_2CO_3 content (here in Na_2O eq.)(Yuan, 2017)

A non-linear relationship between W/B ratio and hydration rate can be observed. In addition to the impact on the dissolution/precipitation process (concentration of ions described previously), increasing the water amount in the system also leads to a higher inter-granular distance. It means that a higher amount of hydrates is required to fill this porosity, i.e. longer hydration period to achieve equivalent strength with higher W/B ratio. In the case of a binder with low degree of slag dissolution and/or a low amount of amorphous hydrates (like C-S-H to fill the heterogeneous voids), this can significantly affect the mechanical properties (see Figure 1.19).

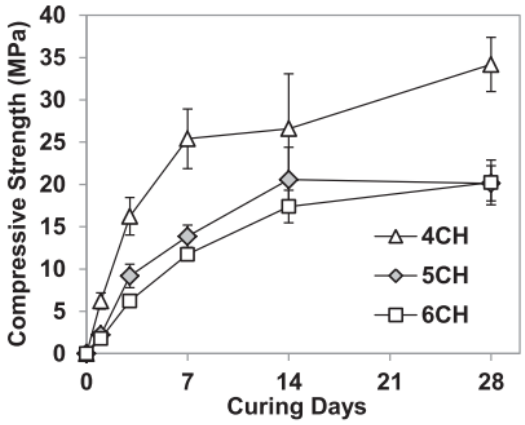

Figure 1.19: Influence of W/B ratio (0.4, 0.5 and 0.6 for 4CH,5CH and 6CH respectively) on strength evolution of GGBS activated by 6.25% $Ca(OH)_2$ (Jeong et al., 2016)

Water that is not used for the hydration process will be evaporated (if RH<100%), leaving porosity and causing drying shrinkage. The results of (Shi, 1996) indicate that lower strength was obtained at equivalent porosity for 3 types of alkali-activated slags compared to OPC (Figure 1.20). It means that a lower W/B ratio should be used to achieve the same strength. It must be partially related to the denser and finer hydrates structure, reported in the literature. Decreasing the porosity in general leads to better mechanical strength and durability properties. Thus, modification of the setting time or rheology by playing on the water content is the worst option.

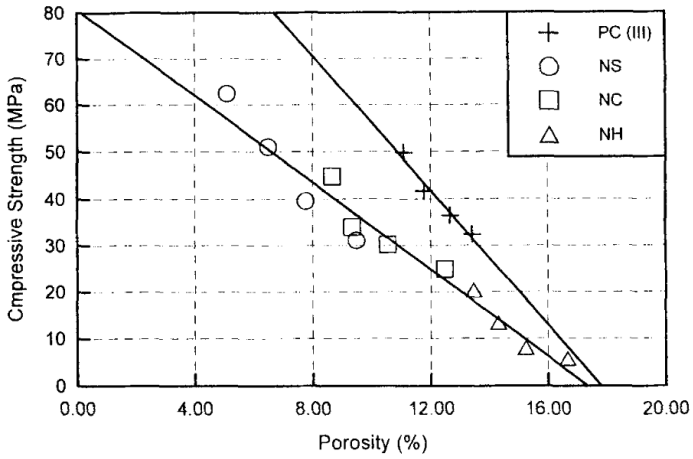

Figure 1.20: Correlation between compressive strength versus porosity of OPC and Alkali-activated GGBS (Shi, 1996)

Insufficient water content can also lead to degradation of the final properties of the product according to our opinion. Firstly, it can significantly affect the rheology, if no (super) plasticizer was used to compensate for the lack of water. High viscosity and yield stress might significantly decrease the final product density and its homogeneity due to problems regarding mortar/concrete compaction. *Macro-scale* structural defects (porosity) will lead to lower mechanical properties. At the same time, saturation of the solution which occurs too quickly due to a lower water content can lead to a heterogeneous fast precipitation of hydrates (if no supplementary additives were used). As was already mentioned before, it leads to a further slowing down of the water access to the slag surface (passivation layer). A *micro-scale* heterogeneous structure leads to defects and lower mechanical and durability properties (Fagerlund, 1999; Holt, 2001). Therefore, a compromise must be found in each specific cases.

Conclusions

GGBS is an excellent candidate to be the main constituent of a very low-carbon binder. Its high mechanical and durability properties provide not only ecological, but also economic benefit. Nevertheless by itself, GGBS, without having been ground to ultra-high fineness, has a very slow reaction with water. Additional chemical supplements (activators) are needed to accelerate this process. The nature of this activator has a very high influence on the ongoing properties. This is similar to the case with many other parameters like slag composition and fineness, curing conditions, W/B ratio, etc. The issue of the availability of the GGBS can be resolved in part by its dilution by other supplementary materials (limestone, other types of slags, ashes, etc.) and its optimised utilisation (high degree of hydration and optimisation of its amount in concrete).

The most promising activator is Na_2CO_3. It provides an optimal ratio between environmental friendliness, price, high mechanical and durability properties. This type of activation has been already used in the past and therefore its long term suitability has been proven. Nevertheless, in modern times, a number of problems such as low early age strength and poor rheological properties significantly limit its use at large industrial scale. The main objective of the present work is to find a solution to improve this type of alkali-activated binder.

Chapter 2 Main Properties of Na_2CO_3-activated GGBS Binders revisited

Introduction

As it was described in the previous chapter, the Na_2CO_3 activation of GGBS represents a compromise between safety, eco-friendly type of activation and high physical/durability properties. At the same time, some drawbacks are often reported in the literature. The main problems are low early strength and poor rheology. Some others are often just side effects of these two main issues. A solution is then required in order to obtain a commercially viable very low-carbon binder. Several studies have been reported in the literature on Na_2CO_3 activated GGBS. The rheological issue is particular generally ignored. In this chapter, the state of the art regarding the properties of these binders is briefly reported. At the same time those studies are completed, in particular by considering the fresh state properties. The main objective is to determine the reference data for the next chapters in which various improvement routes are explored.

First a study of the rheological and strength properties was performed. As previously stated, various factors have an impact on these properties. Among them is the slag fineness, amount of sodium carbonate, W/B ratio, and the curing conditions. Various experimental techniques like surface charge measurements, micro-calorimetry, XRD analysis, and SEM observations allow investigating the origin of the two main issues indicated above.

2.1 Materials

All the GGBS grades considered here are produced by the company ECOCEM. In particular, three different fineness grades were considered.

2.1.1 Standard slag

The main slag grade used (designated below as *GGBS, standard or conventional slag, GGBS 4400 cm^2/g*) was provided by ECOCEM from the Fos-sur-Mer plant, France. It was manufactured according to the European standard (NF EN 15167-1, 2006).

The chemical composition is presented in Table 3 (data provided by ECOCEM France, determined by X-ray florescence (XRF)). The slag has M_o = 1.05 (basicity modulus) and M_a = 0.27 (activity modulus), therefore it can be classified as basic type with normal hydraulic properties. SEM-EDX analysis in our laboratory confirms this composition (Figure 2.1). Taking into account that EDX analysis has lower accuracy than XRF, a good correlation of Ca/Si ratio between the two methods can be observed:

XRF method: $$\frac{m_{Ca}}{m_{Si}} = \frac{43.9*71.469\%}{37.6*46.743\%} = 1.785$$

EDX method: $$\frac{m_{Ca}}{m_{Si}} = \frac{28.5}{16.08} = 1.772$$

Table 3: Chemical composition of the standard GGBS used (XRF provided by ECOCEM France)

CaO	SiO_2	Al_2O_3	Fe_2O_3	TiO_2	MgO	Na_2O	K_2O
43.9	37.6	10.26	0.33	0.81	6.93	0.22	0.26

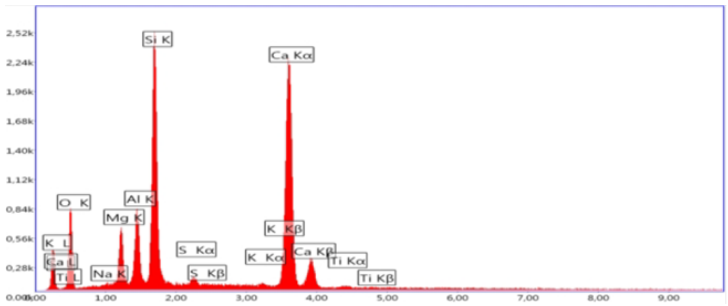

Element	Wt %	Atomic %
O	27.08	44.18
Na	0.06	0.07
Mg	3.95	4.24
Al	5.41	5.24
Si	17.3	16.08
S	1.08	0.88
K	0.6	0.4
Ca	43.76	28.5
Ti	0.75	0.41

Figure 2.1: Global EDX analysis of standard GGBS

The Blaine fineness of the provided sample is about 4400 cm^2/g (data from ECOCEM France). The granulometry was measured using the particle size analyser Cilas 1090 in ethanol solution under ultrasound dispersion. The results, presented in Figure 2.2, shows that $d_{(50)}$=11µm., which is in agreement with the ECOCEM data.

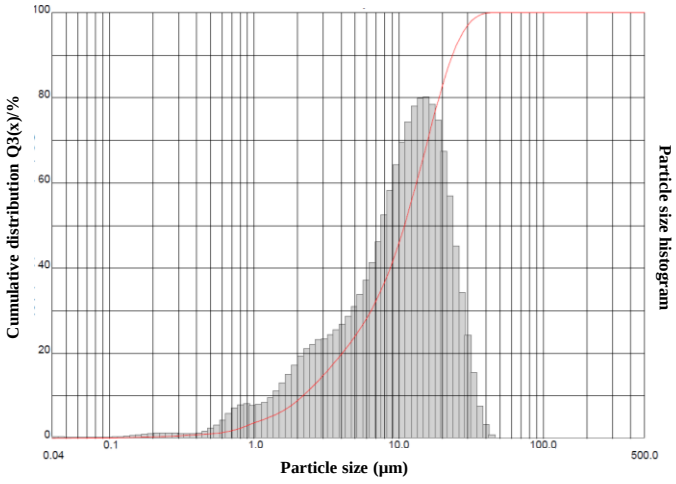

Figure 2.2: Particle size distribution of Standard GGBS

The slag has a high glass content (more than 95%). The XRD analysis is presented in Figure 2.3.

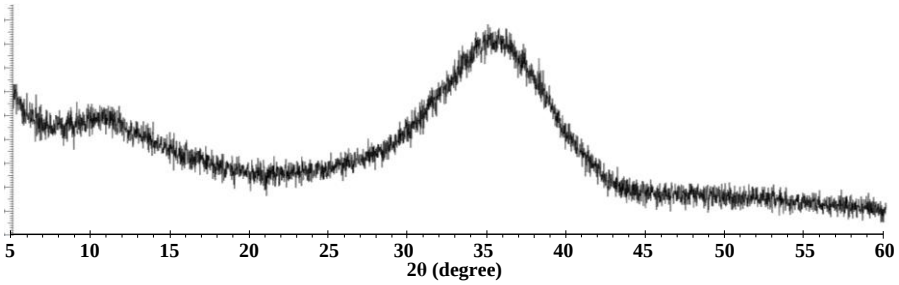

Figure 2.3: X-ray diffraction patterns of the Standard GGBS

SEM images of the GGBS powder are presented in Figure 2.4. It can be noticed that the coarse particles have a rather angular shape. This shape should be due to the fact that the grains themselves have a very high strength and during grinding there is a split along the defect lines of raw granules of slag sand. The very fine particles (less than 2 μm) are located on the surface of the larger ones and are possibly held by van der Waals or by capillary moisture forces.

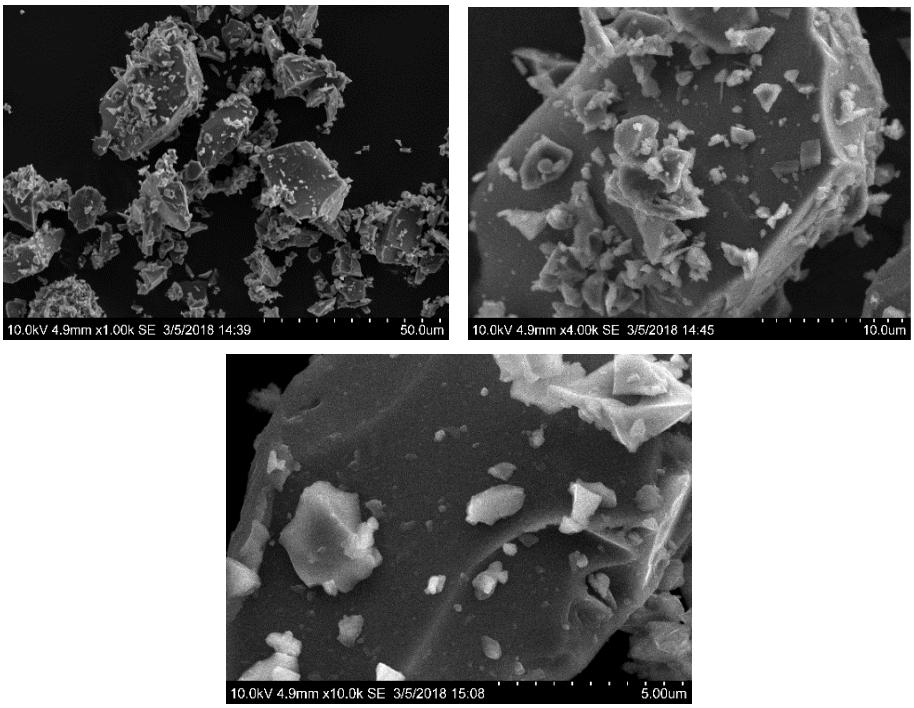

Figure 2.4: SEM images of the Standard GGBS particles at different zooming factors

2.1.2 Fine GGBS

Fine slag from the same source (ECOCEM, Fos-sur-Mer) and with a same chemical composition as the standard GGBS was also used in this study. The fine GGBS was obtained by increasing the grinding time. This includes lower production rates and this needs to be taken into account in the economical and CO_2 footprint calculations. Fine GGBS has a specific surface (in

terms of Blaine) of about 5600 cm^2/g (data from ECOCEM France). The granulometric analysis is presented in Figure 2.5. The $d_{(50)}$ is about 9 µm. SEM images and XRD analysis of this slag are presented in Figure 2.6 and Figure 2.7 respectively. No apparent difference in the shape of the particles can be observed. The XRD pattern is also similar to that of Standard GGB. Further, this slag will be designated *GGBS 5600 cm^2/g* or *Fine GGBS*.

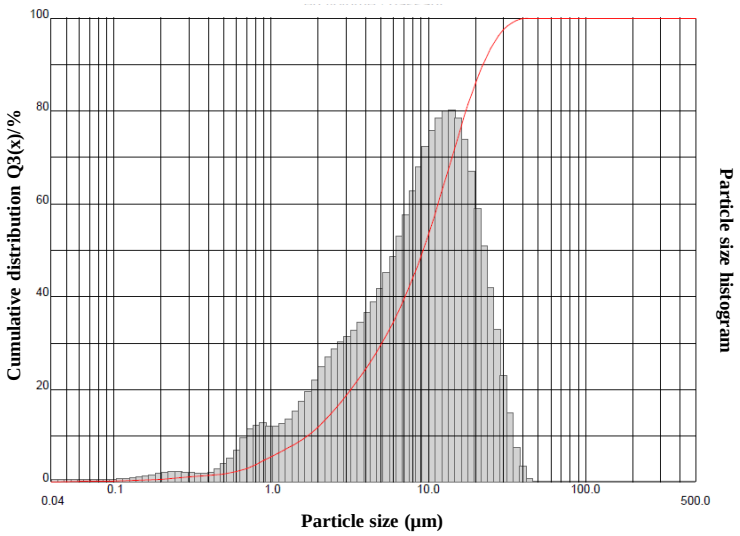

Figure 2.5: Particle size distribution of Fine GGBS

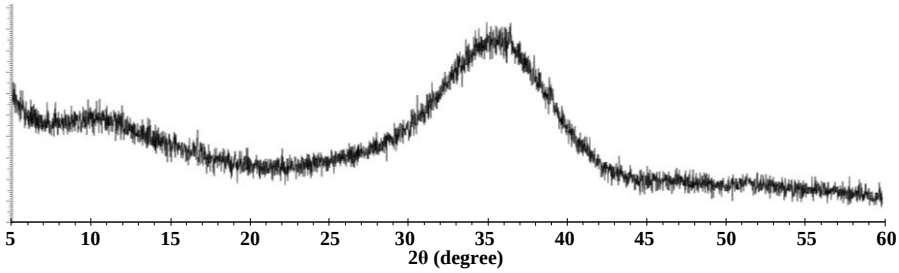

Figure 2.6: XRD analysis of the Fine GGBS

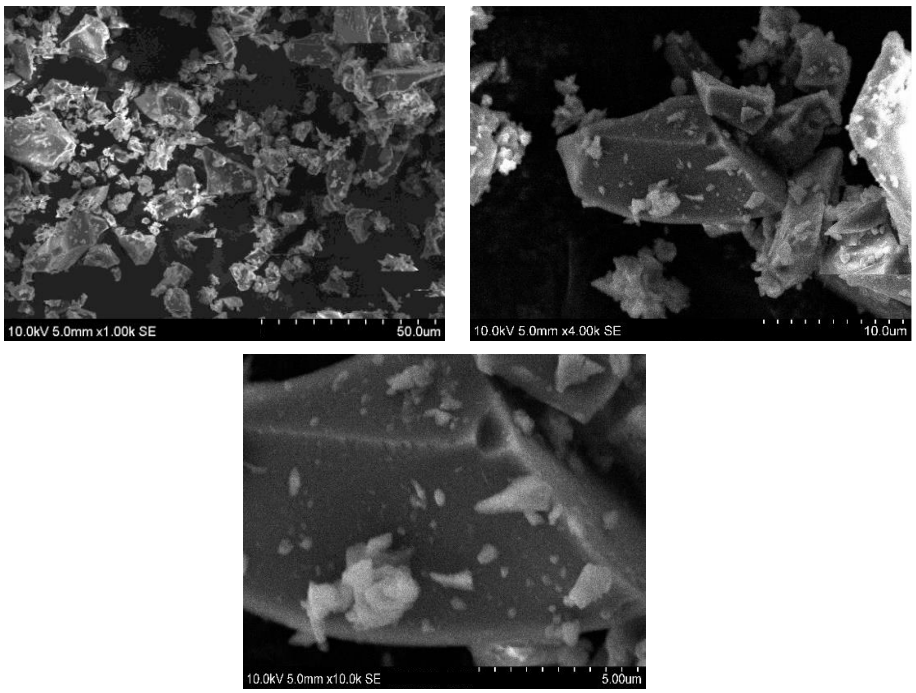

Figure 2.7: SEM images of the Fine GGBS particles at different zoom factor

2.1.3 Ultrafine GGBS

This slag was obtained by a cyclonic sieving method during the production of conventional slag (ECOCEM, Fos-sur-Mer). This slag has a Blaine fineness of about 11000 cm^2/g (data from ECOCEM France). The granulometric analysis is presented in Figure 2.8. $D_{(50)}$ is less than 2 µm. The distribution is bimodal and the proportion of the finer fraction (less 1 µm) is significant (30%). The SEM images and XRD analysis of this slag are presented in Figure 2.9 and Figure 2.10 respectively. From the XRD results, the presence of calcium carbonate can be clearly observed. It was probably formed on the grain surface as a result of the reaction with the humidity and carbon dioxide from the air due to the very high slag reactivity. The SEM images show that the shape of the particles is characterised by higher sphericity than the coarser slags and strong agglomeration can be observed. In the remainder of this document, this slag will be named *Ultrafine GGBS* or *GGBS 11000 cm^2/g*.

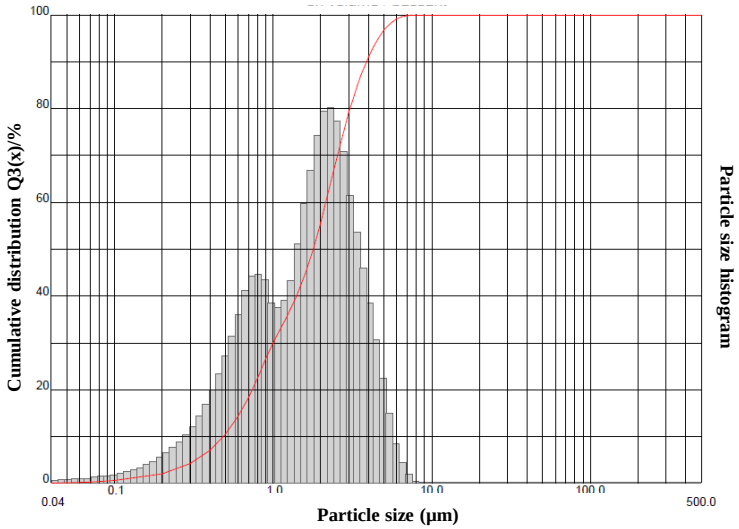

Figure 2.8: Particle size distribution of Ultrafine GGBS

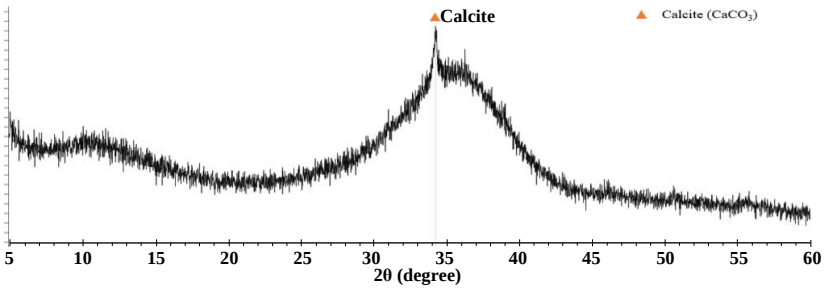

Figure 2.9: XRD patterns of Ultrafine GGBS

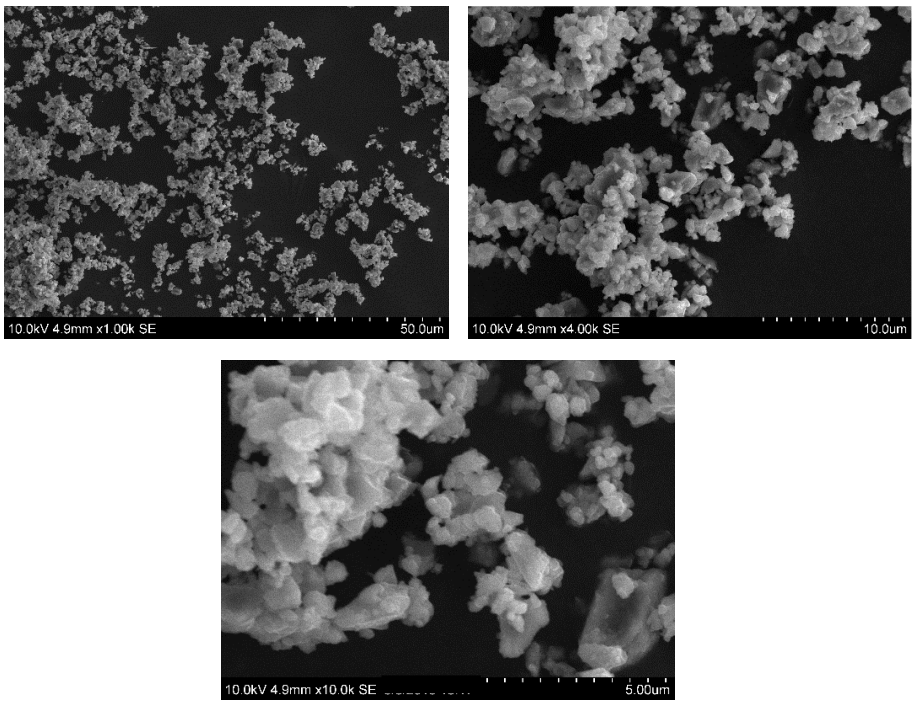

Figure 2.10: SEM images of Ultrafine GGBS particles at different zoom factor

2.1.4 Sodium carbonate (Na_2CO_3)

The sodium carbonate used in this study is a lightly dehydrated white powder of reagent grade from VWR, CAS: 497-19-8 (designated further as *Na_2CO_3*, *NaC* or *Soda Ash*). The particle size is ≤125 microns (80-90%). The solubility versus temperature and pH level versus concentration of Na_2CO_3 solutions in distilled water are presented in Figure 2.11 and Figure 2.12 respectively. We can observe a strong decrease of the solubility below 35°C. This will have some consequences on the sensitivity of these binders to temperature. This implies an exothermic dissolution process as shown in Figure 2.13. This is, on the other hand, a favourable parameter for binder reactivity. The pH level of the Na_2CO_3 solution seems to level off beyond 150g/l. At the same time for example the concentration of 150 g/l or higher can not be achieved at the temperature below 13-14°C.

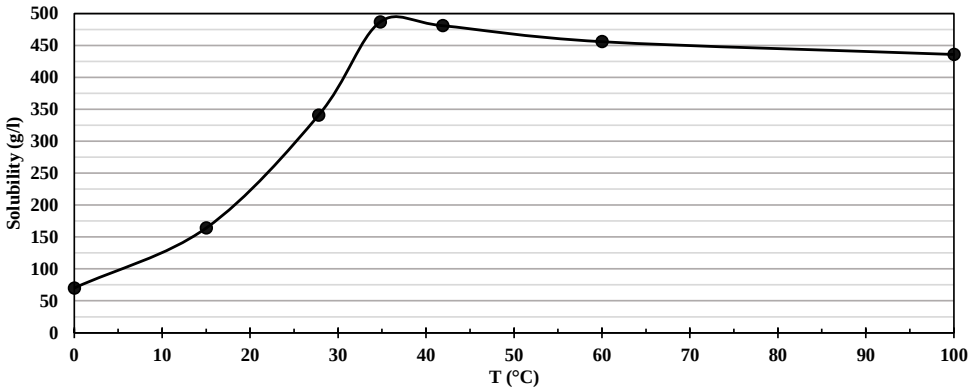

Figure 2.11: Solubility of Na_2CO_3 in water as a function of T°C (GCIP, 2007)

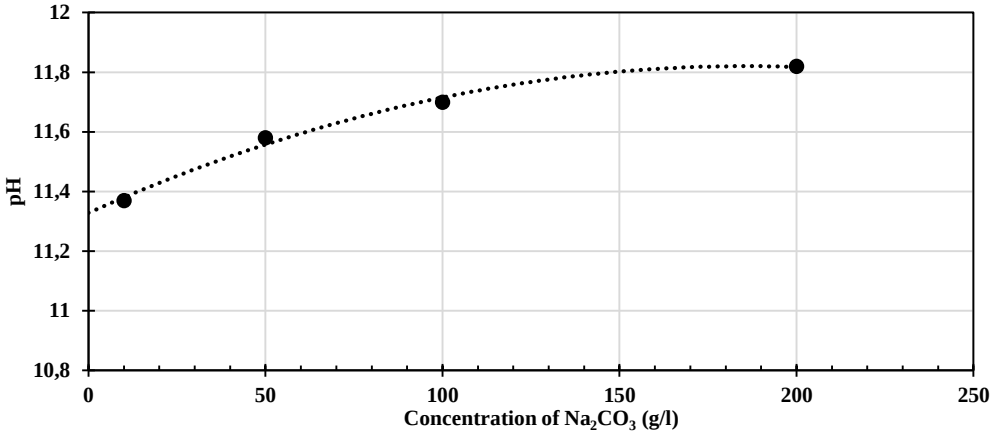

Figure 2.12: pH level of solution as a function of anhydrous Na_2CO_3 concentration in water at 20°C

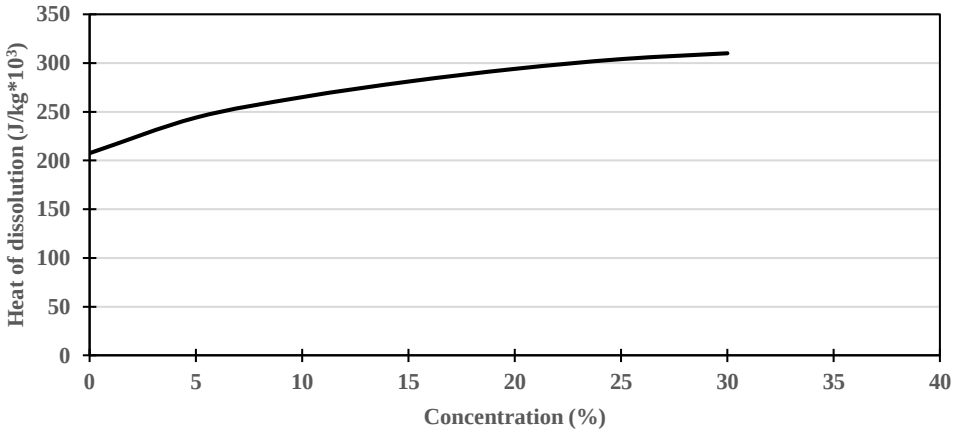

Figure 2.13: Effect of concentration on heat release over Na_2CO_3 dissolution at 25°C (GCIP, 2007)

2.2 Fresh state properties: Zeta potential, pH level and conductivity

As soon as the oxide particles (here slag particles) are put in contact with an aqueous solution, a net charge appears on their surface. The origin of this surface charge is complex and depends on the physicochemical interactions with the solution. This may include specific ion adsorption, isomorphous ion substitution, differential ion dissolution and ionisation of surface sites (Johnson et al., 2000). Ions dissolved in the bulk solution or leached from the mineral particles are then attracted to the surface to compensate for the surface charge. This leads to the formation of an electrical double layer (EDL), which controls many suspension properties through its impact on the interactions among the particles (Safi et al., 2011; Lowke and Gehlen, 2017). In particular the EDL controls the flocculation state of the particles and consequently the rheological properties. It also determines dispersant ((super-) plasticizer)

efficiency (Daimon and Roy, 1979; Plank and Hirsch, 2007; Rickert, 2012), as well as being an indicator of the particles' reactivity and other specific properties (Pointeau et al., 2006). The EDL comprises two main regions (Figure 2.14): A region in which the counter -ions are tightly adsorbed on the surface (Stern layer) and a diffuse region comprising the sliding layer on which the potential (Zeta potential or ζ-potential) is measured. Indeed the ζ-potential is determined through relationships based on the Smoluchowski equation which relates the particle electrophoretic mobility and an applied potential. Then the ζ-potential is related to the charge density at a virtual surface (sliding surface) around the particle, not at the actual surface of the particle. When the absolute value of the ζ-potential is close to zero the (repulsive) electrostatic forces are weak and they can be overcome by the (attractive) van der Waals forces leading to agglomeration of the particles. On the other hand, when the ζ-potential is high the (repulsive) electrostatic forces can overcome the van der Waals forces leading to the dispersion of the particles. This is described quantitatively by the DLVO (after Derjaguin, Landau, Verwey and Overbeek) theory (Russel et al., 1989). The working mechanism of the ionic plasticisers as those comprising the sulfonate group is based in this principle. These anionic polymers adsorb on positive sites (rich in Ca^{2+}) of the particles leading to an increase of the absolute value of the ζ-potential, then to an increase of the repulsive electrostatic forces and dispersion.

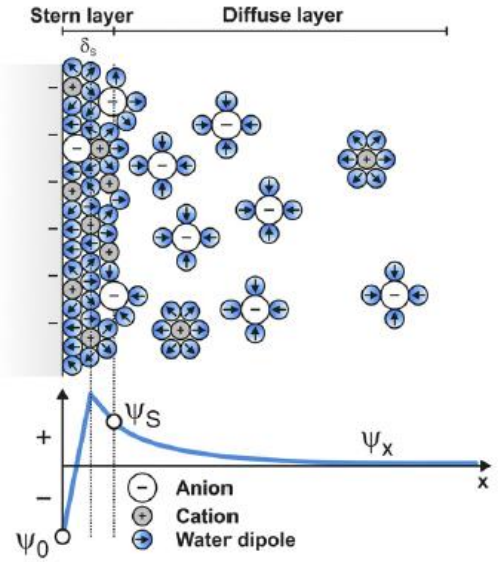

Figure 2.14: Definition of the Zeta potential denominated Ψs (from Lowke and Gehlen, 2017).

The sign of the ζ-potential controls, in particular, the adsorption ability of dispersants depending on their charge.

Measurement of the ζ-potential was undertaken using a Zetaprobe Analyser from Colloidal Dynamics (Figure 2.15) performing through the electroacoustic method. This

apparatus allows performing measurements at high particle concentrations. Yet in this investigation, relatively dilute (although opaque) suspensions are considered (1g powder per 100 ml of deionized water in general). Dry components were added into water with different additives (such as sodium carbonate) and mixed manually in a closed flask for about 30 sec. Then the suspension was transferred to a cell for measurement over permanent stirring at 270 rpm. The values of the ζ- potential, conductivity and pH were recorded every 5 minutes.

Figure 2.15: ZetaProbe Analyser for measurement of particle surface charge

The results of ζ-potential time evolution for the three GGBS grades dispersed in deionized water are presented in Figure 2.16. As it can be seen, all fineness types of GGBS have a similar behaviour and have a negative zeta potential, with fluctuations in time. In the case of Ultrafine GGBS, the fluctuations are more frequent and stronger compared to the other grades, which might indicate higher reactivity if we assume that the fluctuations are related to dissolution/precipitation. Differences among the three types of slag were also observed with pH and conductivity (Figure 2.17 and Figure 2.18). For the three cases the pH increases with time. The pH level increases significantly with fineness. The pH of the Ultrafine GGBS approaches 13 after about 1 hour. Taking into account the fact that the measurements are performed with dilute solutions (about a factor of 200 compared to a paste with water/slag ratio of 0.5), the corresponding pH for a typical cement paste should be different (due to enhancement of the dissolution/precipitation process at lower Water/Binder ratio). This slag is then expected to react sufficiently fast without any activation. Yet, although the pH level is more than enough for slag dissolution, to reach sufficient mechanical strength development the hydration process should be controlled in order to get an appropriate distribution of the hydration products.

Similar to the pH, the conductivity increases with slag fineness which might be related to an increase in dissolution rate (Figure 2.17).

These results are in agreement with those already reported in the literature (Kumar et al., 2008; Elakneswaran et al., 2009; Habbaba and Plank, 2012). Negative values of zeta potential for slag particles are related to the deprotonation of silanol and aluminol groups after contact with water at high pH:

$$>Si\text{-}OH + OH^- \rightarrow >Si\text{-}O^- + H_2O$$

$$>Al\text{-}OH + OH^- \rightarrow >Al\text{-}O^- + H_2O$$

The symbol '>' indicates that the compound is located on the particle surface. The number of these negative sites should be higher compared to that of OPC clinker due to higher Si and Al contents in slag. In addition, less dissolved cations (Ca^{2+}) are available for surface charge compensation than in the case of OPC. This explains why the ζ-potential is negative with GGBS and positive with OPC (Figure 2.19). With the increase of the slag fineness and the corresponding increase of dissolution rate, the ζ-potential is less negative overall due to faster leaching of Ca^{2+} (and other alkali) leading to more charge compensation. The fluctuations can be associated with both the measurement artefacts (particle sedimentation for instance) and the changes in surface charge due to the process of dissolution/precipitation, for instance between Ca leached from the slag and CO_3^{-2} from dissolved CO_2.

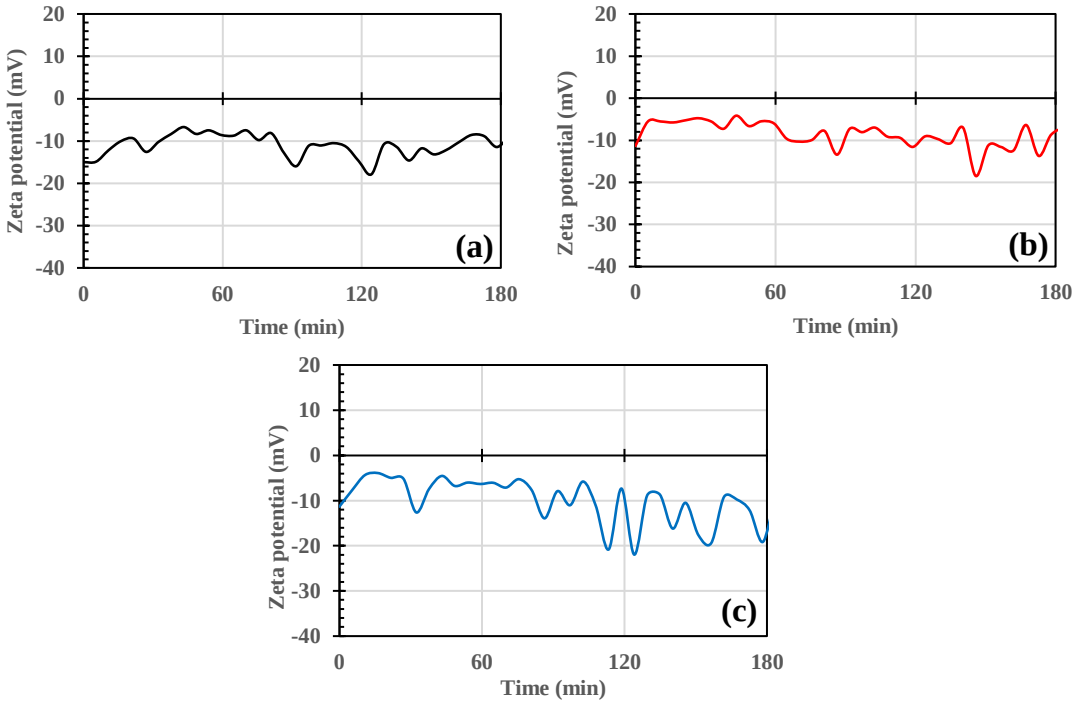

Figure 2.16: Zeta potential evolution of Standard 4400 cm^2/g (a), Fine 5600 cm^2/g (b) and Ultrafine 11000 cm^2/g(c) GGBS in deionized water (W/B=100)

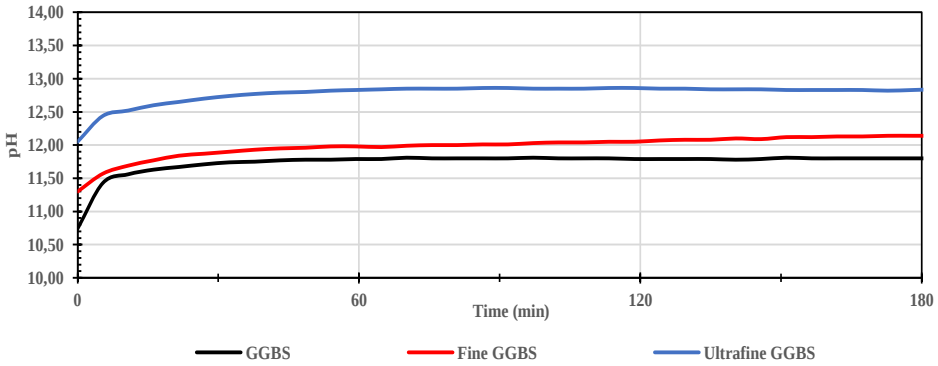

Figure 2.17: pH level of Standard, Fine and Ultrafine GGBS in deionized water

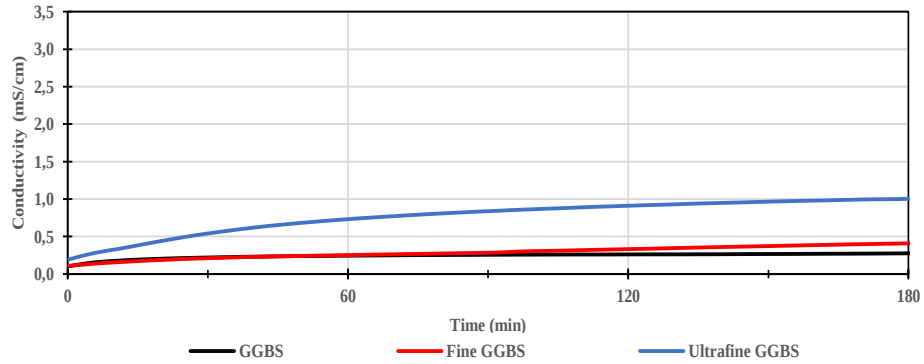

Figure 2.18: Conductivity of Standard, Fine and Ultrafine GGBS in deionized water

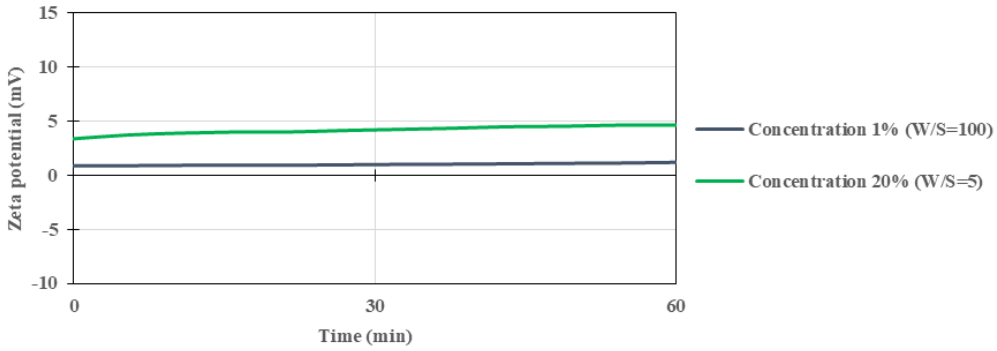

Figure 2.19: Zeta potential evolution of OPC in deionized water

The addition of Na_2CO_3 leads to a significant change in the time evolution of ζ-potential (Figure 2.20), both *quantitatively* and *qualitatively* (except in the case of the ultrafine GGBS). The addition of Na_2CO_3 makes the ζ-potential start much more negative. This can be related in particular to increased deprotonation of the silanol/aluminol groups due to a higher pH level (Figure 2.21). In addition, rapid adsorption of the carbonate ions (characterised by a high negative charge density) on the positive sites (mainly Ca^{2+}) on the particle surface should contribute to this negative value. Actually this implies very early precipitation of Ca^{2+} with the carbonates will also render the surface more negative. Over time, more Ca^{2+} ions are dissolved from the slag and may re-adsorb on the (negative) surface leading to an increase of the ζ-potential (which is observed only in the case of the first two GGBS grades). One can observe a sudden growth of the ζ-potential at a certain moment, which eventually reaches positive values. If we

assume that the ζ-potential evolution is mainly controlled by Ca^{2+} release and precipitation (Habbaba and Plank, 2012), the steep growth may reflect a kind of bursting phenomenon in the Ca^{2+} leaching process. This may reflect an eventual rupture of a hydrated membrane on the grain surface due to osmotic pressure. Such a mechanism has been suggested in the case of early clinker hydration (Birchall et al., 1978). Later on, an approximate equilibrium seems to take place between dissolution and precipitation, and finally an eventual increase of the precipitation rate (compared to dissolution) leads to a decrease of the ζ-potential, which reaches more or less negative values depending on slag fineness. Note that the "bursting' phenomenon is not observed in the case of the ultrafine GGBS. Yet, since the moment at which this transition is observed decreases with slag fineness, it might then have been missed in the case of the ultrafine GGBS.

Increasing the slag particle concentration leads to the ζ-potential values near to zero (Figure 2.22) over the duration of the measurement period. This suggests that for actual slag pastes (with water/binder around 0.40) the particles should be highly agglomerated due to low strength electrostatic (repulsive) forces compared to the van der Waals attractive forces. This will have consequences on the rheological properties as discussed further in this document.

Since the sign of the ζ-potential at high slag concentration is hard to anticipate, the appropriate choice of dispersant type (anionic or cationic) is not clear. One can anticipate that the adsorption capacity of the slag surface should be low. This is in contrast with OPC for which the particle surface seems to become more and more positive when the particle concentration is increased (Figure 2.19 and Figure 2.22), implying high capacity for adsorption of ionic dispersants.

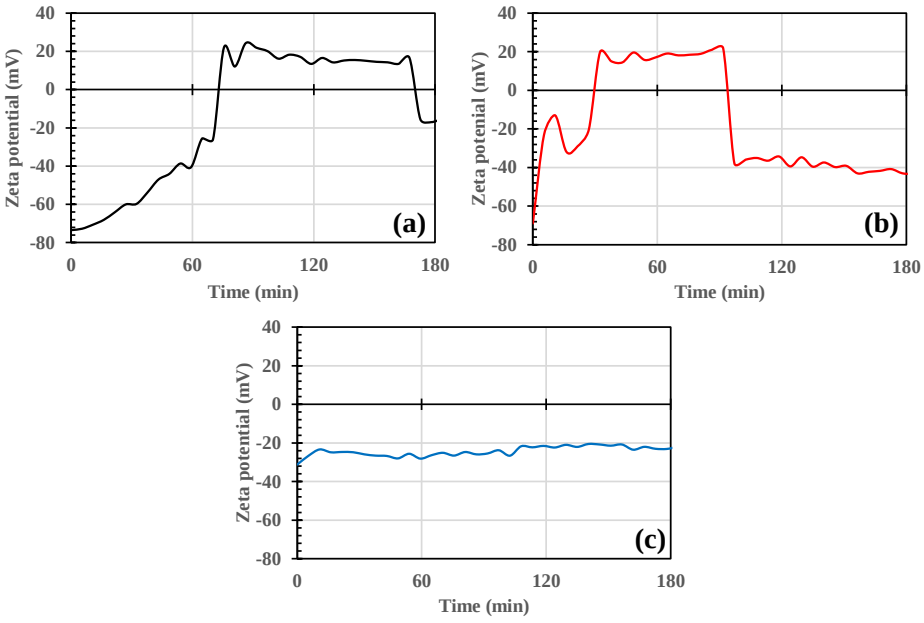

Figure 2.20: Evolution of the ζ– potential of Standard (a), Fine (b) and Ultrafine (c) GGBS dispersed in deionized water in the presence of 8% of Na_2CO_3 (W/B=100)

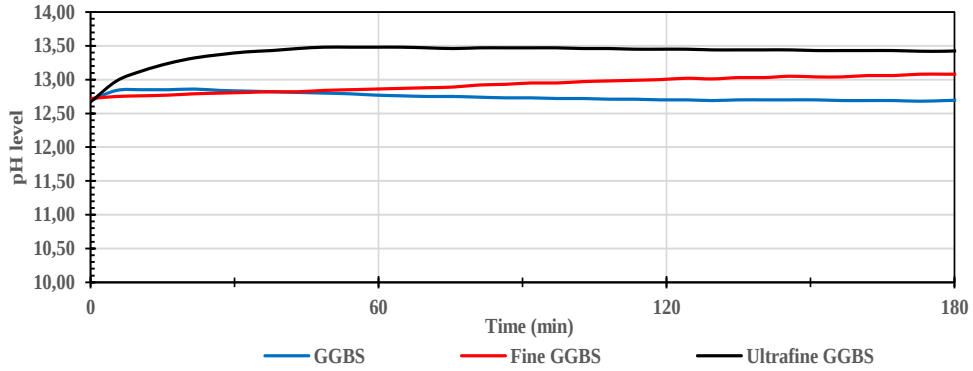

Figure 2.21: pH level of Standard, Fine and Ultrafine (c) GGBS in deionized water with 8% of Na_2CO_3

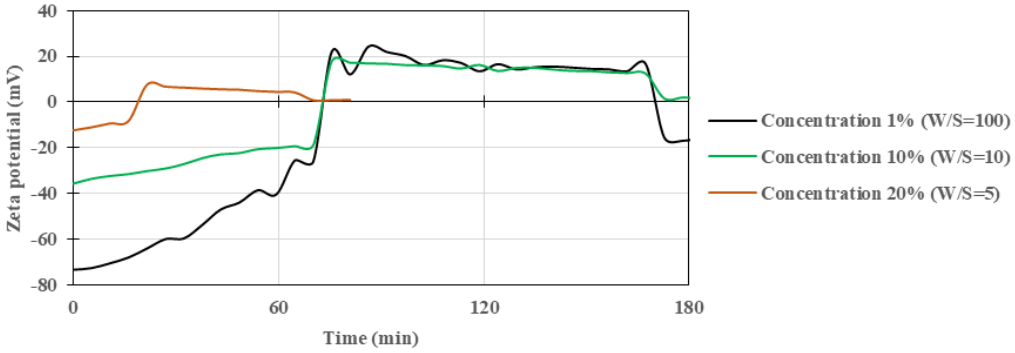

Figure 2.22: Impact of slag concentration on the ζ-potential time evolution

2.3 Rheological properties

Cementitious materials are characterized by at least two rheological parameters: *yield stress* and *viscosity*. From a practical point of view, the yield stress is related to the capacity of the material to resist flow initiation while the viscosity characterizes the resistance of the material to maintain flow at a given rate. At the very beginning, the rheological properties are mostly governed by the interactions among the anhydrous particles which are controlled, as discussed above, in great part by the ζ-potential. However, over time the hydration products start precipitating leading to the evolution of the rheology.

In the case of concrete/mortars, some simple methods are used for the evaluation of rheological properties, such as the Marsh cone test for high fluidity products and the Abrams cone test for stiff concrete. These tests are straightforward and easy to be performed in the field. However, the most accurate and suitable method for laboratory study, in particular for cement pastes, is a rheometer. In the present study all measurements were performed on paste samples with AR2000ex laboratory rheometer from TA Instruments. The temperature was controlled by a Peltier system. A vane-in-cylinder geometry was used (Figure 2.23) in order to minimize wall-slip.

Figure 2.23: Rheometer from TA Instrument with vane-in-cylinder geometry used in this study

Sample preparation consisted of mixing the dry powders with the water solution for 2 minutes at 500 rpm with an IKA Eurostar 40 mixer (Figure 2.24). All measurements started at the age of 3 minutes, corresponding to the duration of placement within the rheometer. Two types of tests were performed.

Figure 2.24: Preparation of paste sample

The first test consisted of the determination of the flow curves at different ages, which allowed for the inference of the yield stress evolution in time. For this, a paste sample was firstly pre-sheared for 30 s at constant shear rate of $25s^{-1}$. The (controlled) shear rate was then increased step-by-step up to 5 s^{-1}. Only low shear rates are considered here, since the yield stress is of primary interest as well as mimicking a slump test with concrete. In particular, this rheological study may not be relevant for the pumping process. The measurements were performed at 10 minute intervals. An example of flow curves at different time periods is presented in Figure 2.25. The minimum that can be observed on some flow curves can be attributed to either fast evolution of the material and/or flow localisation. This phenomenon precludes a simple identification of the yield stress from common rheological models, such as Bingham's or Herschel–Bulkley's. Instead the yield stress value was arbitrarily assumed to be the stress at a shear rate of $0.1s^{-1}$.

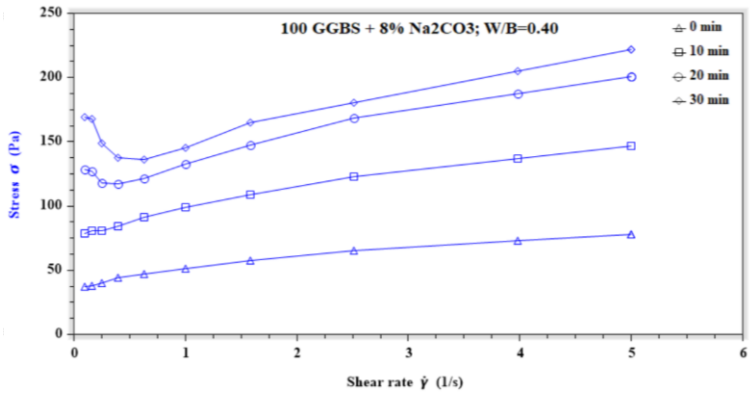

Figure 2.25: Example of flow curve evolution in time

The second rheological test consisted of following the time evolution of the linear viscoelasticity (or storage modulus) (G') at a frequency of 1Hz. The vane-in-cylinder geometry was used. Measurements were taken each minute at an oscillatory strain of 0.2%, which is located within the linear viscoelastic region (Figure 2.26). The final results were represented in the form of storage modulus as a function of time. Mini-cone tests were also considered.

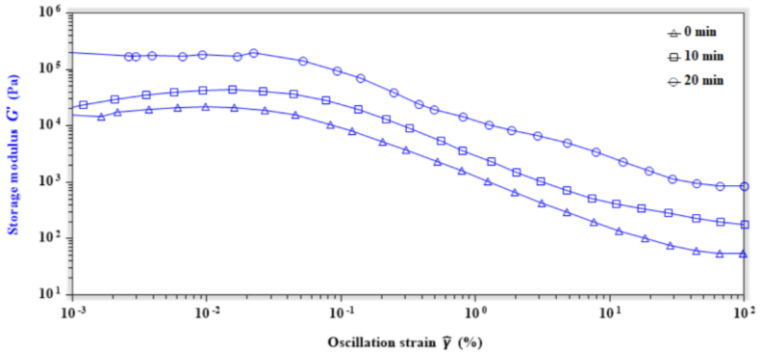

Figure 2.26: Example of storage modulus evolution in time as a function of oscillation strain (f=1Hz)

2.3.1 Rheological properties of the Standard GGBS pastes

In Figure 2.27 the results of the yield stress measurements according the procedure described previously are presented. In all cases (except 0% Na_2CO_3), a monotonic increase of the yield stress over time can be observed. The evolution rate depends on increases of the Na_2CO_3 dosage. It can be noticed that the yield stress at t=0 decreases strongly in the presence of the activator. This can be explained by taking into account the results from the $\zeta-$ potential measurements. The addition of Na_2CO_3 leads to initial values which are significantly more negative, leading to strong repulsion among the particles and then dispersion. During hydration, the yield stress increases due to the precipitation of hydration products (Na/Ca carbonates). This process increases with Na_2CO_3 dosage. It is to be noticed that the high values of the yield stress (especially without the activator) can be also partially attributed the angular shape of GGBS particles (Figure 2.4) (Land and Stephan, 2012).

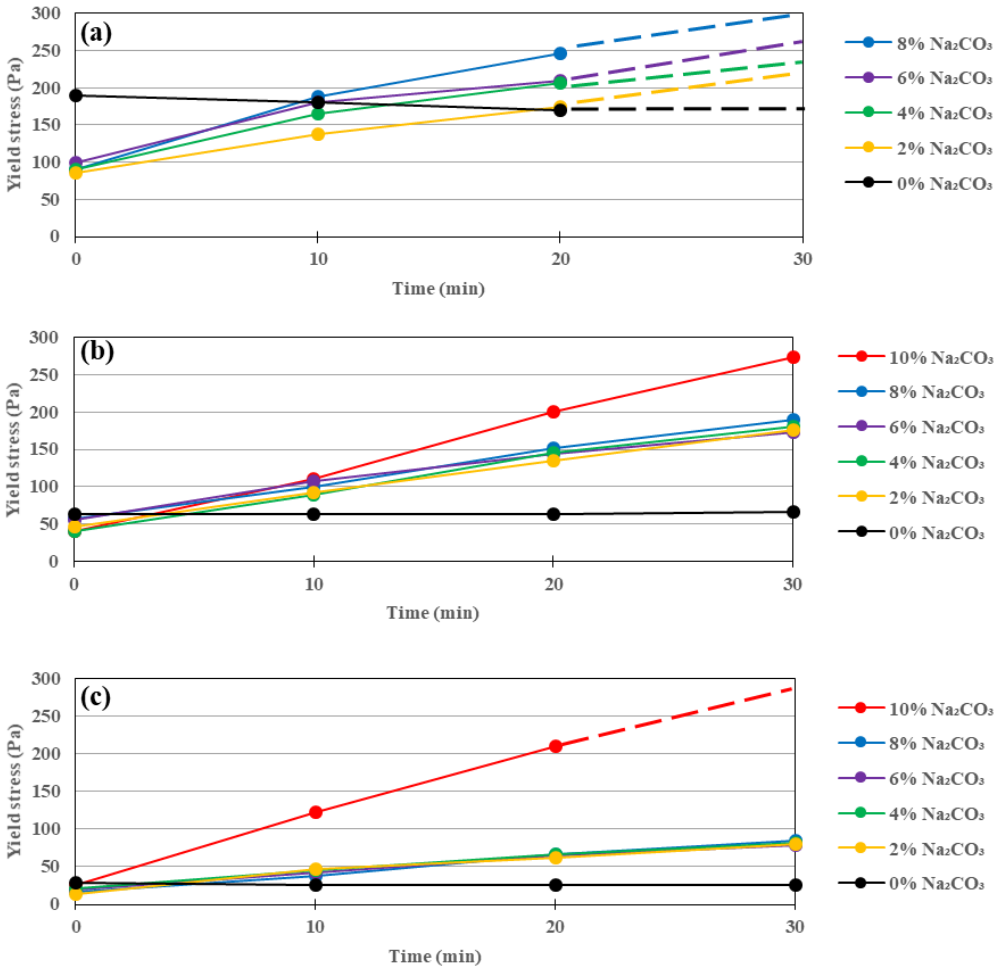

Figure 2.27: Yield stress evolution in time for Standard GGBS with different dosage of Na_2CO_3 and at different W/B ratio: 0.35 (a); 0.40 (b) and 0.45 (c)

One can observe a strong influence of the water/binder ratio on the yield stress. The initial yield stress is divided by a factor about 4 when increasing the W/B ratio from 0.35 to 0.45. The rate of its evolution is also enhanced when decreasing the W/B ratio. Yet this depends on the Na_2CO_3 concentration. At concentrations commonly used to properly activate the GGBS (8-10%), the paste reaches almost the same level of yield stress independent of the W/B ratio. In this case, the yield stress evolution is fast and this represents a crucial issue in practice. This actually represents the main issue addressed in the study presented in this document.

The evolution of the storage modulus allows for the mechanical probing of the evolution of the paste microstructure over time at rest. The evolution of G' over time for different Na_2CO_3 concentrations and different W/B ratios is reported in Figure 2.28. Although G' measurements are related to the yield stress, they can be performed for longer time periods since the deformation is low and sliding can be avoided even for a stiff product.

The initial value of G' seems to be independent of the activator concentration (similar to the yield stress). The impact of the dosage increases over time due to the difference in the hydration kinetics.

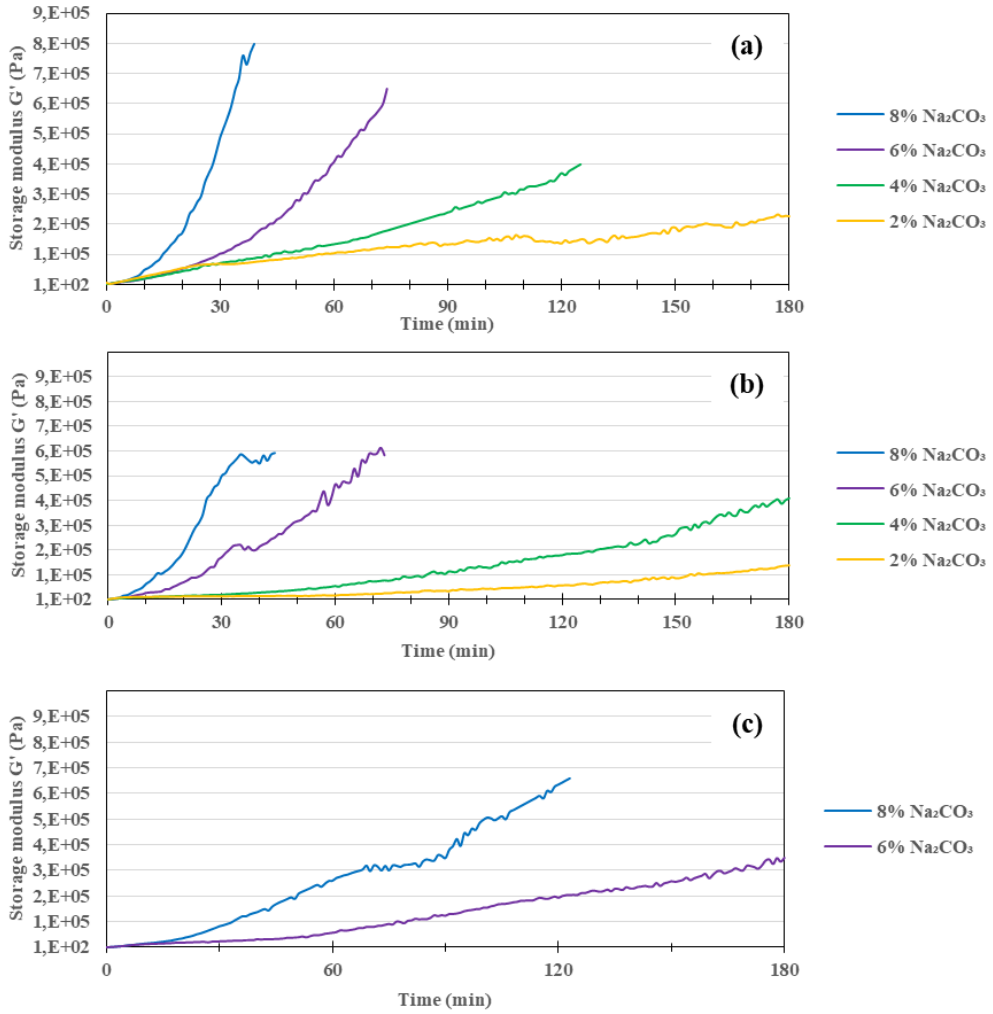

Figure 2.28: Storage modulus evolution for standard GGBS with different Na_2CO_3 dosages and Water/GGBS ratios of: 0.35 (a); 0.40 (b) and 0.45 (c)

Mini-cone slump tests were performed for comparison with the rheological measurements (Figure 2.29). A moistened metal cone with dimensions H=60 mm, d=36mm and D=60 mm was filled with paste and placed on a smooth wet metal surface on a vibration table. The cone was raised and the values of the spreading diameter and slump height were recorded. Then a vibration (50Hz) was applied for 5s. The values of spreading after vibration were measured.

The results in the case of 8% of Na_2CO_3 and W/B=0.40 are reported in Table 4. It should be pointed out that after only 10 minutes a significant spread loss occurred. Nevertheless, higher values after a short vibration time were obtained, indicating that this is mostly related to the particles' physical agglomeration/flocculation. However beyond about 30 minutes, the spread could not be fully recovered with vibration indicating that the hydration process was starting to become significant.

Table 4: Mini-cone slump test results: pastes with 8% Na_2CO_3 activated GGBS at W/B=0.40

Time	Slump, cm	Spreading, cm	Spreading after vibration, cm
0	3,6	18	28,9
10	2,1	11,8	27
20	1,6	11,2	23,6
30	1,5	10,6	21,4
40	1,4	10,4	21,1
50	1,2	10,3	20,7
60	1,1	10,3	19,3
70	1,1	10,3	19,1

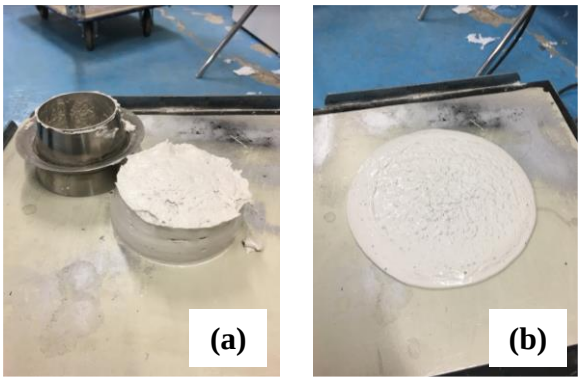

Figure 2.29: Mini-cone slump test: GGBS paste with 8% Na_2CO_3 at W/B=0.40 before (a) and after (b) vibration at the age of 50 minutes.

To characterise the loss of rheology and beginning of stetting, the Vicat test was used. This method consisted of the free penetration of a needle into a sample at different time intervals. A plastic mould of 40 mm height was filled with fresh paste. The beginning of the setting time was recorded when the needle fails to penetrate the paste, placed in the Vicat's mould, 4 ± 1 mm from the bottom of the mould. The sample preparation procedure was the same as for the rheological study above.

The results reported in Figure 2.30 indicate that the W/B ratio plays a more significant role on setting than the dosage of Na_2CO_3. This is in agreement with the results of the previous rheological tests.

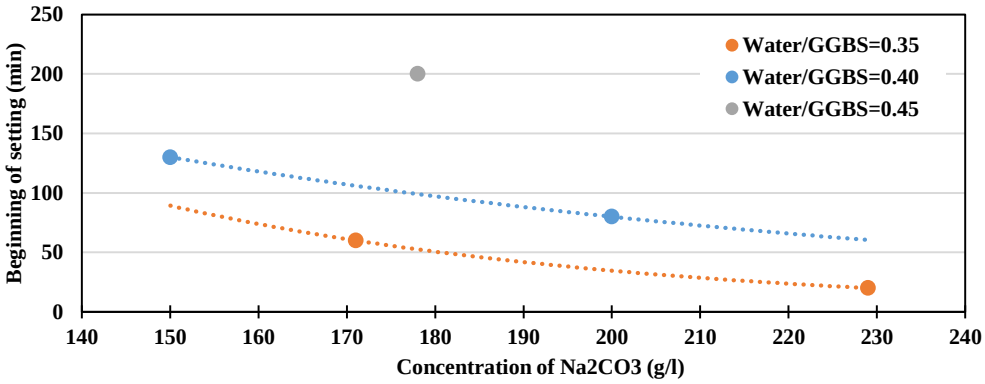

Figure 2.30: Influence of Water/GGBS ratio and initial concentration of the alkaline solution on the beginning of setting

2.3.2 Impact of the slag fineness on the rheological properties

Pastes with Fine GGBS

The results for the time evolution of the yield stress at different activator concentrations and for three different W/B ratios are presented in Figure 2.31. The measurements were performed following the same procedure as with Standard GGBS and are then to be compared with the results in Figure 2.27. Similar trends can be observed, however increasing the slag fineness leads to a significant increase of the yield stress at all times and at any given activator concentration. This may be attributed to the faster precipitation of early hydration products, reflecting the higher reactivity of this slag grade.

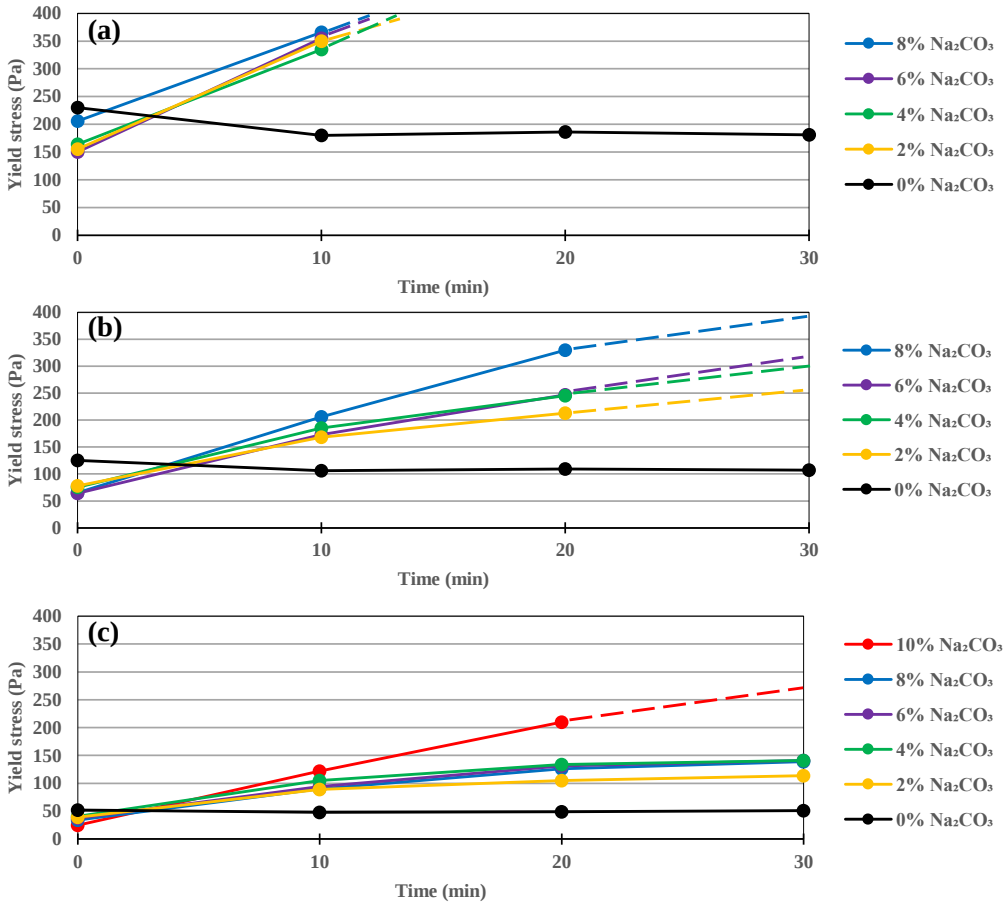

Figure 2.31: Yield stress evolution of GGBS 5600 cm^2/g with different dosages of Na_2CO_3 and at W/B ratio of: 0.35 (a), 0.40 (b) and 0.45 (c)

The results of the evolution of the storage modulus over time are presented in Figure 2.32. By comparison with Standard GGBS (Figure 2.28), it can be noticed that at low W/B ratio (0.35) the results are quite similar. However, in the case of a higher W/B, the rate of the paste structuration is higher with finer GGBS.

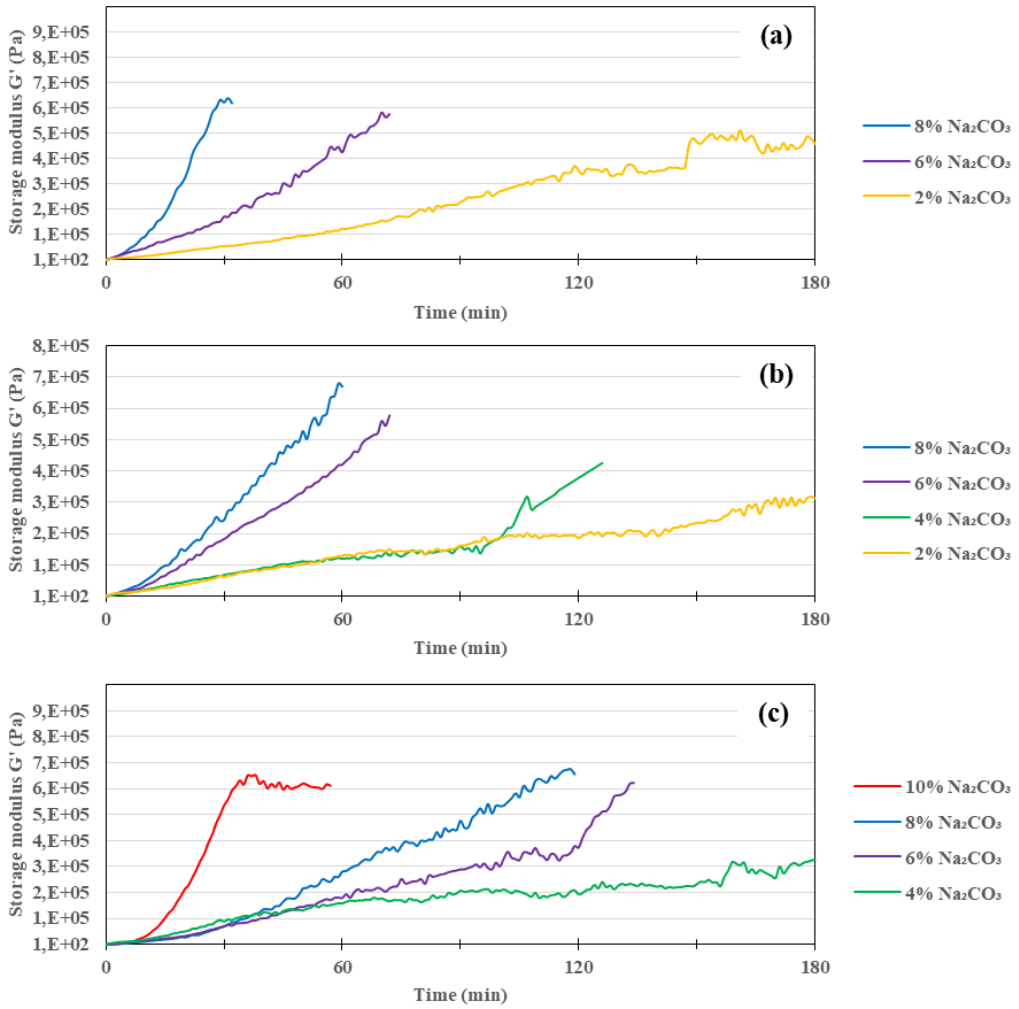

Figure 2.32: Storage modulus evolution of Fine GGBS with different amount Na_2CO_3 and W/B ratio of: 0.35 (a), 0.40 (b) and 0.45 (c)

Pastes with Ultrafine GGBS

In this case the pastes consisted of mixtures of 5% or 10% (by mass) of Ultrafine with the remainder being Standard GGBS. Such replacement levels are related to what can be done in practice since this ultrafine grade can be produced only in limited amounts as it has a higher cost and CO_2 footprint.

The yield stress evolution of the different pastes is reported in Figure 2.33 and Figure 2.34. Despite the fact that only a small fraction of the standard GGBS was replaced with the ultrafine, the rate of evolution and the initial values are on the order of those of fine GGBS. This is also clearly visible with storage modulus evolution (Figure 2.35).

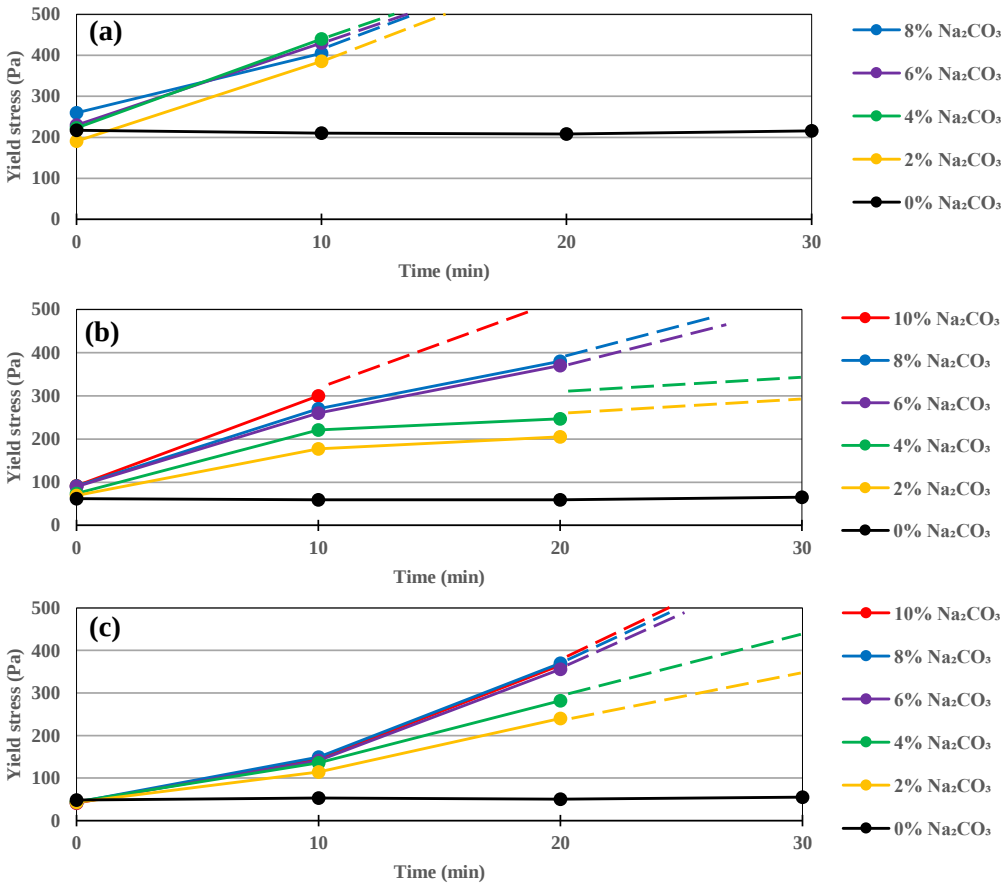

Figure 2.33: Yield stress evolution for GGBS with 5% replacement by Ultrafine GGBS with different dosages of Na_2CO_3 and at different W/B ratios: 0.35 (a); 0.40 (b) and 0.45 (c)

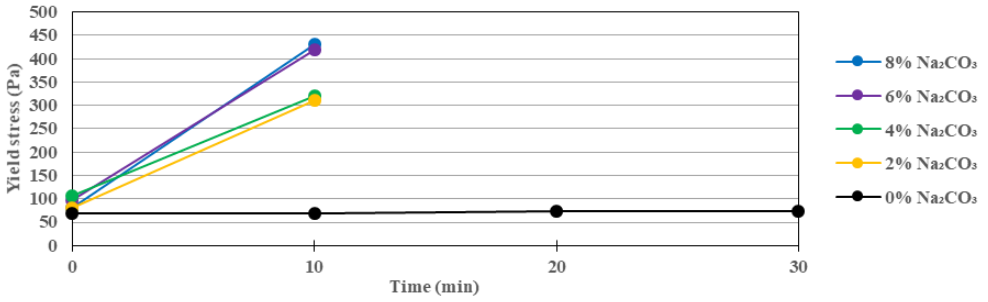

Figure 2.34: Yield stress evolution for GGBS with 10% replacement by Ultrafine GGBS with different dosages of Na_2CO_3 and W/B=0.40

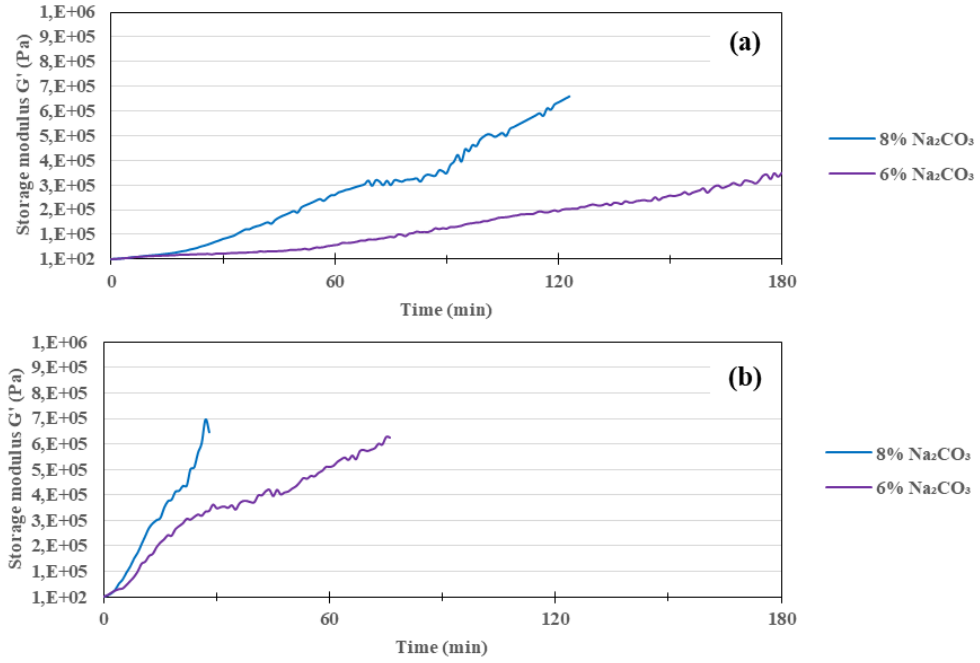

Figure 2.35: Comparison of storage modulus evolution in case of 100% GGBS (a) and with 10% replacement by Ultrafine GGBS (b) with different amounts of Na_2CO_3 and W/B=0.45

General observations regarding the rheological behaviour

- The yield stress values and their evolution are highly dependent on the W/B ratio of the paste.
- The impact of Na_2CO_3 dosage on the yield stress increases with time due to the hydration process.
- Increasing the slag fineness leads to an increase of the rate of the yield stress evolution.
- In all cases, the evolution of yield stress (leading to loss of rheology) is quite fast for conventional concrete. In addition, even immediately after mixing, appropriate flowability is expected to be achieved only with high water content.
- At the same time, high water content may significantly delay setting. In practice, the setting is also one of the important parameters, not only because of the strength requirements for economic reasons, but also regarding durability. With a very long setting period, the risk of shrinkage due to the water evaporation is higher if the curing conditions are not optimal. In addition, bleeding and segregation are expected if a high W/B is used.

Appropriate rheological admixtures to increase the open (workability) time and to reduce W/B ratio are then required. This will be discussed in the forthcoming chapters.

2.4 Hydration kinetics

The hydration kinetics of the slag pastes was evaluated through the evolution of heat release using a TAM Air Isothermal Calorimeter from TA Instruments (Figure 2.36). The temperature was fixed at different values with an accuracy of ±0.02°C. The sample preparation procedure was the same as in the above rheological study. 20 ml plastic bottles were used to sample approximately 5g of paste. The reference product used to into account parasitic temperature variations is composed of 5g of silica sand and 2.5g of water. All results were normalized to the mass of dry binder, excluding sodium carbonate. Since the mixing was performed outside the instrument, the measurements started approximately 3 min after the powder made contact with water.

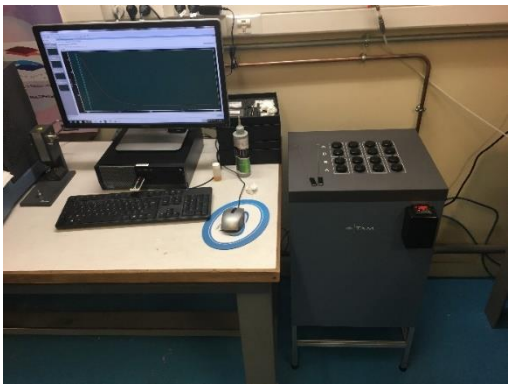

Figure 2.36: TAM Air Isothermal micro-calorimetry equipment for heat evolution recording during the binder paste hydration process

In Figure 2.37 an example of isothermal micro-calorimetry results is presented. In agreement with (Shi. et al., 2006), in the case of sodium carbonate activation the heat evolution curves are of *Class III*. That is, 3 main peaks can be observed. The first one (first pre-peak) is related with the wetting of particles and ions, the dissolution of sodium carbonate, and the formation of the very first hydrates. It is generally characterized by a release of large amounts of heat in a short period of time. Since this peak starts to appear right at the moment of contact with water and the measurement starts after 3 minutes, almost only the deceleration part of this pre-peak can be observed.

Then another peak appears, designated hereafter as the “first peak”. Depending on the formulation, an induction period can be observed between the pre-peak and the main hydration peak. Often the two peaks (pre-peak and first peak) superimpose. The first peak is related mainly to the formation of Ca-based hydration products. According to several studies (Bernal et al., 2015; Ke et al., 2016; B Yuan et al., 2017a), this corresponds to carbonate based phases including calcium carbonate polymorphs ($CaCO_3$) and Gaylussite ($Na_2Ca(CO_3)_2$*5 H_2O), and sometimes

Afm type phases are detected. The formation of these first hydrates are responsible for the setting and the appearance of the first strength properties. Since the main hydrates within this period of time are (big) crystals, the strength is very low (this will be demonstrated in the following chapters). Despite the fact that the process of thickening begins a short time after mixing, the beginning of the setting is rather related to the beginning of the rise of the first peak. The end of the setting is mostly related to the magnitude of the first peak (FP) and its deceleration. The open time is expected to be longer when the first peak is delayed prominently.

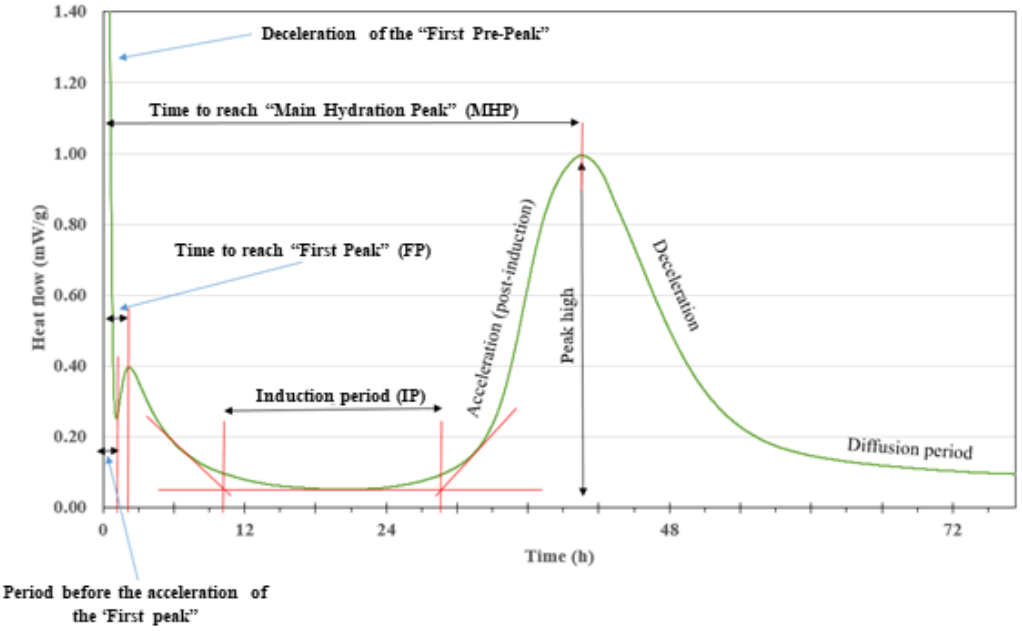

Figure 2.37: Schematic representation of heat evolution during Na_2CO_3 activated GGBS hydration with indication of zone of interest

Similar to OPC, the first peak is followed by an induction period, which is much longer in this case. The origin of the induction period, which is a key parameter for early age strength, will be discussed further. The third peak (acceleration period) is related to a massive formation of C-S-H type hydrates (Shi. et al., 2006), which are responsible for significant strength development.

Beyond the third peak, the hydration process slows down (deceleration), because the structure becomes more and more compact as a result of space filling with amorphous (or nano-crystalline) gel of C-(A)-S-H type and a decrease of water availability. Although at a very low rate, the hydration process continues at long term leading to a monotonic increase of the strength, even at very long term (see further).

2.4.1 Hydration kinetics of the Na_2CO_3 activated Standard GGBS

The calorimetry curves (performed at 22°C) are presented in Figure 2.38 for different activator dosages and different W/B ratios. The first hydration peak can hardly be distinguished from the dissolution (wetting) peak and appears rather as a shoulder. At low W/B ratio (0.35), this peak can be distinguished only at a sufficiently low Na_2CO_3 dosage (2%). Increasing the W/B ratio leads to a decrease of the activator concentration for which the first peak separates from the first pre-peak. This may be related to the increase of open time (precipitation of the first hydration products) with the increase of W/B ratio. Increasing the activator concentration (by weight of GGBS) and/or decreasing the W/B ratio leads to a decrease of the induction period and an increase of the height of the strength-giving peak (third or main hydration peak). Note that at very low activator dosage (2%), the main peak splits into two peaks indicating a modification in the hydration path. Table 5 summarizes the main calorimetric data.

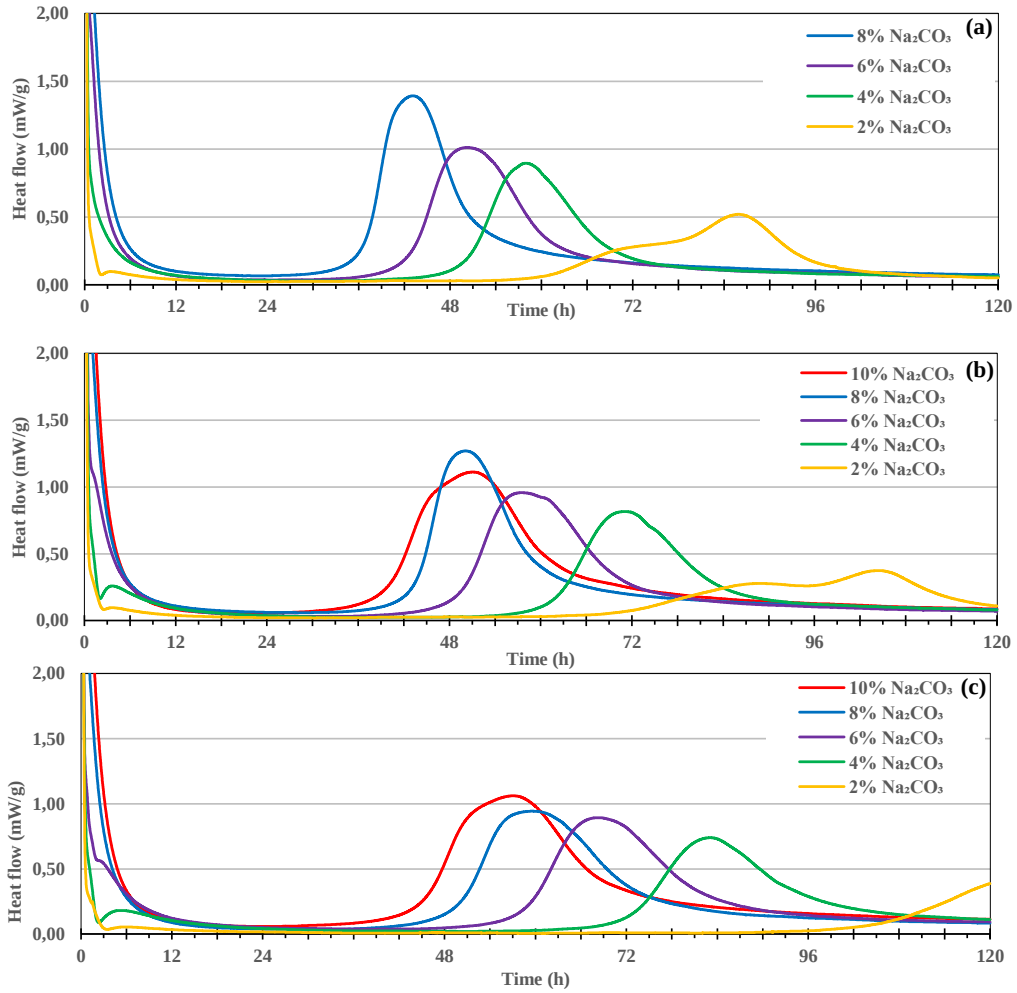

Figure 2.38: Heat evolution of GGBS with different Na_2CO_3 dosages at W/B ratio of: 0.35 (a), 0.40 (b) and 0.45 (c)

Table 5: Summery of heat evolution of GGBS at different W/B ratios and Na_2CO_3 concentrations

Water/GGBS	% Na_2CO_3 of GGBS mass	Concentration of Na_2CO_3	First peak (FP)	Main hydration peak (MHP)	Peak high
	%	g/l	h	h	mW/g
0.35	2	57	3.5	72/86	0.28/0.52
	4	114	N.D.	58	0.90
	6	171	N.D.	50	1.00
	8	229	N.D.	43	1.39
0.40	2	50	4	88/104	0.28/0.37
	4	100	4	71	0.82
	6	150	1	57	0.95
	8	200	N.D.	51	1.26
	10	250	N.D.	51	1.11
0.45	2	44	6	125	0.43
	4	89	5.5	83	0.74
	6	133	2.5	68	0.89
	8	178	N.D	59.5	0.94
	10	222	N.D.	57	1.06

In Figure 2.39 the time to reach the strength-giving hydration peak is presented as a function of the aqueous activator concentration for different W/B ratios. These results show that the appearance of the early strength is expected to be highly dependent on water content. Indeed the induction period depends on the water content through both the W/B ratio and aqueous activator concentration. Products based on such a binder are expected then to have low robustness regarding mixing water dosage.

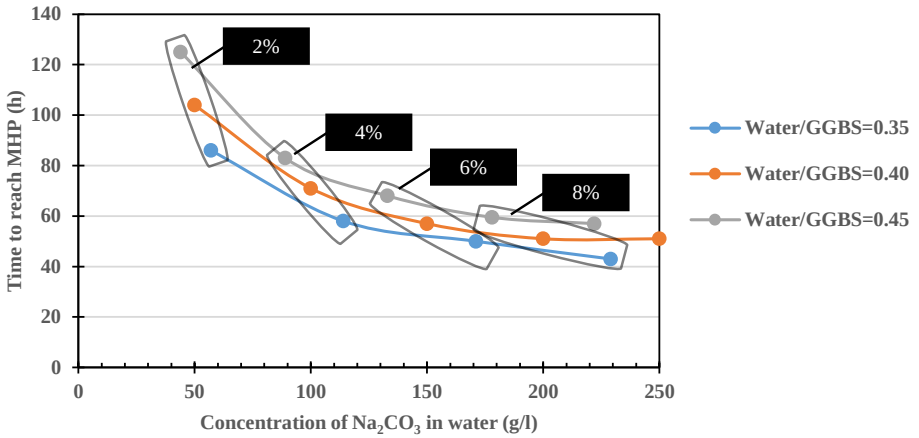

Figure 2.39: Time to reach the main hydration peak (MHP) as a function of Na_2CO_3 aqueous concentration. The black squares indicate the percentage of the activator relative to GGBS mass

To characterise the early degree of hydration, cumulative released heat curves are presented in Figure 2.40. Higher values indicate a more advanced degree of hydration (slag dissolution and the precipitation of hydration products). At any given time, a monotonic increase of the hydration level can be observed when increasing the Na_2CO_3 dosage and/or reducing the W/B ratio.

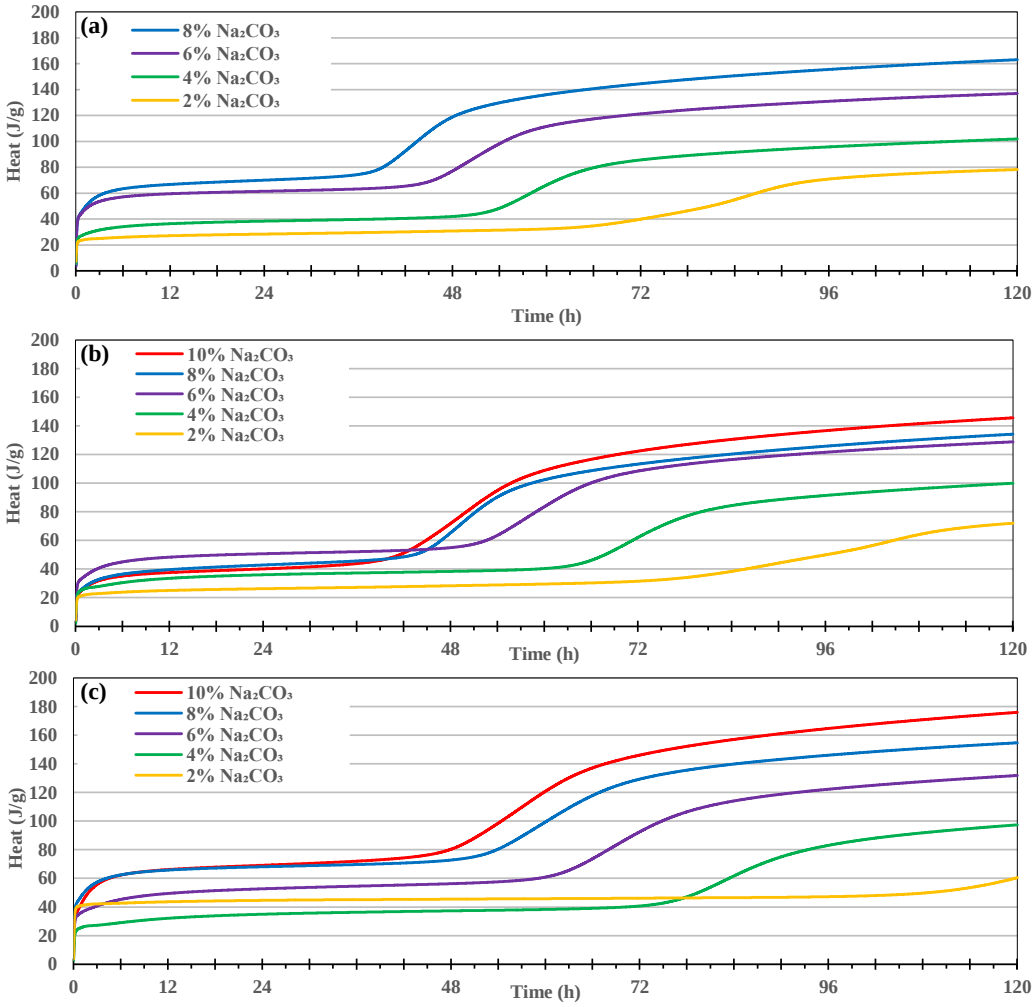

Figure 2.40: Heat released by hydration of GGBS with different Na_2CO_3 amount at different Water/GGBS ratio: 0.35 (a); 0.40 (b) and 0.45 (c).

Total heat released after 120h *versus* aqueous activator concentration for the three W/B ratios considered is presented in Figure 2.41. The aqueous concentration of the activator seems to be the key parameter regarding the early age degree of hydration (no crucial impact of pure W/B ratio from some moment).

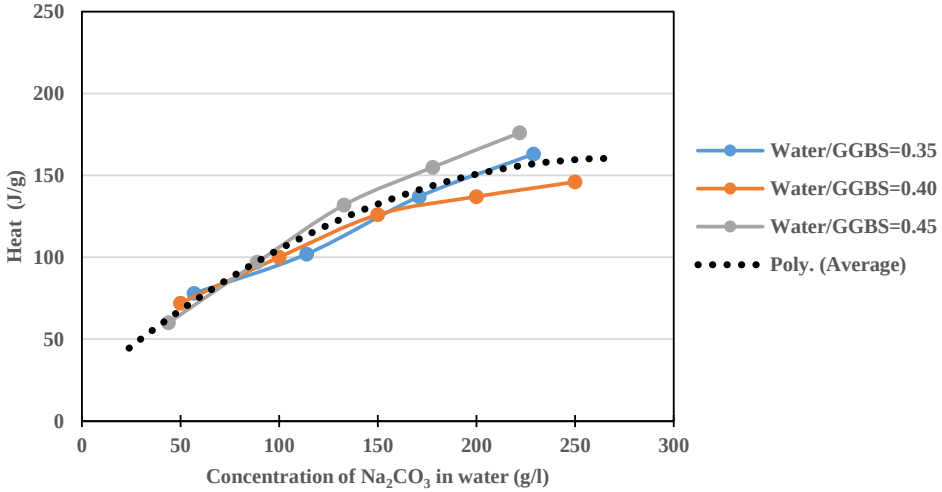

Figure 2.41: Heat released after 120h of hydration process as a function of initial Na_2CO_3 concentration in water.

2.4.2 Hydration at low temperature

All previous results were obtained with a fixed environmental temperature at 22°C. Several studies (Wang et al., 1994; Castellano et al., 2016) showed that alkali-activated slag binders are highly sensitive to curing temperature (storage or short treatment). This is known to have a positive effect on the strength development. The impact of low temperature curing has been much less frequently considered. This is an important issue to take into account, especially in colder northern climates.

The impact of a reduced curing temperature on the hydration kinetics for two different W/B ratios is reported in Figure 2.42. A significant slowing of the reaction can be observed when the temperature is decreased to 15°C. The induction period is significantly extended and the shape of strength-giving peak is modified. Yet the first peak is not substantially impacted. Even at low W/B ratio, the induction period is quite long (the main hydration peak occurs after 4-5 days of hydration).

In addition, low robustness regarding the amount of mixing water and a lack of robustness regarding concreting temperature are also expected for products based on this binder.

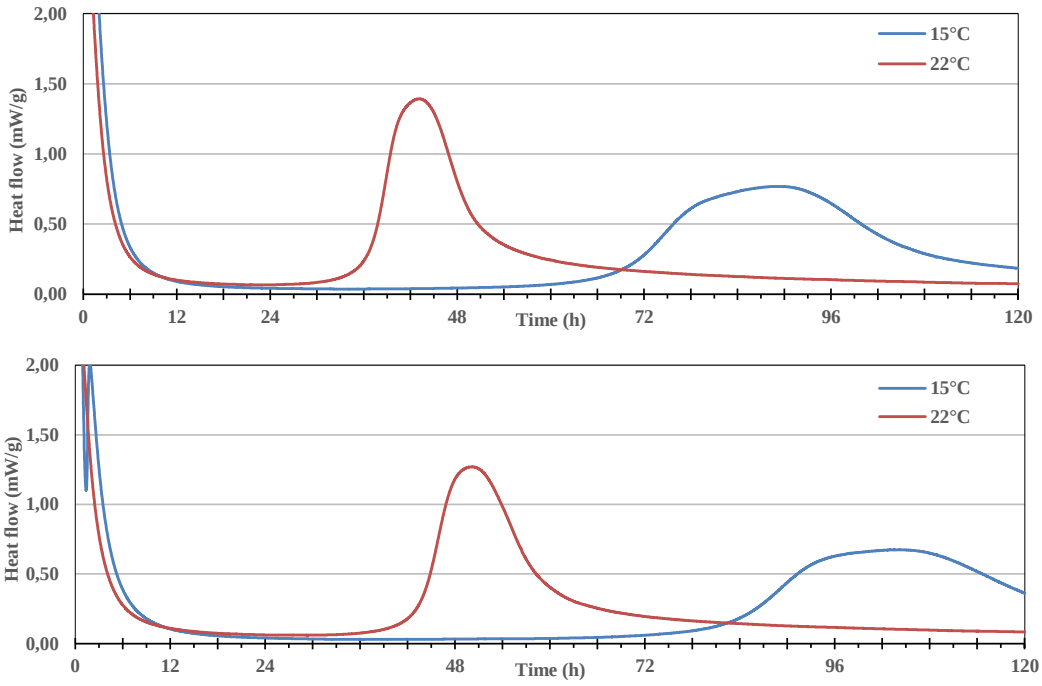

Figure 2.42: Heat evolution of GGBS with 8% of Na_2CO_3 at Water/GGBS=0.35 (a) and 0.40 (b) at different curing temperature

2.4.3 Influence of slag fineness on hydration kinetics

Case of Fine GGBS

The results of the released heat evolution throughout the hydration process of the Fine GGBS pastes for different W/B ratios are reported in Figure 2.43. Increasing the fineness accelerates the appearance of the main hydration peak in all cases. In addition, a lower influence, compared the Standard GGBS, of the activator content on the induction period can be observed. A particularly positive effect is noticeable at lower concentrations. The main characteristics of the released heat curves are reported in Table 6.

Figure 2.44 represents the evolution of the time to reach the main hydration peak as a function of the Na_2CO_3 concentration for different W/B ratios. These curves highlight the fact that the induction period is less sensitive to the aqueous activator concentration than in the case of Standard GGBS (hence it has a high influence). Again, the amount of mixing water is crucial, contributing to both the *aqueous* dosage concentration and the W/B ratio.

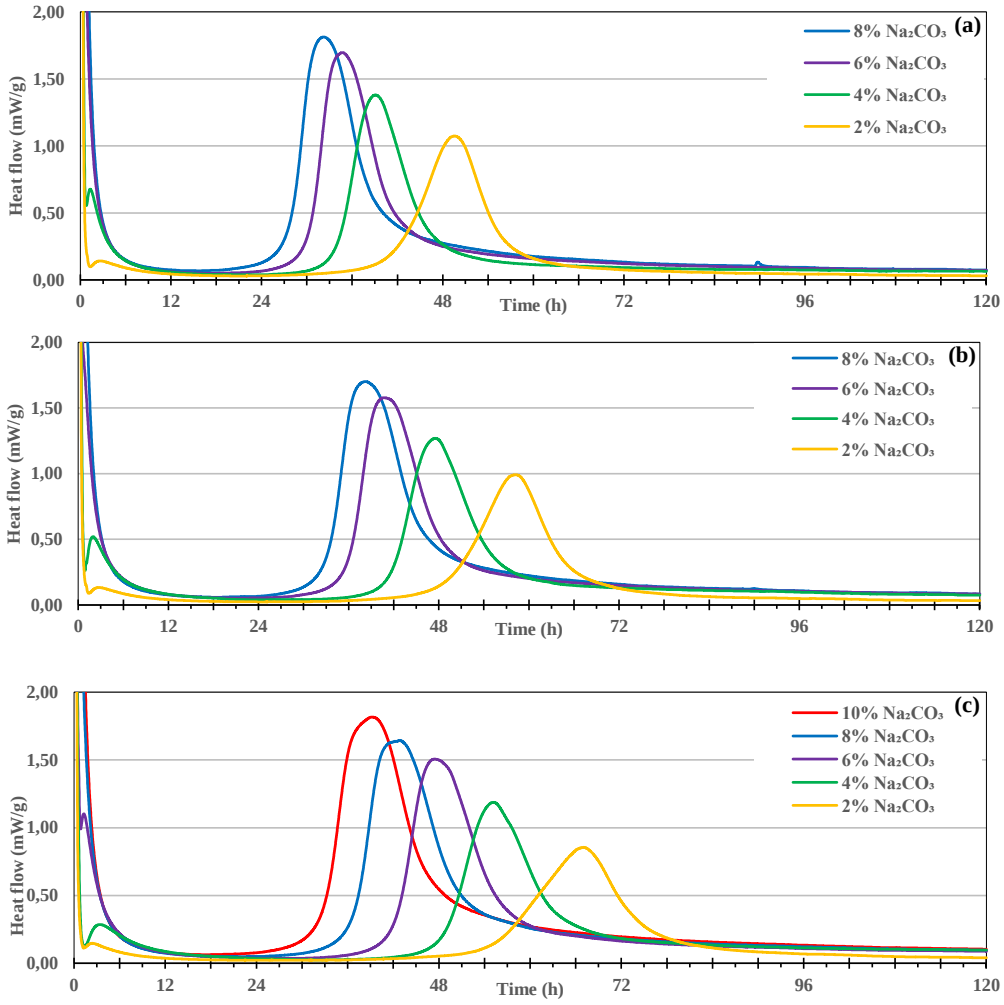

Figure 2.43: Heat evolutions of GGBS 5600 cm²/g with different Na_2CO_3 dosage at W/B ratio of 0.35 (a); 0.40 (b) and 0.45 (c).

Table 6: Summery of heat evolution of Fine GGBS at different W/B ratios and Na_2CO_3 amounts

Water/ GGBS	% Na_2CO_3 of GGBS mass	Concentration of Na_2CO_3	First peak (FP)	Main hydration peak (MHP)	Peak high
	%	g/l	h	h	mW/g
0.35	2	57	3	50	1.06
	4	114	0.5	39	1.37
	6	171	N.D.	35	1.68
	8	229	N.D.	32	1.81
0.40	2	50	3.5	59	0.98
	4	100	2	47	1.25
	6	150	N.D.	41.5	1.57
	8	200	N.D.	38.5	1.70
	10	250	-	-	-
0.45	2	44	3	68	0.85
	4	89	4	56	1.18
	6	133	0.5	48	1.51
	8	178	N.D.	43	1.64
	10	222	N.D.	40	1.81

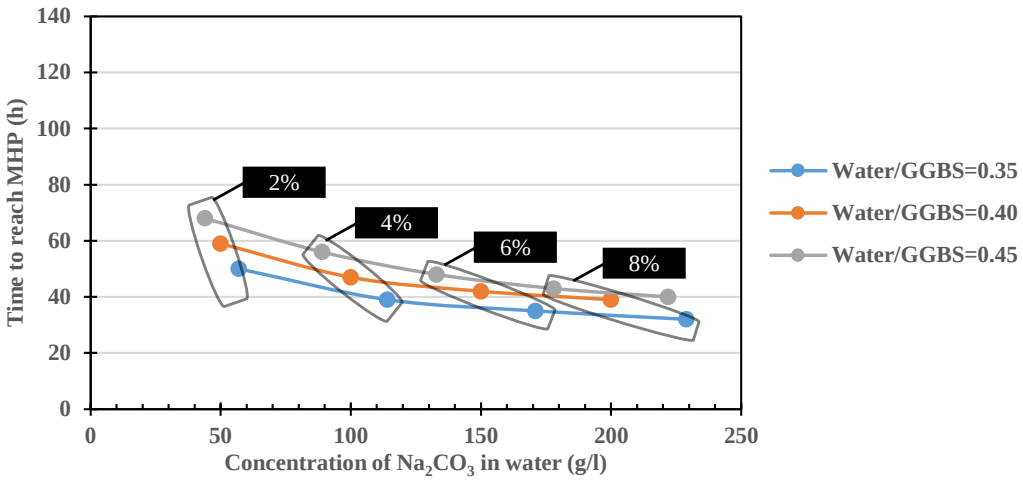

Figure 2.44: Time to reach the main hydration peak (MHP) for GGBS 5600 cm²/g as a function of Na_2CO_3 concentration in water

The cumulative heat released curves are presented in Figure 2.45. The final values at 120h of hydration are presented in Figure 2.46. The total heat released is higher compared to that of Standard GGBS (Figure 2.41) in all cases. In addition, the effect of the aqueous concentration of the activator is lower.

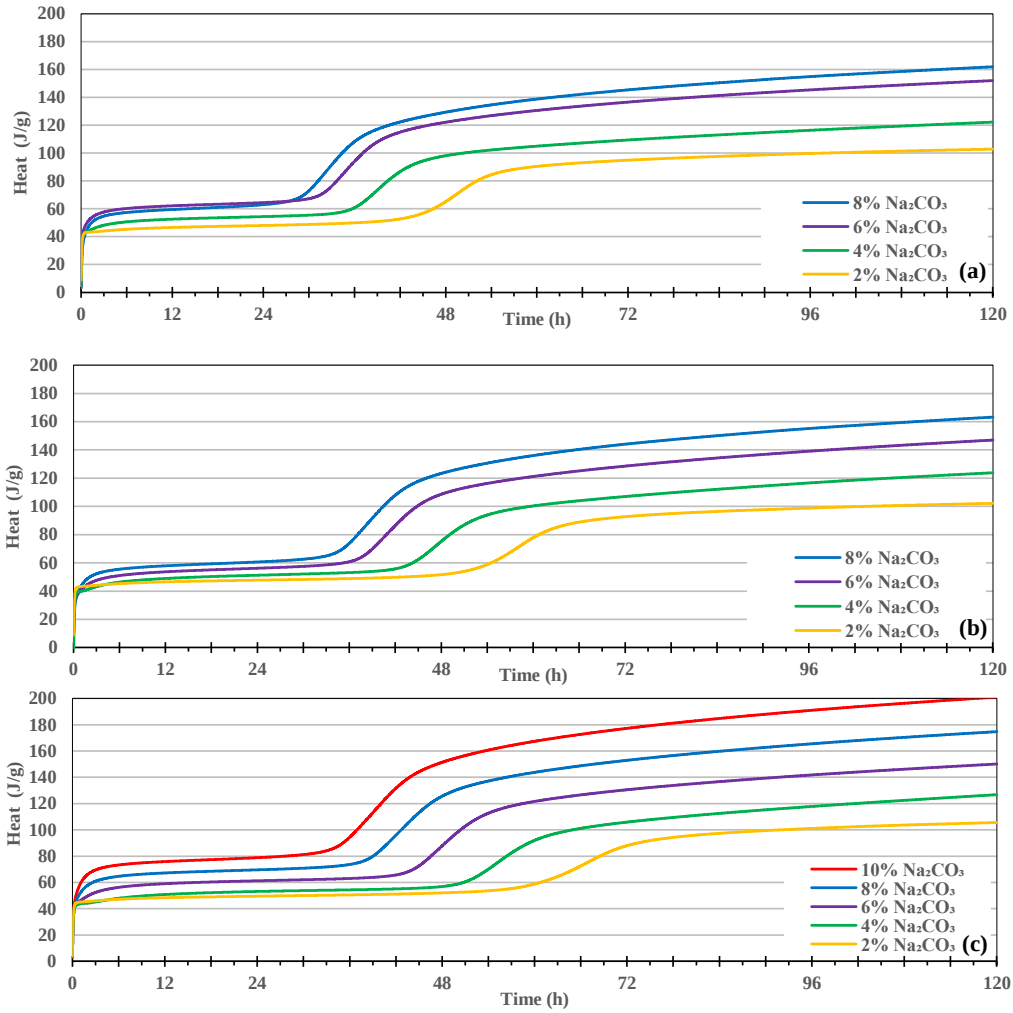

Figure 2.45: Heat released after hydration of GGBS 5600 cm^2/g with different quantity of Na_2CO_3 at Water/GGBS ratio: 0.35 (a); 0.40 (b) and 0.45 (c).

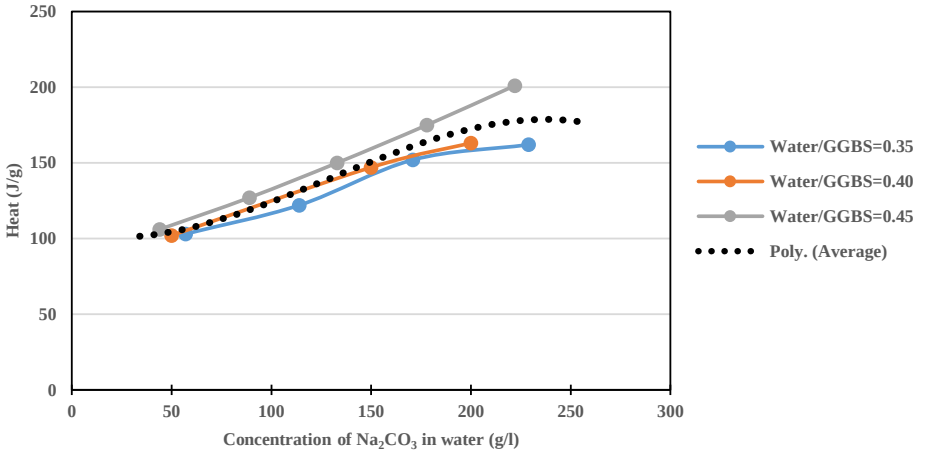

Figure 2.46: Heat released after 120h of hydration process of GGBS 5600 cm²/g as a function of initial sodium concentration in water.

Case of Ultrafine GGBS

The released heat flow curves for 5% and 10% of Standard GGBS replacement by Ultrafine are presented in Figure 2.47 and Figure 2.48 respectively. Such replacement leads to a noticeable decrease of the induction period and an acceleration of the main hydration peak. In addition, the binder with Ultrafine GGBS can be characterized by a lower sensitivity to the hydration kinetics and to the activator concentration. Increasing the substitution level leads to an increase this effect.

With a 10% replacement of Standard with Ultrafine GGBS, the hydration kinetics are even faster than in the case Fine GGBS.

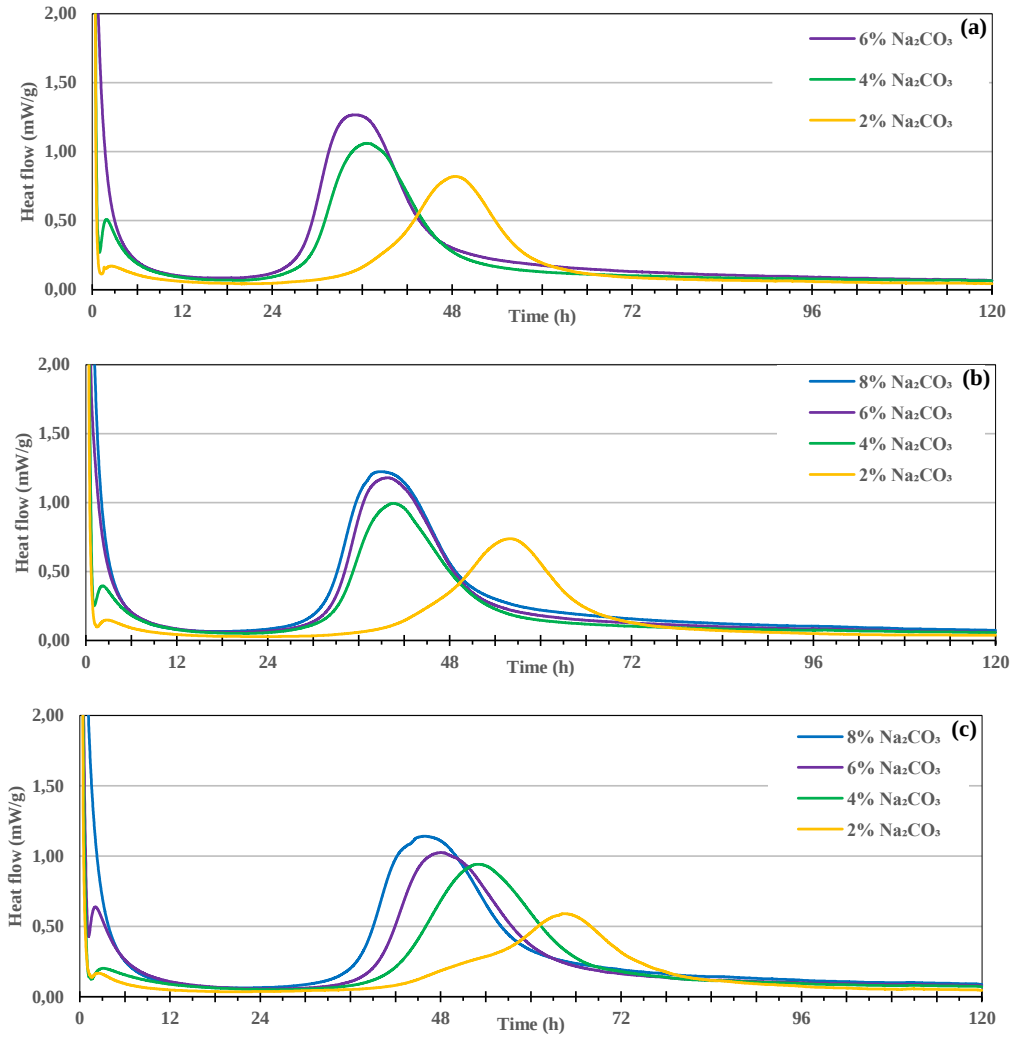

Figure 2.47: Heat evolution of GGBS pastes with 5% replacement of Standard by Ultrafine GGBS with different Na_2CO_3 amounts at W/B ratios of: 0.35 (a); 0.40 (b) and 0.45 (c).

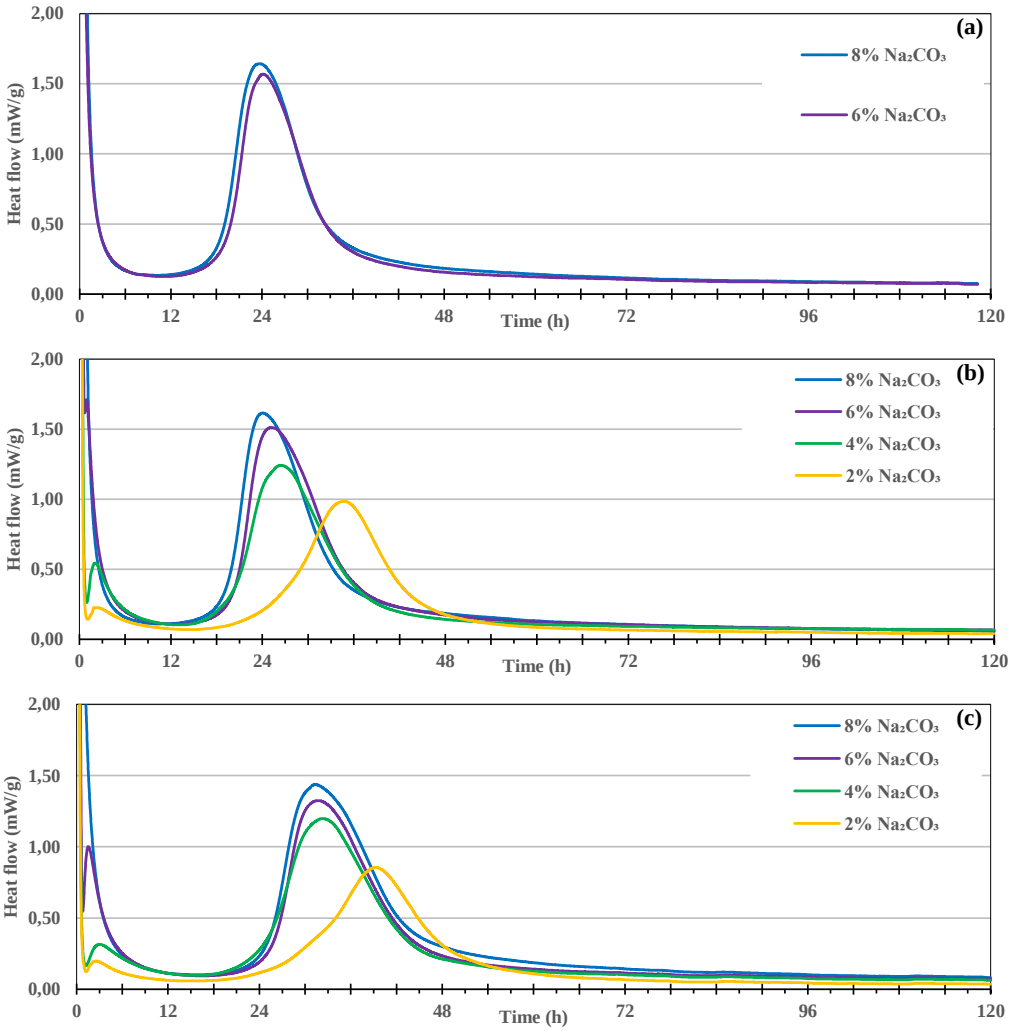

Figure 2.48: Heat evolutions of GGBS with 10% replacement of Standard by Ultrafine GGBS with different Na_2CO_3 dosages at W/B ratios of 0.35 (a); 0.40 (b) and 0.45 (c).

In examining the time to reach the main hydration peak as a function of the aqueous activator concentration (Figure 2.49 and Figure 2.50), the following observations can be made:

- As for the other GGBS grades, the critical influence of the W/B ratio can be observed. Decreasing the water content leads to a significant acceleration of hydration. Yet when increasing the substitution level of Ultrafine GGBS, the water sensitivity decreases. In the case of 10% replacement, almost no difference between a W/B ratio of 0.35 and 0.40 could be observed, and a much lower difference between 0.40 and 0.45 compared to 100% Standard GGBS.
- Similar observations can be made regarding the sensitivity to the activator dosage. For example, in the case of 10% replacement, there is almost no difference between 100 and 200 g/l of Na_2CO_3 for the same W/B ratio.
- The two results above reflect some type of self-activation of the Ultrafine GGBS.

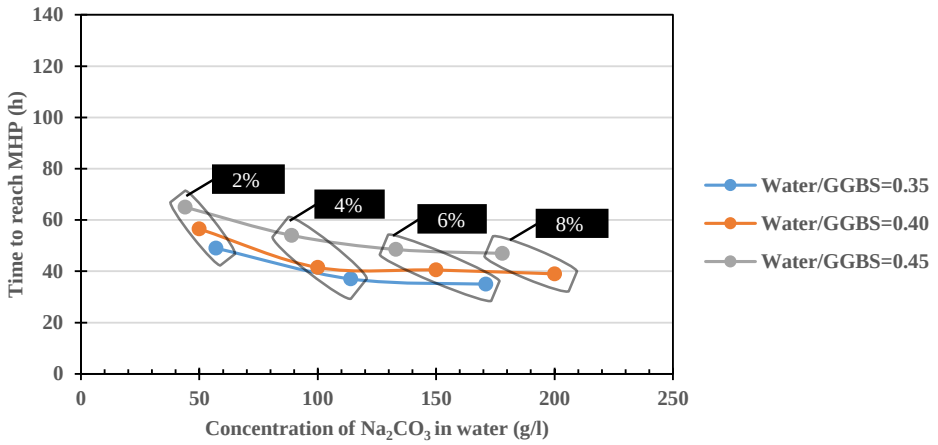

Figure 2.49: Time to reach the main hydration peak (MHP) for GGBS with 5% replacement by Ultrafine GGBS by mass as a function of Na_2CO_3 concentration in water.

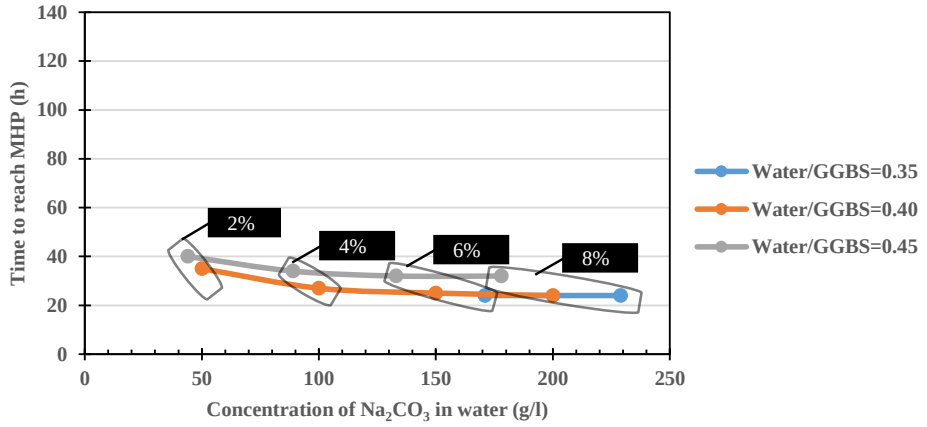

Figure 2.50: Time to reach the main hydration peak (MHP) for GGBS with 10% replacement by Ultrafine GGBS by mass as a function of Na_2CO_3 concentration

The cumulative heat released after 120h of hydration as a function aqueous activator concentration for the two Ultrafine substitution levels is presented in Figure 2.51 and Figure 2.52. Even at a 5% partial replacement of Standard with Ultrafine GGBS, a similar total heat released over the range of activator dosage considered. At higher replacement levels (10%), the released heat becomes less sensitive to the activator dosage. As stated above, the Ultrafine seems to play the role of an activator for Standard GGBS.

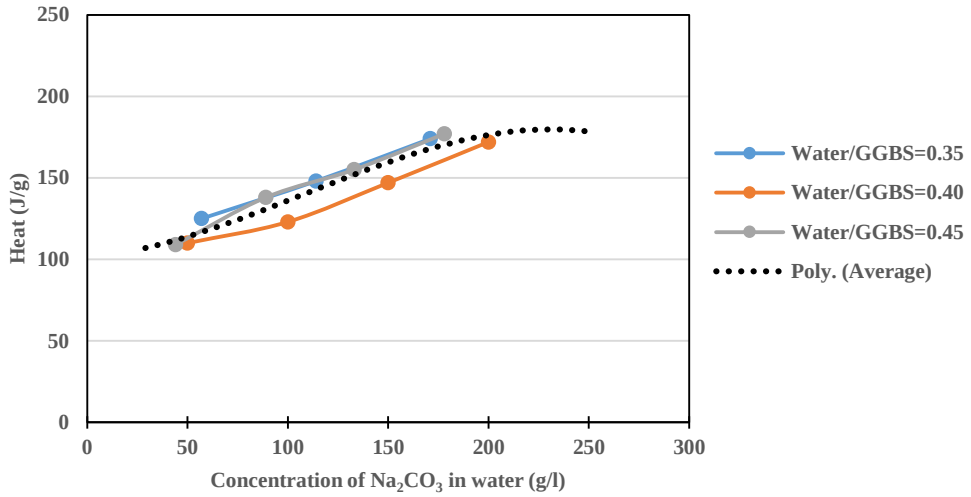

Figure 2.51: Cumulative heat released after 120h of hydration of GGBS with 5% replacement by Ultrafine GGBS as a function of initial sodium concentration in water.

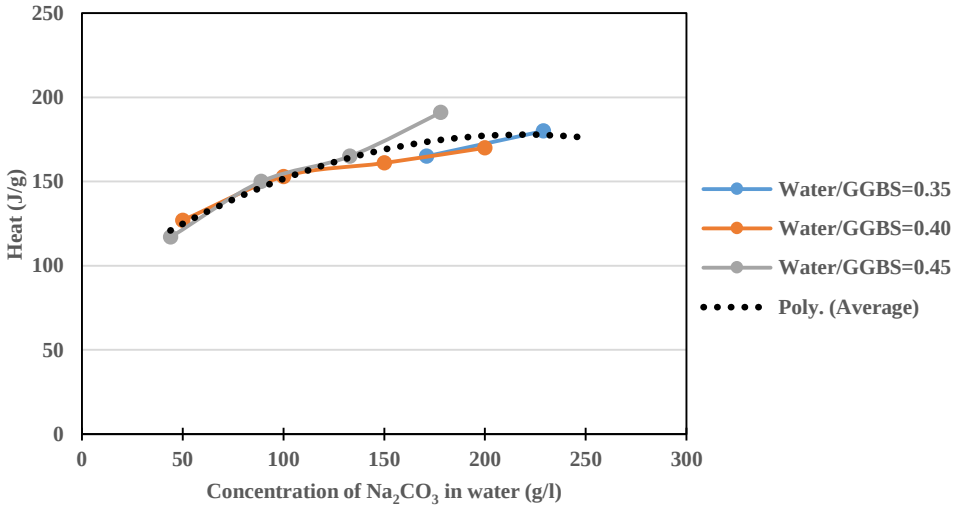

Figure 2.52: Cumulative heat released after 120h of hydration of GGBS with 10% replacement by Ultrafine GGBS as a function of initial sodium concentration in water.

2.4.4 Summarizing the micro-calorimetry results

The results related to the hydration kinetics are summarised in Table 7. Representing the time taken to reach the main hydration peak (MHP) as a function of sodium carbonate concentration (Figure 2.53) allows for the highlighting of the positive effect of increasing the slag fineness. This effect can also be seen through the total released heat after 120h of hydration (Figure 2.54). A particularly positive effect of fineness for low activator concentration can be observed. It can be observed that the results of 100% Fine GGBS and 95% Standard with 5% Ultrafine GGBS replacement are similar. This can be attributed to the value of the specific surface that might be on the same order for the two powders. Yet one cannot be sure that the difference in reactivity is related only to the difference in specific surface.

Table 7: Summery of hydration kinetics of GGBS 4400 cm2/g, GGBS 5600 cm2/g and Ultrafine GGBS at different W/B ratio and sodium carbonate concentration

			GGBS 4400 cm^2/g		GGBS 5600 cm^2/g		95% GGBS 4400 + 5% Ultrafine		95% GGBS 4400 + 10% Ultrafine	
W/B	% Na_2CO_3 of GGBS mass	Concentration of Na_2CO_3 in mixing water	Main hydration peak (MHP)	Peak height	Main hydration peak (MHP)	Peak high	Main hydration peak (MHP)	Peak height	Main hydration peak (MHP)	Peak height
	%	g/l	h	mW/g	h	mW/g	h	mW/g	h	mW/g
0.35	2	57	72/86	0.28/ 0.52	50	1.06	49	0.82	-	-
	4	114	58	0.90	39	1.37	37	1.06	-	-
	6	171	50	1.00	35	1.68	35	1.27	24	1.57
	8	229	43	1.39	32	1.81	-	-	24	1.64
0.40	2	50	88/104	0.28/ 0.37	59	0.98	56.5	0.78	34.5	0.98
	4	100	71	0.82	-	-	41.5	0.99	27	1.24
	6	150	57	0.95	41.5	1.57	40.5	1.17	25	1.51
	8	200	51	1.26	38.5	1.70	39	1.22	24	1.61
	10	250	51	1.11	-	-	-	-	-	-
0.45	2	44	125	0.43	68	0.85	52/65	0.25/ 0.58	40	0.85
	4	89	83	0.74	56	1.18	54	0.94	33.5	1.18
	6	133	68	0.89	48	1.51	48.5	1.02	32	1.32
	8	178	59.5	0.94	43	1.64	47	1.13	32	1.43
	10	222	57	1.06	40	1.81	-	-	-	-

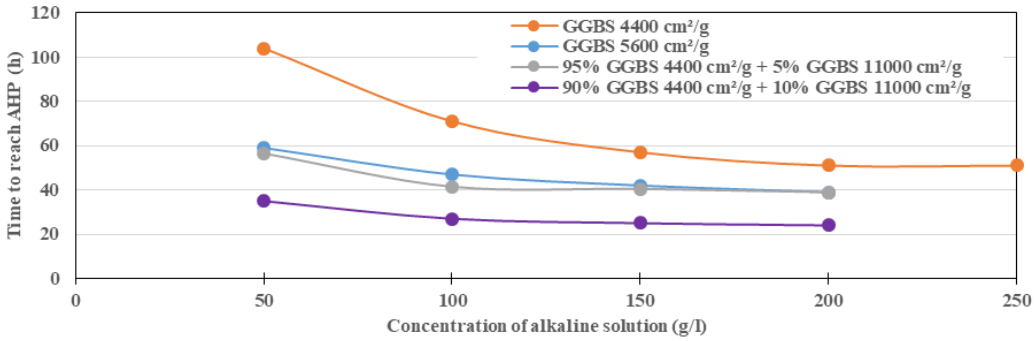

Figure 2.53: Time to rich the main hydration peak for different GGBS fineness at constant Water/GGBS ratio of 0.40 as a function of sodium carbonate concentration

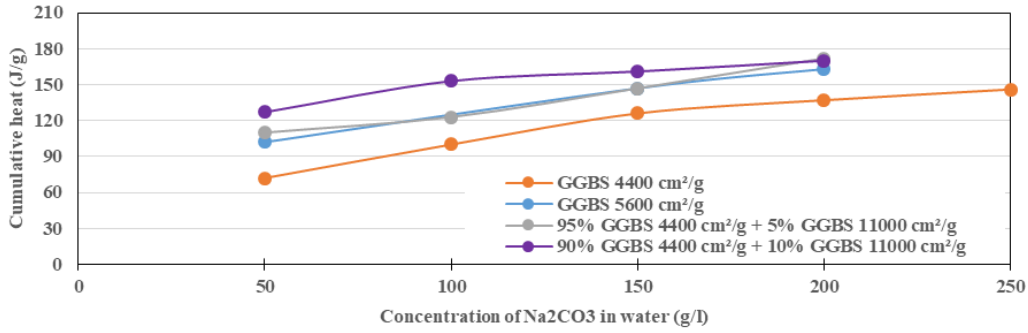

Figure 2.54: Cumulative heat released after 120h of hydration as a function of aqueous sodium carbonate concentration for different GGBS fineness at the same Water/GGBS ratio of 0.40

Concluding remarks regarding hydration kinetics

- As one can expect, increasing the sodium carbonate dosage leads to a decrease of the induction period and the appearance of the strength-giving hydration peak. Yet this effect is not monotonic. There is a minimum activator dosage above which the hydration kinetics become less dependent upon this parameter. The value of this minimum dosage decreases with increasing slag fineness.
- Decreasing the W/B ratio leads also to an acceleration of the appearance of the main hydration peak. In addition, the impact of this parameter seems to be more important. Decreasing the water content leads to a shorter induction period at any fineness and Na_2CO_3 content. Nevertheless, increasing the slag fineness and activator concentration (increasing the hydration rate/reactivity of the system) leads to a decrease of its importance.
- Decreasing the curing temperature leads to an increase of the induction period, in a very critical way even for high concentrations of activator and a low Water/GGBS ratio. This can be due to an eventual crystallization of the sodium carbonate and subsequently the decrease of the alkaline concentration. Other usual reasons may be invoked, such as a slower rate of dissolution/precipitation, transformation of low-temperature metastable phases, etc.
- Another important parameter is the slag fineness. Its increase significantly reduces the induction period. In addition, the system becomes less sensitive to sodium carbonate dosage and W/B ratio. This is especially noticeable with a high W/B ratio (0.45). In other words, the system becomes more robust. The most positive results were obtained with the partial replacement of conventional GGBS by 10% of Ultrafine GGBS. However even in case 100% GGBS 5600cm^2/g or 5% Ultrafine replacement of standard GGBS, the improvement is noticeable.

2.5 Compressive strength evolution

To determine the compressive strength, prismatic standard mortar samples with dimensions of *40x40x160 mm* were prepared following the procedure below:

- Weighing all the required components
- Mixing of the dry components of the binder for XX minutes (450 g in total, if not otherwise indicated)
- Addition of the normalized sand (1350 g) and further mixing for 1 min
- Addition of water at the required Water/Binder ratio (including all the components that are added in solution form as Na_2CO_3 or retarder)
- 1 min of mixing at low speed followed by 30 s at high speed (NF EN 196-1, 2016)
- 30 s pause for cleaning tank walls and hand mixing
- Mixing during 30 s at low speed, then 30 s at a high speed

The different steps of the preparation procedure are presented in Figure 2.55.

Figure 2.55: Procedure of the mortar preparation

Stainless steel moulds conforming to the standard (NF EN 196-1, 2016) were used. An inert lubricating oil was used for easy demoulding of samples. The moulds were filled on a vibrating table at a frequency of 55Hz (Figure 2.56).

Figure 2.56: Filling procedure of the prismatic moulds

After preparation, the moulds were wrapped with a plastic film to prevent any water evaporation and then cured under specific temperature conditions (Figure 2.57).

Figure 2.57: Storage of the samples before demoulding

Between 23 and 24 hours (47/48h for some cases), the samples were demoulded for further storage in closed plastic bags under different temperature conditions (Figure 2.58). Storage in closed bags permitted avoiding drying (due to a high relative humidity (RH>95%)) and carbonation. In all cases, the curing humidity is indicated and achieved by storage in climatic chamber. By default, the standard storage temperature in the present work is 22°±1°C. In some cases curing was performed at 15°C or under heat treatment.

Figure 2.58: Further storage of the samples in plastic bags after demoulding

The mechanical tests (mainly compressive strength) were performed using an appropriate press with a load area of 40*x*40 mm (Figure 2.59). The load was applied at a constant speed of about 2.2 kN/s until complete sample failure, according to NF EN 196-1. Two specimens were tested for each curing age.

Figure 2.59: Hydraulic press used for compressive tests (a) and the sample after breakage (b)

In Figure 2.60, the results of the compressive strength development are presented for standard GGBS with different activator dosage rates. The strength results are correlated with those of micro-calorimetry: increasing the Na_2CO_3 dosage leads to an increase in strength at all

terms. The impact of the activator dosage is particularly significant at early age. Increasing the dosage from 8 to 10% leads to a twofold increase in strength at two days (20MPa vs. 10MPa).

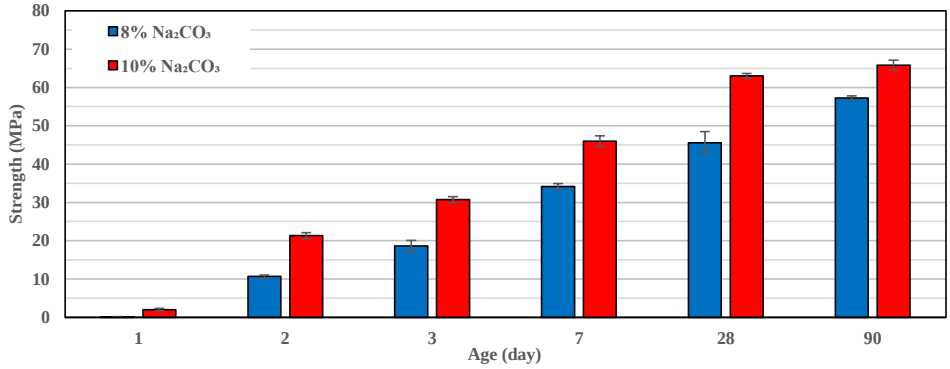

Figure 2.60: Influence of Na_2CO_3 amount on compressive strength development of mortars based on 100% GGBS 4400 cm^2/g at W/B=0.40

The influence of the W/B ratio on strength development is illustrated in Figure 2.61. Similar to activator dosage, the strength is highly sensitive to W/B, in particular at early age. Decreasing the amount of mixing water may lead to early strength development through two mechanisms: (i) increase of the aqueous concentration of the sodium carbonate, and (ii) the critical concentration of the ionic species for the precipitation of hydration products can be reached faster. In addition, similar to other cementitious materials, decreasing the W/B will lead to faster percolation of the hydration products (lower inter-grains distance) leading to faster development of strength, and eventually lower porosity implying improvement of strength. The only drawback that can be expected when decreasing the W/B is an eventual degradation of the rheology. This may lead to the formation of large defects during mould filling and then the degradation of strength. It is interesting to note that the increase in strength over time of products based on Na_2CO_3 activated binder seem to be boundless (up to 1 year here).

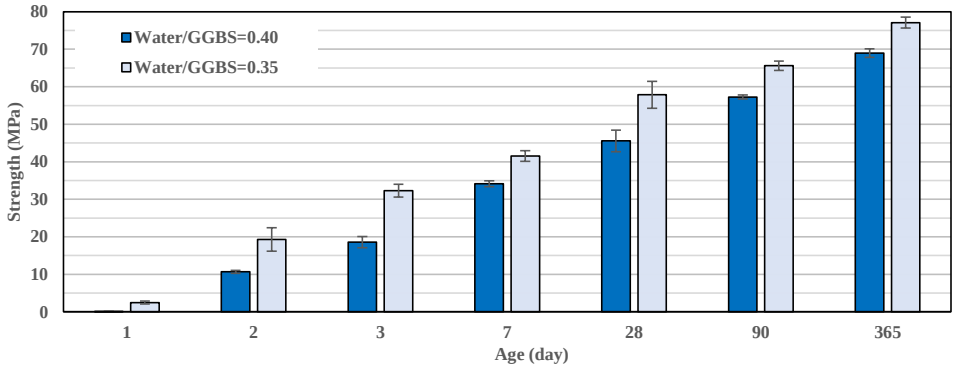

Figure 2.61: Influence of W/B ratio (0.40 and 0.35) on compressive strength development for Standard GGBS with 8% of Na_2CO_3

By comparing Figure 2.60 and Figure 2.61, the same strength results are obtained with 10% of Na_2CO_3 at W/B=0.40 (250 g/l) and 8%Na_2CO_3 at W/B=0.35 (230 g/l). Reducing the amount of sodium carbonate by decreasing the W/B allows for keeping high aqueous activator

concentration and appropriate compressive strength development. This will lead to positive consequences for durability (by minimizing Na content) and economical aspects.

Although in terms of strength these results are quite promising for industrial applications, it should be noted that the rheology of these mortars were quite poor (low slump, short open time). This correlates with the results obtained from the rheology of the binder paste. To fill the moulds, it was necessary to spend considerable time on vibration to reach the appropriate fresh density (2300-2350 kg/m^3). It was also necessary to prepare the samples immediately as these mortars quickly lose their plasticity, which could lead to microstructure heterogeneity and degradation of strength if too much time elapsed before placement. The strength development for finer GGBS grades was not considered for those reasons. An increase of the W/B ratio could allow enough open time and improve the mould-filling ability of the product. Yet this would negatively affect the early age strength. It is well-known that playing with the W/B is not the best method to improve the rheology of concrete and other cement-based products. One of the main objectives of this study is to improve the rheology of Na_2CO_3 products through an appropriate chemical admixture. This is discussed in the forthcoming chapters.

2.6 *In-situ* Synchrotron X-ray diffraction

The crystalline hydrates precipitation from the first seconds up to 24 hours of hydration was followed in *real time* using a Synchrotron XRD (Beamline SWING, SOLEIL Synchrotron, France). The advantage of Synchrotron radiation is its high brilliance (high photon flux) and coherence (well-defined wavelength). In this way, high temporal and angular resolution scans can be obtained. Two types of experiments were performed.

The first series of experiments consisted of recording the XRD pattern scans from the very first seconds of hydration (from the moment the solid particles made contact with the added solution). A special set-up was used to remotely inject a given aqueous solution into a cell with a Kapton film (transparent to X-ray) containing the dry binder powder (Figure 2.62 and Figure 2.63). The total duration of measurements was approximately 16 minutes. The average intensity over 10 scans per second was used for the determination of the XRD pattern evolution over time. In the present work, for clarity reasons, only 16 scans are presented (an average of one scan every 1 min). The results in terms of diffraction angle were converted using the Bragg law to 2θ scans (wavelength of 1.789 Å, Co Kα radiation) for comparison with laboratory measurements.

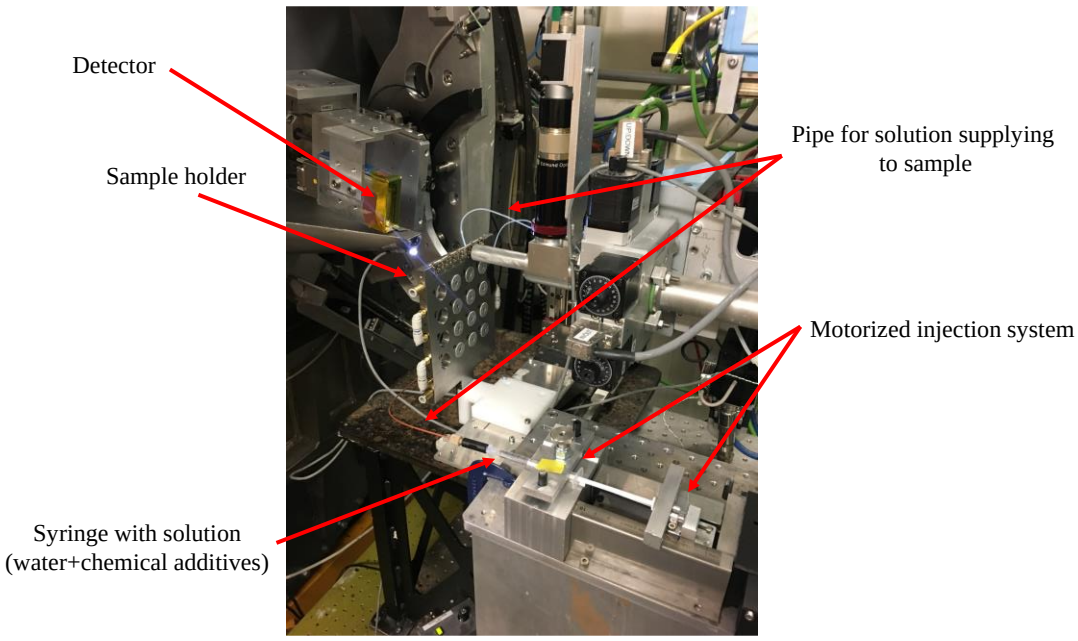

Figure 2.62: General view of the experimental set-up for in-situ Synchrotron XRD scanning starting immediately after powder/solution contact

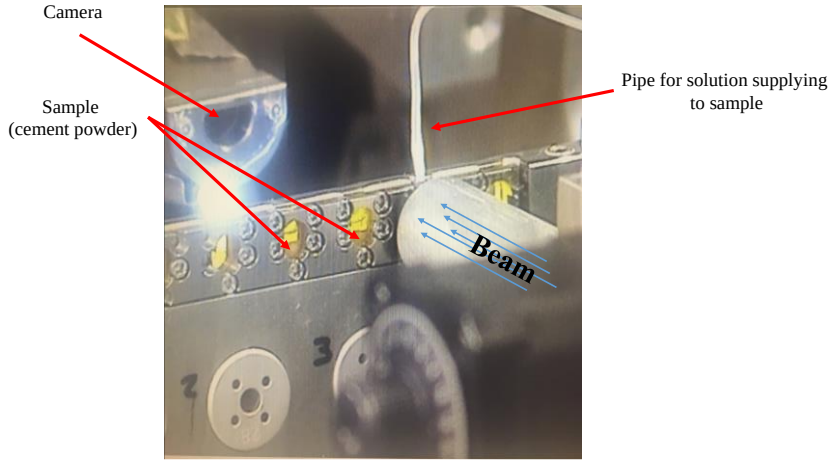

Figure 2.63: View from the external camera during the in-situ X-ray diffraction scanning test from the moment when binder powder and solution come into contact.

The weakness of this set-up is that it was not possible to stir in order to homogenize the powder-solution mix. Thanks to a camera the X-ray beam could be displaced and placed within the liquid/powder contact zone (Figure2.64). Hence the local W/B ratio is not controlled and should be higher than that in the previous tests. Due to this higher water content, the solid particles could easily move against each other. It led to constant changes in the scanned area leading to fluctuations in the intensity of the XRD peaks. For example some peaks could appear and disappear during scanning. Nevertheless, from these experiments some precious qualitative observations about the hydration process from the very first seconds could be obtained, which is not possible with a standard laboratory X-ray diffractometer.

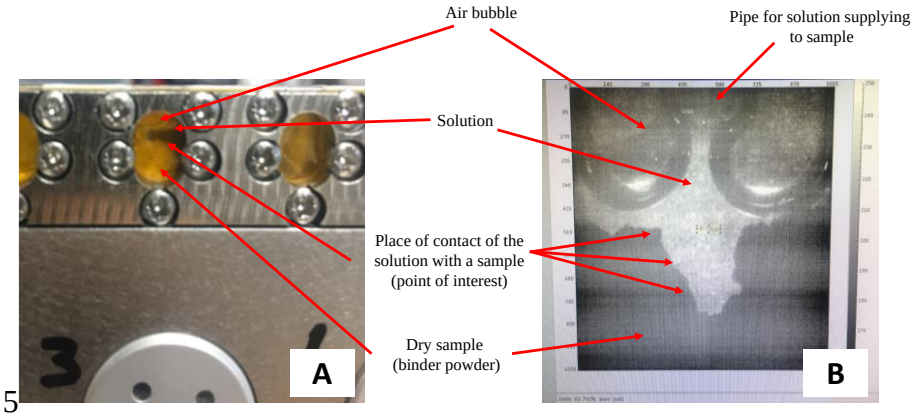

Figure2.64: Setup for in-situ X-ray diffraction scanning from the moment of binder powder and solution contact. View of the set-up after measurements (a) and from camera during scanning (b)

A second type of experiment was performed to consider the hydration process over a few hours. Freshly prepared binder samples were inserted into cylindrical cells covered with Kapton films (Figure 2.65). The set up included a holder containing 12 cells. An average of 10 scans every 1h was used to follow *in-situ* the development of the crystalline phases up to 24 hours.

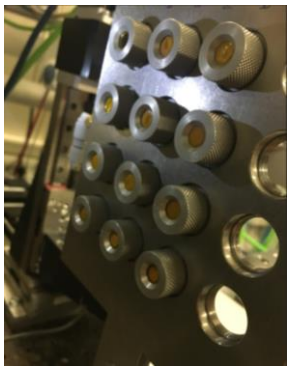

Figure 2.65: Holder for in-situ X-ray diffraction of the paste samples during the first 24h of hydration

2.6.1 Hydration products in case of high Na_2CO_3 concentration

Figure 2.66 presents the *in-situ* XRD scans of a standard GGBS paste in plain water or with Na_2CO_3 at a concentration of 200g/l. In the absence of the activator there are no detectable crystalline hydrates within the first 16 minutes after contact with water. Nevertheless, it doesn't mean that any amorphous phases or extremely low amount of low crystalline phases were not formed. In the presence of Na_2CO_3 crystalline hydration products appear from the first minute following contact with water. The main hydration products at very early are Gaylussite, Calcite and hydroxyl-Afm phases such as C_2AH_6 and C_2AH_8. Some Ca-Monocarboaluminate can be also detected after a few minutes. The peaks are quite large compared to the case in which the hydration process is more advanced (see further). This may reflect a poor degree of crystallisation of the phases. In agreement with most observations reported in the literature (Abdalqader et al., 2016; Bernal et al., 2015), the main hydration product that precipitates within

the first minutes is Gaylussite. Calcium is expected to be the first element (beside other minor alkalies and sulfur) to be leached from the slag. Ca^{2+} should combine with dissolved CO_3^{2-} and Na^+ from the sodium carbonate solution to precipitate this phase. At a high ratio of Na^+ over Ca^{2+} available in solution, Gaylussite is favoured over calcium carbonate polymorphs (Bury and Redd, 1933). Depending on the relative availability of Na^+, Ca^{2+}, which depends on the Na_2CO_3 concentration and temperature through its solubility, different Na/Ca salts may form (Figure 2.67). In this case the availability of Ca^{2+} depends on the solubility of the slag.

Formation of the hydroxyl-Afm phases and Ca-Carboaluminate indicates that Al is released almost as early as Ca. On the other hand the absence of Hydrotalcite indicates that the concentration of released Mg remains low over this early period of hydration.

The phase diagram in (Figure 2.67) may qualitatively explain the origin of the existence of a minimum value of the activator concentration (150 g/l) for appropriate hydration (through calorimetry). This might be related to the fact that Calcite precipitation is favoured over Gaylussite beyond this minimum value. Precipitation of this transient phase seems to be necessary in order to promote appropriate hydration of the slag. This will be discussed throughout this document.

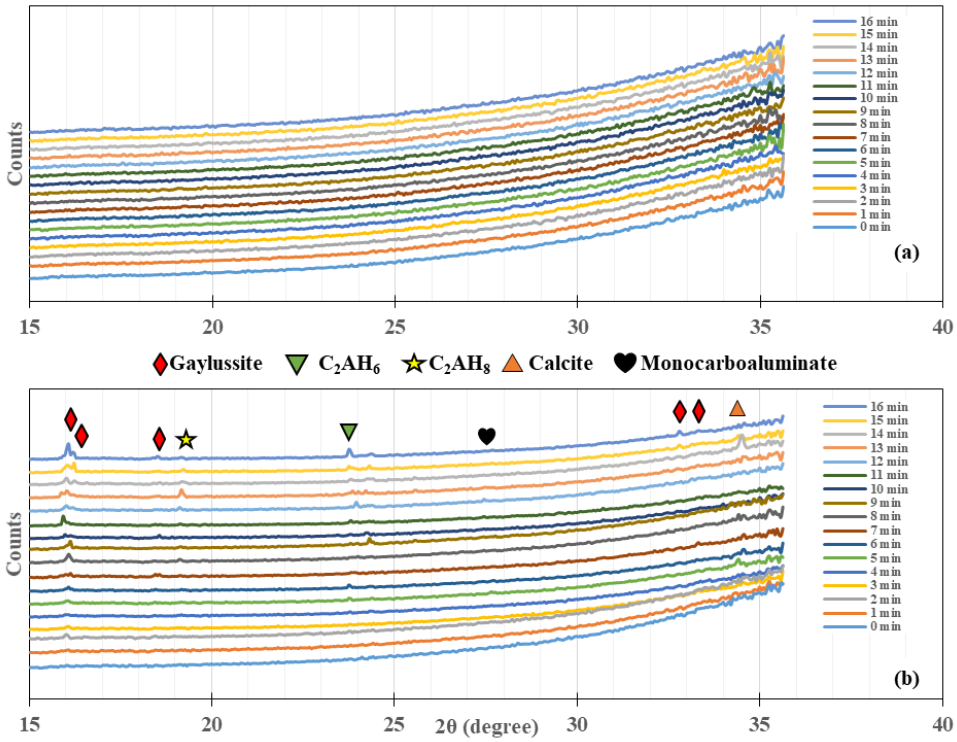

Figure 2.66: In-situ XRD patterns using a synchrotron radiation of GGBS hydration for the first 16 minutes after contact with pure water (a) or 200g/l of Na_2CO_3 solution (b)

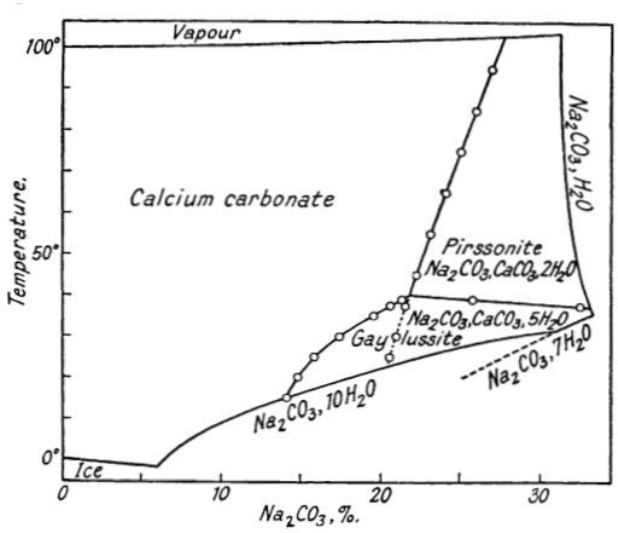

Figure 2.67: Diagram of phase stability in a system $CaCO_3$-Na_2CO_3-H_2O as a function of Na_2CO_3 concentration and temperature (Bury and Redd, 1933)

XRD scans corresponding to subsequent phase development from 1h to 1 day are reported in Figure 2.68. Over this period of hydration, the main crystalline phase remains Gaylussite. At the beginning the Gaylussite peaks are quite large, indicating a low crystallisation degree (small crystals and/or with structural defaults). Over time, these peaks become more and more well defined, indicating an increase in the degree of crystallisation and/or amount. Small amounts of Hydrotalcite can be detected beyond 1h without any significant increase up to 24 h. Massive consumption of Na by Gaylussite precipitation should avoid any eventual formation of NaOH that should trigger high dissolution rate of the slag. This may be reminiscent of the long induction period of Na_2CO_3 activated slag binder.

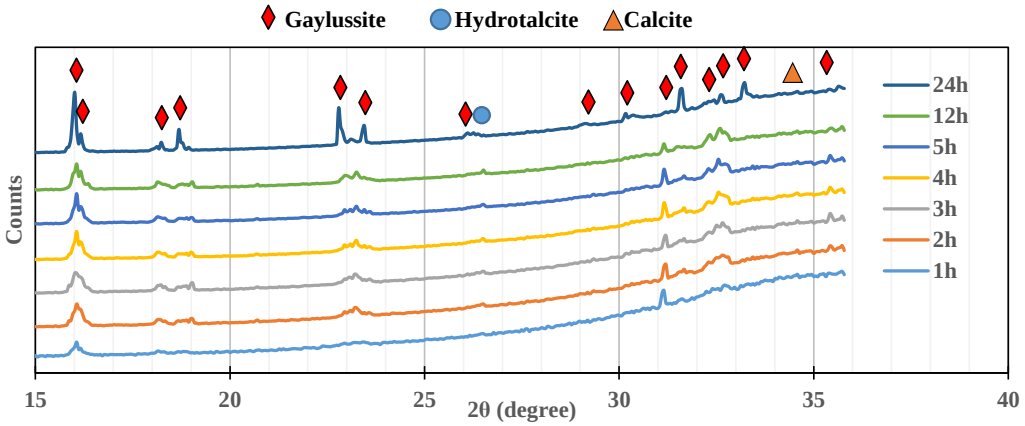

Figure 2.68: Synchrotron in-situ XRD patterns. GGBS activated with 200g/l of Na_2CO_3 for the first 24h

2.6.2 Hydration products in case of low Na_2CO_3 concentration

Based on the phase diagram of (Bury and Redd, 1933) Gaylussite should not form at low Na_2CO_3 aqueous concentration. To verify this, samples of slag pastes activated with Na_2CO_3 at 50 g/l were considered. In this case no Gaylussite can be observed for the first 24 hours of hydration (Figure 2.69). At the same time a very large peak at around 34.3° may indicate the precipitation of poorly-crystallised Calcite. The absence of Gaylussite, or any other Ca-Na carbonate phases, suggests that in this case NaOH should be readily formed upon dissolution of the activator. In this case the situation is similar to NaOH activation. A rise of pH caused by the in-situ formation of NaOH leads to an immediate attack of the slag surface, leading to early leaching of Si/Al. Indeed a small peak in the region of 2Theta=24.0°-24.4° appears and can be attributed to a very low crystallised Stratlingite (yet additional tests are required to confirm this hypothesis). Formation of Stratlingite is indeed observed in the case of NaOH activation from the first hours of hydration (Wang and Scrivener, 1995; Haha et al., 2012). In the absence of any seeding, the formation of these two poorly crystallised phases should take place on the slag surface leading to the hindering of dissolution and then a long induction period.

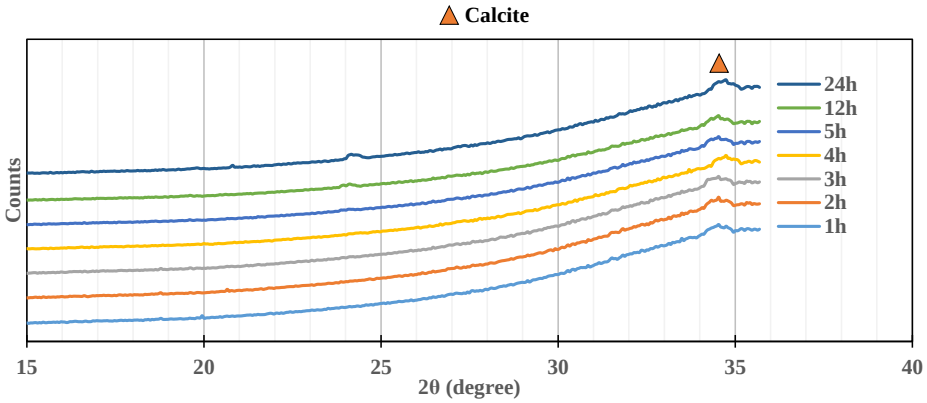

Figure 2.69: Synchrotron in-situ X-ray patterns evolution of GGBS activated with 50g/l Na_2CO_3

2.7 *Ex-situ* Laboratory X-ray diffraction

Ex-situ XRD was carried out on powder paste samples using a Bruker D2-phaser wide-angle diffractometer with Co Kα radiation (1.78897 Å). The same sample preparation procedure as for the above rheological measurements was used. The samples were stored in closed plastic test tubes to avoid drying or carbonation (Figure 2.70). At different ages, a sample was extracted from the tube, ground in a hand mill and sieved with a 100µm sieve. The hydration was stopped by the solvent exchange method. After the sample were centrifuged and dried at 35°C in a

conventional stove. The XRD scans were performed over 2θ angle range between 5° and 60° with a step of 0.02° with 10 rpm sample rotation.

Figure 2.70: Paste samples for ex-situ Laboratory XRD analysis

In order to compare with the Synchrotron *in-situ* XRD analysis, the Laboratory XRD was performed over the first 24h of hydration. The XRD patterns for a GGBS activated with 8% Na_2CO_3 (or 200g/l) in the case of W/B=0.40 are reported in Figure 2.71. The results for the two measurement methods are similar. Yet, with the ex-situ method the presence of some amount of hydrated sodium carbonate as a result of sample drying can be detected. Nevertheless, the amount of the recrystallized Na_2CO_3 decreases with time of curing, and this is correlated with the increase of Gaylussite content.

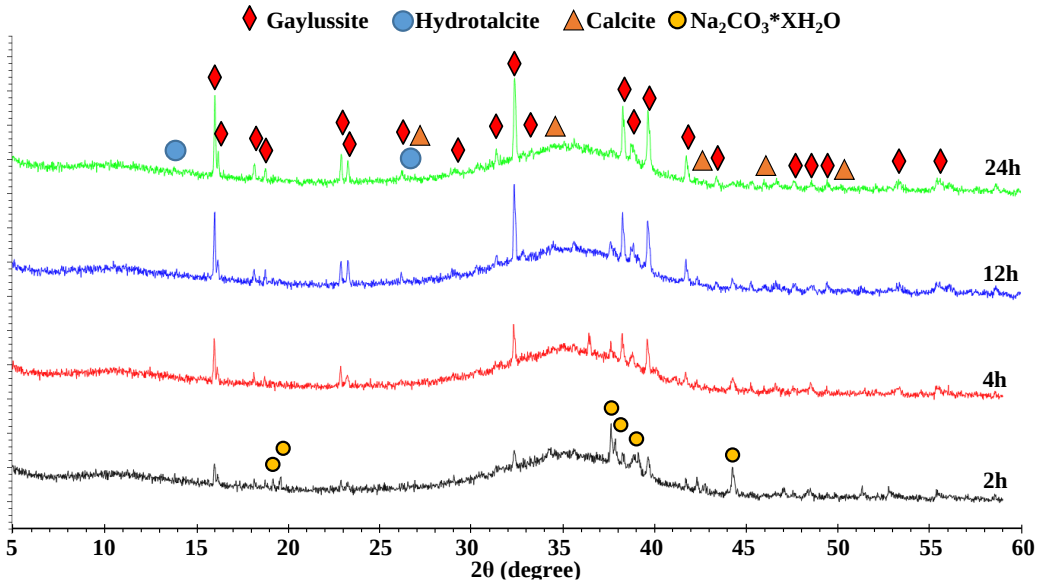

Figure 2.71: XRD patterns evolution of GGBS with 8% Na_2CO_3 at W/B=0.40 during the first 24h

Decreasing the water content (W/B=0.35) and keeping the same amount of sodium carbonate by weight leads to an acceleration of the development of hydration products (Figure 2.72). In particular more Gaylussite can be observed after the first 4 hours. It might be related to both an increase in the sodium carbonate concentration (from 200 to 230g/l) and faster saturation of solution by leached Ca^{2+} ions caused by water reduction. After 24 hours of hydration no significant difference can be observed for both W/B ratios.

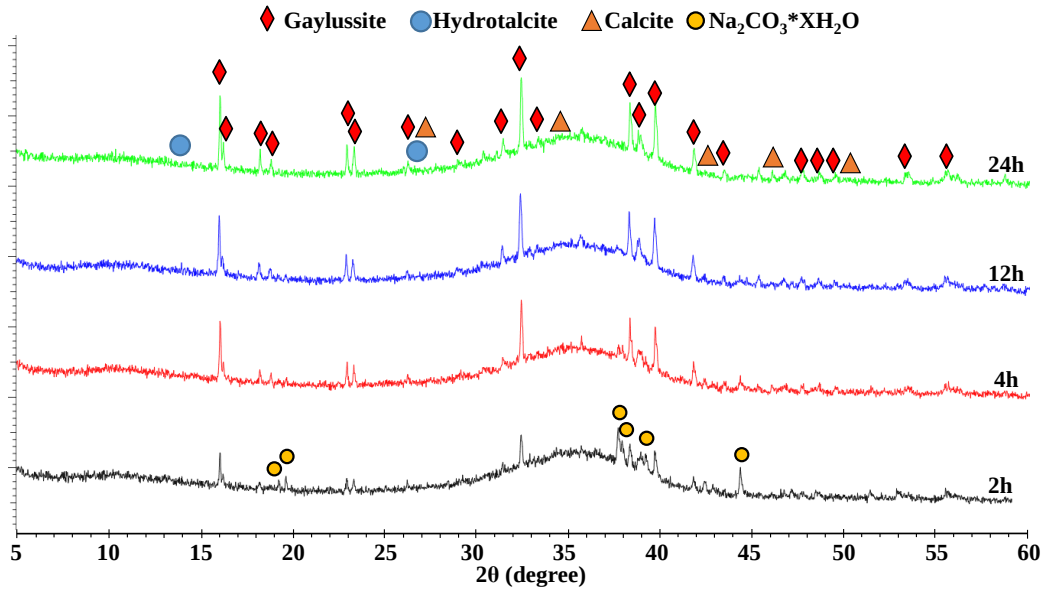

Figure 2.72: XRD patterns evolution of GGBS paste with 8% Na_2CO_3 at W/B=0.35 during the first 24h

Long term, up to 3 months, XRD analysis shows qualitatively similar results for both W/B ratios of 0.35 (Figure 2.73a) and 0.40 (Figure 2.73b), with a slightly higher amount of crystalline hydrates in the case of lower water content. Beyond 1 to 2 days, the intensity of the Gaylussite signal starts decreasing and that of calcite starts to grow. Such a massive consumption of calcium in the form of calcite ($CaCO_3$) might lead to the formation of high density C-S-H with a low Ca/Si ratio, which might be the reason for higher strength and excellent durability (Pelisser et al., 2012; Krivenko, 2017; Kunther et al., 2017). Beyond 7 days a noticeable formation of different Afm-type phases (such as Hydrotalcite and Monocarboaluminate hydrate), calcite and low nanocrystalline C-(A)-S-H can be observed. Low amounts of crystalline phases might indicate a high amount of amorphous C-(A)-S-H gel formation, which explains a high strength (for example compared to NaOH activation as reported in the literature).

The hydration mechanisms of Na_2CO_3 slag have already been discussed in the literature (Bernal et al., 2015; Abdalqader et al., 2016; Ke et al., 2016a; B Yuan et al., 2017). In the case of a sufficiently high aqueous Na_2CO_3 concentration, and up to about 24 hours, the main hydration product is Gaylussite. Once the Na^+ concentration in solution becomes sufficiently low, additional leached Ca^{2+} from the slag will form Calcite (see the phase diagram in Figure 2.67). Besides the calcium carbonates polymorphs, the precipitation of the Afm-type phases, including the carboaluminates and Hydrotalcite, will also contribute to the consumption of carbonate ions. When the CO_3^{2-} ions become exhausted, the Gaylussite is destabilised, releasing Na^+ ions into solution leading to an increase in pH (formation of NaOH). Dissolution of the slag is then accelerated leading to the end of the induction period and the formation of the strength-giving hydration products (C-A-S-H). The fate of Na and its distribution among the remaining Gaylussite, hydrated sodium carbonate salts, adsorption for charge compensation

within the C-A-S-H, etc. is beyond this study and is worthy of investigation. Indeed this may have crucial impact the long term properties including efflorescence, freeze-thaw resistance, etc.

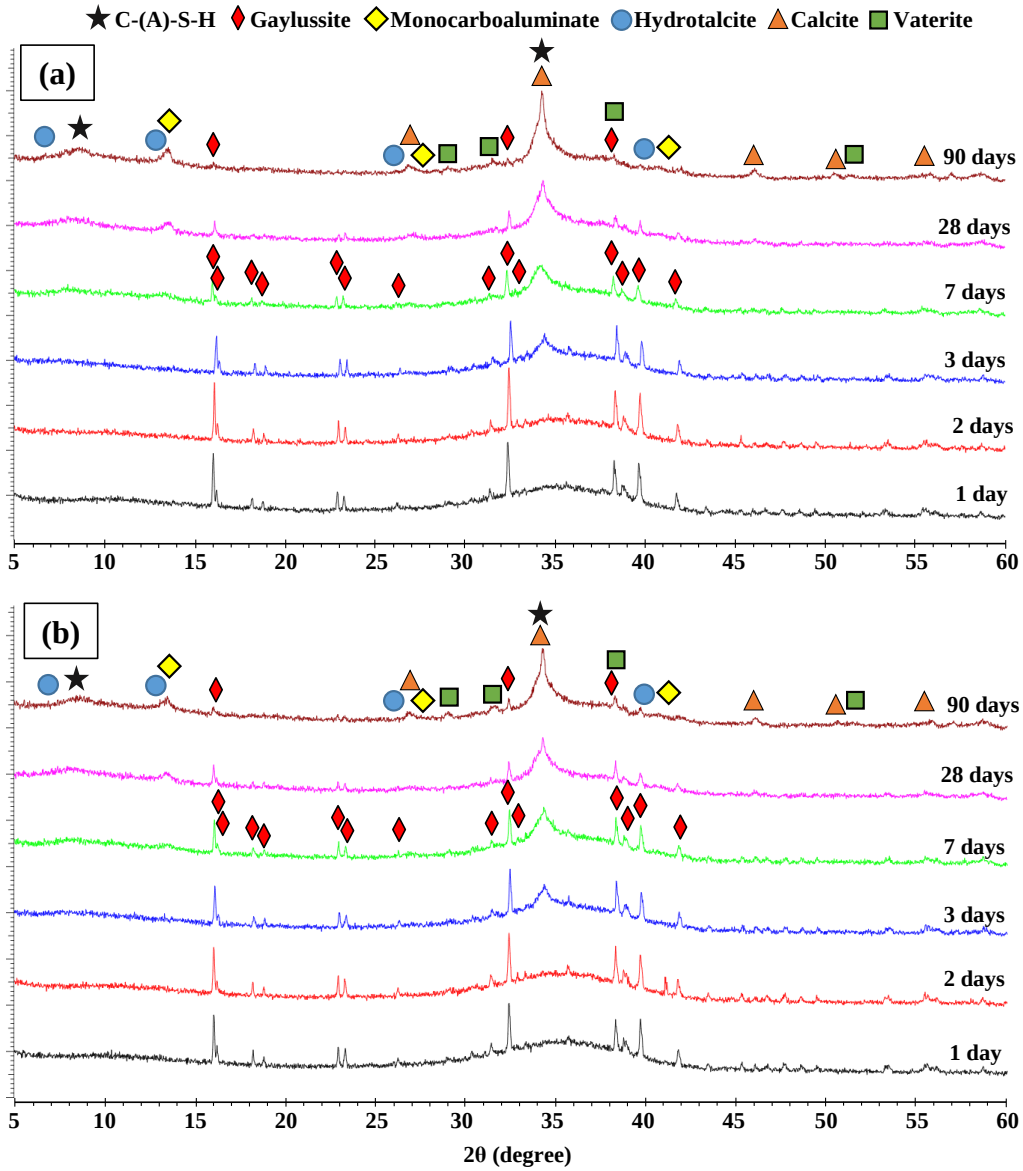

Figure 2.73: Laboratory Ex-situ XRD analyses. Evolution of the crystalline phases of GGBS activated with 8% Na_2CO_3 at W/B=0.35 (a) and 0.40 (b) from 1 to 90 days

2.8 Evolution of pH

The pH level evolution was monitored on the same samples used for XRD analysis before their treatment. The measurements were performed by an ex-situ leaching method (Behnood et al., 2016). The sample was finely crushed by manual grinding. 5g of this powder was mixed with 20 ml of demineralized water. The pH level of the obtained solution after 3 minutes of stirring was recorded. The results of its evolution in time for different Na_2CO_3 concentration are presented in Figure 2.74 . As it can be observed, increasing the amount of

sodium carbonate led to a higher alkalinity at all ages. Higher values can explain the higher reaction rate seen with the micro-calorimetry test as well as higher compressive strength with higher amounts of activator. No significant decrease of the pH occurs in the case of 6% and 8% between 3 and 28 days (the period of intensive hardening), against the clear drop in the case of 2% and 4%. These results are consistent with the assumption that, as a result of the initially favourable soda ash concentration (150-200 g/l), a sufficient amount of Gaylussite was formed. At later age, it plays the role of an alkaline deposit and maintain high hydration rate. The pH like many other factors, affect the hydration process and all other physical parameters.

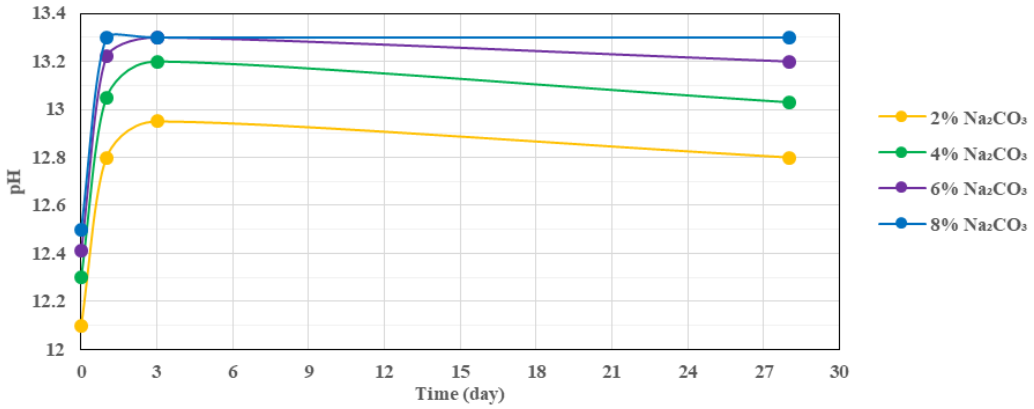

Figure 2.74: Evolution of pH level of past based on 100% GGBS with different amount of Na_2CO_3 at W/B=0.40 (paste:water=1:4, dilution during the measurements)

It is also worth noting that in any case, the initial pH level is between 12 and 12.5, which is a clear advantage in terms of safety on the construction site. The rise of pH to 13-13.2 occurs only at the time of setting and intensive hardening (24-72h). This is due to the reaction of in-situ NaOH formation described earlier. Although even in this case, the values are lower than OPC and especially lower than GGBS activated by pure sodium hydroxide or silicate. At longer term, high pH level (more than 10-11) will protect the steel armature against the corrosion.

2.9 SEM observations

The Hitachi S3400N scanning electron microscope (SEM) coupled with energy-dispersive X-ray spectroscopy (EDX) was used to study microstructural changes and elemental analysis in the hardened pastes. The same hydration stopping procedure as before for XRD was used. The samples were covered by a carbon deposit to enhance their conductivity.

The SEM images for a paste at a W/B=0.35 with 8% of Na_2CO_3 activation are presented in Figure 2.75. At the age of 2h after mixing (Figure 2.75a) GGBS grains can be distinguished with some small crystals. By coupling the SEM images with the EDX analysis (Figure 2.76)

these crystals might represent yet-unconsumed sodium carbonate as pointed out above based on the XRD results and some hydrates. Small deposits on the slag surface might be poorly crystallised Gaylussite/Calcite (Figure 2.77). After 4h an intensification of the process can be observed (Figure 2.75b). Though the GGBS particles are still well distinguishable, the surface is more covered with hydrates. After 1 day of hardening, some grains are completely or very significantly covered by hydrates (Figure 2.75c). Yet, it seems there is not enough or no C-S-H gel to collate all of the grains together. Beyond 7 day, no more naked slag grains can be clearly observed. A large amount of gel was formed, which seems to be denser at 28 days. These observations confirm the previous observations. However, even at 28 days coarse unreacted GGBS grains can be observed (Figure 2.75e). The presence of unreacted slag explains the continuous strength evolution over time for such products.

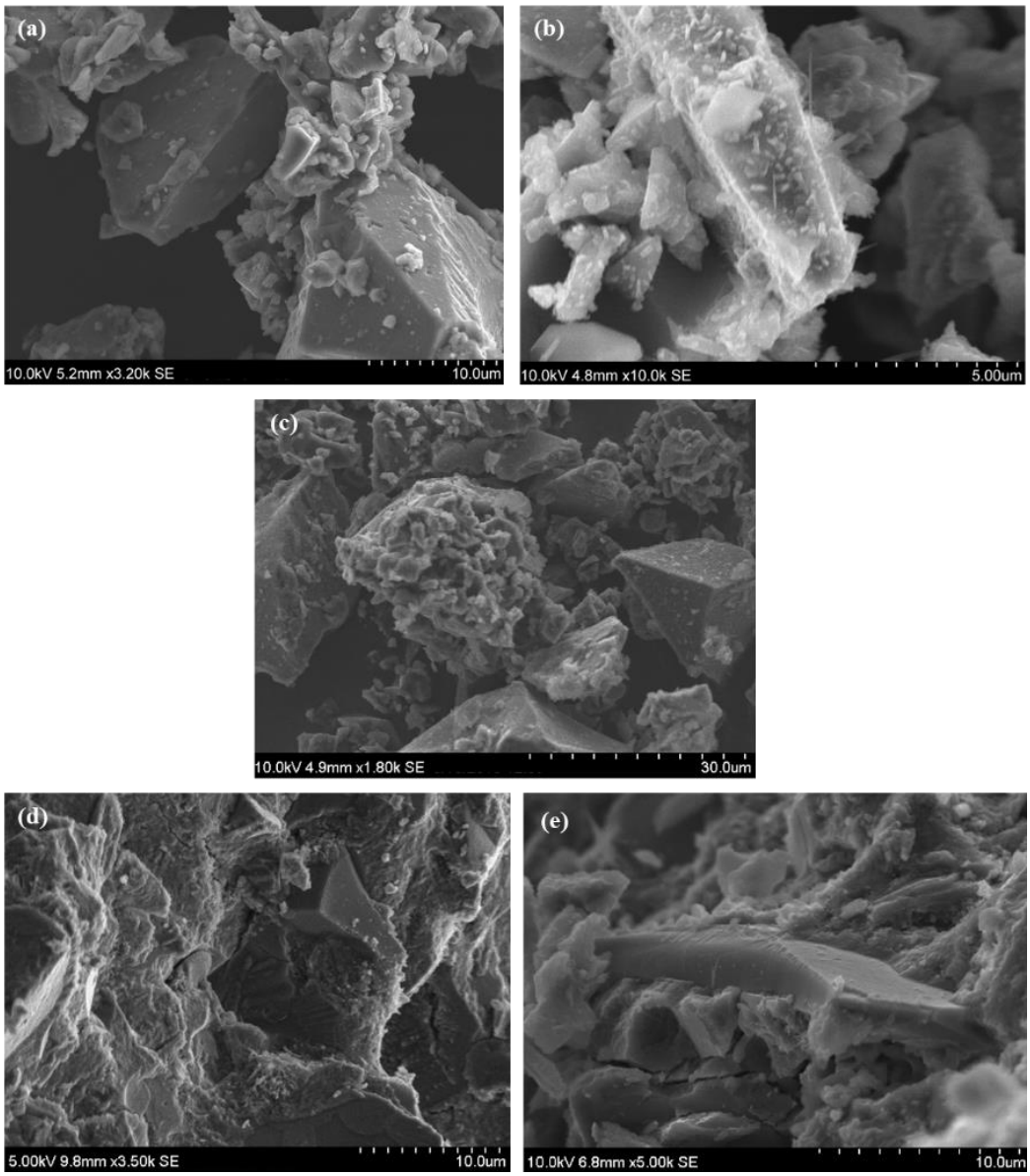

Figure 2.75: SEM images of GGBS pastes surface with 8% Na_2CO_3 and W/B=0.35 at the age of 2h (a), 4h (b), 1 day (c), 7 days (d) and 28 days (e)

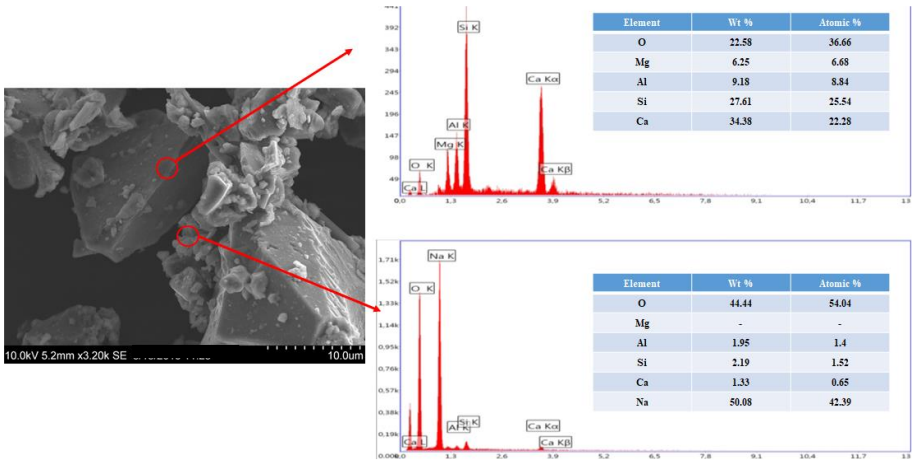

Figure 2.76: Example of SEM-EDX analysis. Paste of GGBS with 8% of Na_2CO_3 and W/B=0.35 at 2h

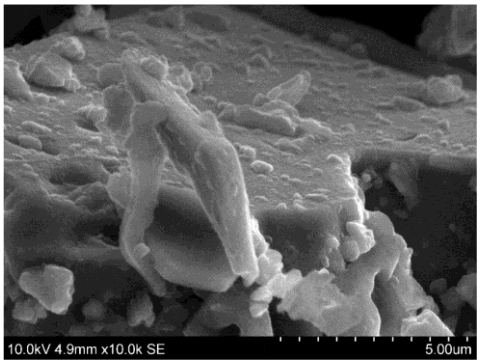

Figure 2.77: Slag surface after 2h of hardening. GGBS activated with 8% of Na_2CO_3 at W/B=0.35

Nevertheless, not only the clearly visible deposit of hydrates on the slag surface can be observed. Regarding the surface of some big slag grains after 28 days of hardening with a high zoom, an additional very thick layer on its surface can be observed (Figure 2.78). This might be the passivation layer of firstly precipitated dense hydrates (nano-crystaline or amorphous), which significantly slows slag's big particle dissolution.

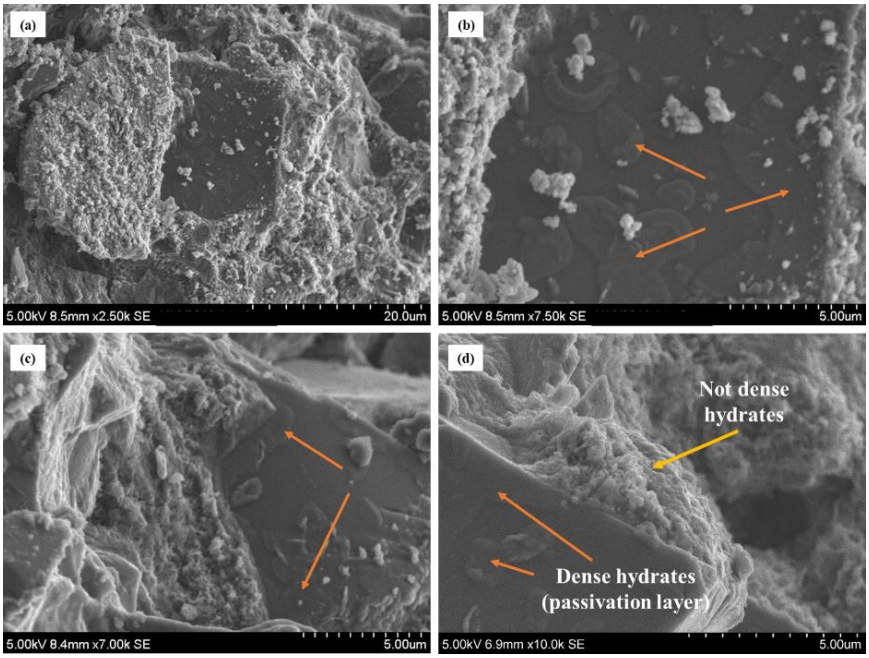

Figure 2.78: SEM observations of 28 day's slag surface. GGBS activated with 8% of Na_2CO_3

Regarding the influence of very low Na_2CO_3 concentration activated slag (here 50 g/l, Figure 2.79), it can be observed that that all grains are covered by small sized hydrates. They cover the entire surface very tightly. At the same time, when examining in detail the intergranular C-S-H gel (Figure 2.80), its very low density can be observed, compared to the sample with high initial sodium carbonate concentration (Figure 2.75). Both of these observations may indicate that in this case, hydration took place primarily on the GGBS surface and not in bulk. Such significant difference in gel density, might be a main reason of compressive strength values decreasing in case of low activator dosage.

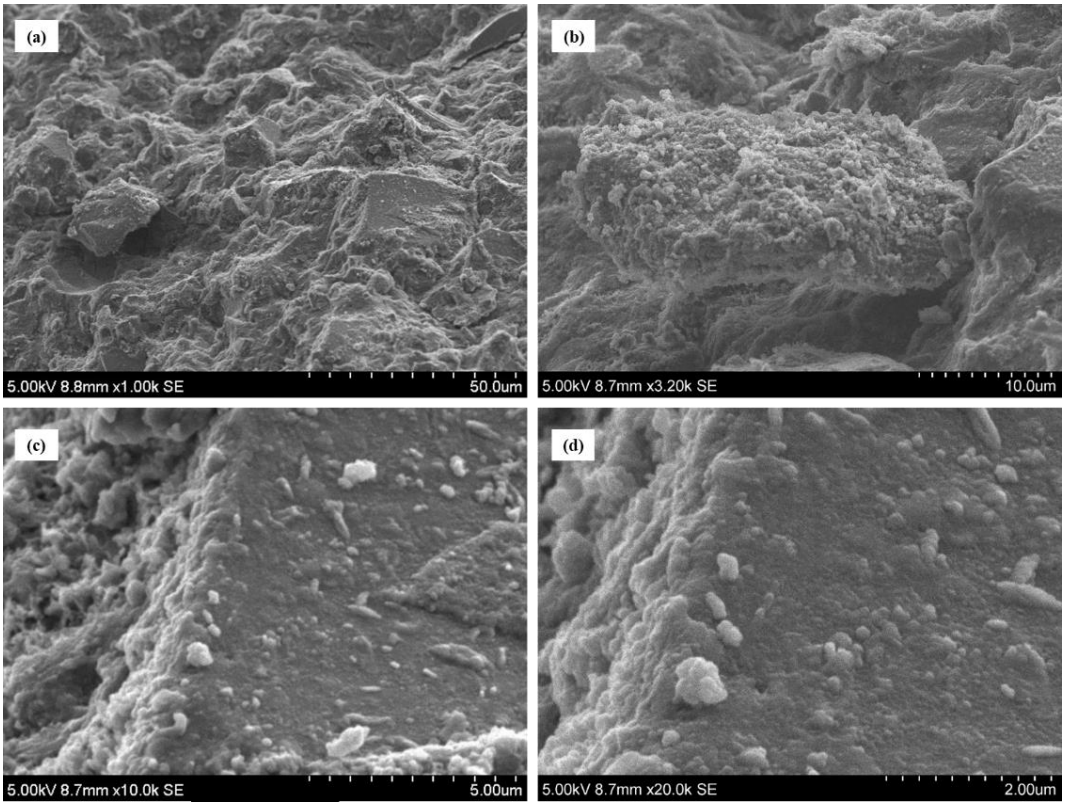

Figure 2.79: SEM observation of 28 day's slag surface. GGBS activated with 2% of Na_2CO_3

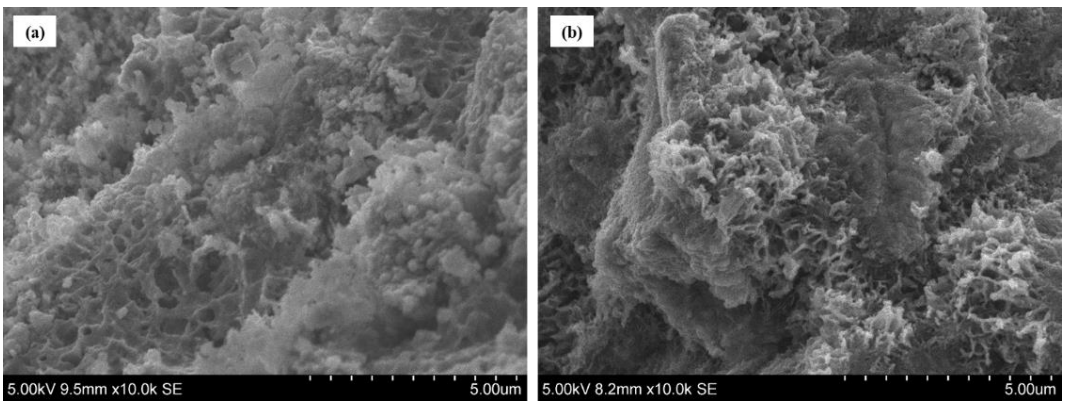

Figure 2.80: SEM observation of 28 day's age sample fracture surface. GGBS activated with 2% of Na_2CO_3 (W/B=0.40)

Conclusions

The obtained results confirmed that Na_2CO_3-GGBS binders have insufficient rheological properties for modern industrial applications. This binder can be characterized by a high initial yield stress and its fast evolution. Increasing the GGBS fineness or decreasing the W/B ratio leads to even poorer properties. The amount of Na_2CO_3 does not have a significant effect on the rheology deterioration rate during the first couple of hours. At the same time, the amount of activator has a significant effect on the induction period and the strength properties both at early and later age.

The results of microcalorimetry indicate that the influence of the amount of Na_2CO_3 at early age is not linear. In all cases (different slag fineness, W/B ratio), there is a certain turning point or minimal concentration required in the system to achieve the high hydration rate. However, for the tested formulations, a very low or no strength was observed after 24h of hardening. At the same time, decreasing the water content in a system or increasing the slag fineness seems to significantly accelerate the hydration process (decreasing the induction period during micro-calorimetry testing). Nevertheless the poor rheology in the case of fine and ultrafine GGBS even prevented the realization of strength measurements due to the impossibility of high-quality homogeneous samples preparation.

Analysis of the precipitated hydrates indicates that at the very beginning the main hydrate is Gaylussite – a double salt of sodium and calcium carbonate ($Na_2Ca(CO_3)_2*5H_2O$). This hydrate plays a double role. Its formation leads to the appearance of an additional surface – nucleation sites. That is why this type of activation is characterized by high strength and durability due to hydration in bulk (compare to some another alkali-activated slag based binders). Consumption of Ca^{2+} by its precipitation should also increase its concentration gradient and accordingly increase its leaching (seen for instance as a sharp change in zeta-potential). In addition, at longer term it maintain a high alkalinity. When the CO_3^{2-} ions are exhausted through precipitation with other hydrates (Afm, Ca-carbonate) the Gaylussite is destabilised. Its decomposition and transformation into different forms of Calcite ($CaCO_3$), leads to an increase in the sodium concentration and thus alkalinity. This phenomenon seems to be the main source of the high hardening rate in the period up to 1 year seen in the present work.

Unfortunately Gaylussite seems also to be responsible for the long induction period and low early age strength. Due to the high amount of added sodium (from Na_2CO_3), the process of Gaylussite formation occurs during the first 24h or more. Its formation inhibits the rise of

alkalinity (capturing of Na^+ in its structure) and an increase in calcium concentration (by capturing Ca^{2+} in its structure), required for C-S-H formation. The acceleration of its decomposition should speed up the hardening process. Decreasing the sodium amount leads to a lower formation of Gaylussite. Nevertheless due to a high amount of calcium leached from the slag and an increased pH, calcite formation occurs. The further low hydration rate might be related with its precipitation on the slag surface. As well as the absence of Gaylussite for supplementary nucleation sites, initial consumption of Ca^{2+} and maintaining of the high pH with time.

As proof of Gaylussite importance, a minimal observed optimum concentration of sodium carbonate in the system after which the reaction rate significantly changes coincides with the minimal concentration for favourable Gaylussite precipitation.

Chapter 3 Improving the rheological properties of Na_2CO_3-activated GGBS binders

Introduction

In the previous chapter it was shown that high aqueous concentrations of Na_2CO_3 are required to decrease the induction period and to have sufficient strength at early age. At the same time, for economical and durability reasons, the amount of Na_2CO_3 should be limited. The best option is then to minimize the W/B ratio. Strength development can also be improved by increasing the GGBS fineness, although this also has some economical drawbacks. However, both solutions lead to the degradation of the rheological properties, in particular a dramatic decrease of the open time (the duration in which the desired rheological properties are maintained). This is crucial, especially for conventional concrete for civil engineering projects where in general the same rheology is required for up to 2 hours. This issue is one of the main reasons why the utilization of this binder has not been generalized beyond the precast concrete industry. Surprisingly, in contrast with other types of activation (for example silicate or NaOH), reported studies on how to control the rheology of Na_2CO_3 slag binders are very limited (Krivenko et al., 2017).

It was shown in the previous chapter that even at low concentrations of sodium carbonate (2%), the yield stress increases significantly within the first 30 mins. This may be attributed in particular to the rapid precipitation of the early hydration products, including the Na/Ca carbonates. Therefore, in order to impede the increase of the yield stress, one is tempted to temporarily inhibit the precipitation of those first hydration products, for example through Ca complexation. Several Ca chelating agents have been then tested. The main challenge was to delay the precipitation of the first hydration products without delaying the strength giving hydration phases such as C-(A)-S-H, which also require Ca to be precipitated.

Another method of retarding hydration is to poison the surface of the anhydrous or/and hydration phases through the adsorption of organic molecules for example sugars. In the case of Na_2CO_3 activated slag binders considered here, both mechanisms of retardation have been explored.

3.1 Selection of the appropriate retarders

Ca-chelating agents as EDTA (Ethylenediaminetetraacetic acid) are known to be excellent retarders for OPC-based products (Thomas and Double, 1983) by interaction with calcium. In the case of the binder considered here, the main challenge is to hinder the precipitation of the carbonates. Phosphonate-type compounds are known to be highly effective in this case (Bishop et al., 2003; Liu, 2011; Lupu et al., 2005; Xyla and Koutsoukos, 1987). The working mechanisms of these compounds in inhibiting calcium carbonate precipitation will be discussed throughout this chapter. Ca^{2+} is sequestered through electrostatic interactions with the ionic groups of the chelating agent (Figure 3.1). In its presence, the first leached Ca^{2+} ions are not available for precipitation of the early hydration products, and hydration is then delayed. For binders with an excess of Ca, such as those based on OPC, a Ca-chelating agent, if used at a sufficiently low dosage, can delay early hydration without significantly impacting strength development. This is not the case for slag-based binders, for which a lack of Ca in solution may turn out to be an issue for C-S-H precipitation. Dosage rate tuning of such retarders in the case of slag binders may reveal themselves to be quite challenging.

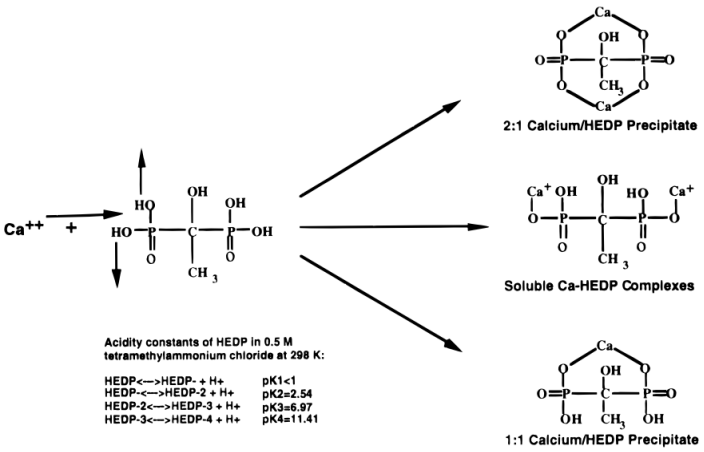

Figure 3.1: Precipitation reaction mechanism between calcium and phosphonate (HEDP) (Browning and Fogler, 1996)

Another working mechanism of retarders is through surface poisoning. This can result from both adsorption of organic compounds such as sugars (Smith et al., 2011) and the precipitation of complexes on the reactive mineral surfaces.

Several phosphonate molecules have been then tested for their impact on rheology and heat released during early age hydration. Most of them are ineffective. The origin of this phenomenon is not understood and requires additional study. In particular different grades of Dequest® phosphonate from Italmach were tested, and the results for the most effective grades are reported. A comparison to certain other types of retarders is also made.

For the selection of the phosphonates, the tests were performed for the case of standard GGBS activated with 200g/l of Na_2CO_3 at a fixed W/B ratio of 0.40. The retarders were added at less than 1% by weight of slag and pre-dissolved in the mixing water.

3.1.1 Case of the EDTMP grade

The molecular structure of the phosphonate 5Na*EDTMP (Penta sodium salt of EthyleneDiamineTetraMethylenePhosphonic acid)) is reported in Figure 3.2. In solution the molecule will ionise and several sites become available for Ca^{2+} complexation.

The influence of the phosphonate on the paste yield stress is presented in Figure 3.2. The rheological protocol is the same as the one used in Chapter 2. The results indicate that this additive is highly effective in reducing the yield stress, but it has a delayed effect. The initial yield stress slightly increases with the additive dosage, while over time it decreases. For instance, for a dosage of 0.3% (which seems to be an optimum) and at 20 min, the yield stress is significantly reduced (more than an order of magnitude). The delayed effect may be attributed in particular to the time required for adsorption of the molecules on the Ca^{2+} rich sites, which is related to the leaching rate of Ca^{2+} from the slag.

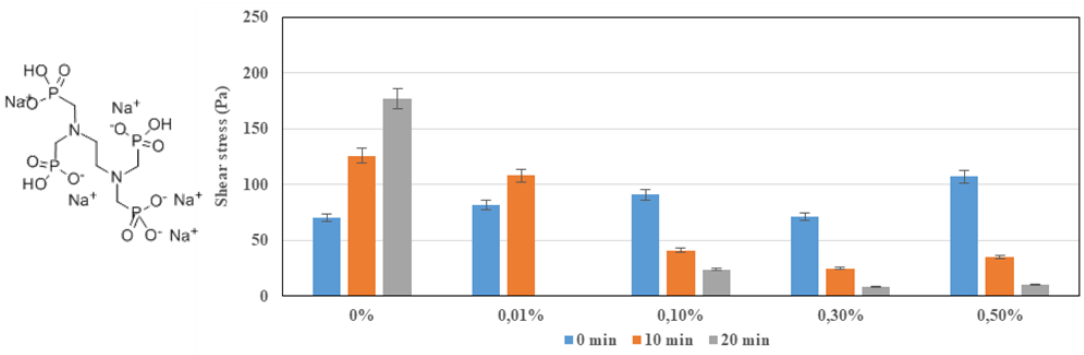

*Figure 3.2: Influence of 5Na*EDTMP dosage on a yield stress evolution of GGBS activated with 200g/l Na_2CO_3 at W/B=0.40*

3.1.2 Case of the HEDP grade

4Na-HEDP (Tetra sodium salt of HydroxyEthylideneDiphosphic acid) molecular structure is reported in Figure 3.3. The number of sites available for Ca^{2+} complexation is lower than in the case of the previous grade.

The influence of HEDP dosage rate on the yield stress evolution over time is presented in Figure 3.3. Similar to the previous grade, the reduction in the yield stress increases with time. A dosage rate of 0.3% seems to be an optimum.

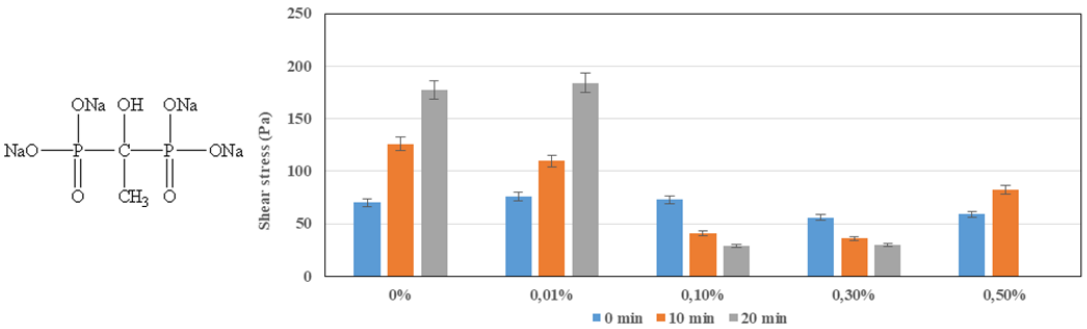

*Figure 3.3: Influence of 4Na*HEDP dosage on yield stress evolution of GGBS activated with 200g/l Na_2CO_3 at W/B=0.40*

Several other phosphonates have been tested including hexa sodium salt of hexamethylenediamine tetra (methylene phosphonic acid) (6Na*HDTMP), tetra sodium salt of phosphonobutan tricarboxylic acid (4Na*PBTC), hepta sodium salt of diethylene triamine penta (methylene phosphonic acid) (7Na*DTPMP), etc. They were less effective in reducing the yield stress and the results are not reported here.

3.1.3 Comparison with other Ca-complexing agents (Sodium Gluconate)

Beyond a certain dosage rate, the addition of Sodium Gluconate seems to have an excellent retardation effect coupled with a significant reduction of the yield stress (Figure 3.4), which confirms results reported in the literature (Krivenko et al., 2017). Sodium Gluconate has only one ionic site, but a Ca^{2+} ion can be sequestrated through the cooperative effects of several molecules. Compared to the phosphonates, a higher dosage is needed to achieve the same effect.

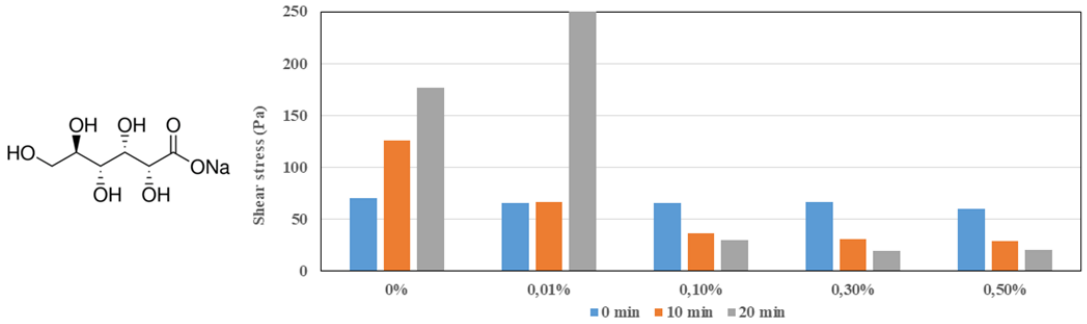

Figure 3.4: Influence of Sodium Gluconate dosage on a yield stress evolution of GGBS activated by 200g/l of Na_2CO_3 at W/B=0.40

Among all the tested additives, three of them showed a significant instantaneous yield stress reduction. In addition, beyond a certain additive concentration, not only is the rheology maintained, but the yield stress even decreased over the 10-20 min time period considered. The choice among the three retarders can be made based their impact on early strength development. This may be determined by considering their impact on the induction period through isothermal calorimetry measurements.

It can be seen (Figure 3.5) that the presence of Sodium Gluconate leads to a significant increase of the induction period. It is a difficult task to determine an optimum dosage of Sodium Gluconate that allows sufficient reduction of the yield stress and an extension of the open time without compromising the early age strength development. On the other hand the phosphonate has a negligible impact on the induction period. Only the results for the 4Na-HEDP grade are reported, those for 5Na-EDTMP are similar. 4Na*HEDP was then used in all the subsequent studies.

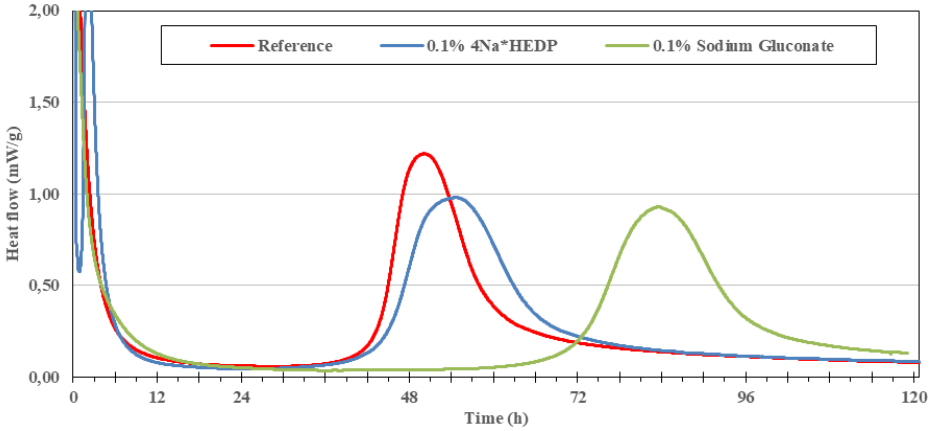

*Figure 3.5: Hydration kinetics of 100% Standard GGBS activated with 8% Na_2CO_3 at W/B=0.40. Influence of 4Na*HEDP and Sodium gluconate addition*

3.2 Detailed study on the impact of 4Na*HEDP on rheological properties

3.2.1 Binders based on Standard GGBS

The impact of phosphonate 4Na*HEDP on the time evolution of the yield stress in the case of GGBS activated with 8% Na_2CO_3 at different W/B ratios is presented in Figure 3.6. The addition of this additive leads to a noticeable retardation effect on the yield stress evolution in all tested cases. The effect can be observed even at a very small dosage (0.05%). Increasing the dosage leads to an increasing of the open time (period over which the yield stress keeps approximately constant). Beyond a certain dosage (for example 0.2% at W/B=0.40) there is no significant additional effect. Increasing further the retarder dosage (results not reported here) leads to an increase of the yield stress. This may be attributed to an eventual precipitation of the phosphonate with Ca^{2+} as Ca-phosphonate (see further) (Bishop et al., 2003). In all cases the yield stress first decreases, remains almost constant over a period that depends on W/B, and then sharply increases. The first period may correspond to the time necessary for the molecule to adsorb onto the mineral phases or/and nucleation of the Ca-phosphonate complexes. Over time the phosphonate should be consumed as precipitate and its effect will vanish. The phosphonate

maintains the rheology, by acting as a retarder and causing the instantaneous yield stress to significantly decrease. The origin of this plasticizing effect will be discussed further.

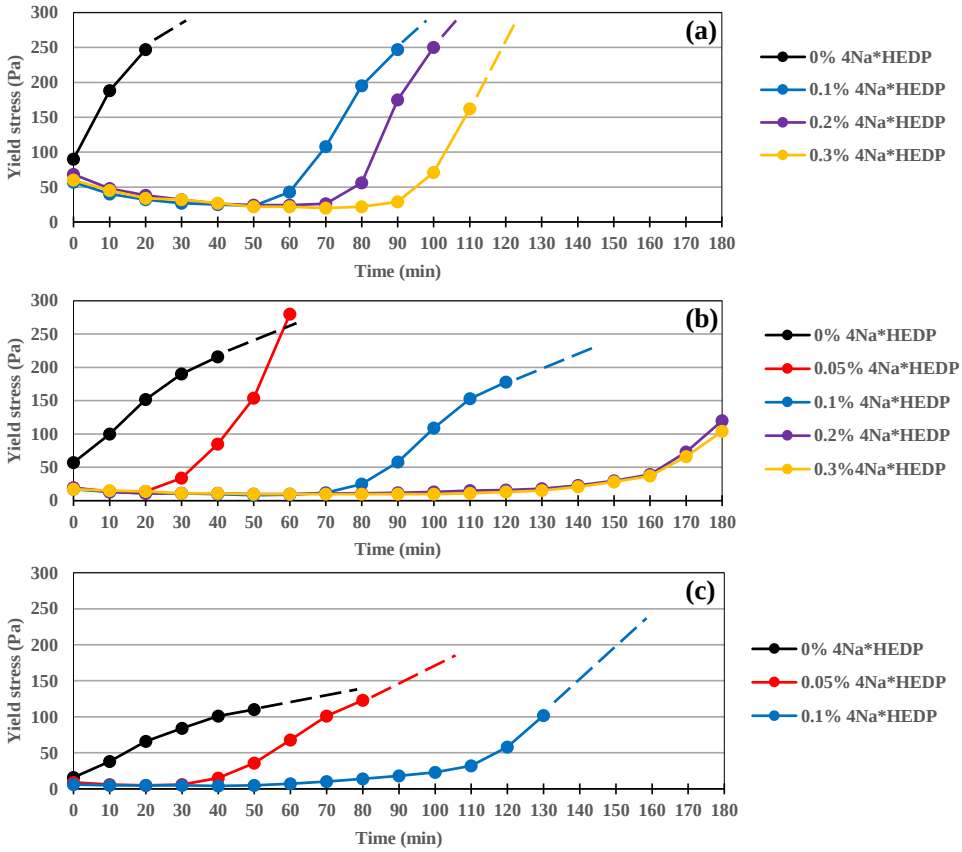

*Figure 3.6: Yield stress evolution of 100% GGBS with 8% Na_2CO_3 at W/B ratio 0.35 (a), 0.40 (b) and 0.45 (c) with addition of different amount of 4Na*HEDP by GGBS weight*

The results regarding the impact of the phosphonate on the yield stress at lower Na_2CO_3 dosages are reported in Figure 3.7 and Figure 3.8. When the dosage of the activator is decreased, the retardation effect of the additive increases. That is, the optimum dosage of retarder increases with activator dosage rate.

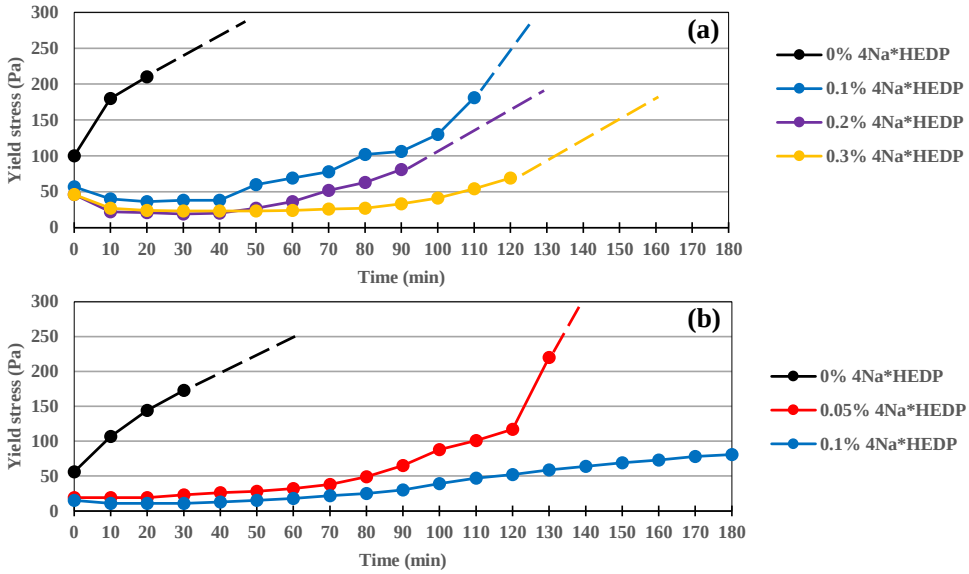

*Figure 3.7: Yield stress evolution of GGBS activated with 6% Na_2CO_3 at W/B ratio 0.35 (a), 0.40 (b) with different dosages by GGBS weight of 4Na*HEDP*

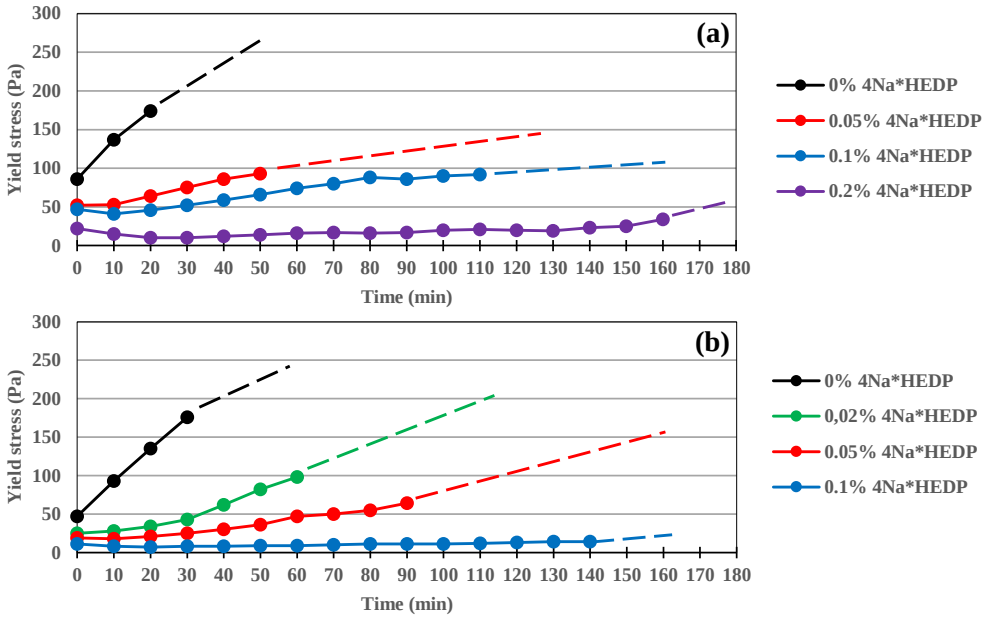

*Figure 3.8: Yield stress evolution of GGBS activated with 2% Na_2CO_3 at W/B ratio 0.35 (a) and 0.40 (b) with addition of different dosages by GGBS weight of 4Na*HEDP*

Figure 3.9 represents the impact of the phosphonate on the plain slag dispersion (devoid of activator, mixed only with pure water). This additive reveals itself to be a very highly effective dispersant for slag.

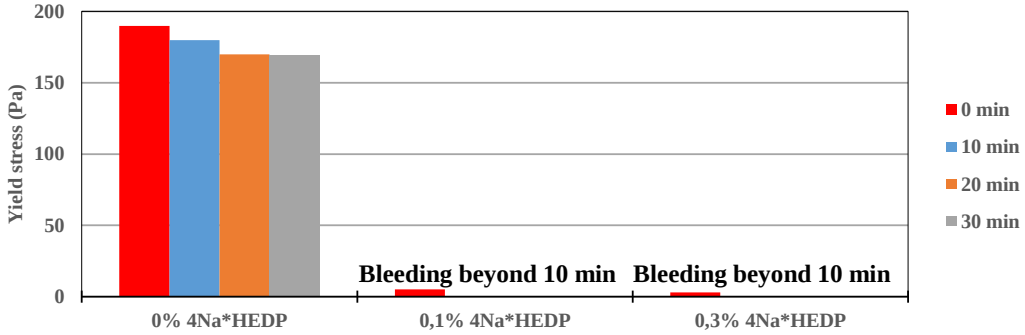

*Figure 3.9: Influence of 4Na*HEDP on yield stress of GGBS with 0% Na_2CO_3 at W/B=0.35*

3.2.2 Increasing slag fineness

It was shown in Chapter 2 that increasing the GBBS fineness led to a noticeable acceleration of hydration. Nevertheless, the rheological properties deteriorated, requiring an appropriate rheological additive. The yield stress evolution in the case of Fine GGBS activated with 8% and 6% Na_2CO_3 is presented in Figure 3.10 and Figure 3.11. A higher amount of retarder is required to obtain the same open time as in the case of Standard GGBS, especially in the case of low W/B ratio. This may be related to higher dissolution rate due to higher specific surface, and then more Ca^{2+} are to be chelated.

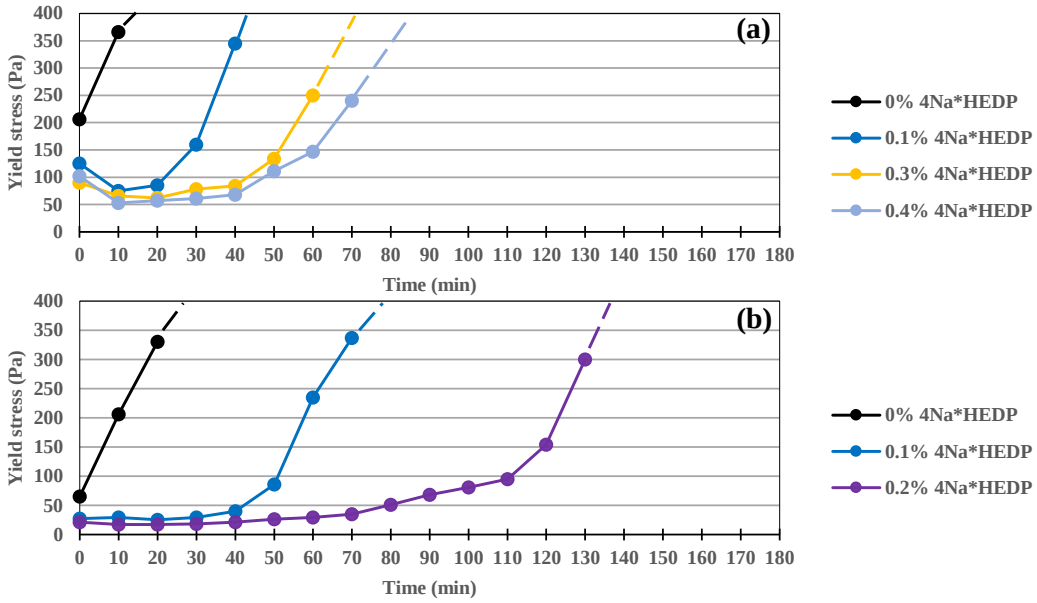

*Figure 3.10: Yield stress evolution of 100% GGBS 5600 cm^2/g with 8% of Na_2CO_3 at W/B ratio 0.35 (a) and 0.40 (b) with addition of different amounts of 4Na*HEDP*

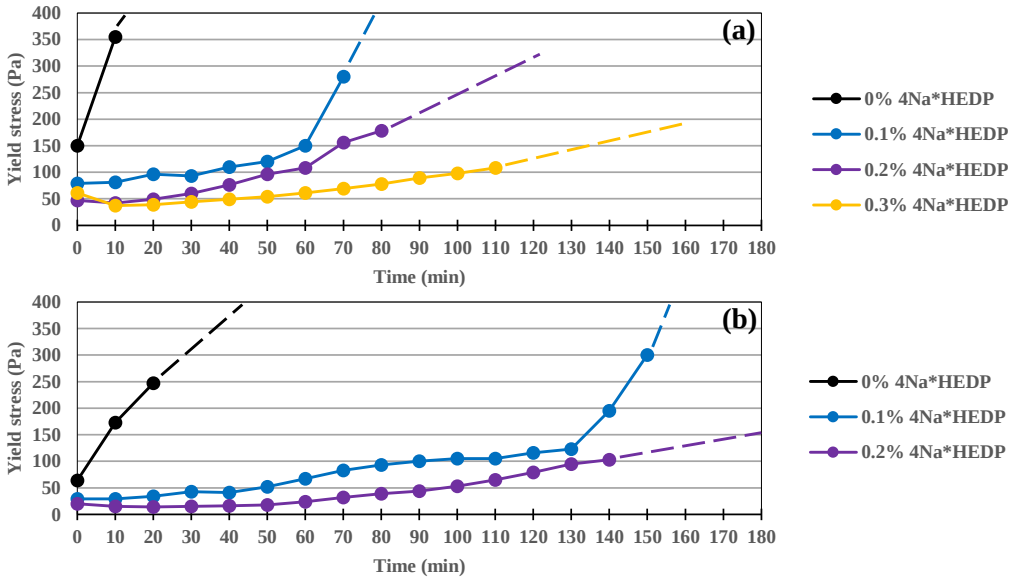

*Figure 3.11: Yield stress evolution of 100% GGBS 5600 cm^2/g with 6% of Na_2CO_3 by GGBS at W/B ratio 0.35 (a) and 0.40 (b) with addition of different amounts of 4Na*HEDP*

In Chapter 2 it was shown that the replacement of 5-10% of ordinary GGBS by Ultrafine GGBS had a strong influence on the hydration kinetics according to micro-calorimetry tests. However, this led to a stronger degradation of the rheology than in the case of 5600 cm^2/g GGBS Blaine fineness. The addition of a retardant/plasticizer is mandatory in this case. Figure 3.12 and Figure 3.13 present the impact of the phosphonate on the evolution of the yield stress in the case of 5% replacement with Ultrafine GGBS and activated with 8% and 6% Na_2CO_3. In this case the short term values of the yield stress seem independent of the phosphonate dosage. The dosage impacts mainly the extension of the open time. The sensitivity of the yield stress to the presence

of the phosphonate seems to increase in the presence of the Ultrafine. This will be discussed further when considering the origin of the plasticizing effects of the phosphonate.

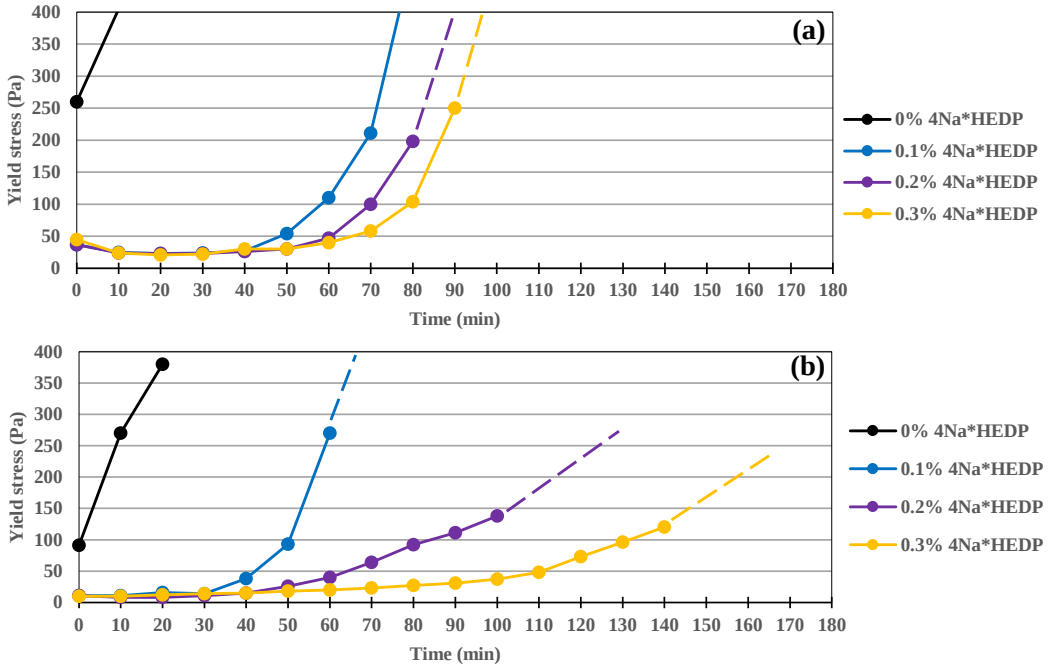

*Figure 3.12: Influence of 4Na*HEDP on yield stress evolution of paste: 95% GGBS + 5% Ultrafine GGBS with 8% Na_2CO_3 at W/B ratio of 0.35 (a) and 0.40 (b)*

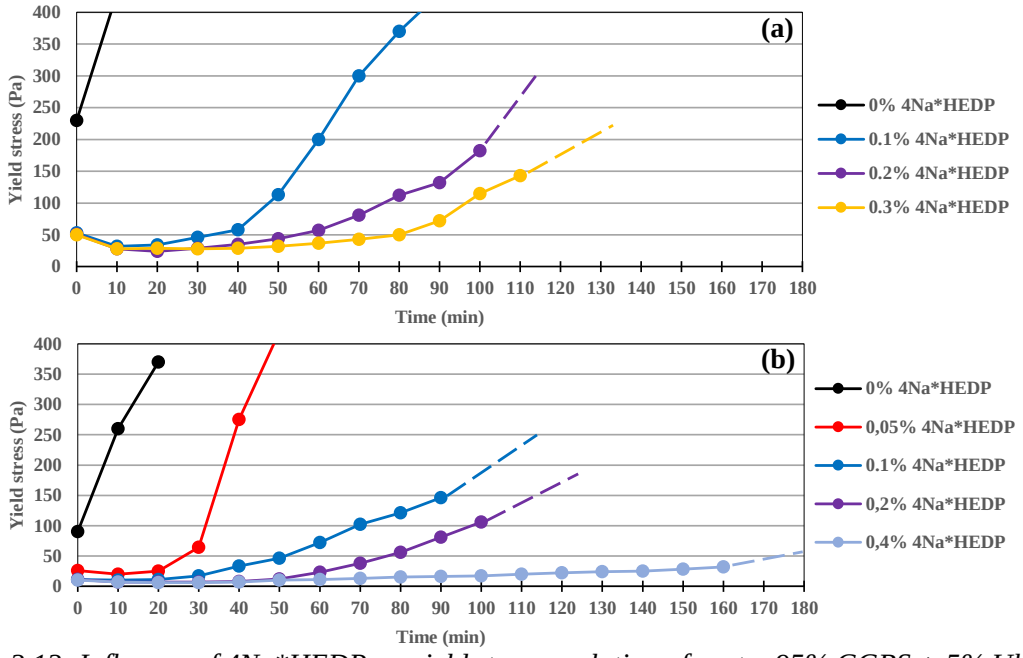

*Figure 3.13: Influence of 4Na*HEDP on yield stress evolution of paste: 95% GGBS + 5% Ultrafine GGBS with 6% Na_2CO_3 at W/B ratio of 0.35 (a) and 0.40 (b)*

3.3 Physical origin of the plasticizing effect of the phosphonate

The decrease of the yield stress of slag dispersion, in particular in absence of Na_2CO_3, upon addition of the phosphonate, indicates that the slag particles are dispersed in the presence of this molecule. This implies that the physicochemical properties of the slag particle's surface is

modified leading to repulsing dispersing forces. This can be investigated through surface charge measurements. The influence of the presence of the phosphonate on the ζ-potential values over two hours for a slag dispersion in demineralized water is reported in Figure 3.14. Addition of the phosphonate turns the initial values of the surface charge of the slag particles more negative. This will lead to an increase in the repulsive electrostatic component of the DLVO potential. This may be attributed to the Ca^{2+} chelating effect of the phosphonate. Indeed, a part of the leached Ca ions from slag cannot re-adsorb onto the negative sites on the surface since they are sequestrated by the phosphonate within the bulk solution. In addition, the phosphonate molecule has several ionic sites, it will then adsorb on the positive sites on the surface leading to a further decrease of the ζ-potential. The phosphonate may then act similarly to the first generation of OPC plasticizers as those are sulfonate-based. One can be then tempted to use such plasticizers in the case of Na_2CO_3 activated slag binders. Yet the solubility of such high molecular weight molecules in the presence of a high concentration of carbonate ions may turn out to be an issue.

It can also be observed that the presence of the phosphonate removes the large fluctuations of the ζ-potential over time. These fluctuations can be related to an eventual Ca precipitation/dissolution process and its re-absorption on the slag surface. The precipitation may take place with dissolved CO_2 for instance. The Ca precipitation process should correspond to the decreasing parts of the ζ-potential. Sequestration of the leached Ca by the phosphonate, in addition to its known $CaCO_3$ growth inhibiting property (Demadis and Lykoudis, 2005), should lead to the removal of the decreasing parts of the ζ-potential.

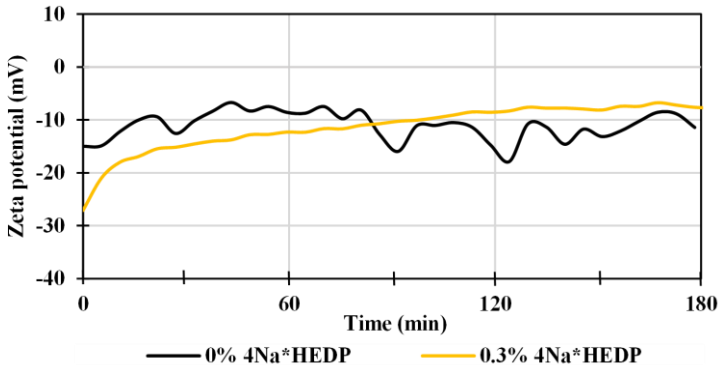

*Figure 3.14: Evolution of the ζ-potential of slag particles without or with 0.3% 4Na*HEDP by GGBS weight only in demineralized water (W/B=100)*

The impact of the phosphonate on the evolution of the ζ-potential in the presence of the activator (at 8% of slag) is reported in Figure 3.15 and Figure 3.16 (corresponding to slag particle concentrations of 1% and 20%). Again, the large variations of the ζ-potential related to dissolution/precipitation disappear in the presence of the phosphonate. In particular, the sharp

increase/decrease of the surface charge is removed (or rather retarded). The presence of the phosphonate seems to smooth out the evolution of the ionic (in particular Ca^{2+}) concentration nearby to the particle's surface. This might be a consequence of Ca^{2+} complexation and carbonate phases growth hindering by the phosphonate. Similar to the plain GGBS dispersions, the ζ-potential starts more negative in the presence of the phosphonate. In addition, it remains negative and with quite a high absolute value, all over the 3h of measurements considered. This should contribute to keeping a low yield stress for a long time. On the contrary, without the phosphonate, the ζ-potential passes through neutral values after about 1h. At that moment, flocculation of the slag particles due to the attractive van de Waals forces should take place, leading to loss of rheology.

It is to be noted that all these events should be accelerated at higher and more realistic GGBS concentrations. This can be determined if the results at W/B=100 (Figure 3.15) and those at W/B=5 (Figure 3.16) are compared. In both cases the ζ-potential remains negative with a high absolute value for a longer time in the presence of the phosphonate, while it tends to be close to zero without this additive. It can be anticipated that superplasticizers (both ionic and cationic), for which the working mechanisms are based on their adsorption on the particles leading to electrostatic or/and steric repulsion, should not be effective in the case of Na_2CO_3 activated slag binders. Since the presence of the phosphonate leads to negative and quite high absolute values, cationic superplasticizers, provided they are soluble in solution with high carbonate ions concentration, should be effective if associated with the phosphonate.

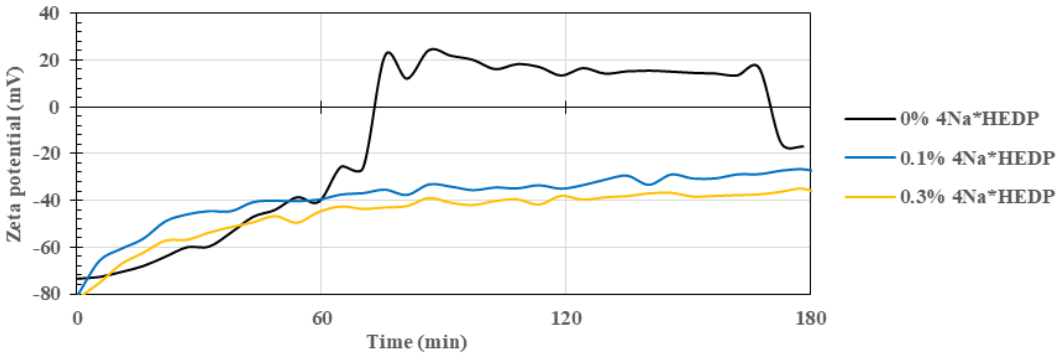

*Figure 3.15: Evolution of the ζ-potential of GGBS dispersions with 8% Na_2CO_3 with different contents of 4Na*HEDP (W/B=100)*

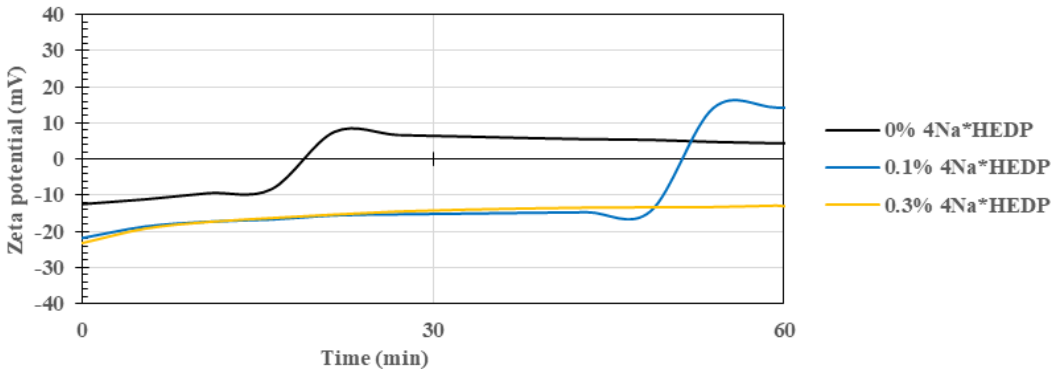

*Figure 3.16: Evolution of the ζ-potential of GGBS dispersions with 8% Na_2CO_3 with different contents of 4Na*HEDP (W/B=100) (W/B=5)*

The presence of the phosphonate leads to the decrease of both pH and ionic conductivity (Figure 3.17). This should be the result of Ca^{2+} complexation by the phosphonate. Nevertheless, these results don't necessarily explain the mechanism of the influence of phosphonates on improving rheological properties. For example, the fact that the minimum yield stresses are achieved after 30-40 minutes while the most negative surface charge seems to take place at the very beginning remains unclear. Other mechanisms may also take place. Addition of phosphonates can also impact the precipitated hydrates (their shape, amount, structure, etc.) and in this way contribute to rheology improving,

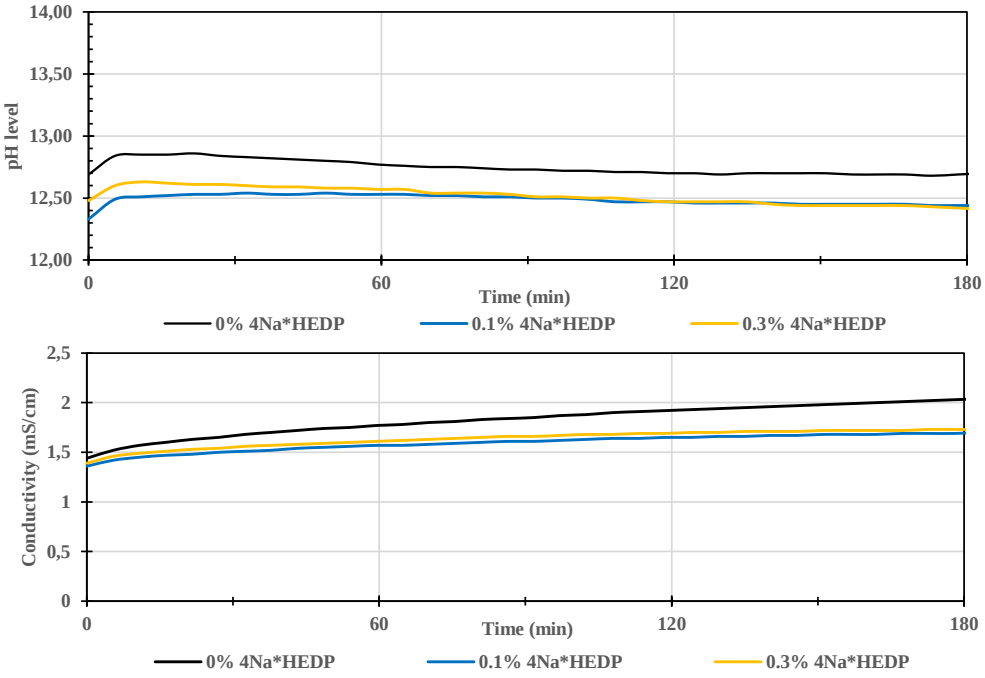

*Figure 3.17: Evolution of pH level and conductivity of Standard GGBS with 8% Na_2CO_3 and different amount of 4Na*HEDP (W/B=100)*

In the case of increased GGBS fineness, the addition of 4Na*HEDP leads to similar effect as in the case of standard GGBS and the same conclusions can be drawn (Figure 3.18 and Figure 3.19). At the same time, greater fluctuations of ζ-potential and higher values of

conductivity indicates a higher slag reactivity, already reported in Chapter 2. These observations might explain why in the case of increased slag fineness, a higher amount of phosphonates is required to maintain correct rheological properties.

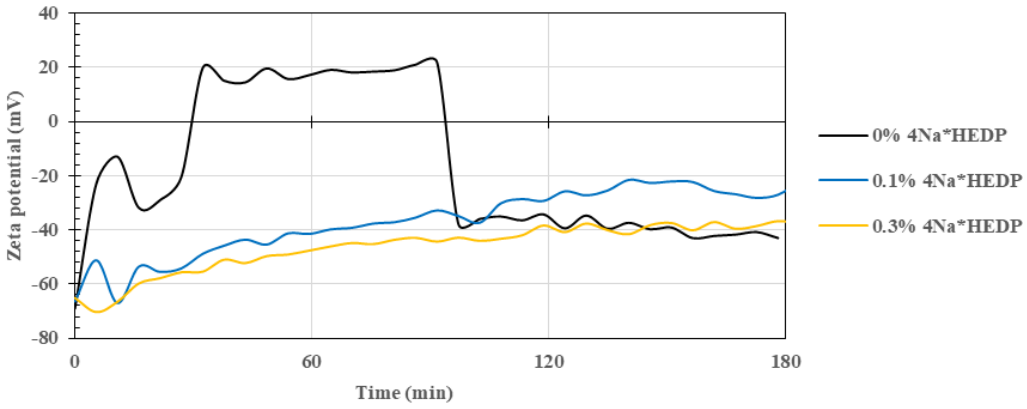

*Figure 3.18: ζ-potential of GGBS 5600 cm²/g with 8% Na_2CO_3 and 0%, 0.1% and 0.3% of 4Na*HEDP by GGBS weight in demineralized water (W/B=100)*

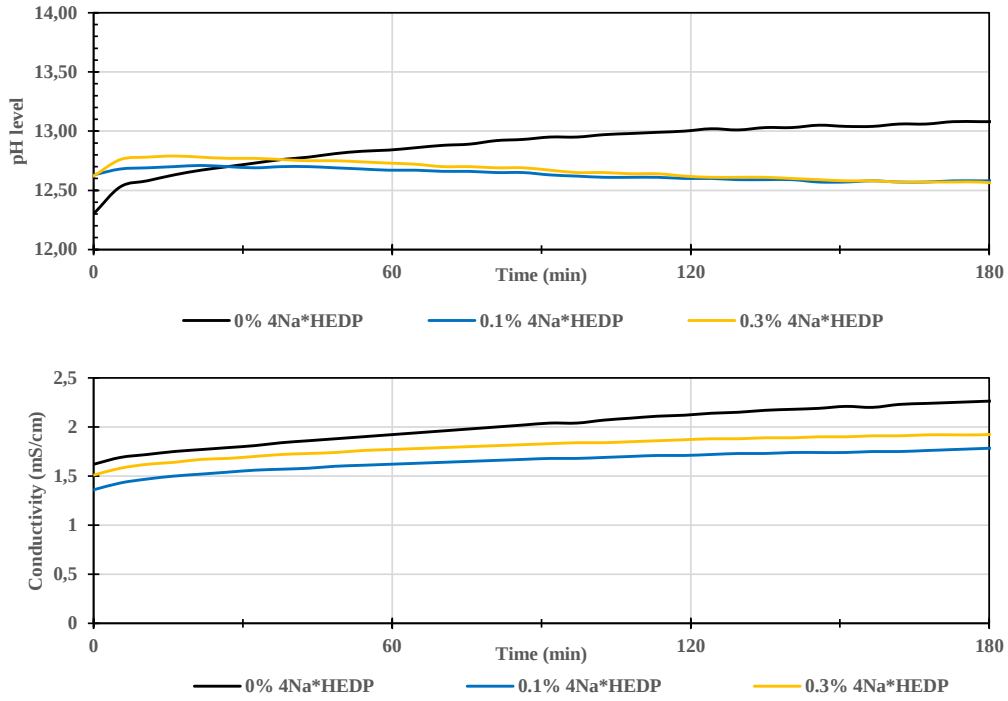

*Figure 3.19: Evolution of pH level and conductivity of GGBS 5600 cm²/g with 8% Na_2CO_3 and different amount of 4Na*HEDP (W/B=100)*

3.4 Impact of the phosphonate on the hydration kinetics

The impact of the phosphonate on the evolution of the heat released upon hydration of Standard GGBS activated with 8% Na_2CO_3 at different W/B ratios is reported in Figure 3.20. It can be observed that the time to reach the strength-giving peak is not significantly impacted by the presence of the phosphonate, at least up to a dosage rate of 0.2%. Hence, the retardation takes

place as it was expected. On the other hand, the peak corresponding mainly to the Ca/Na carbonates is also clearly delayed in the presence of the phosphonate. This correlates with the previous results regarding the increase on open time. The effect of the phosphonate on the delay of the first hydration peak increases with W/B. This implies that the lower the W/B ratio, the higher the required dosage of the phosphonate, as it was also observed with rheological measurements. This may be attributed to the fact that the rate of the leached Ca^{2+} (to be chelated) increases when the W/B is lower since the concentration of activator is higher (higher hydration rate).

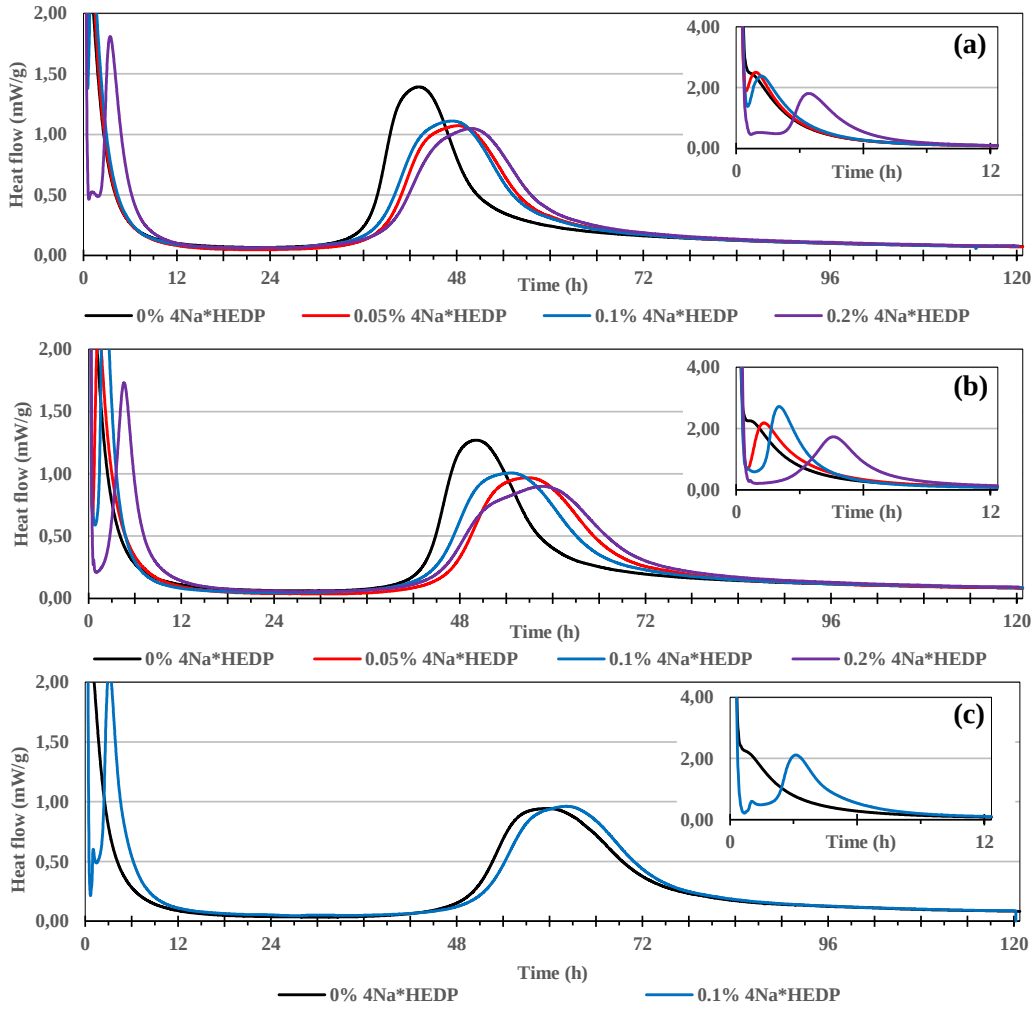

*Figure 3.20: Released heat evolution during hydration of Standard GGBS activated with 8% Na_2CO_3 and with different dosages of 4Na*HEDP at W/B ratio of 0.35 (a); 0.40 (b) and 0.45 (c)*

Figure 3.21 presents the results for the cumulative heat released over time. Overall, the presence of the phosphonate leads to an increase of the heat released, indicating an increased degree of hydration. This may be attributed to several reasons. Through the Ca^{2+} complexation process, the phosphonate plays the role of a Ca sink leading to an increase of the slag dissolution. By preventing Ca^{2+} re-adsorption onto the slag surface the latter remains overall negative and more Ca^{2+} can be pulled out from the particle through electrostatic attraction. A second reason

should be the fact that the phosphonate can precipitate as Ca*HEDP particles (see further) that may play the role of seeds for the growth of hydration products.

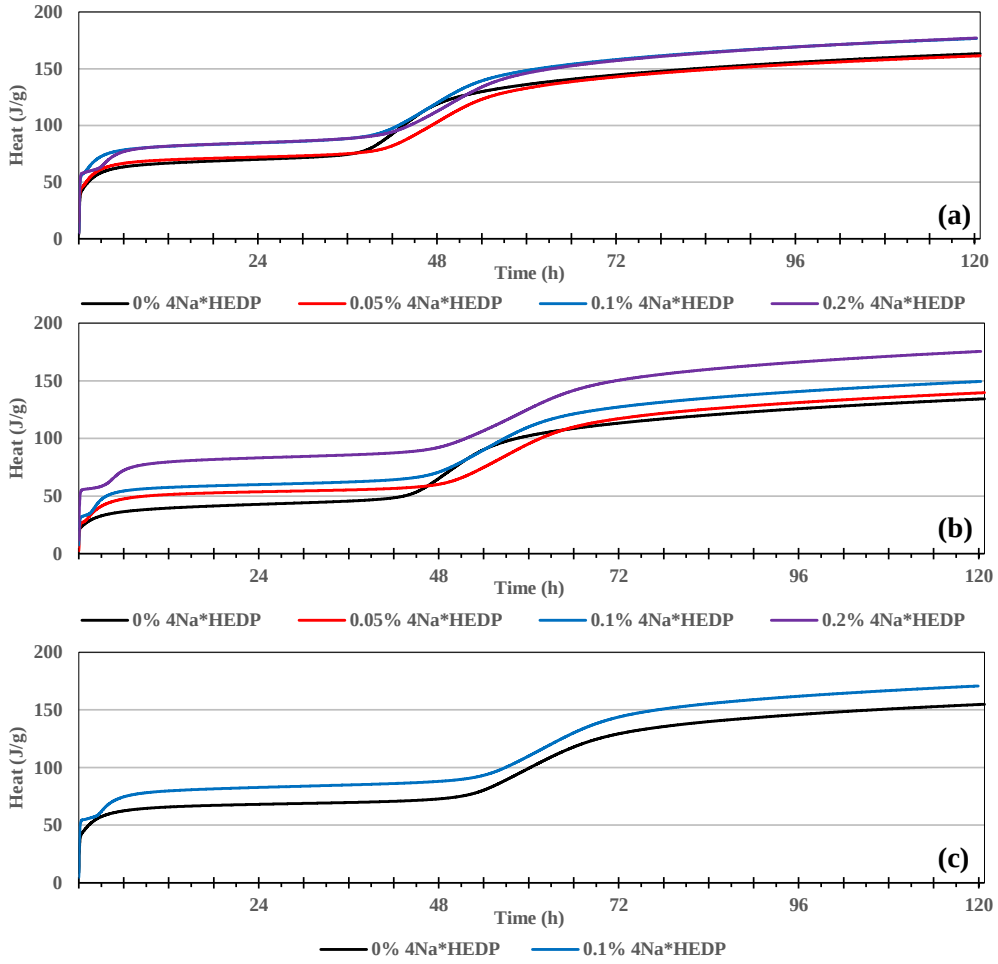

*Figure 3.21: Heat released during GGBS hydration with 8% Na_2CO_3 at different Water/GGBS ratios: 0.35 (a); 0.40 (b) and 0.45 (c) and different amounts of 4Na*HEDP*

3.4.1 Impact of the activator dosage on the phosphonate effectiveness

At a lower activator amount (6%), the retardation effect of the phosphonate is enhanced (Figure 3.22). It is expected that when decreasing the Na_2CO_3 content, the kinetics of formation of the carbonate-based hydrates (to be hindered) and the rate of Ca^{2+} leaching (to be sequestered) decrease. Less retarder is then required. Note that at W/B ratio of 0.35 the strength-giving peak is delayed at a dosage of 0.2%. The optimum retarder dosage is then around 0.1%. For W/B=0.4 the strength-giving peak is delayed even at 0.1%. The phosphonate dosage should be then tuned according to both the activator content and W/B ratio. It can be observed that the first peak can actually be split into two separate peaks. The early hydration mechanism seems then to be affected by the presence of the phosphonate. This will be discussed below when analysing the hydration products.

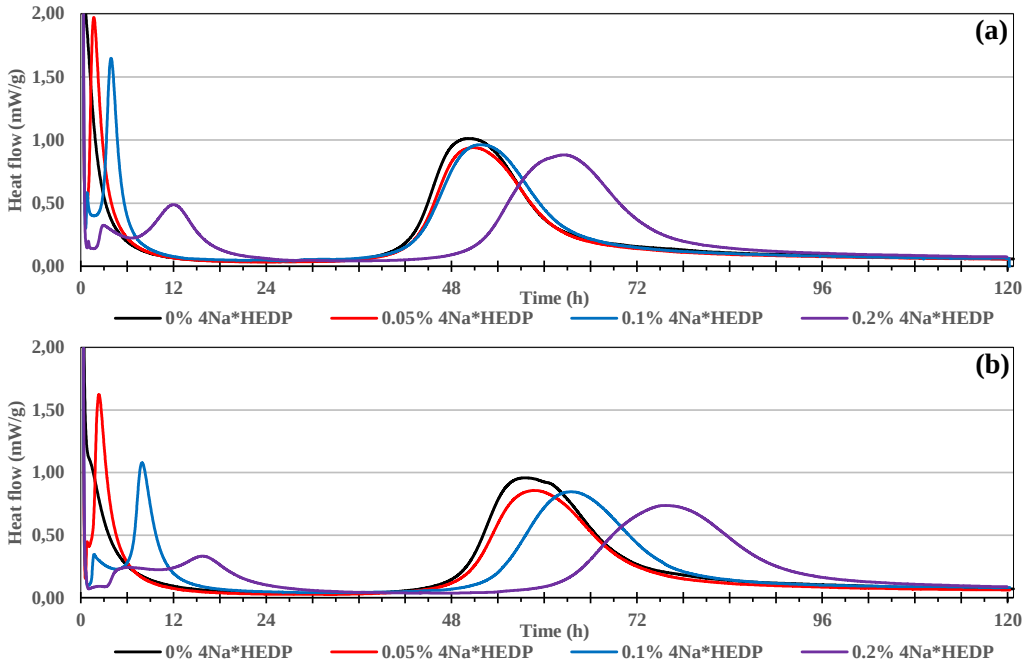

*Figure 3.22: Hydration kinetics of GGBS with 6% Na_2CO_3 and with different dosage of 4Na*HEDP at Water/GGBS ratio of 0.35 (a) and 0.40 (b)*

Further decreasing the amount of the activator (to 2% or 50g/l), even with a very small dosage of phosphonate significantly increases the induction period observed (Figure 3.23). It will be then a difficult task to find an optimum phosphonate dosage at low activator concentrations. Yet, this has no practical interest.

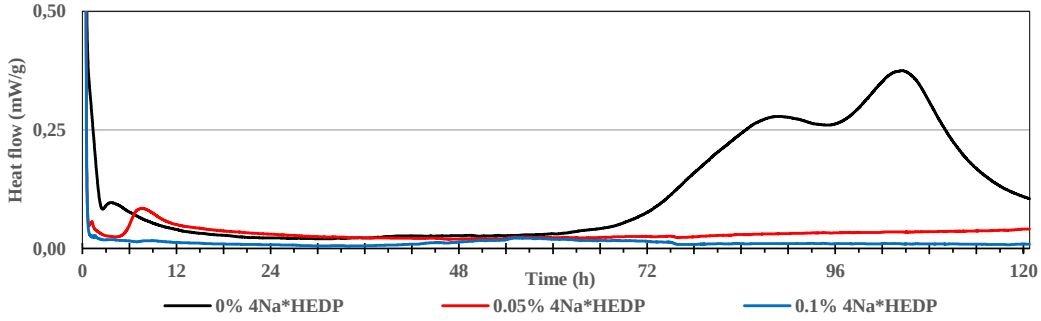

*Figure 3.23: Released heat upon hydration of GGBS activated with 2% Na_2CO_3 in the presence of 4Na*HEDP at W/B=0.40*

3.4.2 Increasing slag fineness

The impact of the phosphonate on the hydration kinetics in the case of finer GGBS (5600 cm^2/g) activated with 8% Na_2CO_3 is presented in Figure 3.24. A higher dosage is required for a significant delay of the first peak compared to GGBS 4400 cm^2/g. This should be directly related to a higher amount of calcium leached into the system from the beginning, which is indirectly confirmed by much higher heat released during the first 6 hours of hydration. In this

case it seems difficult to tune the retarder dosage, in particular at low W/B ratio; that is, to delay significantly the first peak without impacting the strength-giving peak.

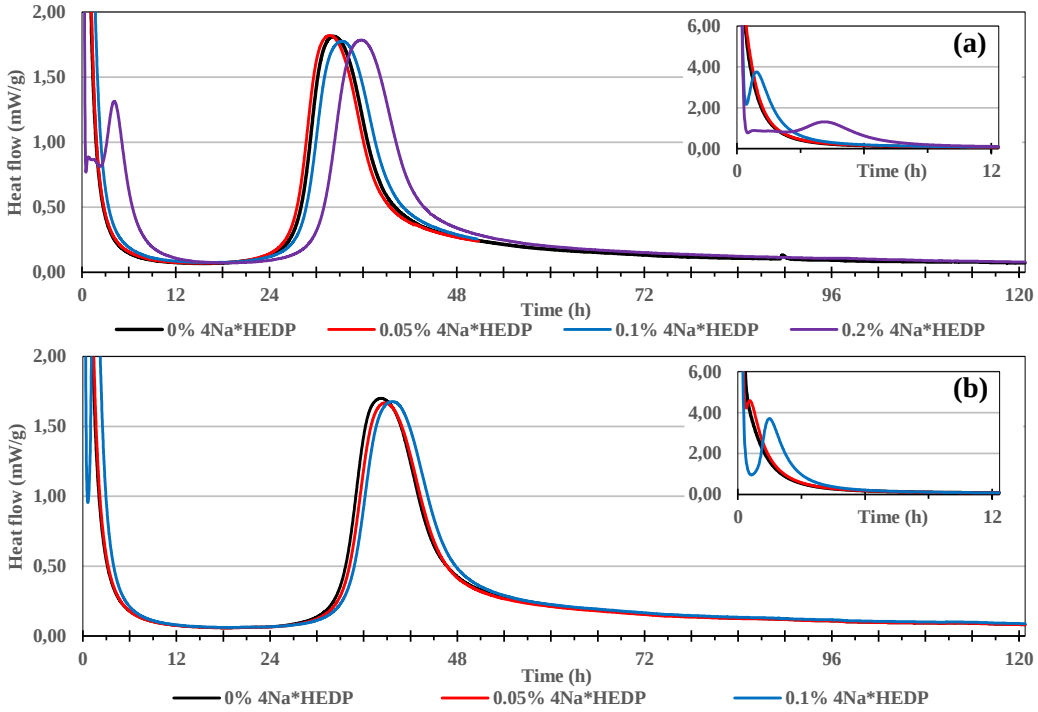

*Figure 3.24: Influence of 4Na*HEDP on the hydration kinetics of GGBS 5600 cm^2/g activated with 8% Na_2CO_3 at W/B ratio of 0.35 (a) and 0.40 (b)*

For a lower Na_2CO_3 dosage (6%) the retarder seems more difficult to be managed. For instance, for a dosage rate of 0.1% the first peak is significantly delayed (to more than 1h), while the strength-giving peak is not significantly affected (Figure 3.25).

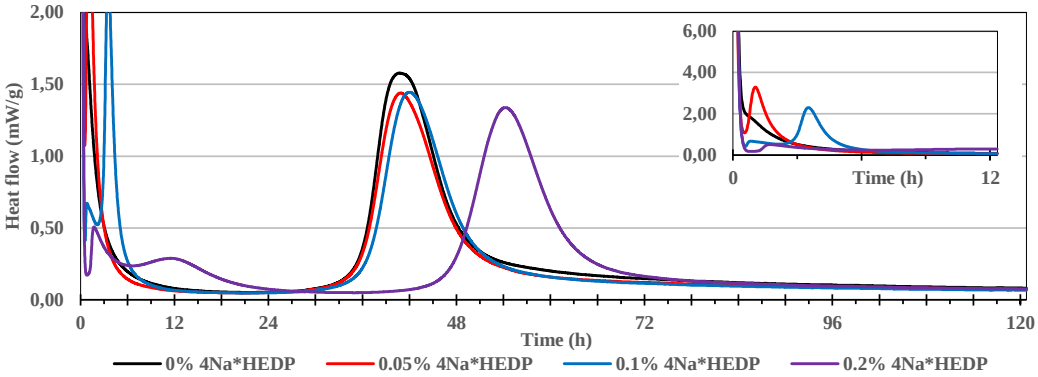

*Figure 3.25: Influence of 4Na*HEDP on the hydration kinetics of GGBS 5600 cm^2/g activated with 6% Na_2CO_3 at W/B=0.40*

The retardation effect of the phosphonate on the hydration kinetics is reported in Figure 3.26 in the case of a binder with standard GGBS replaced by 5% or 10% of ultrafine grade. Up to a dosage of 0.1%, a delay of the first peak can be obtained without any modification of the strength-giving peak. The first hydration peak, which can now be resolved thanks to the

presence of the retarder, is significantly higher than in the case of the two previous grades of GGBS. This reflects again the high reactivity of the Ultrafine GGBS.

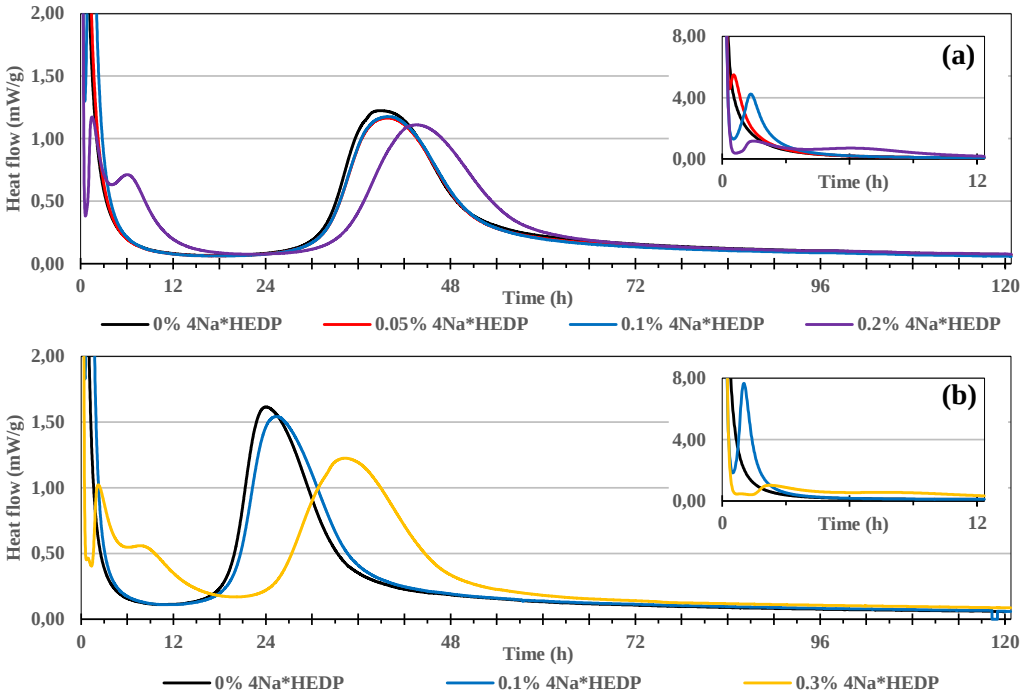

*Figure 3.26: Influence of 4Na*HEDP on the hydration kinetics of GGBS with partial replacement by Ultrafine GGBS: 5% (a) or 10% (b). W/B=0.40 and 8% Na_2CO_3*

3.5 Impact of the phosphonate on the early hydration products development through *In-situ* Synchrotron XRD

The measurements were performed at the Synchrotron SOLEIL, beamline Swing (France) following the procedure described in the previous chapter. The impact of the phosphonate on the hydration products development over the first 16min after contact between the powder and water is reported in Figure 3.27. There is no clearly observed crystalline phase formed in the presence of the phosphonate. In addition less fluctuations compare to the case of pure water can be observed (compared to Figure 2.66 and Figure 2.68). This confirms that the phosphonate affects the precipitation and/or the growth of the Ca-based hydrates (for ex. Gaylussite here) through Ca-complexation.

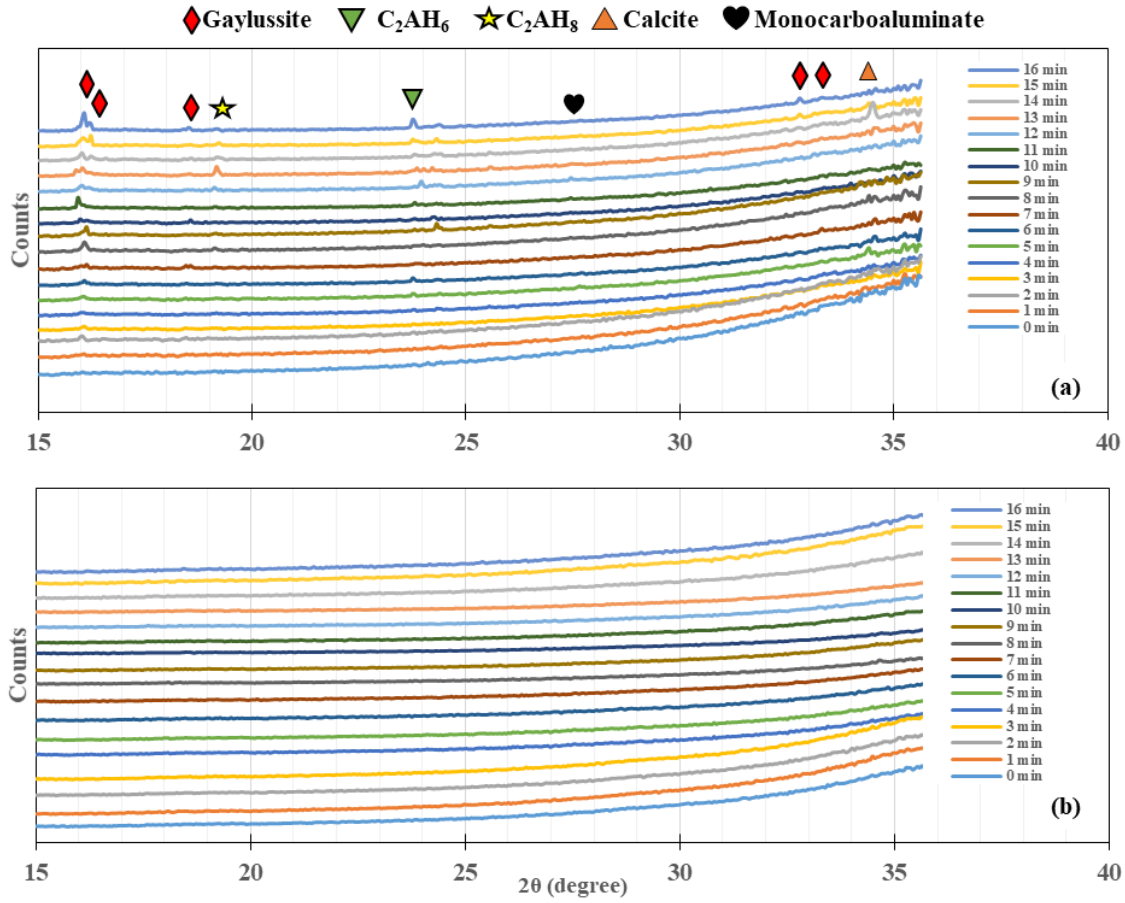

*Figure 3.27: Influence of 4Na*HEDP addition on the hydration phases during the first 16 minutes. GGBS 4400 cm^2/g, solution of 200 g/l Na_2CO_3 and 0% (a) or 0.1% (b) 4Na*HEDP*

The Synchrotron *in-situ* XRD of the pastes over the first 24 hours of hydration is reported in Figure 3.28. Beyond one hour, the effect of the phosphonate seems to have almost disappeared. Within the first hours, one can observe a slightly lower signal of Gaylussite for the first hours. Beyond this time, the Gaylussite becomes clearly more crystalline in the presence of the phosphonate from the first hours. This may be related to an eventual seeding effect of the phosphonate through the precipitation of Ca-phosphonates particles. These seeds may play the role of a template for the growth of Gaylussite, which will then have improved crystallinity.

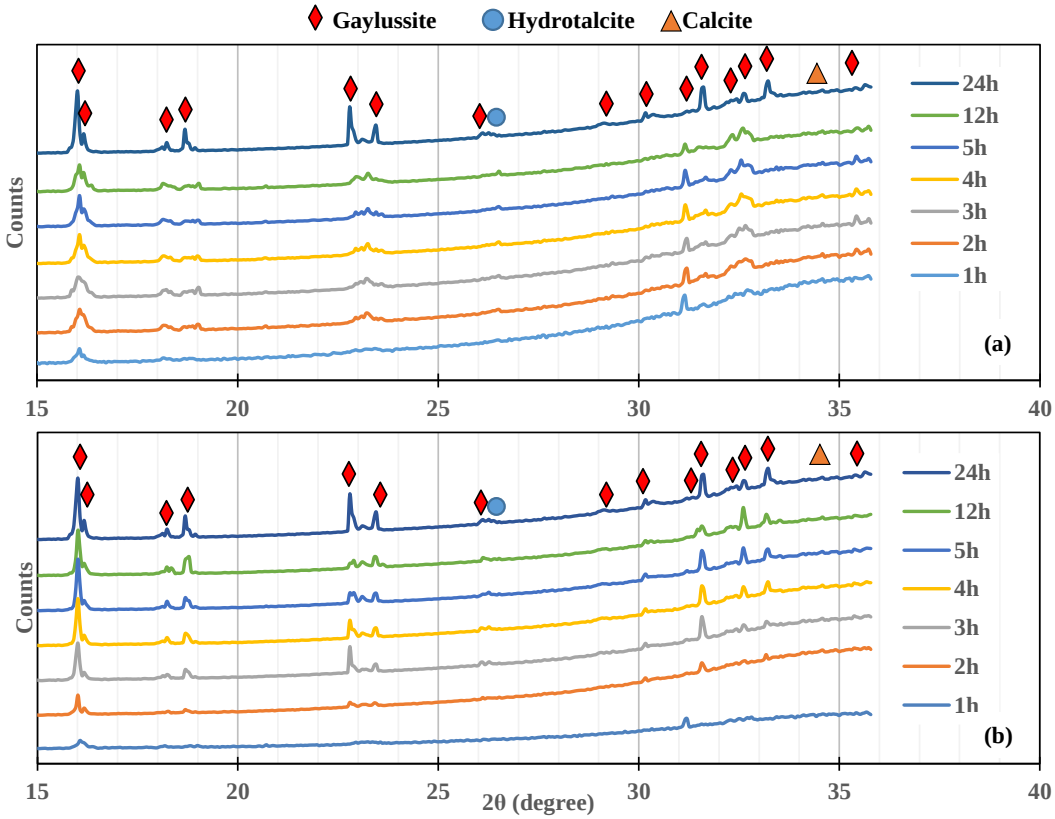

*Figure 3.28: Influence of 4Na*HEDP addition on the first 24 hours of hydration phases the case of Standard GGBS activated with 200 g/l Na_2CO_3 without(a) or with 0.1% 4Na*HEDP (b)*

3.6 Impact of the phosphonate on the long term development of the hydration phases: Laboratory *ex-situ* XRD

The impact of the phosphonate on the evolution over the first 24 hours of the XRD patterns in the case of GGBS activated with 8% Na_2CO_3 at W/B=0.35 is reported in Figure 3.29. These results show clearly that the development of Gaylussite's peak intensity is indeed delayed. It can be seen more clearly at high dosage of phosphonate (0.3%). Over time the Gaylussite signal tends to reach the same level independent of the phosphonate dosage. The main difference between the *in-situ* and *ex-situ* results is the presence of the Na_2CO_3 signal. Sodium carbonate might have precipitated upon drying during the preparation of the samples required for the ex-situ method.

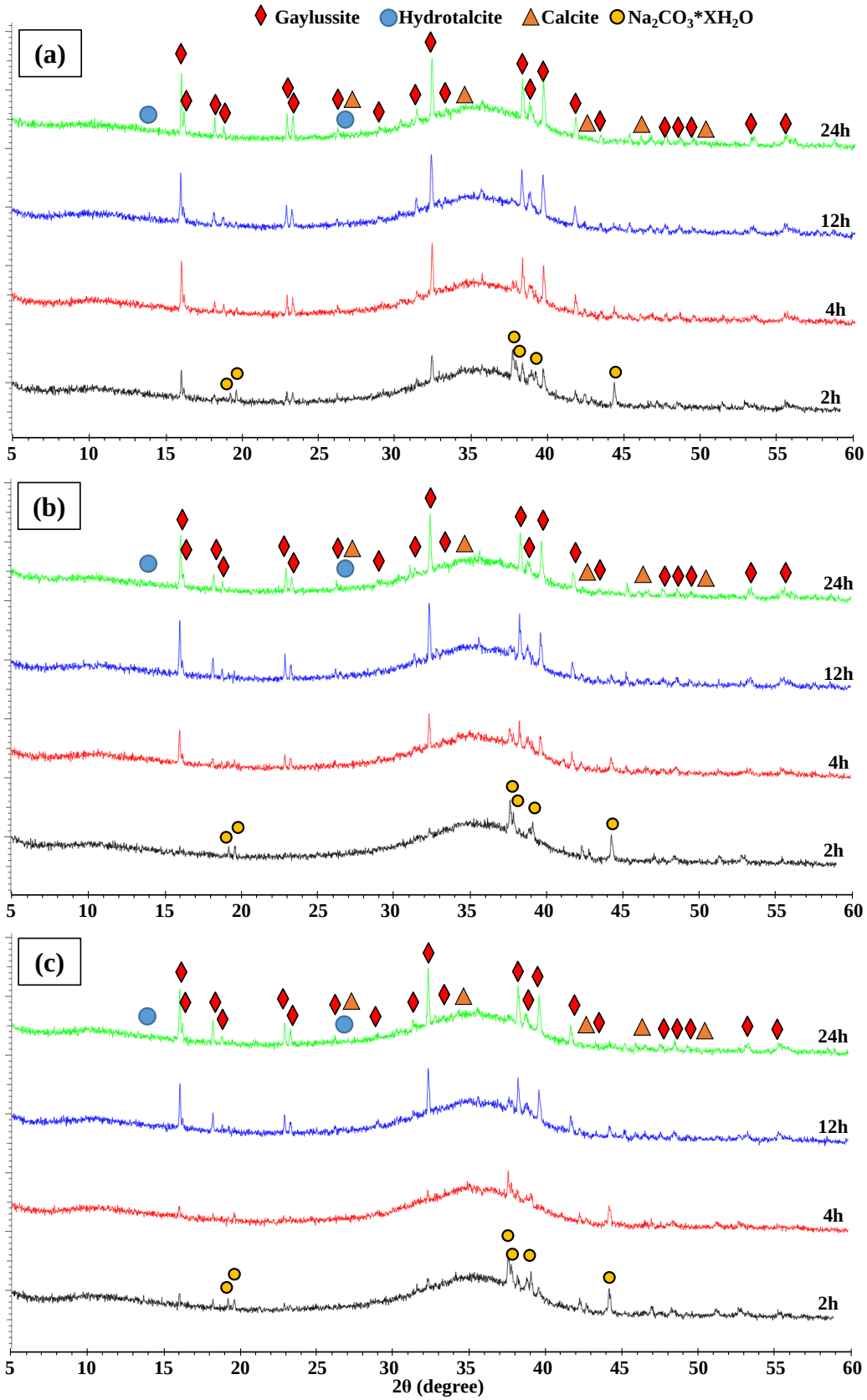

*Figure 3.29: Influence of 4Na*HEDP on the hydrates development over the first 24h. Paste of GGBS 4400 cm^2/g with 8% Na_2CO_3 and 0% (a), 0.1% (b) or 0.3% (c) 4Na*HEDP at W/B=0.35*

The impact of the phosphonate on the evolution of the XRD patterns in the long term (1 to 90 days) is reported in Figure 3.30. The hydration products impacted are mainly those based on calcium carbonate, including Gaylussite and $CaCO_3$ polymorphs. It was shown previously that in the presence of the phosphonate, Gaylussite growth was retarded and displayed improved crystallinity. In addition, it can be observed that in the long term Gaylussite seems more stable in the presence of the phosphonate. This is probably related to its improved crystallinity. More Vaterite and less calcite are formed in the long term in the presence the phosphonate. Usually Vaterite is a metastable $CaCO_3$ polymorph and transforms into the more thermodynamically stable Calcite. It forms only under well-controlled slow rate precipitation conditions, for instance in the presence of organic molecules (Manoli and Dalas, 2000). The phosphonate seems to stabilize Vaterite and hinders its transformation to calcite. Similar phenomena have already been reported regarding the crystallization of $CaCO_3$ in the presence of polymers or oligomers containing phosphonic groups (Wang et al., 2009). This mechanism so can be also responsible for Gaylussite stabilisation.

The content of the Afm phases monocarboaluminate and/or Hydrotalcite are slightly affected by the presence of the phosphonate. At long term their content seems to be diminished. This may be correlated with the stabilisation of Gaylussite by the phosphonate since each of these phases require CO_3^{2-} ions (samples were prevented against external CO_2 contact).

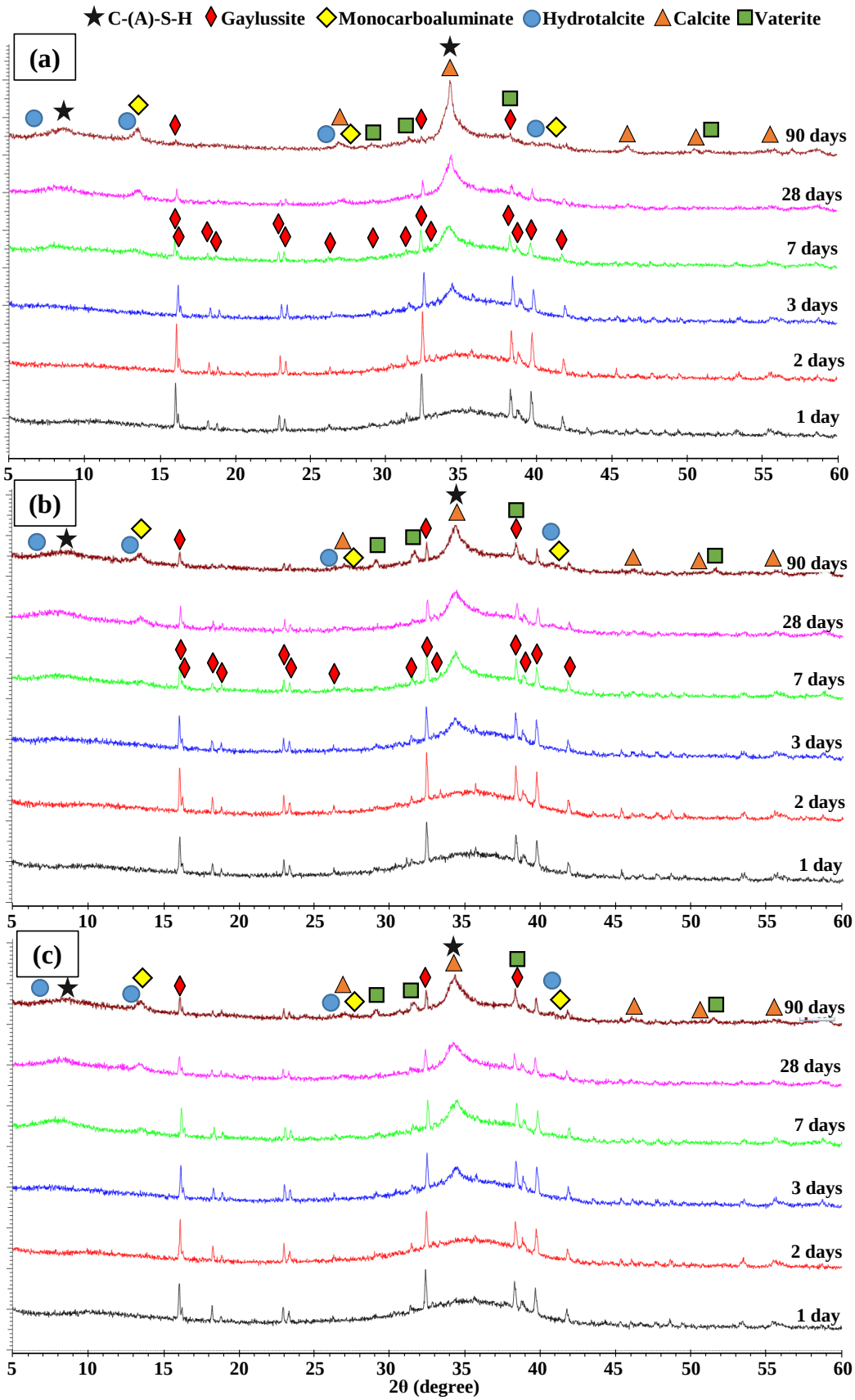

*Figure 3.30: Influence of 4Na*HEDP on XRD patterns evolution over hydration from 1 to 90 days, in the case of Standard GGBS activated with 8% Na_2CO_3 with different phosphonate contents 0% (a), 0.1% (b) or 0.3% (c) at W/B=0.35*

3.7 TGA analysis

Since with XRD analysis only crystalline phases can be examined, complementary techniques should be used to deal with amorphous phases. Here the thermogravimetric analysis (TGA) was used. A Sytsys 16/18 TGA-DSC/TMA instrument was used (Figure 3.31). Approximately 100 mg of crushed sample powder was subjected to a heating rate of 10°C/min from 25°C to 1000°C in an argon atmosphere. The samples of paste were prepared following the same procedure used for the Laboratory XRD analysis.

Figure 3.31: Sytsys 16/18 TGA-DSC/TMA instrument

The results of TGA (TG-DTG curves) for GGBS activated with 8%Na_2CO_3 at W/B =0.40 at 28 days without or with phosphonate (0.1%) are presented in Figure 3.32. As usual most of the water is lost between 50°C and 250°C. Up to about 100°C this corresponds mainly to free water. In addition, in some hydrates such as Gaylussite (Johnson and Robb, 1973) or sodium carbonate hydrates, the water is only weakly linked and it escapes within this temperature range. Beyond this range, the mass loss corresponds to the non-structural bounded water in C-S-H. Since the main peak is at 115-116°C this corresponds rather to C-(A)-S-H. The TG peak on the right hand side corresponds to Ca-Al Afm phases including CAH-type and Ca-carboaluminate hydrates (CAĈH) (Morsy et al., 2008; Jin and Al-Tabbaa, 2015; Collier, 2016). The addition of 0.1% 4Na*HEDP leads to a slightly higher weight loss within this main TG peak (up to 250°C). Consequently a higher amount of the corresponding hydrates was formed, which may explain the greater strength values with phosphonate addition as it will be shown in next chapter. This may be related to an eventual seeding effect of the precipitated Ca-phosphonate particles.

Weight loss at 250-350°C is related to the decomposition of Hydrotalcite with a peak at about 320°C (Frederic, 2012; Frost et al., 2009). The weight loss in the temperature region between 600°C and 800°C is attributed to the decarbonisation of the carbonate phases (Jacquemot, 2014; Jin et al., 2014; Jin and Al-Tabbaa, 2015; B Yuan et al., 2017a). A slight changes in this region in the presence of phosphonates migth be related to a minor changes in Calcite/Vaterite amount seen with *ex-situ* XRD.

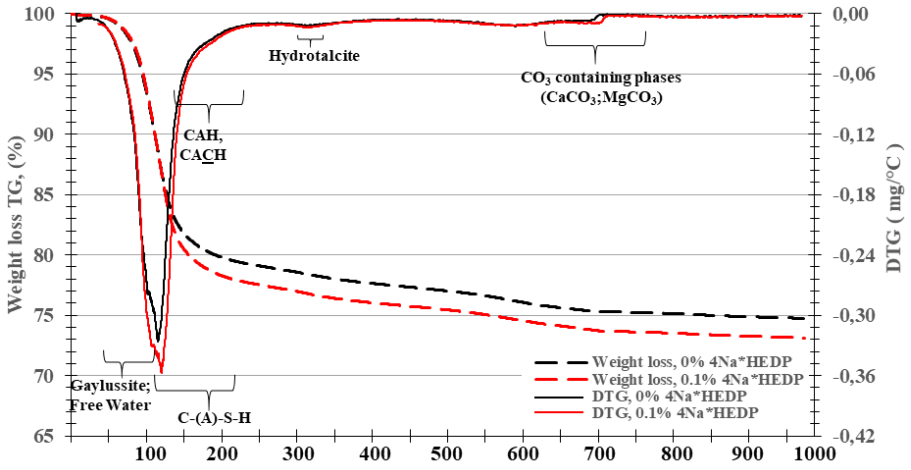

*Figure 3.32: Influence of 4Na*HEDP on TG-DTG curves in the case of GGBS activated with 8% Na_2CO_3 at W/B=0.40 with 0% or 0.1% 4Na*HEDP at 28 days*

TGA measurements at 120 days (in the case of the mix with the phosphonate), show that the hydration process beyond 28 days is non-negligible (Figure 3.33). It can be observed that the mass loss under 105°C decreases between 28 days and 120 days. This may be related to more free water consumed by hydration process and the decrease in the amount of Gaylussite (as shown above with XRD). There is a clear increase in weight loss in the region of 180-250°C. This corresponds to an increase of C-A-S-H, CAH and carboaluminate hydrates.

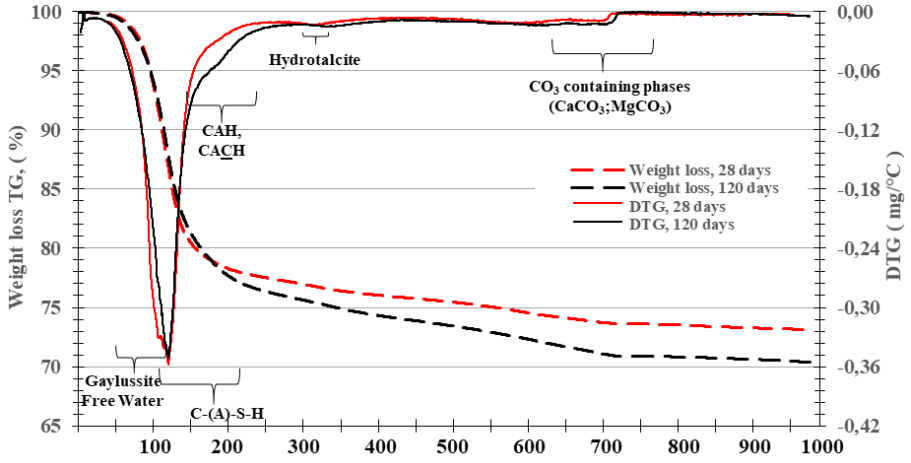

*Figure 3.33: Evolution of TG-DTG curves at long term for GGBS activated with 8% Na_2CO_3 at W/B=0.40 with 0.1% 4Na*HEDP. Comparison between 28 and 120 days*

3.8 Impact of the phosphonate on the microstructure: SEM observations

SEM images of samples of GGBS activated with 8% Na_2CO_3 at W/B=0.35 without and with phosphonate addition are reported in Figure 3.34. An overall high amount of non-reacted GGBS can be observed in both cases (light grey colour, since GGBS is denser than the hydrates). The finest slag grains seem to have reacted more in the presence of the phosphonate.

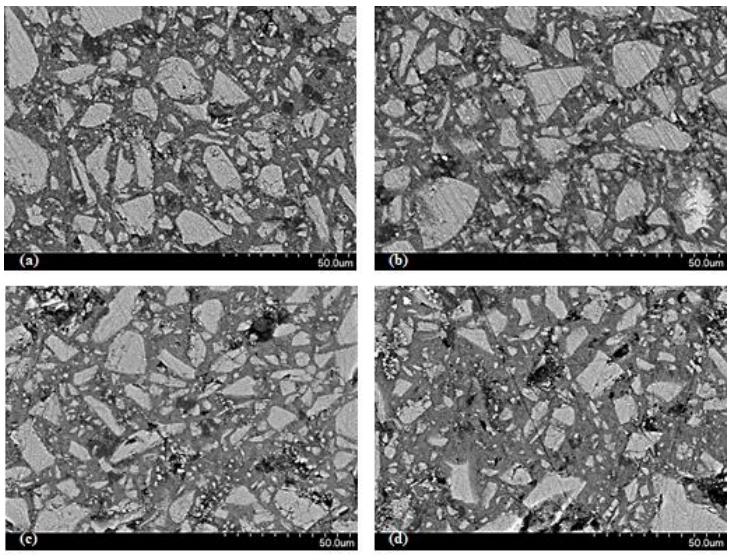

*Figure 3.34: Influence of 4Na*HEDP on the microstructure (through SEM imaging) of GGBS activated with 8% Na_2CO_3 without (a-b) and with 0.3% (c-d) 4Na*HEDP, at the age of 28 days at W/B=0.35*

Evaluation of the amount of unreacted slag was performed by measuring the surface of the 30 treated images corresponding to the grey level of unreacted slag (Baroghel-Bouny et al., 2002). A free program "Mesurim Pro" was used. The amount of unreacted slag can be estimated as the following:

$$A=100\%*(1-(S_{anhydr}/S_0)), \text{ with } S_0=1/(1+(\rho*(W/B))),$$

A – amount of unreacted slag
S_{anhydr} - surface of unreacted slag at the measuring age (in % of image surface)
S_0 – initial surface of unreacted slag (calculated value)
ρ – slag density

Results clearly shows a high amount of unreacted slag in all the samples. A very low dissolution of the slag is noted between 7 and 28 days, which is expected to decrease as time increases. This observation is consistent with the continuous long term hydration process and compressive strength increase for such products. The strength was observed to increase even after 10-15 years of hardening (Shi. et al., 2006). Figure 3.35 shows that even if the difference is quite small, the hydration degree of the slag is indeed higher in the presence of the phosphonate (due to the low accuracy of this method, supplementary measurements are required).

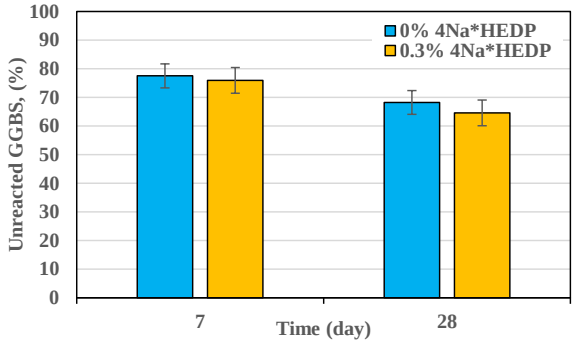

*Figure 3.35: Influence of 4Na*HEDP on the percentage of unreacted GGBS activated with 8% Na_2CO_3 at W/B=0.35, at 7 and 28 days*

3.9 Impact of the phosphonate on the microstructure: X-ray commuted microtomography

SEM observations were completed with X-ray 3D computed micotomography (μCT)). It is a non-destructive method that can be used to characterize the 3D microstructure (porosity, micro-cracking, etc.) at micron scale without any treatment. However the spatial resolution of the laboratory set-up used here (1 pixel=3.8μm) is lower than that of SEM.

The North 130 Star Imaging X50+ scanner available in the researcher's laboratory was used here (Figure 3.36). The X-ray beam was tuned at 180kV and 50μA with tungsten as a source of radiation and target. The values are related to the sample geometry and material characteristics (in particular density).

Figure 3.36: X-ray CT scanner for non-destructive microtomography observation of the sample 3D microstructure

The binder sample was cured in a plastic test-tube and placed, without any treatment, on a rotating platform for tomographic scanning (Figure 3.37). 1200 scans with 20 images per angular position were used. Each scan corresponded to a 360° rotation about the sample's vertical axis. A series of high resolution images of 3073x3889 pixels with a physical voxel size of 3.8 μm^3 has been used for the 3D reconstruction. The acquisition for each pixel, presented by the material's specific X-ray absorption coefficient, was normalized to 16-bit grey values. The brightness intensity of each voxel is directly related to the local density (Bossa et al., 2015). The brightness is higher for higher density. The air voids are represented by black colour (zero on the grayscale). An example of a μCT scan is presented in Figure 3.38.

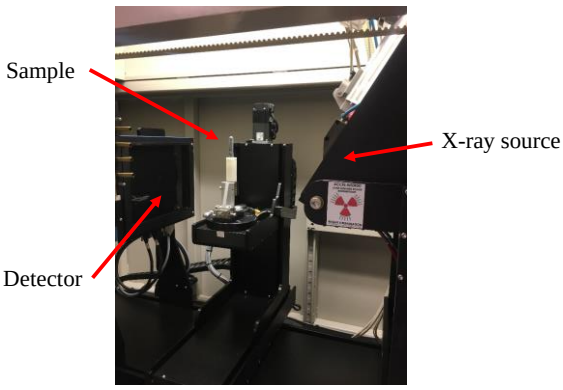

Figure 3.37: Set-up for micrptomography scanning

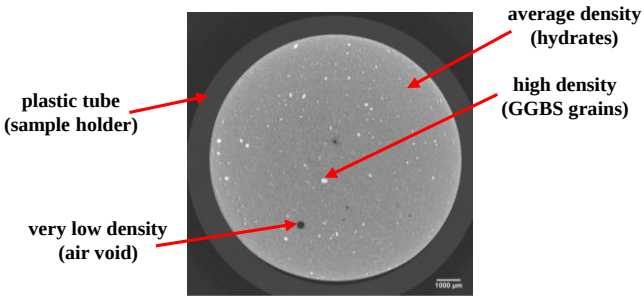

Figure 3.38: Example of CT scan of AA-GGBS paste

By comparing the formulations with and without 4Na*HEDP (Figure 3.39), lower macro porosity (black air voids) can be observed in the presence of the additive. Some cracks can be observed in all the samples. Yet, in the presence of the phosphonate only fewer cracks are observed. This may be the consequence of improved rheology and higher hydration in bulk.

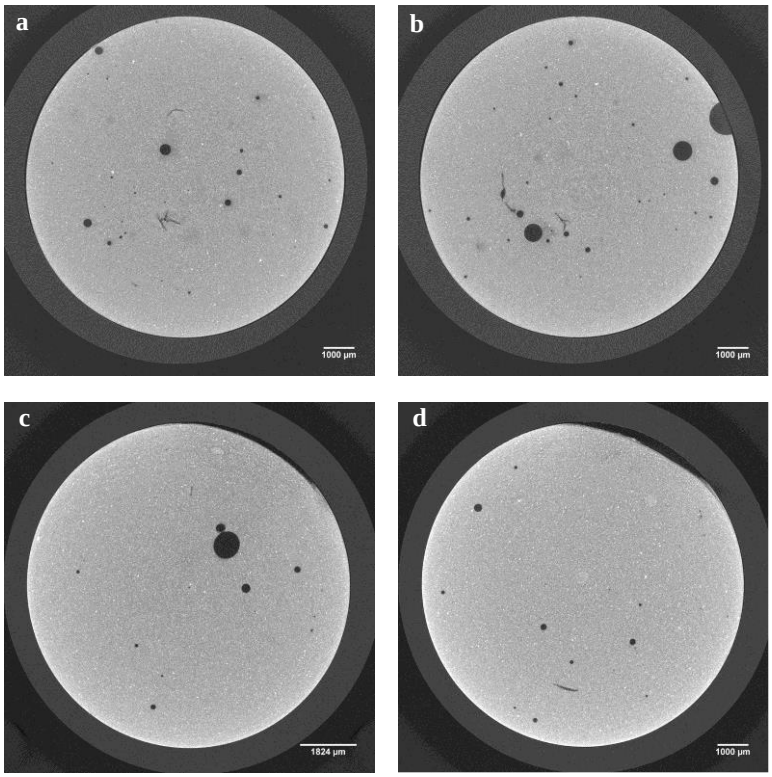

*Figure 3.39: Tomography scans. Comparison between 0% (a,b) and 0.1% (c,d) of 4Na*HEDP for GGBS with 8%Na_2CO_3 and W/B=0.40 at the age of 120 days.*

3.10 Impact of the phosphonate on the Gaylussite precipitation

It was shown through XRD that the presence of the phosphonate impacted the amount and crystallisation degree of Gaylussite. To consider the phenomenon in a more quantitative manner, Gaylussite was synthesized in the presence or absence of the phosphonate in solution.

Gaylussite was synthesized through the following procedure. 5g of $CaCl_2$ was first dissolved in 10 ml of demineralised water at 22°C (concentration of 4.5 mol/l). 10g of Na_2CO_3 was dissolved in 50 ml of demineralised water (concentration 1.9 mol/l or 200 g/l Na_2CO_3). Such a concentration of sodium carbonate within this temperature range should promote Gaylussite formation and inhibit calcite formation (Bury and Redd, 1933; Dheilly and Tudo, 1997). The phosphonate blended samples were prepared by adding 4Na*HEDP at different dosage rates into the sodium carbonate solution. The Na_2CO_3 and $CaCl_2$ solutions were quickly and thoroughly hand mixed. Immediately following contact between the two transparent solutions, the final solution becomes turbid white indicating rapid precipitation of particles. Four different samples were prepared, containing different amounts of 4Na*HEDP: 0 g/l, 1.67g/l (low, 1670 ppm), 5g/l (middle, 5010ppm) and 16.7 g/l (high, 16700ppm) in the final solution. The main challenge is minimizing $CaCO_3$ precipitation and other Na/Ca-Carbonates.

The chemical reaction between the two solutes leading to Gaylussite is:

$$CaCl_2 + 2Na_2CO_3 \xrightarrow{H_2O} 2NaCl + Na_2Ca(CO_3)_2 * 5H_20$$

Figure 3.40 shows the solutions after precipitation, before centrifugation and drying. A white precipitate can be observed in all cases. Without the phosphonate, most of the precipitated particles settle rapidly on the bottom of the container. This indicates that the particles (or aggregates) are quite large. On the other hand, in the presence the phosphonate a significant fraction of particles remain suspended in the liquid. Increasing the phosphonate dosage leads to an increase of the fraction of the suspended particles. This suggests that phosphonate presence leads to the precipitation of finer particles (growth inhibition) and/or prevent their agglomeration.

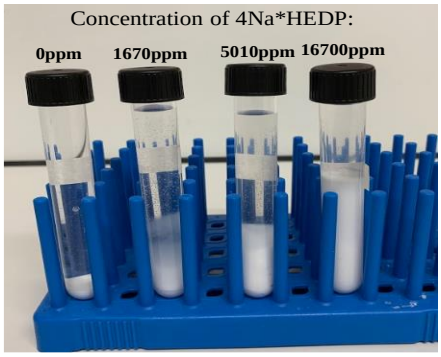

*Figure 3.40: The appearance of the samples one hour after the synthesis of Gaylussite (white precipitates) at different concentrations of 4Na*HEDP*

After 4 hours in an aqueous solution, the samples were centrifuged to separate the precipitate from the liquid. The recovered solid was dried at 35°C to eliminate residual moisture and was immediately analysed. The results of XRD reported in Figure 3.41 show that the main precipitated products are Gaylussite ($Na_2Ca(CO_3)_2*5H_2O$) and Halite (NaCl). Nevertheless, traces of Calcite ($CaCO_3$) and unreacted Sodium Carbonate Hydrate ($Na_2CO_3*xH_2O$) are also detected. The addition of the phosphonate leads to a significant modification of the precipitated products. In the case of low dosage rate of phosphonate (1670 ppm here) a much higher (in terms of XRD signal) amount of all crystalline products were observed. In addition, they have a higher degree of crystallinity or with a much lower amount of structure defects (thinner peaks). Further, by increasing the phosphonate (up to 16700 ppm) the Gaylussite peaks become larger, indicating the presence of significant defects in the crystalline structure. In this case the appearance of a signal from Ca-HEDP can also be clearly observed (Browning and Fogler, 1996). These nano-sized crystals might be embedded in the Gaylussite structure, leading to the decrease of its crystalline order.

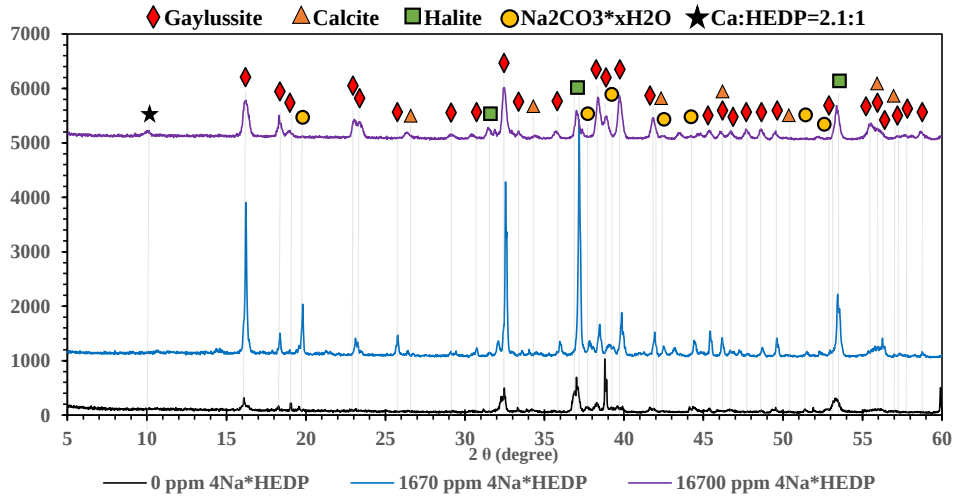

*Figure 3.41: XRD patterns of precipitates particles from direct Gaylussite synthesis throw $CaCl_2/Na_2CO_3$ solution with different amount of 4Na*HEDP*

Examination by SEM was performed on these samples for the determination of particle size and observation of the qualitative aspects. Analysis of the sample without 4Na*HEDP coupled with EDX analysis confirms the presence of Gaylussite crystals (Figure 3.42).

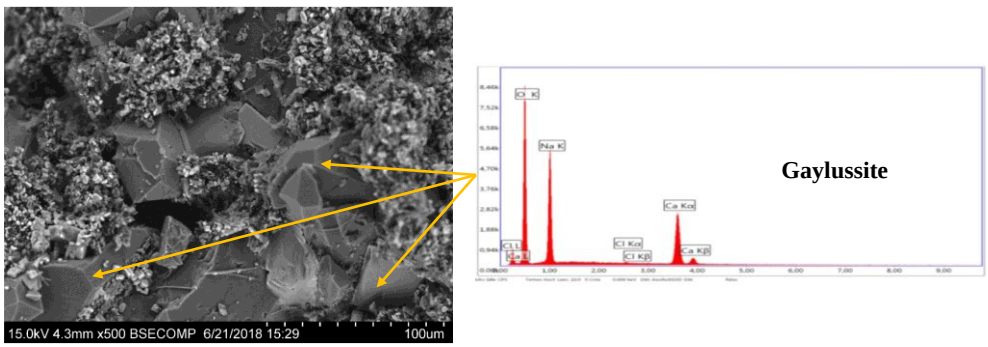

*Figure 3.42: SEM/EDX analysis of synthetized Gaylussite crystals without addition of 4Na*HEDP*

The SEM images of the sample showed that the average particle size is approximately 80-150 μm (Figure 3.43). In addition, all of the crystals have a lot of defects compared to the perfect Gaylussite crystal (Figure 3.44) and they are agglomerated. The small particles deposited on their surface are identified as Calcite ($CaCO_3$), NaCl and different Na_2CO_3*xH_2O crystals.

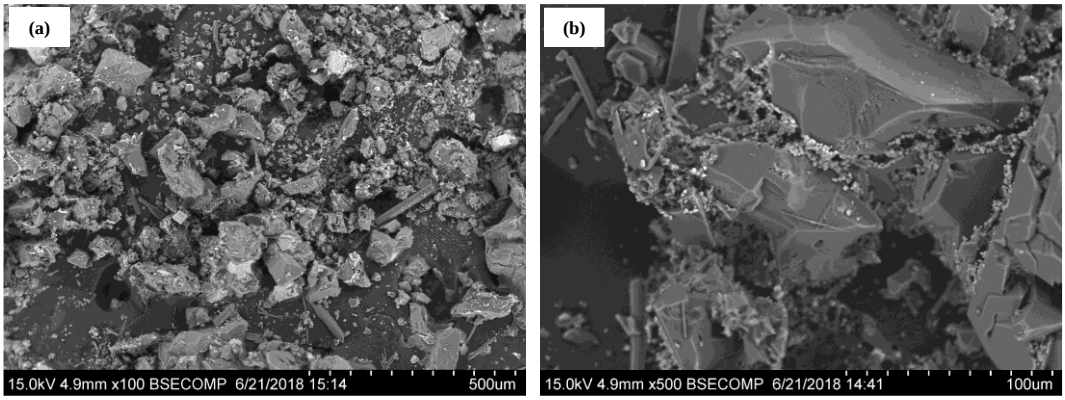

*Figure 3.43: SEM observation of synthetized Gaylussite crystals without addition of 4Na*HEDP*

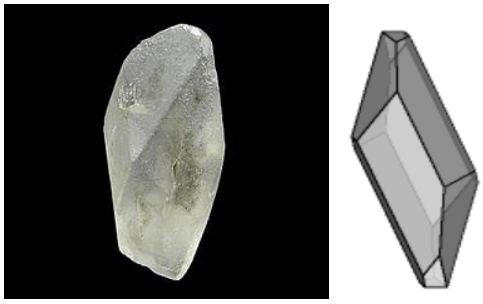

Figure 3.44: Perfect Gaylussite crystal (https://www.mindat.org/min-1662.html)

In the presence of a low amount of phosphonate, significant apparent structural modifications can be observed (Figure 3.45). The shape of the Gaylussite crystals is close to *perfect*; they seem to have minimum structural defects and they are not agglomerated. This is correlated with the XRD results above. Precipitation into individual crystals might be related to the abovementioned seeding effect of the precipitated Ca*HEDP particles.

EDX analysis of the Gaylussite crystals shows that phosphonate molecules are embedded into its structure (revealed by the presence of Phosphorus peak) (Figure 3.46).

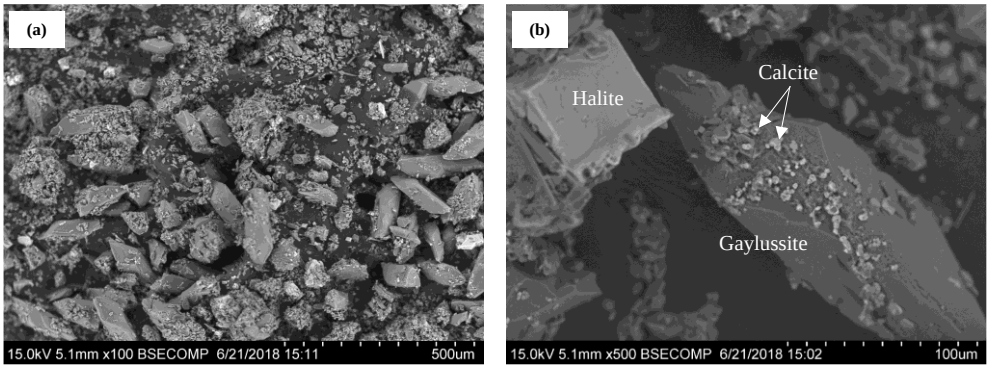

*Figure 3.45: SEM observation of synthetized Gaylussite with low 1670 ppm 4Na*HEDP concentration*

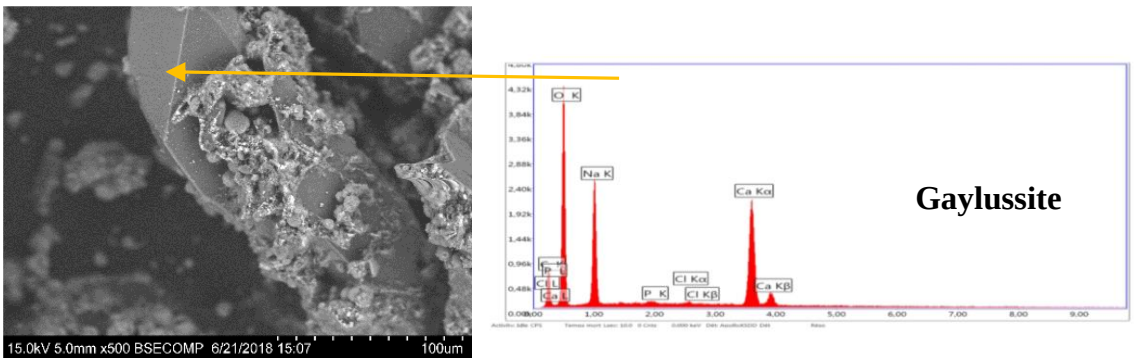

*Figure 3.46: SEM/EDX analysis of synthetized Gaylussite crystals with low 4Na*HEDP concentration*

A further increase in the amount of phosphonate leads to a significant reduction of the average size of Gaylussite crystals (5-20 µm in length) (Figure 3.47). In addition the particle shape becomes plate-like, with and aspect ratio Length/thickness of 3-4. No apparent agglomeration of crystals can be observed. The modification of the form of the crystals is probably related to the possible formation of fibrous Ca*HEDP (with Ca/HEDP=1:1) instead of its isotropic form (Ca/HEDP=2.1:1) and a mix of thereof. This might be due to lack of calcium or due to higher amount of 4Na*HEDP in this case (Browning and Fogler, 1996). The EDX analysis confirms the incorporation of HEDP into the Gaylussite structure (Figure 3.48).

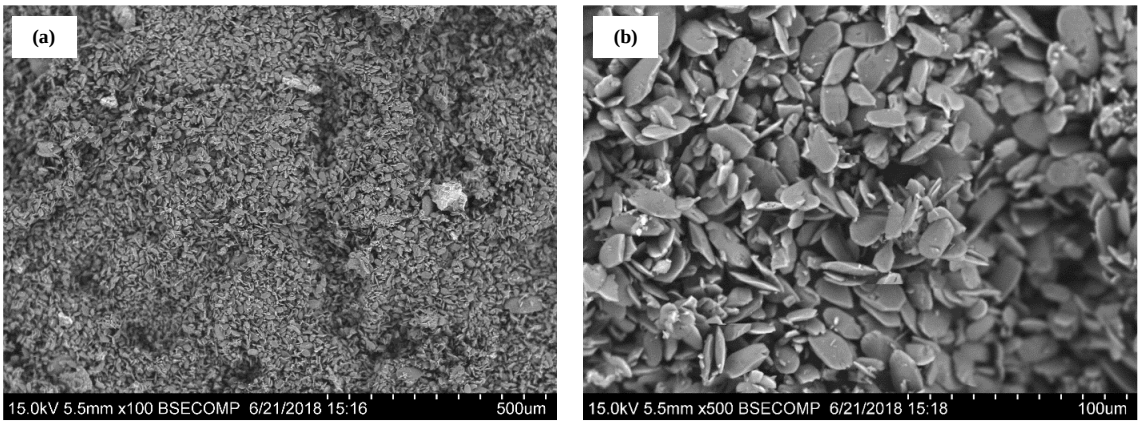

*Figure 3.47: SEM images of synthetized Gaylussite with high 4Na*HEDP concentration (16700 ppm)*

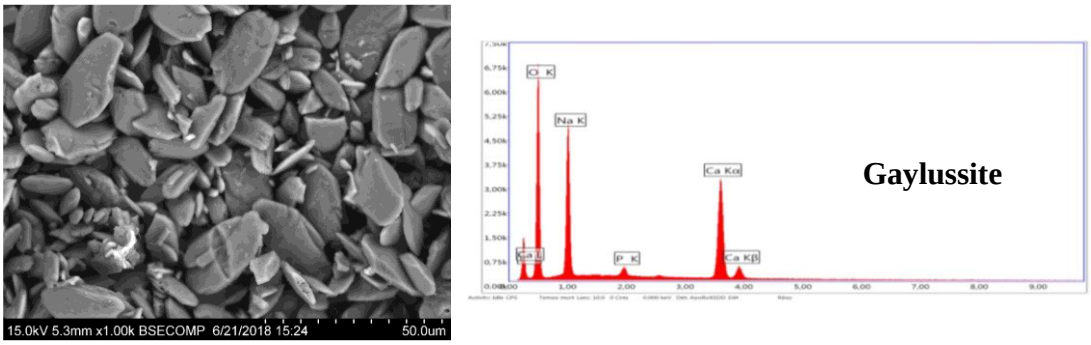

*Figure 3.48: SEM/EDX analysis of synthetized Gaylussite with high 4Na*HEDP concentration*

Through the previous XRD analysis it was also observed that the addition of the phosphonate led to a slower Gaylussite decomposition (higher stability). To verify this effect,

the samples with and without the phosphonate addition were diluted 3 times with deionized water and stored for 48h at 35°C. Such conditions are expected to lead to destabilisation of the Gaylussite due the decreased CO_2 concentration in water (at high temperature). Then, the solution was centrifuged and dried at 35°C. The SEM images are reported in Figure 3.49. Without phosphonate addition, all of the Gaylussite was transformed into calcite (Figure 3.49a and Figure 3.49b). For the samples containing the phosphonate only the beginning of the transformation is observed, i.e. Gaylussite is more stable. In this case all of the small crystals observed on the Gaylussite surface are calcite.

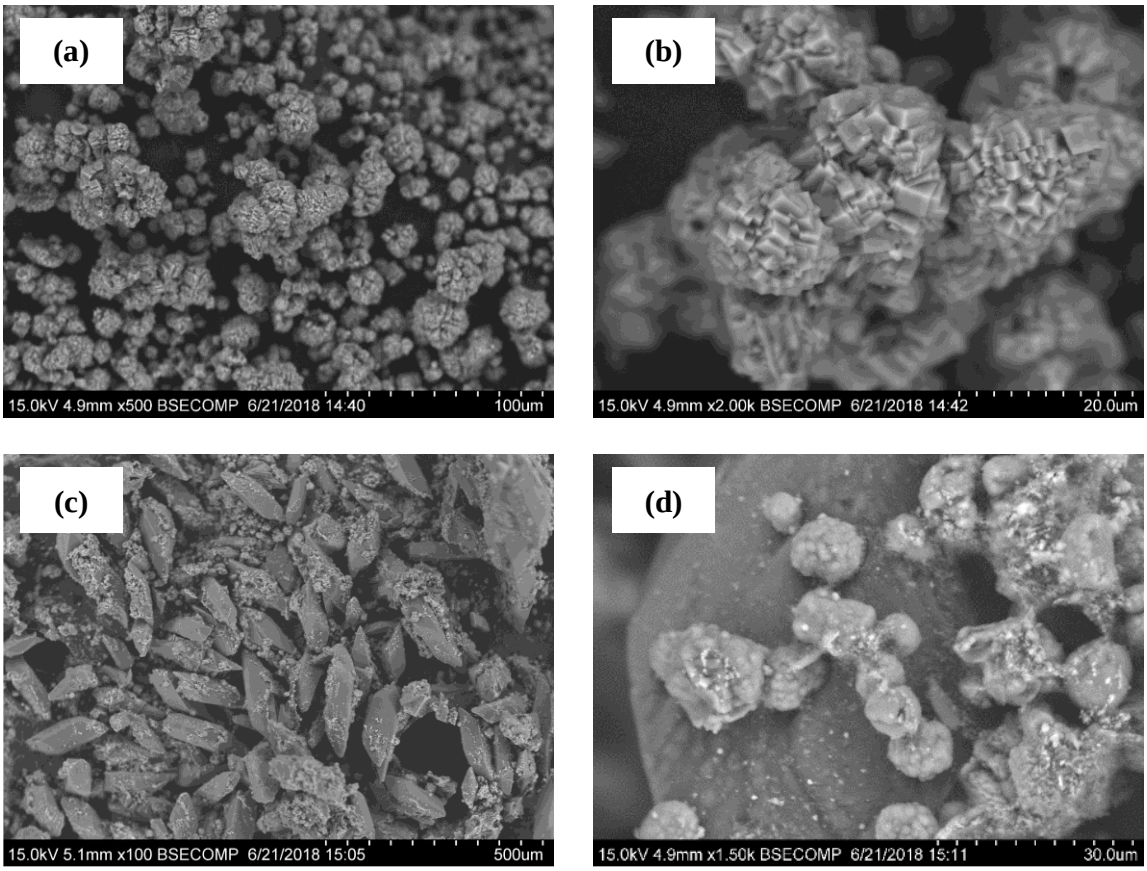

*Figure 3.49: SEM images of the samples after 48h of Gaylussite destabilisation through partial decarbonation without (a-b) and with addition of 1670 ppm 4Na*HEDP (c-d)*

These observations in simplified media are expected to hold in the case of the Na_2CO_3 activated GGBS pastes. It can be concluded that the presence of the phosphonate has several effects on Gaylussite. The phosphonate should play the role of template for Gaylussite growth through precipitation of Ca*Phosphonate particles. This will lead to an improved degree of crystallinity of this hydrate and therefore it becomes more stable. The effect of the phosphonate is then more than the complexation of Ca.

Conclusions

The obtained results showed that the rheological properties of Na_2CO_3 activated GGBS can be significantly improved by the addition of some specific additives, whose principle of action is interaction with Ca^{2+} ions. The most suitable additives are phosphonate salts, due to their possibility of dissolution and interaction in a Na_2CO_3 saturated medium. Depending on the chosen type, not only can an increase in setting time possible, but also a decrease in yield stress can be achieved.

The dosage of phosphonate has a significant influence on the rheology and also on the hydration kinetics. A high dosage leads to a significant increase in the induction period as seen with microcalorimetry, which should have a negative influence of strength evolution (lack of calcium for C-S-H precipitation, more stable Gaylussite). At the same time, no further positive impact of phosphonate over-dosage on decreasing the yield stress was observed. The additional influence of different parameters like slag fineness, W/B ratio and sodium carbonate concentration also take place as before.

Results of the ζ-potential measurements indicate that the addition of phosphonate leads to more negative values of surface charge, which increases the electrostatic repulsive forces of the particles and prevents their flocculation (the action mechanism of first generation plasticizers). This phenomenon is related to the Ca^{2+} complexation/consumption. Indirectly it was confirmed by lower conductivity and pH level. Lack of calcium for calcite/Gaylussite precipitation prevents excessively rapid in-situ formation of NaOH from Na_2CO_3. The results of the XRD analysis confirmed that at the very beginning the precipitation process of such phases was significantly affected (retardation of the precipitation and crystal growth). Increasing the phosphonate dosage leads to increasing of this influence. Phosphonate influence on the rate of crystals growing and/or their shape (seen with synthetized Gaylussite) is supposed also to be responsible to the rheology improving. A longer term phosphonate impact evaluation showed that the Gaylussite decomposition occurs more slowly. At the beginning of hardening, it has been suggested that due to a lack of calcium (consumed by phosphonate), a slower consumption of dissolved CO_2 occurs, leading to a longer Gaylussite decomposition period. In turn, this leads to a slower rise in pH. This fact, coupled one more time with calcium deficit, leads to a delay of C-S-H precipitation at the very early age.

The results of phosphonate influence on synthetized Gaylussite indicate an additional mechanism of its stabilisation at longer term. Through the calcium complexation, phosphonates

become part of Gaylussite. At certain dosages this leads to its higher crystallization degree and accordingly leads to a more stable form. This phenomenon should be related with the seeding effect of phosphonates. In fact, calcium salt of the tested phosphonate are nano-sized solid particles, which provide additional specific surface for nucleation. This phenomenon may mean that phosphonates do not completely prevent the precipitation of calcite/Gaylussite at the very beginning, but prevent their growth at the nano stage by their simultaneous precipitation on the large number of calcium-phosphonate solid seeds/particles. This seeding theory can be confirmed by more advanced (microcalorimetry, TGA) and more uniform hydration (SEM and tomography observations).

Chapter 4 Hardened state properties in the presence of the phosphonate

Introduction

In the previous chapter the positive effect of the phosphonate 4Na*HEDP on the rheological properties was demonstrated. Its addition leads not only to the extension of the open time (the duration in which the desired rheological properties are maintained), but also to the reduction of the yield stress. Thanks to this additive, it is now possible to test the impact of several mix-design parameters on the hardened properties. For example, the investigation of the effect of increasing slag fineness on compressive strength was limited due to the difficulty in preparing the samples, since the rheology is significantly reduced. Since the phosphonate additive plays the role of an effective plasticizer through a significant reduction of the binder yield stress, it should be possible to decrease the W/B ratio and maintain an acceptable rheology. Reducing the W/B ratio will lead to the improvement of strength and other long term properties.

It was also shown that the phosphonate impacted the distribution of the hydration products through, in particular, seeding effects. Hardened properties are then expected to be improved. Yet since we are dealing with early age, strength development may be negatively impacted if the phosphonate dosage is too high. This was seen through the isothermal microcalorimetry results in the previous chapter. Beyond a certain dosage, the evolution of the heat released during early hydration initiated a delay; not only of the first hydration peak (related to the loss of the rheological properties and setting), but also the main hydration peak associated with massive C-S-H formation. This retardation was less significant in the case of higher sodium carbonate concentration or higher slag fineness and was in any case dependent on phosphonate dosage.

In this chapter, the influence of different binder mix-design parameters (such as the activator concentration, W/B ratio and slag fineness in the presence of different dosage rates of the phosphonate) on the compressive strength and shrinkage will be considered. In addition, the impact of curing conditions (temperature and relative humidity) on these properties will be also examined.

4.1 Compressive strength evolution

4.1.1 Influence of the phosphonate dosage

The compressive strength development for a binder based on Standard GGBS (4400 cm^2/g) activated with 8% Na_2CO_3 at W/B=0.35 with different amounts of 4Na*HEDP is presented in Figure 4.1. At low phosphonate dosage (0.1%), a slight decrease in strength up to 2 days is observed. On the other hand, the strength is improved beyond 2 days and up to 1 year. This may be attributed to the previously discussed seeding effects of the phosphonate on the precipitation of Ca*phosphonate particles. In addition, the improvement of the rheology with the phosphonate might have resulted in a more homogeneous distribution of the binder around the sand grains. This will also lead to strength improvement. It is to be noted that lower phosphonate dosages were not considered since the rheology was not sufficiently improved. Increasing the phosphonate dosage to 0.4% leads to a significant degradation of the strength within the first 3 days. These results are correlated with the micro-calorimetry measurements reported in the previous chapter where a retardation of the strength-giving hydration peak was observed. Even with this high phosphonate dosage, the compressive long term strength is improved (beyond 7 days).

Again, it is interesting to note the continuous and remarkable increase of the compressive strength at long term beyond 28 days (here up to 1 year) in the case of Na_2CO_3 activated binders.

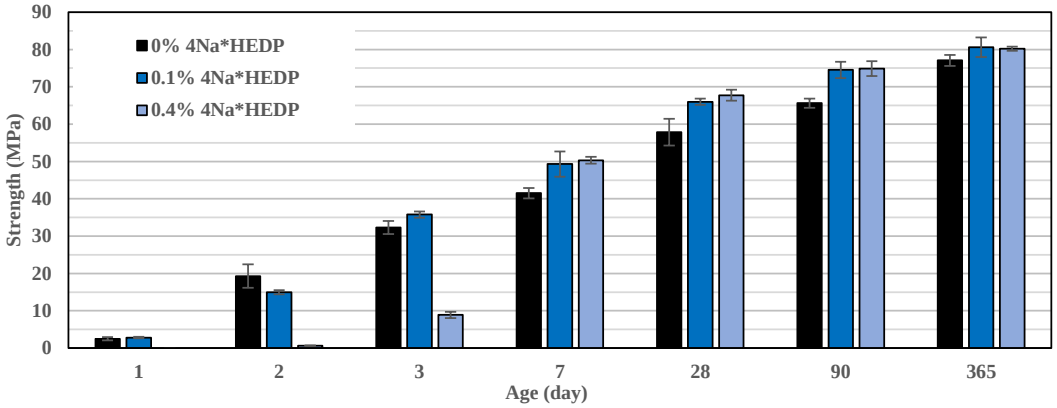

*Figure 4.1: Influence of 4Na*HEDP on strength evolution in the case of a binder based on 100% GGBS 4400 cm^2/g activated with 8% Na_2CO_3 at W/B=0.35*

Increasing the W/B ratio, and keeping the same Na_2CO_3 content by weight of GGBS, leads to a decrease in the strength especially in early age (compare Figure 4.2 and Figure 4.1) in correlation with the previous chapter's micro-calorimetry results. The long term strength tends to be almost independent of the W/B ratio. The impact of the phosphonate remains the same as at a lower W/B: there is a slight degradation at 2 days and improvement beyond.

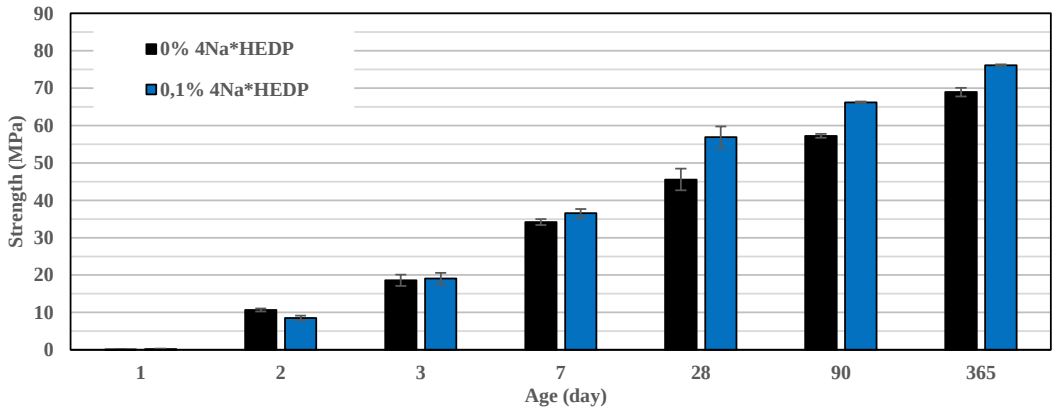

*Figure 4.2: Influence of 4Na*HEDP on strength evolution in the case of a binder based on GGBS 4400 cm^2/g activated with 8% Na_2CO_3 at W/B=0.40*

4.1.2 Influence of Na_2CO_3 concentration

The influence of the amount of activator on the mechanical strength development is reported in Figure 4.3. Increasing the dosage rate of Na_2CO_3 leads to an improvement in strength at all ages. At long term (1 year) the strength seems to become less sensitive to the activator dosage rate (though only 6% and 8% were considered). These results are not novel, however their interpretation is not clear. As discussed in the previous chapters, decreasing the amount of Na_2CO_3 will favour precipitation of calcite over Gaylussite due to an excess of Ca^{2+} relative to Na^+ (Bury and Redd, 1933). Small crystals of calcite are expected to precipitate on the slag surface from which the Ca^{2+} ions are leached. In contrast, Gaylussite, which contains Na^+, should rather precipitate in bulk solution, since the highly hydrated Na^+ (which is only monovalent) should have low tendency for adsorption onto the slag surface (Franks, 2002). Then, two main possible reasons may be put forward to explain the increase of the strength with activator dosage: (i) precipitation of a large amount of Gaylussite within solution, instead of calcite on the slag surface, leading to better distribution of the hydration products through additional nucleation sites, and (ii) large amount of *in-situ* formation of NaOH can be achieved upon destabilisation of the Gaylussite leading to high pH levels, then higher dissolution degree of the slag.

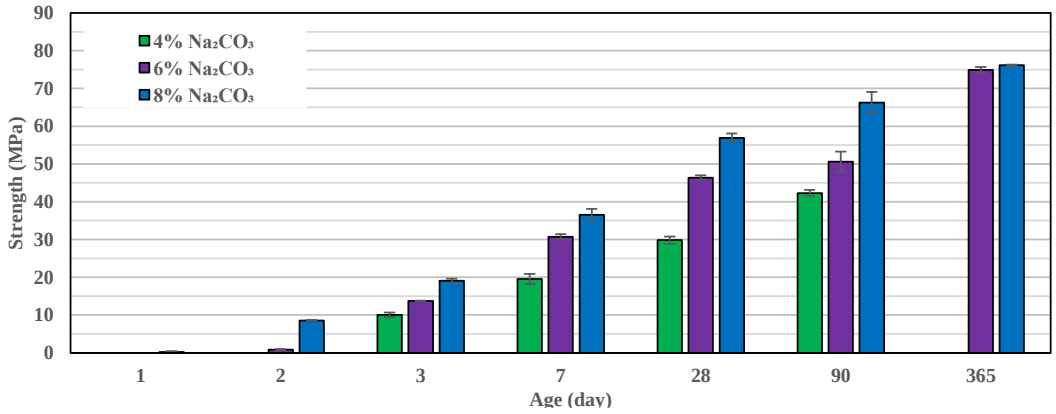

*Figure 4.3: Influence of Na_2CO_3 amount on strength evolution in the GGBS 4400 cm^2/g at different amount of activator (W/B=0.40 and 0.1% 4Na*HEDP)*

As for the microcalorimetry results, the aqueous concentration of the activator, instead of its content by GGBS weight, seems to be the relevant parameter for the strength development for a given phosphonate concentration. Previously micro calorimetry results indicated that the minimum optimal concentration is about 150 g/l to achieve setting after 24/48h and to have the possibility of sample demoulding. The results for the compressive strength versus this aqueous concentration of the activator at different ages is presented in Figure 4.4.

At 2 days the strength increases only slightly with the aqueous concentration of the activator. On the other hand, the strength is highly sensitive to the W/B ratio. At 3 days the sensitivity of the strength to the aqueous concentration of the activator increases, and at the same time it becomes less dependent upon W/B. At 7 days and beyond, the influence of W/B ratio becomes less significant and the strength evolution starts to be mainly controlled by the aqueous activator concentration. At long term (1 year) the strength becomes independent of both mix parameters, at least within the intervals considered. Note that all these observation are applicable only to sufficiently high soda concentration with Gaylussite precipitation. As it was already demonstrated, another phenomena occurs in case of low concentration.

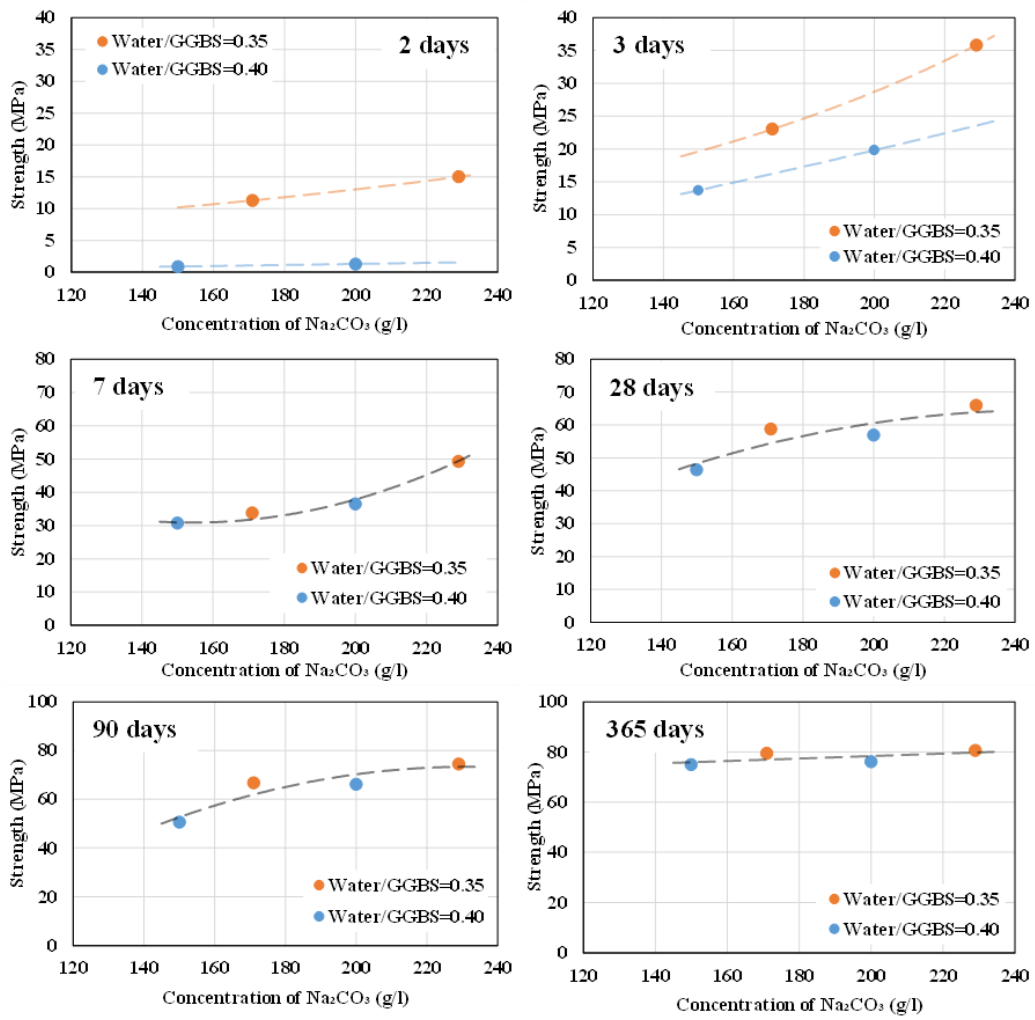

*Figure 4.4: Evolution of the strength versus sodium carbonate aqueous concentration for different W/B ratios at different ages in the case GGBS 4400 cm^2/g in the presence of 0.1% 4Na*HEDP*

4.1.3 Comparison between dry and pre dissolved additions of the Na_2CO_3

Figure 4.5 indicates that method of introducing the activator into the mix has a significant impact. When the activator is pre dissolved in the mixing water, the strength of the corresponding mortar sample is higher at all ages. When used in powder form, the hydration (and then dissolution) of the Na_2CO_3 particles (here D_{50}=125µm) will be in competition with the hydration of the other powders (in particular the slag particles). By taking into account also the precipitation of the early hydration products which consume water, less solvent is then available for the sodium carbonate dissolution. Not all of the activator powder may then be dissolved. This may turn out to be critical. Non-dissolved sodium carbonate might also have impacts on the durability of the product, leading in particular to freeze-thaw and efflorescence issues. Therefore, the use of the activator in pre-dissolved form is highly recommended.

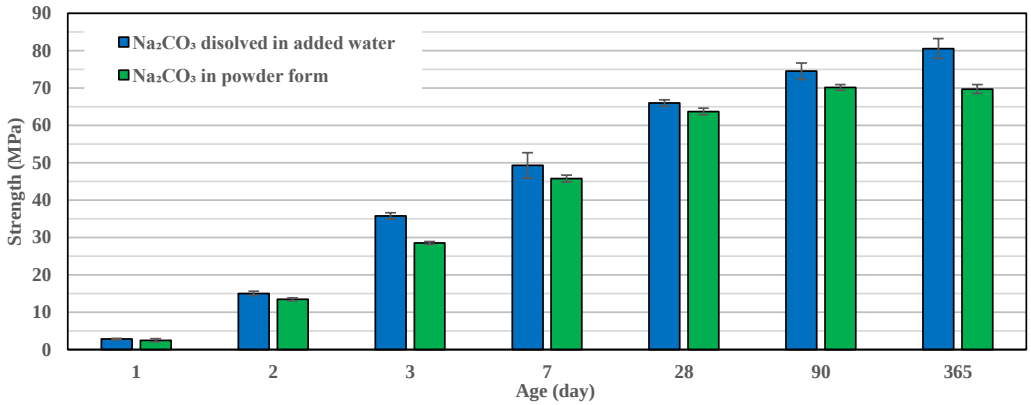

*Figure 4.5: The difference in compressive strength evolution when 8% Na_2CO_3 is added in powder form or dissolved in added water. 100% GGBS 4400 cm^2/g at W/B=0.35 with 0.1% 4Na*HEDP*

4.1.4 Impact of the GGBS fineness on the strength development

Fine GGBS

Increasing GGBS fineness leads to the degradation of the rheological properties. This issue can now be overcome with the addition of the phosphonate. Samples with appropriate rheology were then prepared (at the same phosphonate content: 0.1% by weight of GGBS) and tested for compressive strength development.

In the Figure 4.6 results of the compressive strength evolution for GGBS 4400 cm^2/g and 5600 cm^2/g are compared at W/B=0.35 and 8% Na_2CO_3. After two days, the samples with finer GGBS displayed a significantly higher strength (almost double). Nevertheless, almost no significant improvement was observed at and beyond 3 days. These results are correlated with the previous measurements of released heat evolution, where the increase of slag fineness led to an increase of the heat released over the first 3 days.

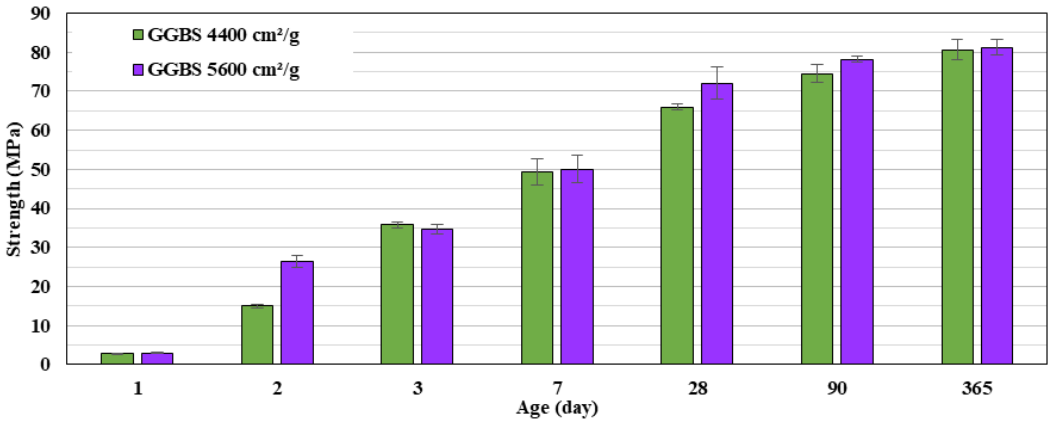

*Figure 4.6: Compressive strength evolution for mortar samples based on GGBS with fineness of 4400 cm^2/g and 5600 cm^2/g, 8% Na_2CO_3 and 0.1% 4Na*HEDP at W/B=0.35*

When the W/B is increased, the positive effect of increasing GGBS fineness is more pronounced and extends to 3 days (Figure 4.7). At longer term, the values become closer as with the lower W/B ratio. Yet, at one year the strength of the samples with finer GGBS becomes higher again. As for the Standard GGBS, increasing the water content leads to a lower compressive strength for the first 3 months. At long term (1 year) the strength becomes almost independent of W/B ratio.

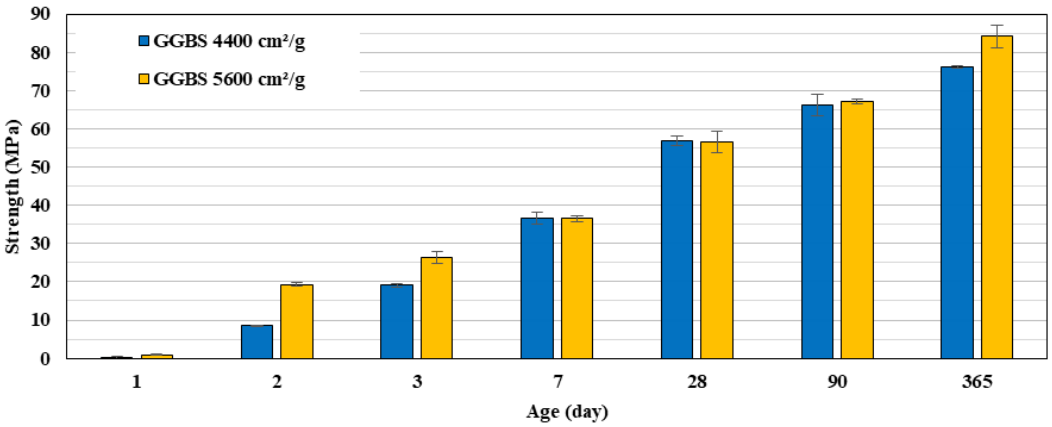

*Figure 4.7: Comparison of compressive strength evolution for the binder based of GGBS with fineness of 4400 and 5600 cm^2/g, 8% Na_2CO_3 and 0.1% 4Na*HEDP at W/B=0.40*

Similar to Standard GGBS, the sodium carbonate amount has a great influence on the compressive strength evolution (see Figure 4.8). Increasing its concentration leads to a higher strength at all ages. At the same time, whatever the concentration, the strength values are higher compared to GGBS with 4400 cm^2/g fineness. In addition the mixes with high GGBS fineness are less sensitive to the amount of activator. Even with a Na_2CO_3 dosage as low as 4%, the strength values are acceptable. It is expected that it should be possible to design a concrete with this binder (with 4% Na_2CO_3) equivalent to those based on CEMIII. Such a low sodium carbonate content should allow for the elimination of several durability issues related to the presence of high levels of alkali.

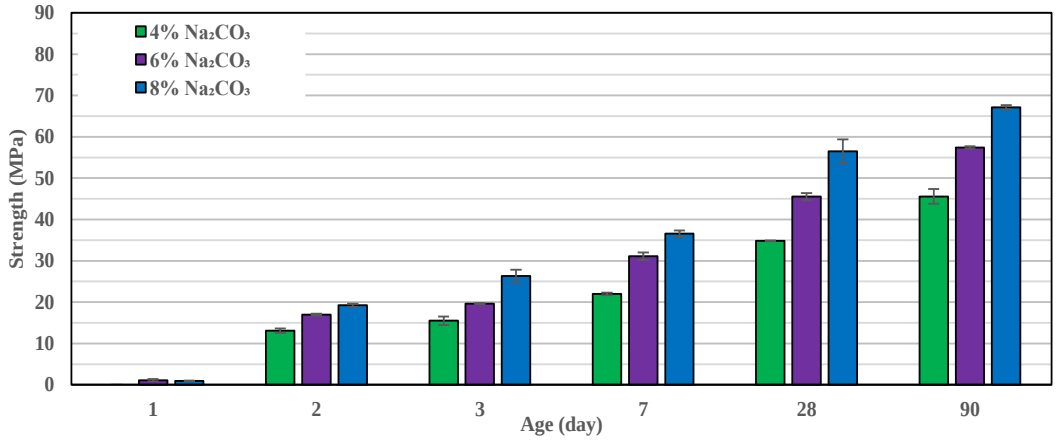

*Figure 4.8: Influence of Na_2CO_3 amount on compressive strength evolution of GGBS 5600 cm^2/g at W/B=0.40 with variable 4Na*HEDP contents: 0.1% for 6% and 8% Na_2CO_3, 0.05% for 4% Na_2CO_3*

Ultrafine GGBS

The previous chapter's micro-calorimetry results showed that the partial replacement, at a level as low as 5%, of Standard GGBS with Ultrafine GGBS leads to a significant acceleration of the hydration process. At the same time, this replacement leads to a very quick setting and poor rheological properties, which makes it impossible to be used without a retarder. The phosphonate 4Na*HEDP allowed for the appropriate rheology and open time to be achieved for such binders. Figure 4.9 represents the evolution of the compressive strength for mortar samples in which Standard GGBS is partially replaced by Ultrafine GGBS at W/B=0.35 and 8%Na_2CO_3. A significant improvement of the strength (in particular at 2 days) can be observed. Yet, at long term the impact is low. Compared to GGBS 5600 cm^2/g, the positive effect was observed from the very beginning. At a replacement level of 10% the strength is increased up to fourfold at 1 day (3MPa vs 13 MPa) and more than twofold at 2 days. The origin of the high reactivity of Ultrafine GGBS is to be investigated. It is not clear whether it is only due to high Blaine fineness, a high specific surface area (BET) or to the specific chemical composition of this grade. It is probable that each of these characteristics is present.

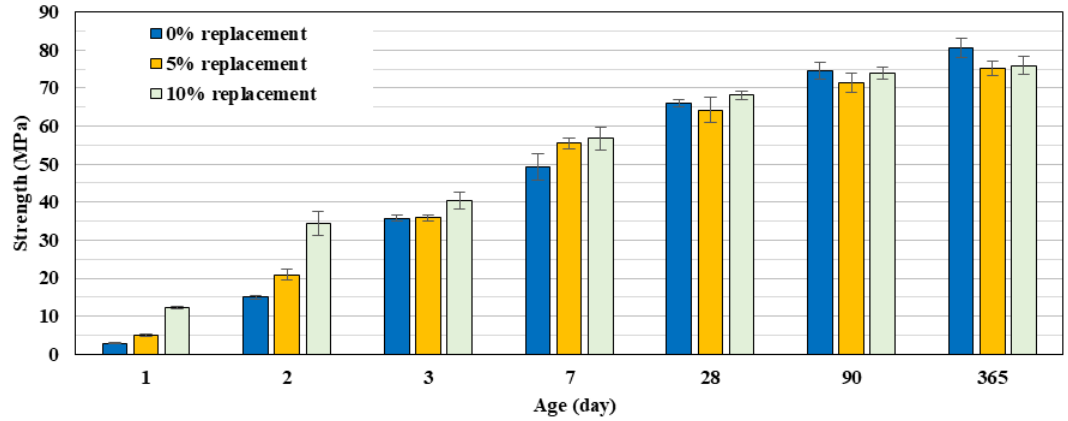

*Figure 4.9: Influence of partial substitution of Standard GGBS with Ultrafine grade (5 and 10%) on compressive strength evolution. W/B=0.35 with 8% Na_2CO_3 and 0.1% 4Na*HEDP*

Independent of Ultrafine replacement level, increasing the W/B ratio leads to a lower compressive strength over the first 3 months (Figure 4.10), with a more significant decrease in the first days of hardening. The addition of Ultrafine GGBS partially compensates for the reduction in strength. Similar to the previous cases, at long term (1 year) the impact of W/B tends to fade.

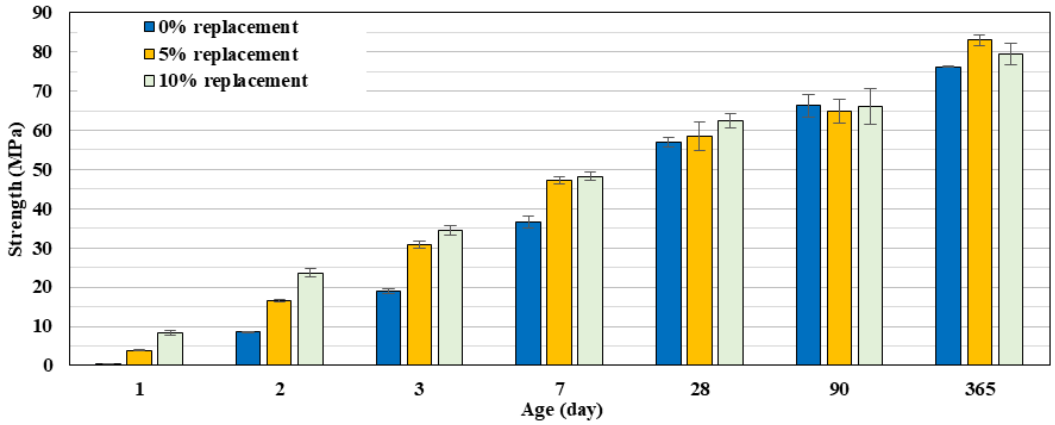

*Figure 4.10: Influence of partial substitution of Standard GGBS with the Ultrafine grade (5 and 10%) on compressive strength evolution. 8% Na_2CO_3 and 0.1% 4Na*HEDP at W/B=0.40*

The impact of the amount of sodium carbonate on compressive strength in the case of the mixes in which Standard GGBS is partially replaced by the Ultrafine grade is reported in Figure 4.11. At early age, the presence of the ultrafine leads to a significant improvement in strength, even at low Na_2CO_3 content. It should be then possible to replace a certain fraction of the activator with Ultrafine without compromising the early strength development. Nevertheless the long term strength (90 days and beyond) seems appears to remain dependent on the activator dosage rate.

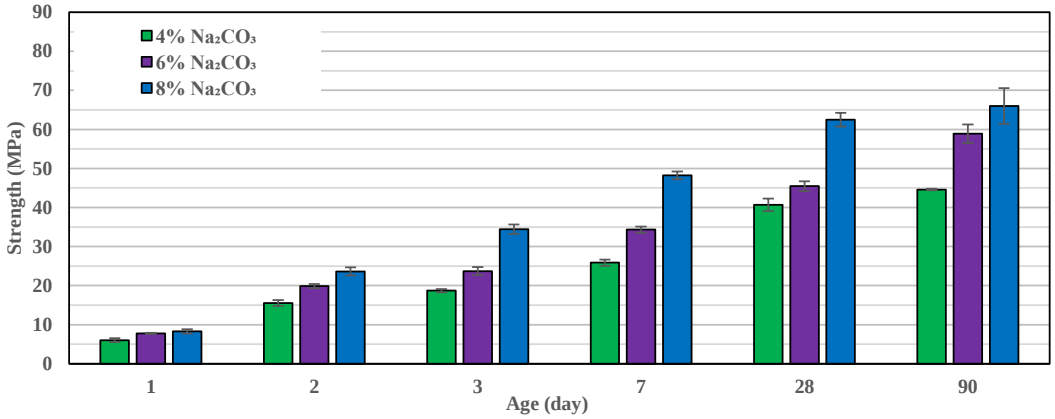

*Figure 4.11: Influence of Na_2CO_3 amount on the compressive strength evolution in case of 90% GGBS 4400 cm^2/g + 10% Ultrafine GGBS at W/B=0.40. 4Na*HEDP dosages are 0.1% for 6% and 8% Na_2CO_3, 0.05% for 4% Na_2CO_3*

Summarizing GGBS fineness impact

Figure 4.12 compiles the results for the impact of GGBS fineness on the compressive strength evolution. The other mix-design parameters (W/B ratio, Na_2CO_3 concentration, 4Na*HEDP dosage, curing temperature) are fixed. It can be noted that the most effective solution to promote early age strength is 10% replacement of Standard GGBS with the Ultrafine grade.

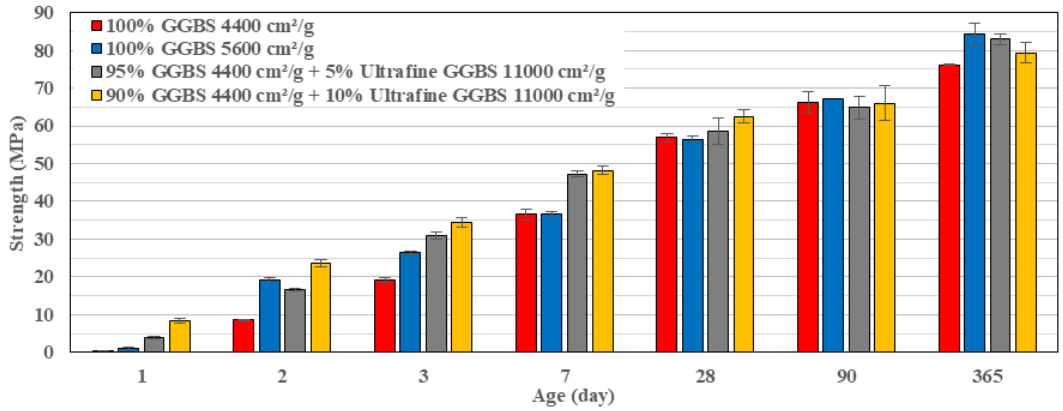

*Figure 4.12: Comparison of strength evolution for different GGBS fineness. 8% Na_2CO_3 and 0.1% 4Na*HEDP were used at W/B=0.40*

At lower W/B ratio and keeping all the other parameters constant, replacement of GGBS by 10% of Ultrafine also provided the best strength results at early age (Figure 4.13). Provided the rheological constraints are overcome, a concrete based on this GGBS binder with 10% Ultrafine has overall better strength development properties that that based on OPC (with standard W/B =0.50).

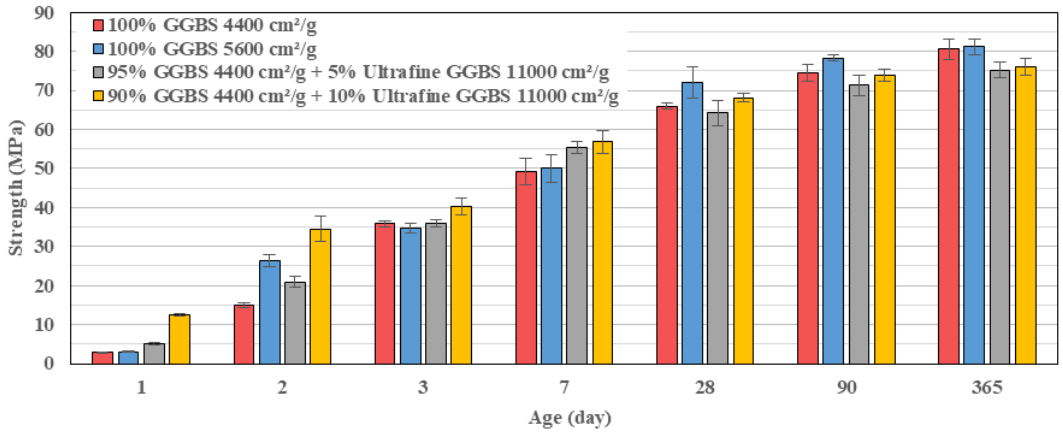

*Figure 4.13: Comparison of strength evolution for different GGBS fineness. 8% Na_2CO_3 (200 g/l) and 0.1% 4Na*HEDP were used at W/B=0.35*

The positive effect of the replacement of Standard GGBS with 10% Ultrafine can be better seen at low Na_2CO_3 content (4%) (Figure 4.14).

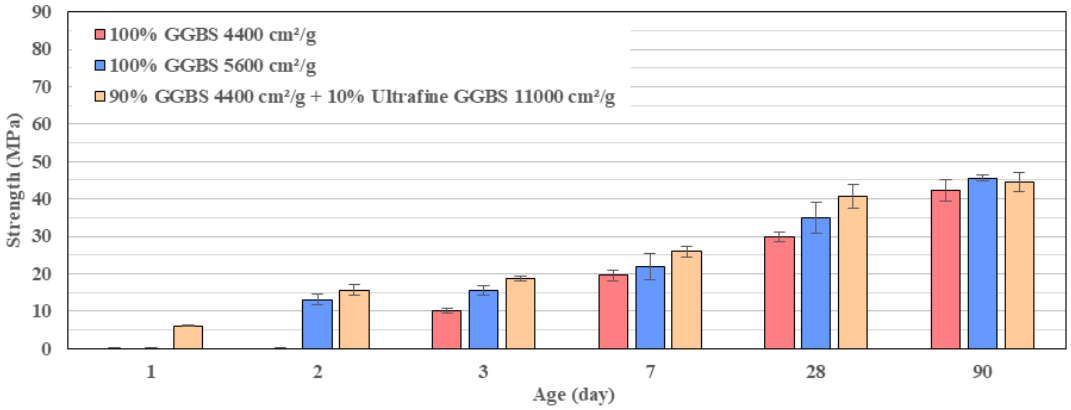

*Figure 4.14: Comparison of strength evolution for different GGBS fineness. 4% Na_2CO_3 (100 g/l) and 0.05% 4Na*HEDP were used at W/B=0.40*

4.1.5 Curing at 15°C

In Chapter 2 the micro-calorimetry results showed that decreasing the curing temperature led to a significant increase in the induction period, without significant influence on the first hydration peak position. The decrease of the early age hydration kinetics at lower temperature may be attributed to both the Arrhenius effect (both dissolution and precipitation are catalysed by temperature) and lower solubility of the sodium carbonate (its recrystallization). In Figure 4.15, a comparison is made between the strength development at 22° and 15°C in the case of a mortar based on Standard GGBS activated with 8% of Na_2CO_3 and with addition of 0.1% 4Na*HEDP. As expected, decreasing the curing temperature leads to a significant reduction of the strength at early age (for ex. 2.5MPa instead of 13.5MPa after 3 days of hardening). However, the long term strength (at and beyond 28 days) is only slightly impacted by the curing temperature.

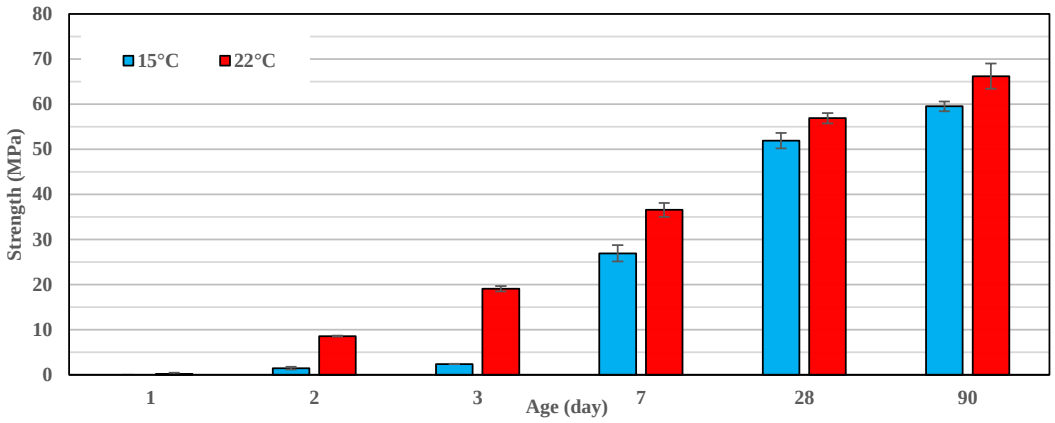

*Figure 4.15: Influence of storage temperature 22°C versus 15°C on strength evolution of GGBS 4400 cm^2/g with 8% Na_2CO_3 and 0.1% 4Na*HEDP at W/B=0.40*

Increasing the GGBS fineness from 4400 to 5600 cm^2/g partially compensates for the reduction of strength at 15°C storage (Figure 4.16). Yet the strength values, in particular at early age, remain significantly lower than those at 22°C.

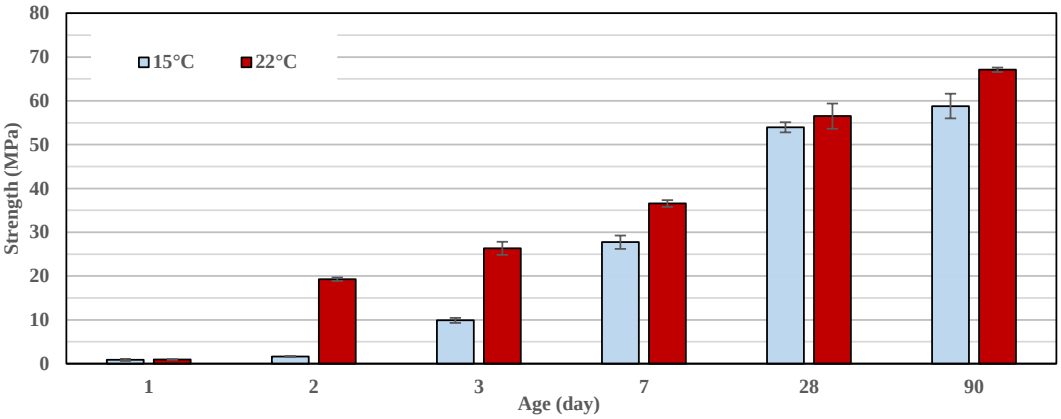

*Figure 4.16: Influence of storage temperature 22°C versus 15°C on strength evolution of GGBS 5600 cm^2/g with 8% Na_2CO_3 and 0.1% 4Na*HEDP at W/B=0.40*

Partial replacement of GGBS 4400 cm^2/g by 5% or 10% of Ultrafine GGBS leads to the same trend (Figure 4.17). Even a 10% replacement with Ultrafine GGBS cannot completely compensate for the decrease in storage temperature.

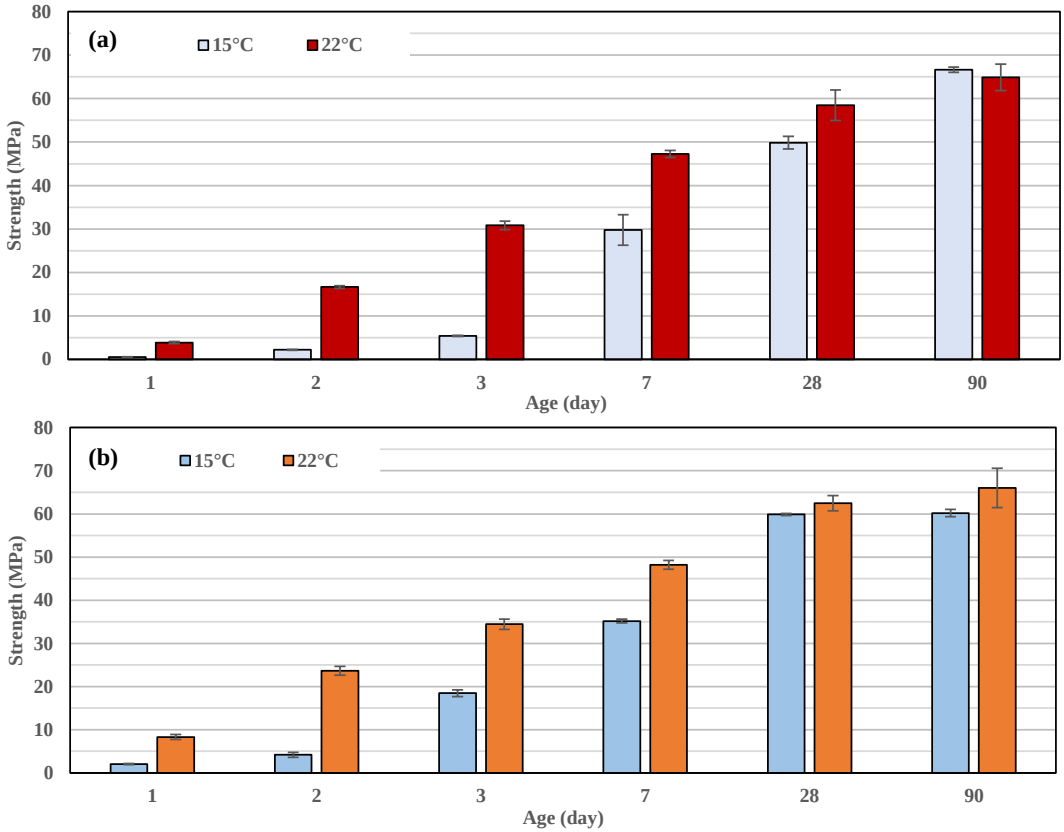

*Figure 4.17: Influence of storage temperature on strength evolution of GGBS 4400 cm^2/g with replacement by 5% (a) or 10% (b) Ultrafine GGBS. 8% Na_2CO_3 and 0.1% 4Na*HEDP at W/B=0.40*

Figure 4.18 summarizes the compressive strength evolution results for GGBS with different finenesses stored at 15°C. As in the case of 22°C, the highest values at early age are attributed to the binder with 10% replacement by Ultrafine GGBS, then to 100% replacement by

GGBS 5600 cm^2/g. As expected, the worst results are observed with Standard GGBS, whose values are highly affected by low temperature storage up to 7 days. In all cases the curing temperature impacts mainly the early age strength development. The strength values at long term (beyond 28 days) are almost independent of temperature or slag fineness. They depend mainly on the activator dosage.

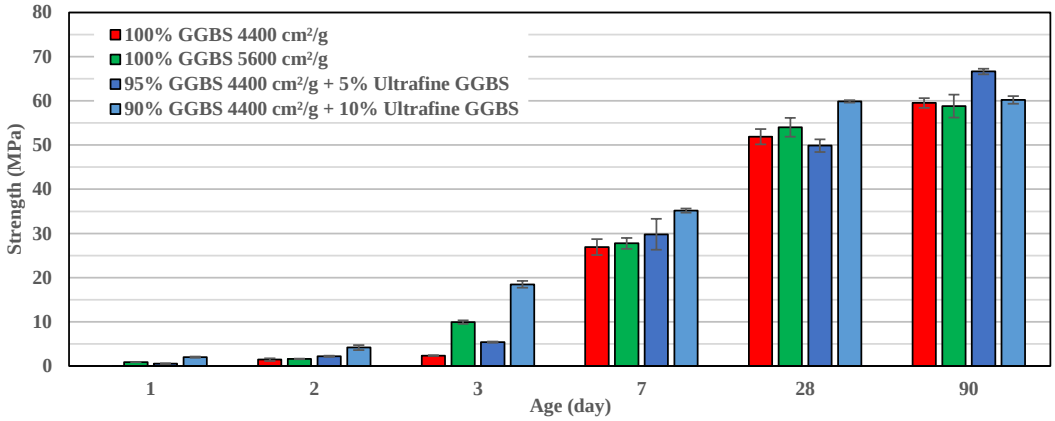

*Figure 4.18: Comparison of compressive strength evolution of GGBS with different fineness stored at 15°C. 8% Na_2CO_3 and 0.1% 4Na*HEDP at W/B=0.40*

4.1.6 Effect of heat treatment

Increasing the curing temperature is expected to lead to the acceleration of the hydration process. To compensate for the negative environmental and economical impacts of heating, a lower sodium carbonate dosage is used.

In Figure 4.19 the impact of heat treatment at 40°C and 80°C over 24 hours is reported in the case of mortar samples based on GGBS 4400 cm^2/g activated with 6% (150g/l) Na_2CO_3 at W/B=0.40. Increasing the curing temperature leads to a substantial improvement in the early age strength development. After only one day of curing at 40°C, the samples reach 37% of the strength value obtained at 28-day's without heat treatment (22°C curing). Curing during 1 day at 80°C led to the samples achieving 68%of the 28-day compressive strength of those made without heat treatment. Yet in both cases, further compressive strength evolution was much slower. A similar phenomenon was also observed in the case of OPC based binders, where the increase of the initial curing temperature leads to an acceleration of the early age strength development, but the long term strength is significantly lower compared those without heat treatment (Klieger, 1958). Hence strength evolution occurs even after 90 days in all cases.

The acceleration mechanisms under heat treatment in our case may be the following description. It was shown previously that at high temperature, Gaylussite is less stable compared to calcite. In addition, the sodium carbonate and the slag are more soluble. Thus, a high level of NaOH will form rapidly upon the reaction of the carbonate ions released from the activator and

the Ca^{2+} leached from the slag. Na_2CO_3 activation at high temperature should then be equivalent to NaOH activation, which is known to lead to high early strength, but poor long term strength. Due to an eventual seeding effect of Ca*HEDP and Gaylussite (formed during sample preparation at 22°C before its placement in curing chamber), the hydration occurs more in bulk than on the slag surface, in contrast with pure NaOH activation. This might explain the relatively high compressive strength achieved in this case. Heat curing may turn out to be an economically valuable process when high early strength is required and moderate long term strength is acceptable. This is the case in the precast industry.

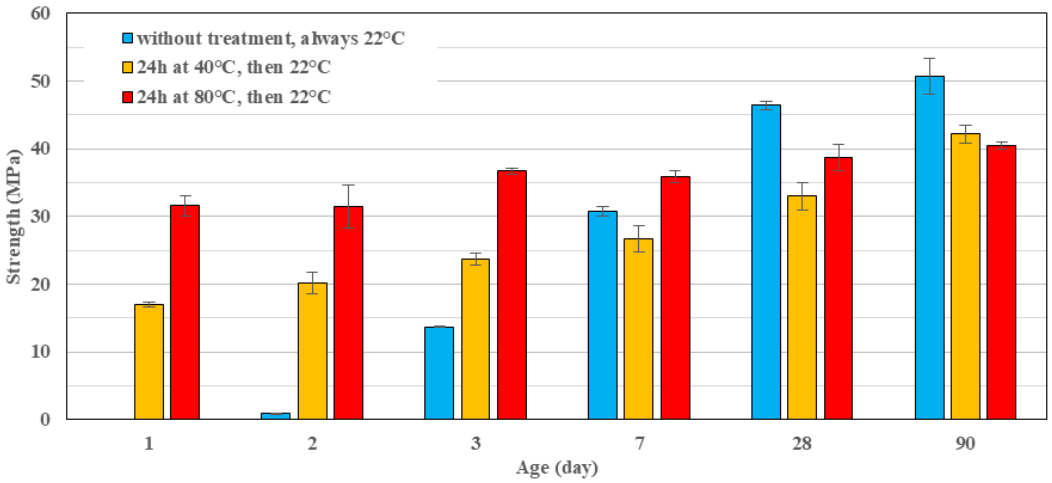

*Figure 4.19: Influence of 24h heat treatment at different T°. GGBS 4400 cm^2/g with 6% Na_2CO_3 (150 g/l) and 0.1% 4Na*HEDP at W/B=0.40*

The influence of heat treatment in the case of much lower sodium carbonate concentration (2% or 50g/l) is reported in Figure 4.20. It can be observed that only at 80°C is a "sufficiently" high compressive strength achieved at 1 day. At the same time, no further strength evolution was observed, probably due to a rapid precipitation of the hydrates (in particular calcite) on the slag surface and complete absence of Gaylussite. In the case of 40°C, no significant strength was observed for the first days of hardening. Yet at long term the strength is relatively high. It is on the same order as with 6% Na_2CO_3.

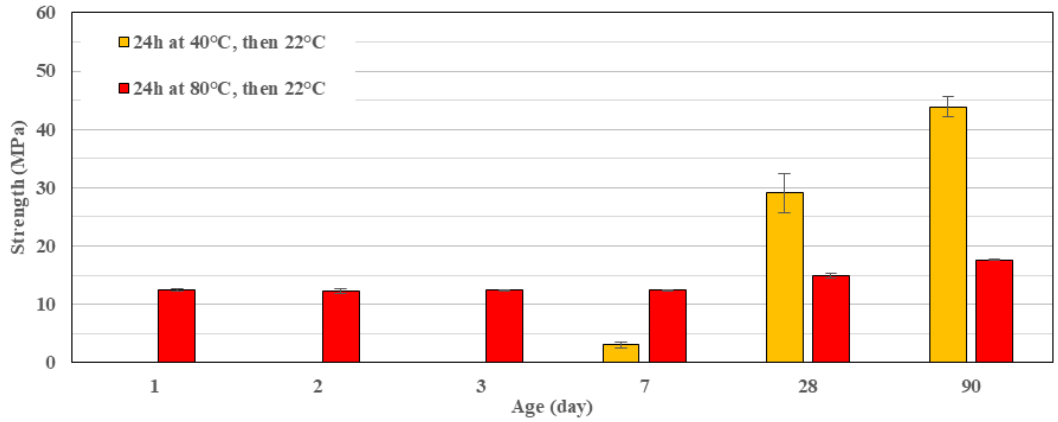

*Figure 4.20: Influence of 24h heat treatment at different T°. GGBS 4400 cm^2/g with 2% Na_2CO_3 and 0.1% 4Na*HEDP at W/B=0.40*

The positive influence of the elevated curing temperature should be related to faster chemical reactions occurring in a system, as well as faster Gaylussite destabilisation at the T°C higher than 40°C for the given soda concentration according to (Bury and Redd, 1933). To clearly illustrate this phenomenon, paste samples for XRD analysis were prepared and stored at 22°C for 28 days, to achieve some hydration rate and some stabilisation of all process. After that, one of the samples underwent 40°C storage for 10 days, while another (reference) was maintained at 22°C for the same 10 days. The results of ex-situ analysis of the two samples are illustrated in Figure 4.21. As it can be observed, the elevated temperature significantly accelerated the process of Gaylussite destabilisation compared to the reference sample. This led to a higher calcite peak intensity as a results of its decomposition. At the same time a clear increase of the low crystalline C-S-H peaks indicate an acceleration of the hydration process and also compressive strength (at least theoretically).

However, in the case of very low soda concentration seen before, no significant impact was observed due to the absence of Gaylussite formed at the beginning (see the results of XRD in Chapter 3). It confirms one more time that in the case of high soda concentration, the induction period is related to Gaylussite formation and its slower decomposition, required for Na^+ liberation. With low soda content, the main reason for an excessive induction period is the absence of nucleation seeds in bulk and the excessively rapid precipitation of hydrates (like low crystalline or amorphous calcite polymorphs) on the slag surface, blocking its further contact with the solution.

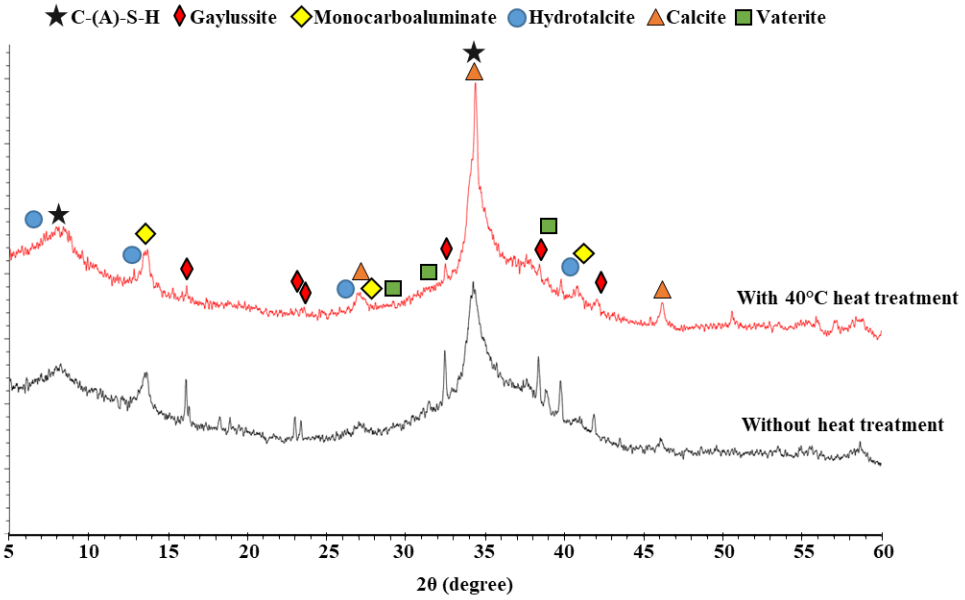

*Figure 4.21: Influence of 10 days heat treatment at 40°C of 28 days old sample of GGBS with 8% Na_2CO_3 and 0.1% 4Na*HEDP at W/B=0.40.*

4.1.7 Influence of storage humidity

A severe drying condition of 50% RH was chosen. Curing under drying conditions started at 3 days for W/B ratio of 0.40 and 2 days for 0.35. It was chosen in accordance with Table 2 (see Chapter 1) and the fact that a significant compressive strength developed at 2 days for W/B=0.35 and 3 days for 0.40. Before curing under drying conditions, all samples were stored in humid conditions (moulds wrapped in plastic). In addition, at the beginning of the drying period, some samples were conserved with adhesive alumina wrapping in humid box from 7 to 28 days.

In Figure 4.22 the results for Standard GGBS activated with 8% Na_2CO_3 in the presence of 0.1% 4Na*HEDP at W/B=0.40 are presented. As it can be clearly observed, increasing the period of curing under humid conditions (RH>95%) led to higher strength development afterward. Drying from 3 days led to a complete cessation of the evolution beyond 28 days. When the dry curing started later, the loss of compressive strength is almost negligible. Yet a slight decrease can be observed at 365 days.

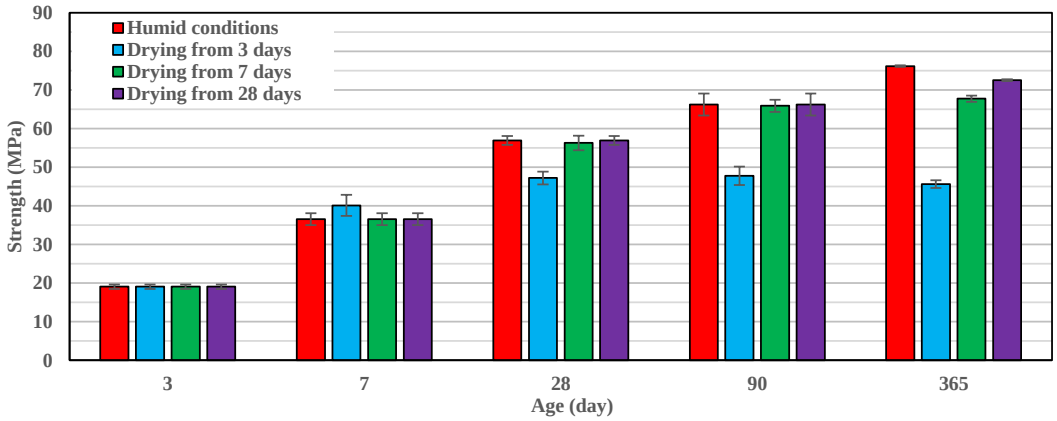

*Figure 4.22: Influence of the duration humidity curing on the strength development under the subsequent dry curing at RH=50% in case of GGBS 4400 cm^2/g with 8% Na_2CO_3 and 0.1% 4Na*HEDP at W/B=0.40*

Decreasing the Na_2CO_3 content to 150 g/l (6%) leads to a larger impact of the duration of humid curing on the subsequent strength development under dry curing (Figure 4.23). For instance, when the samples are cured under humid conditions for only 3 days, the strength loss is about 60% after 1 year, while in the case of 200 g/l Na_2CO_3 the loss is about 40%. This may be due to the fact that with a lower activator dosage, the hydration reaction is slower. Then, when curing under dry conditions, more water will be lost since the sample porosity is more open and there is more free water.

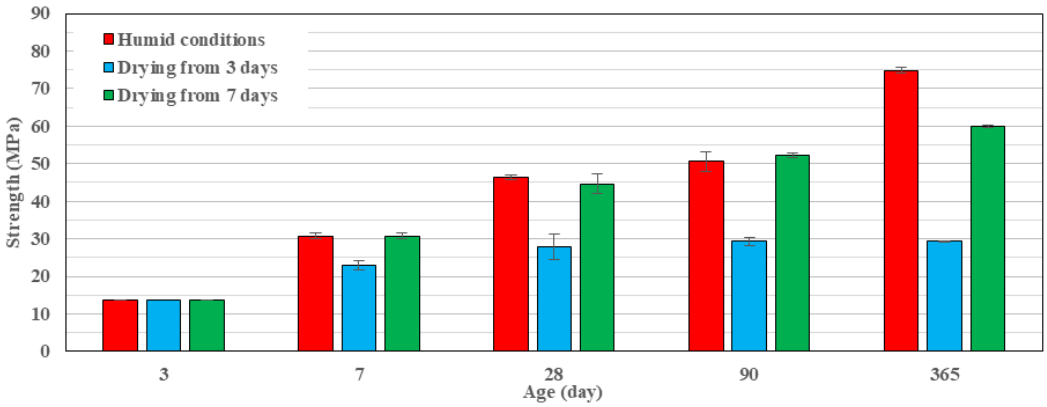

*Figure 4.23: Influence of humidity storage duration on the subsequent strength development under dry conditions (RH=50%) in case of GGBS 4400 cm^2/g, 6% Na_2CO_3 and 0.1% 4Na*HEDP at W/B=0.40*

Figure 4.24 illustrates the impact of W/B ratio decreasing during 50% RH storage. Decreasing water is expected to lead to a lower and less connected porosity. Yet, this is not enough to limit strength loss when the curing is performed under dry conditions. On one hand, lower porosity would lead to lower departure rate of water. On the other hand, this would lead to higher capillarity pressures upon water removal and then higher drying shrinkage. Eventual cracking due to this shrinkage will reduce the strength.

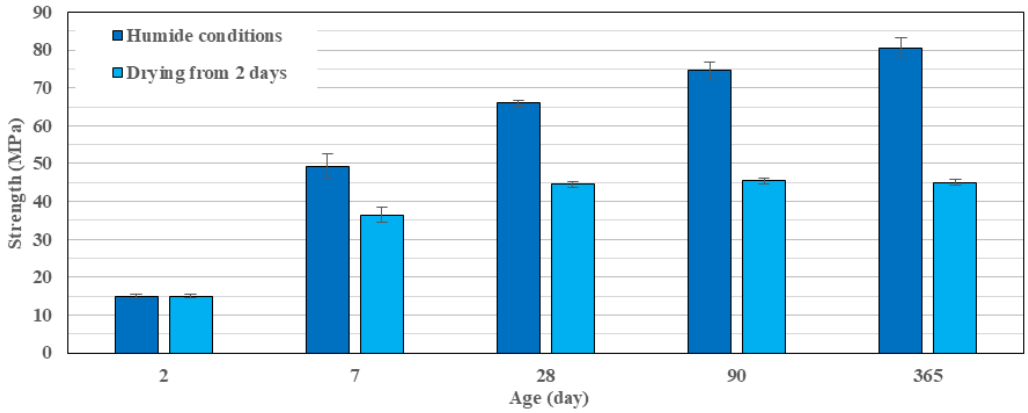

*Figure 4.24: Strength development under dry conditions (RH=50%) following 2 days curing in humid conditions in case of GGBS 4400 cm^2/g with 8% Na_2CO_3 and 0.1% 4Na*HEDP at W/B=0.35*

Decreasing the amount of activator (from 8% to 6%) leads to a more significant loss of strength in the long term (1 year): about 40% for 230g/l and 50% for 170 g/l (Figure 4.25).

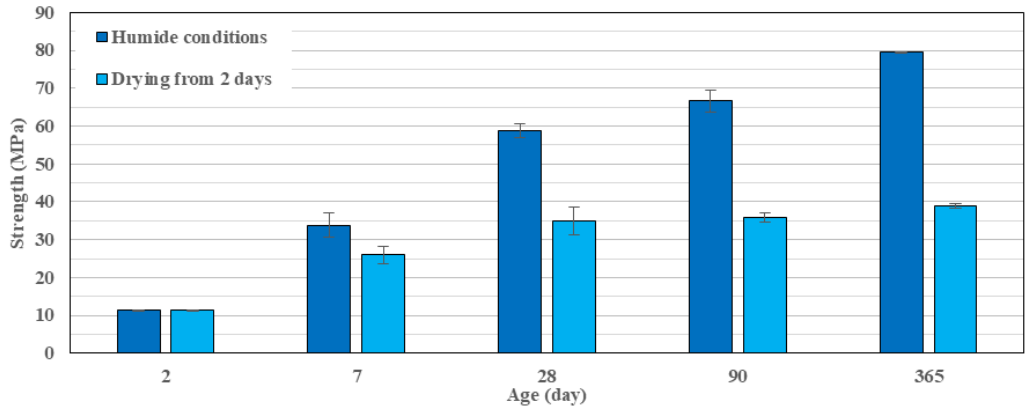

*Figure 4.25: Strength development under dry conditions (RH=50%) following 2days curing in humid conditions in case of GGBS 4400 cm^2/g with 6% Na_2CO_3 and 0.1% 4Na*HEDP at W/B=0.35*

It can be concluded that increasing the duration of the initial humid storage allows for the achievement of better strength development even if subsequent curing occurs under severe drying conditions. Acceleration of the hydration process during humid storage may permit a limitation of the degradation of the strength during the subsequent dry curing. The duration of the initial humid curing may be then reduced. It is also necessary to take into account other environmental factors such as low temperature, which can significantly slow down the hydration kinetics, leading to higher water loss. High temperature curing may also enhance water loss through evaporation. On the other hand the hydration process is faster in this case, which should limit this effect. It is worth expanding that study to an extended range of temperatures.

4.2 Shrinkage

The shrinkage tests were performed on similar samples to those that underwent compressive strength testing. However, in this case special inert shrinkage plugs were incorporated into the mortar. A digital length comparator (±0.001mm) from Controlab (Figure 4.26a) was used to measure the variation of the sample size along the longitudinal axis (initial length about 160 mm). For each formulation, two types of storage conditions were considered: wrapped in a double adhesive alumina foil (to prevent drying) and free drying at RH=50%. All samples were placed in a climate chamber at a temperature of 22°C (Figure 4.26b). The measurements were carried out along two perpendicular sides starting after 3 days of curing for W/B=0.40 and 2 days for 0.35. For each formulation, the instantaneous shrinkage value was taken as the average of measurements over two samples. The results are reported in terms of relative length variations (in µm/m) evolution over time.

Figure 4.26: Procedure for measurements of longitudinal dimensional variation of the mortar samples (a) and sample storage in climatic chamber (b)

4.2.1 Impact of the phosphonate on shrinkage evolution

The influence of phosphonate 4Na*HEDP on the shrinkage development without drying (autogenous shrinkage) is presented in Figure 4.27 for W/B=0.40. The addition of this additive

leads to higher shrinkage almost from the beginning of the measurement period. It might be related to the fact that the phosphonate leads to a higher instantaneous hydration degree and a more dense structure (attributed to eventual seeding effects and rheology improvement of phosphonate). This can be seen from the compressive strength measurements, where the phosphonate addition led to higher strength values (see the results of Chapter 3). A more advanced reaction leads to more free water consumption and consequently higher autogenous shrinkage. It is also worth noting that shrinkage continues even at long term for both mixes. This observation is in agreement with the continuous strength increase up 1 year measurements observed previously. Nevertheless, in the case of 0% phosphonates, no retardation effect takes place and some shrinkage occurs before start of the measurements. Hence, taking into account the compressive strength, which is quite similar at 3 days for both of these formulations, the non-measured shrinkage in the case of 0% phosphonates should be insignificant.

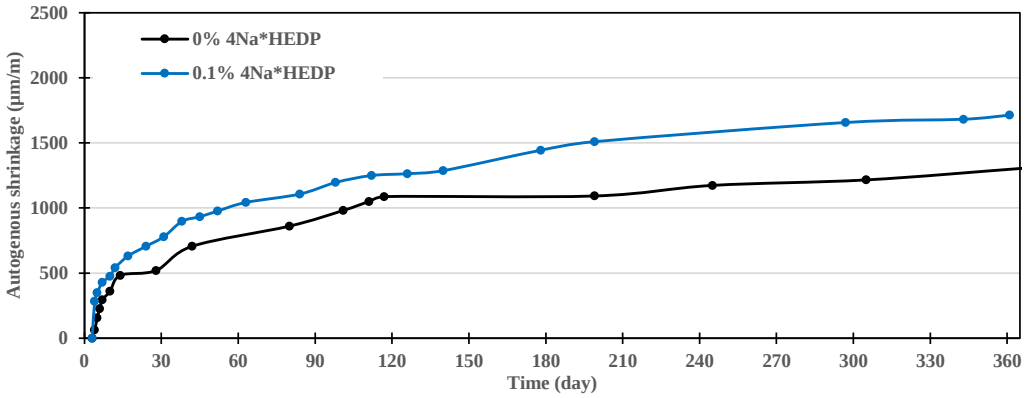

*Figure 4.27: Influence of 4Na*HEDP on the autogenous shrinkage evolution of mortars based on GGBS activated with 8% Na_2CO_3 (200 g/l) at W/B=0.40*

The phenomenon of shrinkage increasing in the presence of phosphonate is also observed for the lower W/B ratio (Figure 4.28). A comparison between the two W/B ratios regarding shrinkage in terms of absolute values is not appropriate since the measurements started at 2 days for 0.35 and 3 days for 0.40.

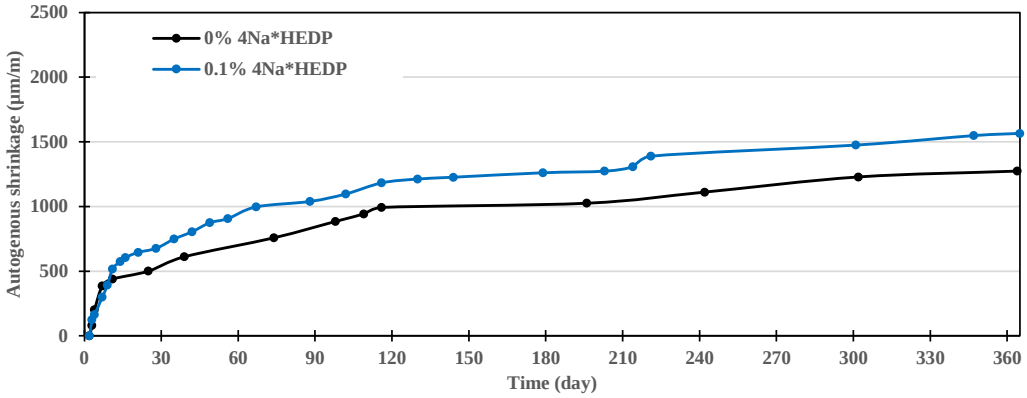

*Figure 4.28: Influence of 4Na*HEDP on the autogenous shrinkage evolution of mortars based on GGBS activated with 8% Na_2CO_3 with (230 g/l) at W/B=0.35*

Under drying conditions both water loss and shrinkage were determined. During the first months, water loss is slightly higher in the presence of the phosphonate (Figure 4.29). This was unexpected since the microstructure was assumed to be denser with the phosphonate. The origin of this phenomenon is not yet understood.

In all cases the mass loss increases with higher W/B. This is, on the other hand, expected since higher W/B implies higher porosity. At W/B=0.35 the mass loss is almost stabilised after 90-120 days, while at W/B=0.40 the samples continue to lose water up to 1 year.

It is worth noting that mass loss is a direct result of water evaporation. 1% of mass loss is almost equivalent to a loss of 11% and 12.5% of the initial water in the system for W/B=0.40 and 0.35 respectively. The sample at W/B= 0.35 loses about 12.5*3.7 = 46% of its mixing water after 1 year of drying. The results are similar for W/B=0.40. Based on such a huge water loss, it can be assumed that the main reason for the blockage of the strength evolution at long term upon drying should be the lack of water available for hydration. An appropriate curing agent is then required for such binders. In contrast with OPC-based binders, there is no hydration product like Ettringite, which may supply a high amount of water upon transformation (to Monosulfate in case of Ettringite). Gaylussite should play this role in part, but it can supply only 5 water molecules (upon its decomposition).

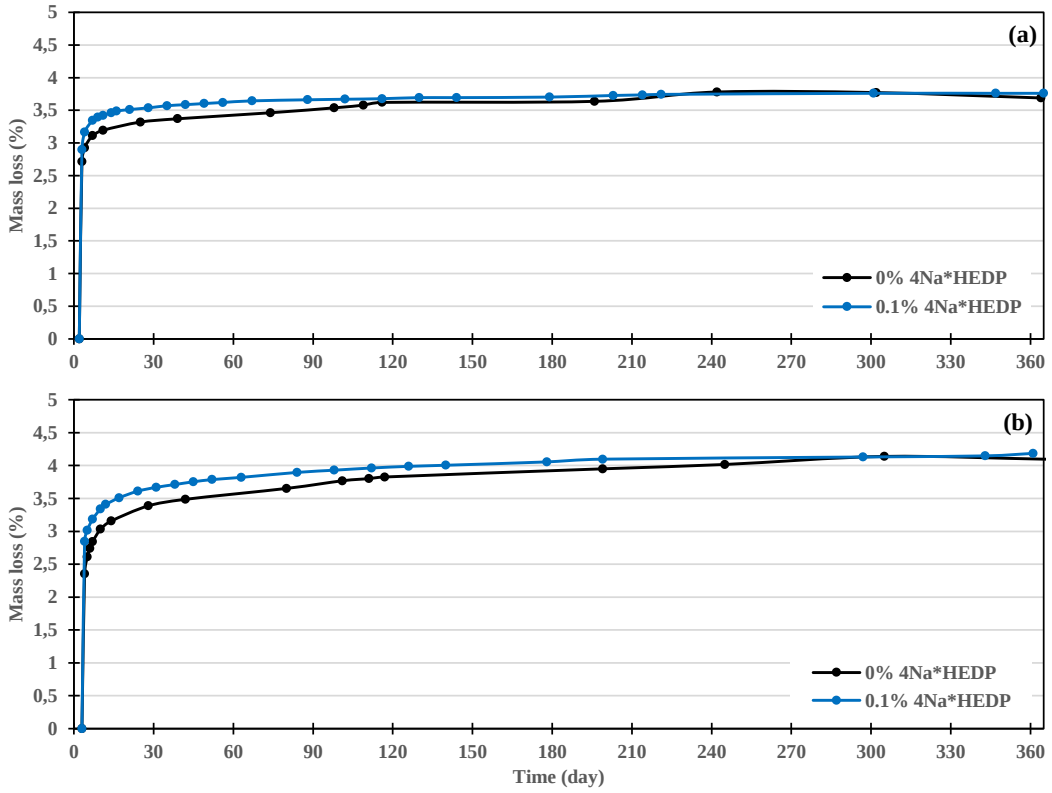

*Figure 4.29: Influence of 4Na*HEDP on mass loss of samples stored at RH=50%, in the case of mortars based on GGBS activated with 8% Na_2CO_3 at W/B=0.35 (a) and 0.40 (b)*

The evolution of the total and drying shrinkages are presented in Figure 4.30. To distinguish the effect of drying alone, the results of autogenous shrinkage were subtracted from total shrinkage (making the assumption that the two processes are additive). Yet, this hypothesis is actually questionable since drying affects hydration. So the autogenous and the drying components of the total shrinkage are not independent in real conditions.

Drying shrinkage is controlled by water departure (mass loss). It can be observed that this type of shrinkage occurs fast at the beginning when most water loss takes place and then levels off (Figure 4.30). On the other hand, total shrinkage continues to grow over a long time since the autogenous component keeps increasing due to continuous hydration.

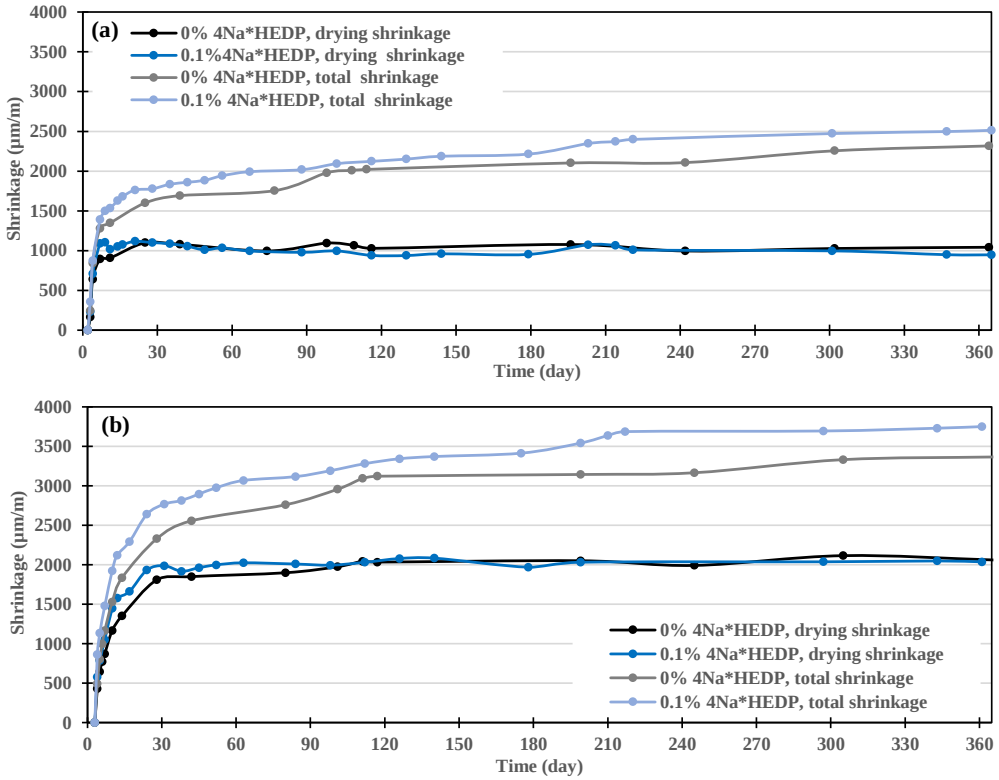

*Figure 4.30: Influence of 4Na*HEDP on drying and total shrinkage for samples stored at RH=50%. GGBS with 8% Na_2CO_3 and W/B=0.35 (a) or 0.40 (b),*

4.2.2 Impact of Na_2CO_3 concentration

The impact of the amount of Na_2CO_3 on the autogenous shrinkage evolution for two different W/B ratios is reported in Figure 4.31. The instantaneous autogenous shrinkage decreases when the activator dosage is decreased. This may be explained by the fact that the hydration degree is lower at all terms. In all cases, the shrinkage values remain high (compared to OPC based products), similar to all alkali-activated binder-based products. This is generally attributed to their finer porosity, than higher capillary pressures induced by water retraction upon hydration. Although the shrinkage level is high, the mechanical properties not significantly affected. The high level of shrinkage does not seem to lead to (significant) damage.

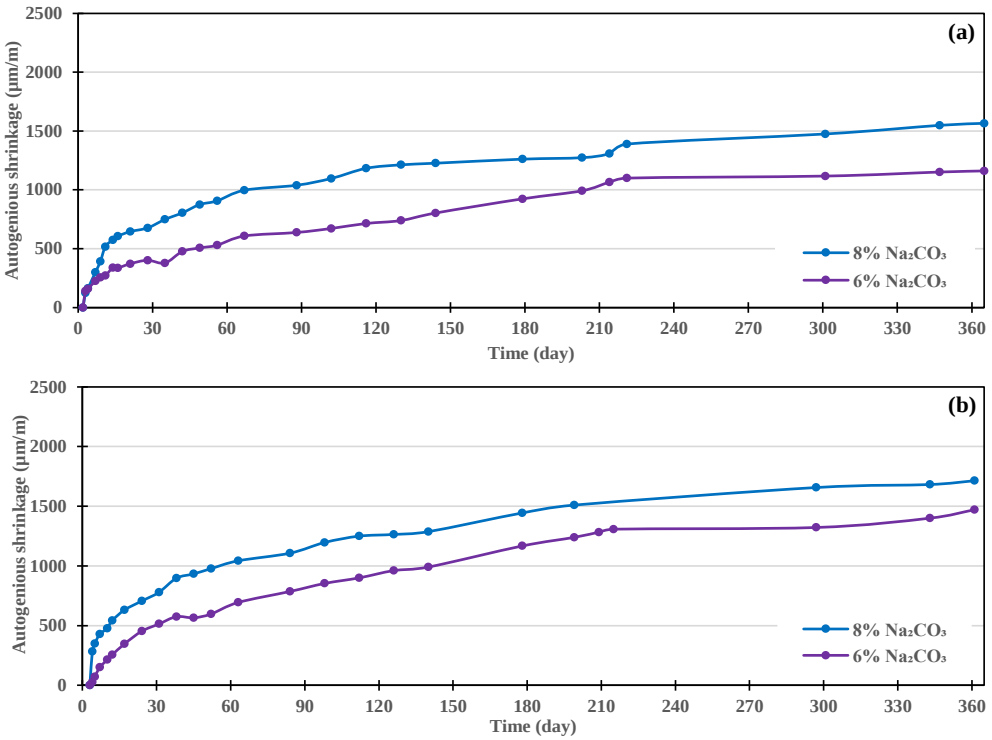

*Figure 4.31: Influence of Na_2CO_3 content on autogenous shrinkage evolution of mortars based on GGBS 4400 cm^2/g at W/B=0.35 (a) or 0.40 (b), in the presence of 0.1% 4Na*HEDP*

Under dry curing conditions, decreasing the amount of the activator leads to significantly higher water loss (Figure 4.32). Since the hydration degree is lower at all times in this case, the porosity is more open and there is less bound water. More water can then escape upon drying. This may explain in great part the increase of the level of strength loss under dry curing seen before in this chapter when the activator content is decreased.

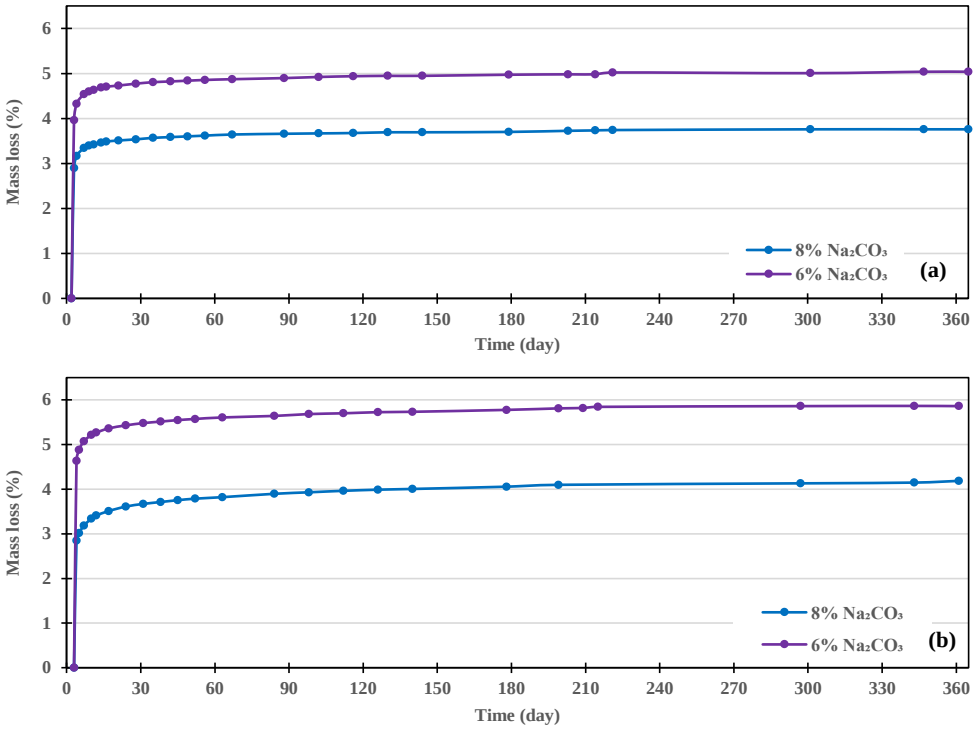

*Figure 4.32: Influence of Na_2CO_3 on a mass loss stored at RH=50%. The binder is GGBS with different amount of Na_2CO_3 in the presence of 0.1% 4Na*HEDP. W/B=0.35 (a) and 0.40 (b)*

The evolution of the total shrinkage and the net drying shrinkage are reported in Figure 4.33 for the two Na_2CO_3 contents. Here again it is assumed that the autogenous and the drying components of the shrinkage are additive. At short term the drying shrinkage increases more rapidly and is higher at low activator content. This can be better seen at W/B=0.40. Over the same period the total shrinkage is lower, which is related to the lower values of the autogenous component. At long term the drying shrinkage component becomes almost the same for the two activator contents. All these results regarding the influence of Na_2CO_3 on dimensional variation are qualitatively in agreement with those reported in the literature (Jacquemot, 2014).

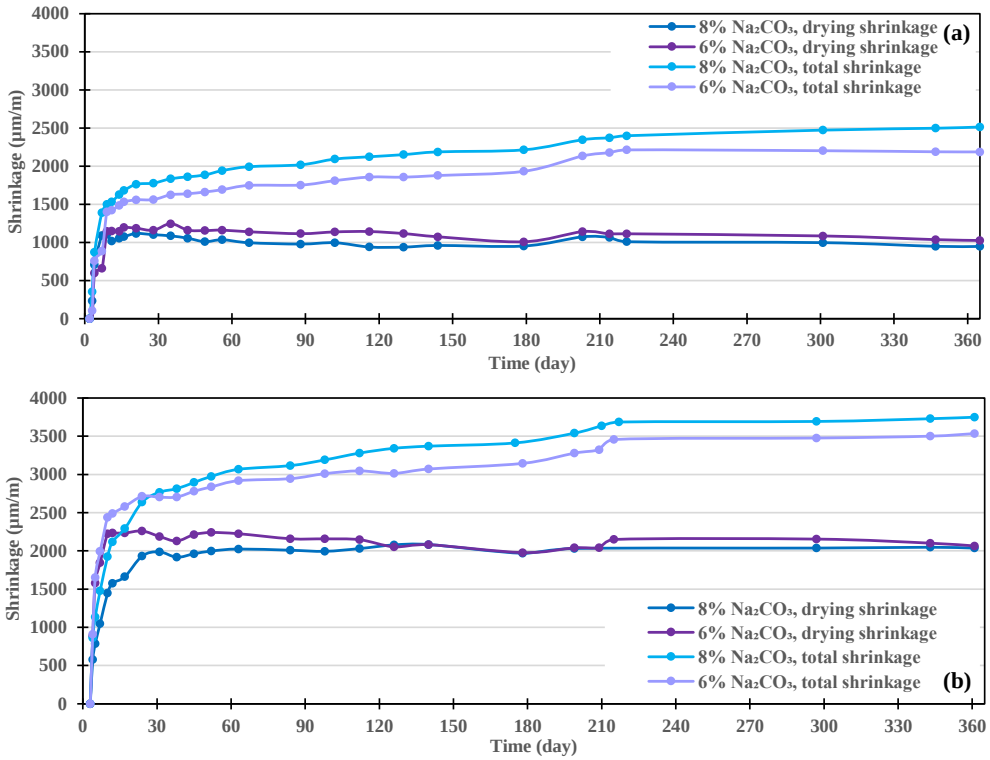

*Figure 4.33: Influence of Na_2CO_3 on total and drying shrinkage for samples stored at RH=50%. GGBS with different amount of Na_2CO_3 in the presence of 0.1% 4Na*HEDP at W/B=0.35 (a) and 0.40 (b)*

4.2.3 Influence of GGBS fineness on shrinkage

Fine GGBS

The impact of the GGBS fineness (4400 cm^2/g *versus* 5600 cm^2/g) on the autogenous shrinkage evolution is reported in Figure 4.34. The *recorded* shrinkage is lower and faster "stabilisation" can be observed in the case of the finer slag. Nevertheless in both cases the autogenous shrinkage keeps increasing, although slowing, after one year of measurement. Since the GGBS grade leads to different hydration kinetics (based on the micro-calorimetry and compressive strength results), it is not straightforward to make comparisons in terms of absolute values. The measurements started after 2 or 3 days of curing, so the early part of shrinkage was not recorded. It is not possible then to conclude that increased fineness leads to a decrease of the

actual autogenous shrinkage. Since the finer GGBS is more reactive, a higher part of unrecorded shrinkage (over the first 2 or 3 days before demoulding and the starting of measurements) might have been missed. If one starts shrinkage measurements earlier, opposite trends may be obtained.

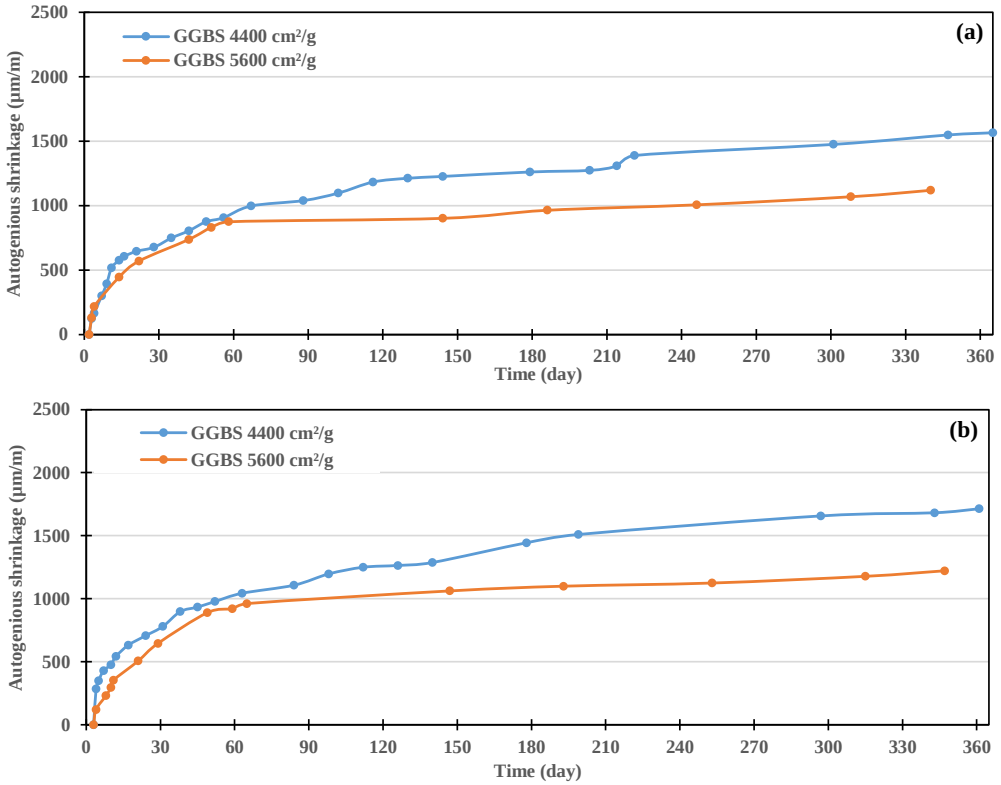

*Figure 4.34: Influence of GGBS fineness on autogenous shrinkage in the case activation with 8% Na_2CO_3, in the presence of 0.1% 4Na*HEDP and at W/B=0.35 (a) and 0.40 (b)*

The higher reactivity of the finer GGBS can be clearly seen through the results of mass loss presented in Figure 4.35. The instantaneous water loss is significantly lower in the case of the finer GGBS.

The time evolution of the total shrinkage and its drying component are presented in Figure 4.36 for the two GGBS grades. The impact of the GGBS fineness depends qualitatively on the W/B ratio. At low W/B (0.35), both the total and drying shrinkages are significantly lower over the two first months with high GGBS fineness. This indicates that over this period the overall shrinkage is mainly controlled by water loss. And the latter is much lower in the case of finer GGBS (Figure 4.35). At long term (beyond about 2 months), the total shrinkage becomes similar for both GGBS grades. There should be a balance between higher autogenous shrinkage (due to higher reactivity) and lower water loss for the finer GGBS. Yet, although the water loss is lower, the drying component of the shrinkage at long term is higher for the finer GGBS. This may be attributed to two reasons: (i) finer porosity implies higher capillary pressures even if less water is lost, (ii) the drying and the autogenous components of the shrinkage are not additive, and the former was underestimated.

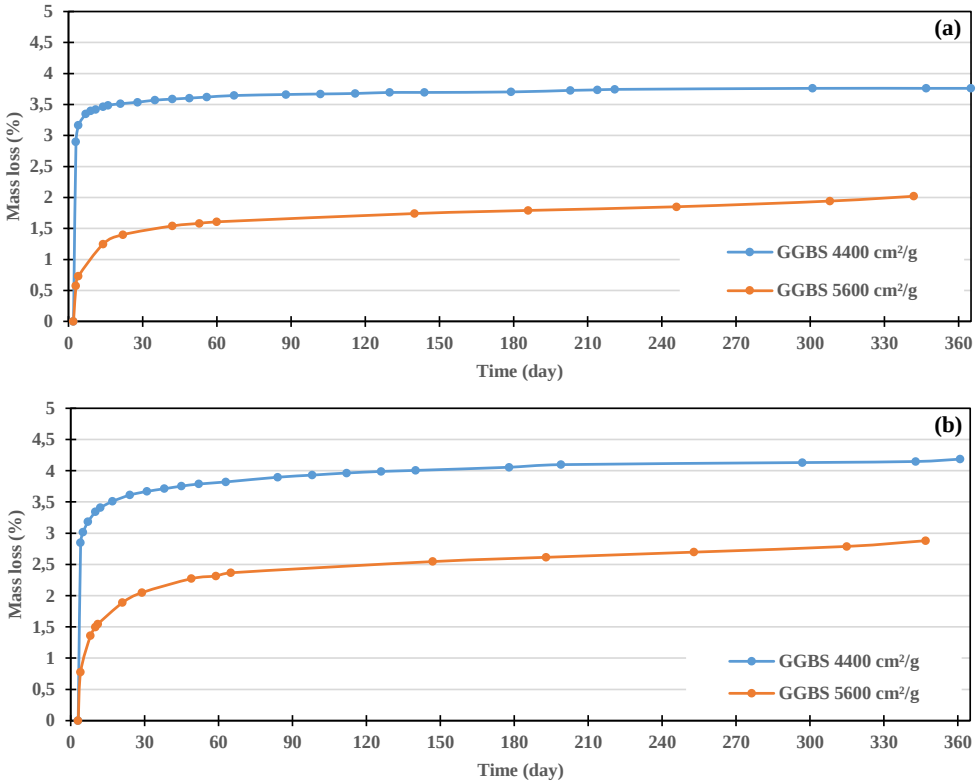

*Figure 4.35: Influence of GGBS fineness on mass loss under dry conditions (RH=50%) in the case of activation with 8% Na_2CO_3, in the presence of 0.1% 4Na*HEDP and at W/B=0.35 (a) and 0.40 (b)*

At higher W/B ratio (0.40), both drying and total shrinkages decrease with GGBS fineness over the duration of the experiment (1 year). Due to the high water amount, the shrinkage seems to be controlled by water loss throughout this period. Also, water loss is lower with finer GGBS due its high reactivity.

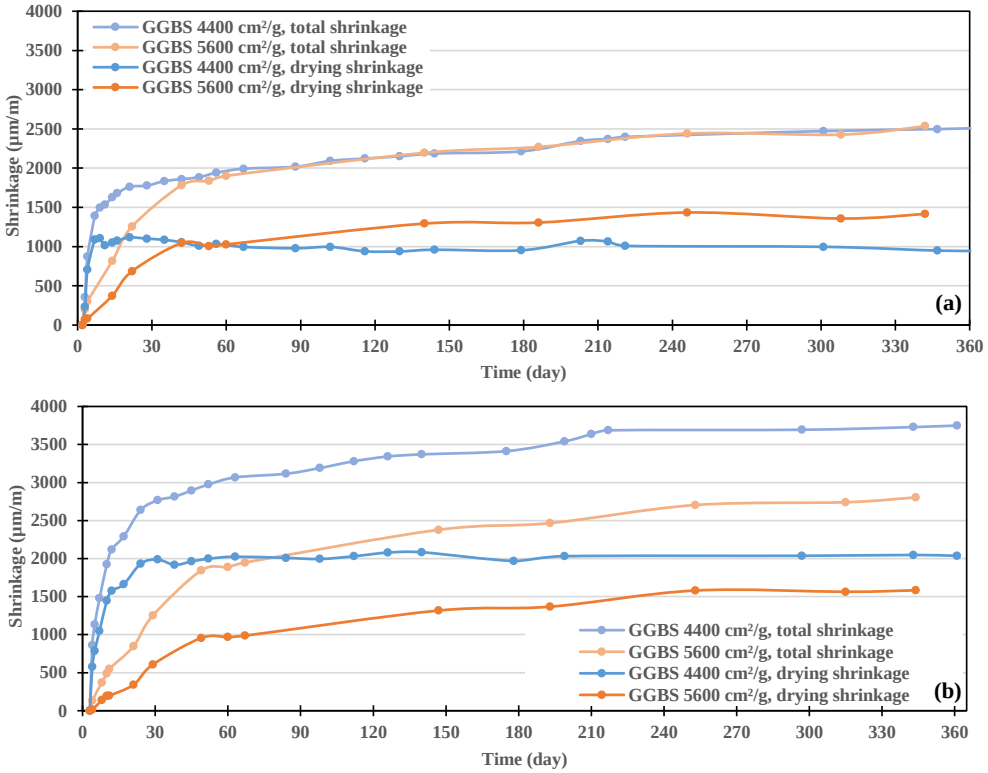

*Figure 4.36: Influence of GGBS fineness on total and drying shrinkage (at RH=50%) in the case of activation with 8% Na_2CO_3, in the presence of 0.1% 4Na*HEDP and at W/B=0.35 (a) and 0.40 (b)*

Ultrafine GGBS

The autogenous shrinkage evolution results between the mixes corresponding 5% Ultrafine replacement of Standard GGBS and the fine GGBS 5600 cm^2/g are very similar (compare Figure 4.37 with Figure 4.34). The autogenous shrinkage is almost independent upon fineness over the first 2 months, during which most of the shrinkage takes place. At longer term, the presence of the Ultrafine leads to a near cessation of shrinkage while with Standard GGBS it continues to shrink. Similar arguments for the case of Fine GGBS can be put forward to explain these trends.

However, suppose that the final shrinkage (after one year) is the same in both cases, it must be observed that a huge part of the autogenous shrinkage with the ultrafine slag was achieved in the first 2 months. In this case, it is in agreement with previously seen strength evolution, which is significantly accelerated at early age by ultrafine slag and almost independent in the long term.

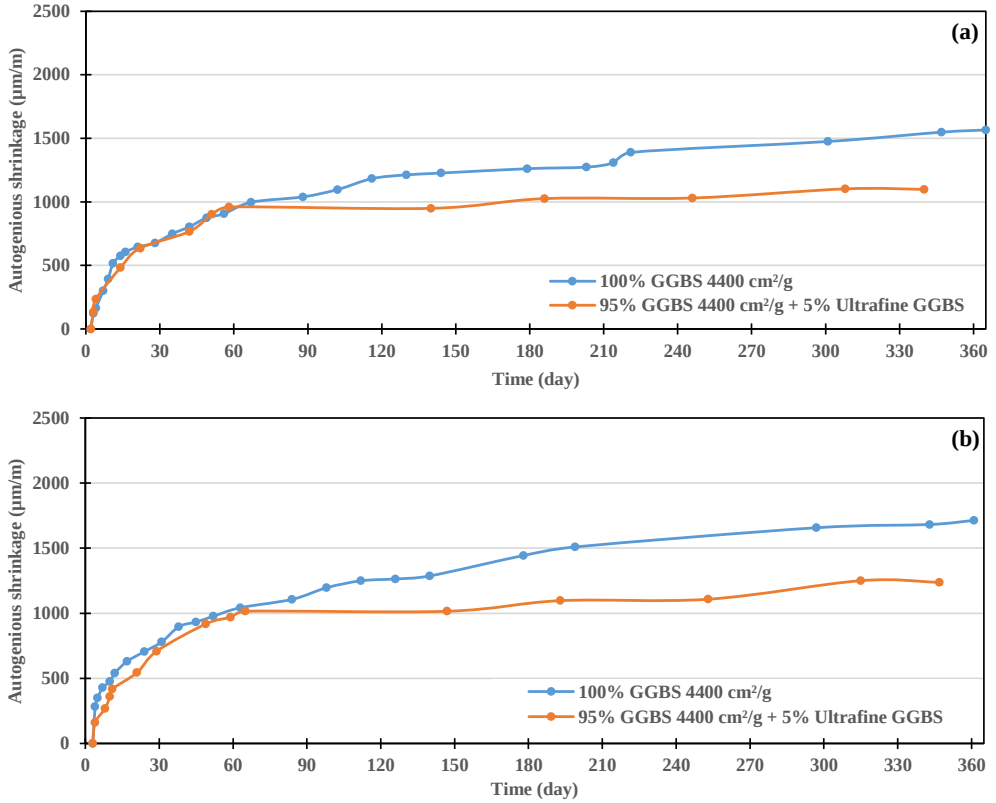

*Figure 4.37: Influence of 5% Standard GGBS replacement by Ultrafine GGBS on autogenous shrinkage in the case of activation with 8% Na_2CO_3, in the presence of 0.1% 4Na*HEDP and at W/B=0.35 (a) and 0.40 (b)*

The results for the evolution of water loss, total and drying shrinkages when 5% Standard GGBS is replaced by the Ultrafine grade are also similar to those for Fine GGBS (Figure 4.38 and Figure 4.39). The same arguments can be developed to explain the different trends observed.

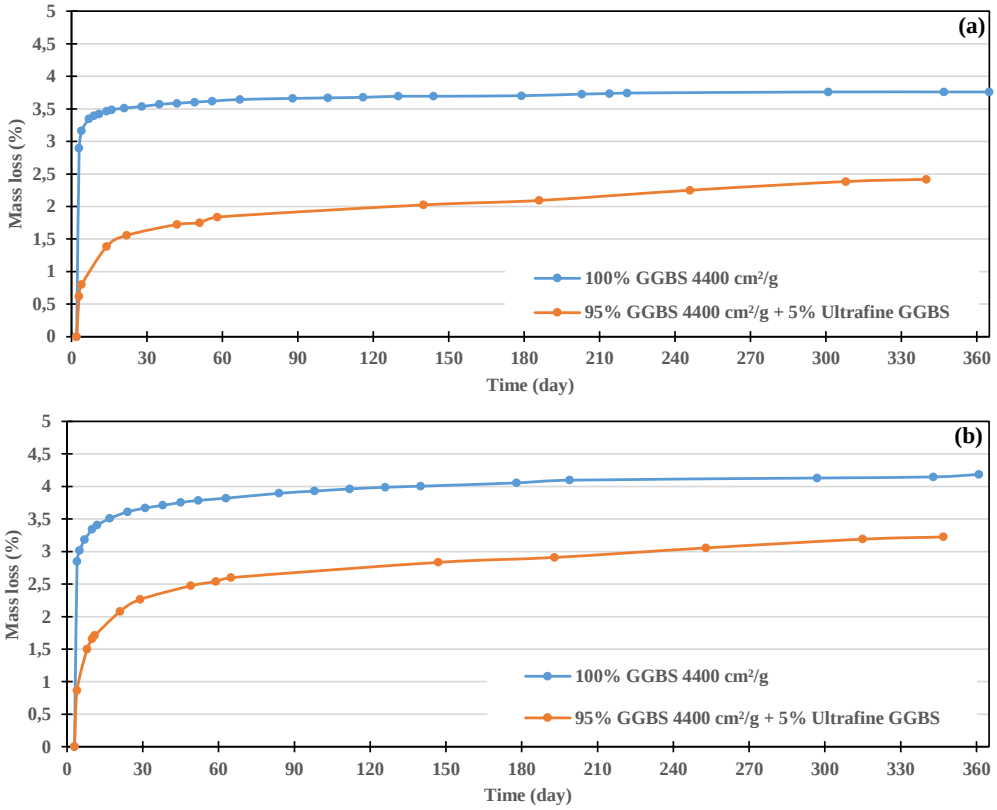

*Figure 4.38: Influence of 5% GGBS replacement by Ultrafine GGBS on mass loss stored at RH=50%. GGBS with 8% Na_2CO_3 and 0.1% 4Na*HEDP. W/B=0.35 (a) and 0.40 (b)*

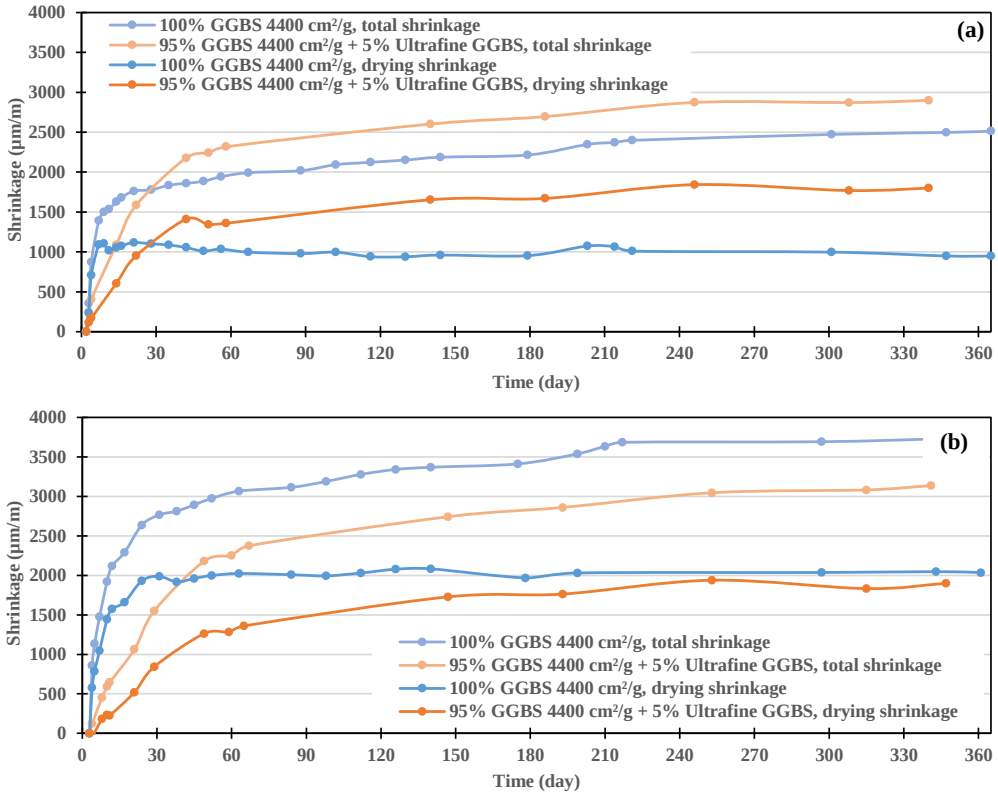

*Figure 4.39: Influence of 5% GGBS replacement by Ultrafine GGBS on total and drying shrinkage stored at RH=50%. GGBS with 8% Na_2CO_3 and 0.1% 4Na*HEDP. W/B=0.35 (a) and 0.40 (b)*

4.2.4 Influence of the humid curing duration

It was observed above that drying may lead to a significant reduction (even cessation) of the strength development, in particular when the hydration process is not sufficiently advanced when the dry curing begins. In was also observed that dry storage conditions (50% RH) may cause the loss of almost half of the mixing water. In the following investigation, the impact of the duration of the humid curing preceding the dry curing is considered.

Figure 4.40 shows that increasing the duration of the period during which the samples are stored under humid conditions leads to a significant reduction in water loss. For example the reduction is about threefold when the samples are pre-cured in humid conditions during 28 days instead of 3 days. This should be related to both the fact that more water is embedded in the hydration products and that a less connected porosity exists due to more advanced hydration.

It is worth noting that even after 28 days of humid curing, there is non-negligible loss of water during the subsequent dry curing (about 17% of the mixing water at the age of 1 year). Therefore even after 28 days of humid curing, a large amount of free water is still present (ignoring the water stemming from the eventual decomposition of the some hydration products such as Gaylussite). So the actual required W/B required for full hydration is significantly lower than 0.40.

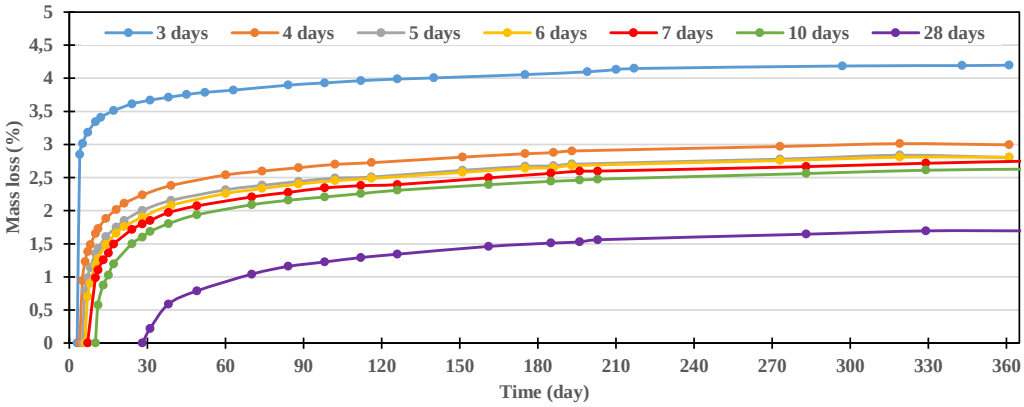

*Figure 4.40: Weight loss of samples cured at 50% RH after varying durations of humid pre-curing, in the case of GGBS activated with 8% Na_2CO_3 in the presence of 0.1% 4Na*HEDP at W/B=0.40*

In Figure 4.41 the total and the net drying shrinkage (the autogenous component subtracted) are presented for different humid pre-curing durations. It can be clearly seen that increasing the humid pre-curing duration leads to a significant reduction of both total and drying shrinkages. Yet the impact is lower than for water loss.

As shown previously, dry curing that starts too early (after 3 days humid curing) led to a significant degradation of the strength and almost complete cessation of its long term development due to high water loss. Pre-curing under humid conditions for a longer duration (up to 28 days) leads to a more advanced reaction (hydration degree), finer porosity and lower water loss, which leads to much less shrinkage. Although the measurements are not performed here, it is expected that the long term strength development should be better when the duration of humid pre-curing is extended.

Figure 4.42 presents the net drying shrinkage versus water loss. It can be seen that for a given amount of water loss, the shrinkage is higher for a longer duration of humid pre-curing. This may be attributed to higher capillary pressures due to finer porosity since the hydration process is more advanced. This assumption of finer porosity is confirmed by the fact that the period of drying shrinkage stabilization is much longer in the case of 28 days pre-curing (Figure 4.41). In any case, in terms of absolute values, increasing the duration of the period of storage under humid conditions leads to lower shrinkage.

An apparent level off of the drying shrinkage can be observed beyond a certain value of water loss (Figure 4.42). This might be related to the fact that the drying shrinkage presented here is assumed to be the difference between the measured total shrinkage and autogenous shrinkage. In this case it is supposed that self-desiccation due to water consumption during hydration takes place before the drying period. The apparent plateau should then be related to the artefact of assuming that the two shrinkage components are additive.

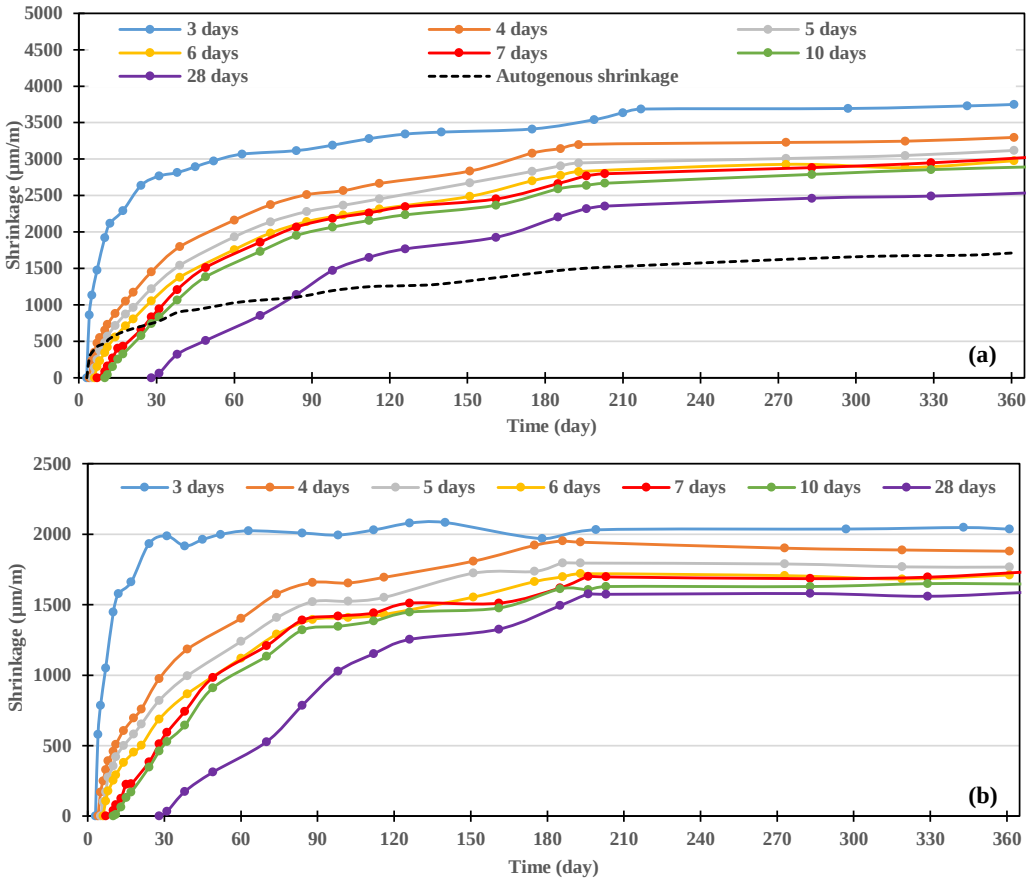

*Figure 4.41: Influence of the duration of humid pre-curing on the afterwards dry curing (RH=50%) on total (a) and net drying shrinkage (b) in the case of GGBS activated with 8% Na_2CO_3 in the presence of 0.1% 4Na*HEDP at W/B=0.40*

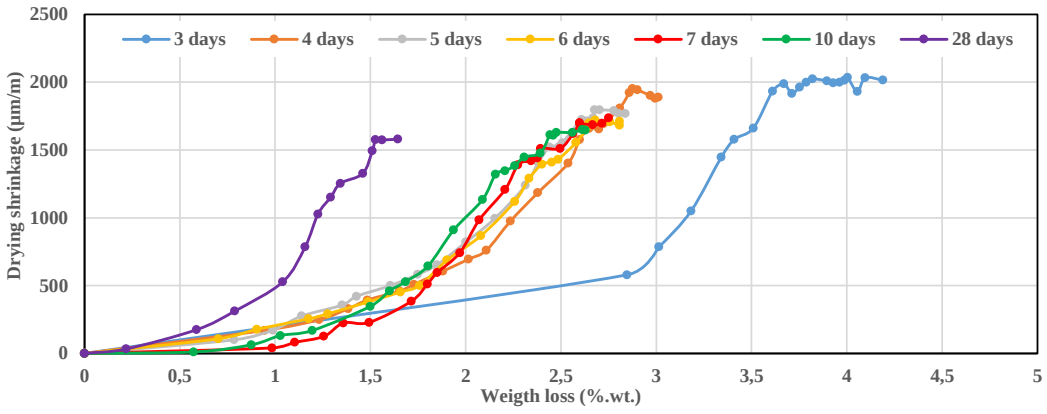

*Figure 4.42: Net drying shrinkage as a function of weight loss for GGBS activated with 8% Na_2CO_3 in the presence of 0.1% 4Na*HEDP at W/B=0.40, for different durations of humid pre-curing preceding curing under dry conditions (50%RH)*

Conclusions

The results of compressive strength evolution confirm the previously observed retardation effect of phosphonate addition at the very beginning. Nevertheless, this effect is almost negligible if the right dosage in each specific case was used. At the same time, its addition allowed for the improvement of the mortar rheology and to clearly determine the impact of different parameters, like low W/B ratio and slag fineness.

Decreasing the water in the system led to a noticeable acceleration of strength evolution in almost all ages. At early age (up to 3 days) this parameter is dominant, even compared to Na_2CO_3 concentration. The influence of reduced water content is more prominent in the period from 2-3 days (higher compressive strength with higher soda dosage). Yet up to one year, almost no significant influence of both parameters was observed (under the condition that the minimum optimal concentration of soda was used).

Concerning the slag fineness, a significant acceleration in early age strength evolution was achieved with finer slag. This should be related to its more rapid dissolution, due to the higher specific surface and more homogeneous distribution due to the lower particle size. Among the tested formulas, the most effective mix is partial standard GGBS substitution by its ultrafine grade (d_{50}=1.8µm), which coincides with the previously observed micro-calorimetry results. This is especially beneficial in the case of high W/B ratio or low sodium carbonate concentration, as well as in the case of sub-optimal curing conditions such as low temperature and/or humidity.

In the case of the curing temperature decreasing from 22°C to 15°C, a significant retardation of strength evolution for the first 7 days of hardening takes place. Acceleration of the reaction by increasing of the slag fineness can decrease this negative influence, but cannot compensate it completely. This phenomenon can be associated with many parameters such as the recrystallization of the activator and the chemical reaction rate (dissolution of the slag and metastable phases, precipitation of new stable strength-giving phases), which drops with decreasing temperature. At the same time a heat treatment for 24h (here 40°C and 80°C) dramatically accelerates the early age strength. This should mainly be due to the acceleration of Gaylussite destabilisation for minimal optimal soda concentration (150 g/l and more). In the case of low activator dosages, such an impressive temperature effect does not take place.

A dry curing condition (here 50% RH) provoked a significant loss of the compressive strength evolution and even further the cessation of the hydration process, if the samples undergo a humid curing period of insufficient duration. This phenomenon should be related to a

significant water evaporation through the non-closed porous system. Due to a slower hydration process and a higher amount of compact C-S-H type hydrates, a longer period is required to close the porosity compared to OPC. Nevertheless, even after long curing period (28 days), 20% of the initial water departs in a period between 28 and 365 days indicating the presence of a high amount of unbound water (useless for hydration at this stage).

The obtained values of shrinkage were higher compared to normally observed OPC values from the literature. This should be related to a finer porosity, higher compressive strength and its constant evolution in time for alkali-activated GGBS. The addition of phosphonates led to even higher shrinkage, confirming the previous observation of a more advanced reaction due to its seeding effect.

Chapter 5 Improving early age strength

Introduction

In the previous chapters one of the main issues generally encountered with Na_2CO_3-activated GGBS binders, the very rapid loss of rheology, was addressed. An appropriate phosphonate-based retarder was selected and its impact on several product properties was considered. Even though this retarder allowed also for a reduction in the yield stress, playing the role of a plasticizer, it was not possible to decrease the W/B sufficiently to achieve an acceptable strength at early age, in particular at low temperature (15°C). This second main issue encountered with such binders is considered in this chapter.

The main early hydration product of Na_2CO_3-activated GGBS binders is Gaylussite. This phase consumes the first Ca^{2+} ions leached from the slag through a reaction with the carbonate ions from the activator. At the same time the Na^+ ions from the activator are embedded in its structure. Yet Gaylussite is unstable against the calcium carbonate polymorphs. Upon Gaylussite decomposition the Na^+ ions are released leading to NaOH in-situ formation. This leads to an acceleration of slag dissolution and C-(A)-S-H precipitation. Therefore, it is expected that the duration of the induction period is controlled by the Gaylussite decomposition kinetics. It was already demonstrated in Chapter 4 that increasing the curing temperature leads to a faster decomposition and a correspondingly higher strength evolution rate. Nevertheless the heat curing is not always feasible on the construction site and is more suitable for precast manufacturing (steam curing). Therefore, the introduction of an accelerating additive is necessary. Theoretically, this can be enhanced specifically by providing supplementary Ca^{2+} ions.

For example (Yang et al., 2012; Jeong et al., 2016;) used $Ca(OH)_2$ as a complementary activator of Na_2CO_3. Yet, they obtained strength development similar to what is generally obtained with pure NaOH. That is, fast early strength development, but low evolution in the long term. This might be related to the dissolution of $Ca(OH)_2$ occurring too quickly and so fast NaOH in-situ formation (since the early pH is about 12) leading to :

$$Ca(OH)_2 + Na_2CO_3 \rightarrow CaCO_3 + 2NaOH$$

Then all the Ca^{2+} provided by the supplementary calcium source is rapidly consumed as $CaCO_3$ and might lead to slag surface blocking, as well as a lower amount of Gaylussite seeds

for the nucleation in bulk. In addition, the presence of lime leads to a high degradation of the rheological properties as will be shown here. Similar results have been obtained by (J. Song et al., 2010) when using NaOH as a complementary activator.

On the other hand, by replacing 50% of Na_2CO_3 with metasilicate, a significant improvement of the strength both at short and long term has been obtained by (Bernal et al., 2016). Yet, a high amount of metasilicate is required, which significantly increases the cost and CO_2 footprint (1.32 t of CO_2 for 1 t of Na_2SiO_3,(Nazari and Sanjayan, 2016)).

Another way to accelerate Gaylussite decomposition in order to release the Na^+ ions is to consume CO_3^{2-} ions through the precipitation of Afm-type phases such as Hydrotalcite. In (Ke et al., 2016) Hydrotalcite (calcined or not) seeds were used to promote its precipitation. It was clearly shown that the calcined Hydrotalcite seeds lead to a significant decrease of the induction period. Nevertheless, no strength results were reported. In addition, quite a high dosage of Hydrotalcite was required which turns out to be a non-valuable acceleration method from an economical point of view.

(Jin and Al-Tabbaa, 2015) also reported studies in which Hydrotalcite precipitation occurs through the addition of reactive MgO. Here again, this is not reasonable from both economical and environmental points of view, due the high price of reactive MgO, high CO_2 emissions during its production (MgO is often obtained by calcination of dolomite $CaMg(CO_3)_2$ and further purification (Yildirim and Akarsu, 2010)).

In this chapter, acceleration through the addition of calcium sources which are economically competitive will be examined (lime, calcium salts, clinker). Various solubilities of the Ca sources are considered (nature and powder fineness). In addition, these sources will be tested in combination with the phosphonate additive to adjust the rheological properties of the binder.

5.1 Materials

Pure powder (analytical grade) calcium oxide (CaO), calcium hydroxide ($Ca(OH)_2$) and calcium chloride ($CaCl_2$) from VWR were used in this study. Clinker from Vicat Company (France) with different levels of grinding was used. Its chemical and mineralogical compositions are reported in Table 8 and Table 9 (results provided by ECOCEM France). The XRD pattern of the clinker powder is reported in Figure 5.1.

Table 8: Main chemical composition of the clinker

SiO_2	Al_2O3	Fe_2O_3	CaO	MgO	TiO_2	MnO	P_2O_5	Cr_2O_3	SrO	Na_2O	K_2O	LOI
21.71	5.0	3.3	65.19	1.49	0.21	0.04	0.06	0.01	0.21	0.18	0.73	0.22

Table 9: Mineralogical composition of the clinker

C_3S	C_2S	C_3A	C_4AF	Na_2O eq.
62.0	15.5	7.7	10.0	0.66

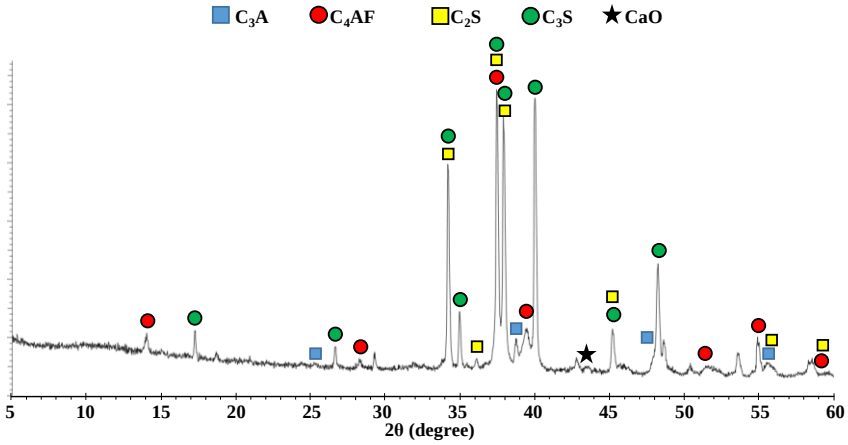

Figure 5.1: XRD patterns of clinker

The raw clinker was first crushed and then ground in a laboratory ball mill. Three fineness grades were obtained denominated hereafter as coarse, fine and very fine clinker. The particle size distribution of the coarse clinker (provided by ECOCEM France) is presented in Figure 5.2, with a $d_{(50)}$ of about 90 µm and the approximate Blaine fineness about 1400 cm^2/g (due to the presence of very coarse particles, these results may be imprecise). SEM observations (Figure 5.3) confirm the presence of a high amount of coarse particles.

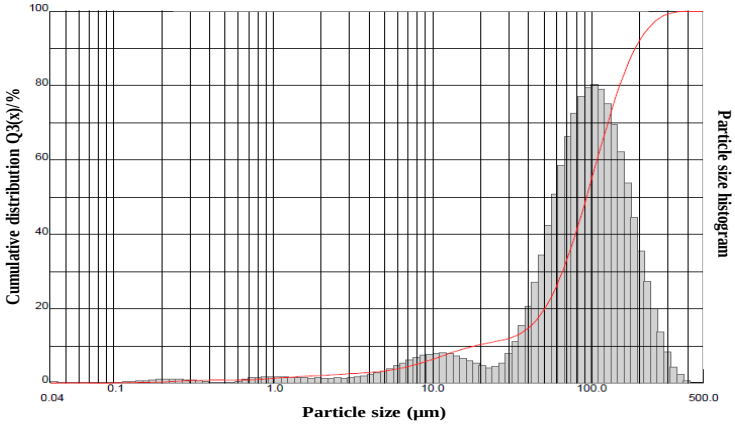

Figure 5.2: Particle size distribution of coarse clinker 1400 cm^2/g Blaine

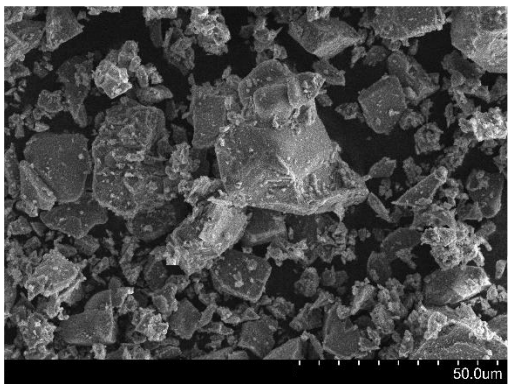

Figure 5.3: SEM image of the coarse clinker 1400 cm^2/g Blaine particles

The particle size distribution of the fine clinker is presented in Figure 5.4. This slag has $d_{(50)}$ about 12.5 µm and the approximate Blaine fineness is about 4000 cm^2/g.

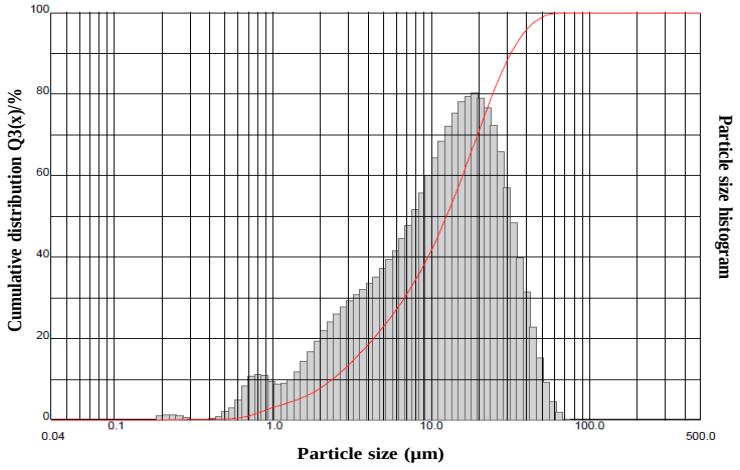

Figure 5.4: Particle size distribution of the fine clinker 4000 cm^2/g Blaine

The particle size distribution of the very fine clinker is presented in Figure 5.5, with $d_{(50)}$ about 8 µm and the approximate Blaine fineness about 6000 cm^2/g. SEM images are reported in Figure 5.6.

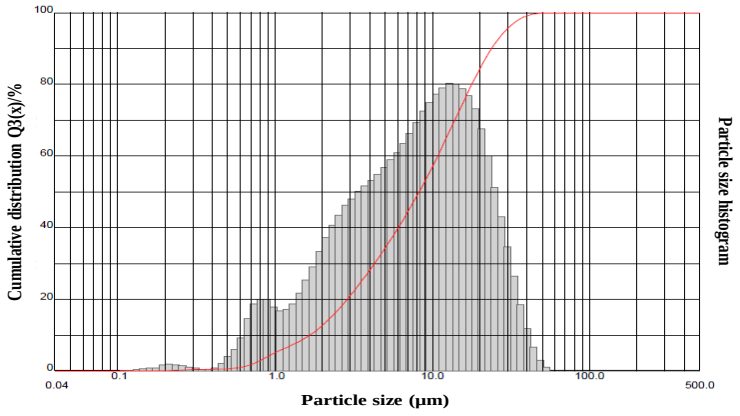

Figure 5.5: Particle size distribution of the very fine clinker 6000 cm^2/g Blaine

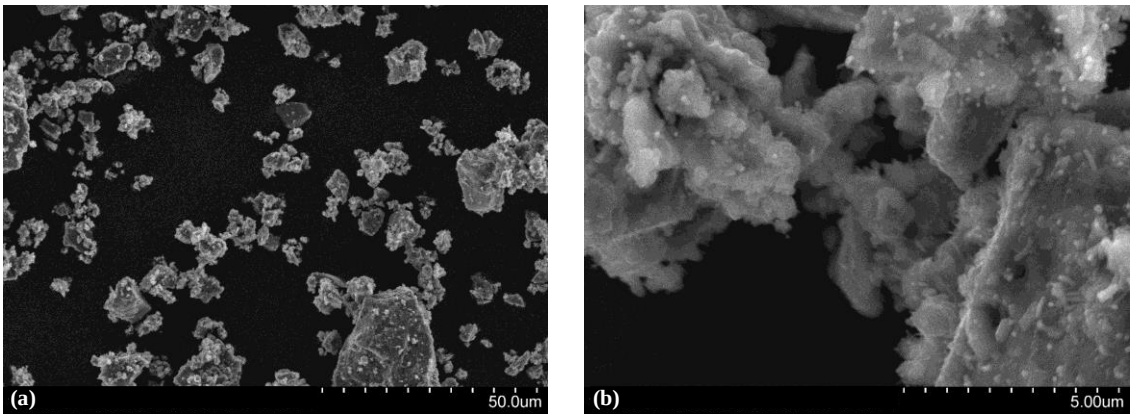

Figure 5.6: *SEM images of the very fine clinker 6000 cm^2/g Blaine*

5.2 Influence of highly soluble calcium sources on early age properties

Three different highly soluble calcium additives were used in partial replacement of GBBS: CaO, $Ca(OH)_2$ and $CaCl_2$. The W/B ratio was fixed at 0.40 and the Na_2CO_3 was kept at a constant aqueous concentration of 250 g/l (10% Na_2CO_3 to total powder, to increase the amount of Na^+).

The microcalorimetry results are reported in Figure 5.7. A significant reduction of the induction period is observed in the case of both anhydrous and hydrated limes. The first peak, which is related to the first hydration products, controls the rheological properties including the open time, which is enhanced. Rheological issues are expected as will be shown below.

In contrast, a noticeable retardation effect on the main hydration peak is obtained in the case of $CaCl_2$ addition. The origin of this unexpected retardation effect of $CaCl_2$ (this additive a good accelerator for OPC based products) was not investigated further. One possible reason might be an eventual decrease of pH through the formation of HCl. Notice that $CaCl_2$ is also a good accelerator in the case of $Ca(OH)_2$ activated slag in which the presence of a high amount of lime maintains a high pH (Bellmann and Stark, 2009).

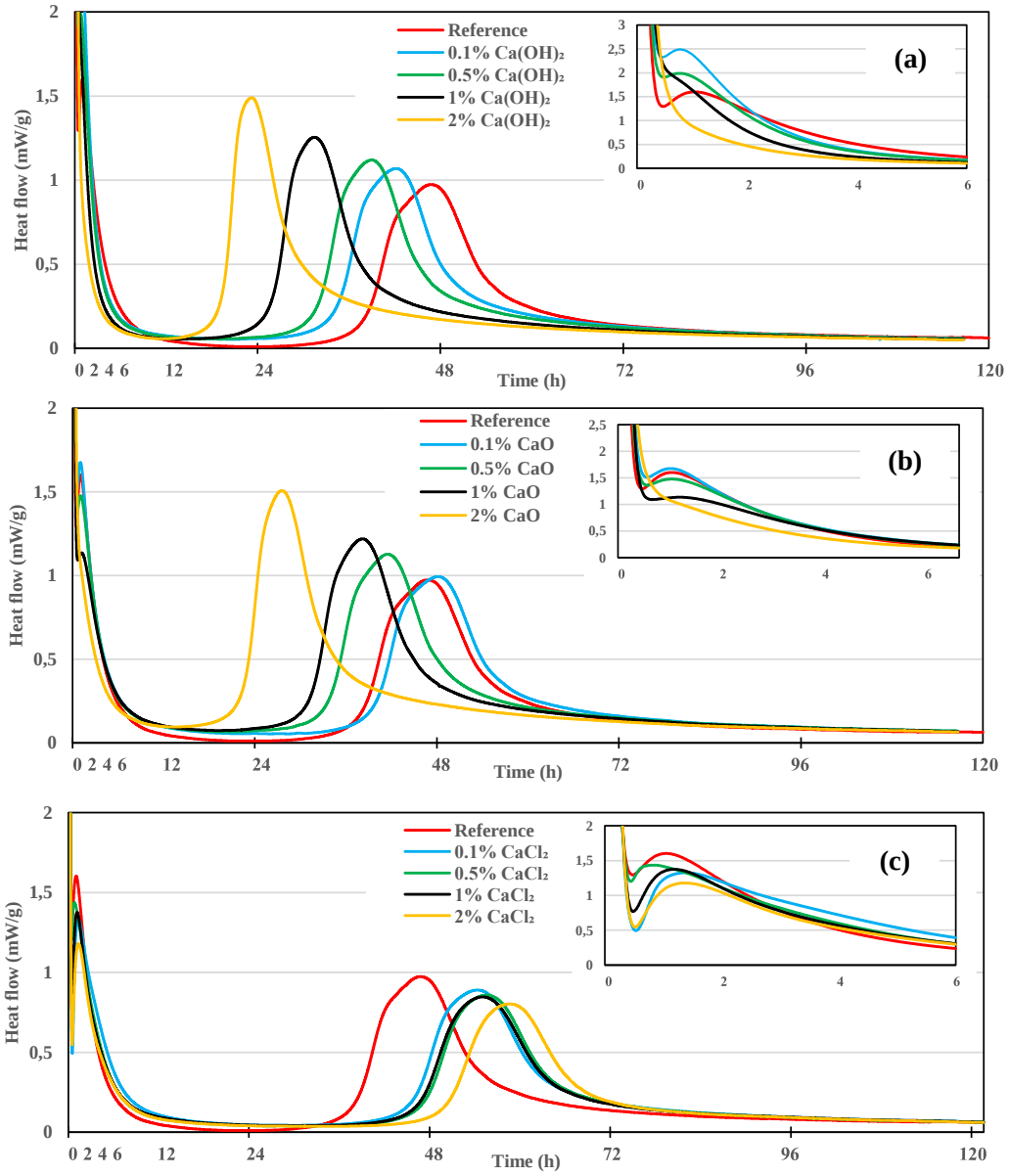

Figure 5.7: Comparison of hydration kinetics in case of partial GGBS replacement by various calcium sources: $Ca(OH)_2$ (a), CaO (b) and $CaCl_2$ (c). W/B=0.40 with 10% Na2CO3 (250 g/l)

The main drawback of $Ca(OH)_2$ is the degradation of the rheology. First, consider the impact of lime without the presence of Na_2CO_3 is considered. The impact of time on the yield stress of a plain GGBS paste is reported in Figure 5.8. The lime leads to an increase of the yield stress from the very beginning. This might be related with the change in the surface charge of the slag particles as shown by the ζ-potential measurements (Figure 5.9). Immediately upon mixing, the pH level is relatively low and the lime is highly soluble, rapidly releasing Ca^{2+} ions. Since the surface charge of the slag particles is negative, the Ca^{2+} ions will adsorb on the surface leading to charge inversion. Yet the ζ-potential remains close to zero, this will lead to particle flocculation and an increase of the yield stress.

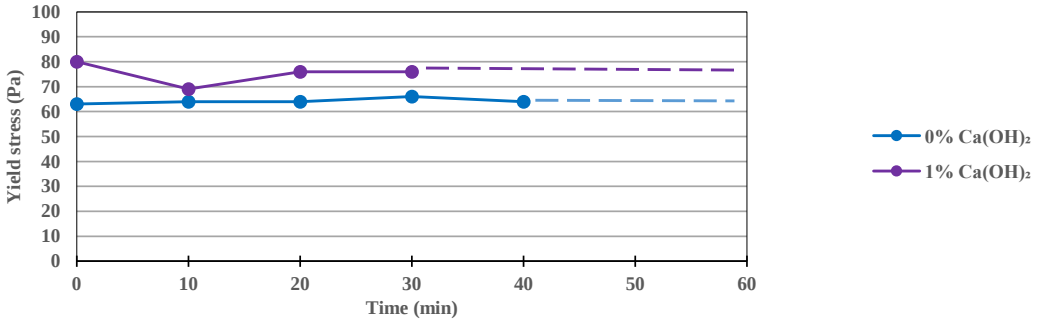

Figure 5.8: Yield stress evolution of GGBS pastes with or without 1% replacement of GGBS by $Ca(OH)_2$ at W/B=0.40, without Na_2CO_3

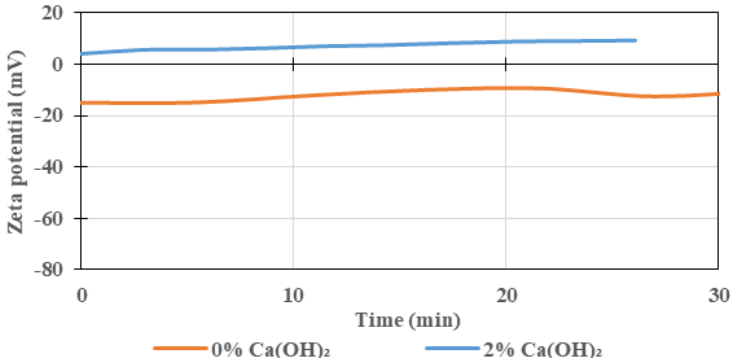

Figure 5.9: Zeta potential of GGBS particles with or without $Ca(OH)_2$ addition W/B=100

In the presence Na_2CO_3 (at 8%), the addition of $Ca(OH)_2$ leads to a significantly faster increase in yield stress(Figure 5.10). In this case, both an eventual flocculation of the slag particles due to the decrease of the absolute values of ζ-potential (Figure 5.11) and rapid precipitation of the first hydration products should come into play.

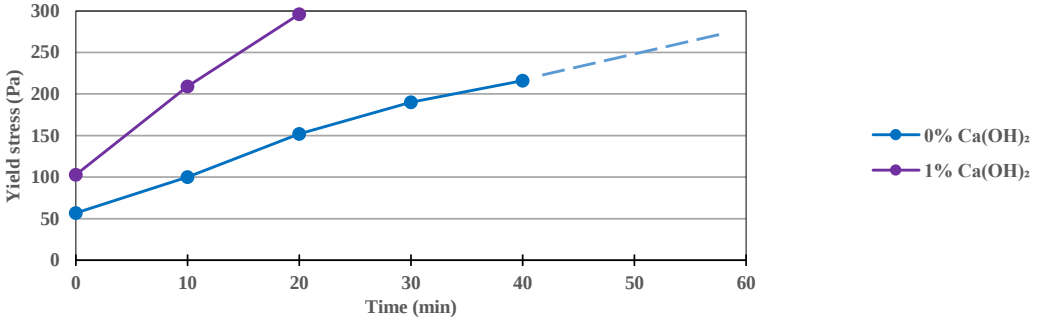

Figure 5.10: Yield stress evolution of GGBS with or without 1% replacement by $Ca(OH)_2$ at W/B=0.40 with 8%Na_2CO_3 (200g/l)

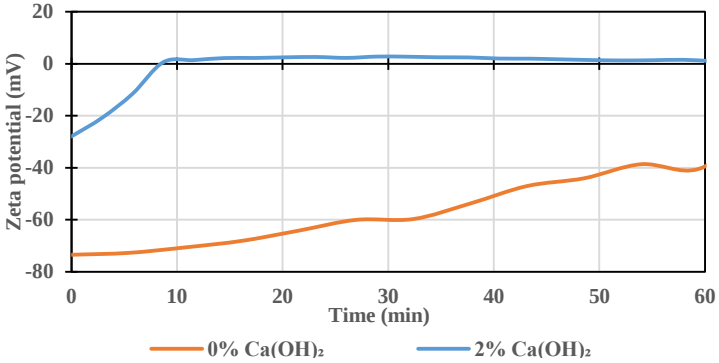

Figure 5.11: Zeta potential of GGBS particles with or without $Ca(OH)_2$ addition at W/B=0.40 with 8%Na_2CO_3 (200g/l)

The phosphonate 4Na*HEDP that allowed the improvement of the rheological properties of the Na_2CO_3 activated GGBS binders is then tested in the presence of lime. The impact of the phosphonate on the yield stress in the presence of lime is reported in Figure 5.12. At a low dosage rate of the retarder (0.1%) the initial yield is significantly reduced. Yet, significant thickening starts after 10 minutes. Before this moment, the mechanism of phosphonate action likely is the same as before. Nevertheless beyond 10 minutes, all phosphonate molecules should be completely consumed and the rheology starts to degrade rapidly. Increasing the phosphonate dosage could extend the open time. However the acceleration effect of the lime on hydration will be then unfortunately eliminated. It turned out to be challenging to manage the thickening effect of the lime with the phosphonate without significantly extending the induction period.

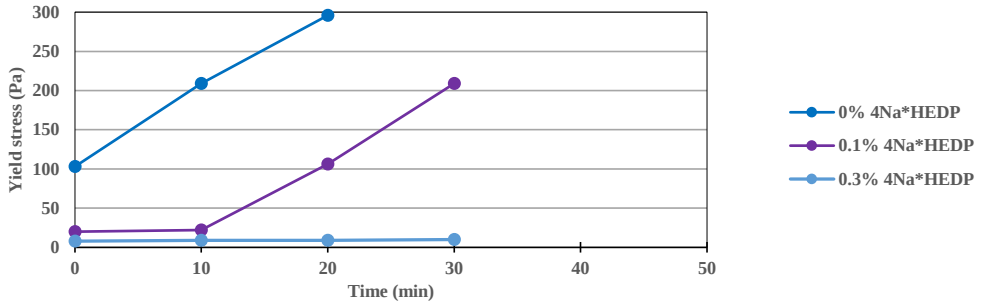

*Figure 5.12: Yield stress evolution of GGBS with 1% replacement by $Ca(OH)_2$ at W/B=0.40 with 8%Na_2CO_3 (200g/l) and 4Na*HEDP*

These results indicate that it should be more convenient to use a calcium source whose solubility kinetics can be controlled. From an industrial point of view the most promising and highly available calcium source, with controllable solubility, is ordinary Portland clinker. Its solubility can be easily varied through its fineness and chemistry during production.

5.3 Rheological properties in the presence of clinker

5.3.1 Influence of partial GGBS substitution by clinker at different W/B ratio and Na_2CO_3 dosages

The yield stress evolution in the case of different levels of partial GGBS replacement by coarse clinker and at different activator contents is presented in Figure 5.13. By comparing Figures 5.13a-c, it can be observed that the addition of coarse clinker leads to a slowing down of the yield stress evolution rate (increase in open time) for any given activator dosage. This effect increases when the Na_2CO_3 amount is decreased. Similar effects can also be observed at a lower W/B ratio (Figure 5.14).

Partial replacement of slag with clinker in the absence of the activator leads to an increase of the yield stress, without evolution over time indicating that there is no high rate hydration

process taking place. The increase of the yield stress in the presence of the clinker may be understood through the ζ-potential. In the case of a dispersion of pure clinker the ζ-potential is positive (Figure 5.15), which is related to a high amount of released and re-adsorbed calcium. Then when GGBS is mixed with clinker heteroflocculation may occur between the negatively charged slag particles and the positively charged clinker particles, leading to an increase of the yield stress.

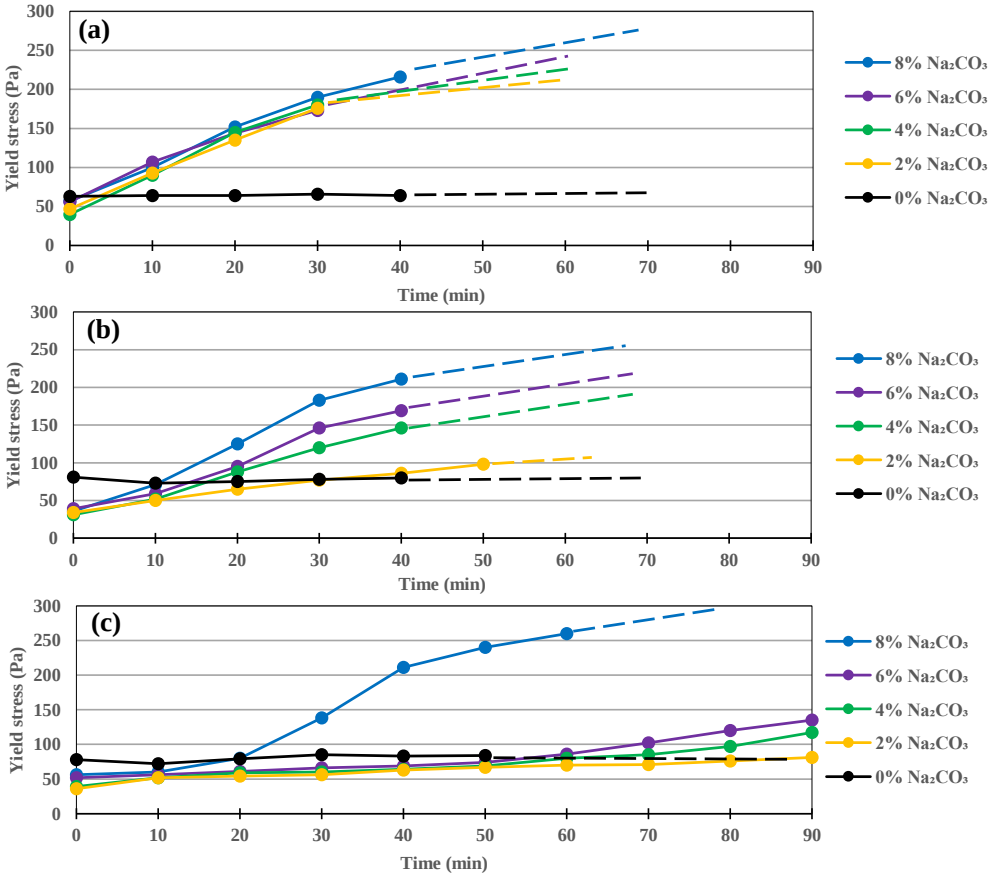

Figure 5.13: Yield stress evolution for different Na_2CO_3 amounts in the case of 100% GGBS (a), with 1% (b) and 5% (c) replacement by Clinker 1400 cm^2/g at W/B=0.40

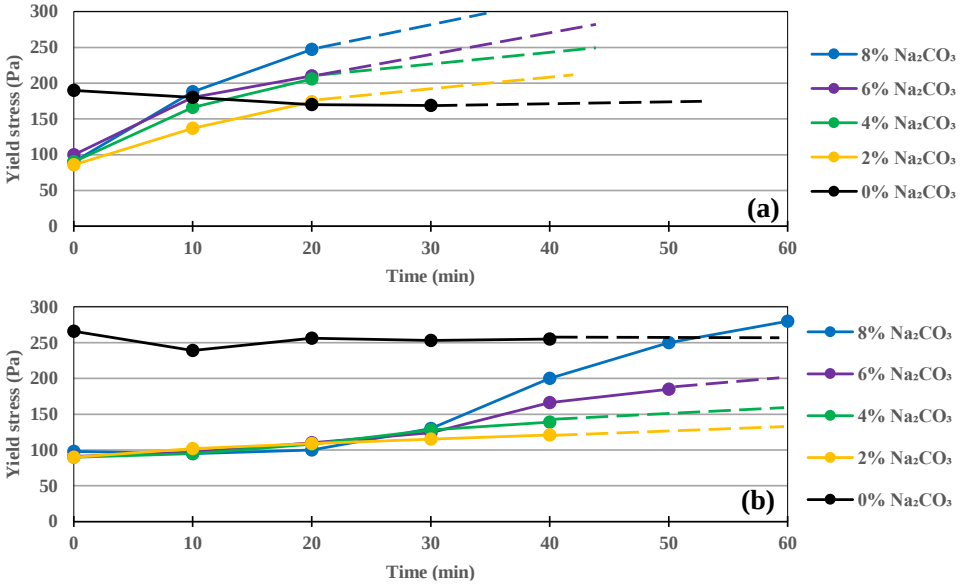

Figure 5.14: Yield stress evolution for different Na_2CO_3 amounts in the case of 100% GGBS (a) and 5% (b) replacement by Clinker 1400 cm^2/g at W/B=0.35

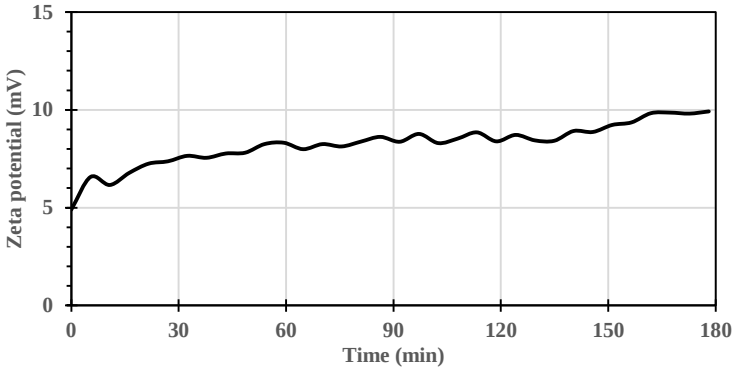

Figure 5.15: Zeta potential evolution of Clinker 1400 cm^2/g in water (Water/Clinker=100)

In the presence of Na_2CO_3 the results of the ζ-potential evolution indicate an initially lower overall negative charge of the particles when clinker is added (Figure 5.16a). A significantly faster increase and transition to positive values takes place in the presence of clinker. This might be related to a greater amount of leached Ca into solution leading to a faster consumption of the CO_3^{2-}. This can also be seen through the higher pH level in the presence of clinker (Figure 5.16b) (due to a higher amount of NaOH in-situ formation). Decreasing the W/B ratio to approach realistic values (those used in the rheological measurements) leads to an acceleration of the transition to the positive values of the ζ-potential (Figure 5.17). Increasing the concentration of Na_2CO_3 also leads to a faster transition to positive values of the ζ-potential (Figure 5.18).

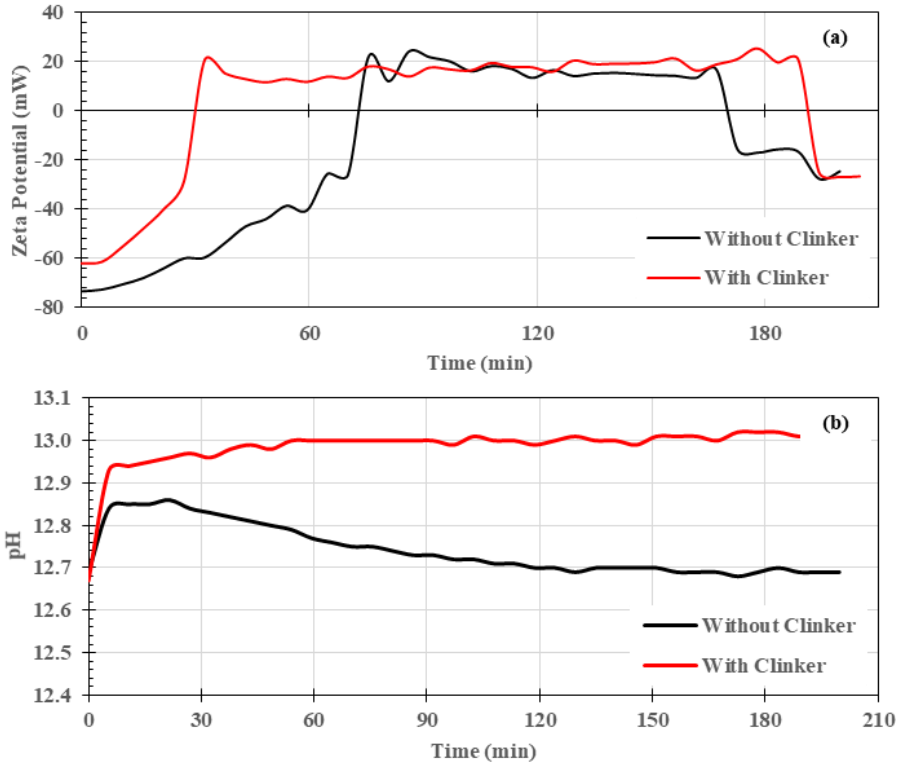

Figure 5.16: Zeta potential (a) and pH (b) evolution of GGBS with and without 5% replacement by Clinker 1400 cm^2/g in the presence of 8% Na_2CO_3 (W/B=100)

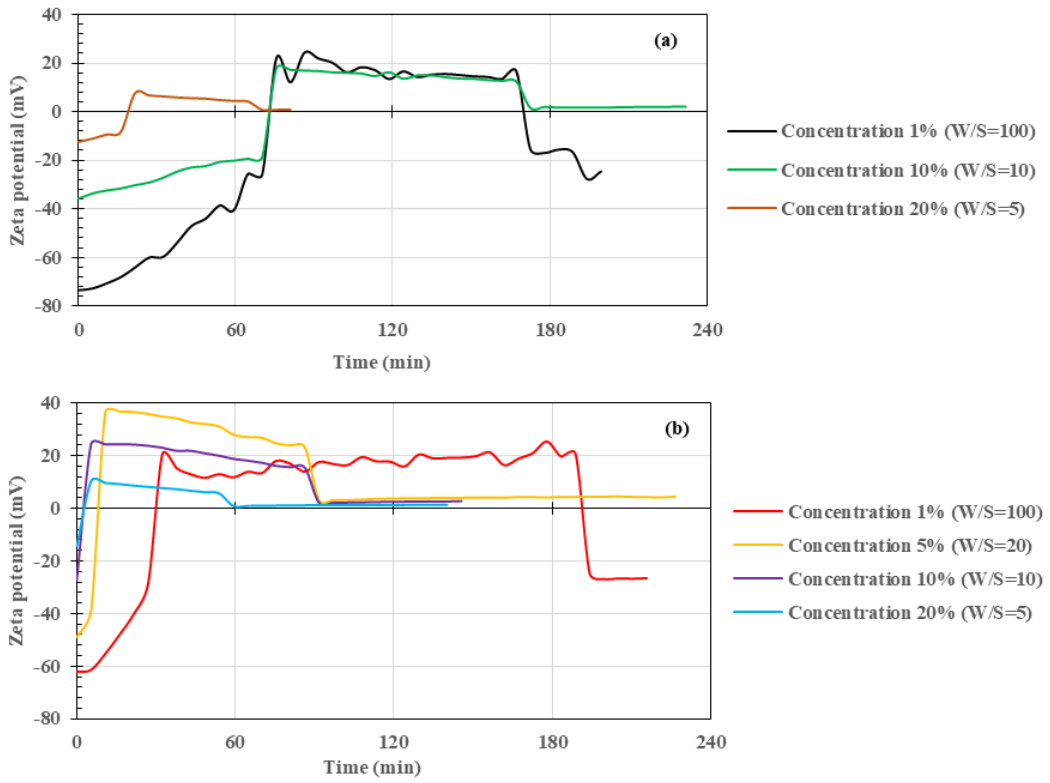

Figure 5.17: Influence of particle concentration for the determination of the ζ-potential without (a) and with (b) 5% replacement of GGBS by Clinker 1400 cm^2/g in the presence of 8% Na_2CO_3

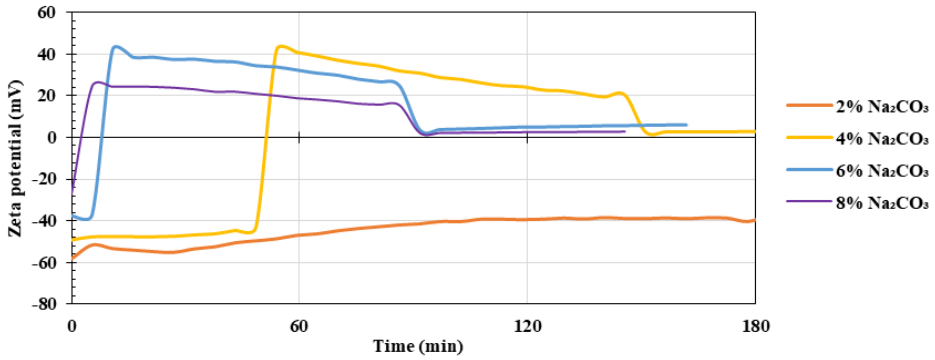

Figure 5.18: Influence of Na_2CO_3 amount on the ζ- potential in case of 5% slag replacement by Clinker 1400 cm^2/g (W/B=20 or 5% concentration)

Increasing the clinker fineness from 1400 to 4000 cm^2/g leads to a significant increase of the yield stress evolution rate for all activator dosages (Figure 5.19), even compared to the case of 100% GGBS. This phenomenon might be related to the high reactivity of the clinker. The yield stress should evolve due mainly to two effects: (i) agglomeration of the particles due to the evolution of the surface charge and the ionic strength, (ii) massive precipitation of the hydration products (carbonates). In the case of low reactive clinker, the evolution should be mainly governed by the first effect, as in case of 100% GGBS (due to calcium leaching). In this case the flocculation should also take place due to a high amount of leached calcium from fine clinker, like in case of lime addition. Due to the significant evolution of the yield stress even without activator addition, precipitation of the hydration products may turn out to be more significant.

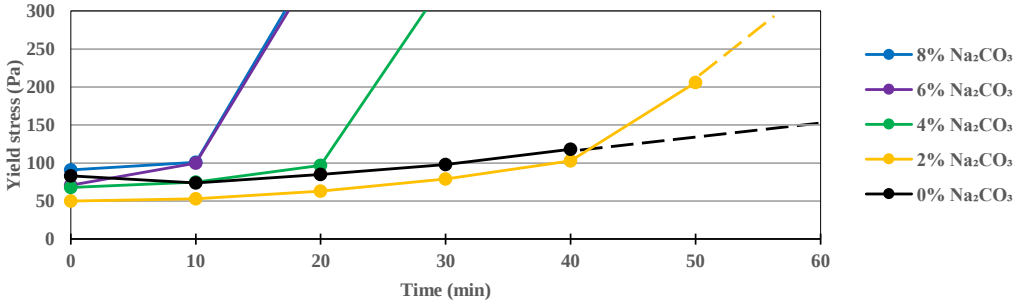

Figure 5.19: Yield stress evolution for different Na_2CO_3 amounts in case of 5% GGBS replacement by Clinker 4000 cm^2/g at W/B=0.40

Further increasing the clinker fineness leads to a faster evolution of the yield stress (Figure 5.20) for all dosage rates of sodium carbonate.

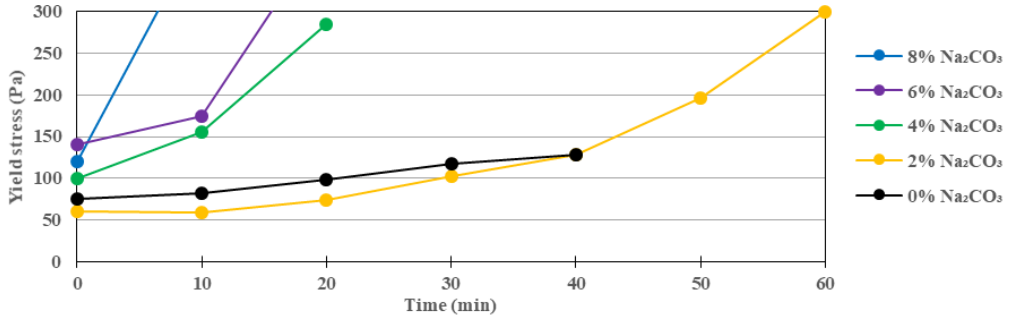

Figure 5.20: Yield stress evolution for different Na_2CO_3 amounts in case of 5% GGBS replacement by Clinker 6000 cm^2/g at W/B=0.40

It was shown that the addition of clinker has an influence on the rheology that depends *qualitatively* on its fineness. In the case of a coarse grade of clinker, its addition leads to a retardation effect on the yield stress evolution. Without the activator, the presence of the clinker leads to an increase of the instantaneous yield stress. On the other hand, with the activator the instantaneous yield stress is decreased when partially substituting GGBS with coarse clinker. Increasing the clinker fineness leads to a significant increase of the yield stress evolution rate.

5.3.2 Impact of different phosphonates on the rheology of the GGBS-Clinker binder

The different retarders considered in the previous chapters with plain GGBS were tested in the case of the GGBS-Clinker mix. The results reported here deal with a mix of 95% GGBS/5% Clinker with 4000 cm^2/g fineness, at W/B=0.35 and activated with 8% Na_2CO_3. The retarders were pre-dissolved in the sodium carbonate solutions at different dosages by mass of (GGBS+Clinker).

Impact the 5Na*EDTMP phosphonate

The influence of the addition of 5Na*EDTMP on the values of the yield stress at different time periods is presented in Figure 5.21. First, it can be observed that the sample without the

retarder has quite a high yield stress at the beginning, which increases significantly after 10 minutes. It was not possible to perform rheological measurements at 20 minutes since the sample became too thick. Addition of the phosphonate at a very low dosage (0.01%) leads to a highly thickening effect. The yield stress at 10 min was too high to be measured. The origin of this phenomenon was not investigated. Beyond a dosage of 0.3%, a significant decrease of the yield stress is observed. In addition, the yield stress decreases over time up to the end of the 20 min measurement duration.

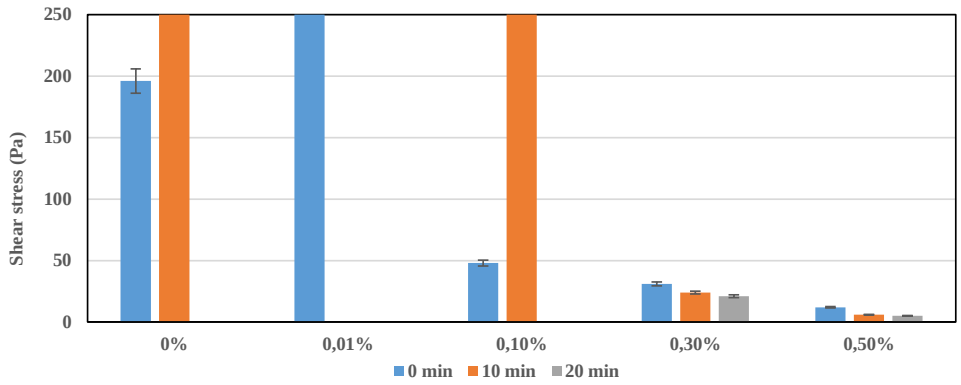

*Figure 5.21 : Influence of 5Na*EDTMP dosage on yield stress evolution for pastes comprising 95% GGBS and 5% Clinker 4000cm²/g at W/B=0.35, activated with 8% Na_2CO_3*

Impact of the 4Na*HEDP phosphonate grade

The influence of 4Na*HEDP different dosages on the yield stress evolution is presented in Figure 5.22. The addition of this molecule leads to a significant decrease of the yield stress evolution, even at a 0.1% dosage. Increasing the dosage up to 0.5% leads to the yield stress increasing again. Nevertheless, the values and the rate of evolution is much lower compared to the reference sample. Similar to the case of the plain GGBS mixes, this may be attributed to the effect of precipitated Ca-phosphonate particles at high dosage. This phosphonate grade seems to have a lower Ca tolerance (higher tendency to precipitate Ca-phosphonates) than the 5Na*EDTMP grade and so it is more appropriate as retarder and plasticizer. Indeed it is effective at lower dosage, which should allow avoiding an eventual delay of the strength development.

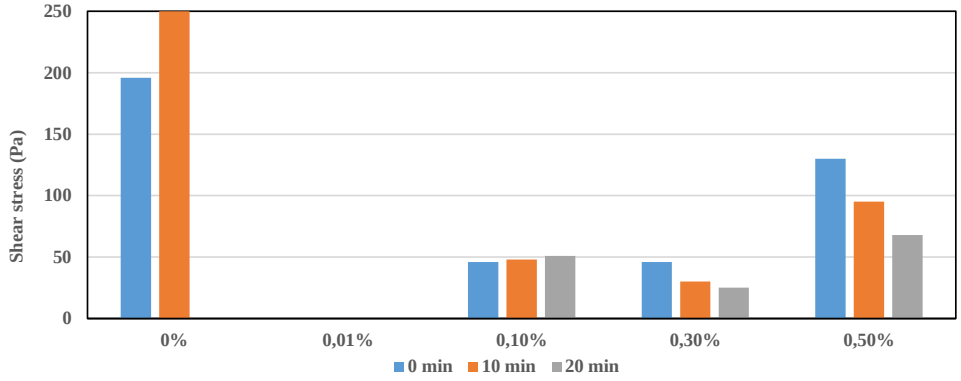

*Figure 5.22: Influence of 4Na*HEDP dosage on yield stress evolution of paste 95% GGBS + 5% Clinker 4000cm²/g at W/B=0.35 with 8% Na_2CO_3*

Several other phosphonate grades have been tested without similar levels of success. The results are therefore not reported here. A further investigation on the GGBS-clinker mixes will be performed with the 4Na*HEDP phosphonate grade. This allows a comparison to be made with the results of the plain GGBS mixes reported in previous chapters.

5.3.3 The rheology of the GGBS-Clinker mixes with phosphonate addition

5.3.3.1 Case of the coarse clinker

The time evolution of the yield stress of the binders for different phosphonate dosages and for different clinker contents is presented in Figure 5.23. By comparing Figure 5.23a-c, it can be seen that the phosphonate is more effective in terms of retardation in the presence of the clinker. There seems to be a synergic effect between the retardation due to the coarse clinker seen above and that of the phosphonate.

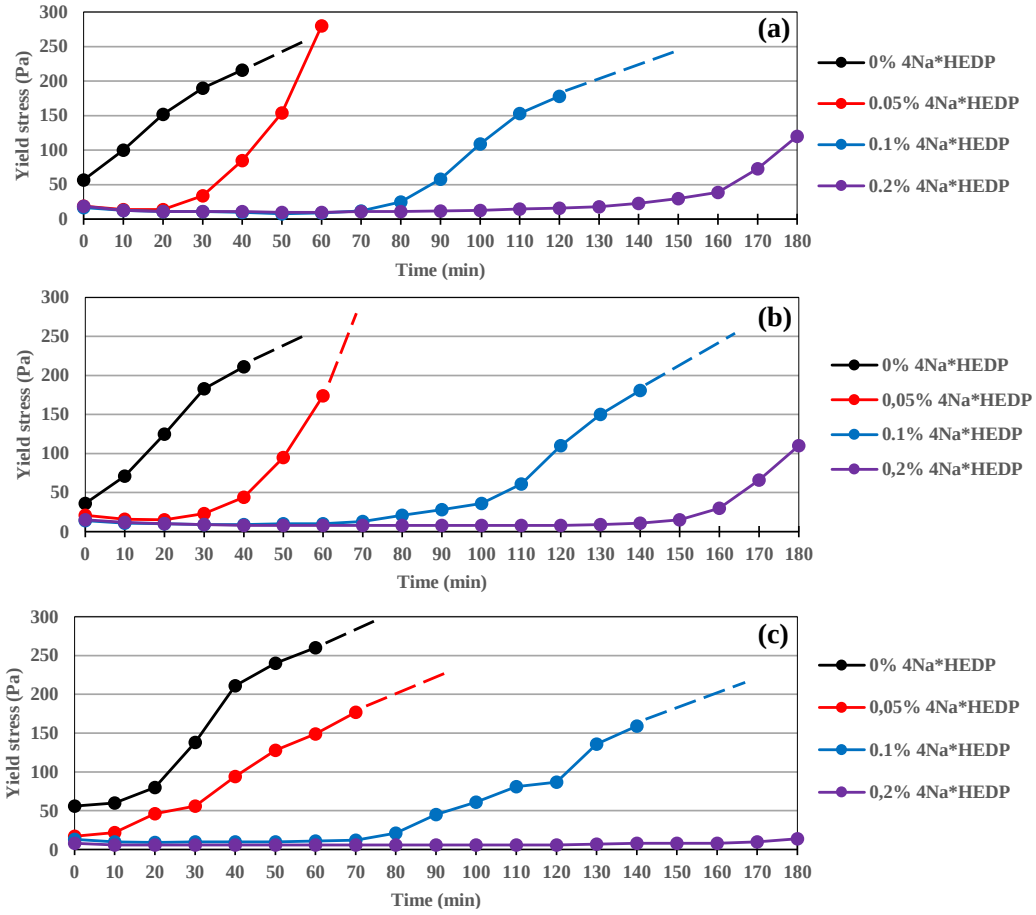

*Figure 5.23: Influence of 4Na*HEDP addition in case of 100% GGBS (a) and 1% (b) or 5% (c) partial slag replacement by Clinker 1400 cm^2/g. 8% Na_2CO_3 at W/B=0.40*

The impact of the phosphonate on the ζ-potential of the GGBS-clinker binder is presented in Figure 5.24. Addition of the phosphonate leads to a delay in the transition of the ζ-potential to positive values. This reflects the Ca complexing effects of the phosphonate and the subsequent

delay in the CO_3^{2-} consumption with the corresponding prevention of rapid NaOH formation. The thickening effect (strong increase of the yield stress at a certain moment), which may be related to both hydration products (carbonates) precipitation and the passage of the ζ-potential through zero (see Figure 5.24) leading to flocculation, is then delayed in the presence of the phosphonate.

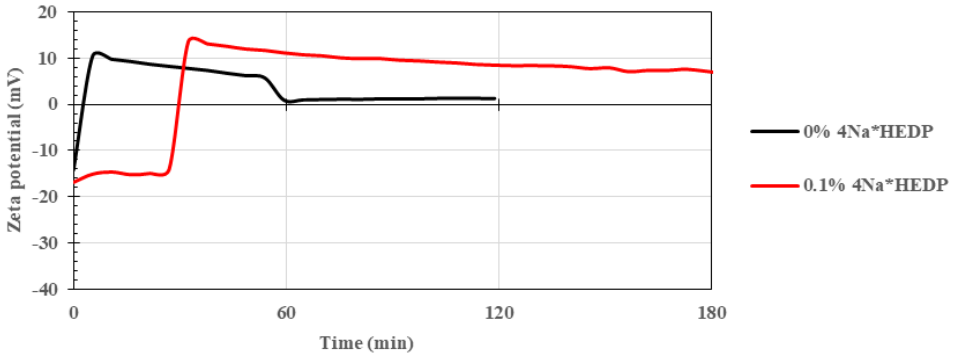

*Figure 5.24: Influence of 4Na*HEDP on the ζ-potential evolution in the case 5% replacement of GGBS by Clinker 1400 cm^2/g at 8% Na_2CO_3 (W/B=5)*

Decreasing the Na_2CO_3 dosage to 6% leads to more retardation and plasticising effects in the presence of the clinker (Figure 5.25). In the case of 5% clinker substitution, an unexpected thickening effect of the phosphonate at low dosage (0.05%) is obtained.

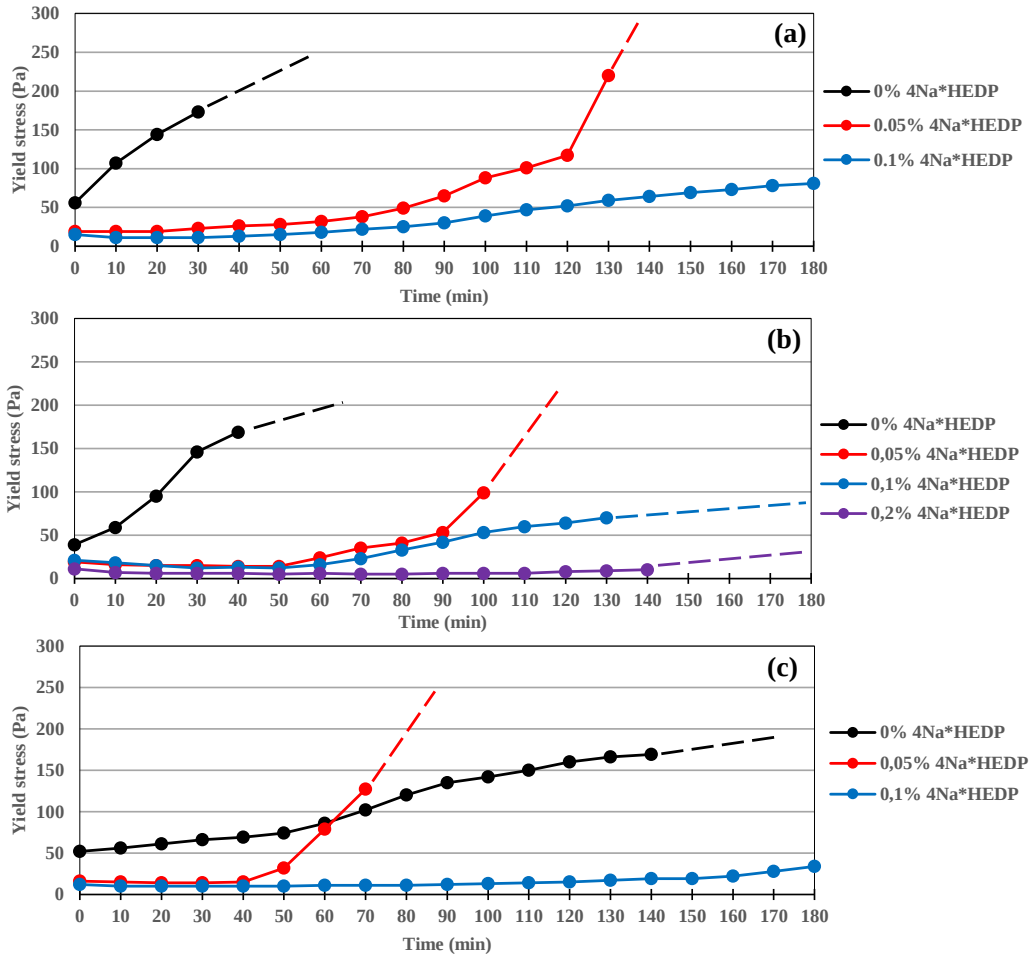

*Figure 5.25: Influence of 4Na*HEDP addition in case of 100% GGBS (a) and 1% (b) or 5% (c) partial slag replacement by Clinker 1400 cm^2/g. 6% Na_2CO_3 at W/B=0.40*

5.3.3.2 Case of Fine clinker

As seen above, the substitution of GGBS with finer clinker (4000 cm^2/g) leads to a higher evolution rate of the yield stress. This was attributed to a higher rate of Ca^{2+} release into solution, leading to both rapid precipitation of the first hydration products and flocculation of the slag particles due to shrinkage of their electrical double layer. Due to a higher amount of calcium ions, a higher dosage of phosphonate is required when the clinker fineness is increased to achieve the appropriate rheological properties (Figure 5.26).

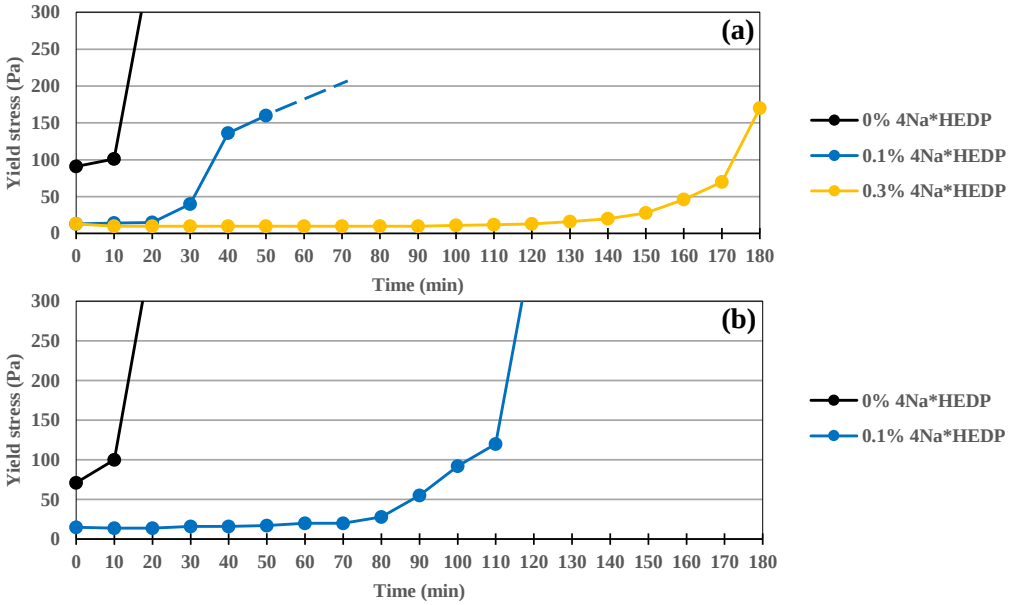

*Figure 5.26: Influence of 4Na*HEDP addition in case of 95% GGBS and 5% Clinker 4000 cm^2/g. 8% (a) and 6% (b) Na_2CO_3 at W/B=0.40*

5.3.3.3 Case of the Very fine clinker

A further increase of the clinker fineness to 6000 cm^2/g Blaine leads to more acceleration of the thickening. Higher amounts of phosphonate are then required (Figure 5.27). As it can be observed that the influence of phosphonate is quite pronounced. This means that unlike with lime, even with very fine clinker, good rheological properties and a sufficient open time can be achieved even if a higher amount of phosphonate is needed.

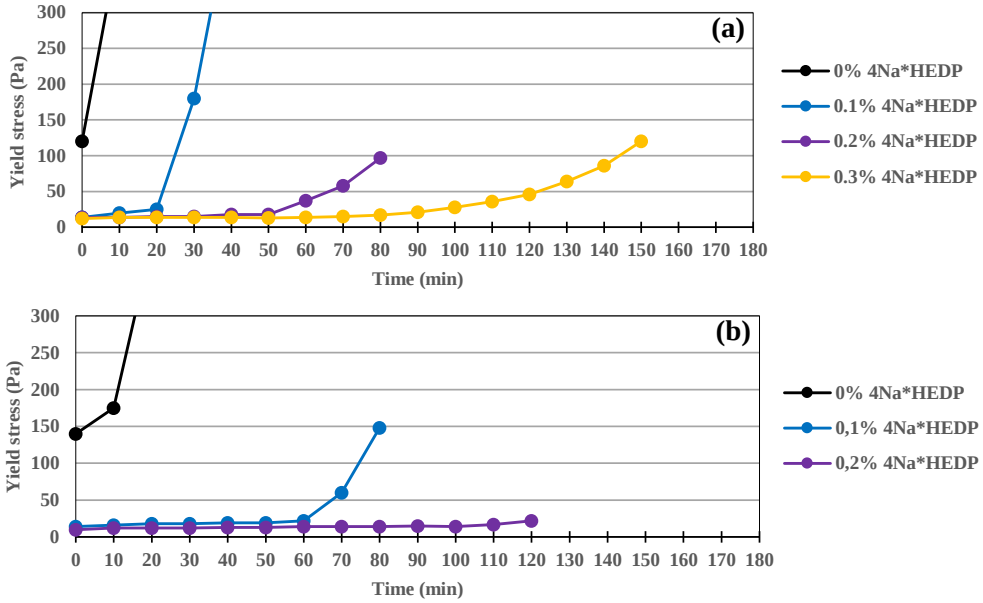

*Figure 5.27: Influence of 4Na*HEDP addition in case of 95% GGBS and 5% Clinker 6000 cm^2/g. 8% (a) and 6% (b) Na_2CO_3 at W/B=0.40*

5.4 Hydration kinetics of the GGBS-clinker mixes

5.4.1 GGBS-clinker mixes without the phosphonate

5.4.1.1 Coarse clinker

The hydration kinetics versus GGBS substitution level by coarse clinker for different amounts of Na_2CO_3 is reported in Figure 5.28. The presence of the clinker leads to a noticeable reduction in the induction period. Yet this acceleration effect depends on the dosage of the sodium carbonate. The reduction of the induction period is more significant at low Na_2CO_3 dosage. For 1% clinker an acceleration is obtained only for 2% Na_2CO_3. In the case of 5% of clinker replacement, a significant reduction of the induction period is observed for all Na_2CO_3 amounts considered. The impact decreases when increasing the activator dosage. However the cumulative heat released increases with activator dosage for all mixes, with or without clinker (Figure 5.29). The reduction of the induction period in the presence of clinker is related (as will be shown later) to the constant Ca^{2+} leaching from clinker. It leads to more rapid Gaylussite dissolution and also provides additional Ca for C-S-H precipitation in the case of high soda concentrations. In the case of low soda dosages, it should provide Ca for C-S-H, as well as increasing the pH level. In addition, it should prevent the slag surface from becoming blocked at the very beginning by fast precipitation of some hydrates in bulk which will play a role of nucleation seeds. This lead to a further higher slag dissolution. In the case of high soda

concentration, the acceleration of the reaction should, on the contrary, lead to greater blocking of the slag surface and further lower slag dissolution (as it also will be demonstrated in the present work).

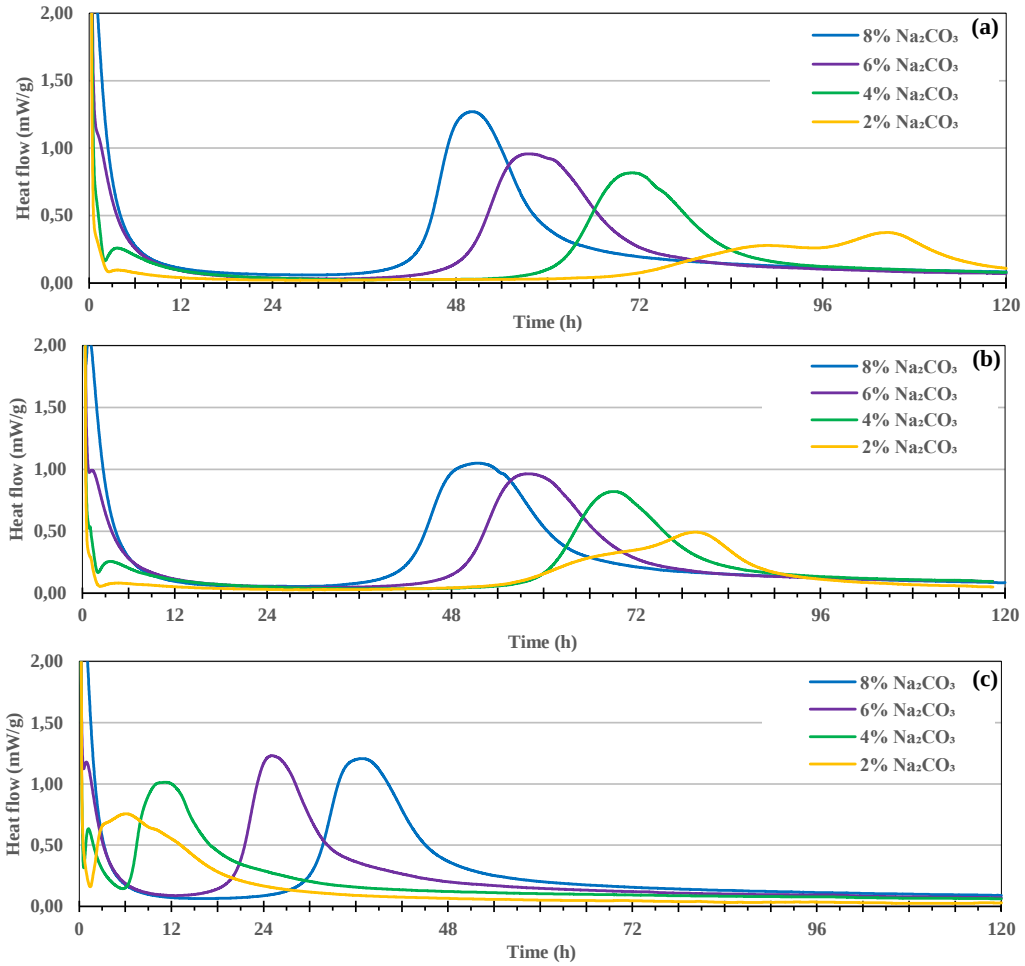

Figure 5.28: Influence of partial GGBS replacement by clinker 1400 cm2/g on hydration kinetics with different amounts of Na_2CO_3 at W/B=0.40. The replacement levels are: 0% (a), 1% (b) and 5% (c)

In Figure 5.29 the heat released after 48 or 120 hours of hydration with different levels of clinker replacement are presented as a function of sodium carbonate aqueous concentration. At short term (48 hours), increasing the clinker percentage leads to a higher amount of heat released for all activator dosage rates considered. On the other hand, at longer term (6 days), the total heat released is lower at 5% than at 1% clinker replacement. This is the first indication that GGBS substitution with clinker leads to an acceleration of the very early hydration, but at longer term the situation may be inverted. The clinker replacement level should be then limited. The replacement level of clinker in the mixes considered this study was limited to 5%.

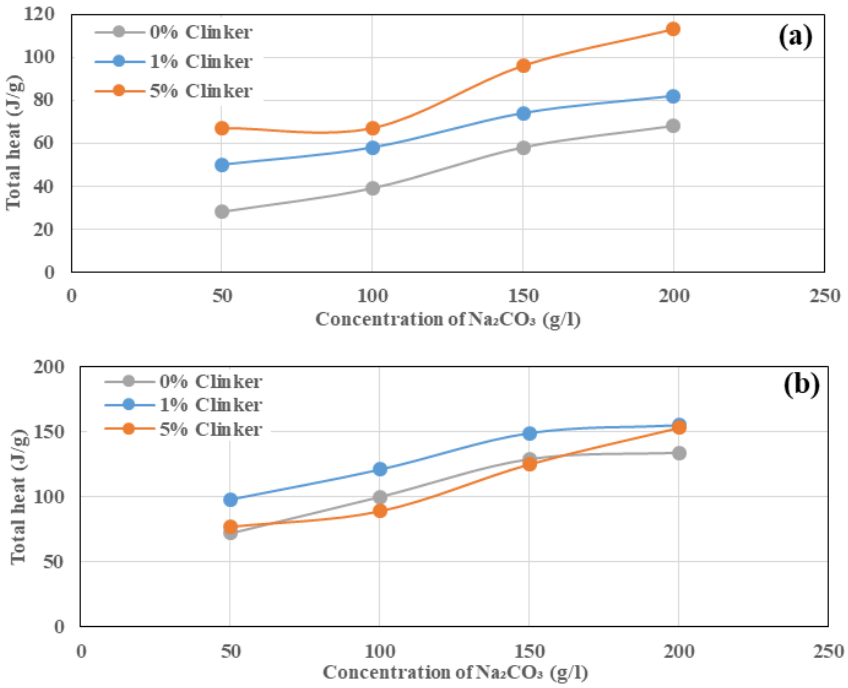

Figure 5.29: Heat released after 48h (a) or 120h (b) of hydration in case of different percentages of GGBS replacement by clinker 1400 cm^2/g as a function of Na_2CO_3 concentration at W/B=0.40

5.4.1.2 Hydration kinetics for the GGBS-Fine clinker mixes

Increasing the clinker fineness up to 4000 cm^2/g leads to a much more significant acceleration of the hydration reaction (Figure 5.30). Two main peaks can still be distinguished, yet no clear induction period can be observed. The first peak might be still related mostly to Gaylussite formation and the second peak to the main hydration process (C-(A)-S-H gel and other hydrates formation). Note that the second peak comprises two separate features. The absence of a clear induction period suggests that a situation similar to NaOH activation is taking place. Due to the rapid release of Ca^{2+} from the fine clinker, calcite precipitation might be preferred to Gaylussite. Once the carbonate ions are consumed, the situation becomes similar to NaOH-activation. This will lead to rapid early strength development, but blockage at long term. This also explains the very fast loss of rheology in this case seen previously.

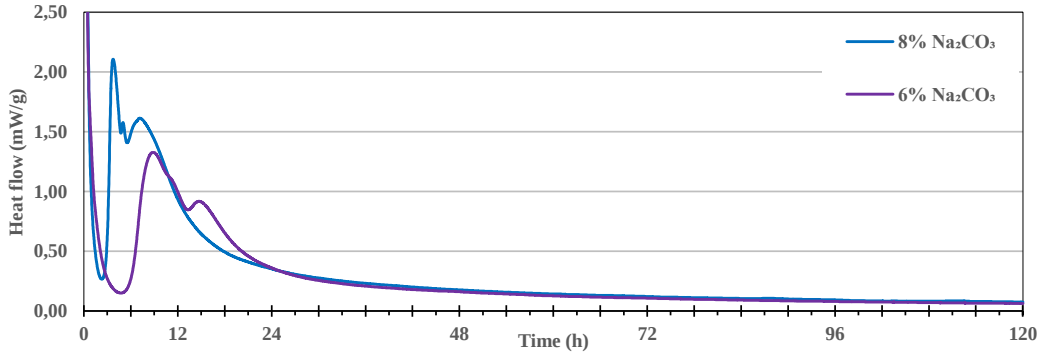

Figure 5.30: Hydration kinetics of GGBS with 5% replacement by clinker 4000 cm^2/g with different amount of Na_2CO_3 at W/B=0.40.

5.4.1.3 Hydration kinetics of the GGBS-Very fine clinker mixes

A further increase of the clinker fineness leads to an even faster hydration process (Figure 5.31). Similar, but enhanced, phenomena compared to the previous case are observed.

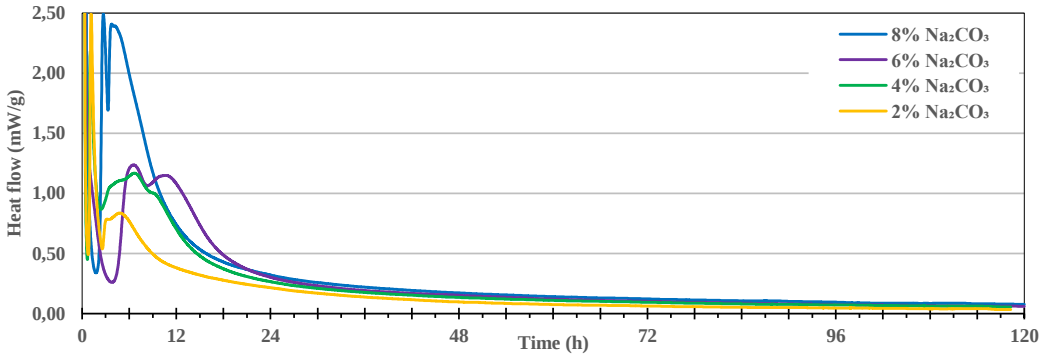

Figure 5.31: Hydration kinetics of GGBS with 5% replacement by clinker 6000 cm^2/g with different amount of Na_2CO_3 at W/B=0.40

5.4.2 Hydration kinetics of the GGBS-clinker mixes in the presence of the phosphonate

5.4.2.1 GGBS-Coarse clinker mixes

In this investigation the GGBS replacement level by clinker was fixed at 5%. Similar to the plain GGBS mix, the addition of the phosphonate leads to a quantitative modification of the hydration process that can be seen through the microcalorimetry results (Figure 5.32). Yet, in contrast with the case of plain GGBS mixes, phosphonate dosage rates up to 0.2% reduce the induction period between the two peaks. At the same time the retardation of the first peak indicates a delay in setting, as before. Further increasing the dosage (0.3%) leads to a delay in hydration (both peaks are delayed). The origin of the accelerating effect of the phosphonate was not investigated further. As was discussed in the previous chapters, the phosphonate may precipitate with calcium leading eventually to acceleration through seeding effects and so also the prevention of slag/clinker surface blocking. The presence of high amounts of Ca^{2+} provided by the clinker may favour the precipitation of the phosphonate. Increasing the phosphonate dosage should lead to an increase of its complexing effects over its precipitation with Ca resulting in retarding effects (lack of free calcium for C-S-H precipitation).

Regarding the first peak (Figure 5.33), it can be seen that the phosphonate leads to its retardation (which corresponds to a longer open time with its addition). This retardation effect increases with the phosphonate dosage rate.

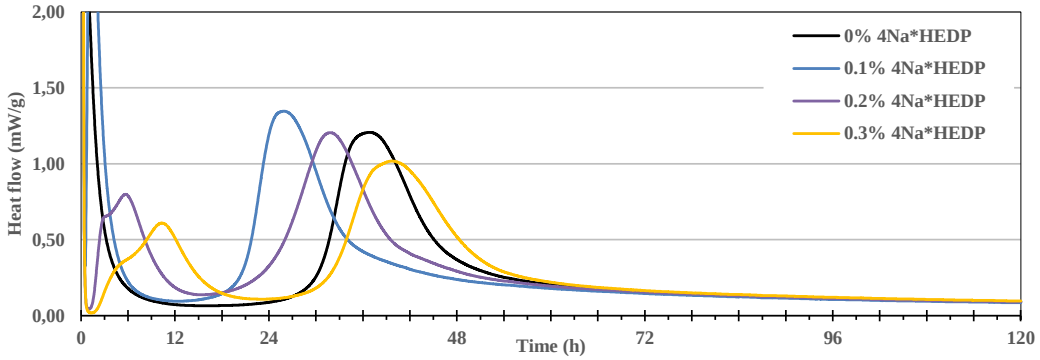

*Figure 5.32: Influence of 4Na*HEDP dosage on hydration kinetics in case of 5% GGBS replacement by clinker 1400 cm^2/g at W/B=0.40 and 8% Na_2CO_3*

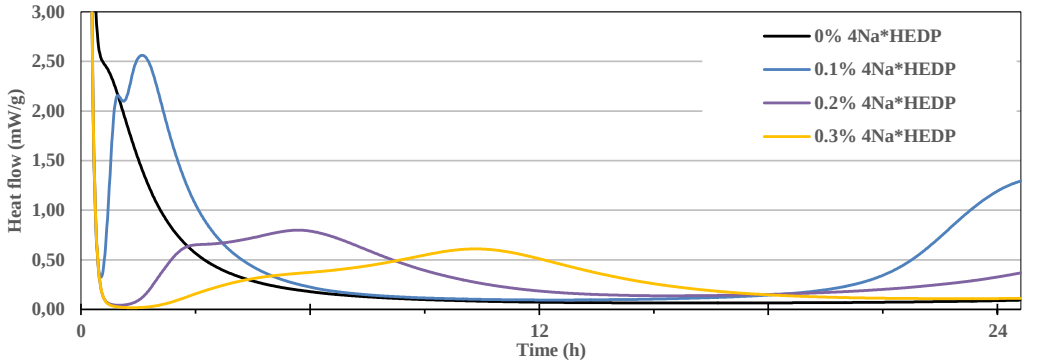

*Figure 5.33: Influence of 4Na*HEDP dosage on hydration kinetics for the first 24h in case of 5% GGBS replacement by clinker 1400 cm^2/g at W/B=0.40 and 8% Na_2CO_3*

The reduction of the induction period in the presence of the phosphonate at low dosage is accompanied by a higher amount of heat released (Figure 5.34), indicating a higher degree of hydration which is expected to lead to higher early strength development.

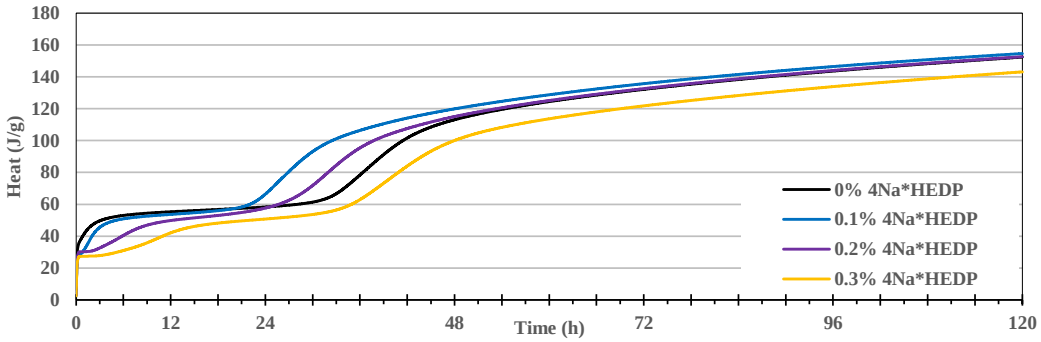

*Figure 5.34: Influence of 4Na*HEDP dosage on heat released during hydration of GGBS with 5% replacement by clinker 1400 cm^2/g at W/B=0.40 and 8% Na_2CO_3*

In the case of a lower amount of sodium carbonate (6%) (Figure 5.35), the accelerating effect of the phosphonate is obtained for a lower phosphonate dosage (0.1%). Beyond this dosage rate, a significant retardation effect can be observed (Figure 5.35 and Figure 5.37). One possible explanation is the following: decreasing the amount of activator should lead to a lower concentration of Ca in solution since the hydration rate of the slag is lower. There is probably

enough phosphonate molecules for complexing all of the available Ca^{2+} at a dosage rate of 0.2%, in contrast with the case of 8% Na_2CO_3.

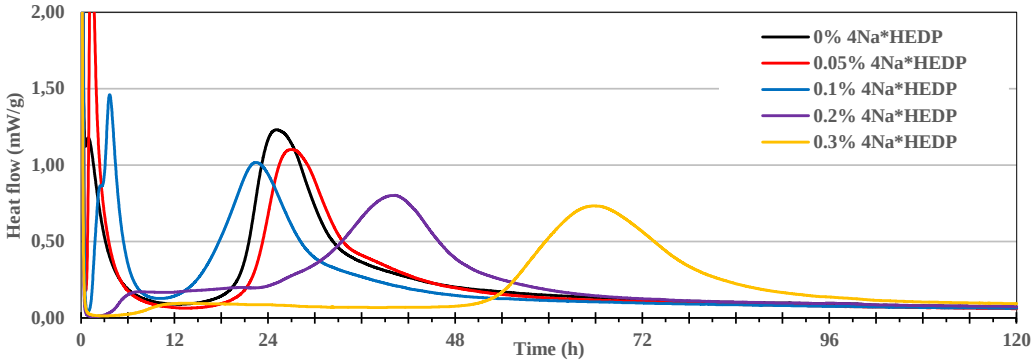

*Figure 5.35: Influence of 4Na*HEDP dosage on hydration kinetics in case of 5% GGBS replacement by clinker 1400 cm^2/g at W/B=0.40 and 6% Na_2CO_3*

Taking into account the retarding effects over the first period of hydration, which is related to the rheology maintenance (Figure 5.36), it is anticipated that the optimum phosphonate dosage for 6%Na_2CO_3 is about 0.1%. Beyond this dosage rate, retardation effects may be an issue.

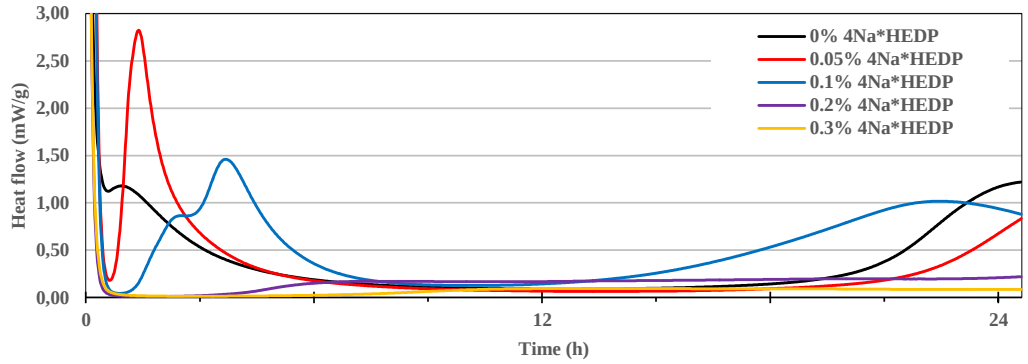

*Figure 5.36: Influence of 4Na*HEDP dosage on hydration kinetics for the first 24h in case of 5% GGBS replacement by clinker 1400 cm^2/g at W/B=0.40 and 6% Na_2CO_3*

This is confirmed by the results of cumulative heat release (Figure 5.37). For dosage rates higher than 0.1% there is a significant decrease of the heat released.

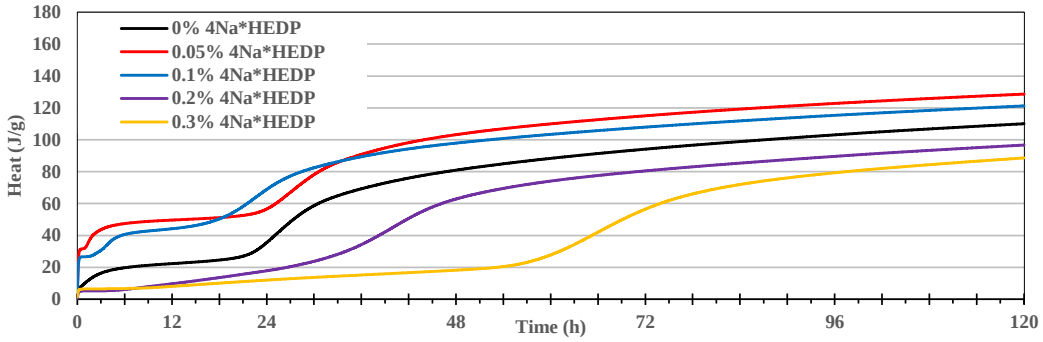

*Figure 5.37: Influence of 4Na*HEDP dosage on heat released during hydration of GGBS with 5% replacement by clinker 1400 cm^2/g at W/B=0.40 and 6% Na_2CO_3*

5.4.2.2 Hydration kinetics of the GGBS - *Fine* Clinker mixes in the presence of the phosphonate

The acceleration effect of the phosphonate is not observed in the case of finer clinker within the dosage rate interval considered (Figure 5.38-Figure 5.39). At the dosage rate for which the strength-giving peak is not retarded (0.1%), a slight delay of the first hydration peak can be observed. This is consistent with the rheological results in which a reduction of the yield stress and a certain extension (insufficient) of open time was obtained (Figure 5.27). In order to maintain sufficient rheology the phosphonate dosage must be increased to a value for which a significant delay of the strength-giving peak occurs. Tuning of the phosphonate dosage rate in the case of fine clinker is challenging (like it was in case of lime). Nevertheless even with a high amount of phosphonate, the main hydration peak occurs in less than 24h (instead of 48h for 100% GGBS), which signifies an acceleration of the hydration process.

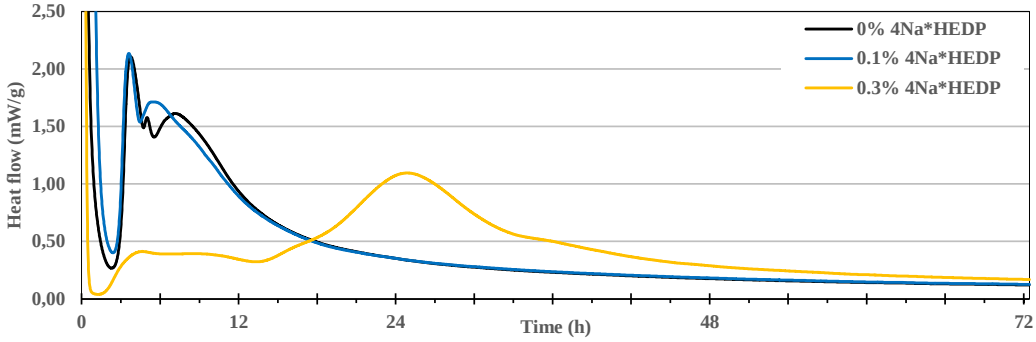

*Figure 5.38: Influence of 4Na*HEDP dosage on hydration kinetics in case of 5% GGBS replacement by clinker 4000 cm^2/g at W/B=0.40 and 8% Na_2CO_3*

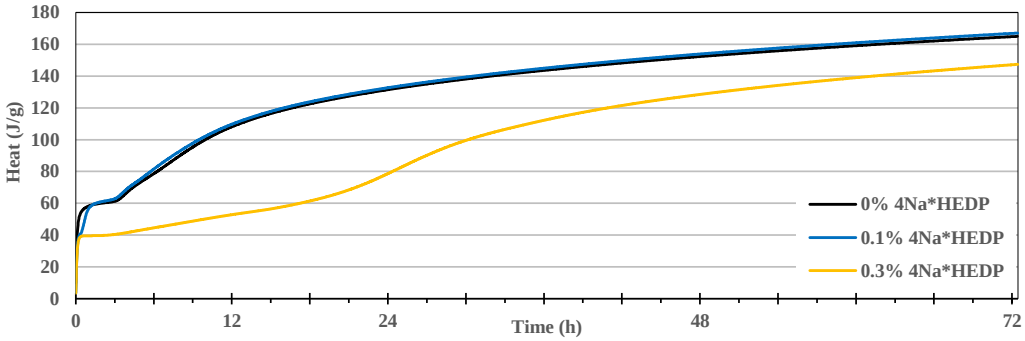

*Figure 5.39: Influence of 4Na*HEDP dosage heat released during hydration process of GGBS with 5% replacement by clinker 4000 cm^2/g at W/B=0.40 and 8% Na_2CO_3*

5.4.2.3 Impact of the phosphonate on the hydration kinetics of the GGBS - *Very fine* clinker mixes

Similar results to the fine clinker are obtained with the very fine grade clinker (Figure 5.40 and Figure 5.41). Here again, tuning the phosphonate dosage in order to get a sufficient open time without significantly impacting the main hydration peak is not easy.

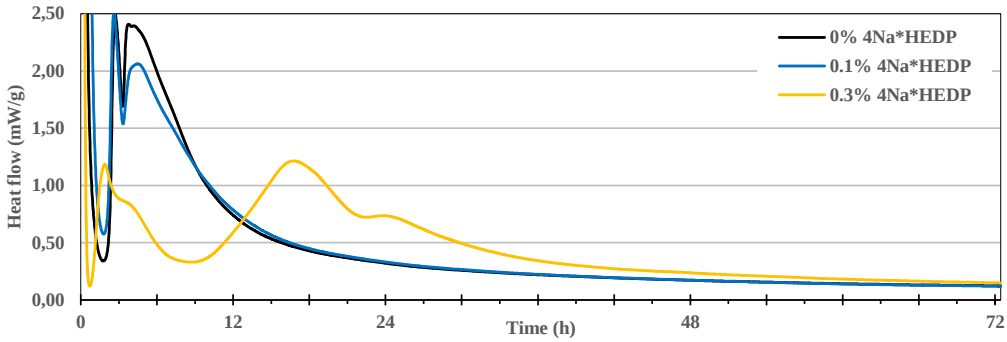

*Figure 5.40: Influence of 4Na*HEDP dosage on hydration kinetics in case of 5% GGBS replacement by clinker 6000 cm²/g at W/B=0.40 and 8% Na_2CO_3*

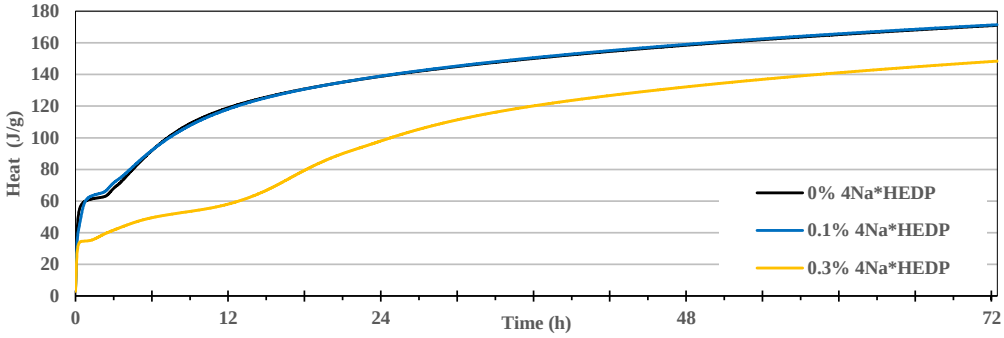

*Figure 5.41: Influence of 4Na*HEDP dosage heat released during hydration process of GGBS with 5% replacement by clinker 4000 cm²/g at W/B=0.40 and 8% Na_2CO_3*

5.4.3 Impact of GGBS fineness

Previously it was shown that increasing the GGBS fineness led to an acceleration of the hydration. When combined with clinker, this acceleration effect can be enhanced. Figure 5.42 illustrates the case of the 5600 cm²/g Blaine GGBS grade. As with the standard GGBS the acceleration effect of the clinker is higher at lower activator dosage.

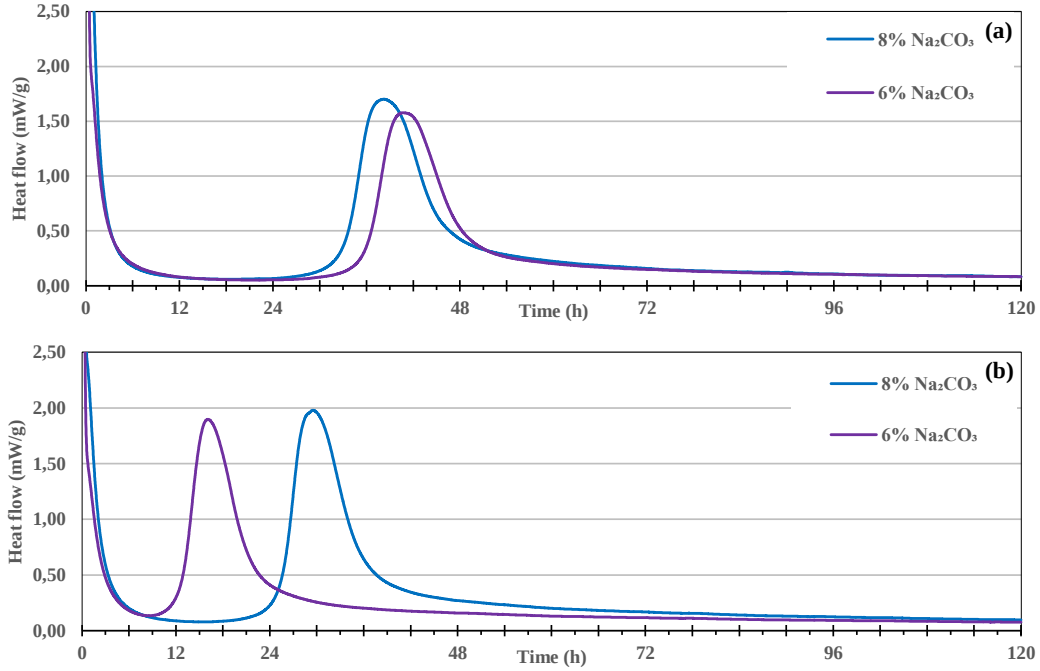

Figure 5.42: Hydration kinetics of GGBS 5600 cm2/g Blaine without (a) and with 5% (b) replacement by clinker 1400 cm²/g at W/B=0.40

Nevertheless, for long term hydration a greater amount of Na_2CO_3 leads to a higher amount of heat released (Figure 5.43), implying higher hydration degree.

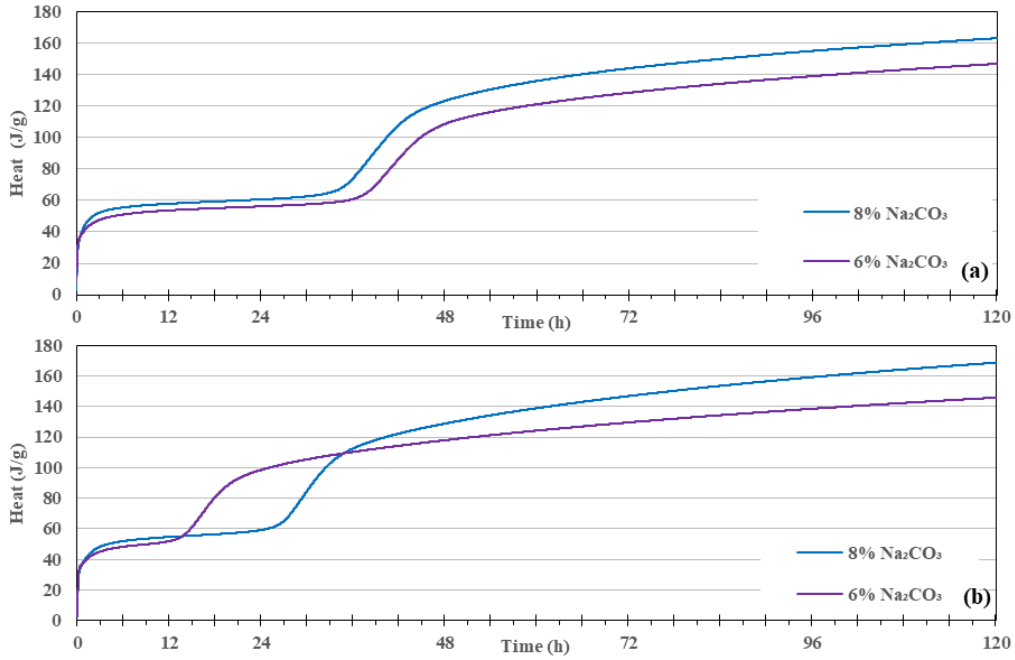

Figure 5.43: Heat released from hydration of GGBS 5600 cm2/g Blaine without (a) and with 5% (b) replacement by clinker 1400 cm^2/g at W/B=0.40

Addition of the phosphonate to the *Fine* GGBS-*Coarse* clinker mix leads to a retardation of the first peak and an acceleration of the strength-giving peak within the dosage interval considered (up to 0.2%) (Figure 5.44). For a lower amount of sodium carbonate (6%) (Figure 5.44b), the phosphonate dosage should be decreased in order to avoid a delay of the strength-giving peak (Figure 5.48b).

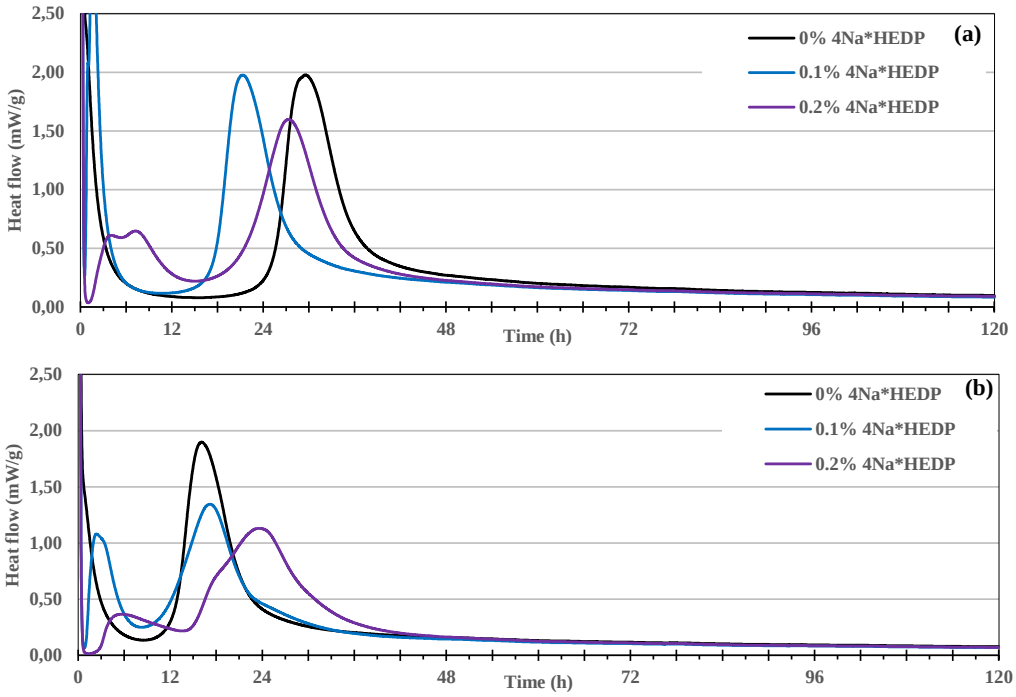

*Figure 5.44: Influence of 4Na*HEDP on the hydration kinetics for GGBS 5600 cm^2/g Blaine with 5% replacement by Clinker 1400 cm^2/g at W/B=0.40 with 8% (a) or 6% (b) Na_2CO_3*

5.5 Compressive strength evolution of the GGBS-clinker binder based mortars

5.5.1 Influence of the phosphonate

Based on the microcalorimetry results on the GGBS-clinker mixes, it was observed that addition of the phosphonate at the appropriate dosage led to an acceleration of the hydration kinetics and the cumulative heat release was increased, indicating a higher instantaneous hydration degree. The phosphonate is then expected to improve the early age strength development. Indeed, a noticeable increase of the compressive strength of the corresponding mortars is obtained at 1 day for a phosphonate dosage of 0.1% (Figure 5.45). The strength is also improved at 2 days. This is then correlated with the microcalorimetry results (Figure 5.32). On the other hand, the impact of phosphonate on the mechanical strength beyond 2 days is less significant. The improvement of the strength can be attributed to eventual seeding effects of the precipitated Ca-phosphonate particles and also to better mould filling since the rheology is improved.

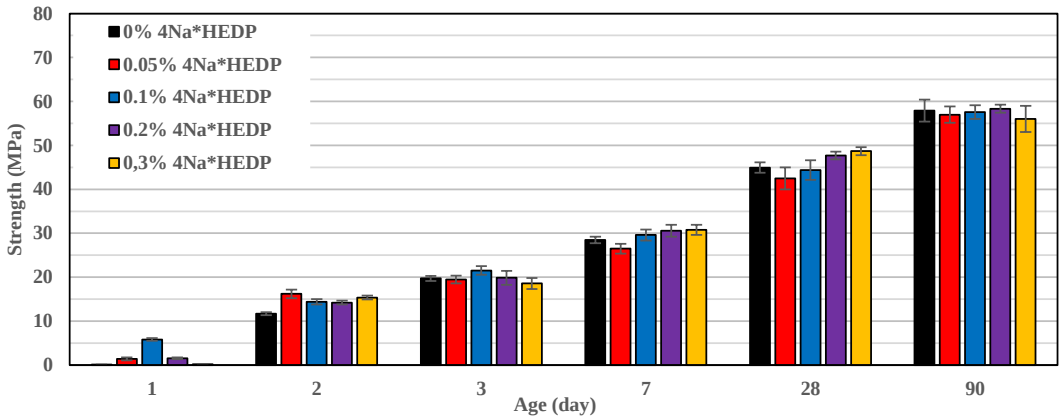

*Figure 5.45: Influence of 4Na*HEDP amount on compressive strength evolution of mortars based on standard GGBS with 5% replacement by clinker 1400 cm^2/g at W/B=0.40 and 8% Na_2CO_3 (200g/l)*

Note that the main expected role of the phosphonate is the extension of the period of the rheology maintenance by delaying the precipitation of the first hydration products. One has to check that there is no negative consequence on the early strength development. Its dosage should be tuned accordingly.

Compared to 100% GGBS, the addition of clinker decreases the retardation effect on compressive strength evolution when too high a dosage of phosphonate (here 0.3%) is used. It means that the binder is more robust against an eventual over dosage of this retarder.

5.5.2 Influence of the amount of slag replacement by clinker

Figure 5.46 represents the results of the compressive strength evolution of mortars based on standard GGBS with different percentages of replacement by coarse clinker at W/B=0.40. A noticeable improvement of the compressive strength at 1 day can be observed with 5% clinker replacement. This is in agreement with the micro-calorimetry results, where a significant acceleration of the main hydration peak was also observed when GGBS is substituted with 5% of clinker. At 2 days, a significant strength improved can be observed with 3% of clinker however the improvement when the substitution level is increased to 5% no longer remains. Nevertheless, beyond 7 days and up to 1 year, substitution with clinker leads to a degradation of the compressive strength, even at only 1% substitution. This negative effect on the long term strength is enhanced when the substitution levels increases. For this reason, the clinker content was limited to 5%.

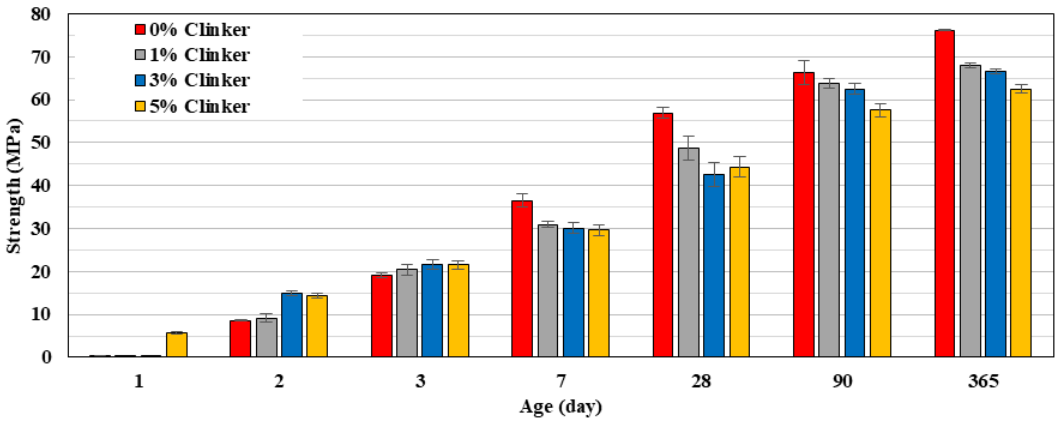

Figure 5.46: Influence of percentage of GGBS replacement by clinker 1400 cm^2/g at W/B=0.40. 0.1% 4NaHEDP and 8% Na_2CO_3 (200g/l) were used

The origin of the long term strength degradation may be attributed to both the modification of the sample microstructure (spatial distribution of the hydration products) and the modification of the nature of the hydration products. In particular, the ratio of Ca/Si in the C-(A)-S-H may be increased due to the higher amount of released Ca in the presence of the clinker. Higher Ca/Si leads to a lower gel density (less reticulated C-S-H) and consequently lower strength values (Kunther et al., 2017; Li et al., 2019).

Decreasing the W/B ratio (Figure 5.47) leads to an acceleration of the strength development and improvement of the strength values both with and without clinker substitution at all terms. Similarly, we observe an improvement of the strength at early age, but degradation beyond 7 days.

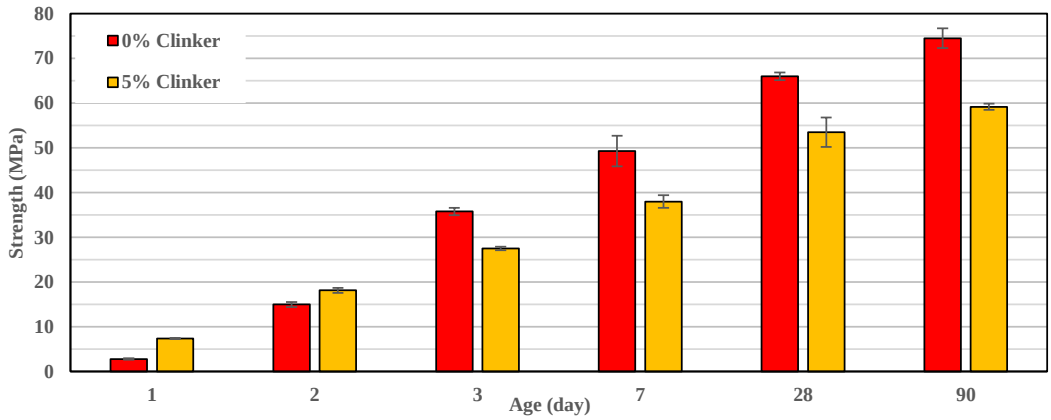

Figure 5.47: Influence on the strength development of GGBS partial replacement by clinker 1400 cm^2/g at W/B=0.35. 0.1% 4NaHEDP and 8% Na_2CO_3 (230 g/l) were used

5.5.3 Decreasing the amount of activator

It was seen in the previous chapters that with 100% GGBS based binders, decreasing the Na_2CO_3 concentration led to an extension of the induction period, lower rate of hydration and lower compressive strength. In contrast, when GGBS is partially replaced by clinker, an early age strength evolution can be observed even with a lower Na_2CO_3 concentration (Figure 5.48). This acceleration is directly related to the amount of clinker, as in the case of high concentration. In addition, as it was seen with micro calorimetry, the effect of 5% clinker is more significant at 1 day with the lower Na_2CO_3 concentration (compare Figure 5.32 and Figure 5.35).

After one day, the strength decreases at all ages when the activator content is decreased. Due to a lower amount of sodium carbonate, a lower compressive strength can be observed in almost all ages compared to a sodium carbonate solution of 200 g/l (compare Figure 5.48 and Figure 5.46).

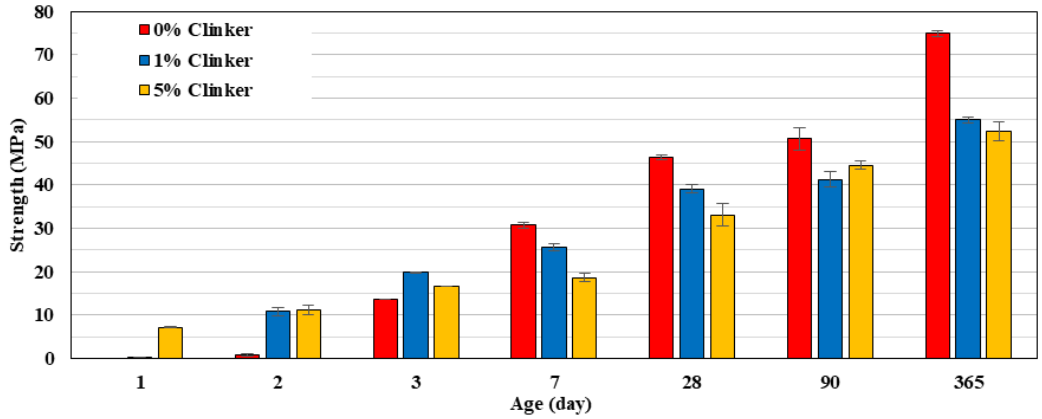

Figure 5.48: Influence of percentage of GGBS replacement by clinker 1400 cm^2/g in case of 6% Na_2CO_3 (150g/l) at W/B=0.40 and 0.1% 4NaHEDP

Decreasing the water content will lead to an increase of the aqueous concentration of the activator and lower inter-grain distance. This has a positive effect on the hydration rate and leads

to greater compressive strength with or without clinker substitution (Figure 5.49). The same quantitative influence of clinker can be observed as the previous concentrations. Yet at later ages, a more significant decrease of the compressive strength can be observed at a lower W/B ratio and a lower amount of Na_2CO_3 when slag is replaced by 5% of clinker.

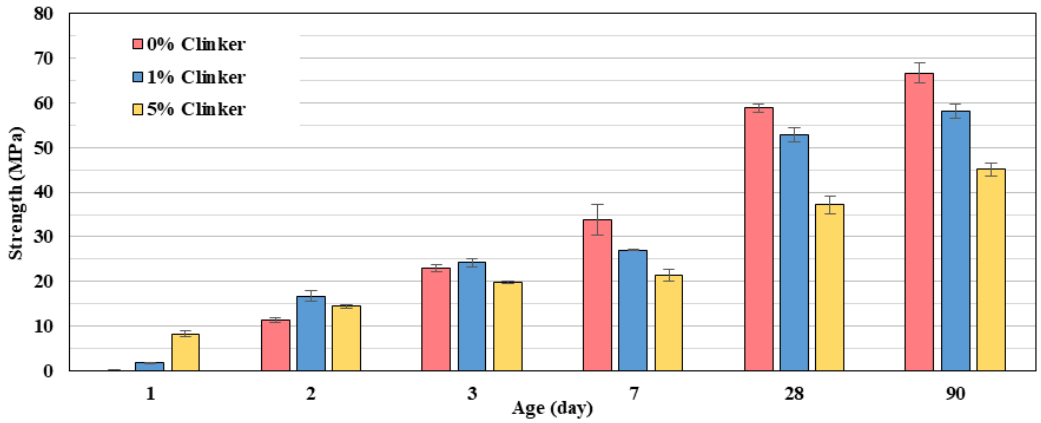

Figure 5.49: Influence of percentage of GGBS replacement by clinker 1400 cm^2/g at W/B=0.35 and 6% Na_2CO_3 (170 g/l), in the presence of 0.1% 4NaHEDP

In Figure 5.50, 3 and 90 day compressive strength is presented for 0% and 5% GGBS replacement by coarse clinker as a function of sodium carbonate concentration. The presence of clinker leads to a higher robustness of the compressive strength evolution against a variation of the water content in the system. At 3 days a strong influence of W/B can be observed for 100% GGBS, which becomes much lower with time. In the case of 5% replacement by coarse clinker, the values are closer to each other at both testing ages. In all cases the strength is still highly dependent on the Na_2CO_3 concentration at the age of 90 days.

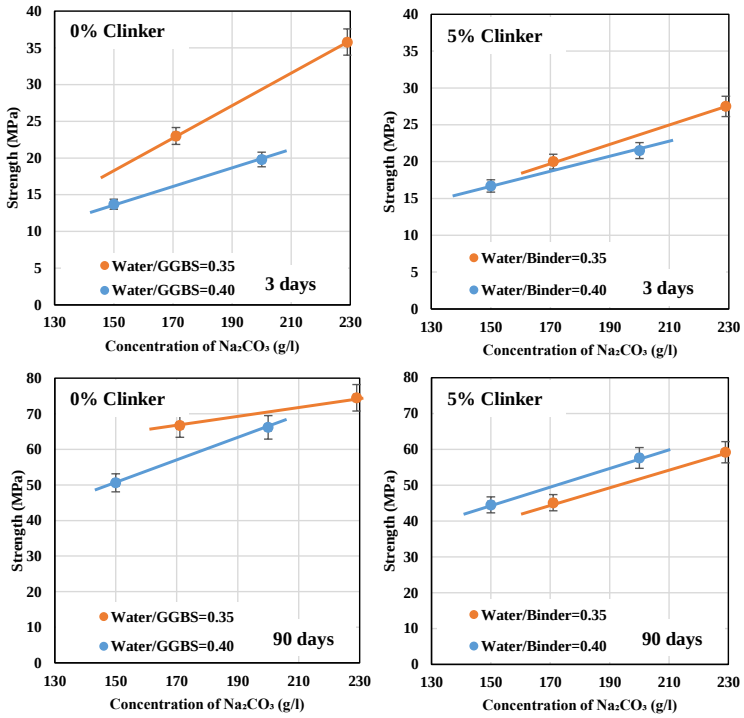

*Figure 5.50: Comparison of compressive strength values at 3 and 90 days of mortars with or without 5% replacement by clinker 1400cm^2/g as a function of Na_2CO_3 concentration. 0.1% 4Na*HEDP*

In Figure 5.51 the impact of clinker on the sensitivity to the aqueous activator concentration is reported. At late ages the trends in strength *versus* Na_2CO_3 concentration with or without clinker substitution are similar. In contrast, at early ages the strength variation is less sensitive to activator concentration for the clinker blended mixes.

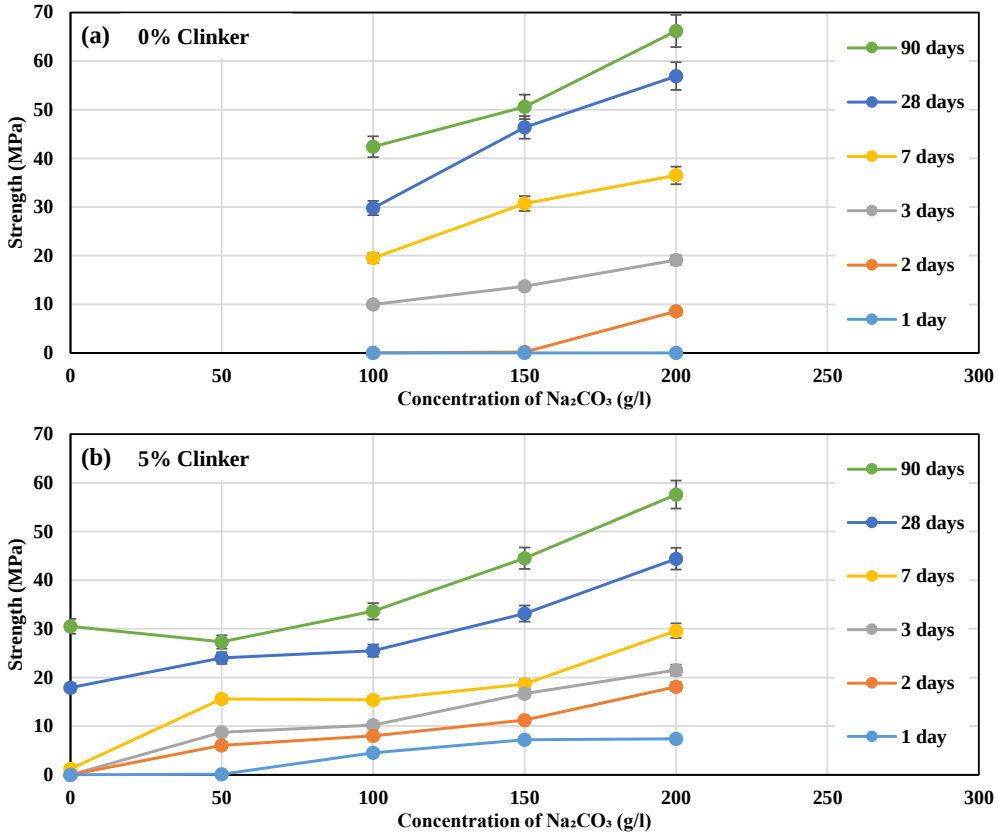

Figure 5.51: Influence of Na_2CO_3 concentration on compressive strength evolution of GGBS without clinker (a) or with 5% (b) replacement by clinker 1400 cm^2/g. Water/Binder=0.40

Decreasing the W/B to 0.35 in the case of clinker blended mortars shows similar results regarding the influence of the sodium carbonate concentration (Figure 5.52) with similar strength values as W/B=0.40 (Figure 5.51b). It means that the addition of clinker increase the robustness of the binder not only against the amount of Na_2CO_3, but also versus variations in mixing water.

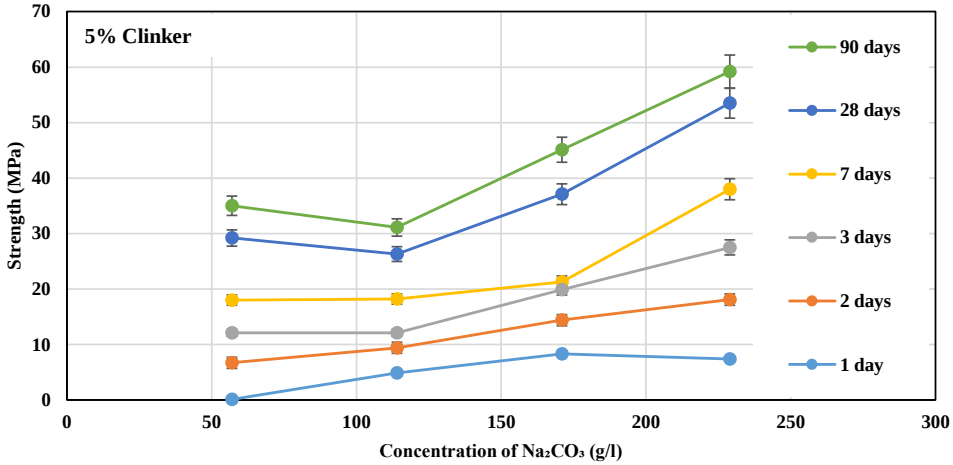

Figure 5.52: Influence of Na_2CO_3 concentration on compressive strength evolution of GGBS with 5% replacement by clinker 1400 cm^2/g. Water/Binder=0.35

The influence of the Na_2CO_3 content was already demonstrated in Chapter 2 with 100% GGBS. It was demonstrated that increasing the activator dosage increases the inner pH level, which presumably affects the rate of hardening. In the case of slag with partial substitution by coarse clinker, the same measurements were performed to establish this effect (Figure 5.53). First of all, compared to 100% GGBS seen previously, the pH level right after mixing is higher in all cases: for 2% Na_2CO_3 it is 12.8 with clinker against 12.1 for 100% GGBS; for 8% Na_2CO_3 it is 13.0 with clinker against 12.5 without it. This observation explains the more rapid loss of rheology and faster hardening due to a higher reaction rate. Regarding the late age values, it is observed that higher sodium carbonate content led to higher alkalinity, which must partly be the reason why the strength evolution is faster in the case of high dosages. However, in all cases, the alkalinity remains high enough to maintain the slag dissolution and precipitation of C-S-H type hydrates. In addition this level is acceptable for reinforced concrete.

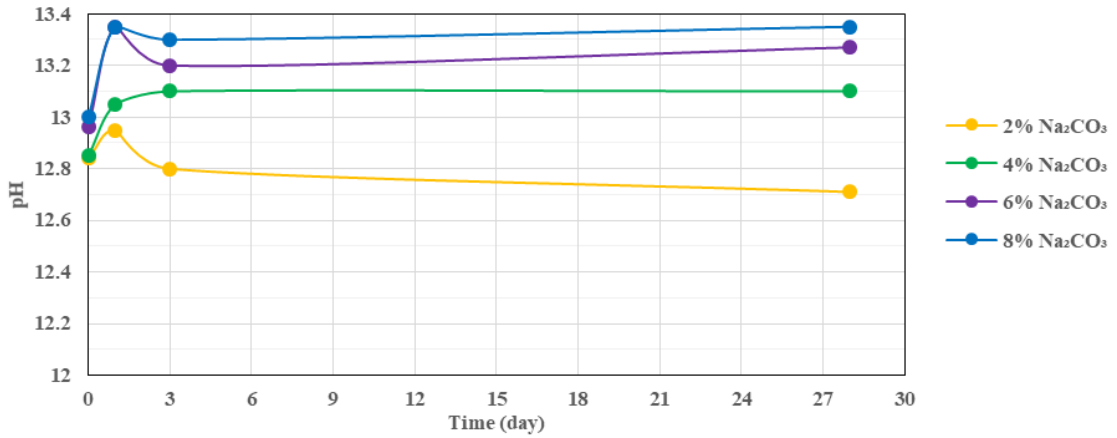

Figure 5.53: Evolution of pH level of past based on 95% GGBS + 5% Coarse Clinker with different amount of Na_2CO_3 at W/B=0.40 (paste:water=1:4, dilution during the measurements)

5.5.4 Increasing clinker fineness

The same mixes as above were considered in which the coarse clinker was replaced with finer grades.

The strength development for the GGBS-clinker based mortars for different clinker fineness grades is presented in Figure 5.54. It can be observed that increasing the clinker fineness leads to higher values of early age strength (1-3 days). At late ages, the opposite is obtained: increasing the fineness leads to the degradation of the strength. In the case of coarse clinker 1400 cm^2/g, the loss of 28 days strength is 22% compared to 100% GGBS. With 4000 cm^2/g and 6000 cm^2/g clinkers the loss is about 40% (see the reference without clinker in Figure 5.46).

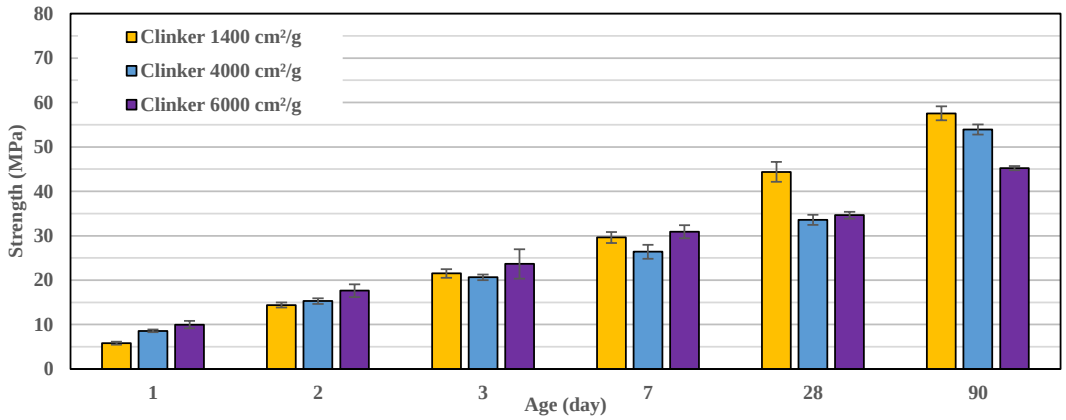

*Figure 5.54: Comparison of the strength evolution in case of 5% GGBS replacement by clinker with different fineness. W/B=0.40, 8%Na_2CO_3 (200g/l) and 0.1% 4Na*HEDP were used*

In the case of lower activator content (4%), the same impact of increasing the clinker fineness can be observed at early age (Figure 5.55). However, in this case there is almost no degradation at late ages. All clinker finenesses lead to a 25% strength loss compare to 100% GGBS with 4% Na_2CO_3 (100 g/l) at 90 days age. At the same time, the absolute strength values remain quite low even after 3 months of hardening (about 30 MPa).

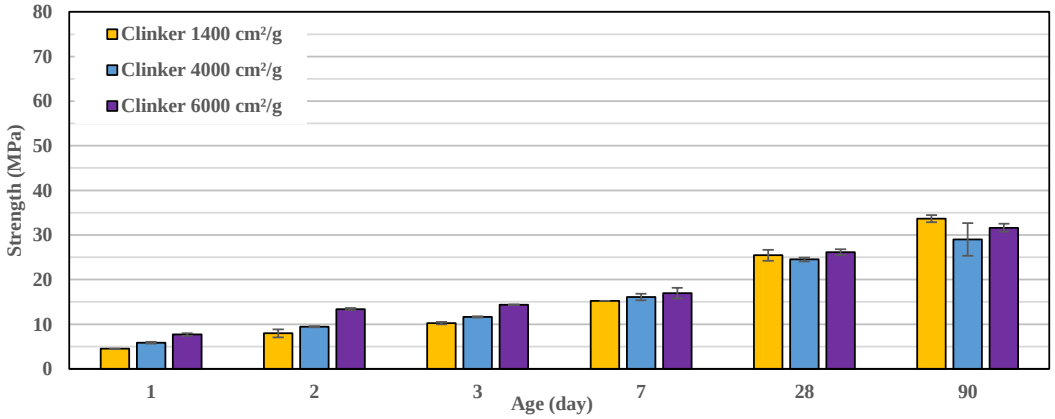

*Figure 5.55: Comparison of the strength evolution in case of 5% GGBS replacement by clinker with different fineness levels. W/B=0.40, 4%Na_2CO_3 (100g/l) and 0.1% 4Na*HEDP were used*

All of the previous strength measurements were performed for mixes with the same amount of 4Na*HEDP. The phosphonate dosage should be modified depending on the rate of precipitation of the first hydration products and the amount of Ca needed to be complexed. For example for very fine clinker (6000 cm^2/g) the amount of phosphonate should be increased. The impact on the strength development is reported in Figure 5.56. Increasing the phosphonate dosage leads to an increase of the long term strength without any degradation of the one-day strength. There is even a slight improvement in the long term strength, which is probably related to the phosphonate seeding effect through the precipitation of Ca-phosphonates particles as discussed previously. Due to the high amount of available Ca in the case of very fine clinker, this seeding effect may be enhanced.

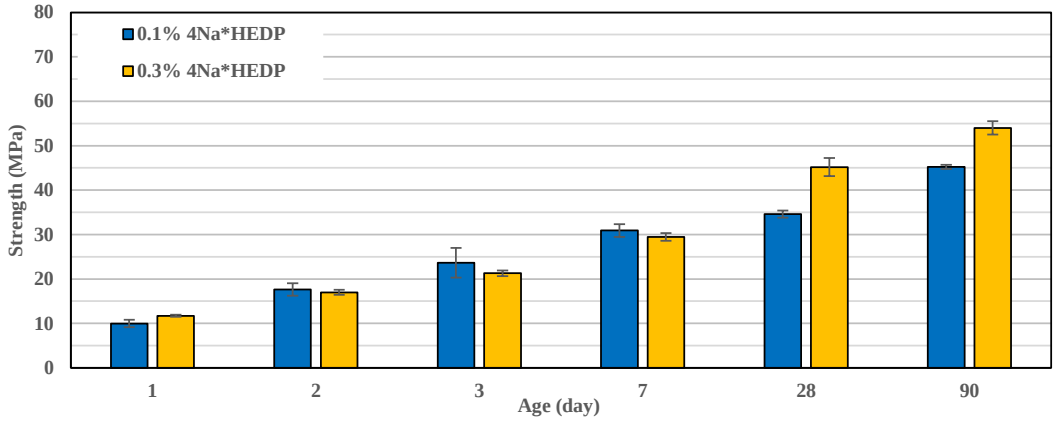

*Figure 5.56: Influence of 4Na*HEDP dosage on compressive strength evolution of GGBS with 5% replacement by very fine clinker 6000 cm^2/g. 8% Na_2CO_3 and W/B=0.40*

5.5.5 Increasing GGBS fineness in the GGBS-clinker mixes

In Chapter 3, it was shown that increasing the slag fineness led to a significant acceleration of the hydration process. Combining partial GGBS replacement by clinker and increasing GGBS fineness might both contribute to the acceleration of the hydration process.

In Figure 5.57 the strength development is presented for mortars in which the effect of lowering the fineness of clinker and GGBS are combined. It can be observed that increasing the GGBS fineness from 4400 to 5600 cm^2/g leads to a significant strength improvement beyond 2 days without clinker substitution and from 1 day for the clinker-blended mixes. At one day the increase in strength is threefold for clinker blended mixes when the slag fineness is increased from 4400 to 5600 cm^2/g. The loss of long term strength in the presence of clinker is almost compensated for (beyond 90 days) by slightly increasing the GGBS fineness.

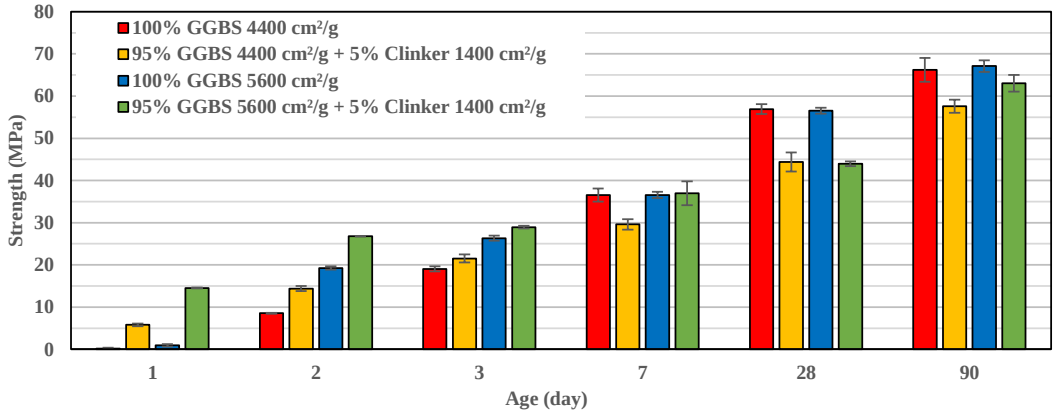

*Figure 5.57: Synergetic effects between clinker substitution and slag fineness increased in case of mortar mixes at W/B=0.40, 8% Na_2CO_3 (200g/l) and 0.1% 4Na*HEDP*

In the case of lower W/B ratio, this synergetic effect of clinker substitution and increased slag fineness is enhanced and takes place at all ages (Figure 5.58). In addition, as previously

demonstrated, decreasing the water content leads to significant acceleration of the compressive strength evolution, especially at early age (1-3 days).

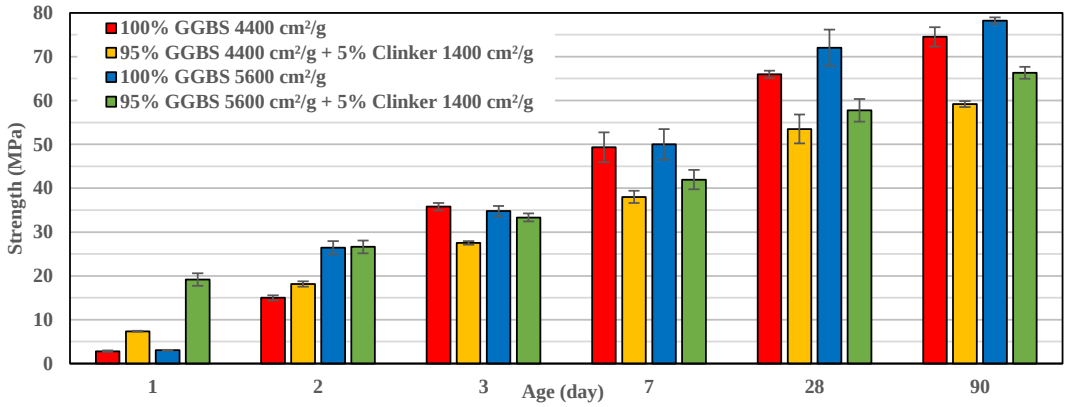

*Figure 5.58: Comparison of 5% GGBS replacement by clinker 1400 cm²/g in case of two different GGBS fineness (4400 and 5600 cm²/g) at W/B=0.35, 8% Na_2CO_3 (230g/l) and 0.1% 4Na*HEDP*

The impact of a partial replacement (5%) of the standard GGBS with ultrafine GGBS on strength development is reported in Figure 5.59. The results are very similar to those obtained when all of the standard GGBS is replaced by the fine GGBS 5600 cm²/g.

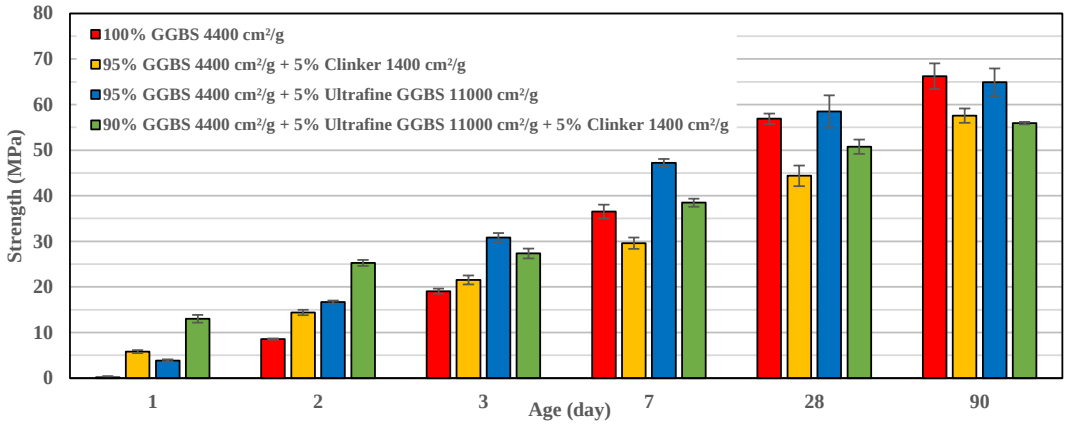

*Figure 5.59: Influence of the combination of Ultrafine GGBS and coarse Clinker 1400 cm²/g substitution on the strength development at W/B=0.40, 8% Na_2CO_3 (200g/l) and 0.1% 4Na*HEDP*

5.5.6 Impact of low temperature (15°C) curing

In a Chapter 3, it was shown that decreasing the storage temperature from 22°C to 15°C led to a significant retardation in compressive strength evolution. This phenomenon can be attributed to two combined effects: the decrease of the dissolution rate of the slag and the precipitation process (decrease of activation energy), and (ii) lower dissolution degree of Na_2CO_3 (its recrystallization).

A comparison regarding strength evolution is made between clinker blended GGBS mortars cured at two different temperatures (15° and 22°C), and the results are reported in

Figure 5.60. A decrease of the strength at all ages is observed for the samples at low temperature. A particularly high decrease of the strength occurs at early age and it becomes less significant beyond 7 days, as in the case of 100% GGBS (see Figure 5.66).

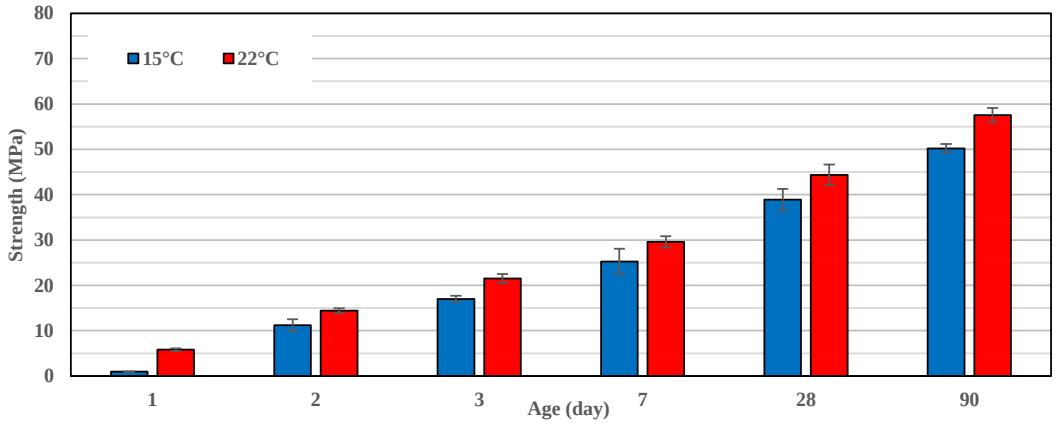

*Figure 5.60: Influence of the curing temperature on strength evolution of GGBS with 5% replacement by Clinker 1400 cm^2/g at W/B=0.40, 8% Na_2CO_3 (200g/l) and 0.1% 4Na*HEDP*

It can be noticed that the presence of the phosphonate is crucial at low temperature (Figure 5.61). Its effect on strength is particularly significant at early age. The origin of this phenomenon is to be investigated.

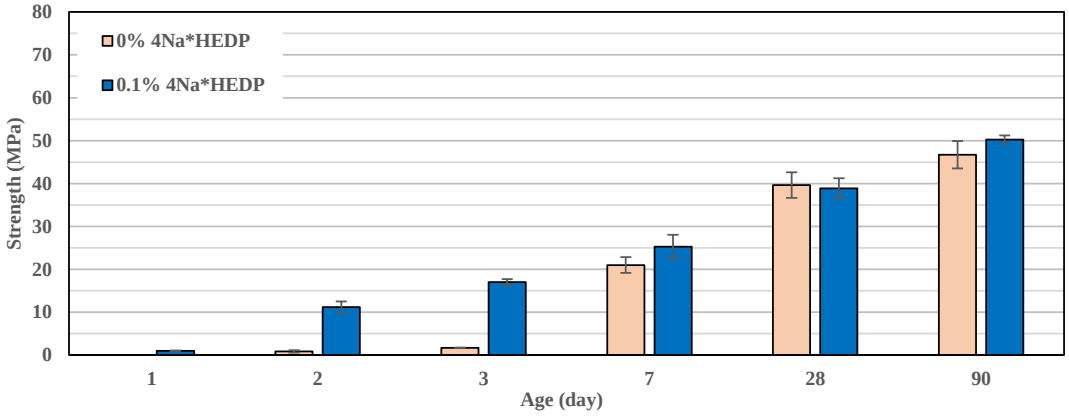

*Figure 5.61: Influence of 4Na*HEDP on strength evolution in case of 15°C storage of GGBS with 5% replacement by Clinker 1400 cm^2/g at W/B=0.40, 8% Na_2CO_3 (200g/l)*

The substitution level of GGBS by clinker also plays an important role in the case of low temperature curing. The results from Figure 5.62 show that the presence of clinker at a sufficient amount (5%) is particularly crucial at low temperature. There is almost no strength up to 7 days without clinker at 15°C, while with a 5% substitution the sample is easily demouldable at 2 days.

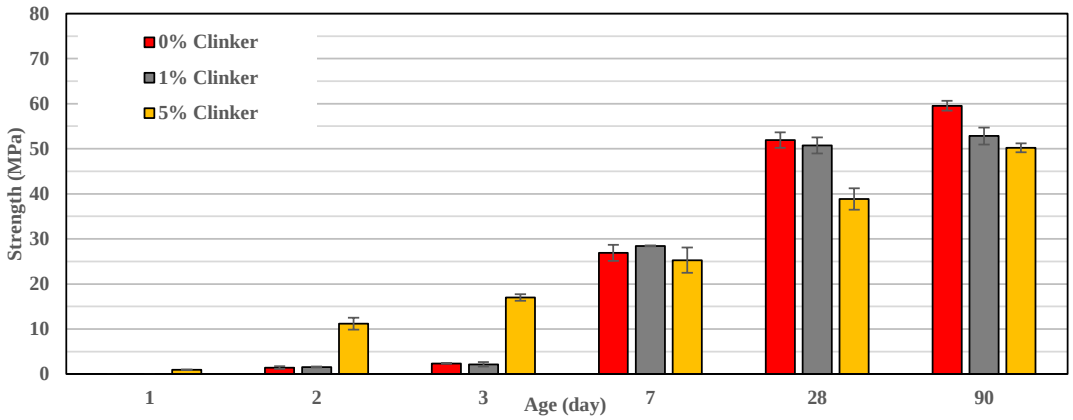

*Figure 5.62: Influence of GGBS replacement by coarse Clinker 1400 cm^2/g on strength evolution in case of 15°C storage at W/B=0.40, 8% Na_2CO_3 (200g/l) and 0.1% 4Na*HEDP*

Increasing the clinker fineness leads (Figure 5.63) to an improvement of the early age strength at low temperature. Nevertheless, the loss of strength at late ages is higher. In addition, one needs to increase the phosphonate dosage to get an appropriate open time. There is then the risk of cancelling out the improvement of early strength development (here the same 4Na*HEDP dosage was used). However, for some applications in which a long open time is not required (as in precast), it may be of interest to use finer clinker at low temperature. One should also take into account the fact that the long term strength is reduced with increased clinker fineness.

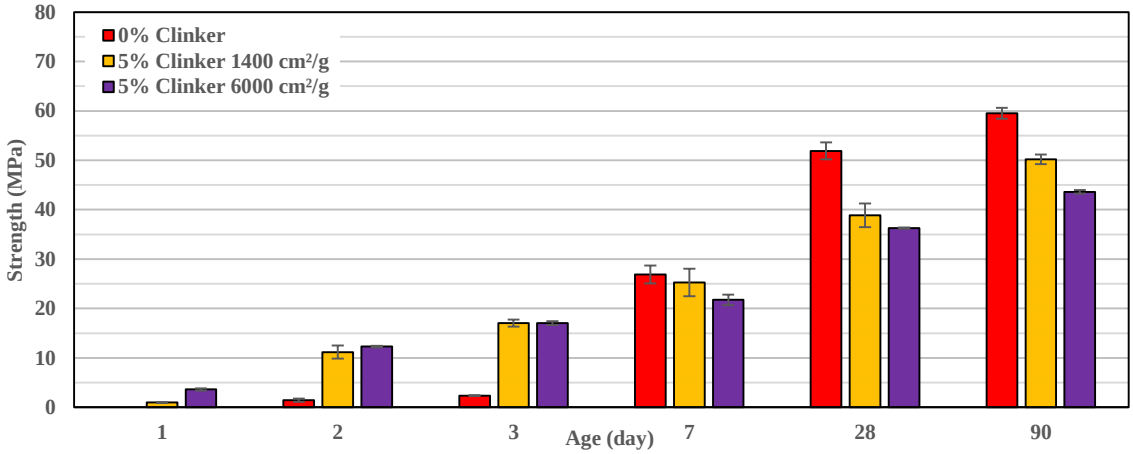

Figure 5.63: Influence of Clinker fineness on strength evolution in case of 15°C storage of mortars with 5% replacement of GGBS by Clinker at W/B=0.40, 8% Na_2CO_3 (200g/l) and 0.1% 4Na HEDP*

5.5.7 Effect of heat treatment

In Chapter 3 the positive effect of the heat treatment on the early age strength of 100% GGBS based mortars was observed. This acceleration is probably related to the lower Gaylussite stability at high temperature, leading to the NaOH activation situation. In addition, the dissolution rate of the slag and the activator is enhanced at high temperature. Unfortunately, similar to NaOH activation, the long term strength is lower.

Figure 5.64 represents the impact of 24 hours of heat treatment in the case of mortars based on GGBS with 5% replacement by coarse clinker activated with 6% Na_2CO_3 in the presence of 0.1% phosphonate. As before, a lower Na_2CO_3 dosage was used to decrease the CO_2 footprint and costs due to the heating process. Heat treatment at moderate temperature (40°C) over 1 day leads to a significant increase of the compressive strength in the first days of hardening. Similar reasons as in the case of plain GGBS can be invoked to explain the strength development behaviour (significant retardation of its evolution for the first 28 days).

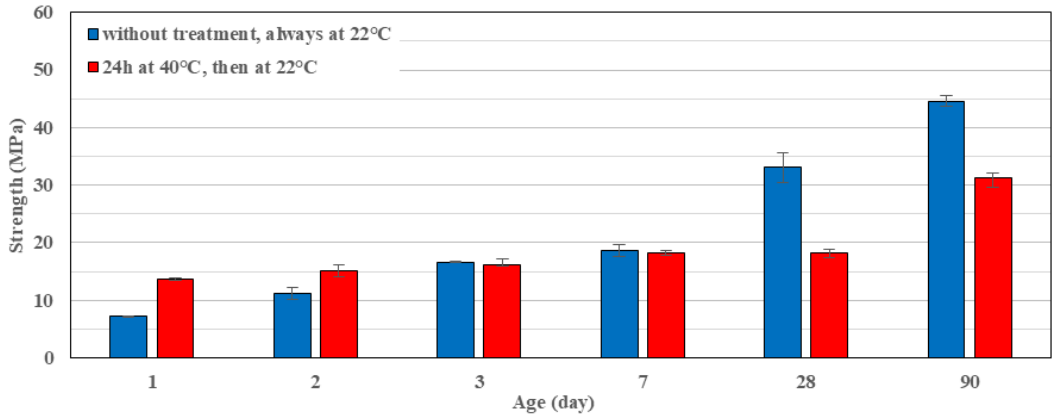

*Figure 5.64: Influence of heat treatment at 40°C over 24h for mortars based on GGBS with 5% replacement by coarse Clinker 1400 cm^2/g at W/B=0.40, 6% Na_2CO_3 (150g/l) and 0.1% 4Na*HEDP*

No significant acceleration can be observed in the case of very low activator concentration (2% Na_2CO_3) (Figure 5.65). In this case, the high amount of calcium provided by the clinker may completely inhibit the formation of Gaylussite since the instantaneous ratio Ca^{2+}/Na^{+} should always be high which favours calcite precipitation. Increasing the curing temperature accelerates clinker dissolution (and then calcium leaching rate) enhancing the above-mentioned phenomenon. Rapid formation of calcite may take place on the anhydrous particles. This will lead to surface pollution and a decrease of the long term hydration rate.

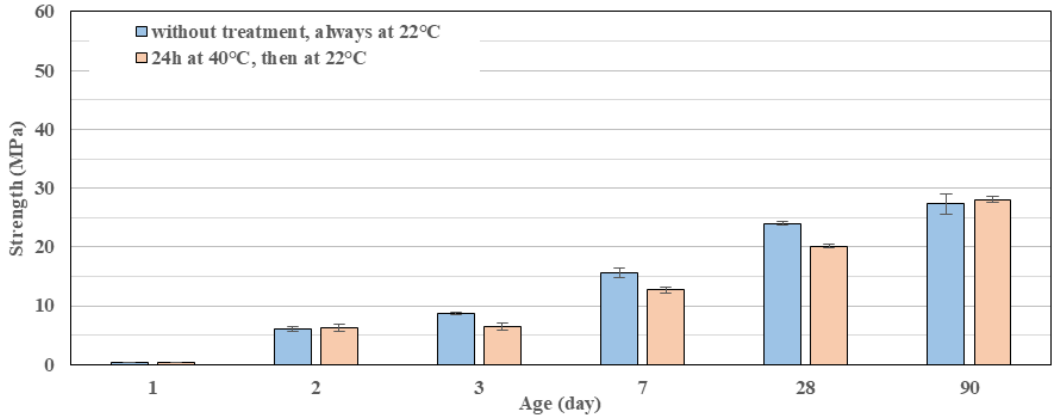

*Figure 5.65: Influence of the heat treatment at 40°C for 24h of GGBS with 5% replacement by coarse Clinker 1400 cm^2/g at W/B=0.40, 2% Na_2CO_3 (50g/l) and 0.1% 4Na*HEDP*

The impact of the presence of the clinker on the strength development in the case of heat-curing is reported in Figure 5.66. The presence of the clinker leads to the degradation of the strength at 1 day. One can conclude that in an industrial processes in which heat curing is frequently employed, plain GGBS based mixes are more appropriate. It is also worth noting that this situation doesn't lead to a complete blockage of the hydration process. In this case, rather a slowing down occurs, since significant strength evolution was observed between 28 and 90 days. It means that in the case of very hot weather, some degradation of the strength can be expected in cases where clinker is present, without any significant problems in the long term.

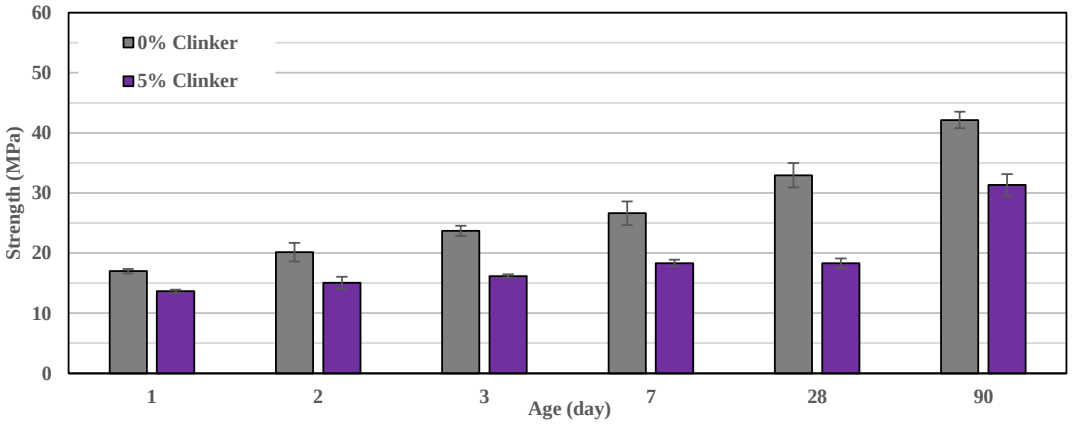

*Figure 5.66: Influence of GGBS replacement by coarse Clinker 1400 cm^2/g at W/B=0.40, 6% Na_2CO_3 (150g/l) and 0.1% 4Na*HEDP in case of heat treatment at 40°C for 24h, than 22°C*

5.6 Shrinkage

5.6.1 Impact of the clinker substitution

The objective of this investigation is to consider whether the acceleration effects of the clinker has negative consequences on shrinkage, which is already high in case of plain GGBS.

Figure 5.67 represents the influence of partial GGBS replacement by clinker on the development of autogenous shrinkage. Increasing the clinker replacement level leads to a significant decrease of the instantaneous shrinkage at all terms. These results are consistent with the lower strength development (beyond the 3 first days) with clinker substitution. In addition, as was indicated above, increasing Ca^{2+} incorporation into the C-S-H gel leads to the decrease of its density, which should result in lower shrinkage levels. The present results should be taken with caution since these measurements started after 3 days. It is expected that the shrinkage should be higher within this period in the presence of clinker since the hydration kinetics are higher.

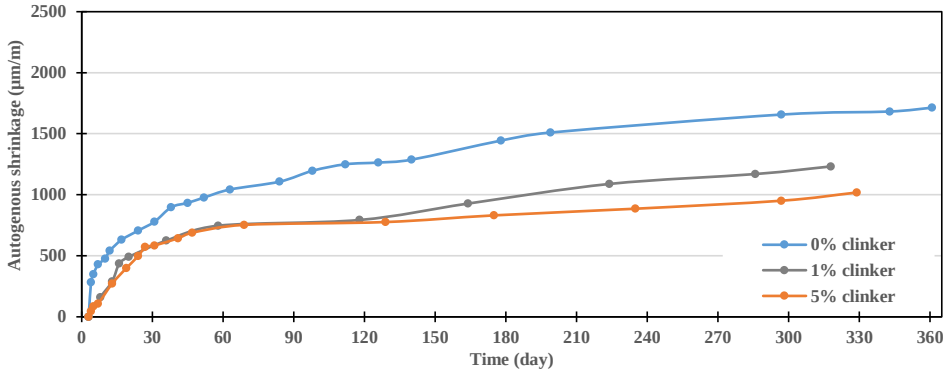

*Figure 5.67: Influence of the percentage of GGBS substitution by clinker 1400 cm^2/g on the development of autogenous shrinkage. W/B=0.40 with 8% Na_2CO_3 (200 g/l) and 0.1% 4Na*HEDP*

The impact of the clinker on water loss under dry conditions (RH=50%) is reported in Figure 5.68. The presence of the clinker leads to a significant reduction in water loss at all ages. This may be attributed to the acceleration of the hydration at early age in the presence of the clinker, which should lead to rapid closing of the porosity. Indeed most of the water is generally lost within the first days.

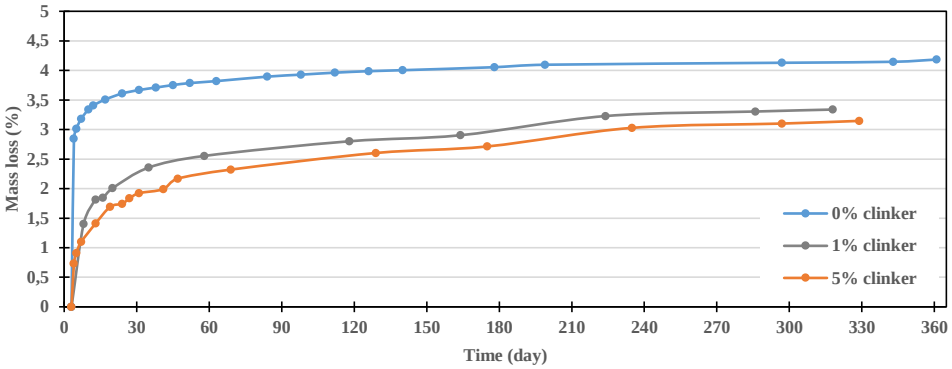

*Figure 5.68: Influence of the percentage of GGBS substitution by clinker 1400 cm^2/g on the mass loss during drying (RH=50%). W/B=0.40 with 8% Na_2CO_3 (200 g/l) and 0.1% 4Na*HEDP*

The results of the total shrinkage for the samples stored at RH=50% are directly correlated with those of water loss (Figure 5.69). Increasing the clinker substitution level leads to a significant decrease of the total shrinkage values. This might be directly related to both lower autogenous shrinkage and drying shrinkage due to lower water loss.

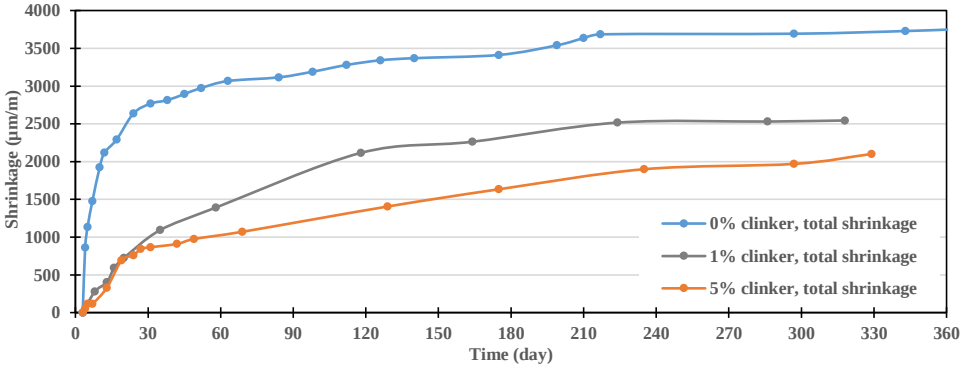

*Figure 5.69: Influence of GGBS substitution by clinker 1400 cm^2/g on the total shrinkage under drying conditions (RH=50%). W/B=0.40 with 8% Na_2CO_3 (200 g/l) and 0.1% 4Na*HEDP*

Similar results for the autogenous shrinkage can be observed in the case of lower W/B ratio and as a consequence, higher aqueous concentration of sodium carbonate (Figure 5.70). Partial GGBS replacement by clinker leads to a significant decrease in the long term shrinkage. There is almost no impact of the clinker on autogenous shrinkage over the first 28 days. In addition there is almost no difference in autogenous shrinkage between the two different amounts of clinker.

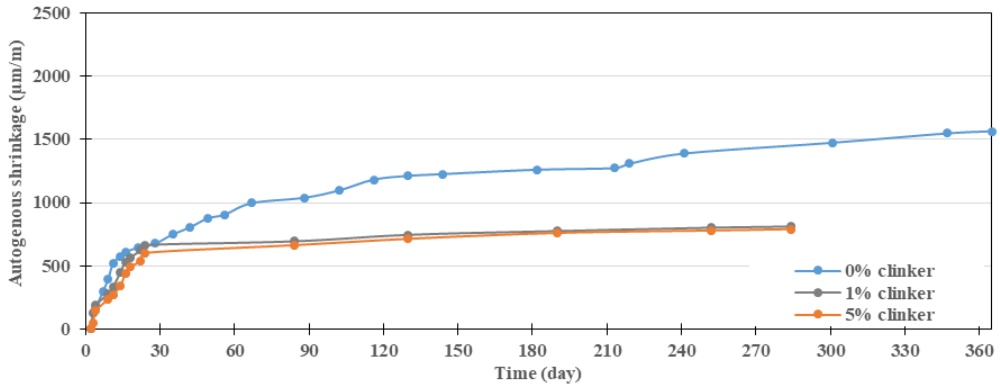

*Figure 5.70: Influence of the percentage of GGBS substitution by clinker 1400 cm^2/g on the development of autogenous shrinkage. W/B=0.35 with 8% Na_2CO_3 (230 g/l) and 0.1% 4Na*HEDP*

The impact of the clinker on water loss evolution over time at W/B = 0.35 is reported in Figure 5.71. The water loss is significantly reduced in the presence of the clinker. As previously stated, this may be attributed to a rapid closing of the porosity in the presence of the clinker. At late ages the evolution is more significant. This may be correlated with the lower long term strength development in the case of the clinker blended mixes.

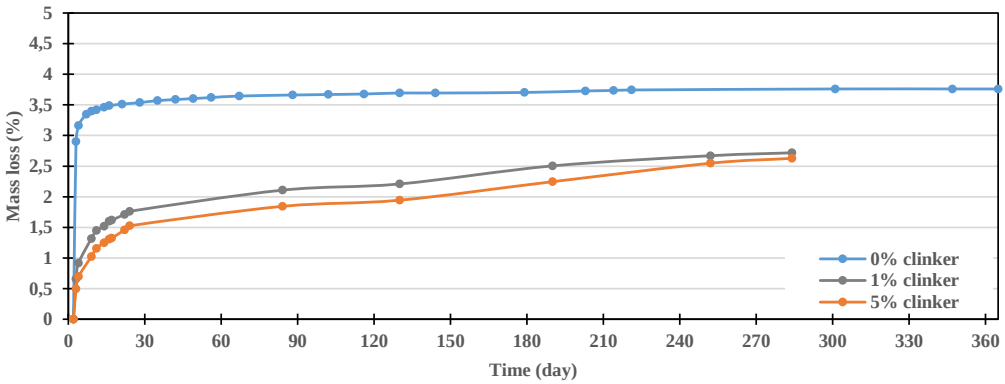

*Figure 5.71: Influence of the GGBS substitution level by clinker 1400 cm^2/g on the mass loss during curing under dry conditions (RH=50%). W/B=0.35 with 8% Na_2CO_3 (230 g/l) and 0.1% 4Na*HEDP*

The early age acceleration of the hydration in the presence of the clinker leads to lower total shrinkage when curing under dry conditions (Figure 5.72).

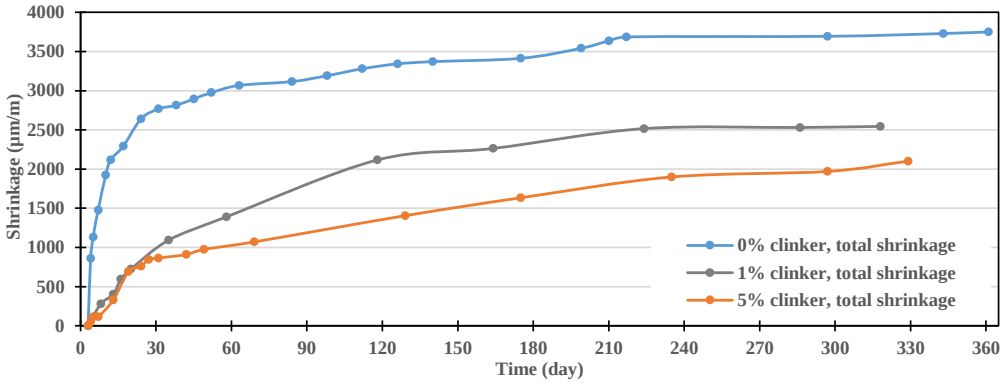

*Figure 5.72: Influence of the GGBS substitution by clinker 1400 cm^2/g on the total shrinkage during curing under dry conditions (RH=50%). W/B=0.35 with 8% Na_2CO_3 (230 g/l) and 0.1% 4Na*HEDP*

5.6.2 Influence of the phosphonate

It was shown above that the addition of 4Na*HEDP, in particular for the clinker-blended mixes, led to an acceleration of the hydration process at early age for certain dosage rates. This has negligible consequences on the autogenous shrinkage as is shown in Figure 5.73. Similar to the effect of clinker, the impact of the phosphonate on shrinkage which is expected to occur at early age (first 3 days) might have been missed since measurements started after 3 days.

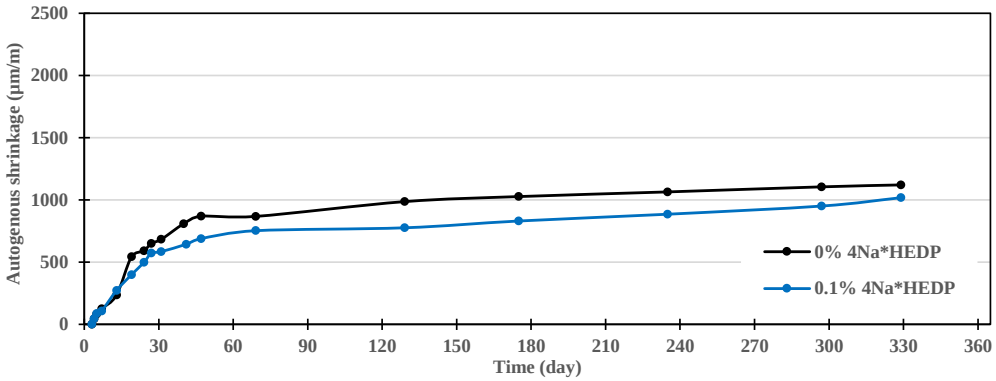

*Figure 5.73: Impact of 4Na*HEDP on autogenous shrinkage in the case of mortars based on GGBS with 5% replacement by clinker 1400 cm^2/g at W/B=0.40 with 8% Na_2CO_3 (200 g/l)*

The mass loss evolution is fairly similar to that of the autogenous shrinkage (Figure 5.74).

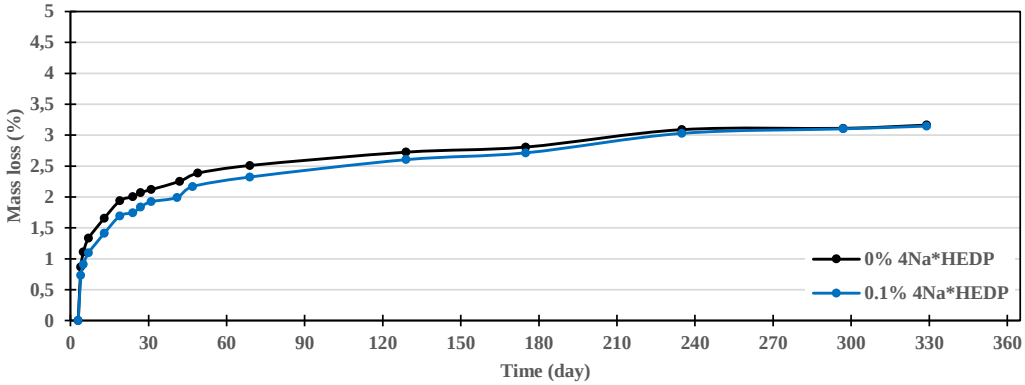

*Figure 5.74: Impact of the 4Na*HEDP on the mass loss under dry curing (RH=50%) in case of GGBS with 5% replacement by clinker 1400 cm^2/g at W/B=0.40 with 8% Na_2CO_3 (200 g/l)*

The presence of the phosphonate in the case of curing under dry conditions (50% RH) leads to the slowing of the shrinkage at early age (Figure 5.75). These results are correlated with the water loss evolution trend, which is the main cause of this shrinkage type through the capillarity forces. However, at longer term the impact of the phosphonate is low.

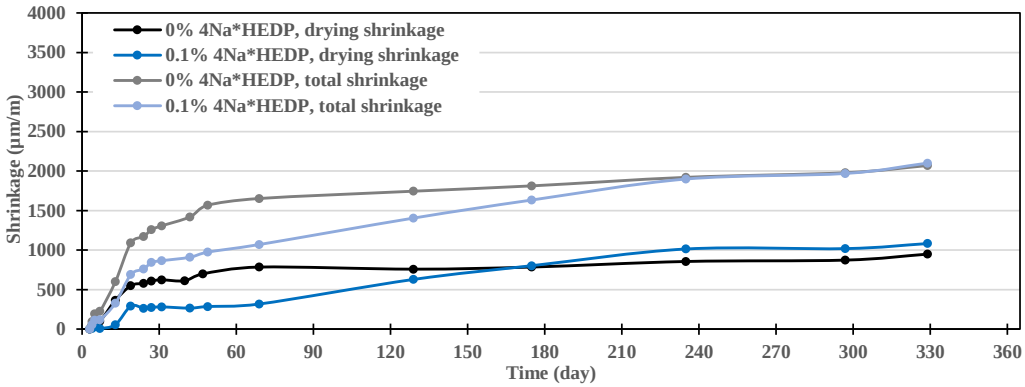

*Figure 5.75: Impact of the 4Na*HEDP on the total and drying shrinkage during curing under dry conditions (RH=50%) in the case of GGBS with 5% replacement by clinker 1400 cm^2/g at W/B=0.40 with 8% Na_2CO_3 (200 g/l)*

5.6.3 Impact of the Na_2CO_3 content

Increasing the Na_2CO_3 content leads to higher autogenous shrinkage (Figure 5.76). This is correlated with the increase of the hydration rate/degree with the activator dosage, as in the case of 100% GGBS.

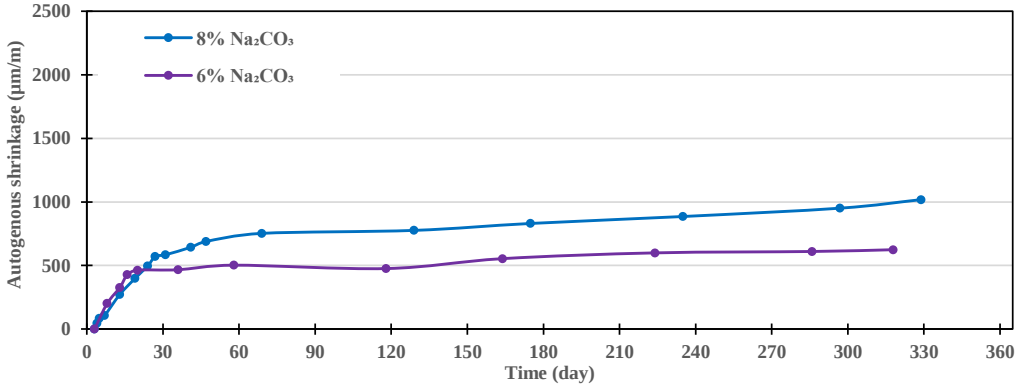

*Figure 5.76: Impact of Na_2CO_3 amount on autogenous shrinkage in the case of mortars based on GGBS with 5% replacement by clinker 1400 cm^2/g at W/B=0.40 with 0.1% 4Na*HEDP*

A higher amount of water loss in the case of low activator concentration was observed (Figure 5.77). This phenomenon, as before for pure slag, should be related to a higher porosity caused by a lower hydration degree and also to a lower amount of formed Gaylussite, which has a capacity to store part of water in its structure (5 water molecules).

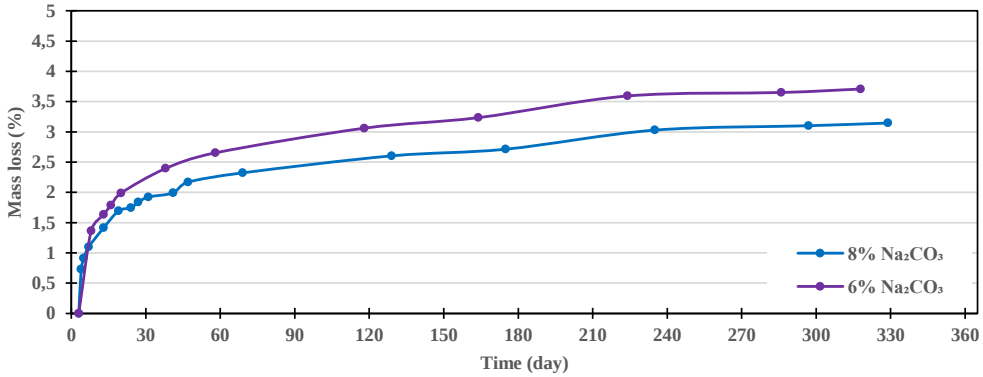

*Figure 5.77: Impact of Na_2CO_3 amount on mass loss during drying (RH=50%). GGBS with 5% replacement by clinker 1400 cm^2/g at W/B=0.40 with 0.1% 4Na*HEDP*

A lower hydration rate and higher amount of water loss in the case of low Na_2CO_3 content caused a higher drying shrinkage (Figure 5.78). A similar total shrinkage in both cases at longer term is related to a significantly lower autogenous shrinkage, due to lower hydration degree in the case of lower sodium carbonate concentration.

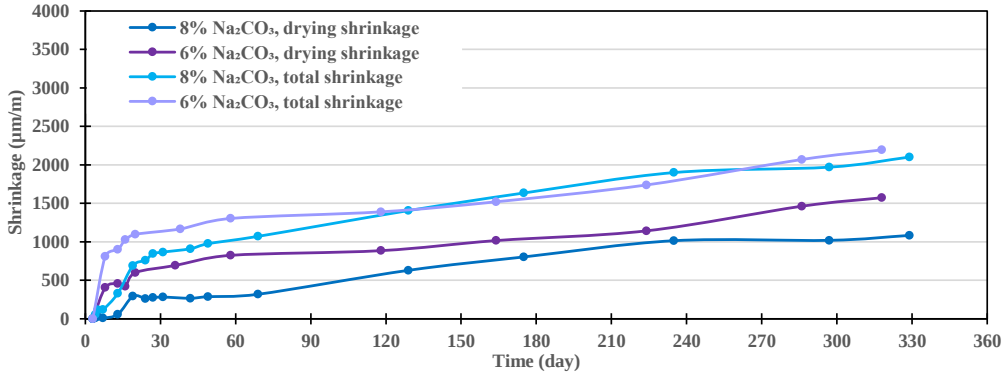

*Figure 5.78: Impact of Na_2CO_3 amount on total and drying shrinkage curing under dry conditions (RH=50%) in case of GGBS with 5% replacement by clinker 1400 cm^2/g, W/B=0.40, 0.1% 4Na*HEDP*

5.7 Real time investigation of the precipitation of the early hydrates using Synchrotron XRD

5.7.1 Influence of the clinker substitution

The in-situ Synchrotron XRD results for the clinker-blended mixes with two different clinker fineness grades are presented in Figure 5.79. The measurement procedure was described in Chapter 2. In the case of coarse clinker, no significant quantitative changes can be observed compared to 100% GGBS (compare Figure 5.79a and Figure 5.79b). A simultaneous formation of calcite and Gaylussite is observed, due to the precipitation between the calcium leached from slag/clinker and carbonates from Na_2CO_3. The two phases are characterised by a poor level of crystallisation. After several minutes the formation of Gaylussite starts to dominate. In addition, its peaks become more pronounced, indicating its crystal growth and increase of its crystallization degree.

On the other hand, in the case of very fine clinker, a significant impact of its presence can be observed (Figure 5.79c). Peaks of Gaylussite and calcite which are much more pronounced are observed immediately after contact with water. In this case a particularly high amount of calcite can be observed, due to a higher amount of calcium ions leached from the very fine clinker. The fast precipitation of Calcite/Gaylussite could be the one of the reasons for the fast loss of rheology in the presence of very fine clinker. The latter is then destabilized when the carbonate ions are exhausted, leading to its transformation to calcite. The results show that over the first few minutes of hydration, both phases precipitate at almost the same time. In addition in the case of very fine clinker, peaks of CAH type hydrates which are slightly more pronounced can be observed, which should also be due to a higher amount of Ca and Al leached ions from clinker.

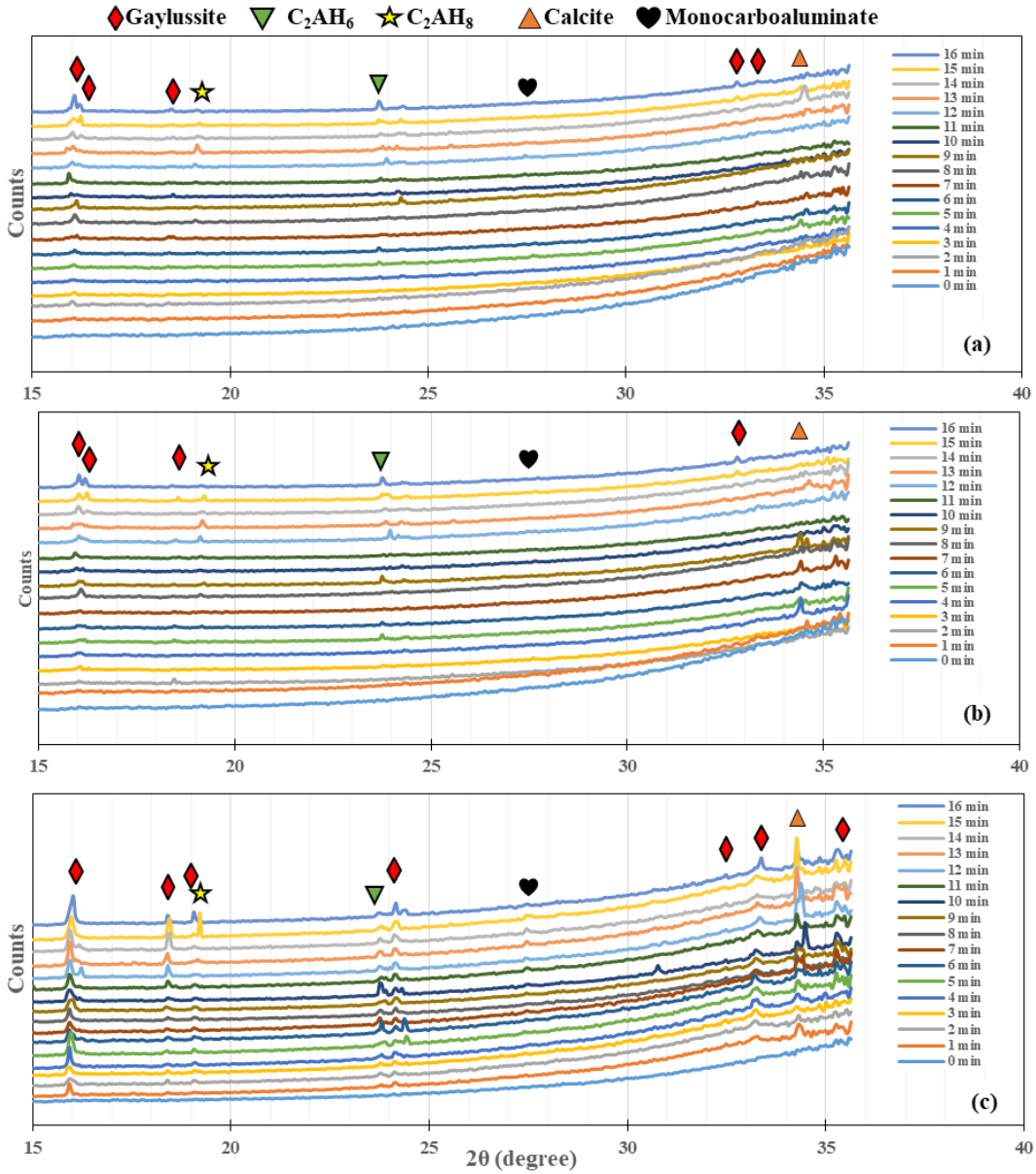

Figure 5.79: In-situ Synchrotron XRD patterns during the first 16min of hydration of 100% GGBS (a) with 5% replacement by coarse clinker (b) and very fine clinker 6000 cm^2/g (c). Solution of 200 g/l

The development of the hydration products was followed further *in-situ* from 1h to 24 h (see procedure described in Chapter 2) (Figure 5.80). In the case of the plain GGBS, up to 24 hours the main crystalline product is Gaylussite. The signal of calcite precipitated during the first few minutes disappeared. In the presence of the clinker, and this is more visible with the very fine grade, the calcite peak appears again after a few hours. The crystalline degree of the calcite is quite low. In addition for both clinker grades, Gaylussite has a lower crystallinity.

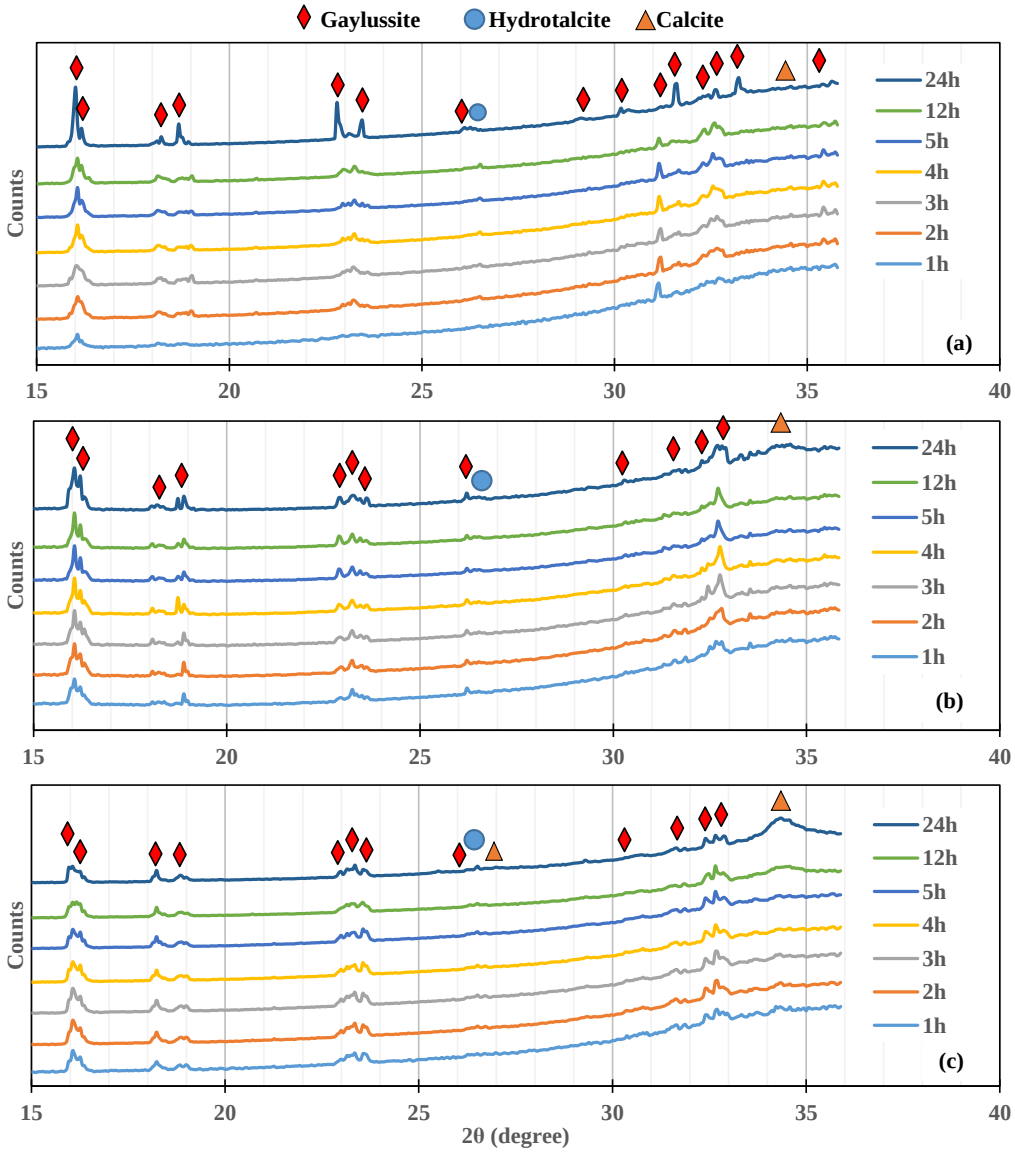

Figure 5.80: In-situ Synchrotron XRD patterns of 100% GGBS (a) and with 5% replacement by clinker 1400 (b) or 6000 cm^2/g (c) over the first 24h of hydration. W/B=0.40 with 8% (200 g/l) Na_2CO_3.

The amount of Gaylussite seems to be lower in the presence of the clinker (in particular the very fine grade). Hence due to the changes in crystallinity degree, it's difficult to compare the intensities. The presence of a sufficient amount of Gaylussite may turn out to be important regarding the hydration process at long term since it may play the role of an alkaline source.

The coarse grade of the clinker may represent a compromise between two conflicting effects: (i) precipitation of a sufficient amount of Gaylussite to serve as an alkaline reservoir,

and (ii) representing a source of calcium with moderate solubility allowing for the precipitation of Calcite, which will lead to the destabilization of Gaylussite (since this allows for the consumption of carbonate ions). The decomposition of Gaylussite leads to the formation of NaOH (see previously demonstrated results, when the addition of clinker led to a higher pH level in the period 0-24h), further dissolution of the slag, and so acceleration of the hydration process.

5.7.2 Influence of the phosphonate addition

The impact of the phosphonate on the precipitation of the first hydration products of the clinker blended GGBS mixes is quantitatively the same as in the case of 100% GGBS. A slowing of the Gaylussite, Calcite and CAH peak growths can be observed (Figure 5.81). Yet this impact is less pronounced in the case of the very fine clinker. This is correlated with the rheological results, in which a low amount of phosphonate little impacted the yield stress of very fine clinker mixes compared to 100% GGBS or coarse clinker blended mixes.

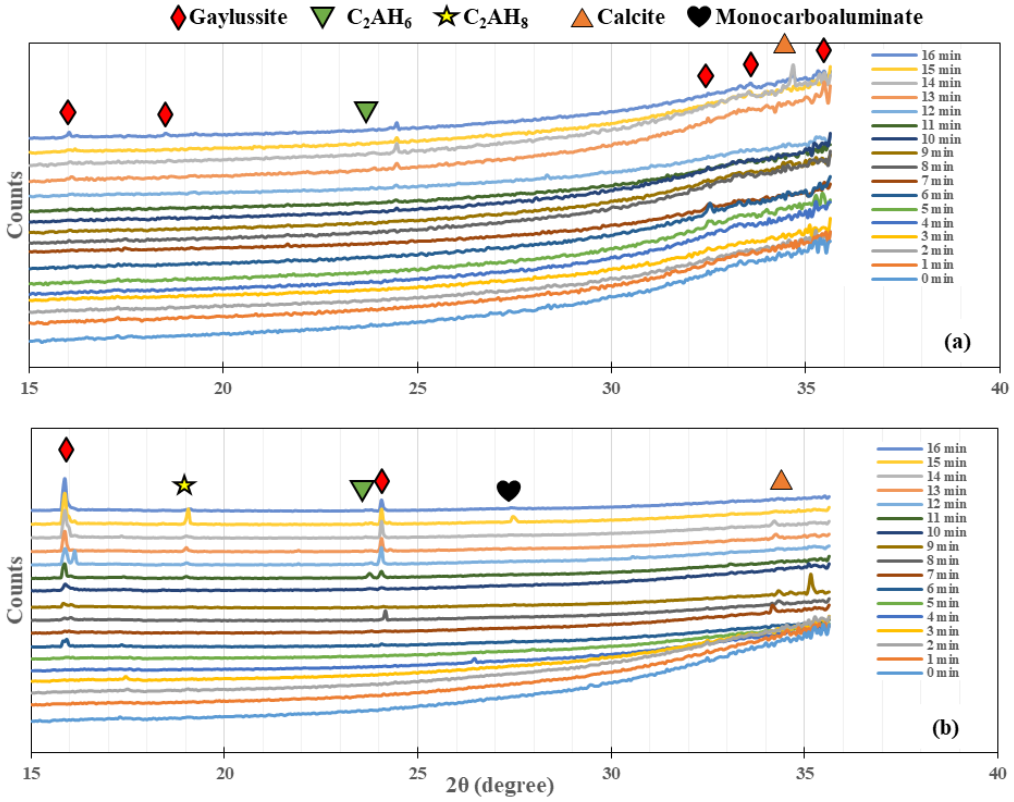

*Figure 5.81: Synchrotron in-situ XRD patterns over the very first minutes of hydration for GGBS with 5% replacement by clinker 1400 (a) or 6000 (b) cm^2/g. Solution: 200 g/l Na_2CO_3 with 0.1% 4Na*HEDP*

Addition of the phosphonate leads to lower calcite formation after 24 hours of hydration (compare Figure 5.82b and Figure 5.80b). A significant modification of the Gaylussite peaks of the clinker-blended mixes can be observed in the presence of the phosphonate. Their growth is accelerated and they become more pronounced. As discussed previously, addition of the phosphonate is expected to prevent excessively rapid calcite formation by calcium complexation

and surface poisoning of the calcite seeds, which consequently leads to an increase of the Na/Ca ratio, favouring Gaylussite formation. In addition, the acceleration of the crystallisation process might be also related to the eventual seeding effects of the phosphonate through the precipitation of Ca*HEDP nano-particles, as discussed in the case of plain GGBS. This may explain the improved strength with phosphonate addition in the case of GGBS-Clinker blended binder.

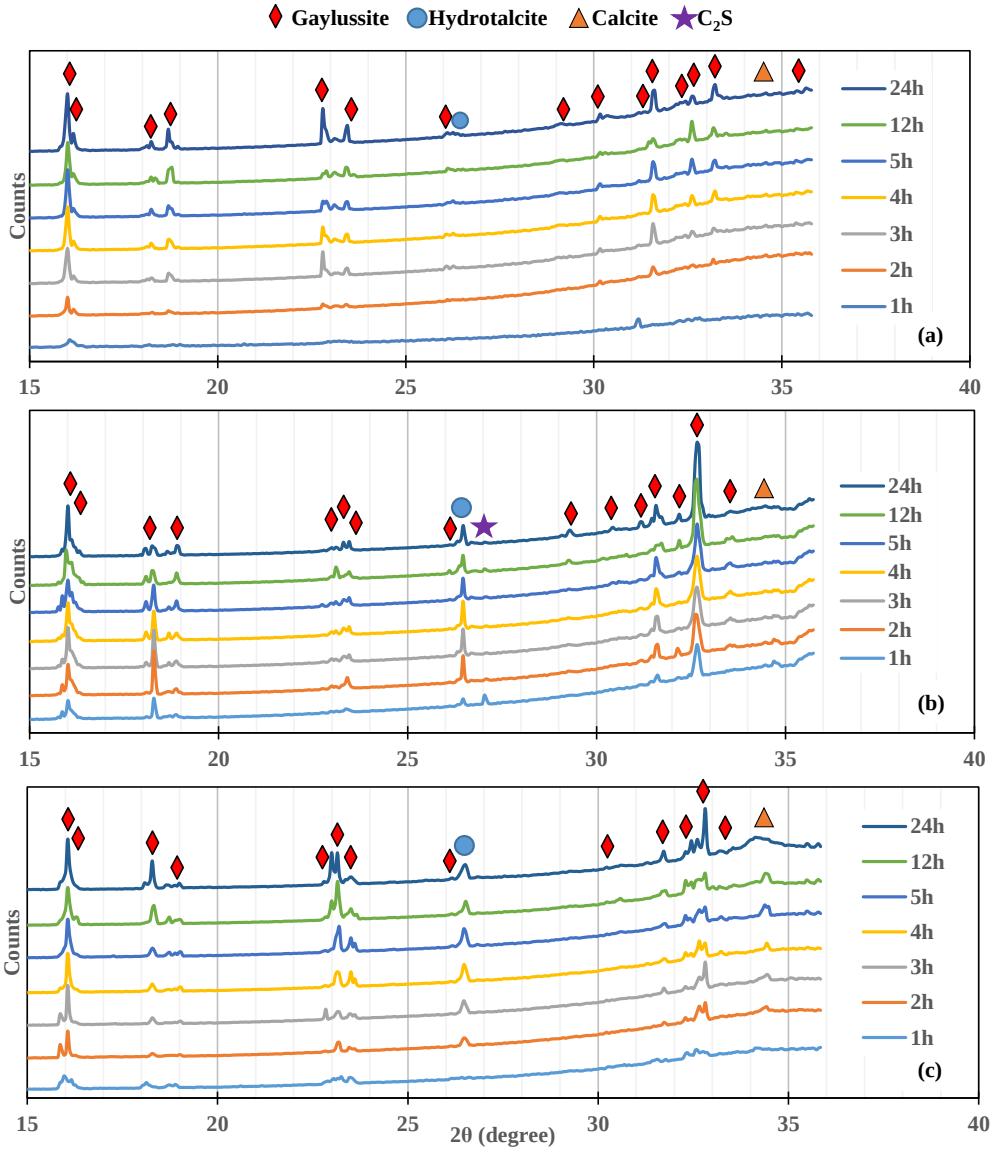

*Figure 5.82: Synchrotron in-situ XRD patterns over the first 24h for plain GGBS (a), 5% clinker 1400 cm²/g (b) and 6000 cm²/g blended GGBS (c). Solution: 200 g/l (W/B=0.40) and 0.1% 4Na*HEDP*

5.7.3 Hydration products in case of very low Na_2CO_3 concentration

In Figure 5.83 the influence of coarse clinker addition in the case of low sodium carbonate concentration (50 g/l) is presented. In both cases no Gaylussite precipitation occurs due to low Na/Ca instantaneous ratios, which is consistent with the Bury's early results (Bury and Redd, 1933). In the presence of the clinker, well-pronounced Calcite peaks can be observed compared to plain GGBS, which indicates its high crystallisation degree. This may

represent a crucial point in explaining how the addition of clinker accelerates the GGBS hydration even in case of very low sodium carbonate concentration (see Figure 5.51, 7 MPa after 2 days of hardening with clinker and zero strength without it).

As suggested previously, the main origin of the long induction period of GGBS activated with low sodium carbonate concentration and in the case of pure water (latent hydraulic properties) should be the precipitation of small sized low crystalline (or mostly amorphous) calcite on the slag grain surface around which the calcium ions are concentrated (passivation layer). This will lead to hydration hindering due the decrease of the slag's effective surface exposed to water. The presence of clinker may limit this effect since the clinker grain's surface is richer in Ca^{2+}, attracting most of the carbonate ions stemming from the activator.

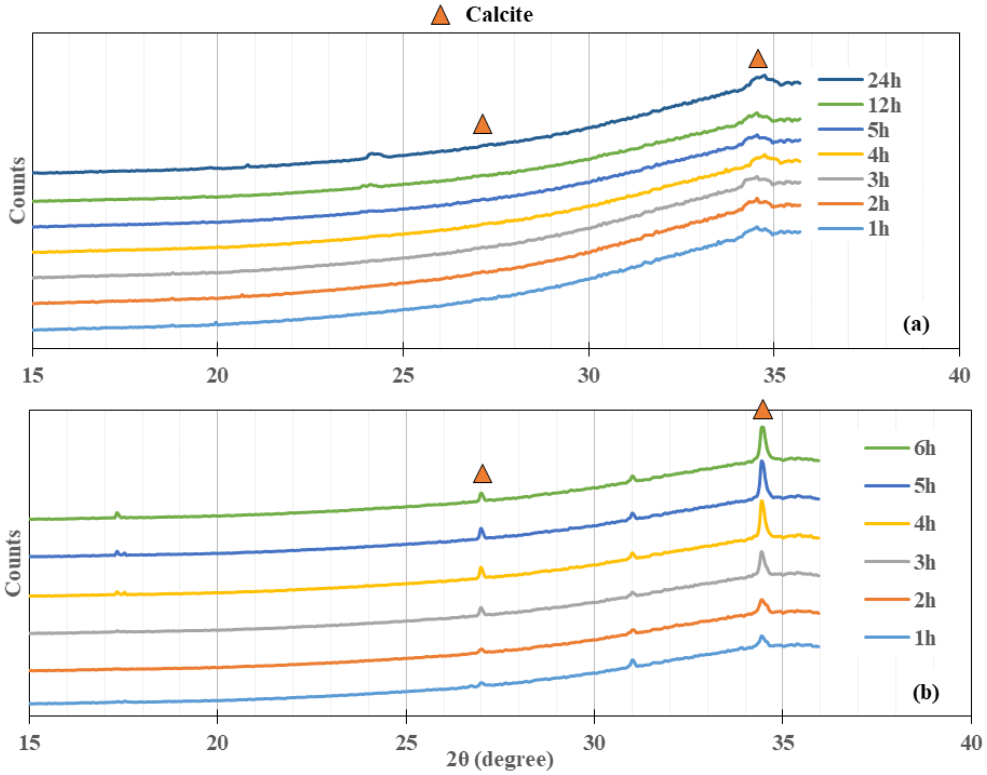

Figure 5.83: *Synchrotron in-situ XRD patterns of GGBS hydration without (a) and with 5% replacement (b) by coarse clinker 1400 cm^2/g at W/B=0.40 with 2%Na_2CO_3 (50 g/l)*

5.8 *Ex-situ* laboratory XRD

5.8.1 Influence of Clinker substitution

The evolution of the XRD patterns for plain GGBS and for 5% coarse clinker blended GGBS mixes up to 28 days is presented in Figure 5.84. Addition of clinker leads to a significantly faster growth of the Calcite peaks and nano-crystalline C-S-H, which correlates with the acceleration of the compressive strength evolution presented above. At long term the amount of

Calcite in the presence of the clinker is higher. In addition a higher amount of Monocarboaluminate can be observed with the clinker blended mixes, and this phase is clearly detected from 3 days in this case. This can be attributed to the higher amount of Ca and Al provided by the clinker.

No significant impact of the clinker on the Gaylussite signal (intensity) can be detected in the case of this coarse clinker grade, similar to what was observed in the above Synchrotron in-situ XRD. However in time, its signal decreases faster, due to its faster decomposition in the presence of clinker.

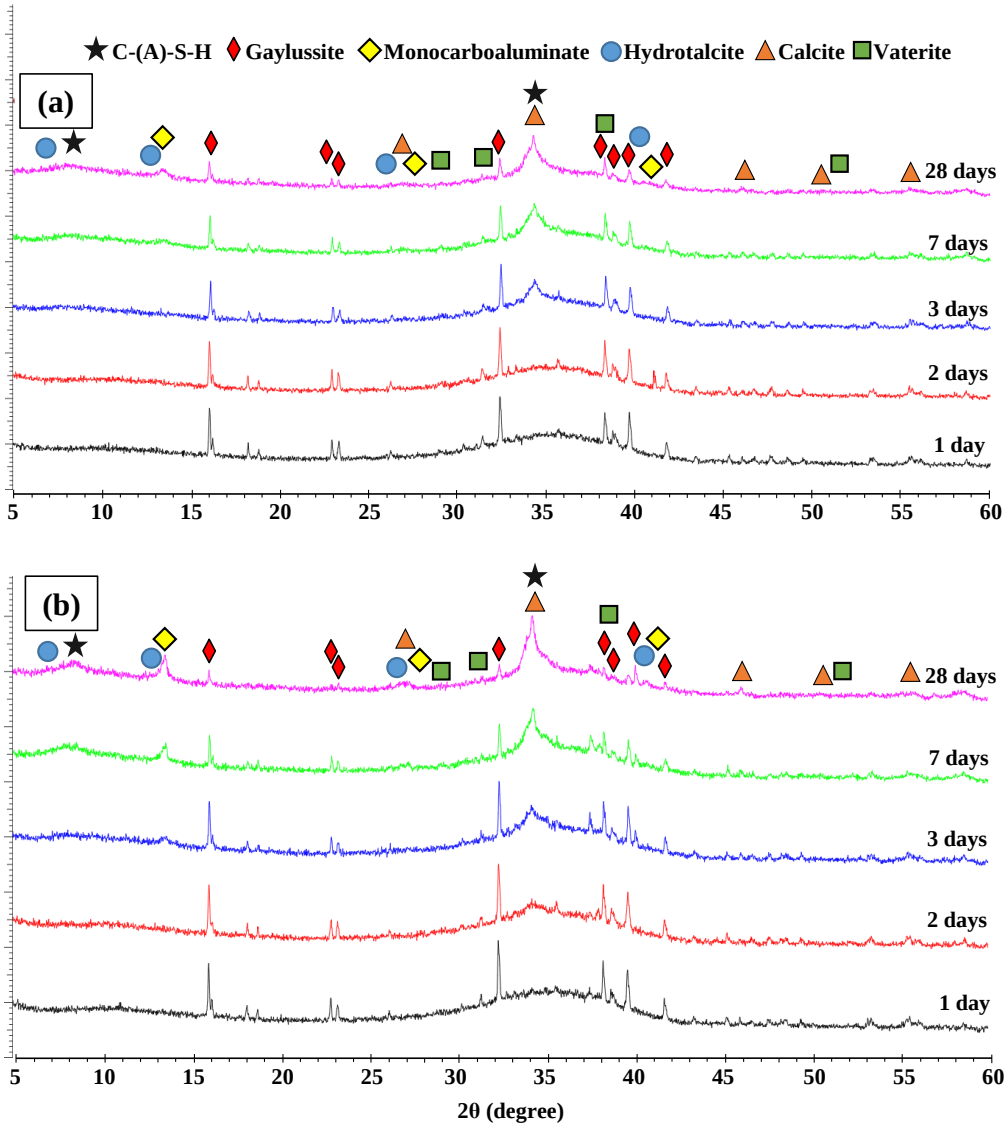

Figure 5.84: XRD patterns of GGBS without (a) and with (b) 5% replacement by coarse clinker 1400 cm^2/g at W/B=0.40 with 8% Na_2CO_3 (200g/l)

Similar quantitative observations can be done regarding the impact of the clinker in the presence of the phosphonate (Figure 5.85). A slower Gaylussite decomposition can be observed in both cases, which nevertheless occurs faster with clinker addition and clearly has already

begun by 2 days. A higher amount of the crystallised phases with clinker addition can be observed also in the presence of 4Na*HEDP.

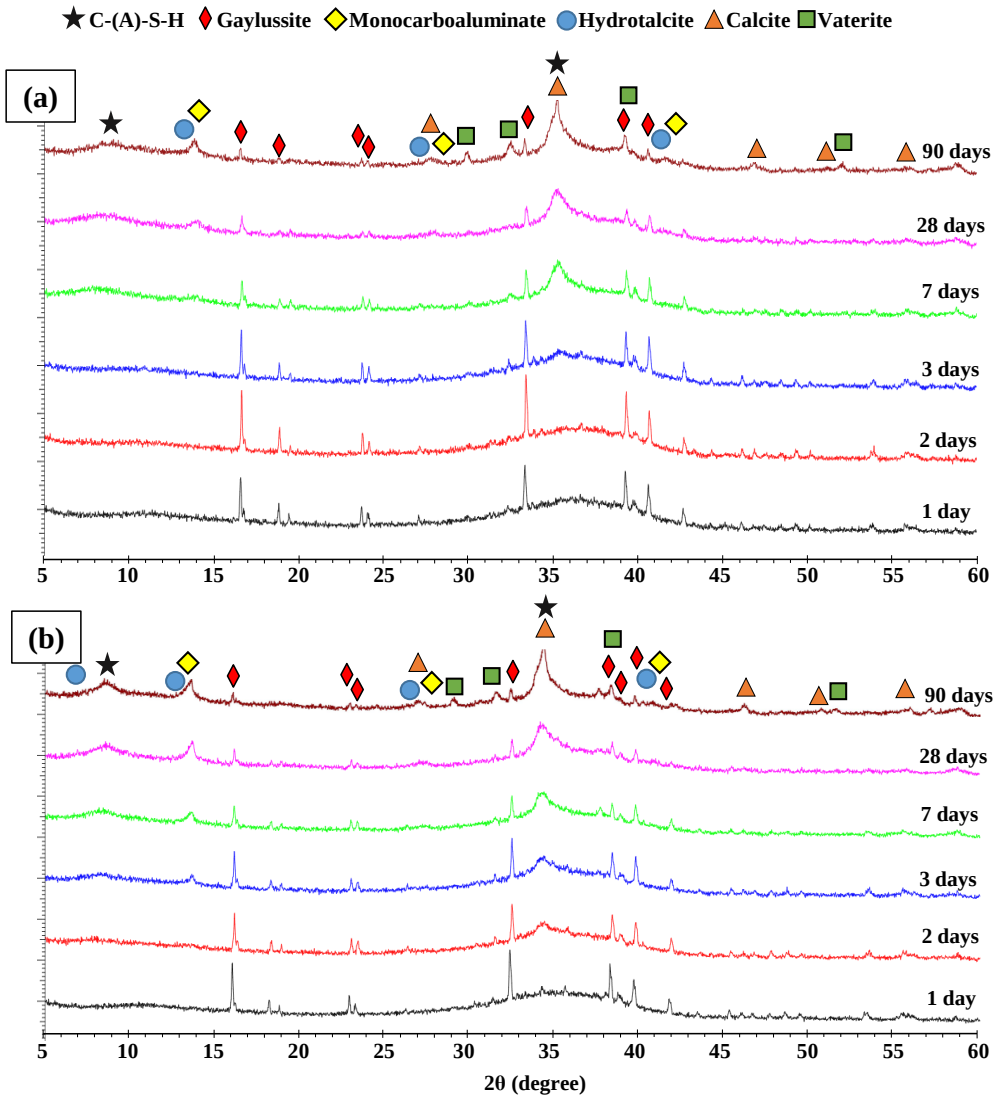

*Figure 5.85: XRD patterns of GGBS without (a) and with 5% (b) replacement by coarse clinker 1400 cm^2/g at W/B=0.40 with 8% Na_2CO_3 (200g/l) in the presence of 0.1% 4Na*HEDP addition*

5.8.2 Influence of the phosphonate dosage

No significant changes in the XRD patterns can be observed at late ages when the phosphonate dosage is increased (Figure 5.86), which explains why no difference in compressive strength evolution was observed. However at 1 day, in the case of high dosage (here 0.3%), a retardation effect of crystal precipitation (crystallisation and/or crystal growth) can be observed and coincides with previous observations with or without clinker. At the same time from the age of 2 days, a higher crystallisation of calcite and Gaylussite was observed with the higher amount of phosphonate.

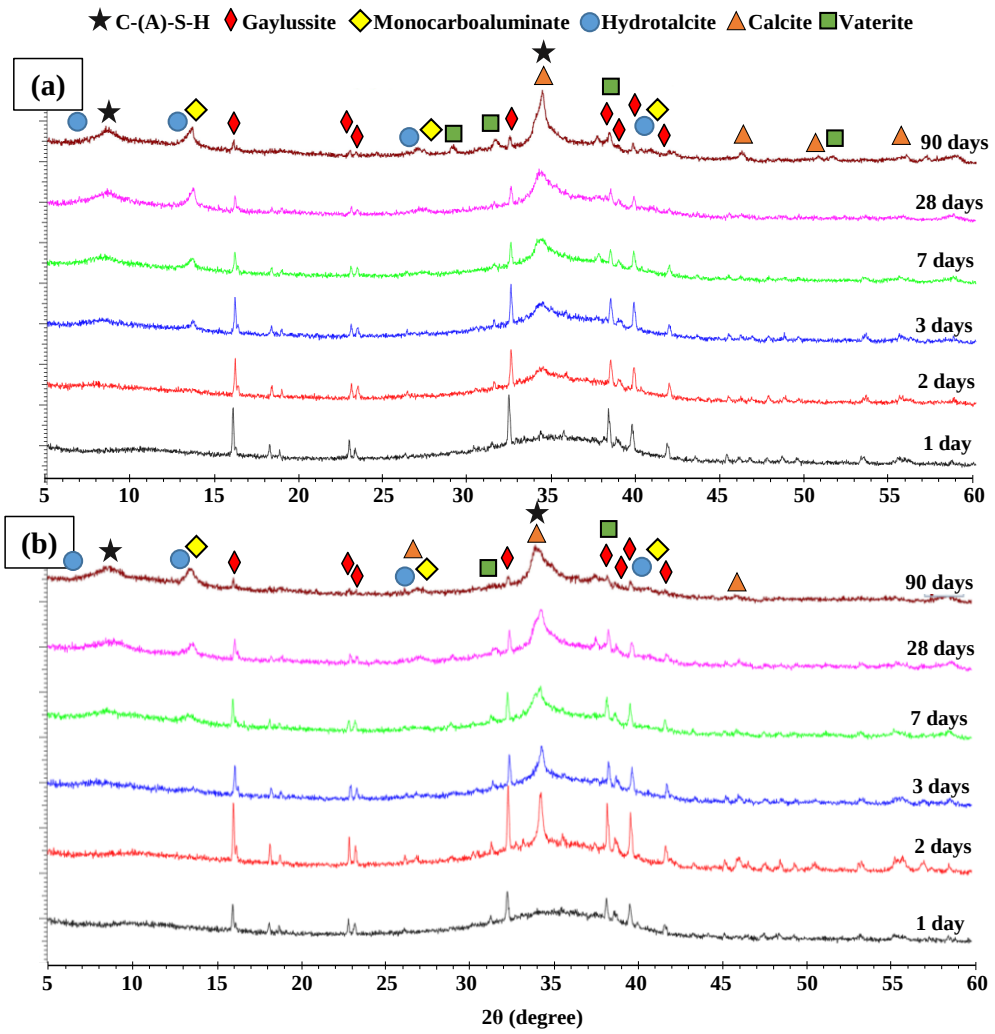

*Figure 5.86: Influence of 4Na*HEDP dosage (0.1% (a) and 0.3% (b)) on the hydration products of GGBS with 5% replacement by clinker 1400 cm2/g at W/B=0.40 with 8% Na_2CO_3 (200g/l)*

5.9 Impact of the clinker on the microstructure using X-ray computed tomography

A comparison between the tomographic images of the samples with and without GGBS replacement by clinker is reported in Figure 5.87. They show a lower amount of air voids, due in particular to lower yield stress.

In addition, a higher amount of unreacted slag/clinker agglomerates can be observed. This agglomeration might be related to a significant difference in surface charge (positive and negative) of the particles, which in some instances results in flocculation. Further, the excess calcium ions leached from the clinker will adsorb on the surfaces on which they precipitate. Over time the largest slag/clinker particles (or mostly agglomerates here) that are the least reactive will be fully covered with hydration products preventing them from contacting the interstitial

water. This observation, in addition to the abovementioned Ca enrichment of the C-S-H gel in the presence of the clinker, may explain the reduction of the mid-term (7-28 days) strength in the presence of coarse clinker.

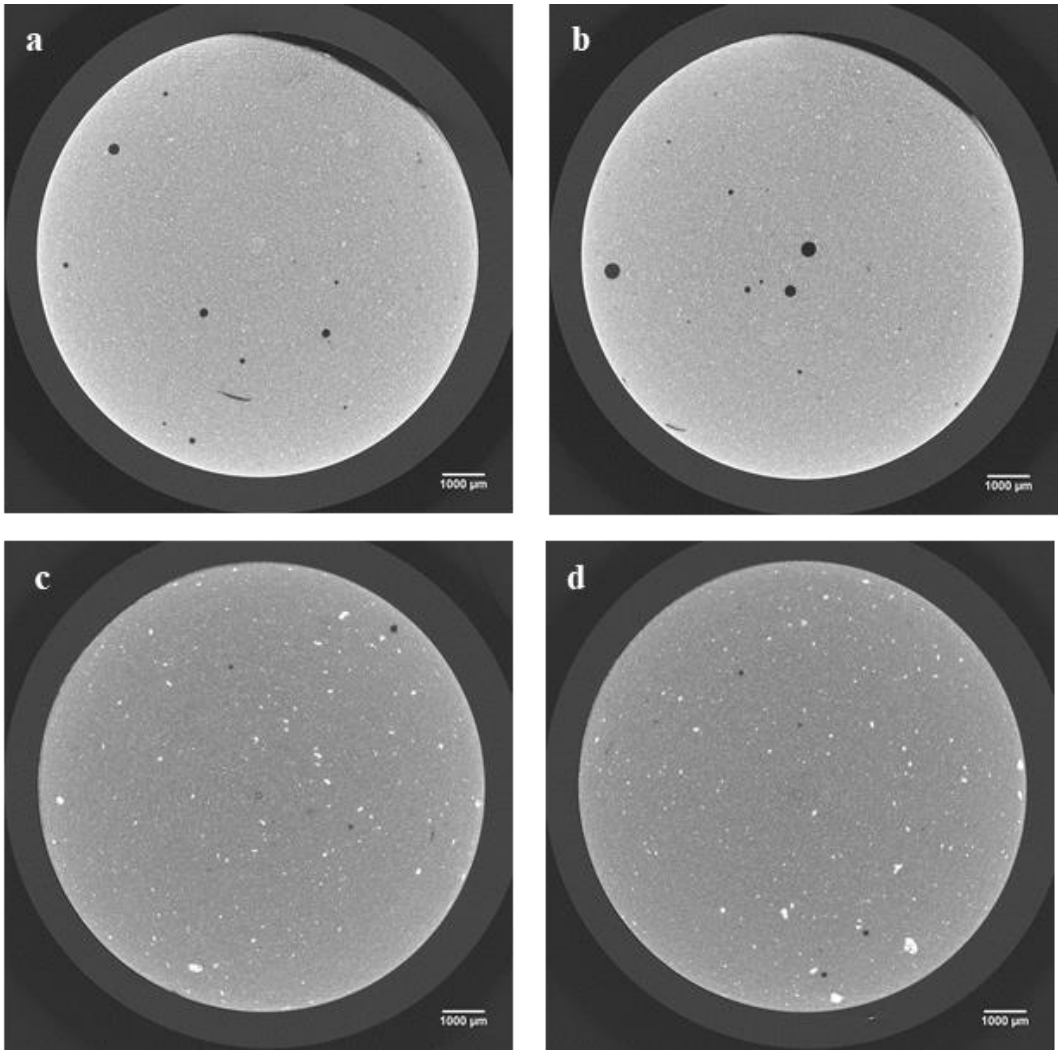

*Figure 5.87: Tomography scans : Comparison between 0% (a,b) and 5% (c,d) GGBS replacement by 5% coarse clinker at the age of 120 days, with 8%Na_2CO_3 and 0.1% 4Na*HEDP at W/B=0.40*

5.10 Impact of the clinker of the microstructure using SEM

SEM images of paste samples of GGBS with and without clinker addition after 28 days of hardening are presented in Figure 5.88. At this finer scale, no significant difference can be observed between the two samples. In both cases, a very high amount of unreacted cement grains can be observed after 28 days of hardening.

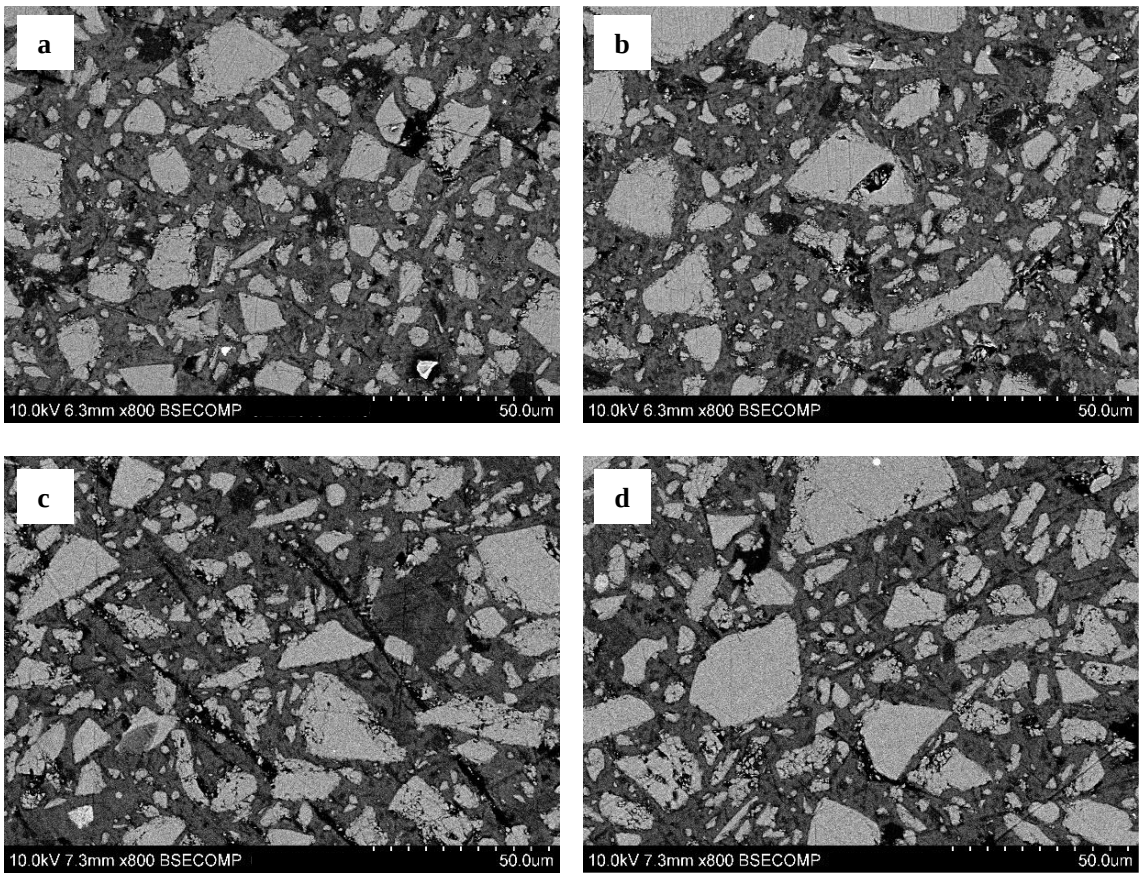

*Figure 5.88: SEM observations of polished surface. Comparison between 0% (a,b) and 5% (c,d) GGBS replacement by coarse clinker at 28 days. 8%Na_2CO_3 and 0.1% 4Na*HEDP at W/B=0.40*

Observations of the same samples fault surface (Figure 5.89) shows that the addition of clinker leads to certain changes in the structure of hydrates. The inter-grain C-S-H gel seems to be less dense. Of course, such structures in the case of 100% GGBS can be observed. However to see these voids in gel, a higher zoom should be used, compared to the samples with clinker. A less dense gel structure may explain the lower strength of the 28 day samples with clinker.

The images illustrated in Figure 5.90 confirmed that in the case of very low Na_2CO_3 content this inter-grain C-S-H gel seems to be even less dense. In addition, as observed, all grains are completely covered with hydration products. This most likely indicates that the precipitation has occurred mainly on the surface of the grains, as it was already seen in the case of pure GGBS (Chapter 2).

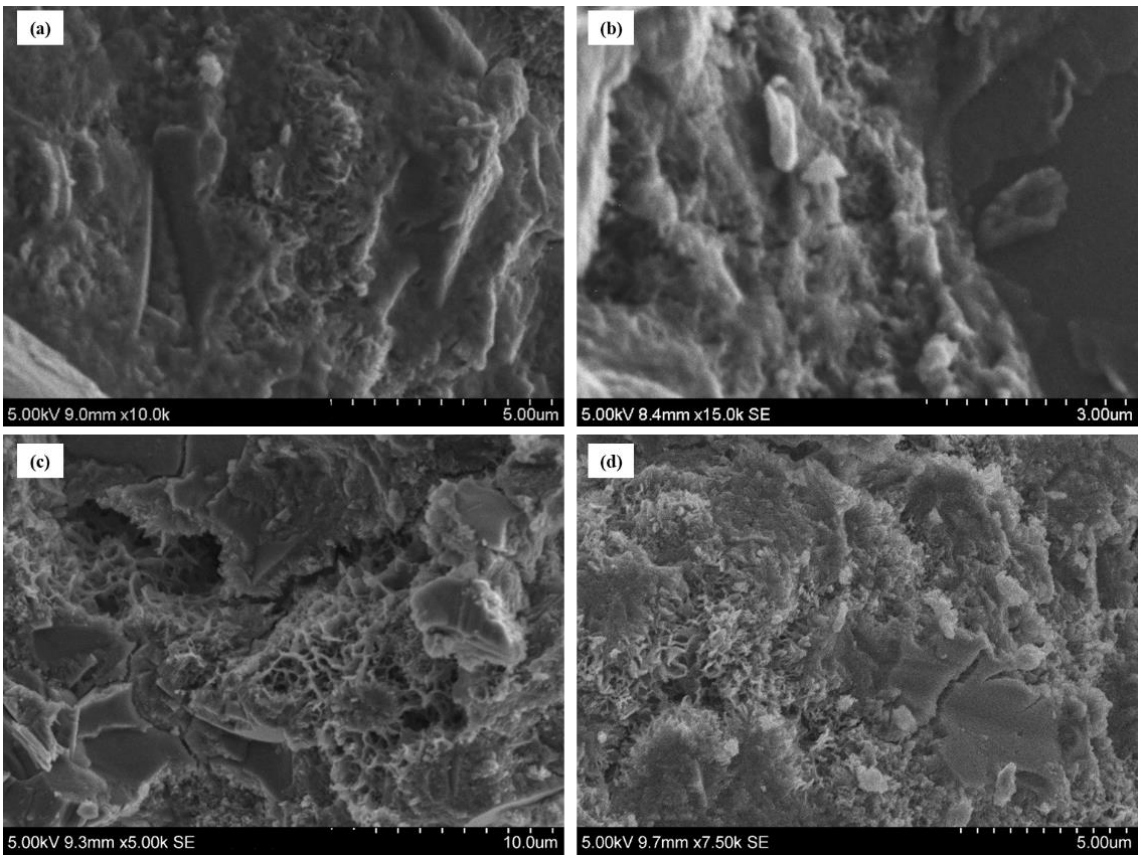

*Figure 5.89: SEM observations of fault surface. Comparison between 0% (a,b) and 5% (c,d) GGBS replacement by coarse clinker at the age of 28 days. 8%Na_2CO_3 and 0.1% 4Na*HEDP at W/B=0.40*

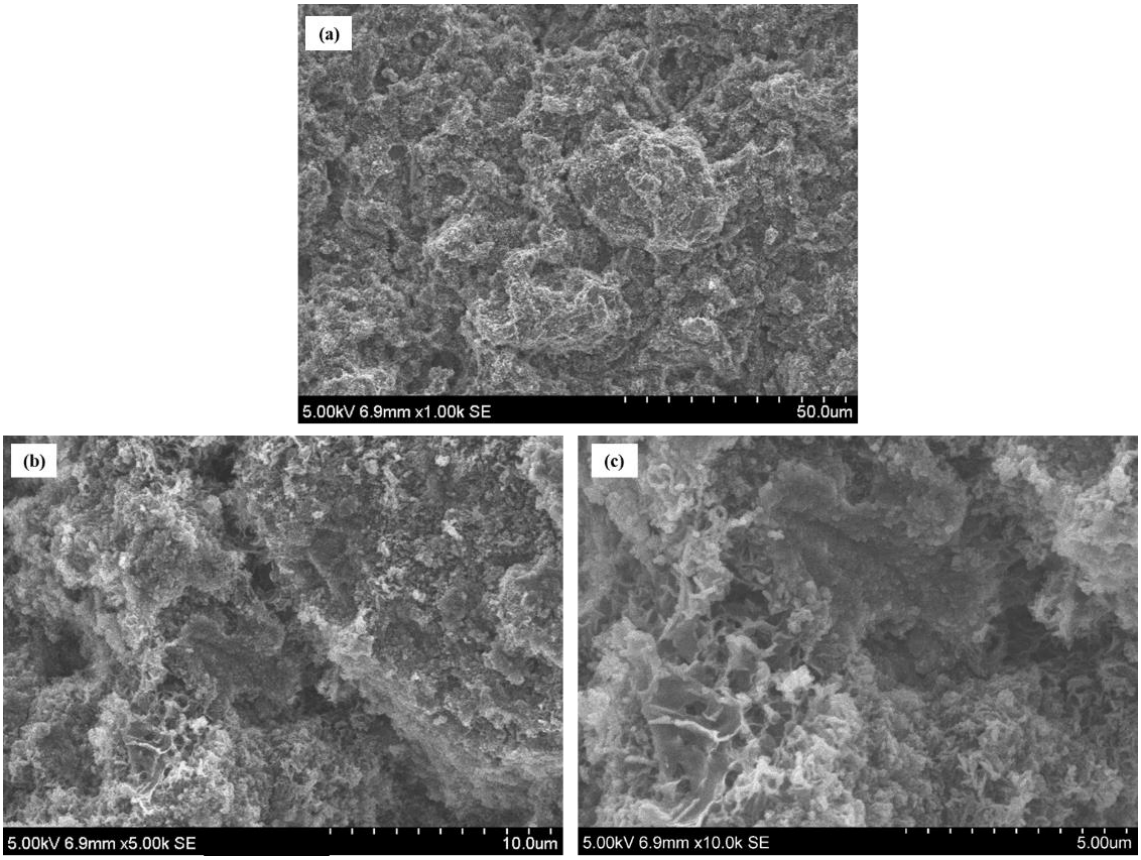

*Figure 5.90: SEM observations of fault surface. GGBS with 5% replacement by coarse clinker at the age of 28 days. 2%Na_2CO_3 and 0.1% 4Na*HEDP at W/B=0.40*

Conclusions

In this chapter, it was shown that the main reason for a long induction period in case of high sodium carbonate concentration is Gaylussite. Its destabilization by the addition of a calcium source (for calcite precipitation and consumption of CO_3^{2-} ions) greatly accelerates the hydration process. This leads to faster increase in alkalinity, which consequently accelerates the hardening. However, the solubility of the source of this calcium is extremely important. In the case of lime addition, a sharp increase in the calcium concentration leads to rheology issues. A lack of time for the precipitation in bulk leads to further decreases in hydration, as seen in the literature. The use of a source with gradual calcium leaching (Portland clinker here) doesn't affect the rheology and at the same time provides an accelerating effect. Nevertheless, its fineness and, accordingly, the dissolution rate play a very important role and should be considered. The use of phosphonates to adjust rheological properties in addition led to better hydration process at the very beginning. However, this acceleration related to clinker addition slightly decreases the compressive strength at longer term compared to plain GGBS, which is more noticeable in the period of 7-28 days. This is most likely associated with less dense hydrate formation. Nevertheless, an increase in the slag fineness can compensate for this phenomenon.

Another positive aspect of hydration acceleration by clinker, which is also worth noting is that such a blended cement is less sensitive to variations in the amount of water. This factor is still very important at the early age. Also, the drop in strength with a decrease in curing temperature is less critical as well as is early age drying impact in the case of low relative humidity. At the same time, although the heat treatment has a synergistic effect with the acceleration from the clinker in the first days, it is rather unnecessary compare to plain GGBS. Excessive acceleration of the reaction leads to a further slowing of the strength development.

However the most important aspect is that the system becomes less sensitive to variations in the Na_2CO_3 concentration, as it was before. The hydration process occurs even in the case of very low (50 g/L) solution. Nevertheless, a slightly different mechanism of positive clinker influence in this case takes place. A higher robustness of the system is a key parameter for industrial applications.

Chapter 6 GGBS dilution with limestone powder

Introduction

Throughout the previous chapters it was shown that it was possible to prepare Na_2CO_3 activated GGBS-based binders with appropriate rheological and mechanical properties, not only for precast, but also for conventional civil engineering applications. The replacement of cement with usually high amounts of clinker by such mixes should contribute to a significant decrease in the amount of CO_2 attributed to the binder, which is the main objective of almost all countries (for ex. agreement COP21, Climate change conference, Paris, 2015). Nevertheless to achieve such ambitious goals, a significant reduction of OPC consumption should take place, to reduce the impact of cement production on global CO_2 emissions. At the same time it is worth noting that GGBS is a limited resource globally (Damtoft et al., 2008) and represents only about 7-10% of OPC production. In addition, its use is economically viable only around the area of its production, e.g. near to the steel factories. Long-term transportation can significantly reduce the positive environmental effect as well as increase its cost. That is why the rational use of this resource is important. It is worth diluting GGBS with other available and low-CO_2 impact materials in the present binder, yet, without negatively impacting the final product properties.

In the previous chapter it was demonstrated that the addition of a small amount of Portland clinker (less than 4.5% in 1t of total binder with Na_2CO_3 already inside) has a positive effect on many properties and increases the binder robustness versus many factors. Unfortunately, it will increase its CO_2 footprint. As a result, it is necessary to reduce this parameter again, by binder dilution.

In the present investigation, limestone powder is used in partial replacement of GGBS. This product is already used for OPC dilution (production of CEM II). Limestone powder is available worldwide. In addition the CO_2 footprint and cost of limestone powder can be extremely low, leading to a further reduction of the CO_2 impact and the cost of the final binder.

Similar investigations have already been reported in the literature, highlighting the positive effect of partial substitution of GGBS with limestone in the case of Na_2CO_3 activated slag binders (Moseson et al., 2012; Rakhimova et al., 2016; B. Yuan et al., 2017). Considered here is the specific case of the developed binder including the partial substitution of slag with clinker in the presence of the phosphonate retarder.

6.1 Materials

Two grades of limestone powder are considered in this first investigation. Both of them are commercially available and supplied by the Omya Company, France. In all cases the limestone powder was mixed in dry form with remaining binder constituents.

The first grade has the commercial name *Betocarb GY* and is denominated hereafter as fine limestone. It has a specific surface of 5400 cm^2/g Blaine and $d_{(50)}$=6µm. Its bulk density is 1600 kg/m^3. The granular distribution provided by Omya is presented in Figure 6.1.

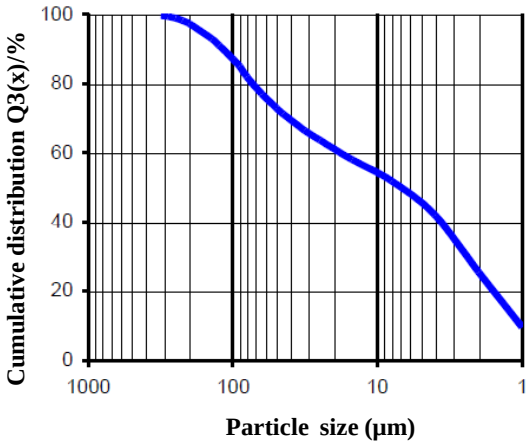

Figure 6.1: Particle size distribution of the fine limestone

The second limestone grade has a commercial name *Omyalite 90 OM*, and is designated hereafter as ultrafine limestone. It has a specific surface of 80 000 cm^2/g BET and $d_{(50)}$=1µm. Its bulk density is 700 kg/m^3. The low value of the density indicates that the particles should be quite porous. The granular distribution provided by Omya is presented in Figure 6.2. The SEM images in Figure 6.3 indicate that the particles are highly agglomerated.

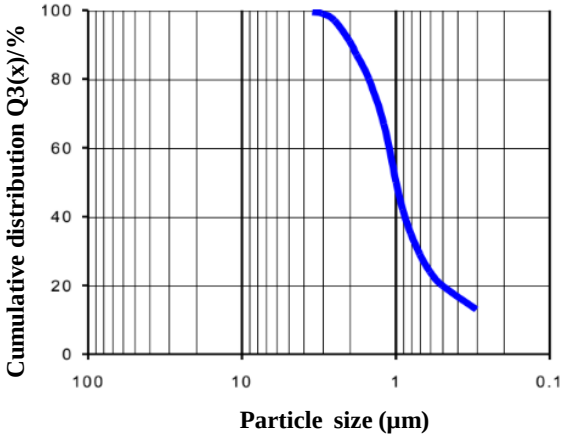

Figure 6.2: Particle size distribution of ultrafine limestone

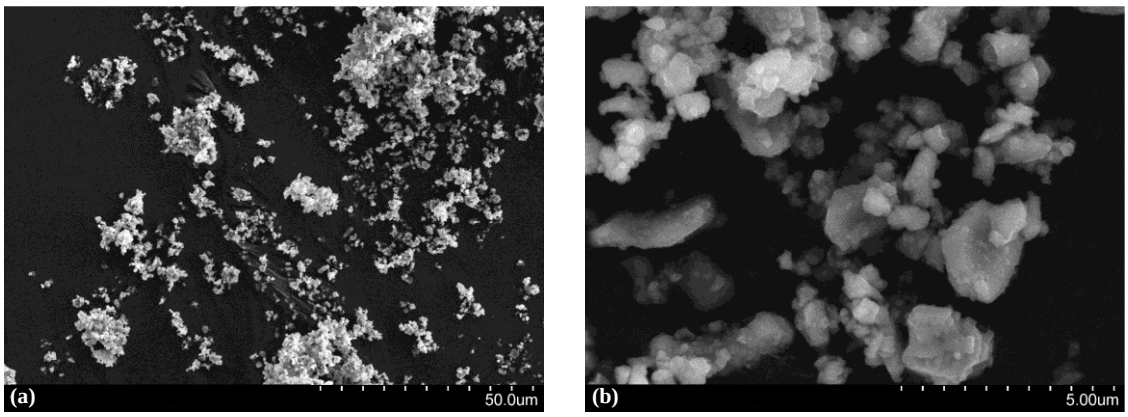

Figure 6.3: SEM images of the ultrafine limestone

The zeta potential of the two limestone grades in the presence or absence of Na_2CO_3 (8% by weight of GGBS) are reported in Figure 6.4. The fine limestone particles have a positive surface charge when dispersed in demineralized water. Several sites can be present on the limestone particles (which are mainly composed of Calcite): CO_3^{2-}, HCO^{3-}, Ca^{2+}, $CaOH^{+}$, etc. depending on the pH and the type and concentration of ions dissolved in the water used (Heberling et al., 2011). In this case the main ions present (in addition to OH^-, H_3O^+) should be carbonates and/bicarbonates stemming from the dissolved CO_2. The measured pH is 8. Under these conditions, an overall positive surface is expected for calcite (Heberling et al., 2011). The addition of Na_2CO_3 is expected to lead to neutralisation of the positive sites by the carbonates ions. Due to their high wetting properties and low charge, the Na ions have less tendency to surface adsorption. The overall surface charge then becomes negative.

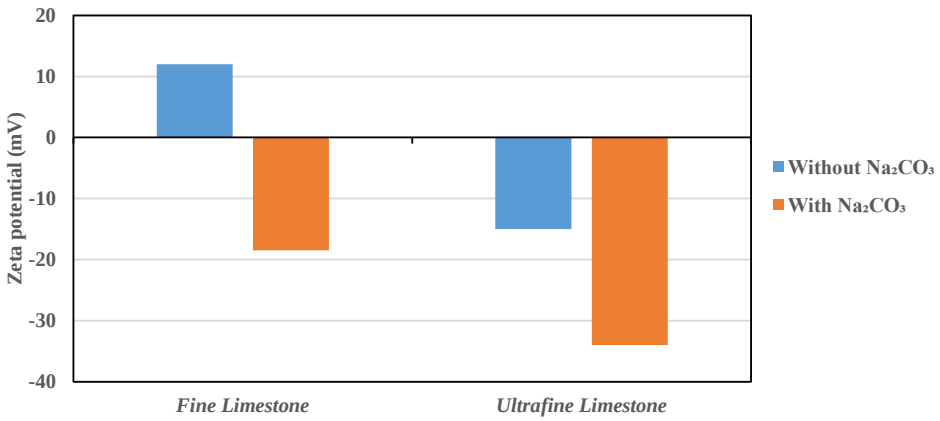

Figure 6.4: Zeta potential of the two types of limestone used, without and with the presence of Na_2CO_3

In the case of ultrafine limestone, the zeta potential is negative in the presence or absence of Na_2CO_3. An unknown grinding-aid agent is included in this grade. The negative value of the zeta potential indicates that this agent is an anionic molecule.

In the case of ultrafine limestone based mixes, a clinker of slightly higher fineness was used. The particle size distribution of this clinker is presented in Figure 6.5. The $d_{(50)}$ is about 18 µm and the approximate Blaine fineness is about 2600 cm^2/g (provided by ECOCEM France).

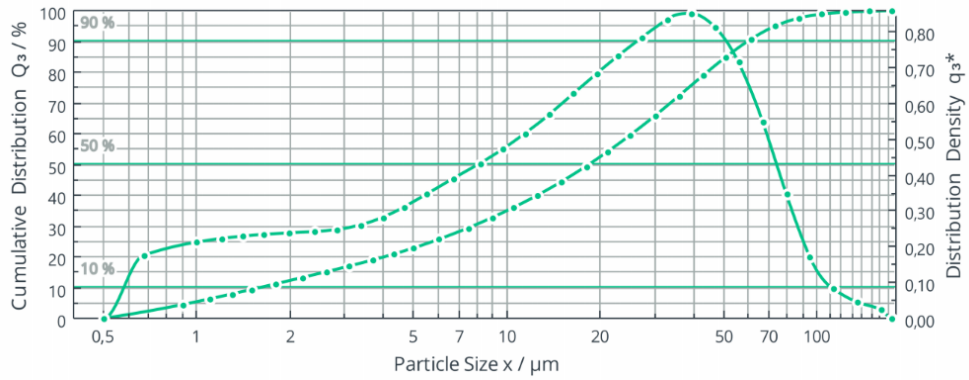

Figure 6.5: Particle size distribution of the 2600 cm^2/g Blaine clinker

6.2 Fine limestone based mixes

6.2.1 Rheological properties

The yield stress time evolution of the mixes in which GGBS is partially replaced by fine limestone is presented in Figure 6.6. A reduction of the instantaneous yield stress values can be observed when the replacement level is increased. This phenomenon was already reported in the literature (Kwow, 2013; B Yuan et al., 2017) in which it was assumed that higher slump values was obtained due to improved granular compaction. Nevertheless, zeta potential results show that yield stress reduction can be also related to an increase in repulsive electrostatic forces due to the highly negative charge of the limestone particles, in particular in the presence of Na_2CO_3. Although the instantaneous yield stress is reduced with limestone substitution its evolution rate remains high. The addition of a retarder is then still required.

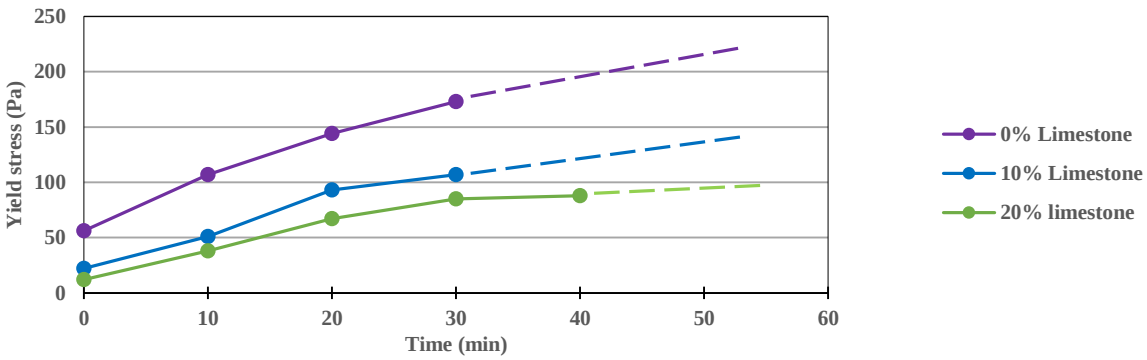

Figure 6.6: Influence of partial GGBS replacement by fine limestone on yield stress evolution at Water/(GGBS+Limestone)=0.40 and 8% Na_2CO_3 to dry components (200 g/l).

Addition of the phosphonate (4Na*HEDP) leads to a significantly extended open time in the case of limestone blended GGBS mixes as well (Figure 6.7). Notice that over time, the reduction of the yield stress due to limestone substitution decreases, leading to almost the same value beyond 20 min.

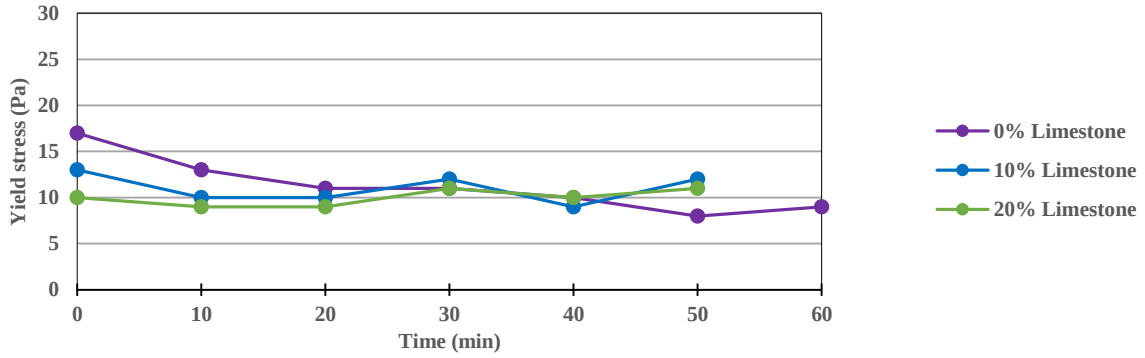

*Figure 6.7: Influence of partial GGBS replacement by fine limestone on yield stress evolution at Water/(GGBS+Limestone)=0.40, 8% Na_2CO_3 (200 g/l) and 0.1% 4Na*HEDP to dry components*

In the case of the presence of the clinker in the binder, addition of the phosphonate is mandatory to extend the open time as it was already demonstrated in the previous chapter. The impact of the partial replacement by fine limestone on yield stress evolution in the case of the clinker-blended mixes is presented in Figure 6.8. Increasing the limestone proportion in the binder leads to the decrease of the yield stress and its evolution over time. Increasing the level of limestone substitution should allow for a decrease in the W/B ratio in order to compensate in part for an eventual loss in strength development.

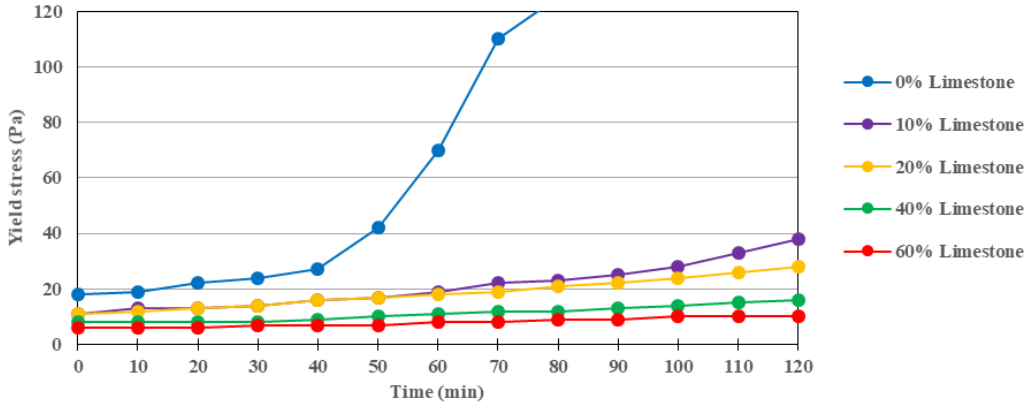

*Figure 6.8: Influence of partial replacement of 95%GGBS+5%Clinker mix by fine limestone on yield stress evolution at W/B=0.40, 0.1% 4Na*HEDP and 6% Na_2CO_3 (150g/l) to total dry mix*

6.2.2 Hydration kinetics

The microcalorimetry results for the paste samples based on GGBS and 5% Clinker 2600 cm^2/g with partial substitution by limestone are presented in Figure 6.9. Increasing the limestone content leads to a retardation of both main hydration peaks. Retardation of the first

peak, related to the formation of the carbonate based hydration products leading to setting, confirms the previous observation regarding the slower yield stress evolution (Figure 6.8). The decrease in the magnitude of this peak could be related to a lower amount of precipitated calcite/Gaylussite at this stage. This may possibly be explained by a lower amount of Ca leached from slag and clinker, due to their dilution with limestone. This should also explain a longer induction period, which is clearly correlated to limestone amount. Since in all cases the water content is constant, a longer period is required to sufficiently saturate the solution with Ca for consumption of CO_3^{2-} and start of the Gaylussite destabilisation. The same argument holds for C-S-H precipitation (second peak). This observation are also in agreement with those reported in the literature in the case of plain GGBS mixes (Rakhimova et al., 2016; B. Yuan et al., 2017).

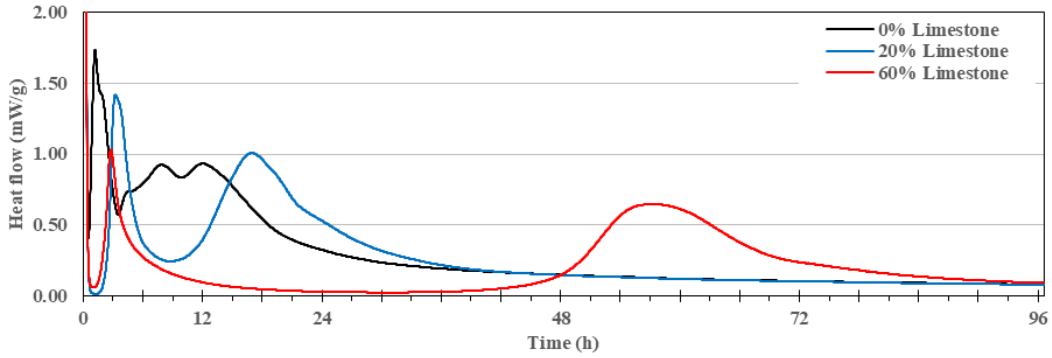

*Figure 6.9: Heat flow of 95%GGBS+5%Clinker binder hydration with different percentage of substitution by limestone at constant W/B=0.40 and 6% Na_2CO_3 (150g/l) with 0.1% 4Na*HEDP*

The results of the cumulative heat released during hydration are presented in Figure 6.10. Increasing the limestone substitution level leads to a lower amount of heat over this period. This is related to a lower amount of reactive binder per unit mass of the dry powder. This means that the binder will release even less of heat for the same period, which can be advantageous in the case of massive element concreting.

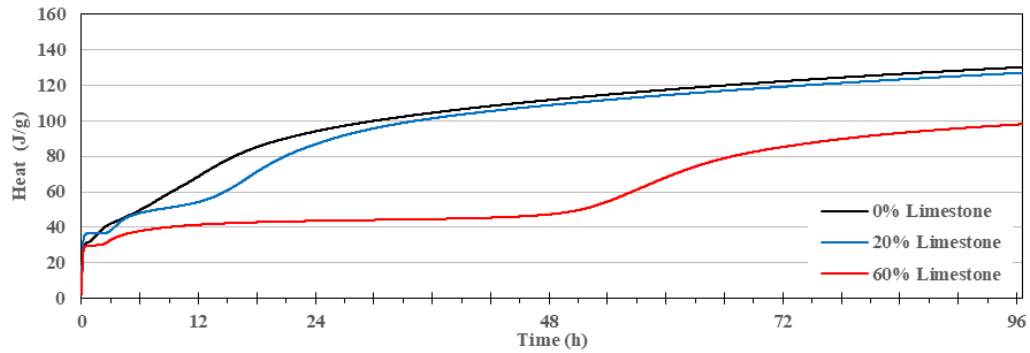

*Figure 6.10: Heat released from 95%GGBS+5%Clinker binder hydration with different percentages of substitution by limestone at constant W/B=0.40 and 6% Na_2CO_3 (150g/l) with 0.1% 4Na*HEDP (normalized to 1g of GGBS+Clinker+Limestone mix binder)*

If the same results are normalized per mass of the reactive binder or per g of 95%GGBS+5%Clinker (Figure 6.11), it can be clearly observed that the addition of limestone led to a greater amount of heat released. This may indicate a higher degree of slag and clinker hydration. Such results should be related to an eventual seeding effect of the fine limestone particles, leading to less precipitation on the anhydrous particles surface. It was shown above that limestone particles in Na_2CO_3 solution have a negative surface charge. This implies that the limestone particles may attract positively charges species (as Ca^{2+}) or hydrates (as Afm-type) playing then the role of templates for hydration products growth.

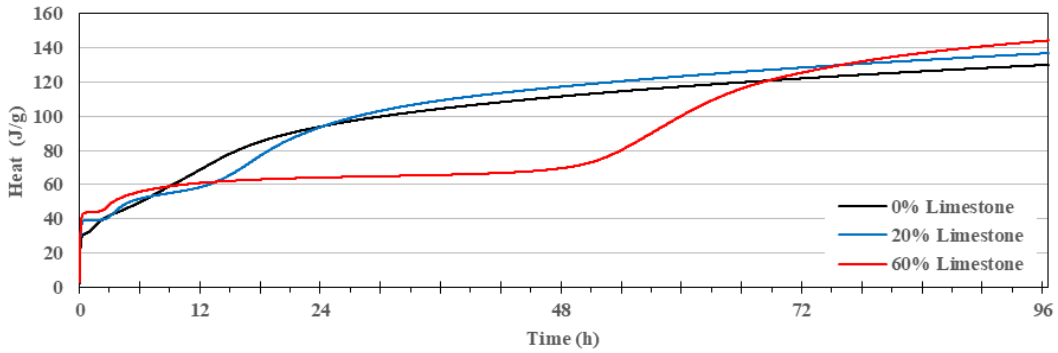

*Figure 6.11: Heat released from 95%GGBS+5%Clinker binder hydration with different percentage of substitution by limestone at constant W/B=0.40 and 6% Na_2CO_3 (150g/l) with 0.1% 4Na*HEDP (normalized only to 1g of GGBS+Clinker mix binder)*

6.2.3 Compressive strength evolution

The mortar mixes considered are reported in Table 10. Note that the amount of water is fixed relative to the total binder including the limestone. With increasing substitution level of limestone, an increasing amount of excess water that is not used for hydration will be present. A significant part of any eventual strength loss might be attributed to this excess water. On the other hand, the *aqueous* concentration of Na_2CO_3 (150 g/l) is fixed since it was shown in the previous chapters that it is the relevant parameter for the activator.

Table 10: Composition of the tested mortar samples to consider the impact of partial binder replacement by fine limestone, in g per 1350g of normalized sand.

	GGBS	***Clinker***	***Limestone***	***Na_2CO_3***	***4Na*HEDP***	***Water***	***Water/ (GGBS+ Clinker)***	***Water/ (GGBS+ Clinker+ Limestone)***
Reference	427.5	22.5	0	27	0.45	180	0.40	0.40
10%	384.75	20.5	45	27	0.45	180	0.44	0.40
20%	342	18	90	27	0.45	180	0.50	0.40
30%	299.25	15.75	135	27	0.45	180	0.57	0.40
40%	256.5	13.5	180	27	0.45	180	0.67	0.40
60%	171	9	270	27	0.45	180	1	0.40

The results of compressive strength development are presented in Figure 6.12. 10-20% replacement of the slag/clinker by limestone leads to a negligible loss in strength at all terms. By comparison, increasing the limestone content to 40-60% led to a significant loss in strength. No measurable strength was detected with a 60% substitution of limestone at 1 day. At 28 days the strength loss is about 40% compared to the reference sample in the case of 60% replacement. The loss of strength when increasing the limestone substitution level can be attributed to the dilution effects, but also to the increase of excess water, leading to higher porosity. In the case of low limestone replacement rates (10-20%), due to the seeding effect referred to above, the acceleration effect may compensate in part for this phenomenon.

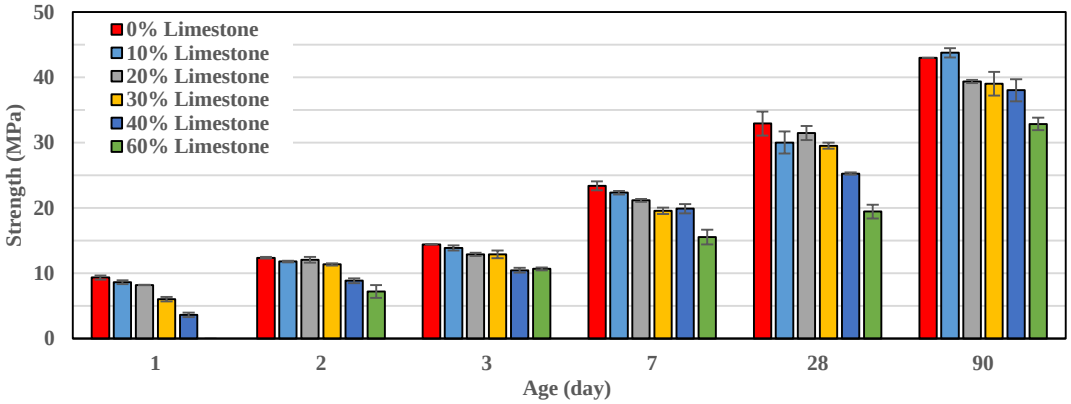

Figure 6.12: Compressive strength evolution of 95% GGBS + 5% Clinker 2700 cm^2/g diluted by different amounts of Fine Limestone. Constant amount of water and Na_2CO_3 concentration (150 g/l) in all cases

The influence of Na_2CO_3 concentration on the compressive strength evolution in the case of dilution by limestone at 40% is then considered. The composition of the mortar samples is reported in Table 11.

Table 11: Composition of the tested mortar samples with or without limestone substitution and different amounts of Na_2CO_3 in g per 1350g of normalized sand.

	GGBS	***Clinker***	***Limestone***	***Na_2CO_3***	***4Na*HEDP***	***Water***	***Water/ (GGBS+ Clinker)***	***Water/ (GGBS+ Clinker+ Limestone)***
Reference-6%	427.5	22.5	0	27	0.45	180	0.40	0.40
40% Limestone -6% Na_2CO_3	256.5	13.5	180	27	0.45	180	0.67	0.40
Reference-8%	427.5	22.5	0	36	0.45	180	0.40	0.40
40% Limestone -8% Na_2CO_3	256.5	13.5	180	36	0.45	180	0.67	0.40

The results of the compressive strength evolution in the case of two different sodium carbonate dosage rates are presented in Figure 6.13. As expected, increasing the Na_2CO_3 dosage

leads to higher strength values at all ages for all conditions. Increasing the hydration rate leads not only to a higher strength values, but also to a lower loss of the strength at 28 days in the case of limestone substitution: about 15% with 200 g/l and 25% with 150 g/l Na_2CO_3.

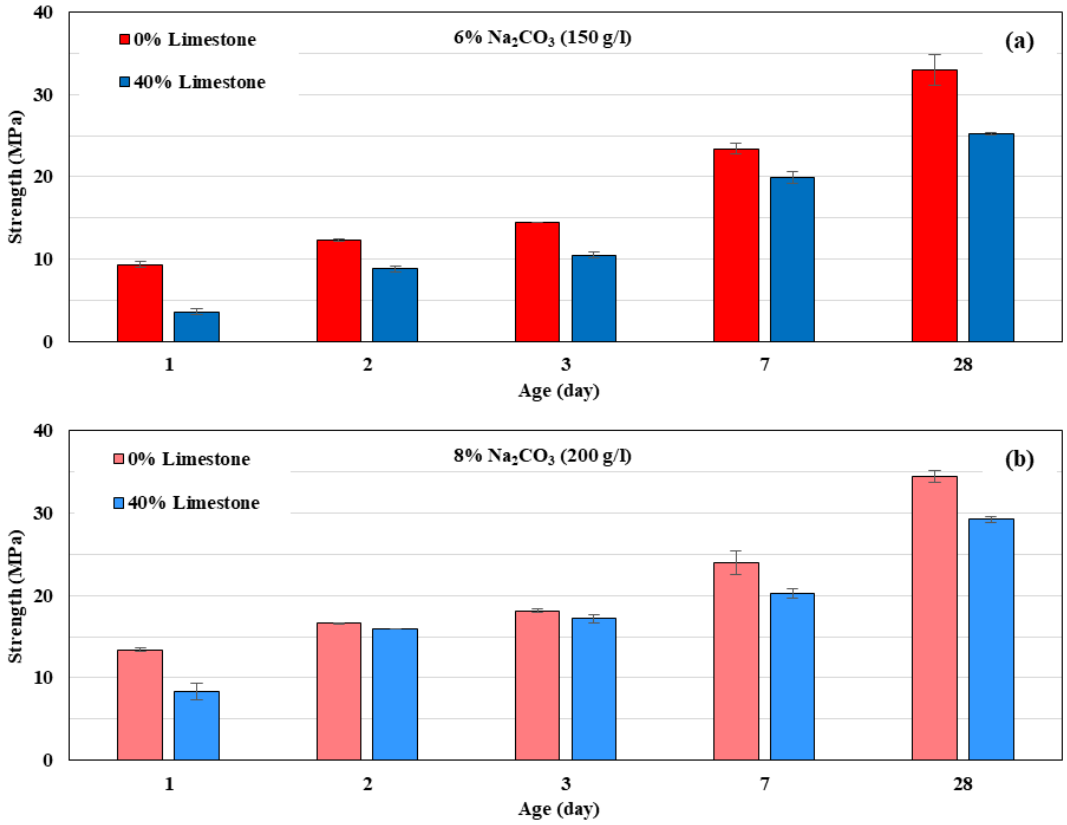

Figure 6.13: Influence of Na_2CO_3 aqueous concentration (150 g/l (a) and 200 g/l (b)) on compressive strength evolution of 95% GGBS + 5% Clinker 2700 cm^2/g diluted by different amount of Fine Limestone. The amount of water was kept constant.

6.2.4 Crystalline hydration products (*ex-situ* XRD)

The results of XRD analysis of the GGBS-clinker mixes with different amounts of replacement (20 and 60%) with fine limestone are presented in Figure 6.14. With the presence of limestone, a significant increase of the Gaylussite intensity peaks at 1 day can be observed. This may be related to a lower amount of available leached calcium from slag and clinker, due to their dilution with limestone, while the aqueous concentration Na_2CO_3 remains constant. In addition, the negatively charged limestone particles may also adsorb Ca ions. The ratio of Ca/Na then decreases in the presence of limestone, favouring Gaylussite against calcite. Beyond 3 days no significant impact of the limestone on the Gaylussite peaks can be observed. This indicates that its decomposition occurs faster in the presence of limestone and should contribute to a higher hydration rate through the seeding effect of the limestone particles. This observation may explain the low strength loss in the case of dilution with 10-20% of limestone, even though the water/active binder ratio is higher.

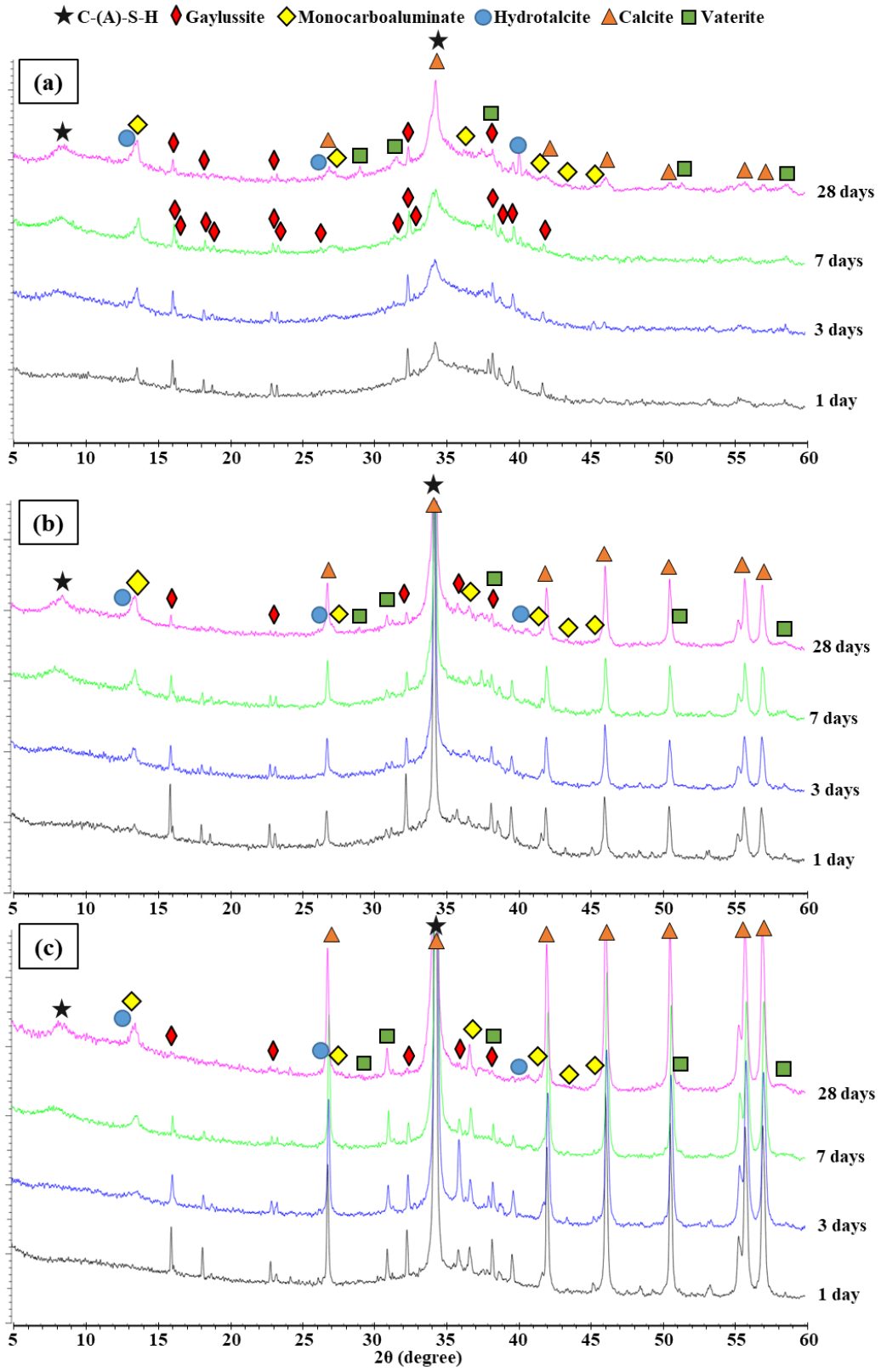

*Figure 6.14: XRD patterns during hydration of (GGBS+Clinker) without (a) and with 20% (b) or 60% (c) replacement by fine limestone. W/B=0.40 with 6% Na_2CO_3 (150 g/l) with 0.1% 4Na*HEDP*

The amount of monocarbonaluminate is lower at early age in the presence of limestone. Here again this may be attributed to a lower amount of available calcium and probably also alumina. At late ages (from 3 days for 20% dilution and 7 days for 60%) all mixes seem to

contain the same amount of crystalline hydration products. This suggests that the main reason for strength loss when increasing the dilution level may be attributed to an eventual increase of the porosity due to excess water.

6.3 Substitution with Ultrafine limestone

In the case of the ultrafine limestone grade only the plain GGBS binders (without clinker) are considered. In addition, due to restricted availability and the high price of ultrafine limestone, only low substitution levels are considered. This limestone grade is rather marketed towards high added value products such as polymer composites, etc.

6.3.1 Impact of the ultrafine limestone on the rheological properties

The impact of ultrafine limestone substitution on the yield stress time evolution on Na_2CO_3 activated GGBS binders is reported in Figure 6.15. A significant reduction of the instantaneous yield stress can be observed in the presence of the ultrafine limestone. It is not clear whether this reduction is due to the highly negative charge of the ultrafine limestone particles, their filling effects, or an eventual dispersing effect of the hidden grinding-aid admixture. More investigation is needed to determine the extent of the different contributions. It is worth noting that the yield stress reduction is almost the same for the two substitution levels of limestone. In addition there is a slight retardation effect of the limestone.

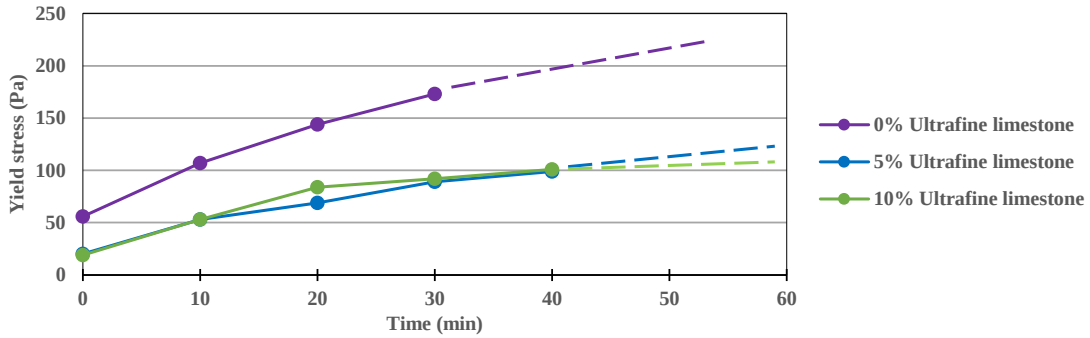

Figure 6.15: Influence of partial GGBS replacement by ultrafine limestone at Water/(GGBS+Limestone)=0.40 and 8%Na_2CO_3 (200g/l)

The phosphonate seems to be less effective in the presence of the ultrafine limestone (Figure 6.16). This phenomenon may be attributed to an eventual acceleration of the slag dissolution due to the seeding effect of the ultrafine limestone particles. The dosage of the phosphonate should be tuned and/or a more effective retarder should be considered in the case of the limestone-blended GGBS mixes.

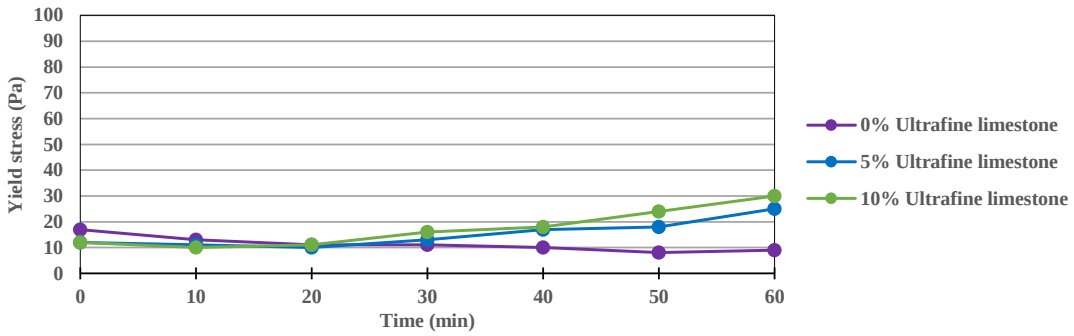

*Figure 6.16: Influence of partial GGBS replacement by ultrafine limestone on yield stress evolution at Water/(GGBS+Limestone)=0.40 and 8%Na_2CO_3 (200g/l) in the presence of 0.1% 4Na*HEDP*

In the above study, the mixes are compared at the same Water/(GGBS+limestone) ratio. Since the presence of the limestone leads to a significant decrease of the initial yield stress, one is tempted to decrease the amount of water, and dose the latter relative to the active binder alone (GGBS). In Figure 6.17 the evolution of the yield stress in both cases is presented. It can be seen that the initial yield stress for Water/(GGBS+Limestone) = 0.36 (Water/GGBS = 0.40) is almost the same than that corresponding to Water/GGBS= 0.40 without limestone substitution. Then, initially, there is almost no water demand of the limestone. Yet, the evolution of the yield stress for the limestone blended mixes is higher, leading to rapid loss of rheology. Further investigation is needed to determine effective retarding admixtures for the limestone-blended mixes.

Another way to compensate for the rapid loss of rheology in the presence of limestone is to decrease the concentration of Na_2CO_3. Yet, this may lead to loss of the eventual gain of strength resulting from the seeding effect of the limestone. The best option should thus be improvement of the rheology.

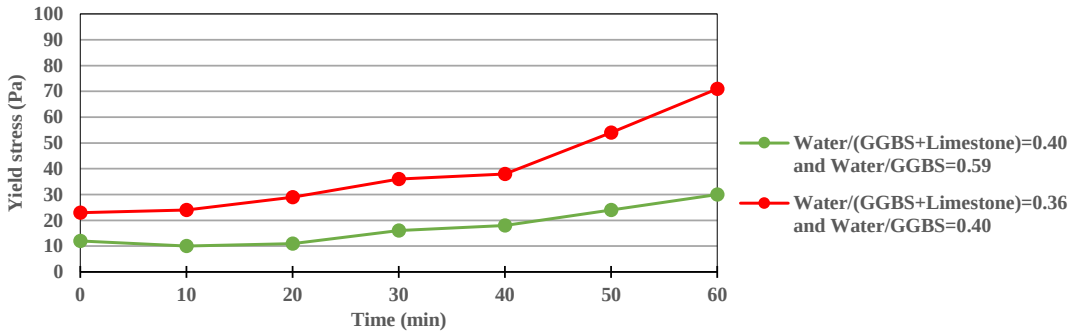

*Figure 6.17: Influence of 10% GGBS replacement by ultrafine limestone at Water/(GGBS+Limestone)=0.40 or 0.36 and 8%Na_2CO_3 to GGBS or to GGBS+Limestone to keep concentration of 200g/l with 0.1% 4Na*HEDP*

6.3.2 Compressive strength development

The mixes with Ultrafine limestone substitution were considered at a constant Water/GGBS ratio. In addition, the phosphonate percentage relative to GGBS and activator aqueous concentration were kept constant. This implies that by increasing the replacement level of GGBS by limestone, the total water in the mortar is lower as well as the amount of sodium carbonate. The compositions of tested mortar mixes are reported Table 12.

Table 12: Composition of the tested mortar samples with partial GGBS replacement by ultrafine limestone, in g per 1350g of normalized sand.

	GGBS	***Ultrafine Limestone***	***Na_2CO_3***	***4Na*HEDP***	***Water***	***Water/ GGBS***	***Water/ (GGBS+ Limestone)***	***Na_2CO_3 concentration, g/l***
Reference	450	0	36	0.45	180	0.40	0.40	200
1%	445.5	4.5	35.6	0.44	178.2	0.40	0.396	200
5%	427.5	22.5	34.2	0.43	171	0.40	0.38	200
10%	405	45	32.4	0.41	162	0.40	0.36	200

The results presented in Figure 6.18 shows that partial replacement of the total binder (GGBS and Na_2CO_3) by ultrafine limestone coupled with lower amount of water in the system leads to an improvement of the strength at all ages. The improvement at 2 days is significant with 10% replacement level. The strength at 1 day remains low, in contrast with clinker substitution. On the other hand, there is strength improvement also at late ages. This may reflect the fact that the acceleration of hydration is mainly due to seeding effects and improved distribution of the hydration products.

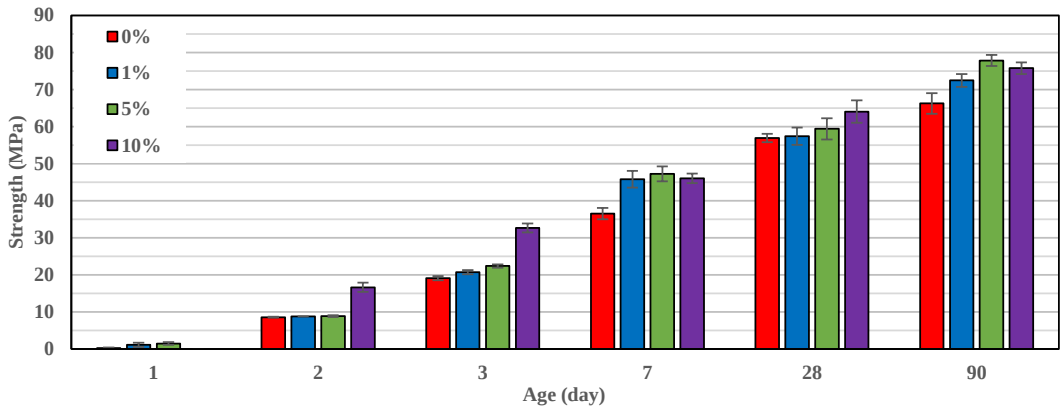

Figure 6.18: Influence of GGBS replacement by ultrafine limestone at different percentage on compressive strength evolution at Water/GGBS=0.40 and 8% Na_2CO_3 to GGBS (200 g/l)

6.3.3 Dry curing in the presence of the ultrafine limestone

The most intriguing aspect of this additive turned out to be its behaviour when cured at low relative humidity. In the previous chapters it was shown that these binders are characterised by a significant decrease in strength when cured under dry conditions (RH=50%). Increasing the period of humid pre-curing permitted a reasonable strength development. However from a practical and economical point of view, increasing the pre-curing period up to 7-28 days is not always possible. In addition, even 3 days of pre-curing, followed by dry conditions (RH=50%), led to a loss of 40-45% of the compressive strength compared to humid conditions throughout. It was also found that there is a correlation between water loss and the decrease of the strength evolution. This was attributed to the slowing of hydration due to less accessible water for unreacted binder grains and eventual cracking due to drying shrinkage. A longer curing period leads to a more advanced reaction and less porosity, which results in lower water loss and better hydration.

The same tests as those described previously were performed in the case of partial slag replacement by 5% ultrafine limestone. The strength evolution under dry conditions (RH=50%) following different durations of pre-curing under humid conditions is considered. The water and all the other additives were added to GGBS weight (see Table 12). The results are reported in Figure 6.19. They show that a decrease of the compressive strength is obtained in all the cases. However the strength loss remains low, even when curing under dry conditions starts after only 3 days.

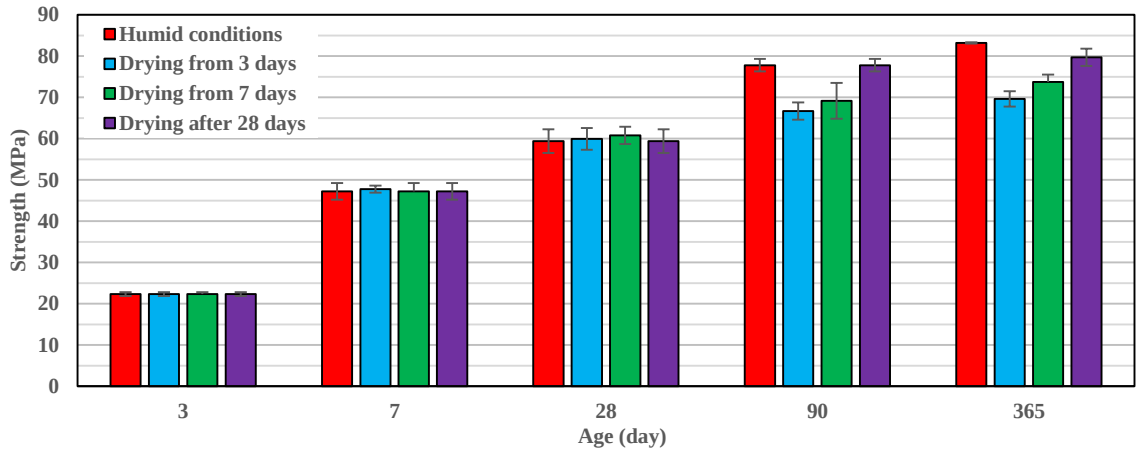

*Figure 6.19: Influence of humidity storage condition (drying at 50% RH) on compressive strength evolution of 95%GGBS and 5% Ultrafine limestone at 8% Na_2CO_3 and 0.1% 4Na*HEDP to GGSB weight at Water/GGBS=0.40*

In Figure 6.20 a comparison is made between the plain GGBS based mix and that in which 5% of GGBS is replaced by ultrafine limestone. The positive effect of the limestone is

clear. A significant improvement can be observed even in the case of the most severe conditions (pre-curing under humid conditions only over the first 3 days). In this case, after 1 year for the plain GGBS, the loss is about 40% when dry curing starts after 3 days compared to humid conditions throughout. In the case of the ultrafine limestone blended mix, the loss is only 16%. In addition, the absolute strength values of mixes with limestone are significantly higher (in particular beyond 90 days) compared to their equivalent mix of plain GGBS.

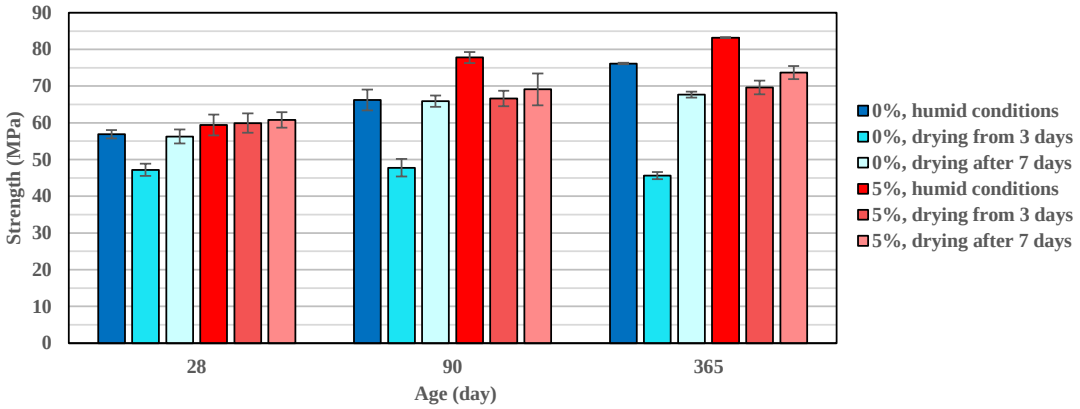

Figure 6.20: Comparison of strength evolution between mortars based on plain GGBS and those with replacement by 5% ultrafine limestone stored at RH=50% beyond different ages during which they are cured in closed plastic bags.

The negative impact of eventual dry curing conditions can be compensated in great part by partial substitution with ultrafine limestone. This also, by the way, leads to a lower CO_2 footprint due to a lower Na_2CO_3 and slag amount.

As expected, the amount of water loss increases when the duration of pre-curing under humid conditions decreases (Figure 6.21). A direct correlation between water loss and decrease in strength can be observed.

A significant decrease of water loss at all ages, in particular under severe drying conditions (from 3 days), with an increase of the ultrafine limestone substitution level can be observed. This may explain the significantly lower decrease in compressive strength loss in this case. With increasing duration of humid pre-curing, the water loss values become less impacted by the presence of limestone, similar to the compressive strength loss. This relatively high amount of water lost even after 28 days of humid pre-curing (almost 20% of initial water was lost over the period between 28 and 365 days) confirms once again the fact that a much lower W/B ratio is required for the hydration of such binders. However, this water may turn out to be useful for further hydration (if not lost), since almost 60-70% of the slag is still unreacted after 28 days.

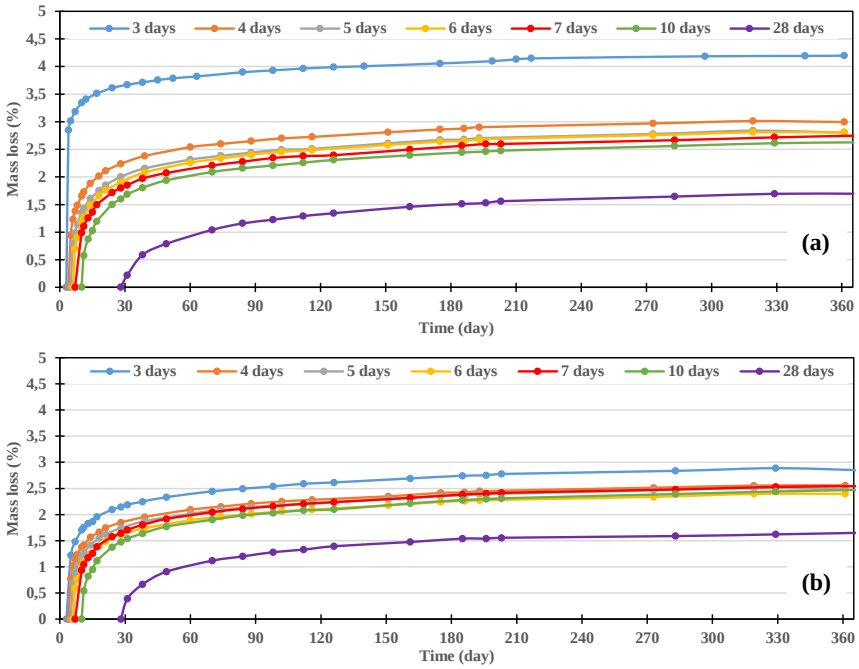

Figure 6.21: The weight loss of samples which undergo 50% RH storage after various durations of pre-curing in humid conditions, without (a) and with (b) 5% GGBS replacement by ultrafine limestone.

The results of the total shrinkage (Figure 6.22) are also correlated with water loss (drying shrinkage) and hydration process (autogenous shrinkage). The ultimate (1 year) shrinkage values are almost independent of the presence of the limestone. This result can be explained by a better water retention and seeding effect of the limestone, the hydration process is more advanced. At the same time, the lower amount of the reactive binder (here GGBS) leads to a lower shrinkage. Both effects might compensate for each other leading to a constant long term total shrinkage.

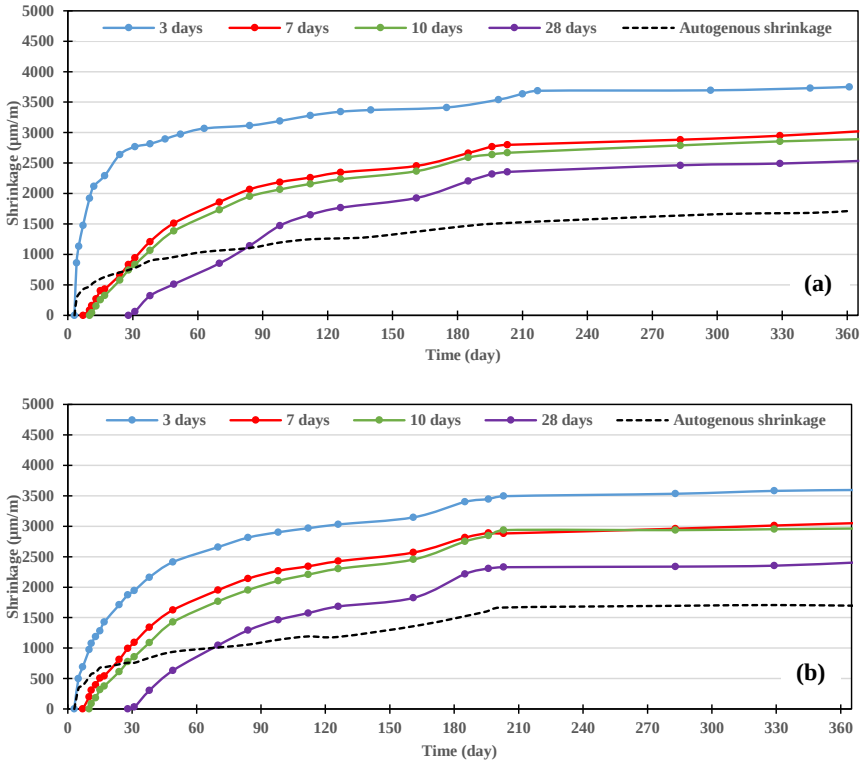

Figure 6.22: Comparison of the total shrinkage of the samples cured under 50% RH after various durations of humid pre-curing, without (a) and with (b) 5% GGBS replacement by ultrafine limestone

6.3.4 Effect of the presence of the ultrafine limestone in the case of low temperature curing

Previously it was observed that decreasing the temperature has a significant negative influence on compressive strength evolution. At the same time, in the case of drying, a longer period of humid storage is required. It means that in case of lower curing temperature, the addition of an accelerator is highly recommended, to reduce humid storage time.

Regarding the acceleration effect of clinker, it was observed that increasing its fineness leads to a higher compressive strength at early age. On the other hand the long term strength is degraded when clinker fineness increases. A clinker with 2600 cm^2/g Blaine fineness was used as a compromise regarding the two opposing effects. The eventual contribution of ultrafine limestone substitution is considered here. The tested formulations are reported in Table 13. The samples were stored in moulds for different periods: 6, 24 or 48 hours. The samples were demoulded at the appropriate ages and placed in the climatic chamber at 50% relative humidity. In all cases the curing temperature was fixed at 15°C (storage of materials and further sample storage).

Table 13: Composition of the tested mortars based on GGBS with clinker and with partial replacement by ultrafine limestone, in g for 1350 g of normalized sand.

Sample	GGBS	Ultrafine limestone	Clinker	Na_2CO_3	Water	4Na*HEDP	Water/ GGBS+Clinker	W/GGBS+ Clinker+ Limestone
Without Limestone	402	-	21	27	189	0.42	0.447	0.447
With Limestone	390	13	20	27	189	0.42	0.461	0.447

The influence of partial replacement by ultrafine limestone on compressive strength evolution of samples stored at 15°C and that started drying at different ages is presented in Figure 6.23. With or without limestone, as was the case previously, increasing the duration of humid pre-curing leads to a significant improvement in compressive strength at all ages. For 48 h pre-curing, the strength values at 2 months are almost the same compared to the reference mix for which the storage was performed in plastic bags. Regarding the influence of ultrafine limestone, a high positive effect can be observed. Even though the replacement is quite low (3%), a significant improvement in strength was achieved (+23% in case of plastic bags storage). In the presence of the limestone a higher hydration rate (strength evolution) was maintained during drying. This is especially remarkable in the case of very short humid pre-curing duration (6 hours). Without ultrafine limestone, almost no further evolution beyond 10 days was observed. In this case drying is responsible for about a 43% loss in compressive strength after 2 months compared to samples cured in plastic bags. Nevertheless, even with ultrafine limestone addition,

about a 30% loss in strength was observed in the case of short duration curing storage. In the case of short term pre-curing of 6 h, only a 3% ultrafine limestone leads to a 50% gain in strength.

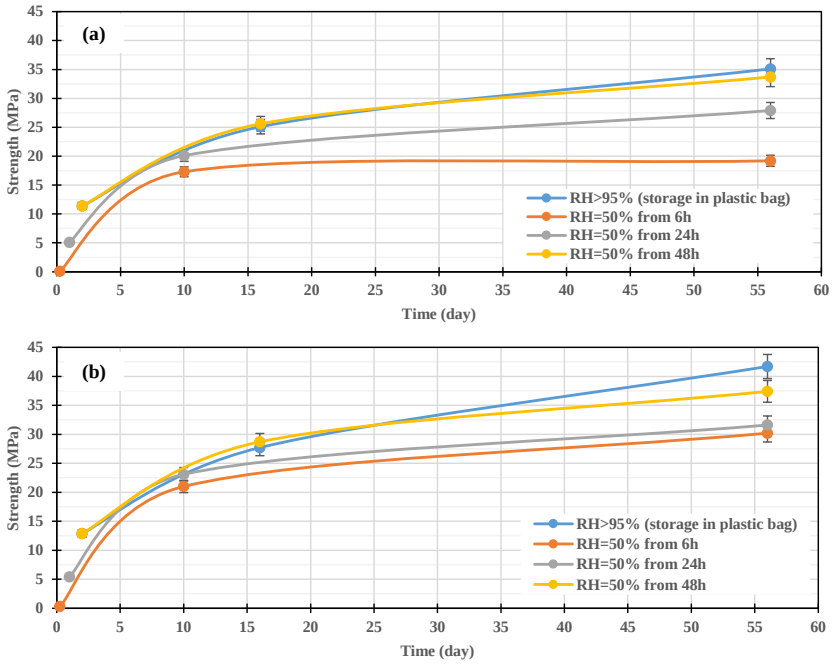

Figure 6.23: Comparison of compressive strength evolution of 95% GGBS + 5% Clinker 2600 cm^2/g without (a) or with (b) partial replacement with Ultrafine Limestone stored at 15°C

The impact of the limestone on the time evolution of water loss is reported in Figure 6.24. Slightly lower values can be observed with ultrafine limestone substitution. Longer humid pre-curing leads to a lower amount water loss, similar to previous results. In the case of drying from 6 hours onward, after 56 days of hardening the mass loss is 4.8% and 4.6% without or with limestone respectively. This mass loss represents about 50.5% and 48.4% of the mixing water, which cannot explain the significant difference in the compressive strength values. This indicates that, regarding the impact of the strength, the seeding effect of ultrafine limestone particles is probably much more important than the capacity for water retention.

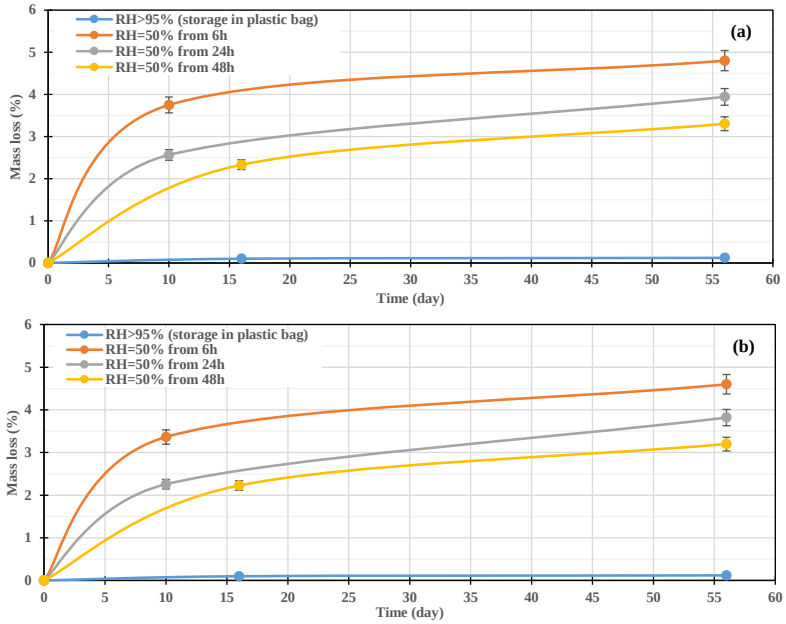

Figure 6.24: Comparison of the evolution of mass loss over time of the samples without (a) or with (b) ultrafine limestone stored at 15°C and starting drying at different ages.

6.4 Crystalline hydration phases

The results of the evolution of the XRD patterns over time are reported in Figure 6.25. As it can be observed, a faster Gaylussite decomposition occurs with ultrafine limestone substitution. This might be related, as suggested prior, to an increase in the rate of calcium leaching into solution, leading to a faster calcite formation and consequently CO_3^{2-} consumption. The supplementary calcium might come from both slag and possible limestone dissolution due to its very high fineness. Due to the possible seeding effect of the ultrafine limestone, a more homogenous hydration in bulk might take place leading to a higher slag dissolution rate. Nevertheless only a very slight difference can be observed. Moreover, in the case of ultrafine limestone, a lower intensity of vaterite peaks can be observed at longer term. No significant changes regarding other hydrates was observed.

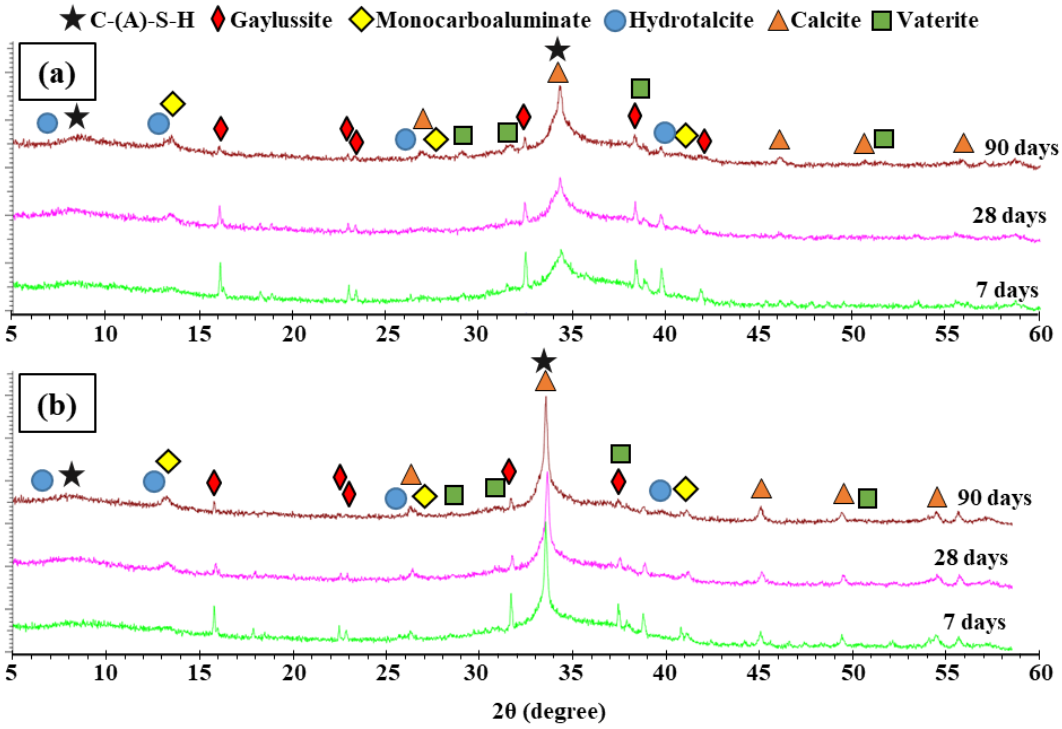

Figure 6.25: XRD patterns of GGBS hydration without (a) and with (b) 5% replacement by ultrafine limestone. Water/GGBS= 0.40 and 8% Na_2CO_3

Conclusions

The obtained results showed that partial dilution of GGBS by limestone can provide not only additional environmental and economical benefits, but also improve the properties of the product. Partial substitution with limestone leads, in general, to improvements in the rheology, which can be an important factor for many applications. This may allow using lower amounts of water, which is beneficial for mechanical and durability properties. These results indicate that this is mostly due to the seeding effect of the limestone particles and consequently a higher rate of binder hydration. The effect of such a supplementary material is strongly dependent on its dosage and fineness. Results with the addition of ultrafine limestone also showed a positive effect in the case of unfavourable storage conditions. Lower loss of strength in the case of drying was observed.

In perspective, increasing the active binder reactivity (in particular though an increase of slag fineness) should lead to obtaining a high performance binder with higher levels of limestone substitution. This requires a significant amount of complimentary studies.

Chapter 7 Improving early strength with an alumina source?

Introduction

As discussed throughout this document the two main drawbacks of Na_2CO_3 activated binders are the lack of sufficient open time and the delay in early age strength development. It was possible to extend the open time up to several hours using a phosphonate based retarder, and early age strength could be improved through a low level substitution with clinker. Yet, clinker leads to an increase of the CO_2 footprint of the binder, and in addition it has a low availability on the market. Other types of hardening accelerators for such binders are then desired. Several OPC-based binders have been tested in the literature; generally in the case other types of activation (mostly Na-silicate). In the present investigation, the case of alumina-based accelerators is considered. Actually, the issue of the presence of alumina in solution in the case of GGBS-based binders goes beyond the objectives considered here regarding how to improve the early strength development of Na_2CO_3 based binders. Indeed, the most widespread utilisation of GGBS is in association with OPC to make up standardized cements such as CEMII/III. The long term properties, such as durability, of concretes made with such cements are enhanced compared to those made with plain OPC. The main drawback of such mixes is similarly the early age strength. When associated with OPC, GGBS acts mainly as a filler at early age, despite the fact that the required pH level (>12) for slag dissolution is readily reached (Kocaba, 2009). The interference with GGBS hydration of the different species released through this association with OPC is still a matter of debate in the literature. For instance, a recent study performed on a single grain showed that the presence of soluble alumina has severe hindering effects on slag dissolution (Suraneni et al., 2016). Even at a high pH level no dissolution and precipitation process was observed in the presence of aluminum in solution. Other studies also pointed out the presence of soluble alumina to explain the retardation of slag hydration, for instance in the case of slag-metakaolin systems (Bernal et al., 2011). Early studies by Glukhovsky (Glukhovsky and Pahomov, 1978) also reported this effect. Actually, because of this phenomenon, using the classical OPC setting accelerator like $NaAlO_2$ in the case of the OPC/GGBS binders (with very high GGBS content) was not recommended. Why the slag is not highly dissolved at early age in the case of GGBS/OPC mixes despite the high pH level remains unexplained. Hence, previously it has been supposed that it is related to the formation of a passivation layer on its surface, due to the high amount of leached calcium (nano-size or amorphous calcite precipitation). However,

other factors might also be present. One possible reason could be that the aluminum is quickly released by the C_3A in the clinker. In this investigation, the impact of the presence of different sources of alumina, with different solubility, on the hydration of Na_2CO_3 activated GGBS is considered. In addition, the case of NaOH activation is considered for comparison.

7.1 Materials and Methods

All the additives were added in powder form in the dry mix. The NaOH was a pure grade (VWR chemicals, ≥99%). Two alumina sources were considered: a highly soluble Sodium aluminate ($NaAlO_2$, technical, Sigma Aldrich) and a Halloysite clay. Halloysite is a nanotube shaped silico-aluminate clay, with 30-70 nm diameter and 1-3 nm length (Figure 7.1). It was added into the dry mixture after 2h of drying at 120°C (non-calcined Halloysite), or after calcination at 750°C for 2h (calcined Halloysite).

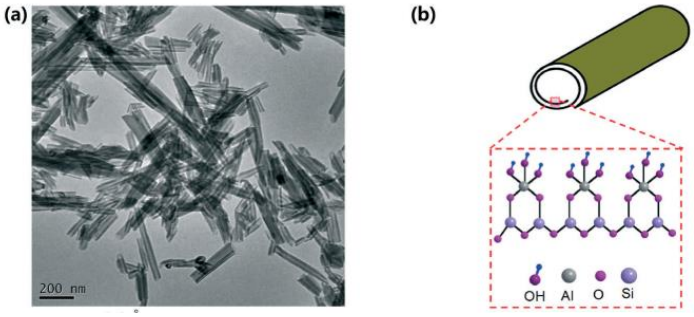

Figure 7.1: TEM images of Halloysite nano-tubes (a) and the representation of its crystalline structure (b) (after Yu et al., 2016).

EDX analysis confirmed the main silico-aluminate composition of the clay: 44% SiO_2 and 56% Al_2O_3. XRD analysis (Figure 7.2) of the clay samples showed the presence of Halloysite with two different distances between the sheets (11 Å and 7 Å). Some impurities consisting of quartz, gibbsite and kaolinite are present (Figure 7.2). Such impurities are always associated with Halloysite even without any special additional treatment.

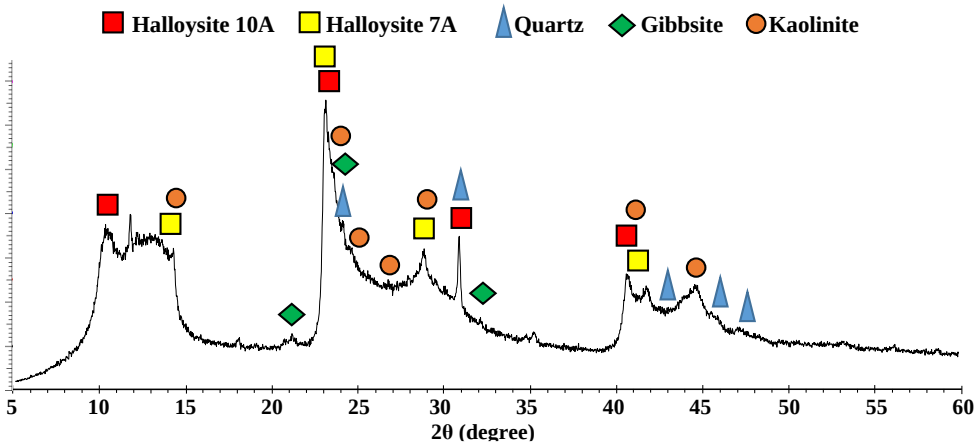

Figure 7.2: XRD pattern of Halloysite used in the present study

The change of the Al coordination of the Halloysite following calcination was characterized using ^{27}Al MAS NMR (see below) (Figure 7.3). Similarly to kaolin/metakaolin, Al in the non-calcined state is mainly in octahedral coordination (indicating that it is mainly hydroxylated). Upon calcination, lower coordination levels (IV and V) appear indicating that partial dehydroxylation and probably degradation of the tube-like structure has taken place.

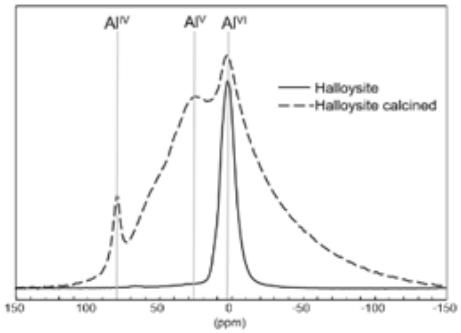

Figure 7.3: ^{27}Al MAS NMR spectra of the non-calcined and calcined Halloysite

^{27}Al high-resolution NMR experiments were carried out on a Bruker AVANCE instrument (principal field 17.6 T–750 MHz) equipped with high speed MAS probe heads (spinning rate of 30 kHz). The 1D MAS spectra have been acquired after a single short pulse ($\pi/10$) ensuring a quantitative excitation of ^{27}Al central transition. Almost 10000 scans were accumulated with a 1s recycling delay. Chemical shifts were referenced relative to a $Al(NO_3)_3$ 1 M solution.

7.2 Impact of the aluminium source on the compressive strength evolution

7.2.1 Na_2CO_3 activation

The compressive strength evolution in the case of Halloysite and calcined Halloysite addition with Na_2CO_3 activation (10 wt. %) is presented in Figure 7.4. The water/binder ratio was fixed at 0.40 for all the mixes. Addition of low amount (< 1%) of low solubility Halloysite (non-calcined) led to a small impact on the strength at all terms. Increasing its dosage to 2.5% leads to a slight decrease of the strength up to 28 days. At longer terms (90 days) the strength is improved.

In the case of more soluble Halloysite (calcined), the strength is slightly reduced at early age. This delay in strength gain may be attributed in particular to the alumina in solution provided by the clay as discussed below. At longer terms (at 90 days) the strength is significantly

improved. The eventual seeding effects of the clay particles may lead to a more compact structure at late ages and thus an improvement of the strength.

Addition of a highly soluble alumina source ($NaAlO_2$) led to almost complete cessation of the hardening process. The strength values were too low (up to 28 days) to be determined and are then not reported here. The origin of this phenomenon will be discussed in details below.

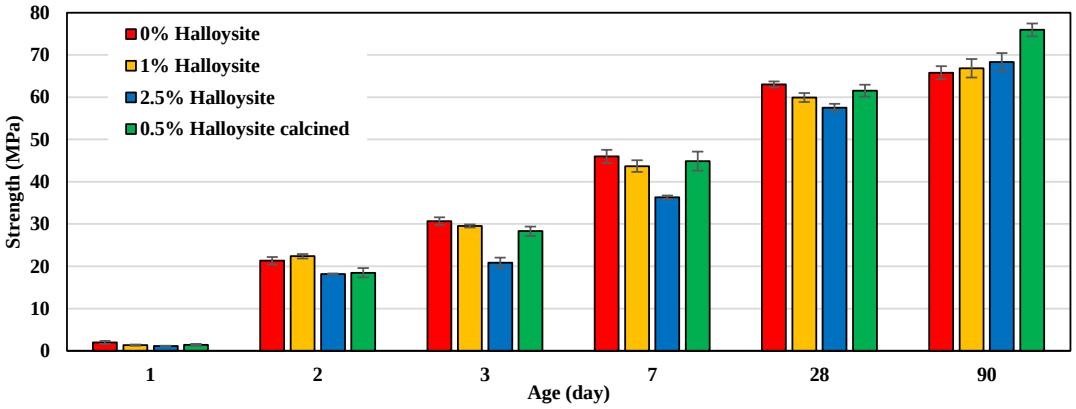

Figure 7.4: Impact of Halloysite and calcined Halloysite on the compressive strength development in the case of 10%Na_2CO_3 activated GGBS at W/B=0.40.

7.2.2 Comparison with the case of NaOH activation

Only one dosage of NaOH was considered (8 wt.%) and the water/binder ratio was fixed at 0.45 for all samples. Note that more water is needed compared to the case of Na_2CO_3 activation to get an appropriate rheology.

The results for the strength development for the Halloysite blended mixes are reported in Figure 7.5. In the case of the plain mix, there is a rapid strength gain at early age while at long term the strength remains modest. This is in contrast with Na_2CO_3 activation. This has already been reported in the literature when comparing for instance NaOH with sodium silicate activation (Shi. et al., 2006; Gebregziabiher et al., 2015). This was attributed to the fast precipitation of hydration products on the slag surface hindering its dissolution. In the case of sodium silicate or Na_2CO_3 activation the presence of seeds made up by early hydration products will lead to a more compact microstructure and higher long term strength.

Addition of a low or moderately soluble aluminate source (Halloysite, calcined or not) leads to an improvement of the strength at all terms. The positive impact is higher when the Halloysite is calcined. The strength improvement may be attributed to two linked phenomena:

(i) *Seeding effects of the clay particles*: the surface charge of the clay particles is expected to be highly negative under these highly basic conditions. The Ca^{2+} ions dissolved from the slag will then be attracted and adsorb on the surface

of the clay particles. The latter should then play the role of framework for heterogeneous nucleation of hydration products combining these Ca^{2+} and aluminates and/or silicates dissolved from the slag (or the clay).

(ii) *Reactivity of the clay*: Under these high pH conditions the solubility of the clay may turn out to be significant, in particular the calcined grade. The silicates and the aluminates dissolved from the clay may combine with the Ca^{2+} ions dissolved from the slag to precipitate hydration products in solution that will play the role of nucleation seeds.

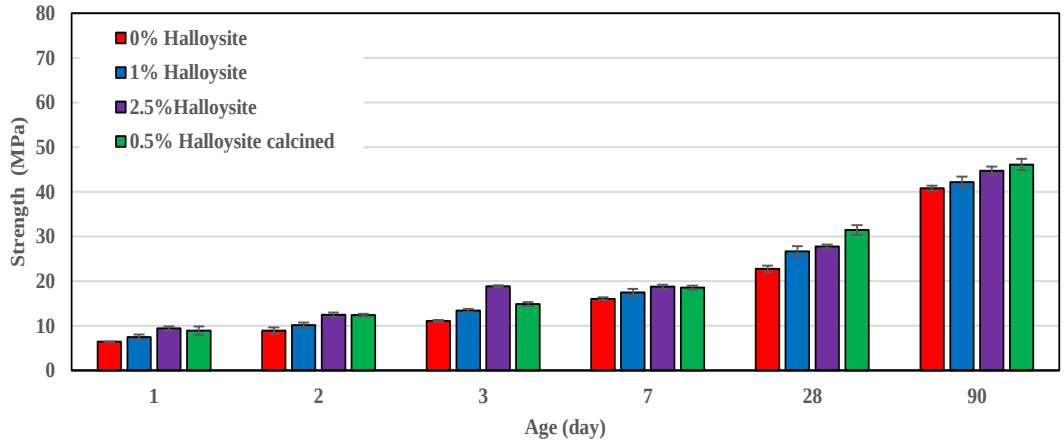

Figure 7.5: Impact of calcined and non-calcined Halloysite on compressive strength development of GGBS at W/B=0.45 and 8% NaOH

Addition of a highly soluble alumina source ($NaAlO_2$) leads to a more significant improvement of the strength at all terms (Figure 7.6). This is in contrast with the case of Na_2CO_3 activation for which the hydration process was almost completely suppressed. The increase of the strength is almost twofold up to 28 days upon the addition of 2% of $NaAlO_2$. The positive effect on strength can be observed even with only a 0.1% dosage of the alumina additive. Strength improvement cannot be attributed to an eventual increase of the alkalinity with $NaAlO_2$ addition (Hashim et al., 2015). The interpretation of these results will be discussed further by considering the impact on the hydration products.

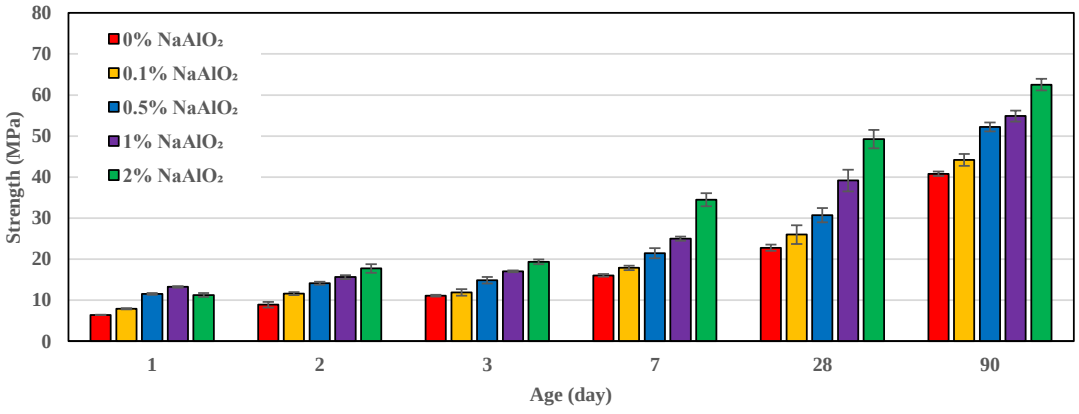

Figure 7.6: Impact of $NaAlO_2$ dosage on compressive strength development of GGBS activated with 8% NaOH at W/B=0.45

7.3 Impact of the aluminium source on hydration kinetics

7.3.1 Na_2CO_3 activation

The microcalorimetry results for the Na_2CO_3 activated mixes with non calcined Halloysite addition are presented in Figure 7.7. At low Halloysite content (in particular at 1%) the hydration process is slightly delayed. The addition of high clay content (5%), leads to an acceleration of both two hydration peaks, including the peak corresponding to the precipitation of the carbonate-based products and the peak corresponding to C-(A)-S-H. As suggested above, this is probably related to an eventual seeding effect of the clay particles.

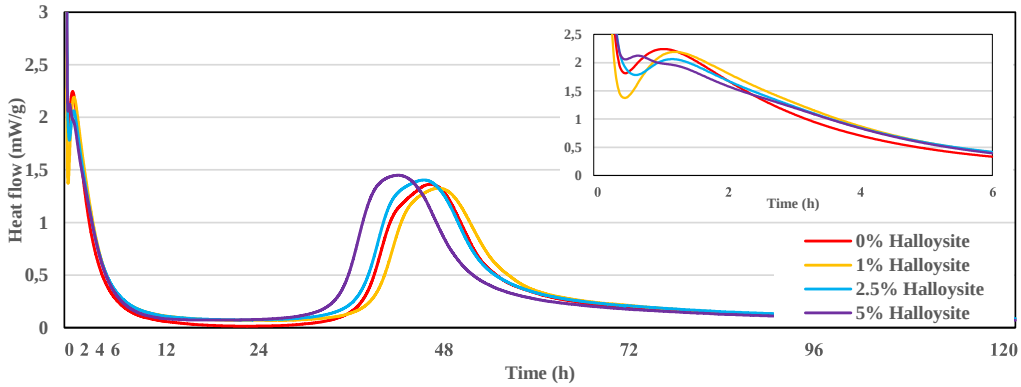

Figure 7.7: Hydration kinetics of GGBS activated with 10% Na_2CO_3 at W/B=0.40 with various amounts of Halloysite

Addition of calcined Halloysite leads to a higher amount of heat released at the very beginning of hydration (Figure 7.8) (first peak). This might be related to a higher amount of formed hydrates due to the supplementary alumina and silica in the system or the seeding effect. At longer term, a slight delay of the main hydration peak is observed (longer induction period). The increase in its width might indicate slower slag dissolution and hydrate precipitation.

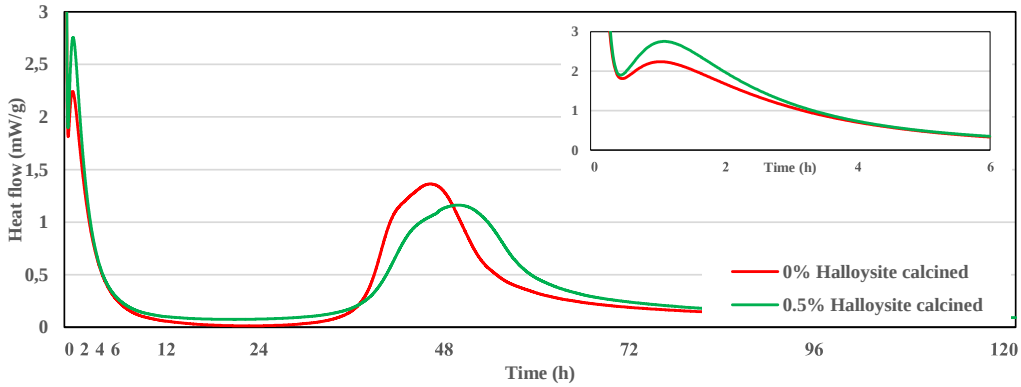

Figure 7.8: Hydration kinetics of 10% Na_2CO_3 activated GGBS with addition of calcined Halloysite (W/B=0.40)

The highly soluble alumina source ($NaAlO_2$) leads to a significant impact on the hydration of the Na_2CO_3 activated samples (Figure 7.9). Even at very low content (0.1%), only the first peak can be observed. In addition, a very small amount of heat is released. Measurements up to 6 days were performed (not reported here) and showed that no further hydration took place. For the plain samples, the first peak is associated with the Carbonate based hydrates. In the presence of Alumina, other Ca-Al based products such as Afm type phases may form (see below). The further lack of heat release indicates that the slag does not dissolve over time. The microcalorimetry results are in agreement with the above mechanical properties in which no measurable compressive strength was obtained.

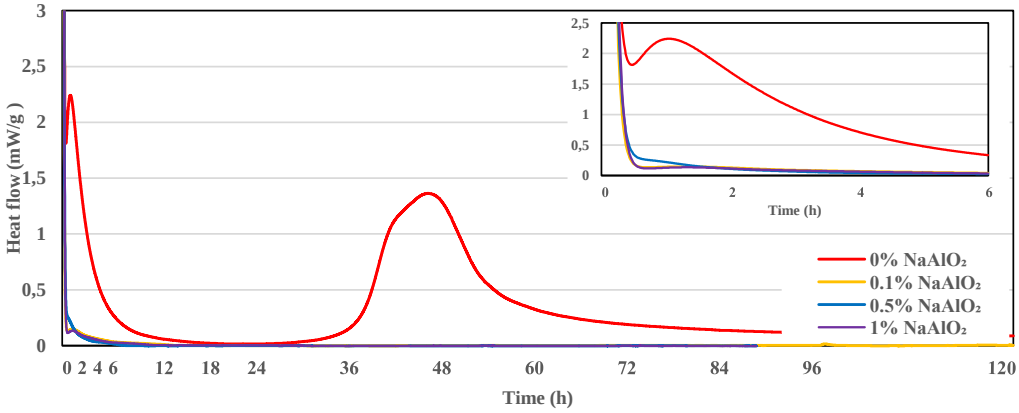

Figure 7.9: Hydration kinetics of GGBS activated with 10% Na_2CO_3 at W/B=0.40 with addition of various amounts of $NaAlO_2$

7.3.2 Comparison with NaOH activation

The heat release curves in the case of NaOH activation with different amounts of Halloysite are presented in Figure 7.10 and Figure 7.11. First it can be noticed that a *qualitatively* different behaviour compared to Na_2CO_3 activation can be observed. Only one main hydration peak appears with almost no induction period (starting from 30 minutes). These results are in agreement with those reported in the literature (Shi. et al., 2006; Haha et al., 2012; Yuan et al., 2014). This behaviour reflects a fast dissolution of the slag due to high pH and precipitation on the particles' surface. This may be in particular at the origin of the blockage of the strength development at late ages. Adding both types of Halloysite led to a slight acceleration and higher amount of heat released at early stage of hydration. This may be in particular attributed to the additional silicate and aluminates provided by the clay whose solubility should be significant under these high pH conditions. Seeding effects can also come into play. However the changes are quite moderate, and this correlates with the impact on compressive strength. Clay calcination seems to lead to a larger impact on hydration, although this should be confirmed at higher dosages.

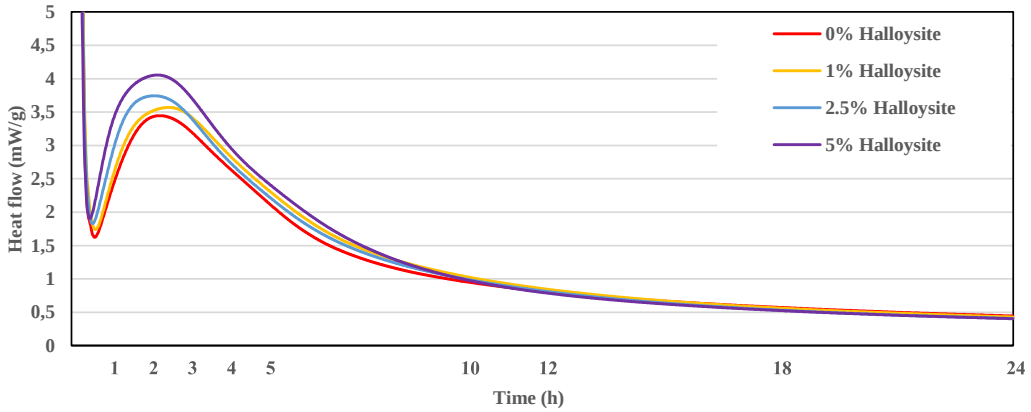

Figure 7.10: Hydration kinetics of GGBS with addition of Halloysite at W/B=0.45 and 8% NaOH

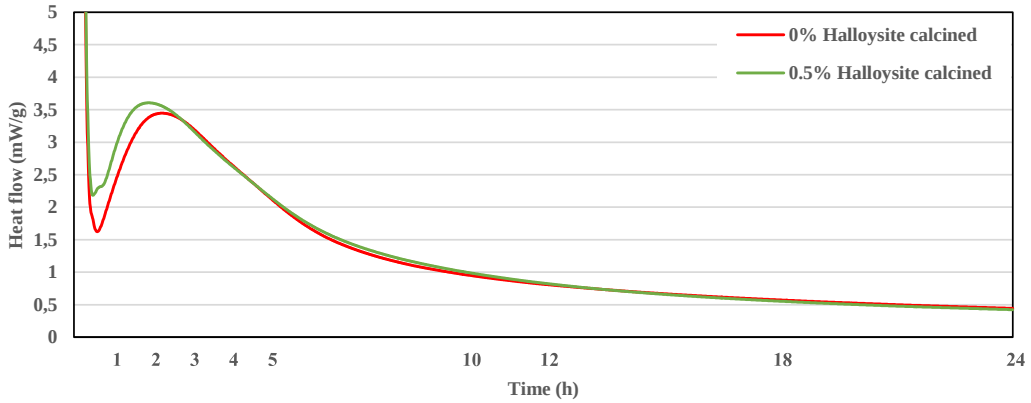

Figure 7.11: Hydration kinetics of GGBS with addition of calcined Halloysite at W/B=0.45 and 8% NaOH

Highly soluble alumina ($NaAlO_2$) leads to a significant increase of the induction period when the dosage is greater than 0.5% (Figure 7.12). With the addition of 1% and 2%, a small pre-peak can be observed at the beginning, followed by an induction period. In this case the hydration process seems to be split into two main steps as is often observed for common cementitious materials. An eventual delay of the slag dissolution due to the presence of alumina may allow for the formation of the first hydrates (related to the first small peak observed with 1% and 2% $NaAlO_2$) that may play the role of seeding for the strength-giving hydration products. This might lead to less precipitation on the slag surface. This will result in a greater degree of slag dissolution and higher long term compressive strength as shown above.

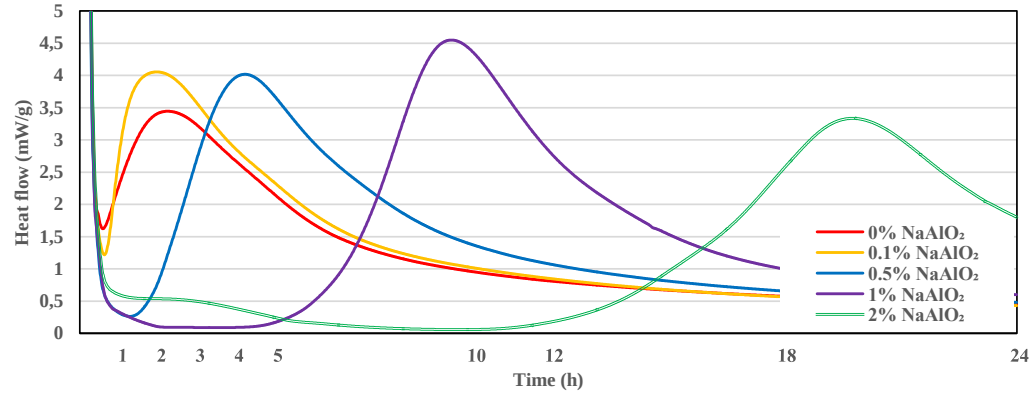

Figure 7.12: Hydration kinetics of GGBS with addition of $NaAlO_2$ at W/B=0.45 and 8% NaOH

A significant retardation effect of $NaAlO_2$ was confirmed through Vicat setting time measurements (Figure 7.13). Increasing the additive dosage up to 1% leads to an increase of the setting time. For further dosage increases, the setting time decreases. This may be attributed to an eventual increase in the amount of the first hydration products. It should be noted that the addition of $NaAlO_2$ will lead to an increase of the pH (through production of NaOH). This should then shorten the setting time. This indicates that it is rather the alumina that should be at the origin of the phenomenon.

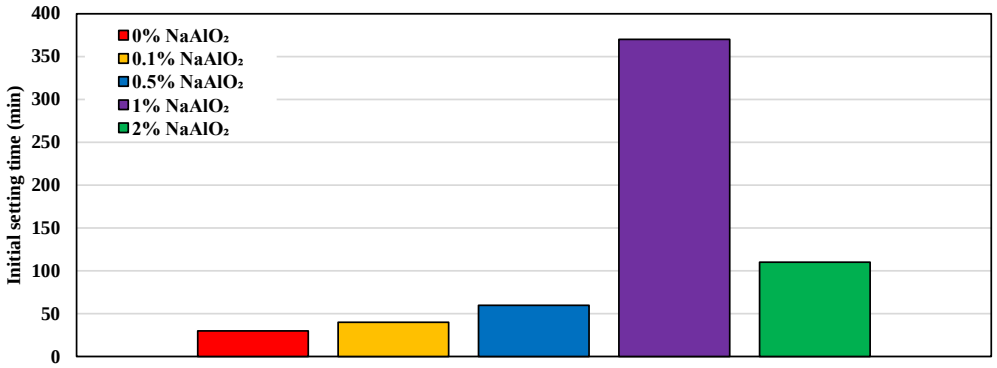

Figure 7.13: Impact of $NaAlO_2$ addition on the beginning of the setting of GGBS activated with 8% NaOH at W/B=0.45

7.4 Impact of the alumina source on the crystalline hydration products

7.4.1 Na_2CO_3 activation

For the reference mix, the main hydration product after 2 hours of hydration is the metastable phase Gaylussite (Figure 7.14a) as already discussed in previous chapters. Beyond 1 day, the intensity of the Gaylussite signal decreases and that of calcite increases. At the same time the peaks of the Afm-type phases (hydrotalcite, carboaluminates) increase.

In the presence of a low soluble alumina source (non calcined Halloysite) (Figure 7.14b), a higher amount of Gaylussite can be observed from the very beginning. Gaylussite seems to be more stable over time. The intensity of the Ca-carbonates peaks decreases which correlates with the increase in the amount of Gaylussite and its stability. This may be explained by an eventual hindering of slag dissolution due to the presence of alumina in solution (see further). Indeed this should lead to a lower concentration of Ca^{2+} in solution, less Ca-carbonate precipitation and then higher carbonate ion concentration in solution. Gaylussite will then be more stable and present in higher quantities due to a higher instantaneous Na/Ca ratio.

Upon the addition of a highly soluble alumina source (Figure 7.14c) only a very small amount of Gaylussite can be detected (contributing in particular to the small first peak shown in the microcalorimetry results above), without a significant evolution in time. It is suspected that the dissolution of the slag is strongly hindered in this case and only a small amount of Ca is released from the slag. Due to the high Na/Ca ratio in solution, only Gaylussite can be precipitated. There is then no way of removing carbonate ions from solution to destabilise Gaylussite and create NaOH as is the case for the plain mixes.

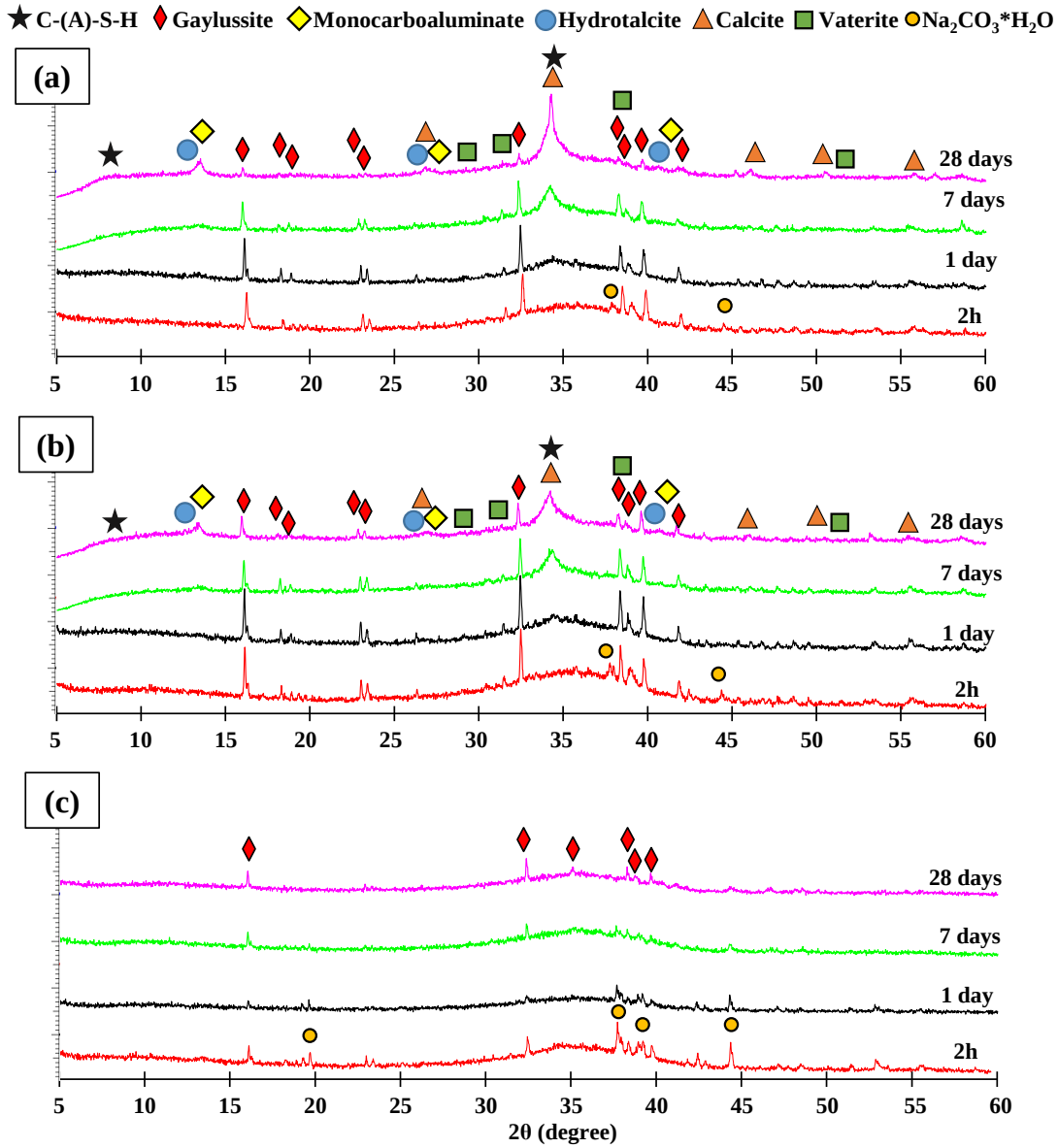

Figure 7.14: XRD patterns of pure GGBS (a), with 2.5% Halloysite (b) and 1% $NaAlO_2$ (c) addition at W/B=0.40 and 10% Na_2CO_3

7.4.2 Crystalline phases in the case of NaOH activation

In the case of slag activation by NaOH solution (Figure 7.15a), the XRD pattern evolution confirms a high rate of early hydration. The presence, even at 2h, of C-A-S-H, Strätlingite and

carboaluminates, which require Si/Al ions, indicates a high slag dissolution rate leading to early strength development. A slightly higher amount of hydrates, in particular at 28 days, can be observed in case of 2.5% Halloysite addition (Figure 7.15b), which correlates with a moderate strength increase. The increase of the hydration peaks is particularly significant with $NaAlO_2$ addition (Figure 7.15c). This is in agreement with the compressive strength results presented above, in which the values were doubled at 28 days.

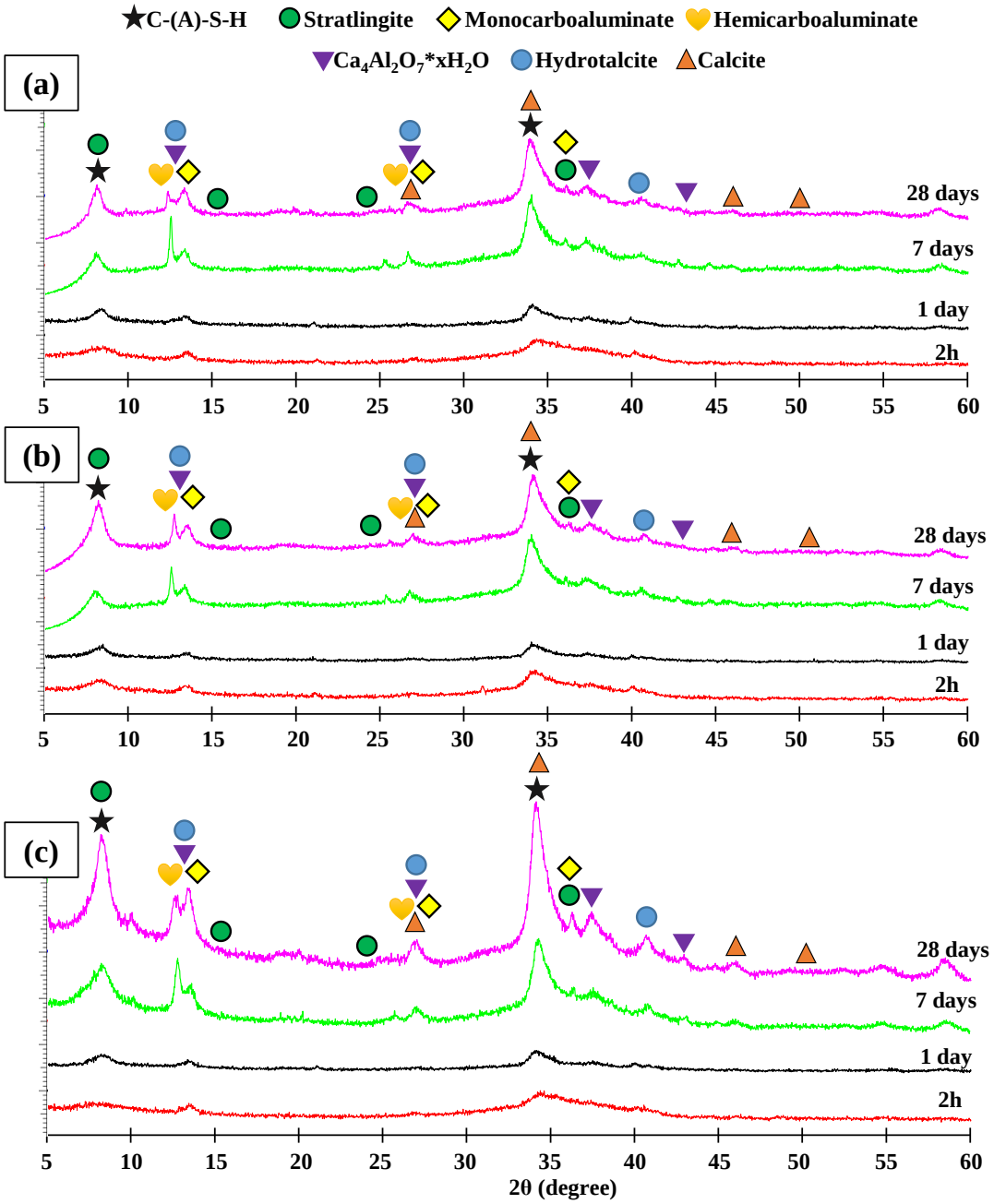

Figure 7.15: XRD patterns of pure GGBS (a) or with 2.5% Halloysite (b) and 1% $NaAlO_2$ (c) addition at W/B=0.45 and 8% NaOH

Although there is some delay in the precipitation of hydration products in the presence of alumina in solution, the slag dissolution and hydration seems to resume and are even enhanced beyond one day (Figure 7.15c). This is probably due to the particularly high pH level in this case

(due to both two additives NaOH and $NaAlO_2$). This is in contrast with Na_2CO_3 activation for which a high pH level can be obtained only upon sufficient slag dissolution (once Gaylussite is destabilized leading to NaOH formation).

7.5 ^{27}Al MAS NMR investigation

7.5.1 Impact of the alumina on the Al-based hydration products in the case of Na_2CO_3 activation

The evolution of the ^{27}Al NMR spectra up to 1 day is reported in Figure 1.16 for mixes without and with an aluminium source. It is known in the literature that the anhydrous GGBS contains mainly Al(IV) sites, but a small amount of Al(V) can also be observed (at 30-40 ppm). Only a small evolution of the Al spectra can be observed within the first day of hydration for the plain mix (Figure 7.16a). This is expected since the dominant phases within this hydration period are Gaylussite and calcium carbonate polymorphs, which do not contain Al. Although at 1 day the appearance of a small amount of Afm-type phases located within the A(VI) region (probably hydrotalcite) is noticeable. The addition of Halloysite (Figure 7.16b) does not lead to a noticeable change in the assemblage of the Al-based phases. Yet, the signal in the Afm region is blurred by that of Halloysite.

Addition of $NaAlO_2$ (Figure 7.16c) leads to a rapid formation (within the first 2 hours) of Afm type phases. There is almost no evolution of the signal beyond this time. A transient increase of the feature corresponding to the Al(V) sites can also be observed (also seen be others (L'Hôpital et al., 2015; Taylor et al., 2010) and probably related to C-A-S-H). From these results two possible origins of the hindering of hydration in the presence of this highly soluble alumina:

(i) Rapid formation of Afm-type phases through the precipitation of the dissolved alumina provided by the additive and the Ca/Mg dissolved from the slag. Since at early stage the Ca/Mg species are rather concentrated nearby the slag grain surface, the Afm precipitation should take place on the surface leading to the hindering of grain dissolution.

(ii) The dissolved alumina may adsorb on the silica rich grain surface and may be eventually incorporated within the silica network leading to its reinforcement (against dissolution). This phenomenon has been shown to occur in various situations, for instance when the issue of alkali-silica reaction and its hindrance in the presence of aluminum is considered (Chappex and Scrivener, 2012).

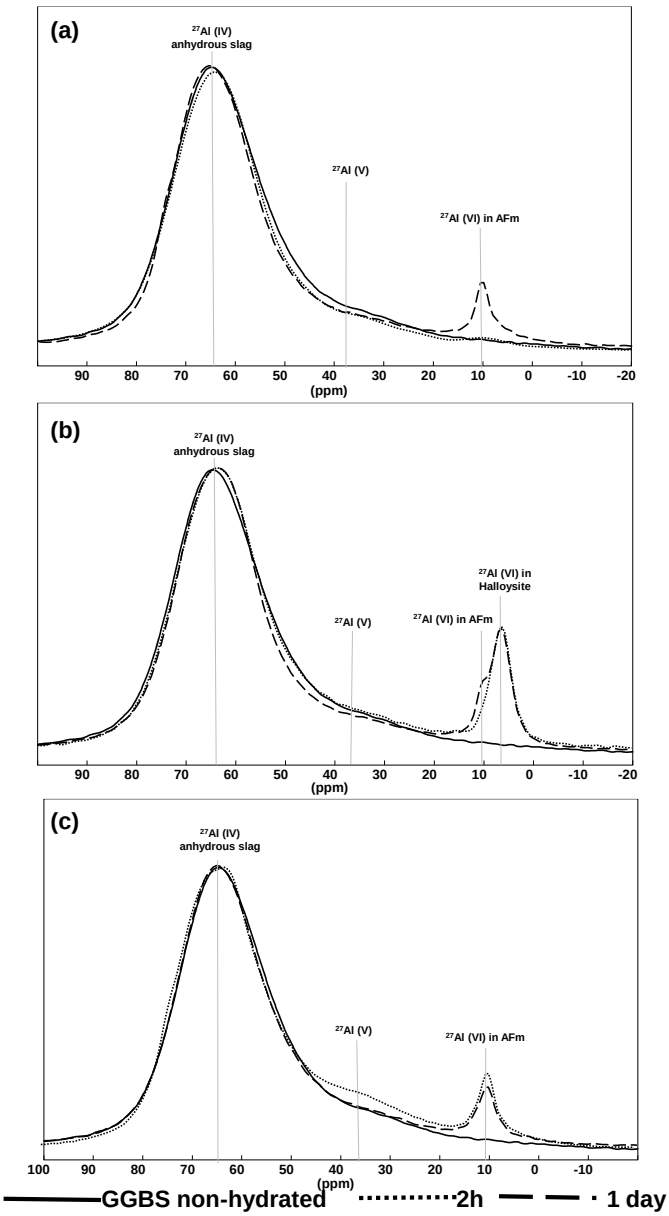

Figure 7.16: ^{27}Al MAS NMR spectra at 2 hours and 1 day for pure GGBS (a) or with addition of 2.5% Halloysite (b) and 1% $NaAlO_2$ (c) at W/B=0.40 and 10% Na_2CO_3

7.5.2 Case of NaOH activation

The evolution of the ^{27}Al MAS NMR spectra of the NaOH-activated samples between 2h and 1 day is reported in Figure 7.17. The peaks at around 74 ppm are assigned to Al substitution in C-S-H. It can be seen that even at 2 h C-A-S-H has already precipitated. This reflects in particular the short duration of the induction period in the case of this activation. Based the above XRD results, the Afm peak centred around 9 ppm may be comprised of, in this case, mainly hydrotalcite and the Al(VI) sites of Strätlingite (Kwan et al., 1995; Santacruz et al., 2015). Indeed Strätlingite is an Afm-type phase which contains both Al(IV) and Al(VI) sites in its structure.

By comparing the spectra in Figure 7.17a with those in Figure 7.17b it can be noticed that the addition of Halloysite leads to an acceleration in the rise of the Al(IV) (C-A-S-H) peak. We

also see that at the age of 1 day, the peak of Halloysite (located up-field) almost disappears (Figure 7.17b). This indicates that even without calcination this clay is reactive under the present pH conditions.

The addition of the highly soluble alumina source ($NaAlO_2$) leads to a significant acceleration of the AFm formation rate, but the C-A-S-H peak height at 2 hours is reduced (Figure 7.17c). This may be related to the delay in setting of these mixes in the presence of soluble alumina. At the age of 1 day, the C-A-S-H peak is much more pronounced in the presence of this additive. This is correlated with the higher strength gain beyond the induction period. The presence of a new feature within the Al(IV) region (at 61-62 ppm) that can be assigned to the Al(IV) sites of Strätlingite can be noticed. Its Al(VI) resonance is superimposed with those of the other Afm phases, such as hydrotalcite, and cannot be resolved.

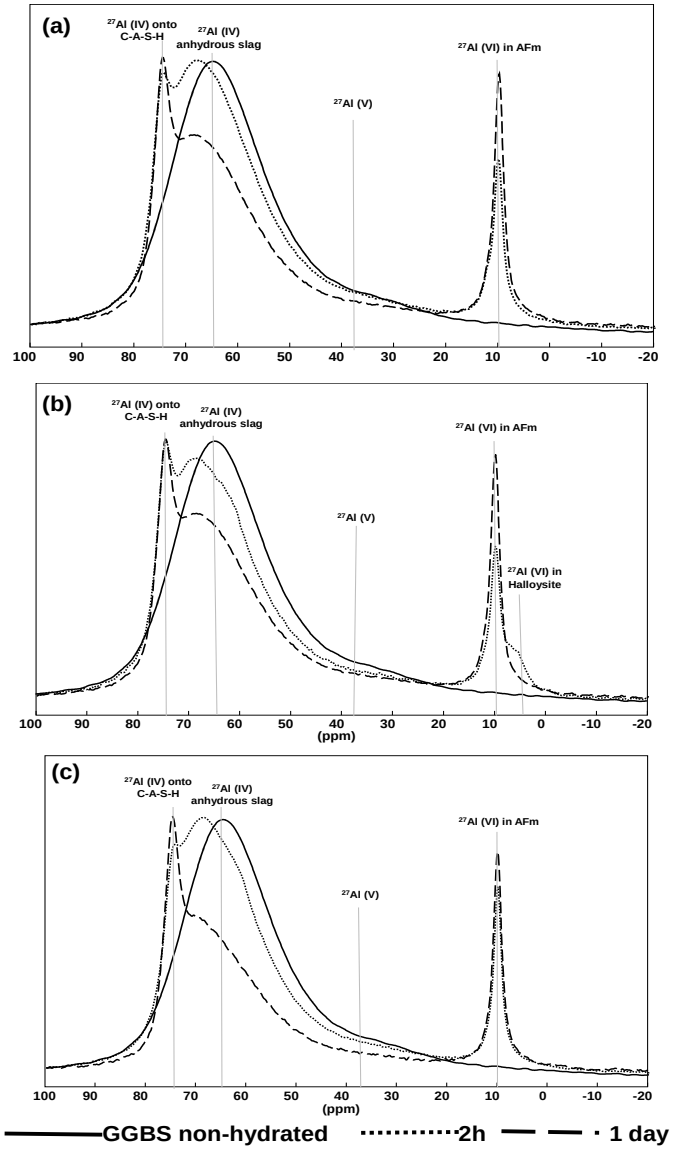

Figure 7.17: ^{27}Al MAS NMR spectra at 2 hours and 1 day for pure GGBS (a) or with addition of 2.5% Halloysite (b) and 1% $NaAlO_2$ (c) at W/B=0.45 and 8% NaOH

7.6 Impact of soluble alumina on the hydration products using TG/DTA analysis

7.6.1 Case of Na_2CO_3 activation

The TG/DTA analysis of the pastes at the age of 28 days is presented in Figure 7.18. The amount of Gaylussite/C-(A)-S-H (region up to 200°C) and different carboaluminates (150-300°C) hydrates decreases significantly with soluble alumina addition. Since no significant compressive strength was detected in this case, mainly dehydration/decomposition of calcium (sodium) carbonate based phases (Gaylussite/calcite) occurs. The TG/DTA analysis confirms the results obtained with the previous analytical techniques.

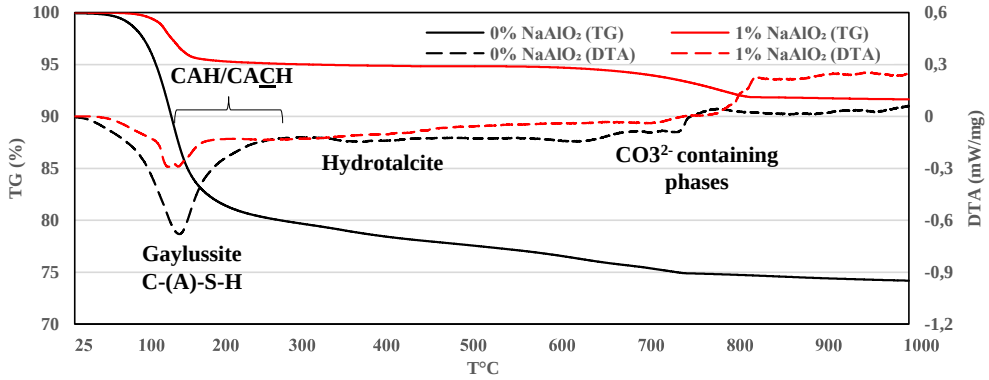

Figure 7.18: TG/DTA of Na_2CO_3 activated GGBS after 28 days with or without addition of $NaAlO_2$

7.6.2 Comparison with NaOH activation

In the case of NaOH activation (Figure 7.19), the thermograms are *qualitatively* different in the presence of $NaAlO_2$ compared to the plain mix. An increase in the weight loss can be observed indicating a higher degree of hydration. The DTA analysis shows that this is mostly due to a higher amount of C-(A)-S-H hydrates and also other carboaluminates. A slight shift to a higher temperature of the peak of C-S-H indicates a higher amount of Al incorporation to form C-A-S-H. Increasing the C-A-S-H amount can explain a higher compressive strength results.

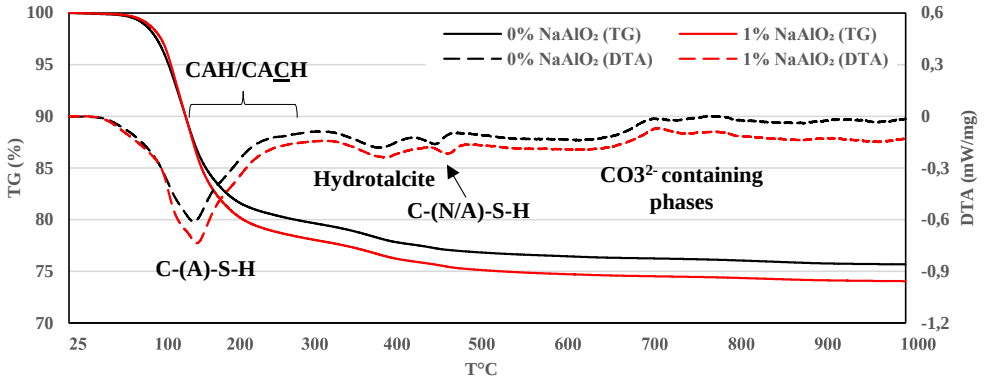

Figure 7.19: TG/DTA of NaOH activated GGBS after 28 days with or without addition of $NaAlO_2$

Conclusions

It was shown that when a slag is activated under quite high pH conditions (NaOH), the addition of an alumina source has a positive effect on hydration kinetics and strength development. When the alumina solubility is high, the additive plays the role of a setting retarder, leading to an improvement of the strength development (probably due to a precipitation of CAH type hydrates in bulk with calcium consumption, further playing a role of nucleation sites). In the case of moderate pH level mixes (Na_2CO_3 activation), moderately soluble alumina sources lead to the delay of early hydration, but strength gain at late ages. On the other hand, highly soluble alumina compounds lead to a complete cessation of the hydration process or to its extreme retardation.

In both cases the retardation effect was attributed to an eventual incorporation of aluminium within the silica network nearby the slag grain surface and therefore its strengthening, which should lead to an increase in the required pH level for slag dissolution. This should explain the significant difference between NaOH and Na_2CO_3 activation in the presence of soluble alumina. In the case of Na_2CO_3, a significant rise in the pH level occurs through CO_3^{2-} consummation by calcite formation and so in-situ NaOH formation. In the case where supplementary alumina hinders the slag dissolution and consequently calcium leaching, this process requires a much longer time. Therefore the influence of added alumina in this case has a much more significant retarding effect. In addition, early precipitation of Afm-type phases in the presence of the alumina source was detected using high resolution ^{27}Al NMR. This is suspected to take place on the grain surface, which can also be the cause of a significant retardation.

General conclusions

The main objective of the present thesis was to significantly improve the rheological and the early age properties (in particular strength evolution) of sodium carbonate activated GGBS based binders. At the beginning, rheological test results confirmed that such binders have insufficient properties for modern industrial applications. They can be characterized by a high initial yield stress and its fast evolution. As often seen in the literature for the cementitious materials, tuning of these values by addition of supplementary water led to an even poorer strength at early age and a significant decrease of durability at longer term. Increasing the GGBS fineness or decreasing of the water/binder ratio led to even poorer rheology. It was determined that the amount of Na_2CO_3 does not have a significant effect on the rheology deterioration rate during the first couple of hours and manifests its influence more in the long term. The main reason for the poor rheology was then attributed to the flocculation and the rapid hydrates precipitation.

A more detailed analysis of the hydration process starting from the first seconds of slag contact with alkaline solution by *in-situ* XRD with synchrotron source revealed that the first precipitates are calcium based: Gaylussite, Calcite, and different calcium-aluminium hydrates. This suggested that this element is possibly responsible for the previously described rheological problems. Taking into account this fact, the addition of additives that act as calcium complexing and/or inhibitors of calcium based crystal growth was tested. The most suitable are phosphonate based additives, due to their possibility of dissolution and interaction in high Na_2CO_3 saturated mediums. An increase of the setting time, as well as a decrease of the yield stress was obtained. Thus, a significant improvement of rheological properties was achieved, as one of the aims of the present work. In addition a higher compressive strength at longer term was observed due to a higher hydration rate with its addition, probably related to a supplementary seeding effect (hydration in bulk). Nevertheless their dosage has a significant influence not only on the rheological properties, but also on hydration kinetics. A high dosage leads to a significant increase of the induction period, due to a calcium complexation in non-soluble precipitates at the beginning required for C-S-H precipitation and other processes.

Regarding the strength evolution, it was observed that different factors affect this process. During the first days, a significant influence of the water/binder ratio was observed. Decreasing of the inter-grain distance leads to an acceleration of the hardening process. Nevertheless, even this does not allow the hardening to achieve a sufficiently high rate, to satisfy modern

requirements. Decreasing of the induction period and a corresponding improvement in early age strength was achieved by increasing the slag fineness. This was especially pronounced in the case of ultra-fine slag. However, these two methods were less effective with decreasing curing temperature. In this connection, the analysis of the subsequent stages of hydration suggested the reason for the long induction period.

The study of sodium carbonate influence has showed that there is a significant difference of the hydration process between low (less than 100 g/l) and high (more than 150 g/l) concentration in water. This indicates the presence of two different reasons for a long induction period.

Analysis of the formed hydrates in the case of high sodium carbonate concentration showed that the dominant hydrate from the first minutes is Gaylussite (double salt of Na and Ca carbonates). This hydrate plays a double role. First, its precipitation leads to a consumption of Ca^{2+}, preventing its reabsorption on the slag surface and further formation of passivation layer. In addition, due to the presence of CO_3^{2-} in solution and the fact that Na^+ ions might hardly get close to the slag's surface, the precipitation of these salts occur mostly in bulk, provided further nucleation sites. At longer term, the gradual dissolution of this hydrate leads to the release of Na^+ ions to maintain a high pH level for slag dissolution rate acceleration. That is why this type of activation is characterized by high strength and durability. At the same time, Gaylussite formation inhibits the growth of alkalinity (capturing of Na^+ in its structure) and an increase in calcium concentration (capturing of Ca^{2+}), required for C-S-H formation at the first 24h of hydration. These last two phenomena are responsible for the long induction period, when significant strength growth is achieved after the end of its precipitation and the beginning of decomposition. From the literature, it is known that this phase is metastable and decomposes under the influence of elevated temperature (from 40°C) and/or a significant decrease in the concentration of carbon dioxide (in solution).

The acceleration of Gaylussite decomposition by heating for 24h showed that the treatment was efficient and confirms the previous assumption regarding the causes of the long induction period. Such method of heat treatment is well-adapted for the precast industry. However for conventional construction the most suitable option is to use a dry or liquid additive to speed up the process.

The addition of a calcium source (for calcite precipitation and consumption of CO_3^{2-} ions for faster Gaylussite decomposition) greatly accelerates the hardening. However, the source of this calcium can significantly affect many parameters at the same time. In the case of lime

addition, a sharp increase in calcium concentration led to problems with rheology and further hydration. The use of a source with gradual calcium leaching (Portland clinker here) seems to be more adapted. Coupled with phosphonate based additives, the provided acceleration effect doesn't affect the rheological properties. In addition, the use of phosphonates led to a better hydration process at the very beginning in the case of a slag-clinker blended binder. Additional Ca/Si/Al leached from clinker can also contribute to faster C-S-H precipitation and be the reason for significant improvement.

However, this acceleration through calcium source addition at the first 3 days of hardening slightly decreases the compressive strength at short term compared to plain GGBS, which is most noticeable in the period of 7-28 days. This is most likely associated with a less dense C-S-H gel formed and slower slag dissolution rate. An increase in the slag fineness can partially compensate for this phenomenon. Hence the results with the addition of different alumina sources indicates, that a more likely reason for this lower slag dissolution is precipitation of some carboaluminates on its surface (passivation layer) or even incorporation of alumina in the slag surface structure which interfere its dissolution.

Among other positive aspects of hydration acceleration by an added calcium source is that such a blended cement is less sensitive to variations in water content. Also, the drop in strength with lower curing temperature is less critical compared to plain GGBS, as well as in the case of low relative humidity storage. A higher robustness of the system is a key parameter for industrial applications.

In case of a very low initial sodium carbonate concentration, the precipitation of very low crystalized/amorphous calcite on a slag surface should be responsible for the very long induction period. No Gaylussite was formed. Therefore the heat treatment at only 40°C doesn't provide any significant improvement in early age strength. Further, the lower alkalinity of such a mix (no internal source to achieve high pH) and the absence of nucleation seeds appears to be responsible for low compressive strength. In this case, the addition of clinker also showed its effectiveness. Possible protection of the slag surface from the amorphous calcite layer and precipitation of some nucleation seeds in bulk led to the strength evolution beyond the first days. However, the results are still modest compared to the sufficiently high Na_2CO_3 concentration which favour Gaylussite precipitation.

To compensate for the additional CO_2 footprint from the previously added additives or other methods of hardening acceleration (increasing of the slag fineness, heat treatment), a binder dilution was performed. The obtained results showed that partial dilution of GGBS by

conventional limestone powder can provide additional environmental and economic benefits, without any degradation of the properties. The results indicate that this is mostly due to the seeding effect of the limestone particles and consequently a higher rate of binder hydration. The effect of such a supplementary material is strongly dependent on its dosage and fineness. In the case of very high fineness, even with a very low amount an amelioration of the properties can be achieved.

Perspectives

Despite significant improvements in the early age properties of such alkali-activated binders for real construction applications, further researches are still needed.

Regarding the rheological properties, it has been demonstrated that novel additives should be used in the case of sodium carbonate activation. Existing solutions (plasticizers) for Portland based cement systems are ineffective or even have the opposite effect. In the case of more effective additives, potentially combined with phosphonates, a more significant decrease in W/B ratio should be achieved with through preserving high fluidity. This should allow a significant increase in the setting and hardening of the system, which will also lead to improvement of the durability properties. In addition, as it was shown, the aqueous concentration of activator and not its total amount plays an important role. Reducing the water content permits a reduction of the activator dosage, leading to ecological and economical benefits.

It is also preferable to find supplementary ways of strength evolution acceleration. At standard curing conditions, it might lead to even greater strengths, which is a definite benefit in the context of modern construction. In addition, this should allow for a reduction in the negative impact of lower temperatures and respectively increase the binder robustness versus this factor. It should also allow for an increase in the dilution rate of the binder with more inert materials, which will have an even greater economic and environmental effect, especially if other industrial wastes and co-products are used for such dilutions. Another source of calcium with a well-controlled dissolution rate will permit the adoption of an OPC free system with the same robustness and potentially eliminate its negative influence on strength evolution in the short term. Also a more in-depth studies are needed for better understanding on how adding a calcium source accelerate the reaction, since an additional mechanisms might take place. For example, the effect of leached Al/Si from clinker remains unknown, and might be in the origins of some strength degradation between 7 and 90 days.

However, even at this stage, the formulations developed in the present work may already be used for a large variety of applications. For this, a more detailed study of durability is required.

Bibliography

Abdalqader, A., Al-tabbaa, A., 2015. Sustainable Binder Based on Sodium Carbonate-Activated Fly Ash / Slag and Reactive Magnesia, in: International Concrete Sustainability Conference, At Miami.

Abdalqader, A.F., Jin, F., Al-Tabbaa, A., 2016. Development of greener alkali-activated cement: Utilisation of sodium carbonate for activating slag and fly ash mixtures. J. Clean. Prod. 113, 66–75. https://doi.org/10.1016/j.jclepro.2015.12.010

Akhter, H., Butler, L.G., Branz, S., Cartledge, F.K., Tittlebaum, M.E., 1990. Immobilization of As, Cd, Cr and Pb-containing soils by using cement or pozzolanic fixing agents. J. Hazard. Mater. 24, 145–155.

Allahverdi, A., Ahmadnezhad, S., 2014. Mechanical activation of silicomanganese slag and its influence on the properties of Portland slag cement. Powder Technol. 251, 41–51. https://doi.org/10.1016/j.powtec.2013.10.023

Allan, M.L., Kukacka, L.E., 1995. Blast furnance slag-modified grouts for in-situ stabilisation of chromium-contaminated soil. Waste Manag. 15, 193–202.

Altan, E., Erdogan, S.T., 2012. Alkali activation of a slag at ambient and elevated temperature. Cem. Concr. Compos. 34, 131–139. https://doi.org/10.1016/j.cemconcomp.2011.08.003

Bae, S., Hikaru, F., Kanematsu, M., Yoshizawa, C., 2018. Removal of Hexavalent Chromium in Portland Cement Using Ground Granulated. Materials (Basel). 11, 1–17. https://doi.org/10.3390/ma11010011

Bakharev, T., Sanjayan, J.G., Cheng, Y., 1999. Effect of elevated temperature curing on properties of alkali-activated slag concrete. Cem. Concr. Res. 29, 1619–1625.

Barnett, S.J., Soutsos, M.N., Millard, S.G., Bungey, J.H., 2006. Strength development of mortars containing ground granulated blast-furnace slag : Effect of curing temperature and determination of apparent activation energies. Cem. Concr. Res. 36, 434–440. https://doi.org/10.1016/j.cemconres.2005.11.002

Baroghel-Bouny, V., Chaussadent, T., Croquette, G., Divet, L., Gawsewitch, J., Godin, J., Henry, D., Platret, G., Villain, G., 2002. Methodes d'essais №58: Caracteristiques microstructurales et propriétés relatives a la durabilite des betons.

Behnood, A., Tittelboom, K. Van, Belie, N. De, 2016. Methods for measuring pH in concrete : A review. Constr. Build. Mater. 105, 176–188. https://doi.org/10.1016/j.conbuildmat.2015.12.032

Bellmann, F., Stark, J., 2009. Activation of blast furnace slag by a new method. Cem. Concr. Res. 39, 644–650. https://doi.org/10.1016/j.cemconres.2009.05.012

Bernal, S., Provis, J.L., Myers, R.J., San Nicolas, R., van Deventer, J.S.J., 2015. Role of carbonates in the chemical evolution of sodium carbonate-activated slag binders. Mater. Struct. 48, 1–13. https://doi.org/10.1617/s11527-014-0412-6

Bernal, S.A., Provis, J.L., Deventer, J.S.J., 2018. Impact of Water Content on the Performance of Alkali-Activated Slag Concretes, in: Sicth International Conference on the Durability of

Concrete Structures. pp. 1–4.

Bernal, S.A., Provis, J.L., Rose, V., Mejía De Gutierrez, R., 2011. Evolution of binder structure in sodium silicate-activated slag-metakaolin blends. Cem. Concr. Compos. 33, 46–54. https://doi.org/10.1016/j.cemconcomp.2010.09.004

Bernal, S.A., San Nicolas, R., van Deventer, J.S.J., Provis, J.L., 2016. Alkali-activated slag cements produced with a blended sodium carbonate / sodium silicate activator. Adv. Cem. Res. 28, 262–273.

Birchall, J.D., Howard, A.J., Bailey, J.E., 1978. On the hydration of Portland cement. Proc R Soc London Ser A 360, 445–453. https://doi.org/10.1098/rspa.1978.0078

Bishop, M., Bott, S.G., Barron, A.R., 2003. A New Mechanism for Cement Hydration Inhibition : Solid-State Chemistry of Calcium Nitrilotris (methylene) triphosphonate. Chem. Mater. 15, 3°74-3088. https://doi.org/10.1021/cm0302431

Black, L., Ogirigbo, O.R., Black, L., 2016. Influence of slag composition and temperature on the hydration and microstructure of slag blended cements. Constr. Build. Mater. 126, 496–507. https://doi.org/10.1016/j.conbuildmat.2016.09.057

Bossa, N., Chaurand, P., Vicente, J., Borschneck, D., Levard, C., Aguerre-Chariol, O., Rose, J., 2015. Micro- and nano-X-ray computed-tomography: A step forward in the characterization of the pore network of a leached cement paste. Cem. Concr. Res. 67, 138–147. https://doi.org/10.1016/j.cemconres.2014.08.007

Bouaziz, A., Hamzaoui, R., Lakhal, R., Achoura, D., Leklou, N., 2017. Efficiency of high energy over conventional milling of granulated blast furnace slag powder to improve mechanical performance of slag cement paste. Powder Technol. 308, 37–46. https://doi.org/10.1016/j.powtec.2016.12.014

Brough, A.R., Atkinson, A., 2002. Sodium silicate-based , alkali-activated slag mortars Part I . Strength , hydration and microstructure. Cem. Concr. Res. 32, 865–879.

Browning, F.H., Fogler, H.S., 1996. Effect of Precipitating Conditions on the Formation of Calcium-HEDP Precipitates. Langmuir 7463, 5231–5238. https://doi.org/10.1021/la9603277

Bury, C.R., Redd, R., 1933. Gaulissite formation. J. Chem. Soc. 1160–1162.

Castellano, C.C., Bonavetti, V.L., Donza, H.A., Irassar, E.F., 2016. The effect of w/b and temperature on the hydration and strength of blastfurnace slag cements. https://doi.org/10.1016/j.conbuildmat.2015.11.001

Chappex, T., Scrivener, K.L., 2012. The influence of aluminium on the dissolution of amorphous silica and its relation to alkali silica reaction. Cem. Concr. Res. 42, 1645–1649. https://doi.org/10.1016/j.cemconres.2012.09.009

Collier, N.C., 2016. Transition and decomposition temperatures of cement phases - a collection of thermal analysis data. Ceramics-Silikaty 60, 338–343. https://doi.org/10.13168/cs.2016.0050

Daimon, M., Roy, D.M., 1979. Rheological properties of cement mixes: II. Zeta potential and preliminary viscosity studies. Cem. Concr. Res. 9, 103–109.

Damtoft, J.S., Lukasik, J., Herfort, D., Sorrentino, D., Gartner, E.M., 2008. Sustainable

development and climate change initiatives. Cem. Concr. Res. 38, 115–127. https://doi.org/10.1016/j.cemconres.2007.09.008

Davidovits, J., 2015. False values on CO2 emission for geopolymer cement/concrete published in scientific papers, Geopolymer institute library, www.geopolymer.org.

Deja, J., 2002. Carbonation Aspects of Alkali Activated Slag Mortars and Concretes. Silic. Ind. 67, 37–42.

Demadis, K., Lykoudis, P., 2005. Chemistry of Organophosphonate Scale Growth Effect on CaCO3 Crystal Growth. Bioinorg. Chem. Appl. 3, 135–150. https://doi.org/10.1155/BCA.2005.135

Dheilly, R., Tudo, J., 1997. Contribution a l'etude de la gaylussite: Na2Ca(CO3)2,5H20. C.R. Acad. Sci. Paris 325, 407–414. https://doi.org/10.1016/S1251-8069(97)80070-X

Elakneswaran, Y., Nawa, T., Kurumisawa, K., 2009. Zeta potential study of paste blends with slag. Cem. Concr. Compos. 31, 72–76. https://doi.org/10.1016/j.cemconcomp.2008.09.007

Fagerlund, G., 1999. Self-desiccation and its importance in concrete technology : proceedings of the Second International Research Seminar in Lund, June 18, 1999.

Fernández-Jiménez, A., Palomo, J.G., Puertas, F., 1999. Alkali-activated slag mortars mechanical strength behaviour. Cem. Concr. Res. 29, 1313–1321.

Fernandez-Jimenez, A., Puertas, F., 1997. Alkali-activated slag cements: kinetic studies. Cem. Concr. Res. 27, 359–368.

Franks, G. V, 2002. Zeta Potentials and Yield Stresses of Silica Suspensions in Concentrated Monovalent Electrolytes : Isoelectric Point Shift and Additional Attraction. J. Colloid Interface Sci. 51, 44–51. https://doi.org/10.1006/jcis.2002.8250

Frederic, L., 2012. Synthesis and Characterisation of Layered Double Hydroxides and their Application for Water Purification. Thesis.

Frost, R.L., Palmer, S.J., Spratt, H.J., 2009. Thermal decomposition of hydrotalcites with variable cationic ratios. J. Therm. Anal. Calorim. 95, 123–129. https://doi.org/10.1080/09593969.2010.491213

GCIP, G.C.I.P., 2007. Soda Ash 46. https://doi.org/10.1002/9780470114735.hawley14648

Gebregziabiher, B.S., Thomas, R., Peethamparan, S., 2015. Very early-age reaction kinetics and microstructural development in alkali-activated slag. Cem. Concr. Compos. 55, 91–102. https://doi.org/10.1016/j.cemconcomp.2014.09.001

Ghiasvand, E., Ramezanianpour, A.A., Ramezanianpour, A.M., 2014. Effect of grinding method and particle size distribution on the properties of Portland-pozzolan cement. Constr. Build. Mater. 53, 547–554.

Glukhovsky, V.D., Pahomov, V.A., 1978. Шлакощелочные цементы и бетоны (Alkali-activated cements and concretes), Budivelnik. ed. Kiev.

Gruskovnjak, A., Lothenbach, B., Winnefeld, F., Figi, R., Ko, S., Adler, M., Mäder, U., 2008. Hydration mechanisms of super sulphated slag cement. Cem. Concr. Res. 38, 983–992. https://doi.org/10.1016/j.cemconres.2008.03.004

Habbaba, A., Plank, J., 2012. Surface chemistry of ground granulated blast furnace slag in

cement pore solution and its impact on the effectiveness of polycarboxylate superplasticizers. J. Am. Ceram. Soc. 95, 768–775. https://doi.org/10.1111/j.1551-2916.2011.04968.x

Haha, M. Ben, Lothenbach, B., Saout, G. Le, Winnefeld, F., 2012. Influence of slag chemistry on the hydration of alkali-activated blast-furnace slag — Part II : Effect of Al2O3. Cem. Concr. Res. 74–83. https://doi.org/10.1016/j.cemconres.2011.08.005

Haha, M. Ben, Saout, G. Le, Winnefeld, F., Lothenbach, B., 2011. Influence of activator type on hydration kinetics , hydrate assemblage and microstructural development of alkali activated blast-furnace slags. Cem. Concr. Res. 41, 301–310. https://doi.org/10.1016/j.cemconres.2010.11.016

Harrabin, B.R., 2017. India's double first in climate battle [WWW Document]. BBC News. URL https://www.bbc.com/news/business-38391034

Hashim, A.N., Hussin, K., Begum, N., Al Bakri Abdullah, M.M., Abdul Razak, K., Ekaputri, J.J., 2015. Effect of Sodium Hydroxide (NaOH) Concentration on Compressive Strength of Alkali-Activated Slag (AAS) Mortars. Appl. Mech. Mater. 754–755, 300–304. https://doi.org/10.4028/www.scientific.net/AMM.754-755.300

Heberling, F., Trainor, T.P., Lützenkirchen, J., Eng, P., Denecke, M.A., Bosbach, D., 2011. Structure and reactivity of the calcite – water interface. J. Colloid Interface Sci. 354, 843–857. https://doi.org/10.1016/j.jcis.2010.10.047

Hodakov, G.S., 1972. Тонкое измельчение строительных материалов (Fine grinding of building materials), Stroyizdat. ed. Moscow.

Holt, E.E., 2001. Early age autogenous shrinkage of concrete. VTT Publ. 2–184.

Houghton, J.., Meira Filho, L.G., Lim, B., Al., E., 1996. IPCC, Guidelines for National Greenhouse Gas Inventories: Refrence Manual, Volume 2.

Humad, A.M., Provis, J.L., Cwirzen, A., 2017. Alkali activation of a high MgO GGBS – fresh and hardened properties. Mag. Concr. Res. 1–9.

Jacquemot, F., 2014. Accélération du durcissement des liants à base de laitier de haut fourneaupour les produits préfabriqués en béton, PhD thesis.

Jahanshahi, S., Pan, Y., Liaoning, T., 2012. Some fundamental aspects of the dry slag granulation process Some Fundamental Aspects of the Dry Slag Granulation Process. 9th Int. Conf. Molten Slag, Fluxes Salts, Beijing, China.

Jeong, Y., Eun, J., Jun, Y., Park, J., Ha, J., 2016. Influence of four additional activators on hydrated-lime [Ca(OH)2] activated ground granulated blast-furnace slag. Cem. Concr. Compos. 65, 1–10. https://doi.org/10.1016/j.cemconcomp.2015.10.007

Jin, F., Al-Tabbaa, A., 2015. Strength and drying shrinkage of slag paste activated by sodium carbonate and reactive MgO. Constr. Build. Mater. 81, 58–65. https://doi.org/10.1016/j.conbuildmat.2015.01.082

Jin, F., Gu, K., Al-Tabbaa, A., 2014. Strength and Drying Shrinkage of Alkali-Activated Slag Pastes Containing Reactive MgO. Second Int. Conf. Adv. Chem. Mater. 51, 395–404.

Johnson, D.R., Robb, W.A., 1973. Gaylussite: Thermal Properties by Simultaneous Thermal Analysis. Am. Mineral. 58, 778–784.

Johnson, S.B., Franks, G.V., Scales, P.J., Boger, D.V., Healy, T.W., 2000. Surface chemistry–rheology relationships in concentrated mineral suspensions. Int. J. Miner. Process. 58, 267–304. https://doi.org/10.1016/s0301-7516(99)00041-1

Ke, X., Bernal, S.A., Provis, J.L., 2016. Controlling the reaction kinetics of sodium carbonate-activated slag cements using calcined layered double hydroxides. Cem. Concr. Res. 81, 24–37. https://doi.org/10.1016/j.cemconres.2015.11.012

Klemm, W.A., 1994. Hexavalent Chromium in Portland Cement. Cem. Concr. Aggregates 16, 43–47.

Klieger, P., 1958. Effect of mixing and curing temperature on concrete strength. J. merican Concr. Inst. 54, 1063–1081.

Kocaba, V., 2009. Development and Evaluation of Methods to Follow Microstructural Development of Cementitious Systems Including Slags, PhD thesis.

Kouassi, S.S., 2011. Etude de la dissolution d'un réseau silicaté en présence d'une solution alcaline, PhD thesis.

Kovtun, M., Kearsley, E.P., Shekhovtsova, J., 2015. Chemical acceleration of a neutral granulated blast-furnace slag activated by sodium carbonate. Cem. Concr. Res. 72, 1–9.

Kravchenko, V.P., Gankevich, V.F., 2013. Поверхностна активность и прочностные (вяжущие) свойства активированных доменных шлаков (Surface activity and strength (binding) properties of ativated blast furnace slags). Enrich. Miner. 55.

Krivenko, P., 2017. Why Alkaline Activation – 60 Years of the Theory and Practice of Alkali-Activated Materials. J. Ceram. Sci. Technol. 8, 323–334. https://doi.org/10.4416/JCST2017-00042

Kryvenko, P., Runova, R., Rudenko, I., Skoryk, V., Omelchuk, V., 2017. Analysis of plasticizer effectiveness during alkaline cement structure formation. J. Enterp. Inf. Manag. 35–41. https://doi.org/10.15587/1729-4061.2017.106803

Kumar, R., Kumar, S., Badjena, S., Mehrotra, S.P., 2005. Hydration of Mechanically Activated Granulated Blast Furnace Slag. Metall. Mater. Trans. B 36, 873–883.

Kumar, S., Kumar, R., Bandopadhyay, A., Alex, T.C., Kumar, B.R., Das, S.K., Mehrotra, S.P., 2008. Mechanical activation of granulated blast furnace slag and its effect on the properties and structure of portland slag cement. Cem. Concr. Compos. 30, 679–685. https://doi.org/10.1016/j.cemconcomp.2008.05.005

Kunther, W., Ferreiro, S., Skibsted, J., 2017. Influence of the Ca/Si ratio on the compressive strength of cementitious calcium-silicate-hydrat binders. J. Maerials Chem. A 2, 17401–17412. https://doi.org/10.1039/c7ta06104h

Kuznetsov, A.M., 1963. Технология вяжущих веществ и изделий из них (Technology of binders and products from them). Vishaya shkola, Moscow.

Kwan, S., LaRosa, J., Grutzeck, M.W., 1995. 29Si and 27Al MAS NMR study of strätlingite. J. Am. Ceram. Soc. 78, 1921–1926.

Kwok, P.S.T., 2013. Slag-Limestone Blends for Sustainable Concrete, Fourth-year undergraduate project.

L'Hôpital, E., Lothenbach, B., Le Saout, G., Kulik, D., Scrivener, K., 2015. Incorporation of

aluminium in calcium-silicate-hydrates. Cem. Concr. Res. 75, 91–103. https://doi.org/10.1016/j.cemconres.2015.04.007

Laar, R. van, Dupon, E., Barel, J., Kamerling, M., 2014. Blast furnace slag granulation plant technology. Millenium steel 28–31.

Land, G., Stephan, D., 2012. The influence of nano-silica on the hydration of ordinary Portland cement. J. Mater. Sci. 47, 1011–1017. https://doi.org/10.1007/s10853-011-5881-1

Li, C., Gao, Z., 2017. Effect of grinding media on the surface property and fl otation behavior of scheelite particles. Powder Technol. 322, 386–392. https://doi.org/10.1016/j.powtec.2017.08.066

Li, J., Yu, Q., Huang, H., Yin, S., 2019. Effects of Ca/Si Ratio, Aluminum and Magnesium on the Carbonation Behavior of Calcium Silicate Hydrate. Materials (Basel). 12, 1268. https://doi.org/10.3390/ma12081268

Liu, D., 2011. Research on Performance Evaluation and Anti-scaling Mechanism of Green Scale Inhibitors by Static and Dynamic Methods.

Lowke, D., Gehlen, C., 2017. The zeta potential of cement and additions in cementitious suspensions with high solid fraction. Cem. Concr. Res. 95, 195–204. https://doi.org/10.1016/j.cemconres.2017.02.016

Lupu, C., Arvidson, R.S., Lu, A., Barron, A.R., 2005. Phosphonate mediated surface reaction and reorganization : implications for the mechanism controlling cement hydration inhibition. Chem. Commun. 14, 2354–2356. https://doi.org/10.1039/b500192g

Magallanes-Rivera, R.X., Escalante-Garcia, J.L., 2014. Anhydrite/hemihydrate-blast furnace slag cementitious composites : Strength development and reactivity. Constr. Build. Mater. 65, 20–28. https://doi.org/10.1016/j.conbuildmat.2014.04.056

Malhotra, V.M., 1987. Matériaux complementaires en cimentation pour le béton. Ministre des Approvisionnements et Services Canada, Ottawa.

Manoli, F., Dalas, E., 2000. Spontaneous precipitation of calcium carbonate in the presence of ethanol , isopropanol and diethylene glycol. J. Cryst. Growth 218, 359–364.

Maraghechi, H., Rajabipour, F., Pantano, C.G., Burgos, W.D., 2016. Effect of calcium on dissolution and precipitation reactions of amorphous silica at high alkalinity. Cem. Concr. Res. 87, 1–13. https://doi.org/10.1016/j.cemconres.2016.05.004

Masoudi, R., Hooton, R.D., 2019. Examining the hydration mechanism of supersulfated cements made with high and low-alumina slags. Cem. Concr. Compos. https://doi.org/10.1016/j.cemconcomp.2019.05.001

Medina, T. de J., Arredondo-Rea, S.P., Gomez-Soberon, J.M., Rosas-Casarez, C.A., Corral-Higuera, R., 2016. Effect of curring temperature in the alkali-activated blast-furnace slag paste and their structural influence of porosity. Adv. Sci. Technol. 10, 74–79. https://doi.org/10.12913/22998624/64021

Michel, M., 2009. Accélération de ciment au laitier par du ciment sulfo-alumineux, PhD thesis.

Mohamed, O.A., 2019. A Review of Durability and Strength Characteristics of Alkali-Activated Slag Concrete. Materials. 12. https://doi.org/10.3390/ma12081198

Moranville-Regourd, M., 1998. Cements made from blast furnace slag. Lea's Chem. Cem.

Concr. 4° edition, 633–674.

Morsy, M.S., Shebl, S.S., Rashad, A.M., 2008. Effect of Fire on Microstructure and Mechanical Properties of Blended Cement Pastes Containing Metakaolin and Silica Fume. Asian J. Civ. Eng. (Building Hous. 9, 93–105.

Moseson, A.J., Moseson, D.E., Barsoum, M.W., 2012. High volume limestone alkali-activated cement developed by design of experiment. Cem. Concr. Compos. 34, 328–336. https://doi.org/10.1016/j.cemconcomp.2011.11.004

Naik, B.T.R., 2005. Sustainability of cement and concrete industies, in: Global Construction: Ultimate Concrete Opportunities.

Nazari, A., Sanjayan, J.G., 2016. Handbook of low carbon concrete, 1st ed. Butterworth-Heinemann.

Newlands, K.C., Foss, M., Matchei, T., Skibsted, J., Macphee, D.E., 2016. Early stage dissolution characteristics of aluminosilicate glasses with blast furnace slag- and fly-ash-like compositions. Am. Ceram. Soc. 1941–1955. https://doi.org/10.1111/jace.14716

NF EN 15167-1, 2006. Ground granulated blast furnace slagfor use in concrete, mortar and grout.

NF EN 196-1, 2016. Méthodes d'essais des ciments — Partie 1 : Détermination des résistances.

Oliveira, K.A., Pedro, A., Oliveira, N. De, Hotza, D., Raupp-pereira, F., 2017. Industrial Wastes as Alternative Mineral Addition in Portland Cement and as Aggregate in Coating Mortars. Mater. Res. 20, 358–364.

Papadakis, V.G., Tsimas, S., 2002. Supplementary cementing materials in concrete Part I : efficiency and design. Cem. Concr. Res. 32, 1525–1532.

Parker, M., Jones, J., Shapiro, J., Bentham, M., 2013. Carbon capture plant turns emissions into baking soda [WWW Document]. Conversat. URL http://theconversation.com/carbon-capture-plant-turns-emissions-into-baking-soda-18847

Pelisser, F., Jean, P., Gleize, P., Mikowski, A., 2012. Effect of the Ca/Si Molar Ratio on the Micro/ nanomechanical Properties of Synthetic C-S-H Measured by Nanoindentation. J. Phys. Chem. C 116, 17219–17227. https://doi.org/10.1021/jp302240c

Plank, J., Hirsch, C., 2007. Impact of zeta potential of early cement hydration phases on superplasticizer adsorption. Cem. Concr. Res. 37, 537–542. https://doi.org/10.1016/j.cemconres.2007.01.007

Pointeau, I., Reiller, P., Macé, N., Landesman, C., Coreau, N., 2006. Measurement and modeling of the surface potential evolution of hydrated cement pastes as a function of degradation. J. Colloid Interface Sci. 300, 33–44. https://doi.org/10.1016/j.jcis.2006.03.018

Powers, T.C., 1958. Structure and Physical Properties of Hardened Portland Cement Paste. J. Am. Ceram. Soc. 41, 1–6. https://doi.org/10.1111/j.1151-2916.1958.tb13494.x

Provis, J.L., Deventer, J.S.., 2014. Alkali Activated Materials,State-of-the-Art Report, RILEM TC 224-AAM. https://doi.org/10.1007/978-94-007-7672-2_5

Rahman, A., Rasul, M.G., Khan, M.M.K., Sharma, S., 2012. Industrial Waste as Alternative Fuel in Cement Industry : Its Impact on Environment. Environ. Geol. Sci. Ind. 108–114.

Rakhimova, N.R., Rakhimov, R.Z., Naumkina, N.I., Khuzin, A.F., Osin, Y.N., 2016. Influence

of limestone content, fineness, and composition on the properties and microstructure of alkali-activated slag cement. Cem. Concr. Compos. 72, 268–274. https://doi.org/10.1016/j.cemconcomp.2016.06.015

Rickert, J., 2012. Zeta potential and rheology of cement pastes – influence of superplasticisers and of granulated blastfurnace slag and limestone. Dusseldorf.

Russel, W.B., Saville, D.A., Schowalter, W.R., 1989. Colloidal Dispersions, Cambridge. ed.

Safi, B., Benmounah, A., Saidi, M., 2011. Rheology and zeta potential of cement pastes containing calcined silt and ground granulated blast-furnace slag. Mater. Construcción 61, 353–370.

San, R., Bernal, S.A., Mejía, R., Gutiérrez, D., Deventer, J.S.J. Van, Provis, J.L., 2014. Distinctive microstructural features of aged sodium silicate-activated slag concretes. Cem. Concr. Res. 65, 41–51. https://doi.org/10.1016/j.cemconres.2014.07.008

Santacruz, I., Torre, Á.G.D. la, Álvarez-Pinazo, G., Cabeza, A., Cuesta, A., Sanz, J., Aranda, M.A.G., 2015. Structure of stratlingite and effect of hydration methodology on microstructure. Adv. Cem. Res. 28, 13–22. https://doi.org/10.1680/adcr.14.00104

Shi., C., Krivenko, P. V., Roy, D., 2006. Alkali-Activated Cements and Concretes. Taylor & F, Abingdon. https://doi.org/10.1017/CBO9781107415324.004

Shi, C., 1996. Strength, pore structure and permeability of alkali-activated slag mortars. Cem. Concr. Res. 26, 1789–1799.

Shi, C.J., Day, R.L., 1995. A Calorimetric Study of Early Hydration of Alkali-Slag Cements. Cem. Concr. Res. 25, 1333–1346. https://doi.org/10.1016/0008-8846(95)00126-w

Shi, Z., Shi, C., Wan, S., Ou, Z., 2017. Effect of alkali dosage on alkali-silica reaction in sodium hydroxide activated slag mortars. Constr. Build. Mater. 143, 16–23. https://doi.org/10.1016/j.conbuildmat.2017.03.125

Singh, M., Garg, M., 1995. Activation of gypsum anhydrite-slag mixtures. Cem. Concr. Res. 25, 332–338.

Smith, B.J., Rawal, A., Funkhouser, G.P., Roberts, L.R., Gupta, V., Israelachvili, J.N., Chmelka, B.F., 2011. Origins of saccharide-dependent hydration at aluminate, silicate, and aluminosilicate surfaces. Proc. Natl. Acad. Sci. 108, 8949–8954. https://doi.org/10.1073/pnas.1104526108

Song, J., Yang, K., Kim, G., Lee, C., Kim, B., Lee, J., 2010. Properties of Sodium Alkali-Activated Ground Granulated Blast-Furnace slag (GGBS) Mortar, in: First International Conference on Sustainability and the Future.

Song, J.K., Yang, K.H., Lee, K.S., 2010. An Expermental Study on Properties of Non-Cement Mortar with Alkali-Activator Combinations, in: International Conference on Sustainable Building Asia. pp. 507–512.

Spanlang, A., Wukovits, W., Weiss, B., 2016. Development of a Blast Furnace Model with Thermodynamic Process Depiction by Means of the Rist Operating Diagram. Chem. Eng. Trans. 52. https://doi.org/10.3303/CET1652163

Sun, Z., Vollpracht, A., 2018. Isothermal calorimetry and in-situ XRD study of the NaOH activated fl y ash , metakaolin and slag. Cem. Concr. Res. 103, 110–122.

https://doi.org/10.1016/j.cemconres.2017.10.004

Suraneni, P., Palacios, M., Flatt, R.J., 2016. New insights into the hydration of slag in alkaline media using a micro-reactor approach. Cem. Concr. Res. 79, 209–216. https://doi.org/10.1016/j.cemconres.2015.09.015

Tan, H., Deng, X., He, X., Zhang, J., Zhang, X., Su, Y., Yang, J., 2019. Compressive strength and hydration process of wet-grinded granulated blast-furnace slag activated by sodium sulfate and sodium carbonate. Cem. Concr. Compos. 97, 387–398. https://doi.org/10.1016/j.cemconcomp.2019.01.012

Taylor, R., Richardson, I.G., Brydson, R.M.D., 2010. Composition and microstructure of 20-year-old ordinary Portland cement–ground granulated blast-furnace slag blends containing 0 to 100% slag. Cem. Concr. Res. 40, 971–983. https://doi.org/10.1016/j.cemconres.2010.02.012

Thomas, N.L., Double, D.D., 1983. The hydration of Portland cement, C3S and C2S in the presence of a calcium complexing admixture (EDTA). Cem. Concr. Res. 13, 391–400. https://doi.org/10.1016/0008-8846(83)90039-X

Thomas, R.J., Lezama, D., Peethamparan, S., 2017. On drying shrinkage in alkali-activated concrete : Improving dimensional stability by aging or heat-curing. Cem. Concr. Res. 91, 13–23. https://doi.org/10.1016/j.cemconres.2016.10.003

Turner, L.K., Collins, F.G., 2013. Carbon dioxide equivalent (CO2-e) emissions : A comparison between geopolymer and OPC cement concrete. Constr. Build. Mater. 43, 125–130. https://doi.org/10.1016/j.conbuildmat.2013.01.023

Turu'Allo, G., 2013. Early Age Strength Development of GGBS Concrete Cured Under Different Temperatures, PhD thesis.

Wang, C., Li, S., Li, T., 2009. Calcium carbonate inhibition by a phosphonate-terminated poly (maleic-co-sulfonate) polymeric inhibitor. Desalination 249, 1–4. https://doi.org/10.1016/j.desal.2009.06.006

Wang, J., Lyu, X., Wang, L., Cao, X., Liu, Q., Zang, H., 2017. Influence of the combination of calcium oxide and sodium carbonate on the hydration reactivity of alkali-activated slag binders. J. Clean. Prod. https://doi.org/10.1016/j.jclepro.2017.10.077

Wang, S., Scrivener, K.L., 1995. Hydration products of alkali activated slag cement. Cem. Concr. Res. 25, 561–571.

Wang, S., Scrivener, K.L., Pratt, P.L., 1994. Factors affecting the strength of alkali-activated slag. Cem. Concr. Compos. 24, 1033–1043.

Winnefeld, F., Haha, M. Ben, Saout, G., Costoya, M., Ko, S., Lothenbach, B., 2015. Influence of slag composition on the hydration of alkali-activated slags. J. Sustain. Cem. Mater. 4, 85–100. https://doi.org/10.1080/21650373.2014.955550

Wortmann, K., 2018. Retarder for Alkali Activated Binder, EP 3 296 278 A1.

Xyla, A.G., Koutsoukos, P.G., 1987. Effect of Diphosphonates on the Precipitation of Calcium Carbonate in Aqueous Solutions. J. Chem. Soc. Faraday Trans. 83, 1477–1484.

Yang, K., Cho, A., Song, J., Nam, S., Al, S., 2012. Hydration products and strength development of calcium hydroxide-based alkali-activated slag mortars. Constr. Build. Mater. 29, 410–

419. https://doi.org/10.1016/j.conbuildmat.2011.10.063

Yang, K., Sim, J., Nam, S., 2010. Enhancement of reactivity of calcium hydroxide-activated slag mortars by the addition of barium hydroxide. Constr. Build. Mater. 24, 241–251. https://doi.org/10.1016/j.conbuildmat.2009.09.001

Yildirim, M., Akarsu, H., 2010. Preparation of magnesium oxide (MgO) from dolomite be leach-precipitation-pyrohydrolysis process. Physicochem. Proplems Miner. Process. 44, 257–272.

Yu, L., Wang, H., Zhang, Y., Zhang, B., Liu, J., 2016. Recent advances in halloysite nanotube derived composites for water treatment. Environ. Sci. Nano 3, 28–44. https://doi.org/10.1039/C5EN00149H

Yuan, B., 2017. Sodium carbonate activated slag : reaction analysis , microstructural modification & engineering application, PhD thesis.

Yuan, B., Yu, Q.L., Broiuwers, H.J.H., 2017. Assessing the chemical involvement of limestone powder in sodium carbonate activated slag. Mater. Struct. 50. https://doi.org/10.1617/s11527-017-1003-0

Yuan, B, Yu, Q.L., Brouwers, H.J.H., 2017a. Time-dependent characterization of Na 2 CO 3 activated slag 84, 188–197. https://doi.org/10.1016/j.cemconcomp.2017.09.005

Yuan, B., Yu, Q.L., Brouwers, H.J.H., 2014. Investigation on the activating effect of Na2CO3 and NaOH on slag. NTCC2014 Int. Conf. Non-Traditional Cem. Concr. 21–25.

Yuan, B, Yu, Q.L., Dainese, E., Brouwers, H.J.H., 2017b. Autogenous and drying shrinkage of sodium carbonate activated slag altered by limestone powder incorporation 153, 459–468. https://doi.org/10.1016/j.conbuildmat.2017.07.112

ÉCOLE DOCTORALE
Sciences mécaniques et énergétiques, matériaux et géosciences (SMEMAG)

Titre : Amélioration des propriétés rhéologiques et à jeune âge des laitiers alcali-activés au carbonate de sodium

Mots clés : Laitier de hauts fourneaux ; ciment à base de laitier ; liant alkali-activé ; Carbonate de sodium ; ciment écologique ; ciment à faible impact CO_2

Résumé : L'un des principaux contributeurs à l'impact environnemental négatif de l'industrie de la construction est la fabrication de ciment Portland ordinaire (OPC), responsable de 5 à 8% des émissions de CO_2 dans le monde. Des matériaux plus écologiques sont maintenant nécessaires. Une possibilité consiste à utiliser du laitier de haut fourneau (GGBS) comme base pour ce ciment de nouvelle génération. Par conséquent, l'ajout d'additifs supplémentaires (activateurs) est nécessaire pour favoriser son hydratation à un taux raisonnable. L'activation par du carbonate de sodium (Na_2CO_3) est l'une des méthodes les plus prometteuses et en même temps les moins étudiées. Ce type d'activation alcaline offre le prix le plus bas, la sécurité la plus élevée, ainsi que d'excellentes propriétés mécaniques et de durabilité. Parmi les principaux problèmes qui entravent son utilisation à l'échelle industrielle, on peut mentionner une évolution de la résistance plutôt lente au cours des premiers jours de durcissement et de rhéologie médiocre. L'objectif principal des travaux de recherche est d'améliorer les propriétés de ce liant à jeune âge, qui répondraient à toutes les exigences modernes du secteur de la construction.

Les paramètres de base de ces types de mélanges ont été établis, comme l'influence de nombreux facteurs tels que le rapport W/B, la concentration de Na_2CO_3, la finesse du laitier et les conditions de cure, à la fois sur les propriétés à l'âge précoce et à long terme. Sur la base de l'analyse du processus d'hydratation, l'utilisation de certains additifs permettant de contrôler très efficacement les propriétés rhéologiques a ensuite été démontrée. Ces additifs permettent non seulement de contrôler le temps de prise, mais procurent également un effet plastifiant. En ce qui concerne l'amélioration des propriétés de résistance au jeune âge, différentes méthodes ont été utilisées. L'utilisation d'un traitement thermique ou d'une augmentation de la finesse du GGBS s'est avérée efficace. Néanmoins, l'utilisation de ces méthodes est souvent limitée. Les résultats du présent travail ont également montré la cause de la longue période d'induction. Une addition de source de calcium avec une cinétique de dissolution contrôlée a permis de résoudre ce problème. Finalement, pour une empreinte carbone finale encore plus faible d'un tel liant, une dilution par du filler calcaire a été considérée.

Title : Improving the rheological and early age properties of sodium carbonate alkali-activated GGBS

Keywords : Ground granulated blast-furnace slag (GGBS); slag cement; Alkali-activated binder; Sodium carbonate; eco-friendly cement; low CO_2 binder

Abstract : One of the major contributors of negative environmental impacts from the construction industry is the manufacturing of ordinary Portland cement (OPC), responsible for 5-8% of global CO_2 emissions. More environmentally-friendly materials are now required. One possibility is to use ground granulated blast furnace slag (GGBS) as the basis for such new generation cements. The addition of supplementary additives (activators) is required to promote its hydration to a reasonable rate. One of the most promising, and at the same time least studied, is sodium carbonate (Na_2CO_3) activator. This type of alkali activation provides the lowest price and the highest safety (low hazard risk), as well as excellent long term mechanical and durability properties. Among the main problems hindering its industrial-scale adoption are a rather slow strength evolution in the first days of hardening and poor rheology. The main objective of the present investigation is to improve the early age properties of this binder, which would allow it to meet all the modern requirements of the construction industry.

The basic parameters of these types of mixtures were established, such as the influence of W/B ratio, Na_2CO_3 concentration, slag fineness and curing conditions both on the early age and long term properties. Based on the analysis of internal processes, the use of some additives that permit the very effective control over the rheological properties was then demonstrated. These additives not only allow control over the setting time, but also provide a plasticizing effect. Regarding the improvement of early age strength, various methods have been used. The use of heat treatment or an increase in GGBS fineness turned out to be efficient. Nevertheless, such methods are often limited. The results of the present work have also shown the cause of a long induction period. A supplementary calcium source addition with controlled dissolution kinetics allowed solving this problem. Ultimately, for an even lower final carbon footprint of such a binder, a dilution by limestone powder was demonstrated.